Lanthanide Molecular Recognition towards Luminescent Labelling of Biomolecules: Application to New Screening Technologies

Linette L Meason

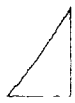

Ph D Chemistry, University of Edinburgh, 2002

I declare that this thesis has been composed by myself and that the research reported has been performed by myself unless otherwise stated.

Linette Meason
May 2002

Acknowledgements

Sincere thanks and appreciation are owed to Dr Zoe Pikramenou. As my academic supervisor, her relentless enthusiasm and continuous support throughout the duration of my Ph D have been an inspiration. In addition, thanks are due to the members of the ZOP group, past and present, including Steven Magennis, Hanna Haider, Murielle Chavarot and Kishore Boodhoo, for creating a friendly and often colourful working environment. Thanks also to the departmental services at Edinburgh and Birmingham Universities, especially to Dr Simon Parsons (Edinburgh) and Dr Benson Kariuki (Birmingham) for X-ray structural analysis and to Dr David Reed for 360 MHz NMR studies. I'd also like to thank my industrial supervisor, Dr Graeme Robertson, and the other members of the research team at GlaxoSmithKline Medicines research Centre, (previously Glaxo Wellcome), Stevenage. My CASE placements with the company were rewarding in many ways. Thankyou to the BBSRC and Glaxo Wellcome for the funds without which this work would not have been possible.

Special thanks to Mark Ruston for covering many miles to share his positive influence, unshakeable optimism and good company with me over the past months, to my family for believing in me, and to Granny M, who'd have loved the chance to become the first Dr Meason in the family.

Abstract

The design of luminescent lanthanide complexes is of great importance in the development of biological labelling systems providing effective alternatives to radioisotopes, and for their application as light triggered sensors and materials. Our approach involves the controlled formation of mixed-ligand Eu(III) and Tb(III) complexes based on specific molecular recognition such that a biological molecular recognition event may be detected. The strategy is based on design of lanthanide systems with controlled coordination around the metal ion. Enhancement of the emission is based on intramolecular energy transfer, which is much more efficient than the FRET mechanism. Our design is based on the arrangement of two different ligands around the metal ion.

A multidentate non-absorbing ligand (NAL) is chosen to form a stable, coordinatively unsaturated complex with the metal, allowing one or two water molecules to occupy the vacant binding sites. Formation of the luminescent ternary complex is achieved by displacement of the remaining inner sphere water molecules upon recognition between the LnNAL chelate and a strongly absorbing, strongly binding light harvesting centre (LHC). This strategy allows flexibility in choosing the antenna ligand. The chromophore, which governs the input energy of light, need not be included in the structure of the encapsulating ligand. Complicated syntheses are avoided and the system can be optimised for maximum emission output.

We have chosen diethylenetriaminepentacetic acid bis(amide) (DTPA-AM_2) ligands as our NAL ligands and simple aromatic carboxylic acids as LHCs to test the design. The DTPA-AM_2 chelates the metal in an octandentate manner via the three nitrogen donors of the diethylenetriamine backbone, the two amide carbonyls and the three remaining carboxylate groups. The amide nitrogen atoms are not involved in coordination and are free to form a binding cavity, ideal for LHC recognition. The binding of the LnNAL chelate (Ln = lanthanide) by the acid moiety is followed by monitoring the emission of the europium ion, triggered by intramolecular energy transfer from the LHC. Electrospray mass spectrometry data and NMR spectroscopic studies provide additional evidence of the controlled formation of ternary complexes. Selectivity of molecular recognition is observed between EuDTPA-bis(ethylamide) and picolinic acid, phthalic acid and benzoic acid binding units, forming mixed ligand species in 1:1, 1:1 and 1:2 stoichiometries respectively.

Combinatorial screening strategies are employed in development of the mixed ligand system, allowing the interaction between a large library of aryl acid potential LHC units and a selection of LnNAL chelates to be evaluated. The DTPA-AM_2 ligands were selected to impart a variety of structural and electronic properties on the binding cavity, including hydrophobicity, rigidity, steric interactions, and π electronic effects. It is demonstrated that the selectivity of molecular recognition is based largely on the aryl-acid binding unit, with additional selectivity imparted by the amide arms of the LnNAL chelate. Equilibrium constants for ternary complex formation, luminescence lifetimes and quantum yields are evaluated for 1:1 mixed ligand species formed upon molecular recognition between LnDTPA-AM_2 chelates and aryl acid LHCs.

Table of Contents

1 Introduction

Supramolecular chemistry,[1] defined as chemistry beyond the molecule, is a growing interdisciplinary research area which studies the non-covalent interactions involved in the spontaneous assembly of complex molecular architectures.

Processes of molecular recognition are vital in nature, perhaps the most celebrated example being the specific hydrogen bonding between nucleic acid base pairs in spontaneous self-assembly of the DNA double helix (Figure 1-1). Accurate transcription and translation of genetic material ensures correct expression of the gene, resulting in the synthesis of the appropriate amino acid sequence of a protein. Molecular recognition between the amino acid side chains in the peptide leads to the secondary structure of the protein, forming α-helices and β-sheets, which in turn influence the ternary structure defining the overall function of the protein in the organism.

Figure 1-1 The DNA double helix

Much of the inspiration for the supramolecular chemist is found in the natural world. Researchers are keen to exploit the concept of molecular complementarity in the design and synthesis of novel and elegant molecular frameworks which exhibit intriguing physical or chemical properties. Such systems have been developed for application as molecular switches, signalling devices and sensors.[2]

Intermolecular forces of recognition such as electrostatic and π-stacking effects, hydrogen bonding and hydrophobic interactions are fundamental to biological function. Enzymatic conversions require specific molecular recognition between the substrate molecule and active site. Similarly, an active pharmacophore must recognise and bind the target receptor for a drug to have the desired therapeutic effect. Specific interactions between antibody and antigen are implicated in immunological responses and can be exploited in biological detection methods. Our interests lie in the development of a luminescent labelling system based on molecular recognition capable of detecting biological macromolecular interactions. Labelling techniques have been widely applied in immunoassay systems. A brief account of some of the methods used to date is given below.

1.1 Immunoassay Methods

The qualitative and quantitative analysis of biologically active molecules is of great importance in clinical applications. Immunoassays[3-5] form a class of highly sensitive, powerful analytical techniques employing the specific molecular recognition between antigen and antibody for the detection of chemically similar species in biological samples. Finding application in areas across the spectrum from routing clinical diagnosis to early drug discovery and development, immunological assays provide sensitive analyses for species such as hormones, proteins, enzymes, drugs and metabolites where traditional chemical or biological analysis may prove ambiguous. The immunological detection of such species in low concentrations using radio-isotope or fluorescence labelling techniques is now standard practice. A typical solid-state immunoassay is schematically represented below in Figure 1-2. An antibody immobilised on a solid support is reacted with a solution containing the free antigen under investigation and a second labelled antibody, forming an immunocomplex on the solid support. Detection of the sample signal following separation of unbound labelled antibody allows quantitative determination of the antigen present in the sample. Direct detection of biological interactions in solution is relatively unusual and somewhat underdeveloped in comparison with the now commonplace solid-phase assay techniques.

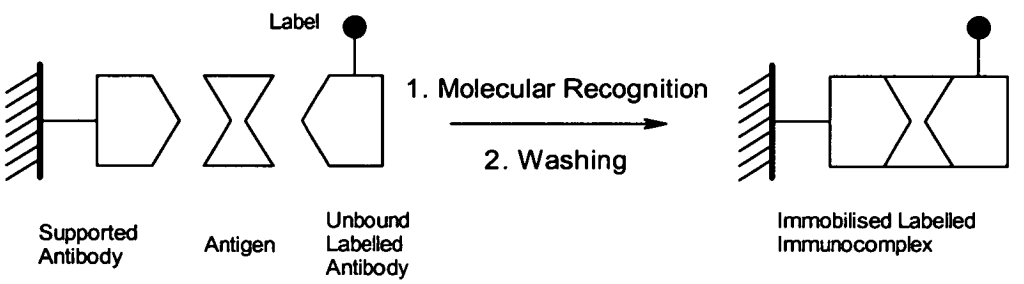

Figure 1-2 Schematic representation of a typical heterogeneous immunoassay

1.1.1 Radioimmunoassay (RIA)

Yalow and Berson first pioneered the use of radioisotopic labelling in the 1960s.[6] Radioisotopes ^{125}I, ^{3}H, ^{32}P, ^{33}P and ^{35}S are frequently employed in immunoassays, providing a distinct signal with a low and stable background count, allowing sensitivities of 10^6 molecules per assay to be achieved in practical applications. The label is robust and unaffected by environmental factors such as temperature, pH and solvent polarity. Its small size allows the immunoreaction to proceed unperturbed by label interference. Radiolabelling techniques are routinely applied in drug discovery and development, often in a Scintillation Proximity Assay (SPA) format, an example of which is given below.

1.1.2 Scintillation Proximity Assay (SPA)

Common in drug discovery and development, the SPA employs the specificity of interaction between the tetrameric protein streptavidin and the soluble vitamin, biotin, (Log $K_{affinity}$ ~ 15)[7] in the formation of a radiolabelled immunocomplex on a solid phase SPA bead. One particularly elegant example of SPA application was developed by Glaxo Wellcome scientists (California, 1999),[8] where high throughput screening technologies were employed in identification of selective enzyme inhibitors in a kinase enzyme cascade.

The cascade requires three enzymes in order to complete a signalling pathway from the cell membrane to the nucleus, regulating gene expression and DNA synthesis. Each enzyme is activated by phosphorylation, mediated by the preceding enzyme in the sequence. Enzyme activated phosphorylation of the biotinylated product peptide in the presence of ^{33}P forms a radiolabelled species in the sample solution. This labelled peptide is recognised by the streptavidin labelled SPA bead, forming a supported immunocomplex. Only phosphorylation by the third enzyme in the cascade results in the labelled peptide product, hence detection of the SPA signal is indicative of the complete cascade. Conversely, the absence of an SPA signal signifies inhibition at some point in the pathway. The SPA is schematically represented in Figure 1-3.

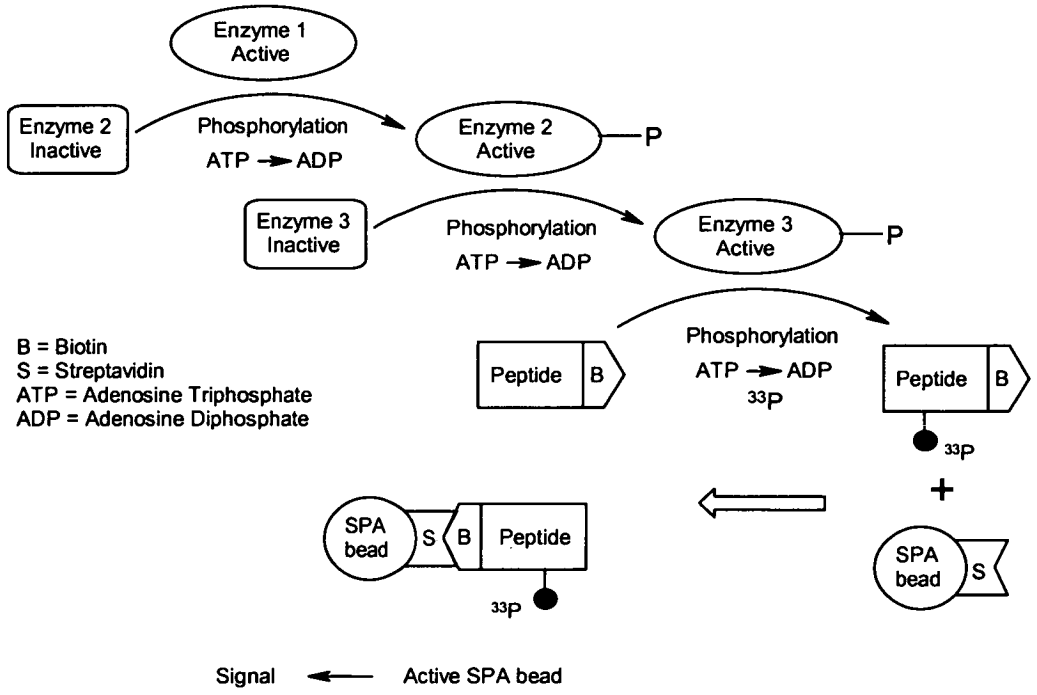

Figure 1-3 Schematic representation of a Scintillation Proximity Assay for a three enzyme cascade

The assay was developed to determine the output from each specific kinase cascade under investigation. Using this SPA 335 000 compounds were screened for inhibitory action against the enzymes, from which 1200 leads were identified. The SPA results allow identification of enzyme specific inhibitors, from which potential therapeutic agents may be developed. Such kinase enzyme cascades have implications in inflammatory responses and in some 30% of human tumours, hence are attractive targets in drug discovery.

Despite the widespread and successful application of RIA, the significant disadvantages associated with the technique have prompted the search for alternative technologies. Increasingly strict legislation surrounding the supply, handling and disposal of radioactive material, and the short shelf life of reagents (^{125}I half-life = 6- days) have together resulted in research into alternative labels. In addition, the heterogeneous nature of the assays, involving several washing steps, is not readily applicable to today's modern automated and miniaturised high throughput screening technologies, now an integral part of the pharmaceutical industry.

In past decades assay methods based on fluorescence technology have emerged as attractive and viable alternatives to radioisotopes in immunoassays.[9-13] The relatively inexpensive technology is clean, safe and versatile. Highly sensitive instrumentation for the detection of light has been developed in recent years and is now commercially available.

1.1.3 Fluorescent Labelling Involving Organic Fluorophores

In 1941 Coons *et al* reported the first use of an organic compound in biomolecular detection, using anthracene isocyanate to label a bacterial protein.[14] Fluoroimmunoassays (FIA) involving organic fluorophores (Figure 1-4) such as dansyl chloride, fluorescein and rhodamine derivatives (Figure 1-5) have achieved sensitivities of 10^{-10} M in routine practice. The organic fluorophore is covalently coupled to the biomolecule of interest as in RIA, its relatively small size not affecting the immunological properties of the antibody. The photophysical characteristics of the probe are sensitive to the environment and changes in the pH and hydrophobicity of the probe's immediate surroundings upon immunoreaction result in changes in the absorption and emission spectra. Such bathochromic or hypsochromic shifts and hyper or hypo-chromic effects allow differentiation between free and bound labelled antibody. Consequently, separation of the labelled immunocomplex from the sample solution is not always necessary reducing the number of steps in the assay. Homogeneous assay methods lend themselves to modern analytical techniques including

high throughput screening of combinatorial libraries, of immense value in the search for novel lead compounds in drug discovery.[15-18] Such technological innovations are discussed further in Chapter 1.3.

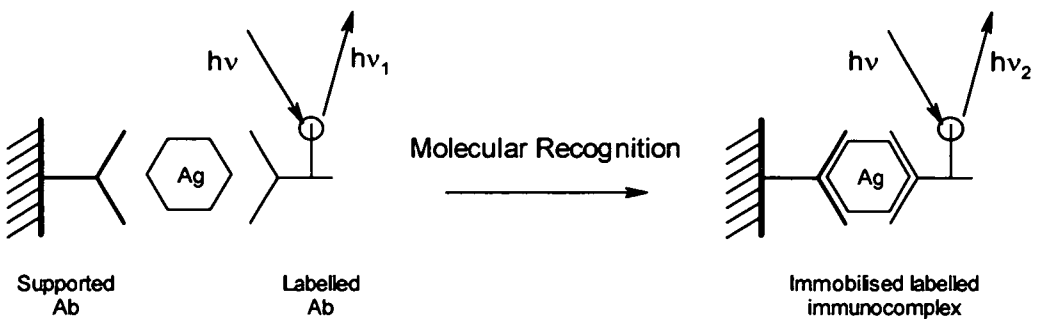

Figure 1-4 Schematic representation of Fluoroimmunoassay (FIA)

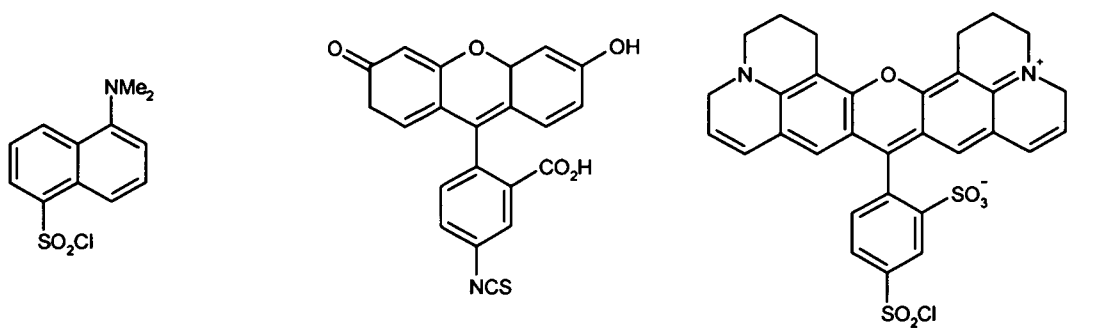

dansyl chloride

λex = 340 nm
λ em =480-520 nm
(Stokes shift ~ 140-180 nm)
ε = 3400 $cm^{-1}M^{-1}$
τ = 14 ns
ϕ = 0.3

FITC
fluorescein isothiocyanate

λex = 492 nm
λ em = 520 nm
(Stokes shift ~ 18 nm)
ε = 72000 $cm^{-1}M^{-1}$
τ = 4.5 ns
ϕ = 0.85

Texas Red (Rhodamine derivative)

λ ex 525 nm
λ em = 615-620 nm
(Stokes shift ~ 80-95 nm)
ε = 85 000 $cm^{-1}M^{-1}$
ϕ = 0.3

Figure 1-5 Structures and photophysical properties of some organic fluorophores commonly applied in FIA

An example of direct replacement of an isotopic label with an organic fluorophore in biological receptor-ligand binding studies is discussed briefly below.

Fluorescein isothiocyanate (FITC) has found application in specific labelling of chemokines,[13] offering sensitivity comparable to that achieved by traditional ^{125}I radio-labelling. Interleukin-8 (IL8), a pro-inflammatory protein implicated in conditions including rheumatoid arthritis, cystic fibrosis, bronchitis, atherosclerosis and a multitude of tumours is the most extensively studied chemotractant cytokine. Targeted labelling of the N-terminus of the IL8 protein with FITC was performed and its binding affinity to specific receptors assessed by fluorescence techniques. The small molecular size of the FITC label allows biological recognition to occur unperturbed thus offering a viable alternative to isotopic detection methods.

1.1.4 Enzyme Linked Immunosorbant Assay (ELISA)

Organic fluorophores are also universally applied in enzymatic immunoassays, an excellent example of which is ELISA (Enzyme Linked Immunosorbant Assay) discussed below (Figure 1-6). Enzymes were first introduced as biological labels in the early 1970s.[19] As with traditional FIA and RIA systems, a supported labelled antibody specifically binds the antigen under investigation. A second antibody covalently conjugated (Scheme1-1) to an enzyme recognises the antigen and forms the immunocomplex. The unbound labelled antibody is separated and removed from the sample prior to enzymatic reaction, which converts a colourless substrate molecule into a coloured (Scheme 1-2) or luminescent (Scheme 1-3) product allowing quantitative detection of the antigen. Enzymes routinely employed in ELISA include alkaline phosphatase (AP), β-galactosidase (GAL) and horseradish peroxidase (HRP).

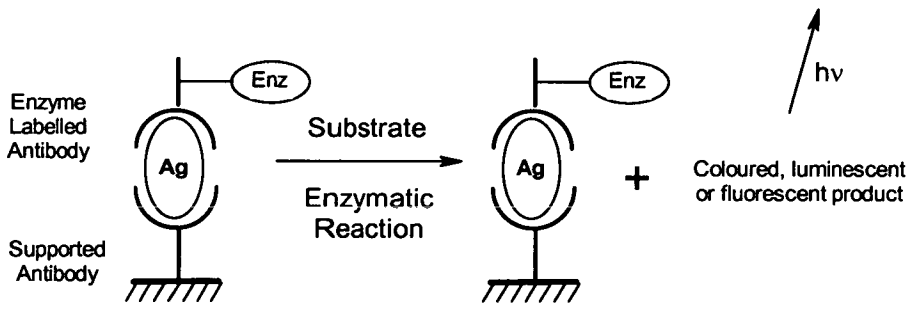

Figure 1-6 Schematic representation of Enzyme Linked Immunosorbant Assay (ELISA)

The main disadvantage associated with these heterogeneous fluoroimmunoassay systems is the laborious multistep nature of the processes involved. Separation of immunocomplex from the sample solution and several thorough washings are required to remove the remaining free labelled antibody prior to fluorescence measurement.

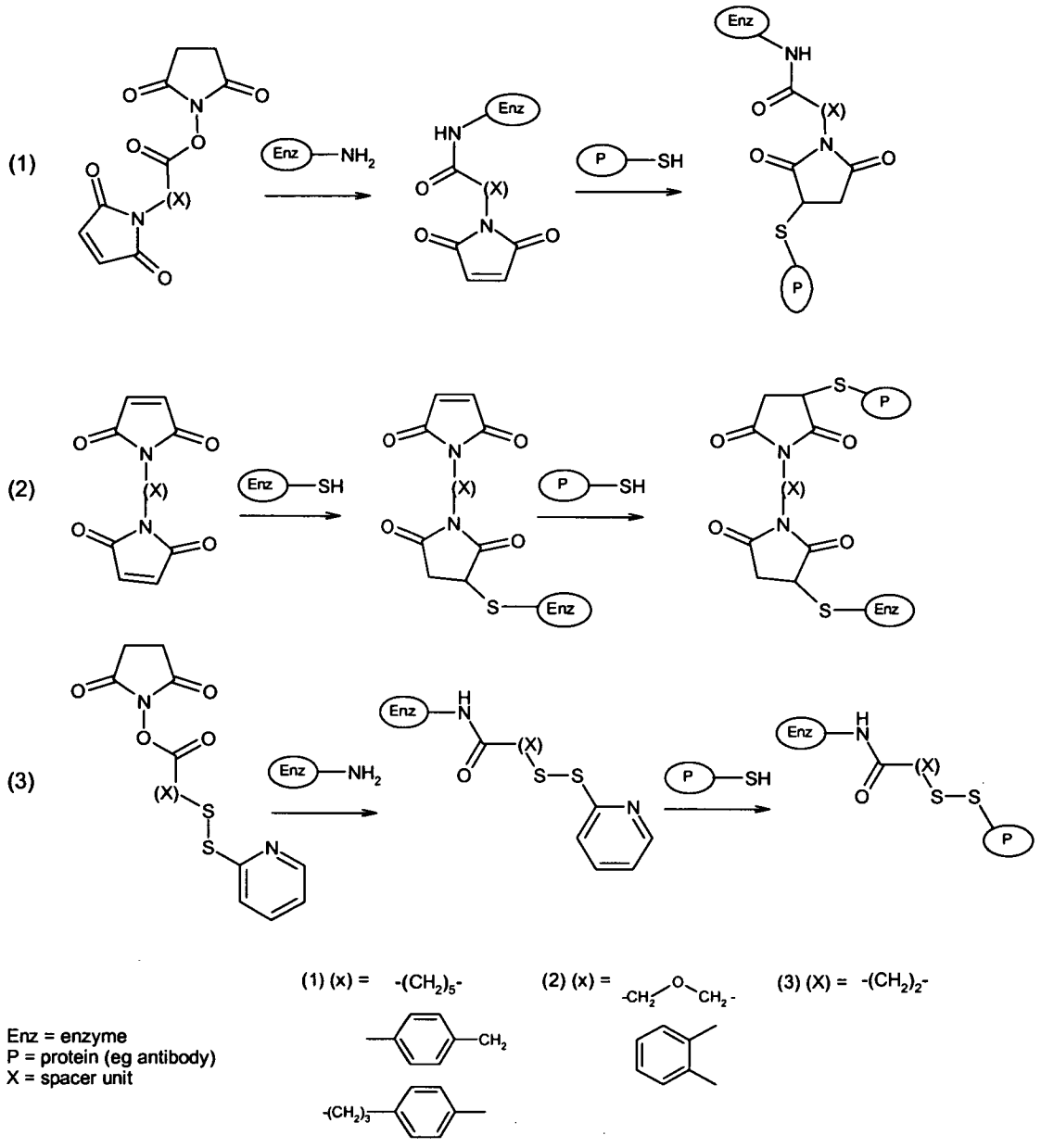

Scheme 1-1 Bifunctional coupling reagents used in enzymatic labelling of an antibody

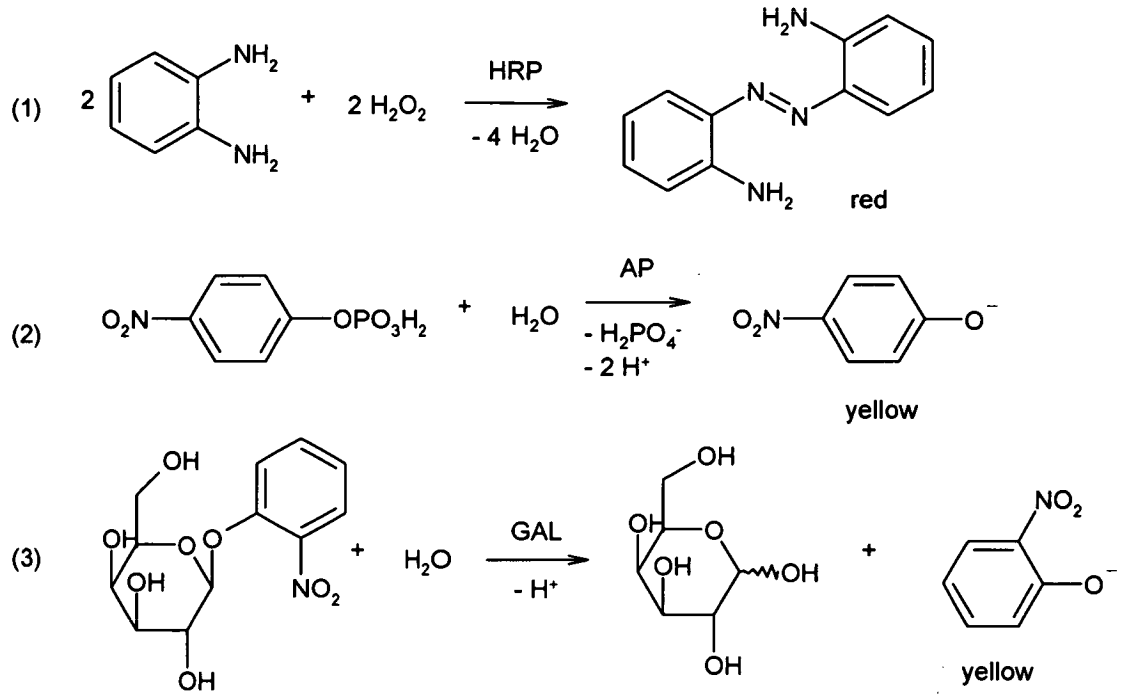

Scheme 1-2 Schematic representation of enzymatic reactions resulting in coloured products commonly employed in ELISA assay methods

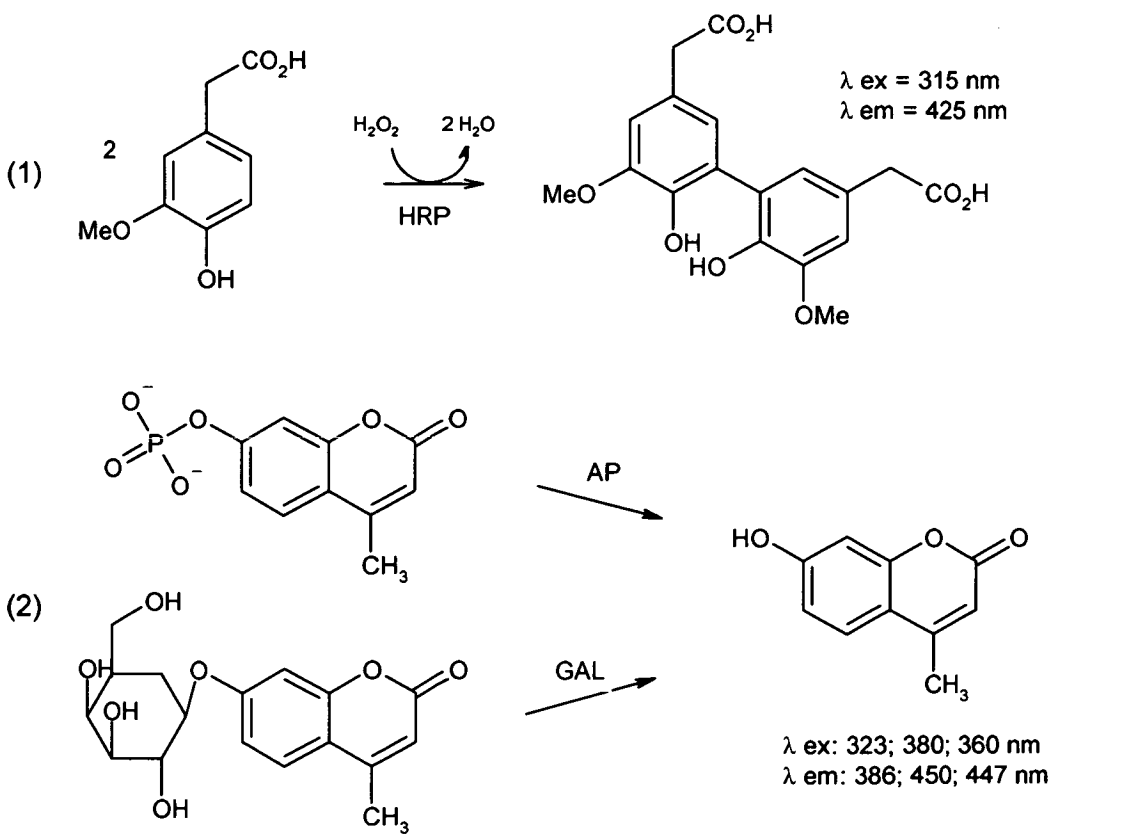

Scheme 1-3 Schematic representation of enzymatic conversions resulting in organic fluorogenic products commonly applied in ELSIA assay systems

The use of organic fluorophores in immunoassays has resulted in a reduction in the number of steps in heterogeneous assays and has facilitated development of simple homogeneous methods. The latter have been vitally important in the mechanisation, miniaturisation and automation of immunological detection methods, offering obvious economic advantages. One such example is the Fluorescence Polarisation (FP) assay summarised briefly below.

1.1.5 Fluorescence Polarisation Assay (FP)

Fluorescence polarisation[20] was initially introduced as an alternative labelling method in the immunoassay field in the early 1960s.[9] An antibody labelled with a fluorescent dye, such as fluorescein isothiocyanate (Figure 1-5) will emit polarised light when excited by a plane polarised excitation source. The degree of polarisation observed is a function of rotational relaxation time and thus related to molecular size. Small molecules, tumbling more rapidly than their larger counterparts, have shorter relaxation times hence the light emitted is polarised to a lesser extent. Molecular recognition between the labelled antibody and antigen under investigation forms the immunocomplex in solution. The greater molecular size of the product immunocomplex slows molecular tumbling, in turn increasing the degree of polarisation detected. As with FIA, the changes in photophysical properties of the dye upon macromolecular recognition render the separation steps associated with traditional assays unnecessary, allowing discrimination between free and bound antibody in solution. Consequently, the assay can be carried out in a "mix-and read" format and is readily applicable to modern automated technologies. The fluorescence polarisation assay is, however, restricted to the study of relatively small antigens, since the rotation of large molecular weight species in solution is slow and changes very little upon immunocomplexation.

Despite the advantages presented by the homogeneous assay format, the use of organic dyes as labels is hindered by the high level of background fluorescence from serum proteins at wavelengths comparable to that of the probe employed, causing significant signal overlap. Rayleigh and Raman scattering by solvated macromolecules and scattering by colloidal particles or solid supports also contribute to high background signals. In addition, the small Stokes shifts (20-50 nm) of organic molecules renders distinction between the excitation source and emitted light difficult. Problems are also incurred due to overlapping spectral bands, which can result in self quenching of the excited state by adjacent fluorophores. Consequently fluoroimmunoassays employing organic probes are in general less sensitive than the corresponding radioimmunoassay methods and the search for alternatives continues.

1.2 Lanthanides as Labels

The unique photophysical properties of lanthanide trivalent cations[21] make them ideal candidates in the search for efficient non-isotopic alternative labels in biological assays. The characteristic emission in the visible region of the electromagnetic spectrum is long-lived, providing a clean, safe, readily detectable signal. Currently finding application in structural determination and analyses,[22] rare earth cations are routinely utilised as probes in a variety of biological[23, 24] and chemical systems in addition to their use as components of photoactive signalling devices[25, 26] and sensors.[27, 28]

Perhaps the most common application of lanthanide cations is as luminescent labels in immunological detection methods,[3-5, 9-12, 29, 30] examples of which are discussed later in 1.3. Instrumentation has been developed allowing lanthanide luminescence to be used in flow cytometry[31] and microscopic imaging,[32] capillary electrophoresis[33] and in nucleic acid sequencing studies.[34] Long-range electron transfer, fundamental to many physiological processes, including photosynthesis and respiration, can be studied by isomorphous replacement of the spectroscopically silent Ca^{2+} or Zn^{2+} with redox active rare earth ions.[35] Similarly, information can be gained regarding the nature of these metal ion binding sites employing luminescent lanthanide cations as structural probes in proteins,[36-39] as the Ln(III) ions employed are of comparable ionic size.

In addition to their ubiquitous application in biological assays, rare earth cations provide robust, sensitive analytical handles in NMR as chiral shift reagents,[40] structural probes of crystalline materials[41] and in clinical Magnetic Resonance Imaging (MRI) as contrast agents.[42]

1.2.1 Lanthanide Luminescence

Only four trivalent lanthanide ions, europium, terbium, samarium and dysprosium, emit light in the visible region of the electromagnetic spectrum, their characteristic luminescence the result of radiative decay of the excited state competing efficiently with other non-radiative de-excitation pathways.[21] In contrast to the lanthanides, most transition metals absorb UV light but very few re-emit the energy in the visible region. Strong coupling between the d-electron excited state and the ligand, field leading to charge transfer processes, provides an efficient depopulation pathway.

Spectroscopic transitions of the lanthanides involve the 4f electrons, shielded from the environment by the outer 5s and 5p orbitals. Although formally forbidden by the Laporte

selection rule ($\Delta L \neq 0$) prohibiting the redistribution of electrons within a single electronic subshell, f → f transitions become allowed due to the large degree of spin-orbit coupling present. The degeneracy of the electronic configuration of the spherical Ln(III) ion is removed by interelectronic repulsions, splitting the energies into spectroscopic terms (S, P, D, F...), which are then further split by spin orbit interaction into spectroscopic levels. For Eu(III) and Tb(III) ions, ($4f^6$ and $4f^8$ configurations respectively) the ground state term is given by ^7F_J where J = 0 (Eu(III)) and J = 6 (Tb(III)) as determined by application of Hund's rules and the Russell-Saunders coupling scheme.[43] The spectroscopic transitions occurring in Eu(III) and Tb(III) ions are shown below in Figure 1-7.

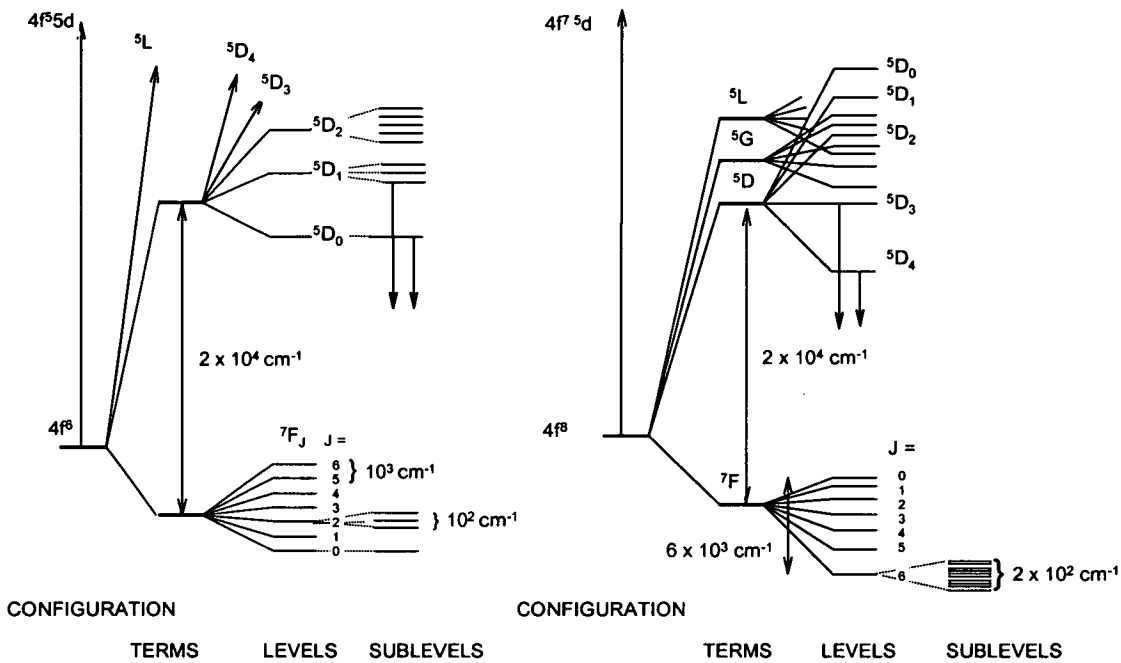

Figure 1-7 Partial energy diagram for Eu(III) ($4f^6$) and Tb(III) ($4f^8$) ions showing the relative magnitude of the interelectronic repulsion, spin-orbit coupling and ligand field effects. Downward arrows indicate luminescence.[21]

Emission spectra are narrow and line-like, with long luminescence lifetimes, in the order of milliseconds, in contrast to organic molecules whose emission lifetimes are typically in the order of nanoseconds. Large Stokes shifts (generally 200-300 nm) prevent overlapping absorption and emission spectra thus minimising scattering effects. Molar extinction coefficients of the lanthanides are intrinsically weak, typically less than 10 $M^{-1}cm^{-1}$ reflecting the forbidden nature of the f-f transitions, presenting significant problems in the application of lanthanide ions as spectroscopic probes. A typical Eu(III) emission

spectrum, showing radiative decay of the $^5D_0$ luminescent level following excitation to the $^5L_6$ excited state at 394 nm, is shown in Figure 1-8.

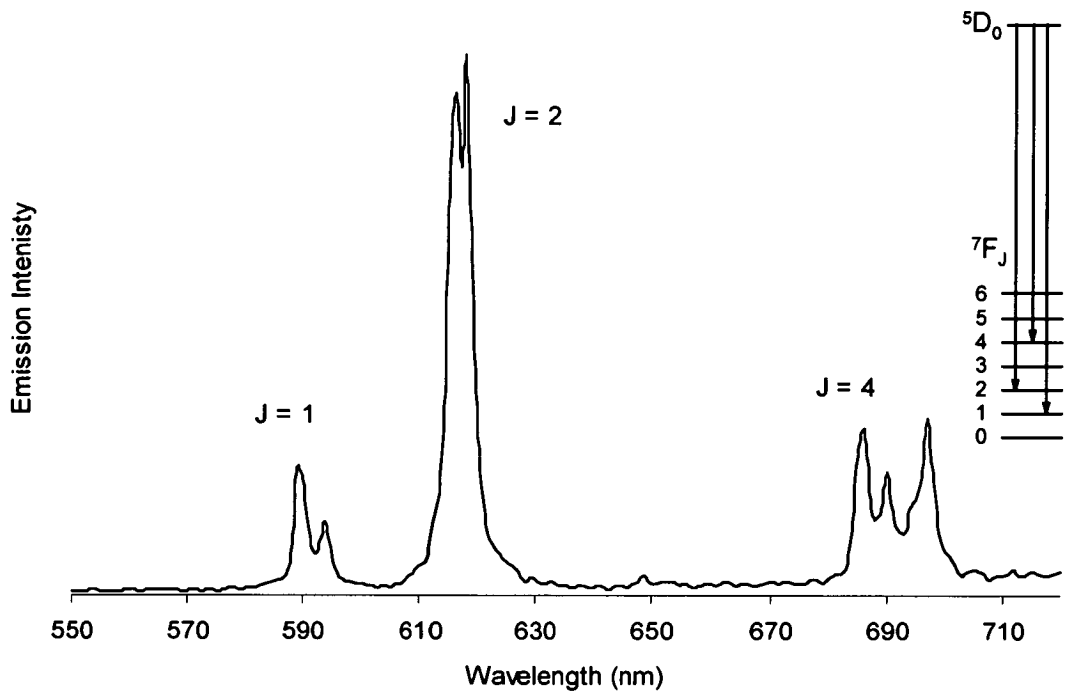

Figure 1-8 Typical Eu(III) emission spectrum showing the electronic transitions resulting in characteristic red luminescence of the ion

A significant disadvantage associated with lanthanide luminescence is the inherently weak emission observed from the free ion in aqueous solution. This is due to low absorbance and the quenching effect of coordinated water molecules,[21, 44, 45] a phenomenon first investigated by Kropp and Windsor in the 1960s.[46] Vibronic coupling with vibrational overtones of high energy O-H oscillators in the primary coordination sphere provides an efficient de-excitation mechanism, depopulating the emissive state via non-radiative energy transfer[47] (Figure 1-9).

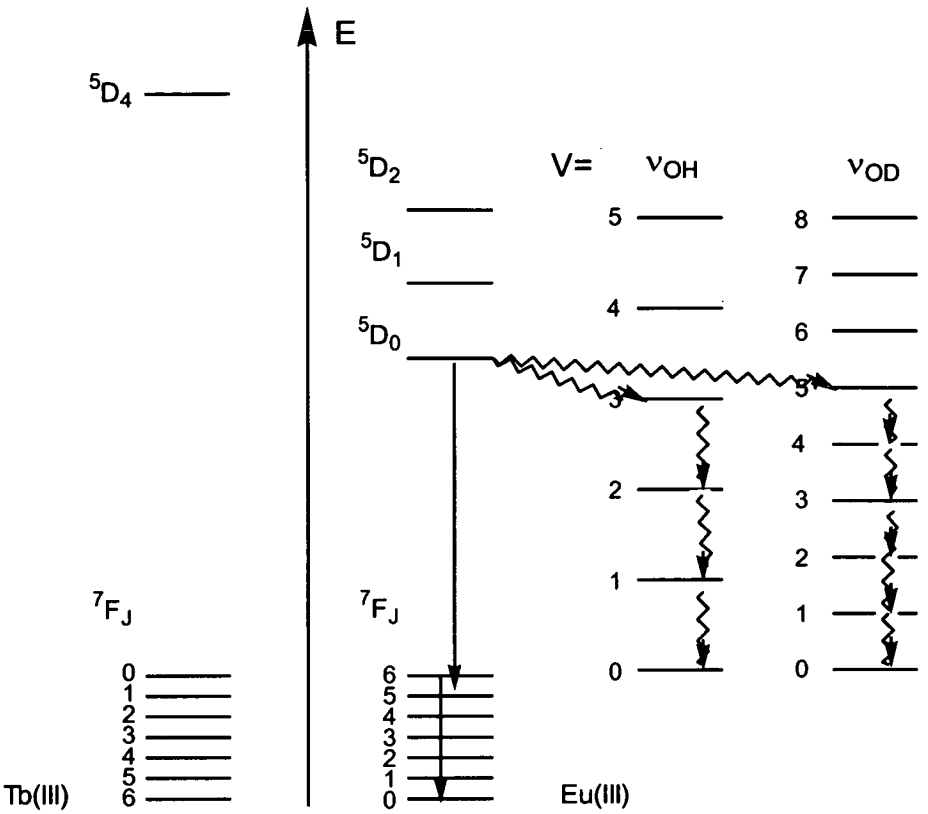

Figure 1-9 Partial energy diagram illustrating the relative quenching abilities of H_2O and D_2O in depopulating Eu(III) and Tb(III) excited states

The luminescence lifetime of a lanthanide excited state is dependent on the efficiency of the de-excitation mechanisms and is therefore proportional to the number of coordinated O-H oscillators. The observed rate of luminescence decay (k_{obs}) comprises several terms (Equation 1-1) where k_{nat}, and $k_{non\text{-}rad}$ are the rate constants for natural photon emission and non-radiative de-excitation respectively. Σk_{XH} represents the contribution of non-radiative energy transfer to proximal high energy X-H oscillators (X = O, C and N: Stretching frequencies: $\nu_{OH} \sim 3400\ cm^{-1}$; amide NH $\nu_{NH} \sim 3310\ cm^{-1}$; methylene CH $\nu_{CH} \sim 2950\ cm^{-1}$). The lifetime, τ_{obs}, is expressed as the reciprocal rate constant.

$$k_{obs} = k_{nat} + k_{non\text{-}rad} + \Sigma k_{XH} \qquad \textbf{Equation 1-1}$$

An estimate of the hydration state of the metal (q) can be gained from lifetime measurements performed on luminescent species in quenching H_2O and non-quenching D_2O. For the lower energy O-D oscillator to provide an efficient deactivating pathway, higher overtones must become involved, energetically unfavourable due to poor overlap of the wavefunctions, as stated by the Franck-Condon principle. The relative quenching power of

an X-D oscillator is approximately 200-fold less than that of the corresponding X-H bond, hence the much longer observed luminescence lifetime of Eu(III) in non quenching D_2O relative to that of the free ion in water. This phenomenon can be applied to provide a measure of the number of coordinating water molecules in the inner sphere of the metal.

The rate constant for depopulation of the excited state by non-radiative energy transfer to coordinated X-H bonds can be obtained by difference (Equation 1-2).

$$k_{H2O} - k_{D2O} = \Sigma k_{XH} \qquad \textbf{Equation 1-2}$$

Application of an empirical formula determined by Horrocks[44] (Equation 1-3) allows the number of coordinated water molecules (q) to be calculated.

$$q = A_{Ln(III)} \bullet (\tau^{-1}_{H2O} - \tau^{-1}_{D2O}) \qquad \textbf{Equation 1-3}$$

The parameter $A_{Ln(III)}$ is an empirically determined factor, 1.05 for Eu(III) and 4.2 for Tb(III). The $^5D_0$ luminescence excited state of Eu(III), of lower energy (17 250 cm^{-1}) than the corresponding $^5D_4$ luminescent level of the Tb(III) ion (20 430 cm^{-1}), is more susceptible to quenching by the solvent environment. τ^{-1}_{H2O} and τ^{-1}_{D2O} are the reciprocal luminescence lifetimes (ms^{-1}) for the species in H_2O and D_2O respectively. Values of q can be obtained to ± 0.5 water molecules.

In addition to solvent quenching effects, an important consideration in the design of luminescent lanthanide complexes for application as probes in biological or chemical systems is the inherently weak absorption coefficient of the metal ions.[48]

Weissman,[49] in 1942, observed that a europium (III) β-diketonate complex emitted characteristic red light upon exposure to sunlight. Although initially believed to be the result of electron transfer, this was later explained as the "Antenna Effect" (Figure 1-10) whereby the diketonate ligand absorbs UV radiation then transfers the energy to the metal ion. Excitation to the ligand singlet excited state is followed by intersystem crossing to the longer lived, lower energy triplet state facilitated by the heavy atom effect. Intramolecular energy transfer to the excited state of the lanthanide populates the emissive level of the metal, from which radiative decay to the ground state manifold results in emission of characteristic light (Eu(III) = red, Tb(III) = green). The widely accepted Absorption Energy Transfer Emission (AETE) mechanism was established by Balzani *et al*[50, 51] on studies with the $[Eu(bipy)_3]^{3+}$ cryptate and is represented schematically in Figure 1-11.

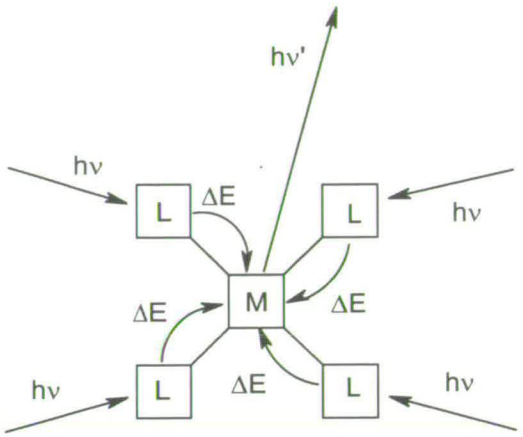

Figure 1-10 Schematic representation of the "antenna effect" whereby light is absorbed by ligand chromophores, then the energy transferred to the central luminescent metal

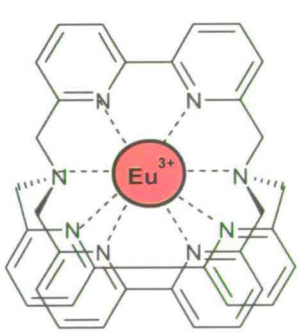

[Eu(bipy.bipy.bipy)]$^{3+}$ cryptand

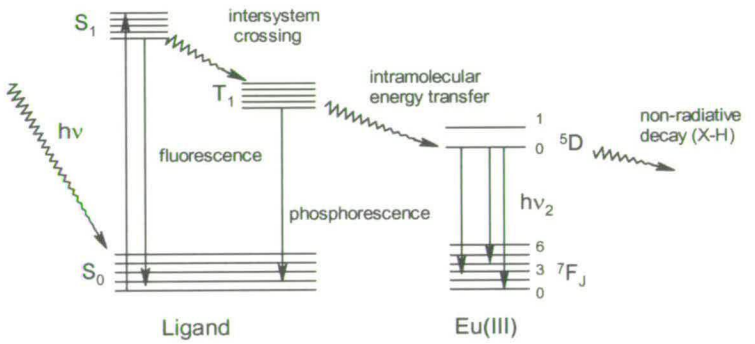

Sensitised Eu(III) Emission by AETE

Figure 1-11 Schematic representation of the Absorption Energy Transfer Emission (AETE) "Antenna Effect" mechanism

1.2.2 Coordination Properties

Classified as "hard acid" in character by the Pearson scheme,[52] Ln(III) ions will preferentially coordinate "hard donor" ligands such as anionic oxygen and nitrogen atoms, forming predominantly non-covalent, electrostatic bonds. The metal ions are hydrated in aqueous solution, and negatively charged oxygen donor ligands are required to displace water molecules from the primary coordination sphere. Neutral O and N donor atoms in general only bind the metal as components of multidentate ligands.[53] Water molecules can be excluded from the primary coordination sphere of the ion by encapsulating it in the cavity of a cryptand or macrocyclic ligand, or by using a polydentate aminopolycarboxylate chelator. Since the f orbitals are shielded from the environment by the outer s and p electrons and are only minimally involved in coordination, complex geometries take on the characteristics of the ligand and are not dictated by the electronic configuration of the metal. The coordination properties of trivalent lanthanide cations are similar to those exhibited by the alkali and alkaline earth metals, with the ions readily forming stable complexes with multidentate and macrocyclic ligands. These multidentate chelators will adopt the conformation of lowest energy around the spherical cation. Coordination numbers between 6 and 12 have been reported with eight and nine most common.

By careful choice of chromophoric ligand such that excited state energies are suitably matched for intramolecular energy transfer to occur, and exclusion of quenching moieties from the inner coordination sphere of the metal, highly luminescent chelates can be prepared, several of which now find application in biological detection methods. Diketonate complexes were initially tried as luminescent labels in biological systems but instability and poor solubility in aqueous media have limited their direct application in immunoassays.[54, 55] In order to overcome these problems, polydentate aminopolycarboxylate ligands have been exploited in the design of luminescent lanthanide chelates for biological labelling. Chelates formed with EDTA (ethylenediamine tetraacetic acid) and DTPA (diethylene triamine pentacetic acid) are highly stable (Log K > 20) and water soluble. Such stability prevents non-specific ionic exchange with biological cations such as Ca^{2+}, Mg^{2+} and Zn^{2+}. These aminopolycarboxylate ligands have been employed in radiolabelling of biomolecules,[56, 57] magnetic resonance imaging[58] and luminescent immunoassays involving mixed ligand Eu(III)[59-64] and Tb(III) chelates.[65-69] A few examples of lanthanides in immunoassays are briefly discussed here.

1.3 Time Resolved Fluoroimmunoassay (TR-FIA) Involving Lanthanides

A highly sensitive fluorescence immunoassay technique was developed based on the characteristic long lived luminescence of the europium and terbium cations.[59, 65] These trivalent lanthanides are employed as versatile labels in time resolved immunoassays. Three currently available TR-FIA kits are briefly discussed here. Sensitivities comparable to RIA, unobtainable with organic fluorophores can be achieved with lanthanide labels in routine practice. The sensitivity is based on minimisation of short-lived background signal by implementing a fixed time delay between the excitation flash and signal detection. The long emission lifetimes of the lanthanide species allow strong signal detection after the delay, during which the short-lived fluorescence of serum proteins decays (Figure 1-12).

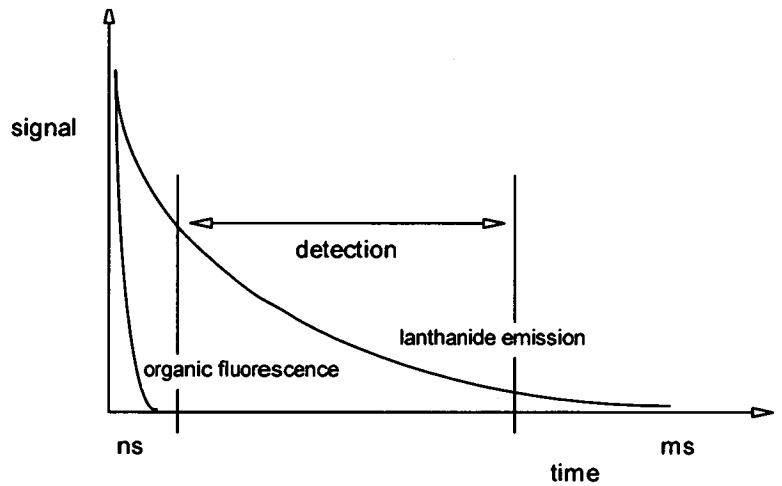

Figure 1-12 Schematic representation of the principal of Time-Resolved Fluorescence Detection

Time resolution, in combination with careful use of filters gives a distinct signal with relatively low background noise levels.

1.3.1 Dissociation Enhanced Lanthanide Fluoroimmunoassay (DELFIA)

A popular time resolved immunoassay method employing europium (III) luminescence is the Dissociation Enhanced Lanthanide Fluoroimmunoassay or DELFIA system[70-72] (Figure 1-13). An antibody is covalently coupled via a protein to an aminopolycarboxylate (EDTA) derivative forming a stable Eu(III) chelate. Multiple labelling of the antibody, with up to 15 chelates per molecule is possible increasing the sensitivity of the system. Molecular

recognition between the labelled antibody, free antigen and supported antibody in solution forms the desired immobilised immunocomplex. Free antigen and unreacted labelled antibody are then washed from the sample. The EuEDTA chelate is non-luminescent, and treatment of the supported complex with an acidic "enhancing" solution is required. The low pH of the enhancing solution facilitates dissociation of the chelate, liberating Eu(III) into the solution, containing an aromatic β-diketone sensitizer ligand and a hydrophobic tris(octyl) phosphate which together form the luminescent species[73] (Figure 1-14). The amount of antigen present in the sample is indirectly determined by comparison with a luminescent Eu(III) standard. Care must be taken to avoid contamination as small europium impurities will also form luminescent species falsifying results.

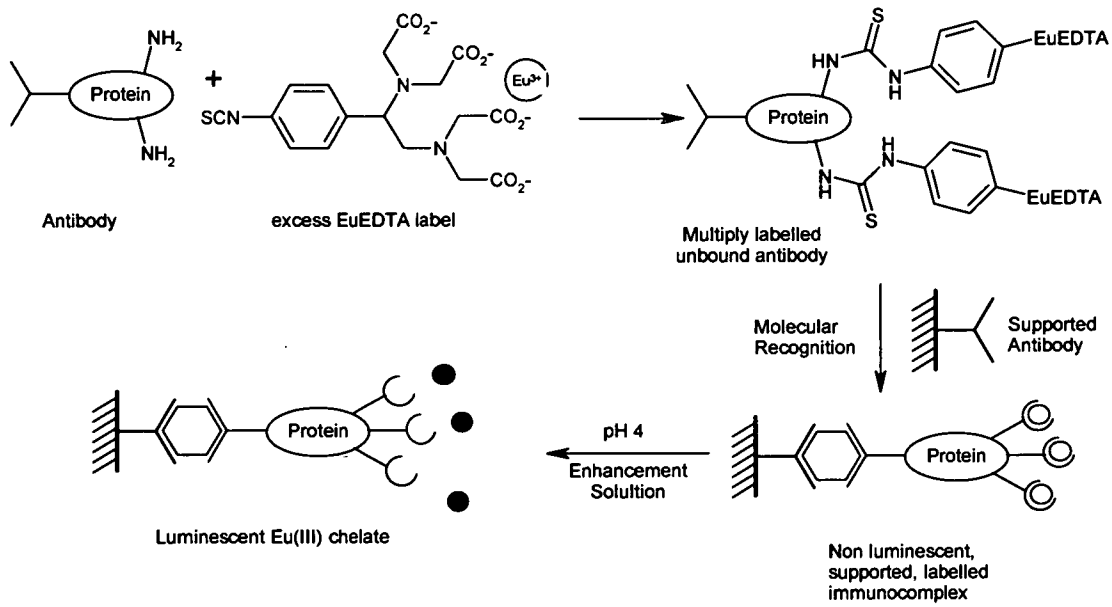

Figure 1-13 Schematic representation of the Dissociation Enhanced Lanthanide Fluoroimmunoassay (DELFA) system

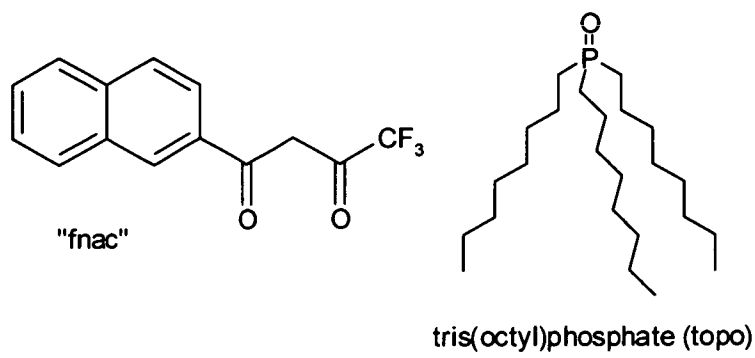

Figure 1-14 Structures of the sensitising "fnac" and hydrophobic "topo" ligands present in the "enhancement" solution for the DELFIA assay

The exact nature of the emissive complex is unknown, but it has been proposed that two sensitising ligands chelate the metal, in combination with two tris(octyl)phosphates, each of which form a hydrophobic umbrella around the inner coordination sphere, thus excluding water molecules and preventing quenching of the luminescence by OH^-. The sensitivity of the assay is improved by employing time resolved techniques.

Despite its popularity the DELFIA assay system is not without disadvantages. The assay is heterogeneous and several washing steps are required to ensure complete removal of unbound labelled antibody prior to treatment with the enhancement solution. Excess ligand is employed in formation of the luminescent chelate, the presence of which contributes to the background fluorescence detected.

Europium DTPA derivatives have also been employed in luminescence assays as direct alternatives to FITC and ^{125}I for detection of IL-8 receptor-ligand interactions.[74] The assay can be performed in high throughput format, exhibiting enhanced sensitivity over the traditional organic or isotopic labelling methods. IL-8 is covalently coupled to the [EuDTPA] chelate *via* a sulphonamide linker and N-terminal cysteine residue forming a labelled ligand. A monolayer of cells immobilised on the surface of a microplate is treated with the labelled IL8 ligand solution, upon which molecular recognition occurs. A non luminescent labelled monolayer is thus formed on the solid support. Treatment of the sample with the DELFIA enhancement solution releases the ion, allowing the highly luminescent β-diketonate chelate to form. Time resolved detection of the luminescence in the lanthanide assay offers enhanced sensitivity over the corresponding assay employing the FITC probe.[13]

1.3.2 Cyberfluor

Like the heterogeneous radiolabelled SPA system (1.1.2) the Cyberfluor method[12, 65] utilises the highly specific molecular recognition between the soluble vitamin, biotin, and the tetrameric protein streptavidin, and offers a versatile assay commonly used in DNA hybridisation.[75] A labelled single strand of DNA can be used as a specific gene probe since it will only bind with the corresponding complementary nucleic acid sequence to form the double helix. The technique, as commonly used in heterogeneous assay systems is schematically represented below (Figure 1-15). For DNA hybridisation the antibody is replaced with a specific nucleic acid sequence.

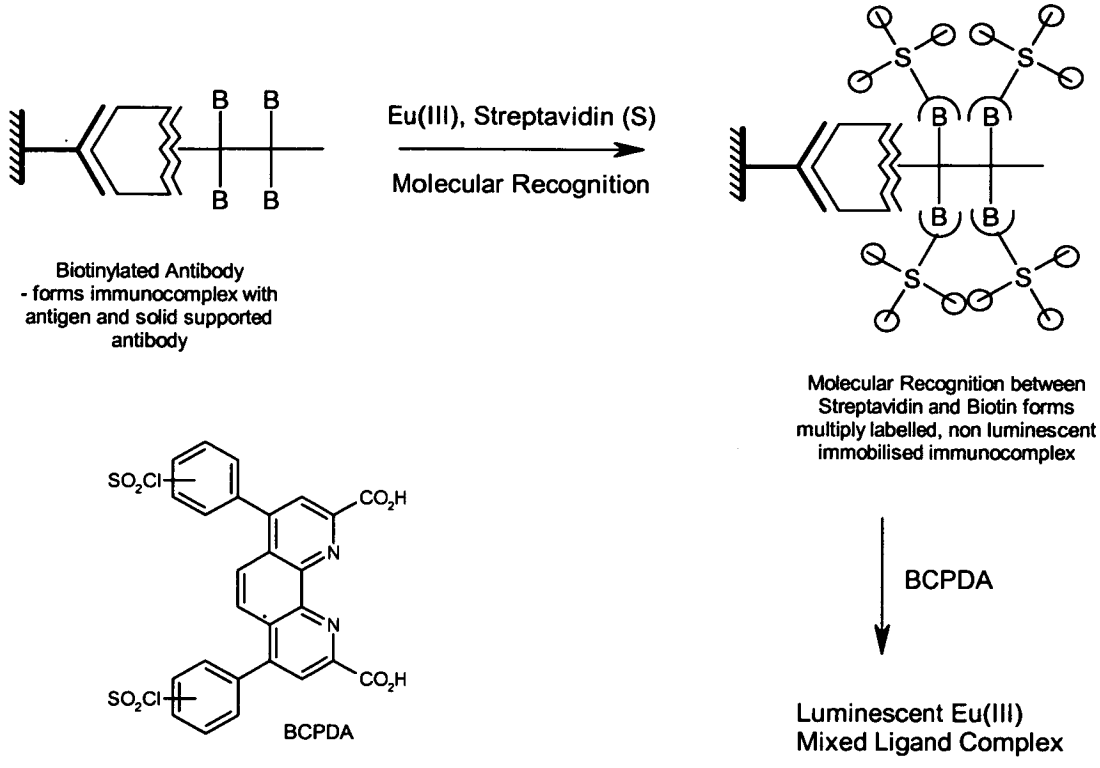

Figure 1-15 Schematic representation of the Cyberfluor assay system

The biotinylated antibody forms an immunocomplex with the supported antibody/antigen. Molecular recognition between biotin and streptavidin produces a multiply labelled species. The Eu(III) luminescent complex is formed upon addition of the sensitising ligand, BCPDA (4,7-bis(chlorosulphophenyl)-1,10-phenanthroline-2,9-dicarboxylic acid (Figure 1-15)),[55] the mechanism of which is not understood. Qualitative analysis of the antigen present is achieved indirectly by time resolved detection of the Eu(III) sensitised emission and comparison with an external Eu(III) standard. The Eu(III)BCPDA chelate is less luminescent than the β-diketone employed in the DELFIA system, but background fluorescence is reduced since excess ligand is removed from the sample prior to analysis. In common with DELFIA, the Cyberfluor method offers indirect, heterogeneous analysis of biological species under investigation.

1.3.3 Enzyme Amplified Lanthanide Luminescence (EALL)

Like ELISA (1.1.4), the commercially available Enzyme Amplified Lanthanide Luminescence (EALL) assay system[65] utilises the enzymatic conversion of a substrate to its corresponding product in analyte detection (Figure 1-16). The enzyme amplified lanthanide luminescence assay is based on formation of a mixed ligand luminescent complex between a Tb(III) aminopolycarboxylate species and the product of the enzymatic reaction. In this case, the enzyme is Alkaline Phosphatase (AP) and the substrate the phosphate ester of 5-fluorosalicylic acid (5-FSAP), which prior to enzymatic hydrolysis does not interact with the $[TbEDTA]^-$ chelate and no luminescence is detected.

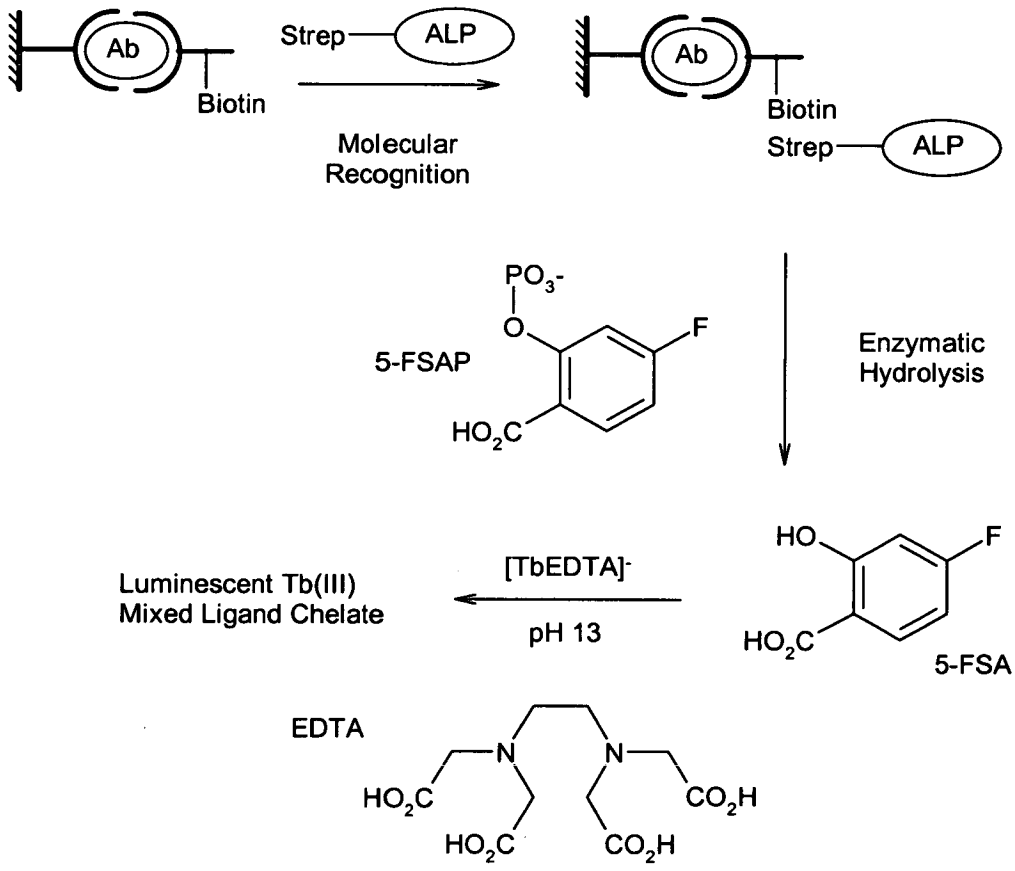

Figure 1-16 Schematic representation of Enzyme Amplified Lanthanide Luminescence (EALL) in immunoassay

A solid-supported antibody forms an immobilised immunocomplex with the antigen under investigation and a biotinylated detection antibody, which then undergoes specific molecular recognition with the streptavidin labelled enzyme (see Cyberfluor, 1.3.2) as shown in Figure 1-15. The immobilised enzyme is then treated with the substrate, 5-FSAP, which is hydrolysed liberating 5-FSA. The product salicylate then forms an intensely luminescent mixed ligand complex with [TbEDTA]$^-$ under alkaline conditions. Quantitative analysis of the antigen of interest is achieved by comparison of the observed luminescence intensity with that of a known standard. This assay has been demonstrated with a number of enzyme substrate pairs and can achieve sensitivities comparable to that of traditional RIA by employing time resolved detection methods.

The exact nature of the emissive [TbEDTA.FSA] chelate is unknown, however, the high stability of the Tb(III) aminopolycarboxylate chelate prevents release of Tb(III) thus formation and precipitation of terbium hydroxide species under the alkaline assay conditions is avoided.

An analogous mixed ligand chelate between a Tb(III) aminopolycarboxylate and 4-aminosalicylic acid (pAS) has been applied to DNA hybridisation allowing development of a homogeneous system, discussed below.

1.3.4 Homogeneous Nucleic Acid Hybridisation Assay

Oser and Valet[76] employed TbDTPA and pAS in specific labelling of oligonucleotide strands such that a nucleic acid could be detected by fluorescence resonance energy transfer (FRET). Two nucleic acid probes of known base sequence are employed, one labelled with the TbDTPA chelate at the 5' terminus. The other is labelled at the 3'end with a salicylic acid derivative. Only upon hybridisation are the two components of the label brought into close proximity allowing energy transfer to occur from the pAS donor to the TbDTPA acceptor (Figure 1-17). Hybridisation is confirmed by observation of characteristic green Tb(III) emission. The assay can be performed in solution, under time resolved conditions, minimising background fluorescence. The homogeneous nature of the assay eliminates the need for laborious pre-hybridisation incubation periods (since the hybridisation kinetics are more favourable in solution) and washing steps, therefore presents itself as an attractive candidate in the development of automated high throughput systems.

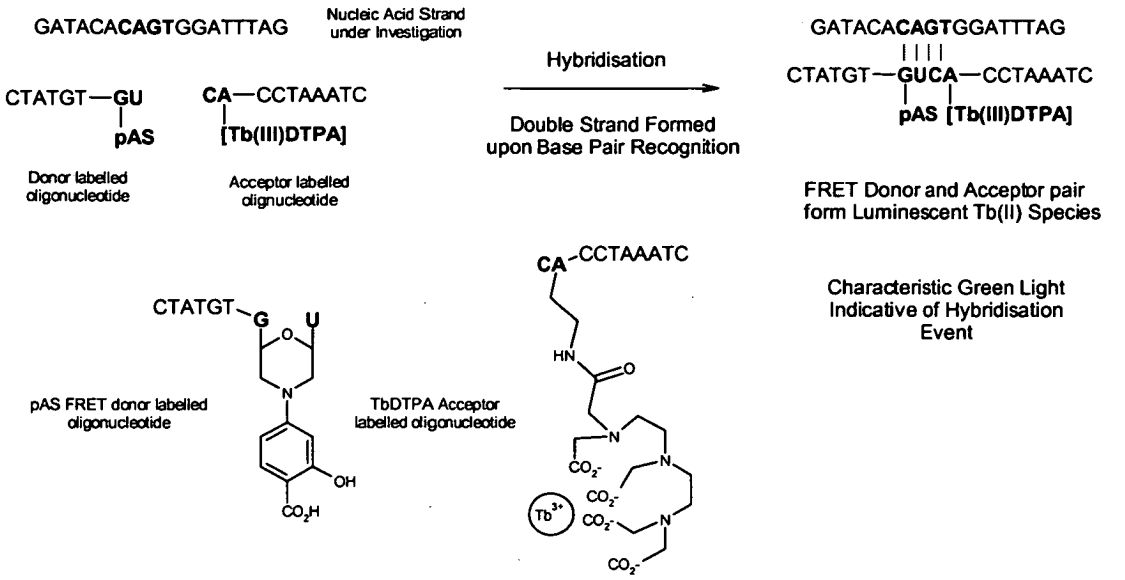

Figure 1-17 Schematic representation of lanthanide labelling in nucleic acid hybridisation assay

The hybridisation assay discussed here demonstrates the applicability of FRET pairs and time resolved detection methods to probing nucleic acid sequences,[77-83] of great importance in detecting mutations and modifications to genetic material.

1.3.5 Homogeneous Time Resolved Fluorometric Assay (HTRF)

Much of the effort devoted to the development of biological detection methods has focused on the search for highly sensitive homogeneous assay systems that are readily adaptable to automation and mechanisation. One success story, termed Homogeneous Time Resolved Fluorometric Assay (HTRF) developed by CisBio International[54] is discussed below. The system (Figure 1-18) utilises a Fluorescence Resonance Energy Transfer (FRET) pair comprising of a europium bipyridine cryptand and an allophycocyanin dye.[54] The donor, a $[Eu\subset(bipy.bipy.bipy)]^{3+}$ chelate (Figure 1-11), incorporates the selectivity of metal binding and complex stability offered by a macrobicyclic polyaza ligand with the chromophoric properties of the organic bipyridine unit. The donor is covalently coupled to the biomolecule (antibody or antigen) using conventional labelling methodology (see Scheme 1-1), without the loss of immunological reactivity or photophysical characteristics of the probe. Depopulation of the metal excited state by components of the serum, such as uric acid, is prevented by incorporation of excess fluoride ions in the sample media. The fluoride ions occupy the remaining vacant coordination sites of the metal preventing association of quenching moieties. The acceptor, an allophycocyanin dye, is also coupled to an antibody

such that formation of the immunocomplex brings the FRET pair into close proximity. Resonance energy transfer from the donor to the acceptor by the Förster mechanism[84] can be observed over distances of 5-10 nm, comparable to those of the immunocomplex. Laser excitation at 337 nm populates the singlet excited state of the tris(bipy) ligand, which undergoes intersystem crossing to the triplet state, from which intramolecular energy transfer populates the metal excited state. Characteristic Eu(III) emission at 620 nm is observed from free labelled antigen in the assay media. Upon immunocomplexation radiationless de-excitation of the donor excited state populates the emissive state of the allophycocyanin dye, from which fluorescence at 665 nm is observed.

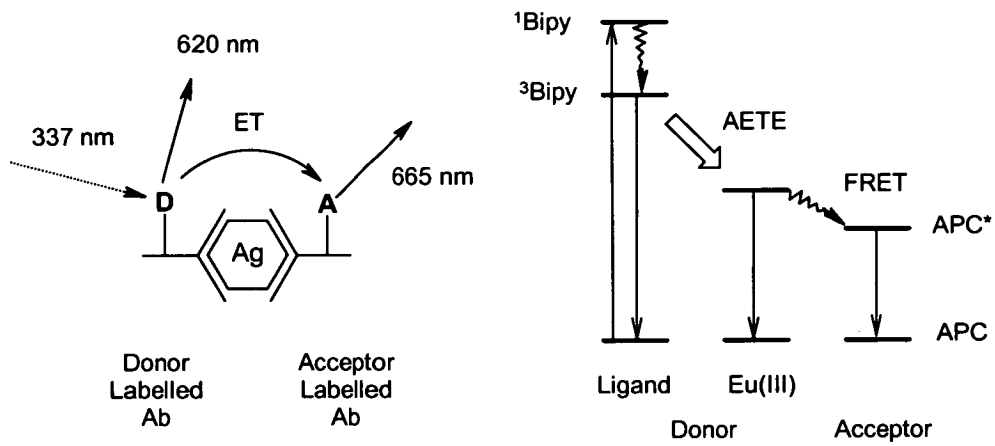

Figure 1-18 Schematic representation of the HTRF FRET based assay

Background fluorescence by serum components and free acceptor-labelled antibodies is minimised by implementing time resolved detection. Dual wavelength detection is performed at 620 nm (donor) and 665 nm (acceptor). The ratio of observed intensities is dependent solely on the concentration of the immunocomplex in solution, allowing quantitative analysis of the antigen. The assay is completely homogeneous, thus negating the tedious washing and separation steps necessary in comparable heterogeneous fluoroimmunoassays.

HTRF systems are now routinely applied in clinical situations, in complex assays involved in drug discovery[85-90] and are continually evolving to meet the demands of the pharmaceutical industry. The efficiency of the FRET assay is proportional to the distance between donor and acceptor (proportional to $1/r^6$, where r = distance). Due to the long-lived metal excited state which populates the APC emissive level, APC fluorescence, the result of biological

molecular recognition, can be detected after a time delay following the excitation pulse. Fluorescence from un-complexed APC is short-lived and decays on timescales comparable to that of serum proteins.

Development of such important homogeneous assay methodology has paved the way forward for rapid technological evolution in pharmaceutical drug discovery and detection.

1.4 Combinatorial Technologies – Synthesis and Screening

Fluorescence based sensing technologies are now routinely employed in identification and optimisation of target and lead compounds for potential drug development and optimisation.[85-90] Cell based fluorescence assays are common in pre-clinical and toxicological studies allowing the behaviour of potential therapeutic agents to be monitored in a cellular environment. Advances in genomics now provide researchers with an abundance of information on disease areas, and supply potential target proteins almost as fast as chemists can validate them. Thanks to evolution of new screening technologies it is now possible to evaluate the activity of large libraries of potential therapeutic agents against these targets quickly and effectively.

The demand for compound libraries has in turn lead researchers to investigate and develop novel synthetic strategies to generate large numbers of small, chemically diverse molecules of high purity to supply such screening programmes.

In the 1960s Merrifield[91] devised an automated system for generation of peptidic molecules employing polymeric supports. This resin based chemistry remained limited to peptidic syntheses until the early 1990s when interest turned to widening the applicability of the automated system. Synthetic strategies are discussed briefly in Chapter 1.4.2.

Crucial to effective drug discovery and optimisation is careful library design.[92] Libraries for early discovery, designed to identify potential agonists and antagonists in general are chosen to maximise chemical diversity. In contrast, smaller, more focussed libraries of chemically/structurally similar compounds are important in lead optimisation in order to maximise the potency of the pharmacophore identified by initial diversity screening.

Advances in computational chemistry[92] enable such libraries to be designed based on molecular similarity or diversity.[93] A molecule can be described mathematically as a set of vectors in space, representing the 2D structure.[94] A target receptor, such as a protein, can be described correspondingly by a 3D descriptor. Computationally, the interaction between the two can be predicted or estimated.[95] Chemically similar compounds in general exhibit

comparable 2D descriptors, enabling faster and more efficient database searching. Chemical diversity can also be represented and searched for in the same way, identifying species with differing 2D descriptors.

1.4.1 Combinatorial Synthesis – an overview

Despite the rapid evolution of combinatorial chemistry technologies[92] in the field of drug discovery limitations still exist. Several semi or automated systems are widely applied throughout the pharmaceutical industry but their use is often restricted to well-established and reliable chemical conversions. Reaction kinetics often differ unpredictably between solid and solution phase syntheses and substantial investment is required at the development stage.

1.4.2 Parallel Synthesis

Conventionally, solid phase library generation enables the assembly of a product molecule on an inert polymeric support by sequential reaction of monomeric units. Excess reagents can be employed without the need for laborious purification procedures since their removal can be facilitated by careful washing of the resin. The product is obtained in good yield and high purity following cleavage from the solid support. Solid phase synthesis can be applied to "split-and-mix" chemistry (schematically represented below, Figure 1-19) rapidly generating large chemical libraries.

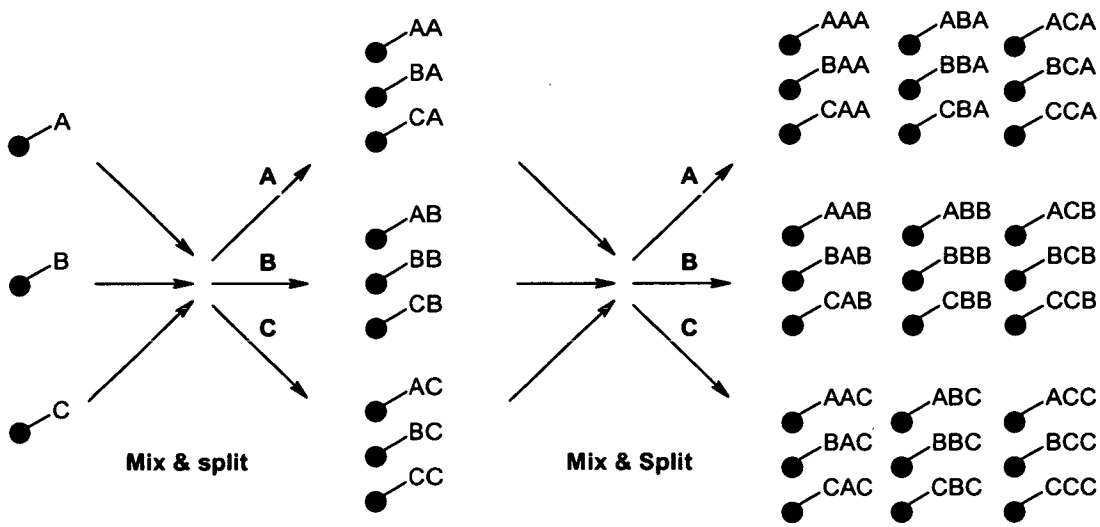

Figure 1-19 Schematic representation of parallel "spit and mix" solid phase synthesis

Using parallel synthetic strategies a large array of compounds can be generated quickly and easily, with control over the monomer sequence in the final product. For example, three starting materials, reacted twice, in sequence with three different reagents will yield twenty-seven distinct products for testing in a high throughput screen.

Such syntheses can be followed by a radiofrequency tagging system developed by IRORI[96] which tracks the inert support as it progresses through many reaction steps. Specialised polymeric supports such as MicroKans and Pins are available. The radio-frequency labelled tag slots directly into the Pin and the molecule is created directly on the functionalised polymer support. With the Microkans the resin beads and tag are held within a polymeric container. These systems reduce the effort required in the often complicated deconvolution of library product mixtures since only one compound per solid support is formed, of which the monomer sequence is recorded.

Where a particular reaction may not be suitable for solid phase synthesis, a modified version of the traditional solution phase synthesis may be employed.[97] Scavenger resins and solid-phase purification systems are available for facile removals of excess reagents. Scavenger resins are employed after the reaction to covalently couple the excess reagent, immobilising it on a solid support and allowing filtration of the clean product or intermediate solution. Common scavengers include amine based resins and aldehydes.

In addition to this, solid supported reagents and catalysts may be used with product filtration. Not surprisingly, combinatorial chemistry and HTS have also found application in catalysis research.[98-101, 103] Similarly, combinatorial screening methods have been applied in development of novel materials[102] exhibiting interesting photophysical and magnetic properties.

1.4.3 Combinatorial Chemistry in Catalysis Research

Traditionally the development of novel catalytic species was achieved through trial and error. Over time, a series of iterative experiments would be performed in order to maximise the efficiency of ligand and metal components in facilitation of chemical conversions and to optimise reaction conditions. With the introduction of combinatorial technologies[98-101] it became possible to perform experiments in parallel, modifying only one or two variables per reaction. Optimum conditions can be established rapidly and the effect of subtle ligand/metal modifications can be evaluated. An excellent example of combinatorial

chemistry in catalysis research is given by Hartwig *et al.*[103] Novel catalysts for palladium mediated coupling of aryl and alkyl halides with alkenes (Heck chemistry) were prepared and screened for activity. Active species identified on the solid phase were then prepared and tested in solution, and found to exhibit retained and improved enantioselectivity.

1.4.4 Combinatorial Techniques in Materials Research

Luminescent materials find application in a variety of systems from lamp phosphors and light emitting displays to photonic devices and consequently attract much interest. The tricolor lamp phosphors, employing lanthanide ions doped into host metal oxide lattices to produce a material emitting light at three individual wavelengths, are perhaps the most celebrated examples of inorganic luminescent materials.[104] The trivalent lanthanides are attractive dopants since their luminescence properties arise from spectroscopic transitions involving the f electrons, shielded from, and thus affected little by, the host lattice environment.

Discovery of novel luminescent materials has traditionally been achieved by trial and error making the experimental processes slow and laborious. Developments in instrumentation for detection of light, made largely in association with the pharmaceutical industry in response to the need for sensitive, automated equipment applicable to high throughput screening technologies have enabled such techniques to be applied in materials research. The search for novel phosphors can now be undertaken using a combinatorial approach, applied to the synthesis and screening of high density compound libraries.[106] Aimed at identification of the best lattice-dopant mixtures or optimisation of stoichiometries thin film or powder libraries can be quickly and effectively generated and their photophysical properties evaluated.

The importance of fluorescence based sensing technology in combinatorial chemistry, drug, materials and catalysis discovery chemistry cannot be underestimated. Without the advances in fluorometric and spectroscopic detection technology of recent years high throughput screening would be limited to radio-isotopic heterogeneous type assays with long incubation periods, complicated and laborious preparation procedures. Improvements can still be made and research into luminescent species applicable to screening technologies is very much alive. Our approach to the design of luminescent lanthanide chelates is outlined below.

1.5 Our Approach

1.5.1 Strategy

As outlined previously, several commercial fluoroimmunoassay detection methods employing lanthanide chelates are available. These methods, such as DELFIA (1.3.1) and EALL (1.3.3) are heterogeneous and formation of the luminescent species is not mechanistically understood. With the homogeneous FRET based assay systems (HTRF, 1.3.5) the transfer of energy is non specific through space. The donor and acceptor need only be in close proximity to one another for ET to occur, the efficiency of which is dependent on the distance between the two components of the FRET pair. Consequently, a drawback of the system is potential interference effects from solvated species in serum samples. Furthermore, the synthetic difficulties encountered in preparation of rare earth polypyridine cryptand species add interest to the search for novel chelators applicable as biological probes. In our approach we aim to develop a system to detect biological molecular recognition by means of specific lanthanide molecular recognition. In contrast to the FRET system of HTRF the lanthanide chelate will be non-luminescent in the absence of biological molecular recognition, only forming a luminescent species upon the macromolecular binding event (Figure 1-20).

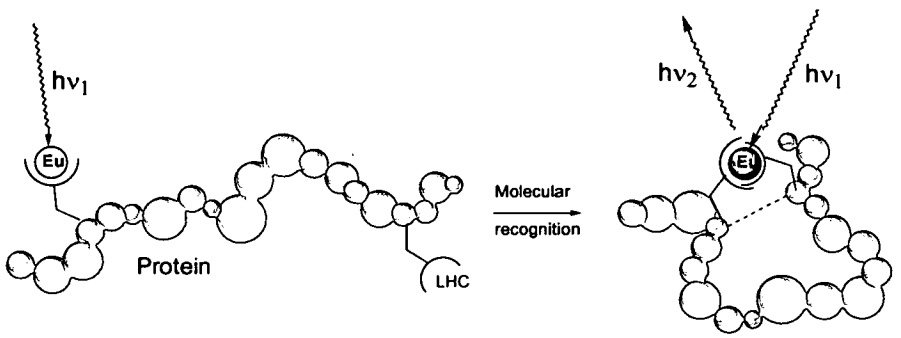

Figure 1-20 Schematic representation of lanthanide molecular recognition for direct detection of a biological event

The system will comprise two components: a stable, water soluble, non-luminescent rare earth chelate (LnNAL) and a separate aromatic moiety. The preformed chelate is attached to the biomolecule under investigation. The sensitising aromatic ligand, or light harvesting centre (LHC), bearing a binding site that recognises the lanthanide site is attached close to the corresponding biological recognition site. No signal is observed prior to biological molecular recognition, upon which the LHC and the LnNAL are brought together

and intramolecular energy results in lanthanide signalling. The close proximity of the two separate components of the luminescent label allows lanthanide molecular recognition to occur. Excitation of the LHC with UV light triggers the characteristic metal emission.

Ternary complex formation is achieved by controlling the arrangement of ligands around the ion, based on replacement of coordinating water molecules from the inner sphere of the metal. Previous studies on mixed ligand lanthanide luminescent assemblies have achieved little or no control in their formation.[106, 107]

On a molecular basis, the problem centres on the design of mixed ligand lanthanide species. Due to the coordination properties of the lanthanide, the NAL (non absorbing ligand) should be polydentate, therefore able to surround the metal displacing most of the coordinated quenching solvent water molecules, forming a highly stable, but non luminescent chelate. The second component, the LHC (Light Harvesting Centre) should be an aromatic strongly absorbing species, with a triplet excited state of appropriate energy for efficient intramolecular energy transfer to the emissive state of the metal centre. The LHC must bear a coordinating group, capable of displacing coordinated water molecules from the inner sphere of the Ln(III) cation chelate, (Figure 1-21).

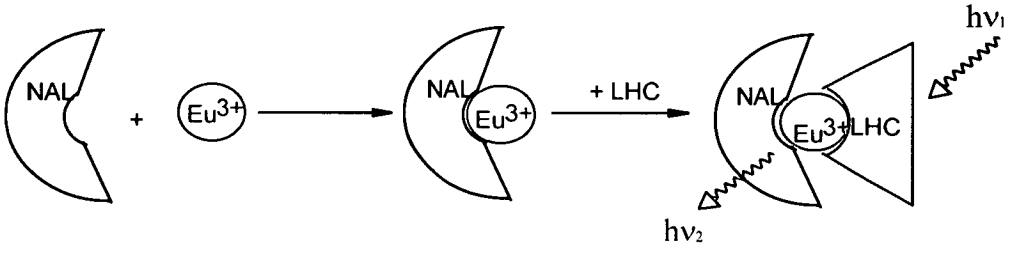

Figure 1-21 Schematic representation of luminescent ternary complex design

1.5.2 Choice of Ligands

Simple, commercially available aminopolycaboxylate[108-116] ligands have been chosen in our ternary complex design, offering obvious advantages over macrobicyclic cryptand species. Syntheses are uncomplicated and inexpensive as the chromophoric unit is not required to be incorporated into the NAL structure. Since a wide variety of LHC units are possible, molecules that offer potential as DNA intercalators may be considered,[107] allowing the potential to develop methods to detect protein–DNA interactions. In addition to complicated syntheses, another disadvantage associated with the bipyridine units of the cryptand employed in CisBio's HTRF method is their ability to quench the lanthanide excited state by non-radiative energy transfer to thermally populated low lying charge transfer states. We

have selected DTPA-AM_2 ligands as our NALs and simple aromatic carboxylic acids as LHCs to test the design.

1.5.2.1 The NAL

Preliminary investigations undertaken in our research group showed simple aminopolycarboxylate ligands to be capable of forming anionic mixed ligand luminescent species. Europium EDTA and DTPA chelates were employed in luminescence studies with the aromatic β-diketone, dibenzoylmethane (DBM), and with simple aromatic carboxylic acids. Assembly of mixed ligand species in 1:1 stoichiometry was observed in aqueous solution by emission and excitation spectroscopy. Similarly, cationic ternary complexes were successfully formed with macrocyclic lariat crown ether NAL chelates. Initial studies showed the mechanism of formation to differ between positively and negatively charged NAL species. This work centres on molecular recognition employing a series of neutral lanthanide chelates prepared from DTPA-bis(amide) ligands (DTPA-AM_2) (Figure 1-22).

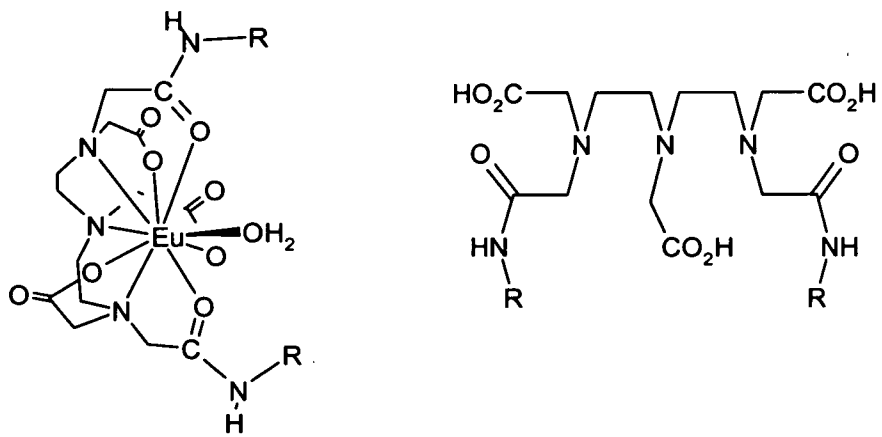

Figure 1-22 Structures of DTPA-AM_2 ligand and Eu(III) chelate

The multidentate aminopolycarboxylate DTPA-bis(amide) derivatives form a class of well known ligands for lanthanide complexation,[117-136] developed for application as contrast agents in Magnetic Resonance Imaging (MRI). Several preparative methods are reported, describing formation of the bis(amides) from the cyclic dianhydride of DTPA upon reaction with the relevant amine. Straight chain alkyl, adamantyl, benzyl, aniline and boronic acid DTPA-AM_2 derivatives (Figure 1-23) have been prepared targeting different relaxation properties of their Gd(III) complexes, except for a few cases where transition metal binding has been reported. A uracil derivative has been prepared[136] for introduction of a hydrogen bonding interface to the amide arms.

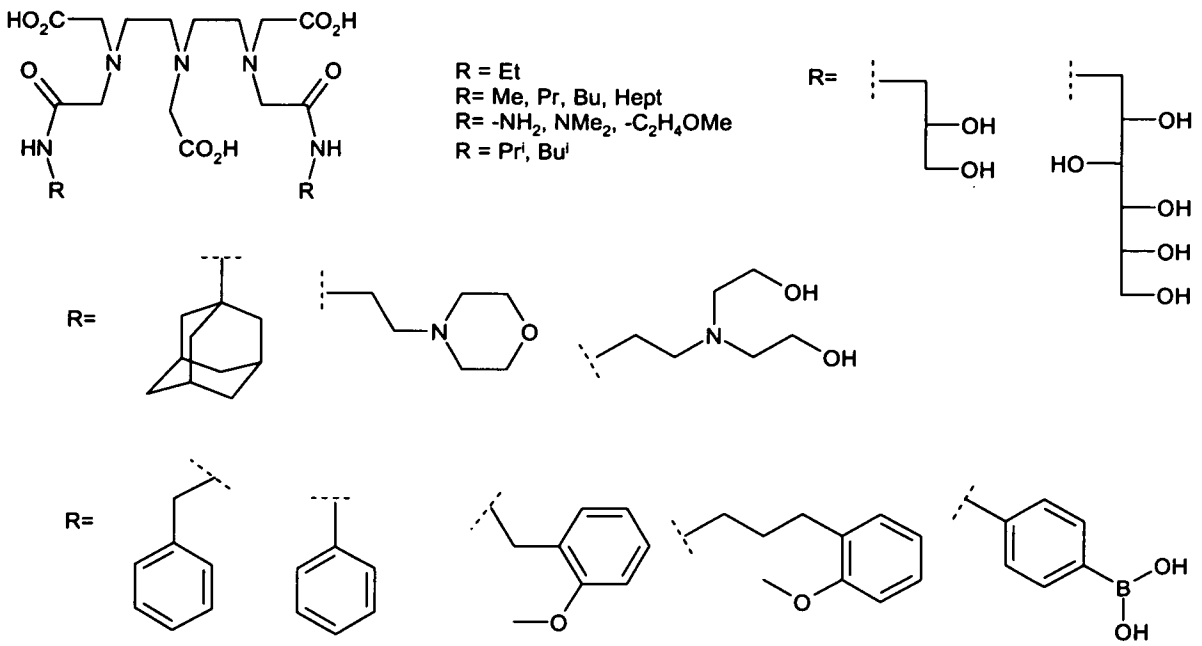

Figure 1-23 DTPA-AM_2 ligands reported in the literature

To the best of our knowledge, these ligands have not been investigated as components of luminescent signalling systems, with the exception of a study into the luminescence lifetime and hydration state of the methyl substituted derivative.[128] Macrocyclic DTPA-bis(amide) complexes have been extensively studied. A molecular switching system based on photoinduced electron transfer (PET) using DTPA ligands has also been reported.[129]

Several reports exist on the non-specific bioconjugation of monosubstituted Ln(III) chelates to oligonucleotides and proteins as luminescent probes. The photophysical characteristics of these aminopolycarboxylate derivatives have been evaluated as potential components of fluorescence resonance energy transfer (FRET) systems.[137-146] In these systems the antenna unit is non-coordinating and energy transfer to the lanthanide is weak and non specific.

The reported crystal structure of [GdDTPA-bis(ethylamide)][117] shows octadentate coordination of the Gd(III) ion, via the three carboxylate anions, the two amide carbonyls and the three nitrogen donors of the diethylenetriamine backbone. The amide nitrogen atoms are not involved in complexation and leave the ethyl arms of the ligand free to form a binding cavity, occupied by one coordinating water molecule. Stability constants for lanthanide complexation in the order of $LogK_{ML}$ 15 have been reported for several DTPA-AM_2 derivatives.

1.5.2.2 The LHC

Several features are required for a good choice of antenna ligand. The LHC should bear a characteristic binding unit with sufficiently high affinity for the lanthanide cation so as to competitively coordinate in aqueous solution. The triplet excited state should lie at an energy level appropriate for efficient intramolecular energy transfer to occur such that sensitised luminescence of the rare earth ion employed is observed upon molecular recognition. A good absorption cross section in the UV region is required for efficient excitation to the ligand singlet state such that intersystem crossing can occur prior to the intramolecular energy transfer event. Aromatic carboxylic acids have been chosen as potential LHCs, offering a variety of simple, model binding units with the potential to vary the chromophore as required.

1.5.3 Studies Undertaken

The controlled formation of mixed ligand luminescent complexes upon binding of the NAL chelate by the acid moiety is followed by monitoring the emission of the europium ion, triggered by intramolecular energy transfer from the LHC. Electrospray mass spectrometry and NMR provide supporting evidence for controlled assembly of ternary complexes. Specific molecular recognition is demonstrated between the model chelate EuBEA and simple carboxylic acids. These results, validating our ternary complex design, are reported in Chapter 3. Experimental details are given in Chapter 2 and the synthetic methods employed discussed in Chapter 4. Combinatorial screening strategies, employed in development of the mixed ligand system, allowed the interaction between a large library of aryl acid potential LHC units and a selection of LnNAL chelates to be evaluated. Results are presented in Chapter 5. It is demonstrated that the selectivity of molecular recognition is based largely on the aryl acid binding unit, with additional selectivity imparted by the amide arms of the chelate. Equilibrium constants for ternary complex formation, luminescence lifetimes and quantum yields are evaluated for 1:1 mixed ligand species formed upon molecular recognition between LnDTPA-AM_2 chelates and aryl acid LHCs. These results of the binding studies are discussed in Chapter 6. An unexpected observation, which may ultimately lead to luminescent materials with tuneable photophysical properties, is presented in Chapter 7. The crystal structure of a heterobimetallic, one-dimensional coordination polymer formed between Eu(III), picolinate antenna ligands and sodium counterions is reported. The interesting luminescence behaviour exhibited by the polymer in the solid state is discussed.

2 Experimental

2.1 Acronyms and Abbreviations

Compound Reference	Name	IUPAC Name
2.4.1	DTPA-dianhydride	*N, N*-bis[2-(2,6-dioxomorpholino)-ethyl]glycine
2.4.2.2	DTPA-BEA	1,11-(bis(ethylamino)-1,11-dioxo-3,6,9-triaza-3,6,9-triscarboxymethyl)undecane
2.4.2.3	DTPA-BUA	1,11-(bis(1-butylamino)-1,11-dioxo-3,6,9-triaza-3,6,9-triscarboxymethyl)undecane
2.4.2.4	DTPA-BDA	1,11-(bis(1-decylamino)-1,11-dioxo-3,6,9-triaza-3,6,9-triscarboxymethyl)undecane
2.4.2.5	DTPA-BBZA	1,11-(bis(benzylamno)-1,11-dioxo-3,6,9-triaza-3,6,9-triscarboxymethyl)undecane
2.4.2.6	DTPA-BTA	1,11-(bis(4-methybenzylamino)-1,11-dioxo-3,6,9-triaza-3,6,9-triscarboxymethyl)undecane
2.4.2.7	DTPA-cyHA	1,11-(bis(cyclohexylamino)-1,11-dioxo-3,6,9-triaza-3,6,9-triscarboxymethyl)undecane
2.4.2.8	DTPA-mcyHA	1,11-(bis(methylenecyclohexylamino)-1,11-dioxo-3,6,9-triaza-3,6,9-triscarboxymethyl)undecane
2.4.2.9	DTPA-cyOA	1,11-(bis(cyclooctylamino)-1,11-dioxo-3,6,9-triaza-3,6,9-triscarboxymethyl)undecane
2.4.2.10	DTPA-NBA	1,11-(bis(2-norbornylamino)-1,11-dioxo-3,6,9-triaza-3,6,9-triscarboxymethyl)undecane dihydrate
2.4.2.12	DTPA-BAA	1,11-(bis(1-adamantylamino)-1,11-dioxo-3,6,9-triaza-3,6,9-triscarboxymethyl)undecane
2.5.2.1	EuBEA	{1,11-(bis(ethylamino)-1,11-dioxo-3,6,9-triaza-3,6,9-triscarboxymethyl)undecane}europium(III) dihydrate
2.5.2.3	EuBUA	{1,11-(bis(1-butylamino)-1,11-dioxo-3,6,9-triaza-3,6,9-triscarboxymethyl)undecane}europium(III) monohydrate
2.5.2.5	EuBBZA	{1,11-(bis(benzylamino)-1,11-dioxo-3,6,9-triaza-3,6,9-triscarboxymethyl)undecane}europium(III) tetrahydrate
2.5.2.6	EuBTA	{1,11-(bis(4-methylbenzylamino)-1,11-dioxo-3,6,9-triaza-3,6,9-triscarboxymethyl)undecane}europium(III) trihydrate
2.5.2.7	EucyHA	{1,11-(bis(cyclohexylamino)-1,11-dioxo-3,6,9-triaza-3,6,9-triscarboxymethyl)undecane}europium(III) trihydrate
2.5.2.9	EumcyHA	{1,11-(bis(methylenecyclohexylamino)-1,11-dioxo-3,6,9-triaza-3,6,9-triscarboxymethyl)undecane}europium(III) hydrate
2.5.2.10	EuBPA	{1,11-(bis(2-biphenylamino)-1,11-dioxo-3,6,9-triaza-3,6,9-triscarboxymethyl)undecane}europium(III) trihydrate
2.5.2.11	EucyOA	{1,11-(bis(cyclooctylamino)-1,11-dioxo-3,6,9-triaza-3,6,9-triscarboxymethyl)undecane}europium(III) trihydrate
2.5.2.12	EuNBA	{1,11-(bis(±)2-aminonorbornylamino)-1,11-dioxo-3,6,9-triaza-3,6,9-triscarboxymethyl)undecane}europium(III) trihydrate

Compound Reference	Name	IUPAC Name
2.5.2.13	EuBDA	{1,11-(bis(1-decylamino)-1,11-dioxo-3,6,9-triaza-3,6,9-triscarboxymethyl)undecane}europium(III) hydrate
2.5.2.14	EuBAA	{1,11-(bis(1-adamantylamino)-1,11-dioxo-3,6,9-triaza-3,6,9-triscarboxymethyl)undecane}europium(III) trihydrate
2.5.3.1	TbBEA	{1,11-(bis(ethylamino)-1,11-dioxo-3,6,9-triaza-3,6,9-triscarboxymethyl)undecane}terbium(III) trihydrate
2.5.3.2	TbBUA	{1,11-(bis(1-butlylamino)-1,11-dioxo-3,6,9-triaza-3,6,9-triscarboxymethyl)undecane}terbium(III) trihydrate
2.5.3.3	TbBBZA	{1,11-(bis(benzylamino)-1,11-dioxo-3,6,9-triaza-3,6,9-triscarboxymethyl)undecane}terbium(III) pentahydrate
2.5.3.4	TbBTA	{1,11-(bis(4-methylbenzylamino)-1,11-dioxo-3,6,9-triaza-3,6,9-triscarboxymethyl)undecane}terbium(III) tetrahydrate
2.5.3.5	TbcyHA	{1,11-(bis(cyclohexylamino)-1,11-dioxo-3,6,9-triaza-3,6,9-triscarboxymethyl)undecane}terbium(III) trihydrate
2.5.3.6	TbmcyHA	{1,11-(bis(methylenecyclohexylamino)-1,11-dioxo-3,6,9-triaza-3,6,9-triscarboxymethyl)undecane}terbium(III) trihydrate
2.5.3.7	TbNBA	{1,11-(bis((±)2-norbornylamino)-1,11-dioxo-3,6,9-triaza-3,6,9-triscarboxymethyl)undecane}terbium(III) trihydrate
2.5.4.1	LaBEA	{1,11-(bis(ethylamino)-1,11-dioxo-3,6,9-triaza-3,6,9-triscarboxymethyl)undecane}lanthanum(III) trihydrate
2.5.4.2	LaBUA	{1,11-(bis(1-butylamino)-1,11-dioxo-3,6,9-triaza-3,6,9-triscarboxymethyl)undecane}terbium(III) trihydrate
2.5.4.3	LaBBZA	{1,11-(bis(1-benzylamino)-1,11-dioxo-3,6,9-triaza-3,6,9-triscarboxymethyl)undecane}lanthanum(III) hydrate
2.5.4.4	LacyHA	{1,11-(bis(cyclohexylamino)-1,11-dioxo-3,6,9-triaza-3,6,9-triscarboxymethyl)undecane} lanthanum(III) hydrate
2.5.5.1	YBEA	{1,11-(bis(ethylamino)-1,11-dioxo-3,6,9-triaza-3,6,9-triscarboxymethyl)undecane} yttrium (III) hydrate
2.5.5.3	YBUA	{1,11-(bis(1-butylamino)-1,11-dioxo-3,6,9-triaza-3,6,9-triscarboxymethyl)undecane} yttrium (III) hydrate
2.5.5.4	YBBZA	{1,11-(bis(benzylamino)-1,11-dioxo-3,6,9-triaza-3,6,9-triscarboxymethyl)undecane} yttrium (III) hydrate
2.5.5.5	YNBA	{1,11-(bis((±)-2-norbornylamino)-1,11-dioxo-3,6,9-triaza-3,6,9-triscarboxymethyl)undecane} yttrium (III) hydrate
2.5.5.6	YmcyHA	{1,11-(bis(methylenecyclohexylamino)-1,11-dioxo-3,6,9-triaza-3,6,9-triscarboxymethyl)undecane} yttrium (III) hydrate
2.5.5.7	YcyHA	{1,11-(bis(cyclohexylamino)-1,11-dioxo-3,6,9-triaza-3,6,9-triscarboxymethyl)undecane} yttrium (III) hydrate
2.5.6.1	GdBUA	{1,11-(bis(1-butylamino)-1,11-dioxo-3,6,9-triaza-3,6,9-triscarboxymethyl)undecane} gadolinium (III) hydrate
2.5.6.2	GdBBZA	{1,11-(bis(benzyllamino)-1,11-dioxo-3,6,9-triaza-3,6,9-triscarboxymethyl)undecane} gadolium (III) tetrahydrate
2.5.7.1	LuBEA	{1,11-(bis(ethylamino)-1,11-dioxo-3,6,9-triaza-3,6,9-triscarboxymethyl)undecane} lutetium (III) hydrate

Table 2-1 Ligands and complexes – Abbreviations used and IUPAC names

Acronym/Abbreviation	Definition/Name
DMF	*N,N*-dimethlyformamide
DCM	Dichloromethane
HATU	*o*-(7-azabenzotriazol-1-yl-*N,N,N',N'*-tetramethyl uronium hexafluorophosphate
DIPEA	*N,N*-diisopropylethylamine
DMAP	*N,N,*-dimethyl-4-aminopyridine
TNBSA	2,4,6-trinitrobenzene sulfonic acid
PS-MB-CHO	Polystyrene based aldehyde resin
TBAOH	Tetrabutylammonium hydroxide
TBACl	Tetrabutylammonium chloride
DMSO	Dimethylsulfoxide

Table 2-2 General reagents - abbreviations used

2.2 Materials

All chemicals in the solution phase syntheses of the ligands were of reagent grade, purchased from commercial suppliers and used as received without further purification. $DTPAH_5$ (diethylenetriamine pentacetic acid) (97%); benzylamine (99%); cyclohexylamine (98%) cyclododecylamine (98%) and tetrahydrofurfurylamine (97%) were obtained from Acros Organics. Acetic anhydride (99%); ethylamine (70% wt H_2O); 1-butylamine (98%); 1-decylamine (98%); methylencyclohexylamine (98%); cyclooctylamine (97%); 4-methylbenzylamine (99%) 4-picolyamine (99%); 1-adamantylamine (97%); +/- 2-*exo*-aminonorbornane (99%) and 2-aminobiphenyl (98%) were purchased from Aldrich. All solvents were reagent grade and used without degassing or further drying. Deionised water was used in all synthetic procedures and spectroscopic studies. Concentrated HCl was 35-38% (aq) purchased from Fluka and diluted as required. Sodium Hydroxide pellets were obtained from BDH. Tetrabutylammonium hydroxide (TBAOH) (40% wt H_2O) was purchased from Aldrich or Fluka. The $Ln(III)Cl_3 \bullet 6H_2O$ salts were of >99.9% purity, stored in a dry atmosphere (dessicator) and used as received from Acros or Aldrich. Eu_2O_3 (>99.9%) was purchased from Aldrich.

The aryl acids screened for their interaction with LnNAL chelates, and subsequent binding studies were supplied by Compound Control, GlaxoSmithKline Medicines Research Centre,

Stevenage, and used as received (>98%). Benzoic, phthalic, picolinic, salicylic, dipicolinic and isophthalic acids used in binding studies were purchased from commercial suppliers (Aldrich, Acros and Fluka). Prof. Ioanniou and Dr Lianilou, University of Athens provided 5-fluorosalicylic acid (5-FSA) and 4-aminosalicylic acid (*p*-NH_2AS).

2.3 Instrumentation

Emission and excitation spectra were measured using Photon Technology International QM-1 luminescence spectrometer consisting of a 75-watt PowerArc xenon lamp and single monochromator (350 nm blaze) excitation source. The sample chamber is equipped with focusing lens for detection of emitted light at 90° to the excitation beam by a single emission monochromator (500 nm blaze), and Hamamatsu R928 digital photomultiplier tube. The instrument is computer controlled, with FeliX 1.41 software installed for data analysis. Emission spectra are corrected for monochromator and PMT response. Excitation spectra are corrected for the spectral response of the xenon arc lamp and the excitation monochromator. Light is directed by a beam splitter to a photodiode giving "real time" correction of the excitation part response for each spectrum. Absorption spectra were obtained with a Shimadzu UV.3101-PC spectrometer equipped with a deuterium lamp.

Luminescence lifetime measurements were made using an "add-on" set-up to the PTI QM-1 luminescence spectrometer. A Continuum Surelite (II) Nd:YAG pulsed laser with selection wavelengths 532, 355 and 266 nm (1^{st}, 2^{nd} and 3^{rd} harmonics of 1064nm) was used as the pulsed excitation source. Light at the strongest wavelength emitted by the sample was focussed by lenses of the PTI instrument on to the emission monochromator and detected by an analogue Hamamatsu R928 PMT tube. A LeCroy oscilloscope then treated the signal (external trigger: 50 Ω; coupling for signal: 50 Ω). Lifetime decay curves were averaged over 500 sweeps. Data fitting was performed using Kaleidagraph software.

Proton NMR spectra were measured on Brüker spectrometers at 200, 250 360, 400 and 600 MHz in deuterated solvents purchased from Goss Scientific. Carbon NMR spectra were obtained at 62.9 MHz or 100.6 MHz. FAB-MS was performed on a Kratos MS-50 spectrometer using an I-NOBA or thioglycerol matrix. Electrospray MS were recorded at the EPSRC MS service centre in Swansea. Flow injection ES-MS was performed at GSK Medicines Research Centre, Stevenage using a Micromass LC-TOF instrument. LC-MS were run on a Micromass series II platform with HP1100 LC/Auto injector. Details of the LC methods employed are given in Appendix 1. Elemental analyses were carried out by

departmental services at Edinburgh University on a Perkin Elmer 2400 CHN analyser and by Butterworth Laboratories LTD, Middlesex.

Combinatorial screening of aromatic acids versus LnNAL chelates was performed in 96 well format using black, flat-bottomed NUNC plates. A *Tecan* Ultra Multifunctional Microplate reader consisting of a high energy xenon arc flash lamp, flash lamp monitor, fused silica condensing optics, choice of dichroic or 50% mirror, excitation and emission filter slides and a red sensitive (R928) PMT for fluorescence-intensity (FI) and time-resolved fluorescence (TRF) measurements was employed. Luminescence was recorded from a fixed position above the plate, initially optimised for maximum fluorescence intensity. The PMT gain was set for optimal signal to noise ratios. Signal integration time was delayed against the flash by a pre-defined lag-time of 20 μs, avoiding detection of short lived organic fluorescence.

2.4 Synthesis of DTPA-bis(amide) Ligands

2.4.1 *N, N*-bis[2-(2,6-dioxomorpholino)-ethyl]glycine: DTPA-dianhydride

DTPA-dianhydride, although commercially available in small quantities, was prepared by a modification of the published procedure[146] (Scheme 2-1). Acetic anhydride (65 ml, 0.69 mol) was added slowly via a dropping funnel to a stirring suspension of $DTPAH_5$ (48.0 g, 0.122 mol) in pyridine at 65°C. Stirring was continued at this temperature for 5 hours after which time the new solid that had formed was collected by filtration and washed with acetic anhydride (200 ml) and refluxed in acetonitrile for 1 hour. The solid was filtered, washed with CH_3CN and dried under vacuum to yield the title compound, DTPA-dianhydride (40.7 g, 94%). ^{1}H NMR (200 MHz, DMSO-d_6): δ (ppm) 12.10 (s, $CO_2\underline{H}$); 3.71 (8H, s, $NC\underline{H}_2CO$); 2.77-2.75 (4H, broad t, $NC\underline{H}_2CH_2N$); 2.68-2.63 (4H, broad t, $NCH_2C\underline{H}_2N$); ^{13}C NMR (62.9 MHz, DMSO-d_6): δ (ppm) 172.6 ($\underline{C}O_2H$); 171.9 ($\underline{C}$=O); 54.7 (NCH_2CO_2H); 52.7 ($N\underline{C}H_2CO$); 51.7, 50.7 ($N\underline{C}H_2\underline{C}H_2N$). CHN: Calculated for $C_{14}H_{19}N_3O_8$: 47.04% C; 5.37% H; 11.76% N. Found: 46.83% C; 5.39% H; 11.67% N.

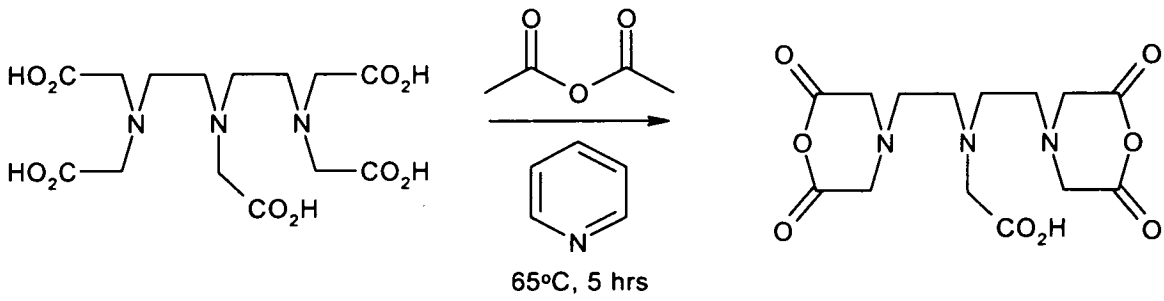

Scheme 2-1 DTPA-dianhydride preparation

2.4.2 Solution Phase Synthesis of DTPA-bis(amide) Ligands

2.4.2.1 General DTPA-bis(amide) preparation

The ligands were prepared according to the literature procedure[117, 118] (Scheme 2-2). DTPA-dianhydride was added in small portions over 30 minutes to an excess amount of the stirring, ice cold amine. The reaction was allowed to warm to room temperature following dilution with water and stirring continued overnight. The solvent was then removed by rotary evaporation, the oily residue re-diluted with water then acidified to pH ~ 2 with conc. HCl. The colourless solid/crystals that formed were collected by filtration, washed with water, ethanol and diethyl ether then dried under vacuum to yield the desired DTPA-bis(amide) derivative. Ligands were characterised by ^{1}H and ^{13}C NMR, FAB-MS and elemental analysis.

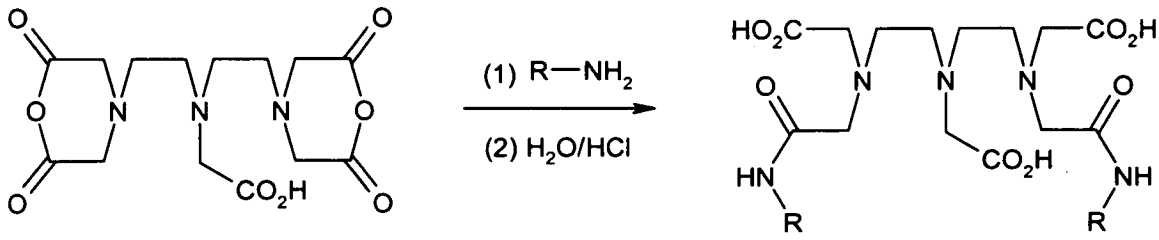

Scheme 2-2 DTPA-bis(amide) ligand preparation

2.4.2.2 1, 11-(bis(ethylamino)-1, 11-dioxo-3,6,9-triaza-3,6,9-triscarboxymethyl)undecane: DTPA-BEA.2H$_2$O

DTPA-dianhydride (15.0 g, 0.042 mol) was added slowly over 30 minutes to a stirring, ice cold solution of ethylamine (30 ml, 0.37 mol, 70% w/w H_2O). The mixture was then diluted with 30 ml H_2O, allowed to warm to ambient temperature and stirring continued overnight. The yellow solution was filtered and the volume reduced to an oil by rotary evaporation. The oil was then diluted with 10 ml H_2O and acidified to around pH 2 with conc. HCl. The colourless crystals that formed were collected by filtration, washed with water (100 ml), ethanol (50 ml) and diethyl ether (50 ml) then dried under vacuum. The solid was recrystallised from H_2O to yield the title compound, DTPA-BEA.2H_2O (4.46 g, 22 %). ^{1}H NMR (360 MHz, D_2O) δ (ppm): 3.84 (4H, s, NC$\underline{H}_2$CO$_2$H, terminal); 3.73 (4H, s, NC$\underline{H}_2$CONH), 3.67 (2H, s, NC$\underline{H}_2$CO$_2$H, central); 3.34-3.38 (4H, t, NC$\underline{H}_2$CH$_2$N); 3.25–3.28 (4H, t, NCH$_2$C$\underline{H}_2$N); 3.19-3.25 (4H, q, NC$\underline{H}_2$CH$_3$); 1.07–1.11 (6H, t, NCH$_2$C$\underline{H}_3$). ^{13}C NMR (62.9 MHz): 172.7 (C$\underline{O}_2$H); 172.4 (C$\underline{O}_2$H); 168.2 (C$\underline{O}$NH); 57.3, 57.1, 55.0 (NC$\underline{H}_2$CO); 52.2, 51.5 (NC$\underline{H}_2$C$\underline{H}_2$N), 35.0 (NC$\underline{H}_2$CH$_3$); 13.9 (C$\underline{H}_3$); FAB-MS $[M+1]^+$ 448 D; CHN:

Calculated for $C_{18}H_{37}N_5O_{10}$: 44.70% C; 7.73% H; 14.49% N. Found: 44.60% C; 7.77% H; 14.49% N.

2.4.2.3 1, 11-(bis(1-butylamino)-1, 11-dioxo-3,6,9-triaza-3,6,9-triscarboxymethyl)undecane: DTPA-BUA.2H_2O

DTPA-dianhydride (10.0 g, 0.028 mol) was added in small portions over 30 minutes to stirring, ice cold neat 1-butylamine (14 ml, 0.14 mol). The mixture was diluted with 10 ml H_2O and stirred at ambient temperature for 24 hrs. The volume was reduced by rotary evaporation and the yellow oil diluted with H_2O (50 ml) before acidification to around pH 2 with conc. HCl. The colourless crystals that quickly formed were collected by filtration and washed with water (20 ml), acetone (100 ml) and ether (100 ml) then dried under vacuum to yield the title compound (12.7 g, 84%). ^{1}H NMR (250 MHz, D_2O): δ (ppm) 3.68 (2H, s, $NC\underline{H}_2CO_2H$, central); 3.47 (4H, s, $NC\underline{H}_2CO_2H$, terminal); 3.31, (4H, s, $NC\underline{H}_2CNH$); 3.26-3.29 (4H, br. t, $NCHC\underline{H}_2N$ & 4H, s, $NC\underline{H}_2CONH$); 3.11- 3.21 (4H, br. t, $NC\underline{H}_2CH_2N$); 1.50 - 1.39 (4H, quintet, $NCH_2C\underline{H}_2CH_2CH_3$); 1.30 - 1.20 (4H, sextet, $NCH_2CH_2C\underline{H}_2CH_3$); 0.87 - 0.81 (6H, t, $NCH_2CH_2CH_2C\underline{H}_3$). ^{13}C NMR (62.9 MHz, D_2O): δ (ppm) 176.9 ($\underline{C}O_2H$ terminal); 171.7 ($\underline{C}O_2H$ central); 171.2 ($\underline{C}ONH$); 58.4, 58.2 ($N\underline{C}H_2CONH$, NCH_2CO_2H terminal); 54.6 (NCH_2CO_2H central); 52.4, 50.7 ($N\underline{C}H_2\underline{C}H_2N$); 38.9 ($N\underline{C}H_2CH_2CH_2CH_3$); 30.4 ($NCH_2\underline{C}H_2CH_2CH_3$); 19.4($NCH_2CH_2\underline{C}H_2CH_3$); 12.9 ($NCH_2CH_2CH_2\underline{C}H_3$). FAB-MS $[M+1]^+$ 504 D; CHN: Calculated for $C_{22}H_{45}N_5O_{10}$: 48.96% C; 8.42% H; 12.98% N. Found: 48.91% C; 8.36% H; 12.89% N.

2.4.2.4 1, 11-(bis(1-decylamino)-1, 11-dioxo-3,6,9-triaza-3,6,9-triscarboxymethyl)undecane: DTPA-BDA.2H_2O

Neat 1-Decylamine (2 ml, 0.01mol) was added slowly to a stirring suspension of DTPA-dianhydride (1.05 g, 3.0 mmol) in 5 ml pyridine and the mixture stirred at room temperature overnight (18 hrs). The resultant yellow solution was filtered to remove any unreacted DTPA prior to reducing the volume by rotary evaporation. The residue was dissolved in water (50 ml) before acidification to around pH 2 with conc. HCl, upon which a colourless solid formed. This was collected by filtration, washed with water (2 x 10 ml), ethanol (2 x 10 ml) and diethyl ether (2 x 10 ml) then dried under vacuum to yield the title compound, DTPA-BDA (1.58 g, 78%). ^{1}H NMR (400 MHz, DMSO-d_6): δ (ppm) 7.75 (3H, $CO_2\underline{H}$); 3.17 (2H, s, $NC\underline{H}_2CO_2H$, central); 3.10 (4H, s, $NC\underline{H}_2CO_2H$, terminal); 2.95 (4H, s, $NC\underline{H}_2CONH$); 2.79 (4H, q, $NHC\underline{H}_2C_9H_{19}$); 2.69 (4H, br, t, $NC\underline{H}_2CH_2N$), 2.56 (4H, br, t, $NCH_2C\underline{H}_2N$); 2.23 (8H, br, $-NCH_2C\underline{H}_2C\underline{H}_2-$); 1.12 (4H, q, $-C\underline{H}_2CH_3$); 0.95 (20H, br, $-C\underline{H}_2-$); 0.59 (6H, t, $-CH_2C\underline{H}3$).

2.4.2.5 1, 11-(bis(benzylamno)-1, 11-dioxo-3,6,9-triaza-3,6,9-triscarboxymethyl)undecane: DTPA-BBZA.2H_2O

DTPA-dianhydride (10.0 g, 0.028 mol) was added in small portions over 30 minutes to stirring, ice cold neat benzylamine (20 ml, 0.18 mol). The mixture was diluted with 10 ml H_2O and stirred at ambient temperature for 20 hrs. The volume was reduced by rotary evaporation and the yellow oil diluted with H_2O (50 ml) before acidification to around pH 2 with conc. HCl. The colourless crystals that quickly formed were collected by filtration and washed with water (2 x 10 ml), acetone (2 x 10 ml) and diethyl ether (50 ml) then dried under vacuum to yield the title compound, DTPA-BBZA (12.9 g, 81%). ^{1}H NMR (360 MHz, D_2O/NaOD): δ (ppm) 7.2-7.3 (10H, m, $C_6\underline{H}_5$); 4.25 (4H, s, PhC$\underline{H}_2$N); 3.1 (4H, s, NC$\underline{H}_2CO_2H$, terminal); 3.0 (4H, s, NC$\underline{H}_2$CONH); 2.85 (2H, s, NC$\underline{H}_2CO_2H$, central); 2.4 (8H, 2 x t. NC$\underline{H}_2C\underline{H}_2$N). ^{13}C NMR: (62.9 MHz, D_2O): δ (ppm) 177.4 ($\underline{C}O_2H$, terminal); 172.4 ($\underline{C}O_2H$ central); 170.8 ($\underline{C}$=O amide); 137.9 (aromatic $\underline{C}$); 129.2, 128.8, 127.5 (aromatic $\underline{C}$H); 58.33, 58.27 (N$\underline{C}H_2\underline{C}H_2$N); 54.6, 52.3 50.4, 42.7 (N$\underline{C}H_2$CON, N$\underline{C}H_2CO_2$ central, N$\underline{C}H_2CO_2$ terminal, N$\underline{C}H_2$Ph). FAB-MS: $[M+1]^+$ 572 D; CHN: Calculated for $C_{28}H_{41}N_5O_{10}$: 55.36 % C; 6.82 % H; 11.53 % N. Found: 55.69 % C; 6.93 % H; 11.44 % N.

2.4.2.6 1, 11-(bis(4-methybenzylamino)-1, 11-dioxo-3,6,9-triaza-3,6,9-triscarboxymethyl)undecane: DTPA-BTA.2H_2O

DTPA-dianhydride (5.0 g, 0.014 mol) was added slowly to neat, ice cold, stirring 4-methylbenylamine (10 ml, 0.078 mol), the reaction diluted with 15 ml water, allowed to warm to room temperature and stirring continued overnight (24 hrs). The volume of the cloudy solution was reduced by rotary evaporation and the yellow oil diluted with 20 ml water. Concentrated HCl was then added dropwise, the solution became clear around pH 5. Further acidification to pH ~ 2 resulted in the formation of colourless crystals, which were collected by filtration, washed with water (50 ml), ethanol (50 ml) and diethyl ether (50 ml), then dried under vacuum to yield the title compound DTPA-BTA•2H_2O (6.8 g, 79%). LC-MS: 599 D (retention time 2.63 mins). ^{1}H NMR (400 MHz, D_2O/NaOD, pD ~ 6): δ (ppm) 6.90 (8H, s $C_6\underline{H}_4CH_3$); 4.02 (4H, s, 2 x NC$\underline{H}_2$PhMe); 3.31 (2H, s, NC$\underline{H}_2CO_2^-$ central); 3.01 (4H, s, NC$\underline{H}_2CO_2$ terminal); 2.85 (4H, s, NC$\underline{H}_2$NCOCH_2PhMe, 2H t, NC$\underline{H}_2CH_2$N); 2.60 (4H, t, NC$H_2C\underline{H}_2$N); 2.00 (6H, s, PhC$\underline{H}_3$). ^{13}C NMR (100 MHz): δ (ppm) 179.0 ($\underline{C}O_2H$ terminal); 173.8 ($\underline{C}$ONH); 170.9 ($\underline{C}O_2H$ central); 137.9 ($CH_2\underline{C}C_5H_4CH_3$ aromatic); 135.4 ($\underline{C}H_3C$); 129.7 ($CH_2\underline{C}CH$); 127.9 ($CH_3\underline{C}CH$); 59.1, 59.0 (N$\underline{C}H_2$CONH, N$\underline{C}H_2CO_2H$); 55.0 (N$\underline{C}H_2CO_2H$); 52.7, 50.4 (N$\underline{C}H_2\underline{C}H_2$N); 42.8 (N$\underline{C}H_2$Ph); 20.5 (PhC$\underline{H}_3$). CHN: Calculated

for $C_{30}H_{41}N_5O_8.2H_2O$: 56.66% C; 7.41% H; 11.01% N. Found: 56.37% C; 7.03% H; 10.78% N.

2.4.2.7 1, 11-(bis(cyclohexylamino)-1, 11-dioxo-3,6,9-triaza-3,6,9-triscarboxymethyl)undecane: DTPA-cyHA

DTPA-dianhydride (10.0 g, 0.028 mol) was added in small portions over 30 minutes to neat ice cold, stirring cyclohexylamine (16 ml, 0.14 mol). The mixture was diluted with 30 ml H_2O and stirred at ambient temperature for 20 hrs. The volume was reduced by rotary evaporation and the yellow oil diluted with H_2O (50 ml) before acidification to around pH 2 with conc. HCl. The colourless solid that quickly formed was collected by filtration and washed with water (100 ml), ethanol (2 x 50 ml) and diethyl ether (100 ml) then dried under vacuum to yield the title compound (13.6 g, 87 %). ^{1}H NMR (250 MHz D_2O/NaOD): δ (ppm) 3.68 (2H, s, $NC\underline{H}_2CO_2^-$ central); 3.56 (2H br, m, $NC\underline{H}C_5H_{10}$); 3.40 (4H, s, $NC\underline{H}_2CO_2^-$); 3.30-3.28 (4H, br, t, $NC\underline{H}_2CH_2N$); 3.25 (4H, s, $NC\underline{H}_2CONH$); 3.09-3.07 (4H, br, t, $NCH_2C\underline{H}_2N$); 1.74-1.66 (8H, br, t. cyhex$\underline{H}_2$); 1.57 (2H, br, d, cyhex$\underline{H}_2$); 1.10-1.30 (10H,br, m, cyhex$\underline{H}_2$). ^{13}C NMR (62.9 MHz): 177.7 (-$\underline{C}O_2$ terminal); 171.2 (-$\underline{C}ONH$); 170.7 (-$\underline{C}O_2$ central); 58.8, 58.5 ($NC\underline{H}_2C\underline{H}_2N$); 54.6 ($NC\underline{H}_2CO_2$ central); 52.1 ($NC\underline{H}_2CO_2$ terminal); 50.7 ($NC\underline{H}_2CONH$); 48.9 ($CONHC\underline{H}$-); 31.8, 24.9, 24.4 (cyhex -$\underline{C}H_2$-). FAB-MS [M+1] 556 D; CHN: Calculated for $C_{26}H_{45}N_5O_8$: 56.18% C; 8.17% H; 12.60% N. Found: 55.98% C; 7.59% H; 12.49% N.

2.4.2.8 1, 11-(bis(methylenecyclohexylamino)-1, 11-dioxo-3,6,9-triaza-3,6,9-triscarboxymethyl)undecane: DTPA-mcyHA

DTPA-dianhydride (12.85 g, 0.036 mol) was added in small portions over 30 minutes to neat ice cold, stirring cyclohexanemethylamine (23 ml, 0.18 mol). The viscous suspension was then diluted with water (20 ml), and allowed to warm to room temperature, at which temperature stirring was continued for 24 hours. The volume of the yellow solution was reduced by rotary evaporation and the oil diluted with 50 ml H_2O before acidification to pH~2 with conc. HCl. The colourless solid which quickly formed was collected by filtration, washed with water (500 ml), EtOH (500 ml) and diethyl ether then dried under vacuum to yield the title compound, DTPA-mcyHA (12.9 g, 62 %). FAB-MS: $[M+1]^+$ 584 D. ^{1}H NMR (360 MHz D_2O/NaOD) δ (ppm): 3.6 (2H, s, $NC\underline{H}_2CO_2$ central); 3.3 (4H, s, $NC\underline{H}_2CO_2$ terminal); 3.2 (8H, s, $NC\underline{H}_2C_6H_{11}$); 3.0-3.1 (2 x broad t, 4H each, $NC\underline{H}_2C\underline{H}_2N$); 2.9-3.0 (2H, br, $CONHCH_2C\underline{H}C_5H_{10}$); 1.6-1.7 (12H, m, cyhex); 1.4-1.5 (2H, m, cyhex); 1.1-1.3 (6H, m, cyhex); 0.7-1.0 (4H, quintet, cyhex). CHN: Calculated for $C_{28}H_{49}N_5O_8$: 57.60% C; 8.64% H; 12.00% N. Found: 57.40% C; 8.64% H; 11.30% N.

2.4.2.9 1, 11-(bis(cyclooctylamino)-1, 11-dioxo-3,6,9-triaza-3,6,9-triscarboxymethyl)undecane: DTPA-cyOA

DTPA-dianhydride (9.0 g, 0.025 mol) was added slowly to neat, ice cold stirring cyclooctylamine (13 ml, 0.095 mol). The mixture was diluted with water (30 ml) and allowed to warm to ambient temperature at which stirring was continued overnight (24 hrs). The volume of the solution was reduced by rotary evaporation then the yellow oil diluted with H_2O (50 ml) before acidification to pH ~ 2 with conc. HCl upon which a colourless solid began to form. This solid was collected by filtration, washed with H_2O (200 ml), EtOH (100 ml) and diethyl ether (100 ml) then dried under vacuum to yield the title compound, DTPA-cyOA (10.9 g, 71%). ^{1}H NMR (200 MHz, D_2O/NaOD) δ (ppm): 3.83 (2H, broad m, NHC$\underline{H}$C$_7$H$_{14}$); 3.6 (2H, broad s NC$\underline{H}_2$CO$_2^-$ central); 3.27 (4H, s, NC$\underline{H}_2$CO$_2^-$ terminal); 3.15 (4H, s, NC$\underline{H}_2$CONH); 2.93 (8H, broad m, NC$\underline{H}_2$C$\underline{H}_2$N); 1.70-1.58 (28H, m, NCHC$_7\underline{H}_{14}$). 13C NMR (62.9 MHz): 178.9 (C$\underline{O}$2$^-$), 171.8 (C$\underline{O}$NH); 58.9 (N$\underline{C}$H$_2$CO$_2^-$, N$\underline{C}$H$_2$CONH); 52.7, 52.1 (NC$\underline{H}_2$C$\underline{H}_2$N); 49.8 (NH$\underline{C}$HC$_7$H$_{14}$); 31.2, 26.6, 25.1, 23.2 (NHCH$\underline{C}_7$H$_{14}$). FAB-MS $[M+1]^+$ 612 D: CHN: Calculated for $C_{30}H_{53}N_5O_8 \bullet 2.5H_2O$ 54.59% C; 8.64% H; 10.60% N. Found: 54.58% C; 8.88% H; 10.61% N.

2.4.2.10 1, 11-(bis(2-norbornylamino)-1, 11-dioxo-3,6,9-triaza-3,6,9-triscarboxymethyl)undecane dihydrate: DTPA-NBA.2H$_2$O

DTPA-dianhydride (2.5 g, 0.007 mol) was suspended in 20 ml chloroform and stirred at room temperature. The amine, (±) 2-*exo*-aminonorbornane (2.1 ml, 0.018 mol), was added slowly to this suspension and stirring continued at room temperature for 30 minutes before heating the reaction to reflux overnight. The mixture was cooled to room temperature, forming an orange oil, which was then diluted with 25 ml of $CHCl_3$. The solvent was removed by rotary evaporation leaving a yellow powder and viscous orange liquid. This mixture was dissolved in 10 ml H_2O before acidification to pH ~ 2 with 2M HCl. No precipitate was observed and the solvent was removed by rotary evaporation. The brown oil was dissolved in methanol, the volume reduced and a white solid obtained by triturating with diethyl ether. This solid was recrystallised from water to yield the title compound, DTPA-NBA (0.94 g, 23%). ^{1}H NMR (400 MHz, D_2O) δ (ppm): 3.8 (4H, s, NC$\underline{H}_2$CO$_2^-$, terminal); 3.7 (4H, s, NC$\underline{H}_2$CONH); 3.6 (2H, s, NC$\underline{H}_2$CO$_2^-$ central); 3.5 (2H, dt, NHC$\underline{H}$C$_6$H$_{10}$); 3.35 (4H, t, NC$\underline{H}_2$CH$_2$N); 3.15 (4H, t, NCH$_2$C$\underline{H}_2$N); 2.22, 2.12 (4H, d, NHCHC$\underline{H}_2$CH); 1.7 (2H, m, Nb); 1.4 (2H, m, Nb); 1.3 (2H, m, Nb); 1.0-1.2 (6H, m, Nb) (Nb = norbornyl). LC-MS: (ES+) 580 D, (ES-) 578 D. (Retention time = 2.51-2.57mins). CHN: Calculated for

$C_{28}H_{45}N_5O_8 \bullet 2H_2O$: 56.25% C; 7.77 % H; 11.71% N. Found: 56.55% C; 8.17% H; 11.70% N.

2.4.2.11 1, 11-(bis(2-norbornylamino)-1, 11-dioxo-3,6,9-triaza-3,6,9-triscarboxymethyl)undecane: DTPA-NBA

The amine, (±) 2-*exo*-aminonorbornane, (5.0 g, 0.045 mol) was added slowly to a stirring suspension of DTPA-dianhydride (5.0g, 0.014mol) in ice cold propan-2-ol. The ice bath was removed after 30 minutes and the reaction mixture allowed to warm to room temperature before heating the mixture at reflux for 1 hr, then stirring at room temperature overnight. The solvent was removed by rotary evaporation forming an orange oil and a white solid. Addition of water (30 ml) resulted in the formation of an orange solution, which was acidified to pH ~ 3 with conc. HCl and refrigerated overnight. Addition of acetonitrile afforded a white solid, which was collected by filtration and recrystallised from water to yield the title compound, DTPA-NBA (1.3 g, 17 %). ^{1}H NMR (250 MHz, D_20/NaOD): δ (ppm) 3.7 (2H, s, $NC\underline{H}_2CO_2^-$ central); 3.5 (2H, dd, $NHC\underline{H}C_6H_{10}$); 3.3 (4H, t, $NC\underline{H}_2CH_2N$; 4H, s $NC\underline{H}_2CO_2^-$), 3.1 (4H, s, $NC\underline{H}_2CONH$); 3.0 (4H, t, $NCH_2C\underline{H}_2N$); 2.2 (2H, br, Nb); 2.1 (2H, br, dd, Nb); 1.6-1.8 (2H, ddd, Nb); 1.2-1.5 (8H, m, Nb); 1.0-1.2 (6H, m, Nb). FAB-MS: $[M+1]^+$ 580 D.

2.4.2.12 1, 11-(bis(1-adamantylamino)-1, 11-dioxo-3,6,9-triaza-3,6,9-triscarboxymethyl)undecane trihydrate: DTPA-BAA.3H_2O

A suspension of the amine, 1-adamantylamine, (2.34 g, 0.0125 mol) in pyridine was added slowly to a stirring suspension of DTPA-dianhydride (1.00 g, 0.0028 mol) in 5 ml pyridine and the mixture stirred at room temperature overnight. The yellow solution was filtered to remove any unreacted DTPA before reducing the volume of the filtrate to an oily residue by rotary evaporation. The oil was then diluted with 20 ml water forming a cloudy solution. Acidification of this solution to pH ~ 3 afforded a colourless precipitate. This solid was collected by filtration, washed with ethanol (20 ml) and diethyl ether (20 ml), then dried in air to yield the title compound, DTPA-BAA (0.55 g, 30 %). ^{1}H NMR (360 MHz, DMSO-D_6) δ (ppm) 3.4 (2H, s, $NC\underline{H}_2CO_2H$); 3.3 (4H, s, $NC\underline{H}_2CO_2H$); 3.1 (4H, s, $NC\underline{H}_2CONHAd$, Ad = 1-adamantyl), 3.0 (4H, br, s $NC\underline{H}_2CH_2N$); 2.8; (4H, br, s $NCH_2C\underline{H}_2N$); 2.55 (8H, m 15H, adamantyl $\underline{H}$). CHN: Calculated for $C_{34}H_{59}N_5O_{11}$: 57.19% C; 8.35% H; 9.81% N. Found: 57.45% C; 8.69% H; 9.25% N.

2.4.2.13 1, 11-(bis(2-biphenylamino)-1, 11-dioxo-3,6,9-triaza-3,6,9-triscarboxymethyl)undecane: DTPA-BPA

The amine, 2-aminobiphenyl, (5.10 g, 0.03 mol) was dissolved in DMF/H_2O (2:1 v/v, 30 ml) forming a red solution at 120 °C. A slurry of DTPA-dianhydride (3.57 g, 0.01 mol) in 20 ml DMF was added and the reaction heated at reflux for 21 hrs. The solution was cooled to room temperature and the solvent removed by rotary evaporation to yield a red/brown oil. Dilution of this oil with 20 ml water afforded a cloudy suspension. The solvent was removed after failed extraction attempts using first DCM then with diethyl ether. The oil was dissolved in DMF, and the solvent removed again. Acidification was attempted using 1M HCl (20 ml). This resulted in the formation of a red/brown organic phase, and a cloudy suspension in the aqueous phase. The aqueous phase was washed with 50 ml DCM and the mixture placed in a separating funnel, upon which a viscous pink solid began to form in the upper aqueous layer. The organic phase was discarded and the aqueous suspension collected then filtered before recrystallisation from methanol. Several crops of product were obtained from the crystallisation media, with overall yield of the title compound, DTPA-BPA, of 3.7 g (53 %). ^{1}H NMR (DMSO-D_6): 200 MHz δ (ppm) 9.59 (3H, br. s, $CO_2\underline{H}$); 8.20-8.24 (2H, br, s, N$\underline{H}$); 7.30-7.47, 7.13-7.27 (18H, m, aromatic $\underline{H}$); 3.17 (br, 8H, $NC\underline{H}_2CO_2H$, $NC\underline{H}_2CON$); 2.83 (2H, s $NC\underline{H}_2CO_2H$, central); 2.39 (4H, br. t, $NC\underline{H}_2CH_2N$), 2.01 (4H, broad. t, $NCH_2C\underline{H}_2N$). The ligand could be further purified by suspension in hot chloroform and filtration to remove any unreacted amine before preparation of Ln(III) complexes.

2.4.3 Solid Phase Synthesis

2.4.3.1 Step 1: Attaching the Linker (Scheme 2- 3)

The resin, ArgoGel-NH_2, (1.0 g, 0.46 mmol, R4273/55) was swollen in DMF for 15 minutes then recovered by filtration. The linker, 4-(3,5-dimethoxy-4-formylphenoxy) butyric acid, GW428586, (0.37 g, 1.38 mmol) was combined with HATU (*o*-(7-azabenzotriazol-1-yl-*N,N,N',N'*-tetramethyl uronium hexafluorophosphate) (0.525 g, 1.38 mmol) and DIPEA (*N,N*-diisopropylethylamine) (0.48 ml, 2.76 mmol) in 3 ml dry DMF, left for 15 minutes before adding to the pre-swollen resin. The mixture was shaken for 3 ½ hours at room temperature, then washed with DMF, DCM, MeOH and DCM. ^{1}H NMR (400 MHz, magic angle spinning): δ (ppm) 10.25 (1H, s, C$\underline{H}$O); 6.10 (2H, s, aryl C$\underline{H}$); 4.1 (2H, t, $C\underline{H}_2O$); 3.88 (6H, s, $OC\underline{H}_3$); 2.40 (2H, t, $NHCOC\underline{H}_2$); 2.18 (2H, t $NHCOCH_2C\underline{H}_2$).

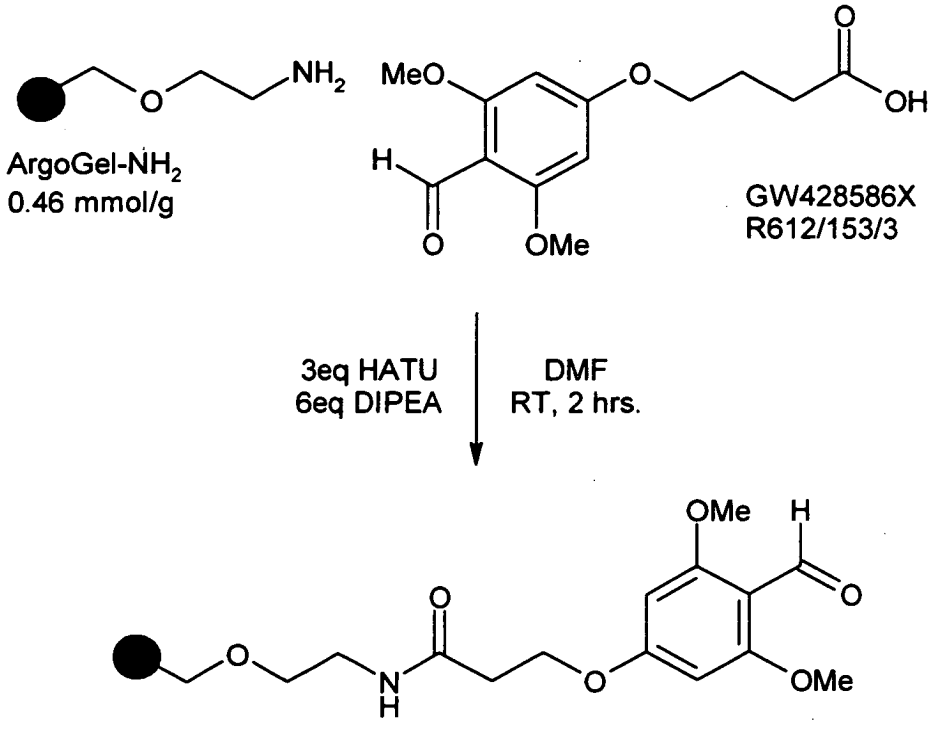

Scheme 2-3 Attaching the linker

2.4.3.2 Step 2: Reductive Amination – 1 4-methylbenzylamine (Scheme 2- 4)

Glacial acetic acid (0.13 ml, 2.3 mmol) was combined with $Me_4NBH(OAc)_3$ (0.60 g, 2.3 mmol) and 4-methylbenzylamine (0.30 ml, 2.3 mmol) in 5 ml DCM then added to the resin. This mixture was left for 1 hr to allow evolution of H_2 before shaking the reaction for 14 hrs. The resin was then washed with DCM, 1:1 DCM/MeOH and finally MeOH before drying under vacuum for 8 hours. ^{1}H NMR (magic angle spinning): δ (ppm) 7.8 (1H broad, N<u>H</u>); 7.15 (2H, d, $CH_2C_6\underline{H}_4CH_3$); 7.05 (2H, d, $CH_2C_6\underline{H}_4CH_3$); 6.0 (2H, s, aryl C<u>H</u>); 4.1 (6H, broad, -NHCO(C<u>H</u>$_2$)$_3$O-); 3.68 (6H, s, OC<u>H</u>$_3$); 2.30 (2H, t,); 2.22(3H, s); 2.00 (2H, t).

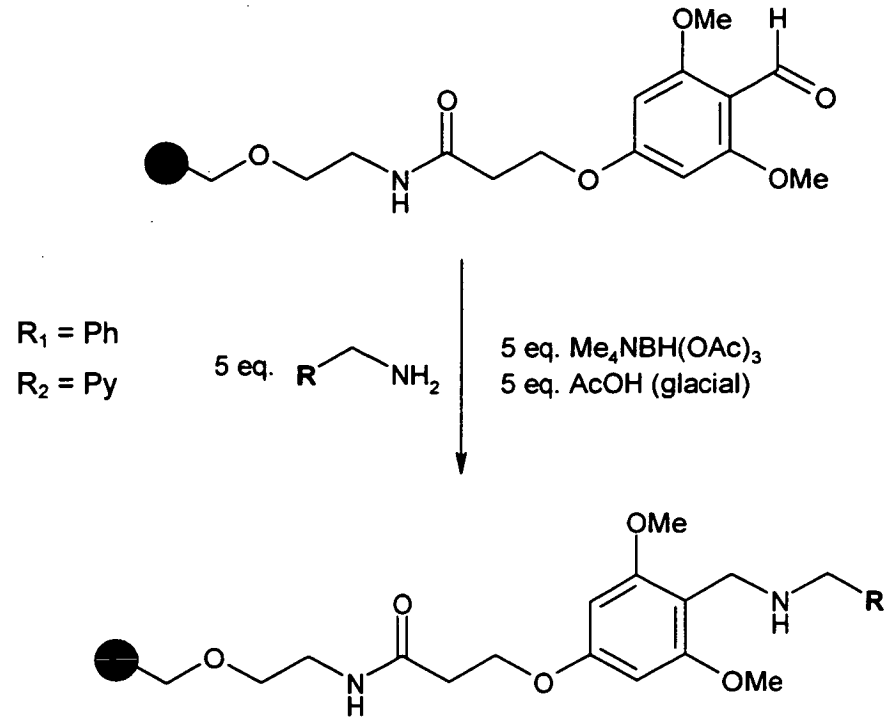

Scheme 2-4 Reductive Amination: attaching 4-methylbenzylamine (R_1) and 4-picolylamine (R_2) to the solid phase

2.4.3.3 Step 2: Reductive Amination – 2 4-picolylamine (Scheme 2-4)

Glacial acetic acid (0.13 ml, 2.3 mmol) was combined with $Me_4NBH(OAc)_3$ (0.614 g, 2.3 mmol) and 4-picolylamine (0..23 ml, 2.3 mmol) in 5ml DCM then added to the resin. This mixture was left for 1hr to allow evolution of H_2 before shaking the reaction for 16 hrs. The resin was then washed with DCM, 1:1 DCM/MeOH and finally MeOH before drying under vacuum for 1 hour. ^1H NMR (magic angle spinning): δ (ppm) 8.45 (2H, d $N(C\underline{H}CH)_2CCH_2$); 7.2 (2H, broad $N(CHC\underline{H})_2CCH_2$); 6.10 (2H, s, aryl C<u>H</u>); 4.00 (2H $NC\underline{H}_2Py$); 3.68 (6H, s, $OC\underline{H}_3$); 2.40 (2H, t); 2.05 (2H, t).

2.4.3.4 Step 3: DTPA-bis(amide) Formation – 1 DTPA-bis(4-methylamide) (DTPA-BTA)

A solution of DTPA-dianhydride (50 mg, 0.14 mmol) and DIPEA (*N,N*-diisopropylethylamine) (24 μL, 0.14 mmol) was added to the resin (100 mg, 0.046 mmol) loaded with 4-methylbenzylamine and the reaction shaken at room temperature for 18 hours.

The resin was then washed with DMF before addition of 4-methylbenzylamine (29 μL, 0.23 mmol) and a catalytic amount of DMAP in 0.5 ml DMF then shaking continued for 2 hrs. The excess reagents were removed by thoroughly washing the beads with DMF, AcOH:EtOAc (1:1 v/v), NH_3:EtOAc (1:1 v/v) and DCM. Cleavage was twice performed with 1 ml TFA.H_2O (95:5), 1 hour each. The solution and washings (DCM and MeOH) were collected and the solvent removed by rotary evaporation. The colourless oily residue was dissolved in MeOH and the solvent removed again before drying under vacuum. This residue was then dissolved in D_2O for ^1H NMR analysis: (400 MHz) δ (ppm) 7.05 (8H, 2d, $CH_2C_6\underline{H}_4CH_3$); 4.22 (4H, s, $NC\underline{H}_2PhMe$); 3.75 (4H, s, $NC\underline{H}_2CO_2^-$, terminal); 3.65 (4H, s, $NC\underline{H}_2CONH$); 3.55 (2H, s, $NC\underline{H}_2CO_2^-$, terminal); 3.15 (4H, t, $NC\underline{H}_2CH_2N$); 3.05 (4H, t, $NCH_2C\underline{H}_2N$); 2.18 (6H, s, $PhC\underline{H}_3$). LC-MS: [M] 599 D. Some DIPEA, DMF, DTPA and 4-methylbenzylamine peaks are observed in the ^1H NMR spectrum. Conventional chromatographic methods cannot be used to purify the ligand and no further characterisation was attempted from this reaction.

2.4.3.5 Step 3: Attempted DTPA-bis(amide) Formation DTPA-bis(4-picolylamide) (DTPA-PYA)

Preparation of the DTPA-bis(4-picolylamide) was attempted using the same procedure as for DTPA-BTA . The amine was successfully attached to the resin via the aldehyde linker as for DTPA-BTA (see Step 2 above) but it was unclear as to whether any product was obtained from subsequent reactions. The nature of the problem was not determined, but is likely to be due to the cleavage of the ligand from the resin and the difficulties experienced in washing the excess amine and DTPA-dianhydride reagents from the reaction.

In both reactions 2.3.3.4 and 2.3.3.5 a plastic residue and orange gum was observed in the crude product following cleavage. We attribute this to decomposition of the rubber stopper by the DCM used in the reductive amination steps. The harsh cleavage conditions may also have resulted in some decomposition of the plastic reaction vessel affording the insoluble colourless residue upon preparation of the NMR sample. An alternative reductive amination procedure was attempted using DMF in place of the DCM.

2.4.3.6 Step 2 – Modified Reductive Amination in DMF

The resin, ArgoGel-NH_2, 0.47 mmol/g loading (1.07g, 0.5 mmol) was swollen in DMF and the solvent removed by filtration. The linker, 4 (3,5-dimethoxy-4-formylphenoxy) butyric acid (0.400 g, 1.5mmol), HATU (hexafluorophosphine azotriazole urea) (0.578 g, 1.5 mmol) and DIPEA (0.523 ml, 3 mmol) were combined in 3 ml DMF and left for 30 minutes prior to

reaction with the resin. This resin mixture was shaken for 3 hours then washed with DMF (6 x 5 ml). The unreacted ArgoGel-NH_2 resin gave a positive TNBSA (trinitrobenzene sulfonic acid) spot test (red beads indicating presence of primary amine). The reacted resin and linker gave a negative TNBSA test (indicting no -NH_2). Reductive amination was carried out in DMF instead of DCM avoiding the decomposition of the rubber stopper observed previously. Five equivalents of the amine, 4-methylbenzylamine, (0.318 ml, 2.5 mmol) were added to the resin in a solution of 4 ml 1% Glacial AcOH/DMF and the reaction shaken for 1 hour. After this time the reducing agent, solid $NaBH(OAc)_3$, (0.644 g, 3 mmol) was added to the reaction, the mixture diluted with a further 2 ml DMF then shaken overnight (18 hrs). The resin was then washed with DMF, MeOH and DCM (4 x 4 ml each), MeOH (1 x 4 ml) and Et_2O (2 x 4 ml), the beads giving a positive Chloranil spot test (deep blue coloured beads) for secondary amine. This aminated resin was used in subsequent attempts to prepare asymmetric DTPA-AM_2 ligands.

2.4.3.7 Alternative Solid Support: Polystyrene Resin - Reductive Amination

The resin, PS-MB-CHO (160 mg, 0.2 mmol; 100 mg 0.13 mmol) was swollen in DMF prior to addition of 1.5 ml 1% AcOH/DMF and 4-methylbenzylamine (5eq, 0.075 ml, 0.65mmol) and the reactions shaken for 1 hour. After this time, 6 equivalents of the reducing agent, $NaBH(OAc)_3$ or $Me_4NBH(OAc)_3$ were added, the mixtures diluted with 1.5 ml DMF and shaken for 18 hours. The resins were then washed with DMF, methanol and diethyl ether. Both gave positive chloranil spot tests for secondary amines. IR analysis of the beads confirmed that conversion of aldehyde to imine followed by reduction to the secondary amine had occurred. The resins were then used without further treatment in subsequent attempts to prepare asymmetric DTPA-bis(amide) ligands.

2.5 Ln(III) Complex Preparation

2.5.1 General Ln(III)DTPA-AM_2 Preparation

Equimolar amounts of the ligand and metal were combined in aqueous (or H_2O/MeOH) solution (20-50 ml, pH 1) before addition of TBAOH (40% w/w H_2O) until pH 5-6 was reached. The volume of the colourless solution was reduced by rotary evaporation (~1 ml) and acetonitrile added forming a white precipitate. The solid was collected by filtration, washed with CH_3CN and Et_2O then dried under vacuum to yield the desired Ln(III)DTPA-bis(amide) complex as a hydrated species (Figure 2-1).

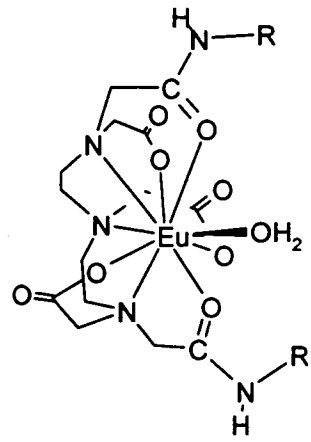

Figure 2-1 General structure of Ln(III)DTPA-AM_2 chelate complex

2.5.2 Europium (III) DTPA-bis(amide) Complexes

2.5.2.1 {1, 11-(bis(ethylamino)-1, 11-dioxo-3,6,9-triaza-3,6,9-triscarboxymethyl)undecane}europium(III) dihydrate: [EuBEA•H_2O]H_2O

The ligand, DTPA-BEA.$2H_2O$, (0.242 g, 0.500 mmol) was combined with 2 ml aqueous $EuCl_3$•$6H_2O$ (0.179 g, 0.489 mmol), the mixture diluted to 20 ml with water before sonicating and heating gently until all of the powder had dissolved (pH ~1). The colourless solution was raised to pH 5 by dropwise addition of TBAOH (40% w/w H_2O) then the volume reduced to ~0.5 ml by rotary evaporation. Addition of CH_3CN to the concentrated solution instantly afforded a colourless solid which was collected by filtration, washed with CH_3CN (50 ml) and Et_2O (50 ml) then dried under vacuum to yield the title complex, [EuBEA.H_2O] (0.288 g, 96%). ES-MS (+): $[M+1]^+$ 596/598 D, $[TBA]^+$ 242 D. The solid was dissolved in methanol (5 ml), the volume reduced and the complex re-precipitated with acetonitrile to remove the excess TBACl. CHN: Calculated for [$EuC_{18}H_{34}N_5O_{10}$]: 34.17% C; 5.43% H; 11.07% N. Found: 34.44% C; 5.26% H; 10.92% N.

2.5.2.2 Alternative preparation of [EuBEA•H_2O]H_2O

Solid DTPA-BEA.$2H_2O$ (0.835 g, 1.73 mmol) was added to a stirring suspension of Eu_2O_3 (0.302 g, 0.858 mmol) in 50 ml H_2O. The mixture was heated at reflux and stirring continued until all the solid had dissolved then filtered before reducing the volume of the colourless solution by rotary evaporation. Addition of 50 ml acetonitrile to the concentrated solution afforded a colourless solid, collected by filtration, washed with CH_3CN and Et_2O,

then dried under vacuum to yield the complex, [EuBEA•H_2O] (0.983 g, 94%). FAB-MS $[M+1]^+$ 598 D. CHN: Calculated for $EuC_{18}H_{34}N_5O_{10}$: 34.17% C; 5.43% H; 11.07% N. Found: 34.10% C; 5.38% H; 11.17% N.

2.5.2.3 {1, 11-(bis(1-butylamino)-1, 11-dioxo-3,6,9-triaza-3,6,9-triscarboxymethyl)undecane}europium(III) monohydrate: [EuBUA•H_2O]

An aqueous solution (2 ml) of $EuCl_3$•$6H_2O$ (0.197 g, 0.54 mmol) was combined with DTPA-BUA.$2H_2O$ (0.292 g, 0.54 mmol) and the mixture diluted to 20 ml, then sonificated and heated until all the ligand had dissolved (pH ~ 1). Addition of TBAOH (40% w/w H_2O) raised the colourless solution to pH ~ 5 before reducing the volume of the solution to 1 ml by rotary evaporation. Acetonitrile (50 ml) was added to the concentrated aqueous solution instantly affording a colourless precipitate, which was collected by filtration, washed with CH_3CN and Et_2O then dried under vacuum to yield the title compound as a monohydrate, [EuBUA•H_2O] (0.313 g, 87 %). LC-MS (ES+) $[M^+]$ 652/654; CHN: Calculated for $[EuC_{22}H_{40}N_5O_9]$: 39.39% C; 6.02% H; 10.44% N. Found: 39.14% C; 6.20% H; 9.53% N.

2.5.2.4 Alternative preparation of [EuBUA•H_2O]

The ligand, DTPA-BUA.$2H_2O$, (1.897 g, 3.48 mmol) was added to a stirring suspension of Eu_2O_3 (0.609 g, 1.73 mmol) in 20 ml water. The mixture was diluted to 50 ml with water and stirring continued at reflux for 17 hours. The volume of the colourless solution was reduced by rotary evaporation before addition of acetonitrile, instantly affording a colourless precipitate. This solid was collected by filtration, washed with CH_3CN and Et_2O then dried under vacuum to yield the complex, [EuBUA•H_2O]0.5H_2O (2.203 g, 95%). FAB-MS: $[M+1]^+$ 652 D. CHN: Calculated for $EuC_{22}H_{41}N_5O_{9.5}$: 38.87% C; 6.09% H; 10.38% N. Found: 38.89% C; 6.23% H; 10.38% N.

2.5.2.5 {1, 11-(bis(benzylamino)-1, 11-dioxo-3,6,9-triaza-3,6,9-triscarboxymethyl)undecane}europium(III) tetrahydrate: [EuBBZA•H_2O]3H_2O

An aqueous solution (2 ml) of $EuCl_3$•$6H_2O$ (0.245 g, 0.67 mmol) was combined with DTPA-BBZA.$2H_2O$ (0.408 g, 0.67 mmol) and the mixture diluted to 20 ml, sonificated and heated until all the ligand had dissolved (pH ~ 1). The colourless solution was raised to pH 5 by dropwise addition of TBAOH (40% w/w H_2O) before the volume was reduced to ~1 ml by rotary evaporation. Addition of acetonitrile (50 ml) instantly afforded a colourless

precipitate, collected by filtration, washed with CH_3CN (20 ml) and Et_2O (20 ml) then dried under vacuum to yield the title compound as a tetrahydrate, [EuBBZA•H_2O]3H_2O (0.436 g, 90%). LC-MS (ES+) [M^+] 719/721. CHN: Calculated for [$EuC_{28}H_{41}N_5O_{12}$]: 42.42% C; 5.34% H; 8.84% N. Found: 42.70 % C; 5.23% H; 8.64% N.

2.5.2.6 {1, 11-(bis(4-methylbenzylamino)-1, 11-dioxo-3,6,9-triaza-3,6,9-triscarboxymethyl)undecane}europium(III) trihydrate: [EuBTA•H_2O]2H_2O

An aqueous solution (2 ml) of $EuCl_3$•6H_2O (0.368 g, 1.0 mmol) was combined with DTPA-BTA.2H_2O (0.639 g, 1.0 mmol). The mixture was sonificated and heated gently until all the ligand had dissolved forming a colourless solution (pH ~ 1). Dropwise addition of TBAOH (40% w/w H_2O) raised the pH of the solution to 5. The volume was reduced to 1 ml by rotary evaporation. Addition of acetonitrile to the concentrated solution instantly afforded a colourless precipitate which was collected by filtration, washed with CH_3CN, Et_2O then dried under vacuum to yield the title compound, [EuBTA•H_2O]2H_2O (0.69g, 87%).

2.5.2.7 {1, 11-(bis(cyclohexylamino)-1, 11-dioxo-3,6,9-triaza-3,6,9-triscarboxymethyl)undecane}europium(III) trihydrate: [EucyHA•H_2O]2H_2O

Aqueous $EuCl_3$•6H_2O (0.194 g, 0.53 mmol) was combined with DTPA-cyHA (0.296 g, 0.53 mmol). The mixture was then diluted to 50 ml, sonificated and heated until all the ligand had dissolved (pH ~ 1). The colourless solution was raised to pH 5 by dropwise addition of TBAOH (40% w/w H_2O). The volume was then reduced to ~ 1 ml by rotary evaporation. Addition of acetonitrile instantly afforded a colourless precipitate, which was collected by filtration, washed with CH_3CN (20 ml) and Et_2O (20 ml) then dried under vacuum to yield the title compound as the trihydrate, [EucyHA•H_2O]2H_2O (0.381 g, 83%). LC-MS (ES+): [M^+] 704; 2.33 mins. CHN: Calculated for [Eu(III)$C_{26}H_{48}N_5O_{11}$]: 41.15% C; 6.39% H; 9.23% N. Found: 40.45% C; 6.16% H; 9.17% N.

2.5.2.8 Alternative preparation of [EucyHA•H_2O]1.5H_2O

The ligand, DTPA-cyHA (0.513 g, 0.922 mmol) was dissolved in 50 ml water in the presence of TBAOH and refluxed for 30 minutes (pH ~ 4). Solid Eu_2O_3 (0.158 g, 0.449 mmol) was added to the hot ligand solution forming a suspension (pH ~ 10). The pH was lowered with HCl (1M aq) and heating continued until the solid had dissolved (pH ~ 1). This solution was filtered and TBAOH added until pH ~ 4 was reached and the volume

reduced by rotary evaporation. Addition of acetonitrile to the concentrated solution afforded a colourless precipitate that was collected by filtration, washed with CH_3CN and Et_2O then dried under vacuum to yield the complex [EucyHA•H_2O]. FAB-MS $[M+1]^+$ 704/706. CHN: Calculated for $EuC_{26}H_{49}N_5O_{11.5}$: 40.66% C; 6.44% H; 9.12% N. Found: 40.72% C; 6.36% H; 8.99% N.

2.5.2.9 {1, 11-(bis(methylenecyclohexylamino)-1, 11-dioxo-3,6,9-triaza-3,6,9-triscarboxymethyl)undecane}europium(III) hydrate: [EumcyHA•H_2O]

Solid DTPA-mcyHA (0.326 g, 0.558 mmol) was added to an aqueous solution (2 ml) of $EuCl_3$•$6H_2O$ (0.203 g, 0.554 mmol). The mixture was diluted to 20 ml with water then heated and sonificated until all the ligand had dissolved (pH~1). TBAOH (40% w/w H_2O) was added dropwise raising the colourless solution to pH 5 before reducing the volume by rotary evaporation. Addition of CH_3CN (20 ml) instantly afforded a colourless precipitate. This was collected by filtration, washed with CH_3CN (50 ml) and Et_2O (50 ml) then dried under vacuum to yield the title compound, [EumcyHA•H_2O]$2H_2O$ (0.339 g, 82 %). LC-MS (ES+): $[M^+]$ 731/733 D (2.57 mins).

2.5.2.10 {1, 11-(bis(2-biphenylamino)-1, 11-dioxo-3,6,9-triaza-3,6,9-triscarboxymethyl)undecane}europium(III) trihydrate: [EuBPA•H_2O]$2H_2O$

The metal salt, $EuCl_3$•$6H_2O$, (0.193 g, 0.527 mmol) was dissolved in 1ml H_2O, combined with the ligand, DTPA-BPA, (0.371 g, 0.527 mmol) and the mixture diluted to 50 ml with H_2O/MeOH forming a pale yellow solution (pH ~1). Aqueous TBAOH (40% w/w) was added dropwise until the pH 5 was reached, then the volume reduced by rotary evaporation. The viscous yellow residue was diluted with 1 ml methanol and the complex precipitated upon addition of acetonitrile (20 ml) to this solution. The solid was collected by filtration, washed with CH_3CN (50 ml) and Et_2O (20 ml) then dried under vacuum to yield the title compound, [EuBPA•H_2O]$2H_2O$ (0.294 g, 65%). LCMS (ES+): $[M^+]$ 844, (2.66mins). CHN: Calculated for Eu(III)$C_{38}H_{38}N_5O_8.3H_2O$: 50.77% C; 4.94 % H; 7.79 % N. Found: 49.67% C; 4.90% H; 7.71% N

2.5.2.11 {1, 11-(bis(cyclooctylamino)-1, 11-dioxo-3,6,9-triaza-3,6,9-triscarboxymethyl)undecane}europium(III) trihydrate: [EucyOA•H_2O]2H_2O

The ligand and the metal were combined in 1:1 stoichiometry ($EuCl_3$•$6H_20$, 0.176 g, 0.480 mmol; DTPA-cyOA, 0.318 g, 0.482 mmol) in 20 ml water and sonificated and heated until all the ligand had dissolved (pH ~ 1). Aqueous TBAOH was added dropwise until pH 5 was reached then the volume reduced to an oil by rotary evaporation. This concentrated solution was diluted with water (10 ml) and filtered to remove insoluble impurities before removal of the solvent, this time forming an off white solid. This solid was dissolved in methanol (5 ml) and the complex then precipitated as a colourless solid upon addition of acetonitrile (50 ml), collected by filtration, washed with CH_3CN (50 ml) and Et_2O (20 ml) then dried under vacuum to yield the title compound [EucyOA•H_2O]2H_2O. CHN Calculated for Eu(III) $C_{50}H_{50}N_5O_8.3H_2O$: 44.22% C; 6.74% H; 8.60 % N. Found: 44.27% C; 6.74 % H; 8.58% N.

2.5.2.12 {1, 11-(bis(±)2-aminonorbornylamino)-1, 11-dioxo-3,6,9-triaza-3,6,9-triscarboxymethyl)undecane}europium(III) trihydrate: [EuNBA•H_2O]

An aqueous solution (2 ml) of $EuCl_3$•$6H_2O$ (0.160 g, 0.437 mmol) was combined with the ligand, DTPA-NBA.2H_2O (0.254 g, 0.438 mmol), the mixture diluted to 20 ml with MeOH/H_2O (1:10 v/v) and heated/sonificated until all of the solid had dissolved (pH ~ 1). Aqueous TBAOH (40% w/w H_2O) was added dropwise until the colourless solution reached pH ~ 6, then the volume was reduced by rotary evaporation. The complex was precipitated from this concentrated solution upon addition of CH_3CN (50 ml), collected by filtration and washed with CH_3CN (20 ml) and Et_2O (20 ml) and dried under vacuum to yield the title compound, [EuNBA•H_2O] 0.236 g, 72 %). LC-MS (ES+): [M^+] 727/729 (2.38 mins). CHN: Calculated for $EuC_{26}H_{50}N_5O_{12}$: 41.99% C; 6.30% H; 8.74% N. Found: 41.99% C; 6.18% H; 8.65% N.

2.5.2.13 {1, 11-(bis(1-decylamino)-1, 11-dioxo-3,6,9-triaza-3,6,9-triscarboxymethyl)undecane}europium(III) hydrate: [EuBDA•H_2O]

The metal salt, $EuCl_3$•$6H_2O$, (0.081 g, 0.22 mmol) was dissolved in 2 ml H_2O and combined with the solid ligand (0.148 g, 0.22 mmol) then the mixture diluted to 20 ml with water. A small amount of methanol was added to aid dissolution of the ligand. The colourless solution (pH ~ 1) that formed following heating/sonification was treated with TBAOH (40% w/w H_2O) until pH ~ 5 was reached. The volume was reduced by rotary evaporation and the complex precipitated from the concentrated solution upon addition of acetonitrile (50 ml).

The colourless solid was collected by filtration, washed with CH_3CN (20 ml) and Et_2O (20 ml) and dried under vacuum to yield the title compound [EuBDA•H_2O] (0.167 g, 90%).

2.5.2.14 {1, 11-(bis(1-adamantylamino)-1, 11-dioxo-3,6,9-triaza-3,6,9-triscarboxymethyl)undecane}europium(III) hydrate: [EuBAA•H_2O]

An aqueous solution of the metal salt, $EuCl_3$•$6H_2O$ (0.159 g, 0.434 mmol) was combined with the solid ligand, DTPA-BAA.$3H_2O$ (0.286 g, 0.434 mmol), the mixture diluted with water/methanol (50 ml) and sonificated/heated until all the ligand had dissolved. Any insoluble impurities were removed by filtration and the colourless solution (pH ~ 1) was treated with aqueous TBAOH until pH ~ 5 was reached. The solvent was removed by rotary evaporation forming a milky white suspension. This solid dissolved upon addition of acetonitrile and the solvent was again removed by rotary evaporation. The colourless solid that formed was collected by filtration and washed with CH_3CN (20 ml) and Et_2O (20 ml) then dried under vacuum to yield the title compound, [EuDTPA-BAA•H_2O] (0.292 g, 82%). ES-MS (+) $[M+1]^+$ 808/810 D; $[M+Na]^+$ 830/832 D.

2.5.3 Terbium (III) DTPA-bis(amide) Complexes

2.5.3.1 {1, 11-(bis(ethylamino)-1, 11-dioxo-3,6,9-triaza-3,6,9-triscarboxymethyl)undecane}terbium(III) trihydrate: [TbBEA•H_2O]$2H_2O$

The metal salt, $TbCl_3$•$6H_2O$, (0.219 g, 0.587 mmol) was dissolved in 2 ml H_2O and combined with 1 molar equivalent of the ligand, DTPA-BEA.$2H_2O$, (0.285 g, 0.589 mol). The mixture was diluted to 10 ml with water, sonificated and heated until all of the ligand had dissolved (pH ~ 1). The base, TBAOH (40% w/w H_2O), was added dropwise until the colourless solution reached pH ~ 5. The volume was then reduced to about 1 ml before precipitation of the complex as a colourless solid upon addition of acetonitrile (20 ml). The solid was collected by filtration, washed with CH_3CN (20 ml) and diethyl ether (20 ml) and dried under vacuum to yield the title compound, [TbBEA•H_2O]$2H_2O$ (0.354 g, 100%). ES-MS (+): $[M^+]$ 604 D. CHN: Calculated for $TbC_{18}H_{36}N_5O_{11}$: 32.88 % C; 5.52 % H; 10.65 % N. Found: 32.28% C; 5.59% H; 10.14% N.

2.5.3.2 {1, 11-(bis(1-butlylamino)-1, 11-dioxo-3,6,9-triaza-3,6,9-triscarboxymethyl)undecane}terbium(III) trihydrate: [TbBUA•H_2O]2H_2O

Solid ligand, DTPA-BUA.2H_2O, (0.321 g, 0.595 mmol) was added to an aqueous solution (2 ml) of the metal salt, $TbCl_3$•6H_2O, (0.222 g, 0.595 mmol), the mixture diluted with water to 20 ml, then sonificated and heated until a colourless solution was formed. Aqueous TBAOH (40% w/w H_2O) was added dropwise until the solution reached pH ~ 6, after which the volume was reduced by rotary evaporation to ~1ml. Addition of CH_3CN (50 ml) afforded a colourless solid, collected by filtration, washed (CH_3CN and Et_2O, 20 ml each) then dried under vacuum to yield the title complex, [TbBUA•H_2O]2H_2O, (0.284 g, 70%). LC-MS: [M^+] 659 D (2.07mins). CHN: Calculated for $TbC_{22}H_{44}N_5O_{11}$: 37.02% C; 6.2% H; 9.81% N. Found: 36.90% C; 6.31% H; 9.51% N.

2.5.3.3 {1, 11-(bis(benzylamino)-1, 11-dioxo-3,6,9-triaza-3,6,9-triscarboxymethyl)undecane}terbium(III) pentahydrate: [TbBBZA•H_2O]4H_20

Equimolar amounts of the ligand, DTPA-BBZA.2H_2O, (0.368 g, 0.605 mmol) and metal salt, $TbCl_3$•6H_2O, (0.266 g, 0.605 mmol) were combined in water/methanol solution (1:10 v/v, 10 ml) and the mixture heated/sonificated until all the ligand had dissolved (pH ~ 1). Aqueous TBAOH (40% w/w H_2O) was added dropwise until the colourless solution reached pH ~ 5, the volume reduced by rotary evaporation and the complex precipitated from the concentrated solution upon addition of acetonitrile (20 ml). The colourless solid was collected by filtration, washed with CH_3CN (20 ml) and Et_2O (20 ml) and dried under vacuum to yield the title complex, [TbBBZA•H_2O]4H_2O (0.348 g, 77%). LC-MS: [M^+] 727 D (2.22mins). CHN: Calculated for $TbC_{28}H_{47}N_5O_{18}$: 40.97% C; 5.78% H; 8.53% N. Found: 41.21% C; 5.24% H; 8.24 % N.

2.5.3.4 {1, 11-(bis(4-methylbenzylamino)-1, 11-dioxo-3,6,9-triaza-3,6,9-triscarboxymethyl)undecane}terbium(III) tetrahydrate: [TbBTA•H_2O]3H_2O

The ligand, DTPA-BTA.2H_2O, (0.350 g, 0.551 mmol) was added to aqueous $TbCl_3$•6H_2O (0.208 g, 0. 551 mmol), the mixture diluted with water to 20 ml, sonificated and heated until all the solid had dissolved. The colourless solution was raised to pH ~ 5 by dropwise addition of aqueous TBAOH (40% w/w H_2O). The volume was reduced by rotary evaporation before precipitation of the complex as a colourless solid with acetonitrile (50

ml). The complex was collected by filtration, washed with CH_3CN and Et_2O (20 ml each) and dried under vacuum to yield [TbBTA•H_2O]4H_2O. CHN: Calculated for $TbC_{30}H_{49}N_5O_{12}$: 43.37% C; 5.95% H; 8.43% N. Found: 43.67% C; 5.47% H; 8.23% N.

2.5.3.5 {1, 11-(bis(cyclohexylamino)-1, 11-dioxo-3,6,9-triaza-3,6,9-triscarboxymethyl)undecane}terbium(III) hydrate: [TbcyHA•H_2O]

An aqueous solution (2 ml) of $TbCl_3$•6H_2O (0.203 g, 0.560 mmol) was combined with DTPA-cyHA (0.315 g, 0.567 mmol), the mixture diluted to 50 ml with methanol/water (1:5 v/v) then sonificated and heated until all the ligand had dissolved. TBAOH (40% w/w H_2O) was added dropwise until the colourless solution reached pH ~ 5. The solvent was removed by rotary evaporation and the pale yellow residue diluted with 1ml methanol, prior to precipitation of the complex upon addition of CH_3CN (50 ml). The solid was collected by filtration, washed with CH_3CN and Et_2O then dried under vacuum to yield the title complex, [TbcyHA•H_2O] (0.327 g, 80%). LCMS: [M^+] 711 D (2.30 min).

2.5.3.6 {1, 11-(bis(methylenecyclohexylamino)-1, 11-dioxo-3,6,9-triaza-3,6,9-triscarboxymethyl)undecane}terbium(III) trihydrate: [TbmcyHA•H_2O]2H_2O

The ligand, DTPA-mcyHA (0.196 g, 0.525 mmol) was added to an aqueous solution (2 ml) of $TbCl_3$•6H_2O (0.306 g, 0.525 mmol), the mixture diluted to 20 ml with MeOH/H_2O (1:10 v/v) and sonificated/heated until all the ligand had dissolved. The colourless solution was treated with TBAOH (40% wt/w H_2O) until pH ~ 5 was reached, then the volume reduced by rotary evaporation to ~1ml. Addition of acetonitrile (50 ml) to the concentrated solution afforded a colourless precipitate, which was collected by filtration, washed with CH_3CN (20 ml) and Et_2O (20 ml) and dried under vacuum to yield the title compound, [TbmcyHA•H_2O]2H_2O (0.329 g, 83%). LC-MS: [M^+] 739 D (2.56mins). CHN: Calculated for $TbC_{28}H_{52}N_5O_{11}$: 42.03% C; 6.56% H; 8.75 % N. Found: 42.27% C; 6.78% H; 8.66 % N.

2.5.3.7 {1, 11-(bis((±)2-norbornylamino)-1, 11-dioxo-3,6,9-triaza-3,6,9-triscarboxymethyl)undecane}terbium(III) trihydrate: [TbNBA•H_2O]2H_2O

Aqueous $TbCl_3$•6H_2O (0.142 g, 0.380 mmol) was combined with solid DTPA-NBA.2H_2O (0.222 g, 0.383 mmol), the mixture diluted with methanol/water to 20 ml then heated/sonificated until all the ligand had dissolved. Addition of TBAOH changed the solution from pH ~ 1 to pH ~ 6 before the volume was reduced by rotary evaporation.

Acetonitrile (50 ml) was added to the concentrated solution and the precipitate that was formed collected by filtration, washed with CH_3CN and Et_2O then dried under vacuum to yield the title compound, [TbNBA•H_2O] (0.245 g, 86%). LCMS: [M^+] 735 D (2.38mins). CHN: Calculated for $TbC_{28}H_{51}N_5O_{11}$: 42.09% C; 6.44% H; 8.76%n. Found: 42.31% C; 6.25% H; 8.53% N.

2.5.4 Lanthanum (III) DTPA-bis(amide) Complexes

2.5.4.1 {1, 11-(bis(ethylamino)-1, 11-dioxo-3,6,9-triaza-3,6,9-triscarboxymethyl)undecane}lanthanum(III) dihydrate: [LaBEA•H_2O]H_2O

The ligand, DTPA-BEA.2H_2O, (0.350 g, 0.72 mmol) was added to an aqueous solution of $LaCl_3$•6H_2O (0.72 M, 1 ml, 0.72 mmol) and the mixture diluted to 5 ml with water (pH ~ 1). Aqueous TBAOH (40% w/w H_2O) was added carefully until the colourless solution reached pH ~ 5, then the volume reduced by rotary evaporation. Addition of acetonitrile (20 ml) to the concentrated solution instantly afforded a colourless precipitate, which was collected by filtration, washed with CH_3CN (20 ml) and Et_2O (20 ml) then dried under vacuum. Analysis (NMR and LCMS) revealed the presence of excess TBA^+. The solid was dissolved in methanol, the solution concentrated and the precipitate that formed upon addition of acetonitrile was collected by filtration, washed (CH_3CN and Et_2O) and dried under vacuum to yield the pure complex, [LaBEA•H_2O] (0.231 g, 54%). ES-MS (+): [M+1]$^+$ 584 D. ^{1}H NMR (400 MHz, D_2O, pD ~ 6): δ (ppm) 1.0(6H, t $CH_2C\underline{H}_3$); 2.3-3.0 (4H, 2H, 2H, 3m, $NC\underline{H}_2C\underline{H}_2NC\underline{H}_2C\underline{H}_2N$); 3.1-3.9 (14H, m, $NC\underline{H}_2CONC\underline{H}_2CH_3$, $NC\underline{H}_2CO_2$). ^{13}C NMR (100 MHz, D_2O): 181.0-180.6 180.2 (5 x $\underline{C}O_2^-$); 175.0-174.4 (2 x $\underline{C}$=O); 61.6, 60.8 ($N\underline{C}H_2CONHEt$, $N\underline{C}H_2CO_2$) 58.5, 57.5, 57.0, 55-56 ($N\underline{C}H_2\underline{C}H_2N\underline{C}H_2\underline{C}H_2N$), 35.5 ($N\underline{C}H_2CH_3$), 13.7 ($NCH_2\underline{C}H_3$). CHN: Calculated for $LaC_{18}H_{22}N_5O_{10}$: 35.94% C; 5.37% H; 11.65% N. Found: 36.07% C; 5.25% H; 11.40% N.

2.5.4.2 {1, 11-(bis(1-butylamino)-1, 11-dioxo-3,6,9-triaza-3,6,9-triscarboxymethyl)undecane}terbium(III) hydrate: [LaBUA•H_2O]

Aqueous $LaCl_3$•6H_2O, 0.72 M, (0.431 ml, 0.311 mmol) was added to the ligand, DTPA-BUA.2H_2O, (0.168 g, 0.311 mmol) and the mixture diluted with 20 ml water before heating and sonification until all remaining solid had dissolved (pH ~ 1). TBAOH (40% w/w H_2O) was added dropwise until pH ~ 5 was reached. The volume of the colourless solution was

reduced by rotary evaporation before precipitation of the complex from the concentrated solution upon addition of acetonitrile (20 ml). The colourless solid was collected by filtration, washed with CH_3CN (20 ml) and Et_2O (20 ml) then dried under vacuum to yield the title compound, [LaBUA•H_2O] (0.204 g, 87%). ^1H NMR (400MHz, D_2O, pD 6): δ (ppm) 32.90-3.20 (14H, m, $NC\underline{H}_2CONHC\underline{H}_2C_3H_7$, $NC\underline{H}_2CO_2H$ (central and terminal)); 3.10-2.95 (4H, broad m, $NC\underline{H}_2C\underline{H}_2N$); 2.85-2.70 (2H, broad, m, $NC\underline{H}_2C\underline{H}_2N$); 2.70-2.50 (1H, broad, m $NCH_2C\underline{H}_2N$); 2.50-2.40 (1H, br, m, $NC\underline{H}_2CH_2N$); 1.55 (4H, quintet, $NHCH_2C\underline{H}_2CH_2CH_3$); 1.35 (4H, sextet, $NHCH_2CH_2C\underline{H}_2CH_3$); 0.95 (6H, t, $NHCH_2CH_2CH_2C\underline{H}_3$). ^{13}C NMR (100 MHz) δ (ppm) 180.1 (5 $\underline{C}O_2^-$); 175 (2 $\underline{C}$=O); 63.1, 62.5, 61.5, 60.9 ($N\underline{C}H_2CO$); 58.5, 58.0, 57.5, 56.1 ($N\underline{C}H_2\underline{C}H_2N$); 40.1, 39.9 ($N\underline{C}H_2CH_2CH_2CH_3$); 30.6, 30.5 ($NCH_2\underline{C}H_2CH_2CH_3$); 19.8, 19.7, 19.5 ($NCH_2CH_2\underline{C}H_2CH_3$); 13.3, 13.2 ($NCH_2CH_2CH_2\underline{C}H_3$).

2.5.4.3 {1, 11-(bis(1-benzylamino)-1, 11-dioxo-3,6,9-triaza-3,6,9-triscarboxymethyl)undecane}lanthanum(III) hydrate: [LaBBZA•H_2O]

An aqueous solution of $LaCl_3$•$6H_2O$ (0.72 M, 0.457 ml, 0.329 mol) was added to DTPA-BBZA.$2H_2O$ (0.200 g, 0.329 mmol) and the mixture diluted with 20 ml H_2O then headed/sonificated until all the ligand had dissolved (pH ~ 1). TBAOH (40% w/w H_2O) was added dropwise to the colourless solution until pH ~ 5 was reached, prior to reducing the volume to ~ 1 ml by rotary evaporation. Addition of CH_3CN (50 ml) instantly afforded a colourless precipitate, which was collected by filtration, washed with CH_3CN (20 ml) and Et_2O (20 ml) then dried under vacuum to yield the title compound, [LaBBZA•H_2O] (0.189 g, 79%). ^1H NMR (400 MHz, D_2O, pD ~ 6): δ (ppm) 7.20 (10H, m, benzyl $\underline{H}$); 4.34-4.12, 4.0-4.1 (4H, m, $NC\underline{H}_2Ph$); 3.55-3.05 (8H, m, $NC\underline{H}_2CO_2$, terminal, $NC\underline{H}_2CONH$); 2.95-1.09 (10H, m, $NC\underline{H}_2CO_2$, $NC\underline{H}_2C\underline{H}_2NC\underline{H}_2C\underline{H}_2N$). ^{13}C NMR (100 MHz): δ (ppm) 181-180 (4 x $\underline{C}O_2^-$); 175-177 (3 x $\underline{C}ONH$); 138 (Aromatic $\underline{C}$); 129.5, 129.3, 128.2, 128.0, 127.5, 127.1 ($\underline{C}H$); 63.1, 61.2, 61.0 ($N\underline{C}H_2CO$); 57.3, 56.3, 55.8 ($N\underline{C}H_2\underline{C}H_2N\underline{C}H_2\underline{C}H_2N$); 43.8, 43.7, 43.4 ($N\underline{C}H_2Ph$).

2.5.4.4 Attempted synthesis of {1, 11-(bis(cyclohexylamino)-1, 11-dioxo-3,6,9-triaza-3,6,9-triscarboxymethyl)undecane} lanthanum(III) hydrate: [LacyHA•H_2O]

To 1.0 ml of aqueous $LaCl_3$•$6H_2O$ (0.72 M 0.76 mmol) was added the solid ligand, DTPA-cyHA (0.421 g, 0.76 mmol). The suspension was diluted to 30 ml with water, heated and

sonificated until most of the solid had dissolved then left to stand for 72 hrs after which time a colourless solid had formed. The reaction was then heated at reflux in the presence of TBAOH (pH ~ 6). Not all of the solid dissolved and the remaining amount was collected by filtration (0.4g) and found to be soluble in concentrated acid, but not in neutral or basic solution or DMSO indicating that the solid was indeed a La(III) complex and not recovered free ligand (soluble in base and DMSO). No analysis was performed on this compound due to the insoluble nature of the species.

2.5.5 Yttrium (III) DTPA-bis(amide) complexes:

2.5.5.1 {1, 11-(bis(ethylamino)-1, 11-dioxo-3,6,9-triaza-3,6,9-triscarboxymethyl)undecane} yttrium (III) hydrate: [YBEA•H_2O]

Anhydrous YCl_3, (0.077 g, 0.39 mmol) was dissolved in 20 ml H_2O and combined with DTPA-BEA.$2H_2O$ (0.191 g, 0.39 mmol). The suspension was heated/sonificated until all the ligand had dissolved (pH ~ 1) and TBAOH (40% w/w H_2O) added dropwise until the colourless solution reached pH ~ 5. The volume was reduced by rotary evaporation and addition of acetonitrile to the oily residue afforded a colourless solid that was collected by filtration, washed with CH_3CN (20 ml) and Et_2O (20 ml) and dried under vacuum to yield the title compound, [YBEA•H_2O] (0.181 g, 84%). ^{1}H NMR (400 MHz, D_2O): δ (ppm) 3.85-3.05 (14H, m, $NC\underline{H}_2CO_2^-$, $NC\underline{H}_2CONH$, $NC\underline{H}_2CH_3$); 3.0-2.80 (4H, broad, $NC\underline{H}_2C\underline{H}_2N$); 2.72-2.60 (2H, broad, $NC\underline{H}_2C\underline{H}_2N$); 2.50-2.38 (2H, broad, $NC\underline{H}_2C\underline{H}_2N$) 1.02 (6H, broad, $NCH_2C\underline{H}_3$).

2.5.5.2 {1, 11-(bis(ethylamino)-1, 11-dioxo-3,6,9-triaza-3,6,9-triscarboxymethyl)undecane} yttrium (III) hydrate [YBEA•H_2O]

The hydrated metal salt, YCl_3•$6H_2O$, (0.355 g, 1.17 mmol) was dissolved in 2ml water, solid DTPA-BEA.$2H_2O$ (0.570 g, 1.18 mmol) added and the mixture sonificated until all the ligand had dissolved (pH ~ 1). The colourless solution was treated with TBAOH (0.5 M aq) until pH ~ 5 was reached then the volume reduced to ~ 1ml by rotary evaporation. The colourless solid which formed upon addition of acetonitrile to the concentrated solution was collected by filtration, washed with CH_3CN (50 ml) and Et_2O (50 ml) then dried under vacuum to yield the title compound, [YBEA•H_2O]•$2.5H_2O$ (0.590 g, 91.5%). FAB-MS: $[M+1]^+$ 534 D. CHN: Calculated for $YC_{18}H_{37}N_5O_{11.5}$: 36.24% C; 6.26% H; 11.74% N. Found: 36.42% C; 6.16% H; 11.35% N. ^{1}H NMR (360 MHz, D_2O): δ (ppm) 3.86-3.13 (14H, m, $NC\underline{H}_2CO_2^-$, $NC\underline{H}_2CONHC\underline{H}_2CH_3$); 2.92 (4H, broad s, $NCH_2C\underline{H}_2N$) 2.73, 2.71 (2H, broad d $NC\underline{H}_2CH_2N$); 2.49 (2H, broad s) ($NC\underline{H}_2C\underline{H}_2N$); 1.06-1.11 (6H, t, $NCH_2C\underline{H}_3$). ^{13}C

NMR (100 MHz): 181.4, 181.1, 180.8, 180.2, 180.0 ($\underline{C}O_2^-$); 175.9, 175.8, 174.7 ($\underline{C}ONH$); 66.6, 63.4, 61.4 ($N\underline{C}H_2CO$); 58.7, 58.6, 56.5, 56.3 ($N\underline{C}H_2\underline{C}H_2N\underline{C}H_2\underline{C}H_2N$); 35.8, 35.4 ($N\underline{C}H_2CH_3$); 13.7, 13.6 ($NCH_2\underline{C}H_3$).

2.5.5.3 {1, 11-(bis(1-butylamino)-1, 11-dioxo-3,6,9-triaza-3,6,9-triscarboxymethyl)undecane} yttrium (III) monohydrate: [YBUA•H_2O]

The ligand, DTPA-BUA.$2H_2O$ (0.430 g, 0.78 mmol) was added to an aqueous solution of the metal salt, YCl_3•$6H_2O$, (0.235 g, 0.77 mmol) and the mixture heated/sonificated until all the solid had dissolved. Aqueous TBAOH (0.5 M) was added carefully until the colourless solution reached pH 5-6, then the volume reduced by rotary evaporation. Addition of acetonitrile to the concentrated solution instantly afforded a colourless precipitate. This was collected by filtration, washed with CH_3CN (20 ml) and Et_2O and dried under vacuum to yield the title complex, [YBUA•H_2O] (0.345 g, 74%). FAB-MS $[M+1]^+$ 590 D, $[TBA]^+$ 242 D. Recrystallisation was attempted from H_2O/CH_3CN but was unsuccessful. The solvent was removed by rotary evaporation and the complex precipitated from the oily residue upon addition of acetone. FAB-MS $[M+1]^+$ 590 D. ^1H NMR (250MHz, D_2O, pD ~ 6): δ (ppm) 3.52-3.14 (14H, m, $NC\underline{H}_2CO_2^-$, $NC\underline{H}_2CONHC\underline{H}_2CH_2CH_2CH_3$); 2.91 (4H, broad, s, $NC\underline{H}_2C\underline{H}_2N$); 2.73, 2.70 (2H, broad, d $NC\underline{H}_2C\underline{H}_2N$); 2.49 (broad, s $NC\underline{H}_2C\underline{H}_2N$); 1.49-1.40 (4H, m, $NCH_2C\underline{H}_2CH_2CH_3$); 1.32-1.23 ($NCH_2CH_2C\underline{H}_2CH_3$); 0.88-0.80 ($NCH_2CH_2CH_2C\underline{H}_3$). ^{13}C NMR (63 MHz) 180.9, 180.4, 179.8, 179.6 ($\underline{C}O_2^-$); 175.7, 175.5, 174.5, 174.4 ($\underline{C}ONH$); 66.1, 62.9, 61.2 ($N\underline{C}H_2CONH$; $N\underline{C}H_2CO_2$); 58.1, 55.9 ($N\underline{C}H_2\underline{C}H_2N\underline{C}H_2\underline{C}H_2N$); 40.0, 39.5, 39.8 ($N\underline{C}H_2CH_2CH_2CH_3$); 30.1 ($NCH_2\underline{C}H_2CH_2CH_3$); 19.5, 19.3, 19.2 ($NCH_2CH_2\underline{C}H_2CH_3$); 12.9 ($-\underline{C}H_3$). CHN: Calculated for $YC_{22}H_{40}N_5O_9$: 43.49% C; 6.65% H; 11.53% N. Found: 43.28% C; 6.32 % H; 11.29% N.

2.5.5.4 {1, 11-(bis(benzylamino)-1, 11-dioxo-3,6,9-triaza-3,6,9-triscarboxymethyl)undecane} yttrium (III) monohydrate: [YBBZA•H_2O]

The metal salt, YCl_3•$6H_2O$, (0.251 g, 0.83 mmol) was dissolved in 5 ml H_2O and solid DTPA-BBZA.$2H_2O$ (0.510 g, 0.84 mmol) added. The mixture was heated and sonificated until all of the ligand had dissolved (pH ~ 1) before dropwise addition of aqueous TBAOH (0.5M) until pH ~ 5 was reached. The volume of the colourless solution was reduced to ~ 1ml by rotary evaporation. Addition of CH_3CN (50 ml) afforded a colourless solid, which was collected by filtration, washed with CH_3CN (50 ml) and diethyl ether (50 ml) and dried under vacuum to yield the title compound, [YBBZA•H_2O] (0.414 g, 76%). FAB-MS: $[M+1]^+$ 658 D. ^1H NMR (250 MHz, D_2O): δ (ppm) 7.47-7.25 (10H, m, aromatic $C\underline{H}$); 4.78-

4.01 (4H, m, CONC$\underline{H}_2$Ph); 3.63-3.08 (10H, m, NC$\underline{H}_2$CONH, NC$\underline{H}_2CO_2^-$ (central and terminal)); 2.81-2.43 (8H, m, NC$\underline{H}_2C\underline{H}_2$N). ^{13}C NMR (63 MHz): 180.7, 180.4, 179.8, 179.6 ($\underline{C}O_2^-$); 176.5, 176.0, 175.0, 174.8 ($\underline{C}$ONH), 137.3, 137.1, 137.0 (aromatic $\underline{C}$); 129.2, 128.9, 128.8, 128.7, 127.8, 127.6, 127.5 (aromatic $\underline{C}$H); 126.8 (Aromatic $\underline{C}$); 66.0, 65.7, 63.1, 61.4, 61.0 (N$\underline{C}H_2$CON; N$\underline{C}H_2CO_2$); 58.0, 55.9, 55.8 (N$\underline{C}H_2\underline{C}H_2N\underline{C}H_2\underline{C}H_2$N); 43.4, 43.1 (N$\underline{C}H_2$Ph). Colourless, monoclinic, single crystals suitable for X-ray diffraction were obtained by slow evaporation of the NMR solution (D_2O). The crystals were of poor quality and the complex was found to be isostructural with a [YBBZA•H_2O]3H_2O structure published by D. Parker[127].

2.5.5.5 {1, 11-(bis((±)-2-norbornylamino)-1, 11-dioxo-3,6,9-triaza-3,6,9-triscarboxymethyl)undecane} yttrium (III) dihydrate: [YNBA•H_2O]H_2O

The ligand, DTPA-NBA.2H_2O, (0.330 g, 0.56 mmol) was added to an aqueous solution of YCl_3•6H_2O (0.165 g, 0.54 mmol), the mixture sonificated/heated until all solid had dissolved (pH ~1) then the pH adjusted (pH ~ 6) by dropwise addition of TBAOH (0.5 M aq) and HCl (1 M). The volume of the colourless solution was reduced to ~1 ml by rotary evaporation. Addition of acetonitrile (20 ml) to the concentrated solution afforded a colourless solid, collected by filtration, washed with CH_3CN, (20 ml) Et_2O, (20ml) and dried under vacuum to yield the title compound, [YNBA•H_2O] (0.326 g, 83%). FAB-MS: $[M+1]^+$ 666 D. CHN: Calculated for $YC_{28}H_{46}N_5O_{10}$: 47.92% C; 6.62% H; 9.98% N. Found: 47.76%C; 6.76% H; 9.61% N.

2.5.5.6 {1, 11-(bis(methylenecyclohexylamino)-1, 11-dioxo-3,6,9-triaza-3,6,9-triscarboxymethyl)undecane} yttrium (III) hydrate: [YmcyHA•H_2O]1.5H_2O

YCl_3•6H_2O (0.327 g, 1.08 mmol) was dissolved in 2 ml H_2O and solid DTPA-mcyHA (0.367 g, 1.09 mmol) added. The mixture was diluted with MeOH/H_2O then heated/sonificated until all of the ligand had dissolved (pH ~ 1) before dropwise addition of TBAOH (0.5M H_2O/MeOH) until pH ~ 6 was reached. The volume of the colourless solution was reduced to ~ 1ml by rotary evaporation. Addition of CH_3CN (50 ml) afforded a colourless solid, which was collected by filtration, washed with CH_3CN (50 ml) and diethyl ether (50 ml) and dried under vacuum to yield the title compound, [YmcyHA•H_2O] (0.587 g, 79%). FAB-MS: $[M+1]^+$ 670 D. ^{1}H NMR (250 MHz, D_2O): δ (ppm) 3.5-2.46 (22H, m, NC$\underline{H}_2C\underline{H}_2NC\underline{H}_2C\underline{H}_2N, NC\underline{H}_2CO_2^-$, NC$\underline{H}_2CO, NHC\underline{H}_2$CH); 1.73-0.86 (22H, m, NCH_2C$\underline{H}$C$_5\underline{H}_{10}$). ^{13}C NMR (63 MHz): 180.8, 180.4, 180.1, 180.0, 179.8 ($\underline{C}O_2^-$); 175.9,

175.6, 174.6, 174.5 (CONH); 66.1, 62.7, 61.2 (NCH_2CON; $NCH_2CO_2^-$); 58.1, 55.9 ($NCH_2CH_2NCH_2CH_2N$); 46.1, 46.0 ($NCH_2C_6H_{11}$); 37.3, 37.0, 36.9 ($NCH_2CHC_5H_{10}$); 30.2, 30.0, 25.8, 25.4, 25.3 ($NCH_2CHC_5H_{10}$). CHN: Calculated for $YC_{28}H_{51}N_5O_{10.5}$: 47.04% C; 7.21% H; 9.80% N. Found: 46.82% C; 6.90% H; 9.68% N.

2.5.5.7 {1, 11-(bis(cyclohexylamino)-1, 11-dioxo-3,6,9-triaza-3,6,9-triscarboxymethyl)undecane} yttrium (III) hydrate [YcyHA•H_2O]

Anhydrous YCl_3, (0.207 g, 1.06mmol) was dissolved in 10 ml H_2O and DTPA-cyHA (0.590 g, 1.06 mmol) added. The suspension was heated/sonificated until all the ligand had dissolved (pH ~ 1), then filtered before addition of TBAOH (40% w/w H_2O) until the colourless solution reached pH ~ 5. The solvent was removed by rotary evaporation to a final volume of ~ 1ml. Addition of acetonitrile to the oily residue afforded a colourless solid that was collected by filtration, washed with CH_3CN (20 ml) and Et_2O (20 ml) and dried under vacuum (0.561 g, 74%). Peaks corresponding to excess TBACl were observed in the proton NMR spectrum of the complex. This solid was dissolved in 10 ml methanol and the volume reduced to dryness by rotary evaporation. The residue was dissolved in MeOH (1 ml) and the white solid that formed upon addition of acetonitrile was collected by filtration, washed and dried to yield the title complex, [YcyHA•H_2O]. ^{1}H NMR (400 MHz, D_2O): δ (ppm) 4.00-3.75 (2H, broad, NCH); 3.75-3.32 (10H, m, NCH_2CO); 3.20-2.90 (4H, broad,); 2.90-2.80 (2H, broad); 2.7-2.45 (2H, broad) ($NCH_2CH_2NCH_2CH_2N$); 1.97-1.85, 1.85-1.72, 171-1.62 (4H, 4H, 2H, broad, cyhexH); 1.48-1.18 (10H, broad, cyhexH).

2.5.6 Gadolinium (III) DTPA-bis(amide) Complexes

2.5.6.1 {1, 11-(bis(1-butylamino)-1, 11-dioxo-3,6,9-triaza-3,6,9-triscarboxymethyl)undecane} gadolinium (III) monohydrate: [GdBUA•H_2O]

The ligand, DTPA-BUA.$2H_2O$ (0.260 g, 0.482 mmol) and the metal salt, $GdCl_3$•$6H_2O$ (0.179 g, 0.482 mmol) were combined in aqueous solution, sonificated and heated until the solid had dissolved (pH ~ 1). Aqueous TBAOH (40% w/w H_2O) was added dropwise until the colourless solution reached pH ~ 5 then the volume reduced to ~ 1ml by rotary evaporation. The colourless precipitate that formed upon addition of acetonitrile to the concentrated solution was collected by filtration, washed with CH_3CN (20 ml) and Et_2O (10 ml) then dried under vacuum to yield the title compound, [GdBUA•H_2O] (0.294 g, 90%). ES-MS (-): $[M]^-$ 655.2, 657.2, 659.2 (characteristic Gd(III) isotopic pattern). $[M+Cl]^-$ 693.2.

CHN: Calculated for Gd(III)$C_{22}H_{40}N_5O_9$: 39.01% C; 5.98% H; 10.36% N. Found: 38.94% C; 5.93% H; 10.42% N.

2.5.6.2 {1, 11-(bis(benzyllamino)-1, 11-dioxo-3,6,9-triaza-3,6,9-triscarboxymethyl)undecane} gadolium (III) trihydrate: [GdBBZA•H_2O]2H_2O

The ligand, DTPA-BBZA.2H_2O, (0.297 g, 0490 mmol) and the metal salt, $GdCl_3$•6H_2O (0.182 g, 0.490 mmol) were combined in aqueous solution, the mixture then diluted with water and heated/sonificated until all solid had dissolved (pH ~ 1). Aqueous TBAOH (40% w/w H_2O) was added dropwise until the colourless solution reached pH ~ 5 before reducing the volume to ~ 1ml by rotary evaporation. Addition of acetonitrile (20 ml) to the concentrated solution afforded a colourless precipitate that was collected by filtration, washed with CH_3N (20 ml) and Et_2O (20 ml) then dried under vacuum to yield the title compound, [GdBBZA•H_2O] (0.349 g, 96%). ES-MS: (-) $[M]^-$ 722.1, 723.1, 725.1, 727.1 (characteristic Gd(III) isotope pattern. CHN: Calculated for Gd(III)$C_{28}H_{42}N_5O_{11}$: 42.15% C; 5.31% H; 8.78% N. Found: 42.03% C; 5.14% H; 8.35% N.

2.5.7 Lutetium (III) DTPA-bis(amide) Complexes

2.5.7.1 {1, 11-(bis(ethylamino)-1, 11-dioxo-3,6,9-triaza-3,6,9-triscarboxymethyl)undecane} lutetium (III) hydrate [LuBEA•H_2O]

The metal, $LuCl_3$•6H_2O (0.069 g, 0.18 mmol) was dissolved in 2 ml water and combined with the solid ligand, DTPA-BEA.2H_2O (0.089 g, 0.18 mmol). The mixture was diluted with water (20 ml) then heated and sonificated until all the ligand had dissolved. TBAOH (40% w/w H_2O) was added dropwise until pH ~ 5 was reached. The volume of the colourless solution was reduced by rotary evaporation to ~ 1ml before addition of acetonitrile to the oily residue. The colourless precipitate was collected by filtration, washed with CH_3CN and Et_2O then dried under vacuum to yield the title compound, [LuBEA•H_2O]. ^1H NMR (400 MHz, D_2O): δ (ppm) 3.79-3.15 (14H, m $NC\underline{H}_2CO_2^-$, $NC\underline{H}_2CONHC\underline{H}_2CH_3$); 2.88, 2.65, 2.44 (4H; 2H; 2H; 3 x broad m, $NC\underline{H}_2C\underline{H}_2N$); 1.01 (6H, m, $NCH_2C\underline{H}_3$). ^{13}C NMR (100 MHz, D_2O): δ (ppm) 181.6, 181.1, 180.6, 180.4 ($\underline{C}O_2^-$); 176.3, 175.0 ($\underline{C}ONH$); 66.6, 66.4, 63.2, 61.5, 61.2, 61.0 ($N\underline{C}H_2CO$); 58.9, 58.8, 56.3, 56.2 ($N\underline{C}H_2\underline{C}H_2N\underline{C}H_2\underline{C}H_2N$); 35.7, 35.3 ($N\underline{C}H_2$); 13.6, 13.5 ($NCH_2\underline{C}H_3$).

2.6 *Ternary Complex Formation*

2.6.1 General Procedure

The mixed ligand [LnNAL.LHC] complexes were formed upon combination of the LnNAL chelate and deprotonated aryl acid in aqueous solution. Chelate solutions (0.1 mM aq) were prepared by dissolution of the isolated complexes (2.4) in deionised water. The aryl acid LHCs (0.01 mmol) were initially dissolved in DMSO (1 ml) forming stock solutions (0.01 M) which were diluted and deprotonated as required. The acid solution (100 µl, 1 $x10^{-6}$ mol) was diluted with deionised water (100 µl) and the pH raised upon addition of NaOH (7.5 µl, 0.1 M) to pH 7-8. Where the LHC compound was supplied as the HCl salt, contained a phenol OH or more than one carboxylate group additional base was charged accordingly.

2.6.2 Combinatorial Screening

Ternary complex formation was performed in black, flat-bottomed NUNC96 microplates. Aqueous chelate solution (0.1mM aq) was dispensed in 100µl aliquots (1 $x10^{-8}$ mol) into each well by auto-pipette. Addition of one molar equivalent of each acid (5mM, 50% v/v H_2O/DMSO pH ~ 7) resulted in a unique LnNAL/LHC combination in each well. Resultant solutions were mixed by aeration with the pipette. The sample luminescence (612 ± 10 nm) following UV excitation (275 ± 10 nm) was detected using a Tecan Ultra Multifunctional plate reader, as detailed in section 2.3. A 20 µs lag time was implemented between the excitation flash and detection of the metal emission allowing decay of background organic fluorescence. The signal was detected over a 40 µs integration time and data recorded using Xfluor software. The relative emission intensity (I/I_0) was calculated as the ratio of ternary complex luminescence (I) to that of the LnNAL complex (I_0). Results from the three iterations of the assay were combined in an MS-Excel spreadsheet (Appendix 2) incorporating both the raw luminescence data and the calculated relative emission intensities for each acid/chelate combination. Analysis of the data following grouping of the acids into clusters of related compounds allows electronic and structural similarities to be identified and correlated with features common to active or inactive species. Due to the large volume of data generated only the more interesting observations are discussed.

2.6.3 Binding Studies – Steady State Luminescence

The LnNAL solution (2 ml, 0.1 mM aq) was titrated with LHC solution (5 mM, 1:1 v/v DMSO/H_2O, pH 7-8) in 0.1 molar equivalent aliquots. Emission and excitation spectra were measured as detailed in 2.3. The increase in sensitised metal emission upon excitation of the

LHC is plotted versus aromatic acid concentration and the data fitted to a 1:1 binding model by non-linear least squares analysis using Kaleidagraph software.

The observed emission intensity, I, is the weighted average of luminescence from the emissive EuNAL and ternary complex species in solution (Equation 2-1).

$$I_{obs} = \frac{[EuNAL]_0 - [EuNAL.LHC]}{[EuNAL]_0} \bullet I_{EuNAL} + \frac{[EuNAL.LHC]}{[EuNAL]_0} \bullet I_{EuNAL.LHC}$$

$$I_{obs}[EuNAL]_0 = ([EuNAL]_0 - [EuNAL.LHC]) \bullet I_{EuNAL} + [EuNAL.LHC] \bullet I_{EuNAL.LHC}$$

$$I_{obs}[EuNAL]_0 = I_{EuNAL} \bullet [EuNAL]_0 - I_{EuNAL} \bullet [EuNAL.LHC] + I_{EuNAL.LHC} \bullet [EuNAL.LHC]$$

$$I_{obs}[EuNAL]_0 = I_{EuNAL} \bullet [EuNAL]_0 + [EuNAL.LHC] \bullet (I_{EuNAL.LHC} - I_{EuNAL})$$

$$I_{obs} = I_{EuNAL} + \frac{[EuNAL.LHC]}{[EuNAL]_0} \bullet (I_{EuNAL.LHC} - I_{EuNAL})$$

$$I_{obs} = I_{EuNAL} + \frac{[EuNAL.LHC]}{[EuNAL]_0} \bullet \Delta I_{max} \qquad \textbf{Equation 2-1}$$

ΔI_{max} is the maximum change in emission intensity observed at complex saturation equilibrium, $[EuNAL]_0$ is the total chelate concentration and [EuNAL.LHC] the concentration of ternary complex in solution, obtained by solving the mass balance equations (Table 2-3) for the equilibrium under investigation (Equation 2-2).

$$EuNAL + LHC \underset{}{\overset{K}{\rightleftharpoons}} EuNAL.LHC$$

$$K = \frac{[EuNAL.LHC]}{[EuNAL][LHC]}$$

$$[EuNAL.LHC] = K[EuNAL][LHC] \qquad \textbf{Equation 2-2}$$

Species	Mass Balance Equation
EuNAL	$[EuNAL] = [EuNAL]_0 - [EuNAL.LHC]$
LHC	$[LHC] = [LHC]_0 - [EuNAL.LHC]$
EuNAL.LHC	$[EuNAL.LHC] = [EuNAL.LHC]_0 + [EuNAL.LHC]$

Table 2-3 Mass balance equations for the formation of the 1:1 complex with EuNAL and LHC (Equation 2-2)

Substituting the mass balance equations into Equation 2-2 and solving the quadratic for [EuNAL.LHC] we obtain Equation 2-3 which in turn is substituted into Equation 2-1.

$$[EuNAL.LHC] = \frac{([EuNAL]_0 + [LHC]_0 + 1/K) - \{([EuNAL]_0 + [LHC]_0 + 1/K)^2 - 4[EuNAL]_0[LHC]_0\}^{1/2}}{2}$$

Equation 2-3

For the curve fit, the change in luminescence intensity ($I_{obs} - I_0$) is plotted versus the total LHC concentration and Equation 2-4 employed in the method of non-linear least squares analysis.

$$I - I_0 = \frac{\Delta Imax}{[EuNAL]_0} \bullet [EuNAL.LHC] \qquad \textbf{Equation 2-4}$$

2.6.4 Time Resolved Luminescence Spectroscopy

The luminescence lifetimes of the chelates and ternary complexes (formed upon combination of the aqueous LnNAL solution with the deprotonated LHC solution as 2.5.1) were measured in aqueous or D_2O solutions (10^{-2} – 10^{-4} M) upon excitation at 532, 355 or 266 nm (chapter 2.2). Luminescence decay was measured at 616 nm ($^5D_0 \rightarrow {}^7F_2$ transition) and at 545 nm ($^5D_4 \rightarrow {}^7F_5$ transition) for europium and terbium respectively. The luminescence decay curves were fitted to mono or biexponential equations (Equations 2.5 and 2.6) using Kaleidagraph software.

$$I = I_{osc} - I_0 \exp(-kt)$$

Equation 2-5 Monoexponential decay equation. I = luminescence intensity at time t (secs), I_{osc} = background correction factor for the oscilloscope, k = decay constant (s^{-1}). Lifetime $\tau = k^{-1}$ (sec)

$$I = I_{osc} - [I_{0(1)} \exp(-k_{(1)} t_{(1)}) + I_{0(2)} \exp(-k_{(2)} t_{(2)})]$$

Equation 2-6 Biexponential decay equation

2.6.5 Ternary Complex NMR Studies

The mixed ligand species were formed upon combination of the diamagnetic LnNAL analogues (Ln = La(III) and Y(III)) with deprotonated picolinic acid in equimolar quantities. The isolated chelate (2.4) (~ 40 mg) was dissolved in ~ 0.5 ml D_2O (pD 6-7) forming a colourless solution to which one molar equivalent of PCA (D_2O/NaOD, pD 7-8) was added. The pD of the resultant solution (pD 4-5) was adjusted to around 7 with D_2O/NaOD.

2.7 *Heterobimetallic Luminescent Polymers*

2.7.1.1 $[EuNa(pca)_4(H_2O)]_n0.5nH_2O$

Picolinic acid (0.62 g, 5 mmol) was dissolved in 3 ml H_2O and 1M NaOH (aq) added until the pH of the solution reached a value of 7-8. Addition of $EuCl_3 \bullet 6H_2O$ (0.185 g, 0.5 mmol) in ~ 2 ml H_2O afforded a colourless solution (pH ~ 2) after mixing. The solution was neutralised with NaOH upon which a colourless microcrystalline solid began to form. This solid was collected by filtration and washed with water and acetone. A substantial amount of the solid dissolved in the water and the filtrate was concentrated under reduced pressure inducing precipitation of the polymer. Recrystallisation of the solid by vapour diffusion with acetone, acetonitrile or methanol also afforded single crystals suitable for structural analysis. Elemental analysis: Calculated for $EuNaC_{24}H_{23}N_4O_{11.5}$: 39.67% C; 3.19% N; 7.71% N. Found: 39.75% C; 2.63% H; 7.48% N. (crystal - sample losing weight). ES-MS (+): $[M+Na]^+$ 684/686 D; ES-MS (-) $[M]^-$ 639/641D.

The polymer, $[EuNa(pca)_4(H_2O)]_n0.5nH_2O$, could also obtained from solutions containing both EuNAL species and picolinic acid. The NAL was dissolved in H_2O/NaOH forming a concentrated colourless solution (pH 7-8) before combination with one equivalent of $EuCl_36H_2O$, also dissolved in water, to give a colourless solution at pH ~ 2. Aqueous NaOH (1M) was added dropwise until the solution reached pH 7-8 before addition of 10 x excess of picolinic acid (pH 7-8, aq/NaOH). Slow evaporation of the solution resulted in the formation of hexagonal colourless crystals of suitable quality for X-ray diffraction. The crystals exhibited strong red characteristic Eu(III) emission upon exposure to UV light.

Formula:	$[EuNa(pca)_4(H_2O)]_n0.5nH_2O$	Unit Cell	
FW	699.39	a = 12.5718(17) Å	α =90°
Wavelength	1.54178Å	b = 12.5718(17) Å	β =90°
T	220(2) K	c = 60.364(19) Å	
Hexagonal crystal system		γ = 120°	
Space group	P6(5)22		

Crystal Data: m = 16.999 mm^{-1} final R = 7.67 % [based on F and 2195 data with F>4s(F)], wR^2 = 16.50 % (based on F^2 and all 3726 unique data used in refinement) for 366

parameters. The structure was solved by Patterson methods (DIRDIF) and refined by full matrix least squares on SHELLXL-97).[157]

2.7.1.2 $[TbNa(pca)_4(H_2O)]_n0.5nH_2O$

A concentrated aqueous solution of picolinic acid (0.54 g, 4.4 mmol) was neutralised with NaOH (1 M aq) before mixing with $TbCl_3 \bullet 6H_2O$ (0.174 g, 0.47 mmol) in 1ml water (pH 2). Addition of 1M NaOH resulted in the evolution of a fine white precipitate that redissolved immediately upon mixing. After approximately 5 minutes a microcrystalline solid precipitated from the solution and was collected by filtration, washed with methanol and ether then dried under vacuum to yield the hetrobimetallic luminescent polymer, $[TbNa(pca)_4H_2O]_n0.5nH_2O$. Elemental analysis: Calculated for $TbNaC_{24}H_{21}N_4O_{10.5}$ (724.39): 40.29% C; 2.96% H; 7.83% N. Found: 40.18% C; 2.615% H; 7.59% N. ES-MS $[MH]^+$ 648 D.

2.7.1.3 $[GdNa(pca)_4(H_2O)]_n0.5nH_2O$

A solution of picolinic acid (0.615 g, 5 mmol) in H_2O/NaOH (pH 7-8) was combined with $GdCl_3 \bullet 6H_2O$ (0.180 g, 0.48 mmol) in 1 ml H_2O. The resultant solution, (pH ~ 2) was neutralised with 1 M NaOH and refrigerated overnight but no precipitate was observed in the flask. Addition of excess base until the pH reached approximately 8 afforded the expected microcrystalline solid, which was collected by filtration, washed with water (5 ml), acetone (5 ml) and ether (2 x 10ml) then dried under vacuum. A few large, colourless hexagonal crystals, suitable for x-ray structural analysis formed in the pasteur pipette used in preparation of the solid and were found to be isostructural with the Eu(III) polymer. ES-MS (-): 643, 644, 645, 646, 648 $[M]^-$ (characteristic Gd(III) isotope distribution pattern). ES-MS (+): 689, 690, 691, 694 $[M+Na]^+$.

X-ray powder diffraction was performed on the bulk microcrystalline samples of the Eu(III), Tb(III) and Gd(III) polymers. The diffraction pattern obtained was the same for each lanthanide, indicating the same unit cell for the three polymers. The pattern also matched that generated from the $[EuNa(pca)_4(H_2O)]_n0.5nH_2O$ single crystal data, confirmation that the bulk samples are isostructural with the single crystals obtained.

2.7.1.4 $[YNa(pca)_4(H_2O)]_n0.5nH_2O$

Mixing aqueous solutions of $YCl_3 \bullet 6H_2O$ and picolinic acid at pH 7-8 did not afford a microcrystalline solid as observed with Eu(III), Tb(III) and Gd(III). Instead, large, well defined, colourless, hexagonal crystals formed overnight. X-ray analysis revealed the compound to be isostructural with the Eu(III) and Gd(III) polymers. Elemental analysis: Calculated for $Y(III)NaC_{24}H_{21}N_4O_{10.5}$: 44.66% C; 3.28% H; 8.68% N. Found: 44.59% C; 3.28% H; 8.69% N.

2.7.1.5 $[NaLa(pca)_4(H_2O)]_n0.5nH_2O$

The La(III) analogue was prepared in the same way as the other Ln(III) polymers and characterised by elemental analysis only as the species was found to be insoluble. Calculated for $La(III)NaC_{24}H_{20}N_4O_{10}$: 42.00% C; 2.94% H; 8.16% N. Found: 41.77% C; 2.66% H; 8.11% N.

2.7.1.6 $[NH_4Eu\ (PCA)_4H_2O]$

Picolinic acid (0.157 g, 1.28 mmol) dissolved in ~ 1ml H_2O and concentrated NH_3 (38% w/w H_2O) added until pH 7 was reached. This solution was then combined with aqueous $EuCl_3 \bullet 6H_2O$ (0.060 g, 0.164 mmol) and the pH adjusted to around 7 with conc. NH_3. A colourless, microcrystalline solid quickly formed and was collected by filtration, washed with water (2 ml), ethanol (5 ml) and diethyl ether (5 ml) to yield the title compound, $[NH_4Eu\ (PCA)_4H_2O]$ (0.057 g, 52%). Large, colourless, well-defined hexagonal crystals of suitable quality for X-ray diffraction were obtained upon slow evaporation of the filtrate.

3 The Ternary Complex Model System

Several DTPA-bis(amide) (DTPA-AM_2) ligands have been prepared from DTPA-dianhydride and are reported in the literature.[117-128, 130-137] Forming highly stable, water soluble, neutral chelates with the lanthanide trivalent cations, these ligands are inexpensive and avoid the synthetic complications associated with macrocyclic crown ethers and cryptands. Neutral Ln(III) chelates are more "biologically compatible" than charged species such as the anionic $[LnDTPA]^{2-}$ complex which can become implicated in membrane transport mechanisms. DTPA-bis(ethylamide) (BEA) was chosen as a ligand on the basis of the well documented gadolinium complex formation, studied as a contrast agent for MRI.

The gadolinium complex, $[GdBEA \bullet 2H_2O]$ was prepared initially by Konings *et al*[117] in 1991. The X-ray crystal structure provides confirmation that octadentate chelation occurs via the three nitrogen atoms of the diethylenetriamine backbone, the three carboxylate groups and two amide carbonyls of the ligand (Figure 3-1). The amide arms do not coordinate the metal and form a binding pocket, occupied by one remaining water molecule, ideal for LHC recognition.

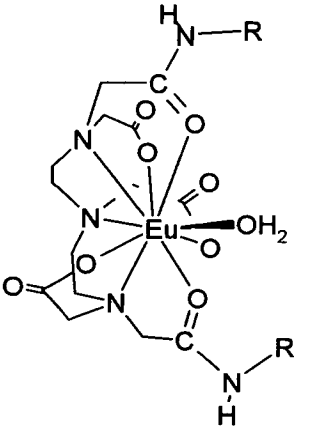

Figure 3-1 Eu(III)DTPA-AM_2 structure

3.1 LnBEA complex formation

The formation of the neutral 1:1 complex between Eu(III) and DTPA-BEA in aqueous solution was studied by luminescence spectroscopy. The binding curve was obtained by integration of the corrected emission spectra (Figure 3-2) for the main Eu(III) peaks between 572 and 640 nm. The weak emission from the free Eu(III) ion in water is increased upon

incremental addition of the ligand. Upon ligand binding parity forbidden f→f electronic transitions become more allowed, as the symmetry of the spherical ion is reduced and quenching water molecules are excluded from the primary coordination sphere. Plotting the relative emission intensity (I/I_0) versus the mole ratio of ligand to metal provides a measure of the strength of binding interaction and the stoichiometry of the species formed.

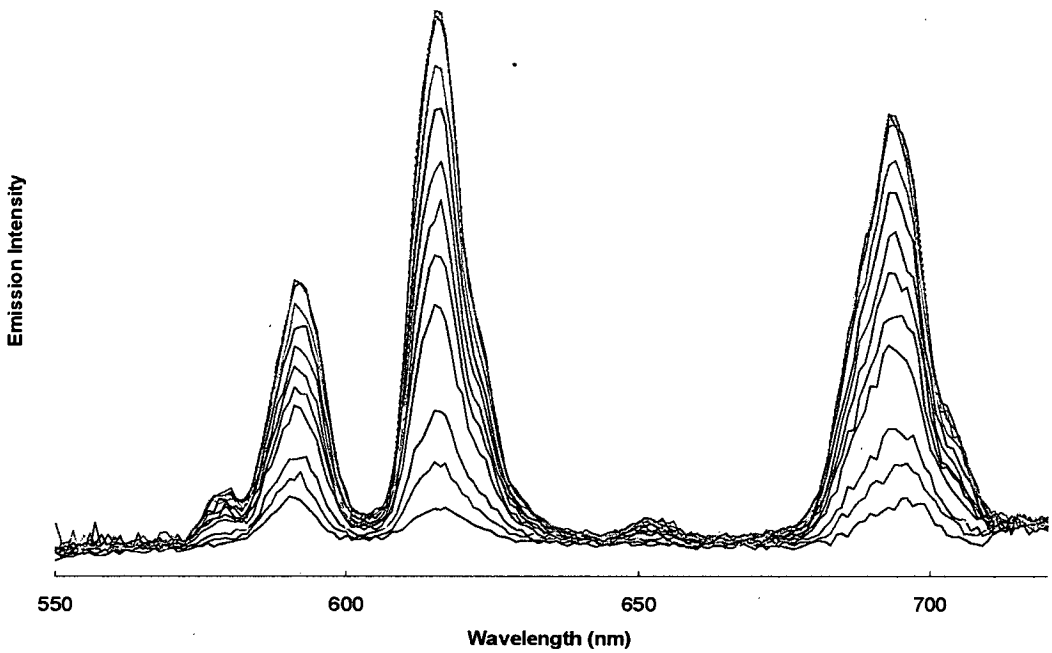

Figure 3-2 Corrected Eu(III) emission spectra (λ ex = 394 nm) for titration of the metal (1.5×10^{-4} M aq) with DTPA-BEA (pH 7).

Titration of an aqueous solution of $EuCl_3$ (pH ~ 6) with DTPA-BEA (pH ~ 7) yields the 1:1 complex, EuBEA, as illustrated by the plateau observed in the emission plot (Figure 3-3) above one equivalent of ligand, indicating saturation of the metal coordination sphere. The sharp inflection at 1:1 stoichiometry is evidence of the strong binding interaction.

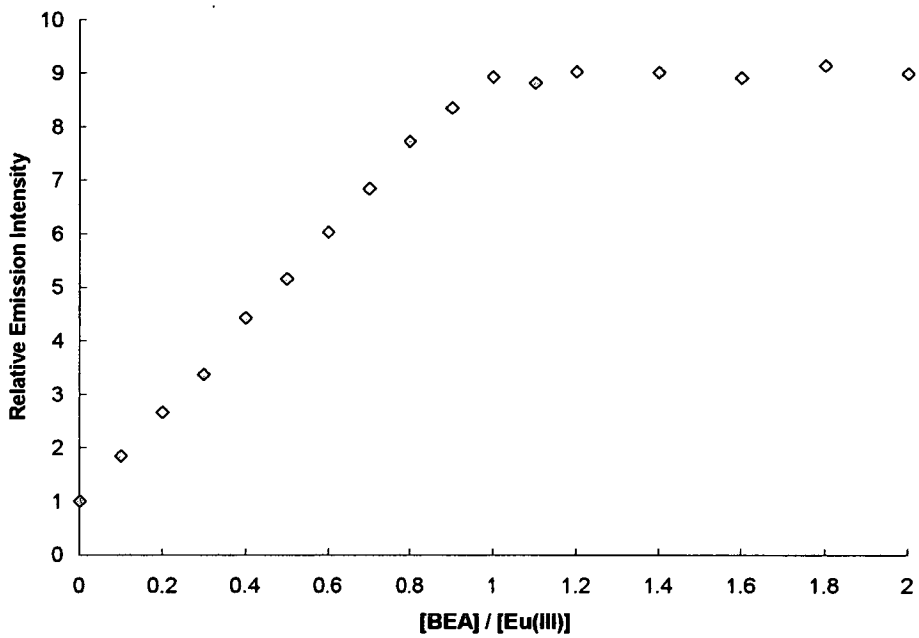

Figure 3-3 Eu(III) emission titration with DTPA-BEA

The 1:1 complex, EuBEA, is also detected in solution by positive and negative electrospray mass spectrometry. Characteristic europium peaks appear in both spectra: ES(+) $[MH]^+$ 596/598 D; $[M+Na]^+$ 618/610 D. ES(-) $[M-H]^-$ 594/596 D; $[M+Cl]^-$ 630/632 D.

Formation of the diamagnetic La(III) analogue was studied by ^1H NMR spectroscopy in accordance with the Eu(III) luminescence studies. The broad, unresolved chelate spectra differ considerably from that of the free ligand. The AB system of the diethylenetriamine methylene protons in the ligand spectrum is broadened and shifted to lower frequency upon chelation to the metal. The quartet signal of the methylene protons of the amide arms is unchanged upon complexation. This observation correlates with the crystallographic evidence indicating that the amide nitrogen atoms are not involved in coordination. The NMR behaviour of LnDTPA-AM_2 complexes has been thoroughly investigated and is well documented in the literature[117, 119, 124, 126-128, 130, 134, 136] as the chelates are frequently employed as contrast agents in MRI. Our studies are in agreement with the literature spectra and were undertaken to investigate the selective molecular recognition involved in ternary complex formation.

3.2 Ternary Complex Formation – Luminescence Studies

Several simple aromatic acids were studied with regard to their binding to the neutral EuBEA chelate. Benzoic (BZA), phthalic (PTA), isophthalic (IsoPTA), picolinic (PCA) and dipicolinic (diPCA) acids (Figure 3-4) were chosen to represent a variety of mono and bidentate LHC binding units. The molar extinction coefficients and pK_a values are shown in Table 3-1.

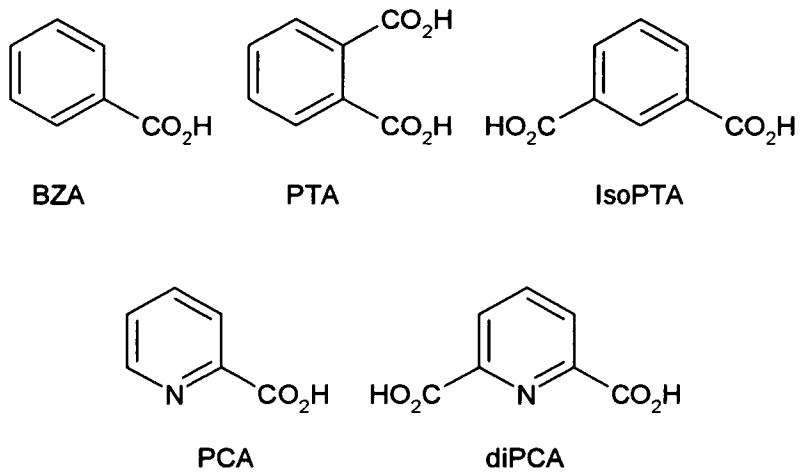

Figure 3-4 Structures of aromatic acid LHCs

The controlled formation of mixed ligand europium complexes with EuBEA and these aryl acid LHCs in aqueous solution was investigated by luminescence spectroscopy. Increasing europium luminescence upon incremental addition of the deprotonated acid to the EuNAL was monitored upon excitation of the aromatic moiety at 270 nm. Emission plots obtained upon integration of the Eu(III) spectra (572-640 nm) allow the stoichiometry of the mixed ligand species to be determined.

Acid	pK_a	ε ($M^{-1}cm^{-1}$)	λ (nm)
BZA	4.19	2930	273
PTA	2.89, 5.51	3200	280
IsoPTA	3.54, 4.60	-	-
PCA	5.52	3830	264
diPCA	1.9, 5.9	-	-

Table 3-1 Aromatic acid pK_a values and molar extinction coefficients

(Ref: See *CRC Handbook of Organic Photochemistry,* Scaiano. J. C. **1989**)

3.2.1 Benzoic Acid Binding

The emission plot (Figure 3-5) shows that benzoic acid (BZA) binds the EuNAL in a monodentate manner. Two equivalents of LHC are required to saturate the metal coordination sphere, as shown by the plateau observed in the binding curve. A ten-coordinate ternary luminescent complex is formed. The 2.5 fold enhancement in emission intensity is relatively low due to the poor light harvesting properties of the acid and the weak nature of the binding interaction. BZA recognition of the EuBEA binding cavity is not well defined, as indicated by the shallow gradient of the binding curve. The characteristic absorption of BZA around 270 nm is observed in the excitation spectrum and provides unequivocal evidence that the increase in luminescence is due to excitation of the acid.

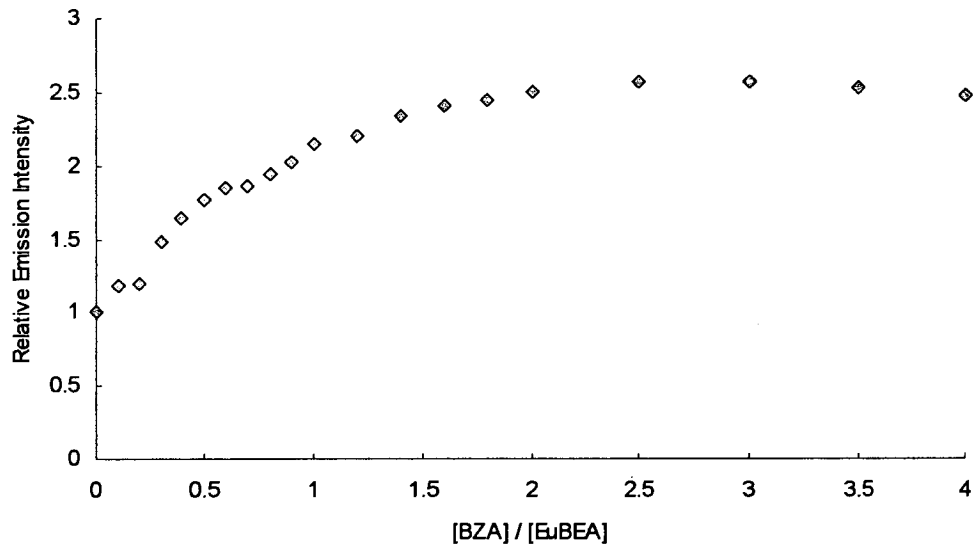

Figure 3-5 Relative emission intensity versus mole ratio for titration of EuBEA (1.5×10^{-4}M (aq), pH 7) with benzoic acid LHC (λex = 270 nm)

3.2.2 Phthalic Acid Binding

The binding interaction between EuBEA and bidentate phthalic acid (PTA) is much stronger than the corresponding interaction with monodentate BZA. Phthalate is able to form a seven membered chelate ring, whereas benzoate cannot, requiring only one molar equivalent to saturate the Eu(III) coordination sphere (Figure 3-6). The eight-fold increase in luminescence can be attributed to sensitised emission upon excitation of the acid (λ_{max} 280 nm, ε = 3200 $M^{-1}cm^{-1}$) confirmed by the characteristic absorption of PTA observed in the excitation spectrum (Figure 3-7).

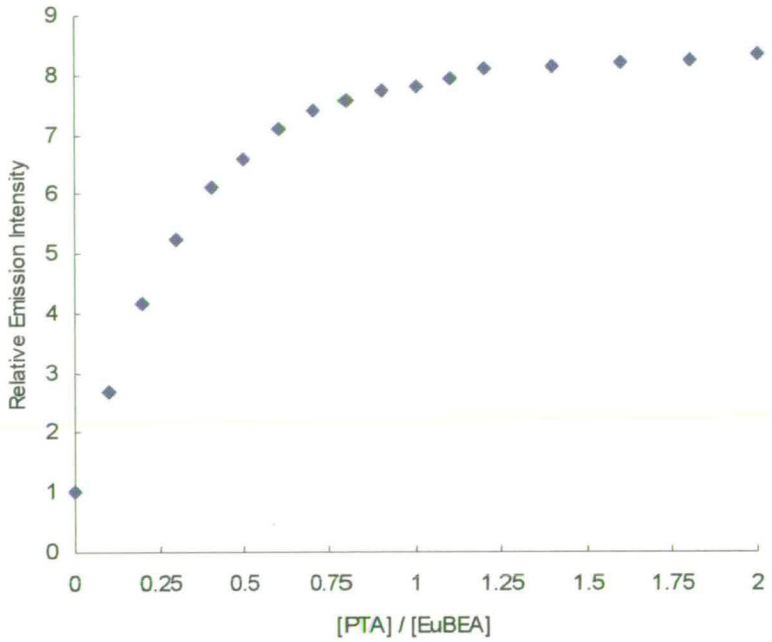

Figure 3-6 Relative emission intensity versus mole ratio for titration of EuBEA (1.5×10^{-4}M) with phthalic acid LHC ($\lambda ex = 270$ nm)

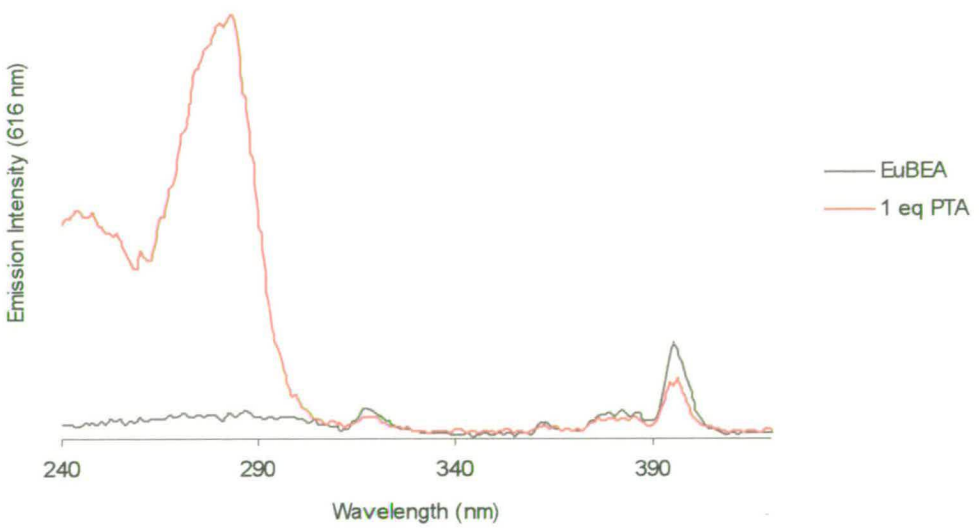

Figure 3-7 Excitation spectrum of $[EuBEA.PTA]^{2-}$, uncorrected for lamp response

3.2.3 Picolinic Acid Binding

Picolinic acid (PCA, pyridine-2-carboxylic acid) was chosen as a light-harvesting centre on the basis of its bidentate binding unit, allowing comparison with the dicarboxylate unit of PTA. PCA is capable of bidentate coordination with the EuNAL involving the carboxylate anion and the heteroatom of the pyridine ring. The acid is observed to recognise the binding cavity of EuBEA forming a ternary luminescent complex in 1:1 stoichiometry as expected. Molecular recognition was followed by luminescence spectroscopy. Intramolecular energy transfer leading to sensitised Eu(III) emission is confirmed by the characteristic PCA absorbance around 270 nm observed in the excitation spectrum of the sample (Figure 3-9). The bidentate interaction between PCA and EuBEA yields a ten coordinate luminescent mixed ligand species. The interaction is strong, reflected by the steep gradient of the emission plot (Figure 3-8). The plateau above one equivalent of PCA, indicative of complex saturation, confirms the 1:1 stoichiometry of the ternary complex.

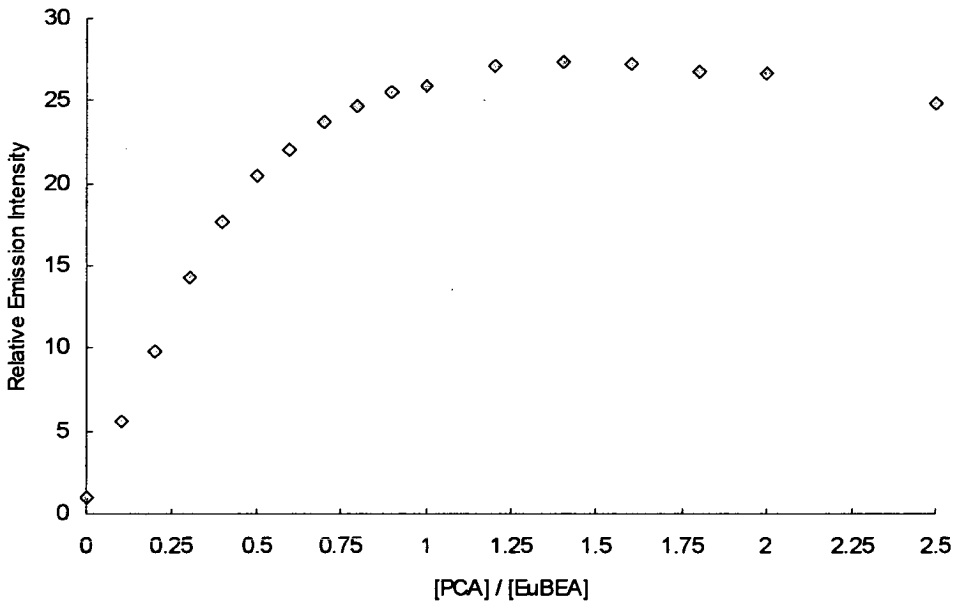

Figure 3-8 Relative emission intensity versus mole ratio for titration of EuBEA ($1.5x10^{-4}M$) with picolinic acid LHC ($\lambda ex = 270$ nm)

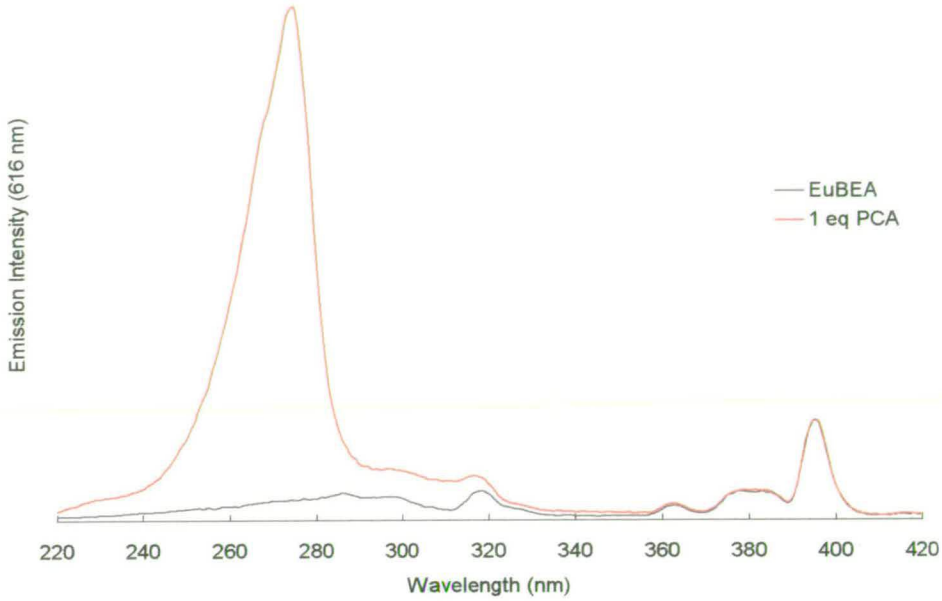

Figure 3-9 Excitation spectrum of [EuBEA.PCA]$^-$ (λ em 616 nm), uncorrected for lamp response

In stark contrast to the well defined stoichiometry of mixed ligand complexes formed upon molecular recognition between EuBEA and BZA, PTA and PCA, isophthalic and dipicolinic acids exhibit quite different binding characteristics as discussed below.

3.2.4 Isophthalic Acid Binding

Isophthalic acid was chosen on the basis of its potential bidentate binding unit and light harvesting characteristics. Containing the same chromophore as both phthalate and benzoate it allows direct comparison of binding modes. Bidentate chelation of EuBEA by IsoPTA is prevented by the steric constraints enforced by the *meta* positioning of the carboxylate ring substituents. Consequently, monodentate binding is expected, as observed with BZA. Formation of the ternary complex is followed by luminescence spectroscopy. Emission of the solution is monitored upon excitation of the aromatic moiety at 270 nm. Sensitised Eu(III) emission is confirmed by the presence of a characteristic aromatic absorbance around 280 nm in the excitation spectrum (Figure 3-11).

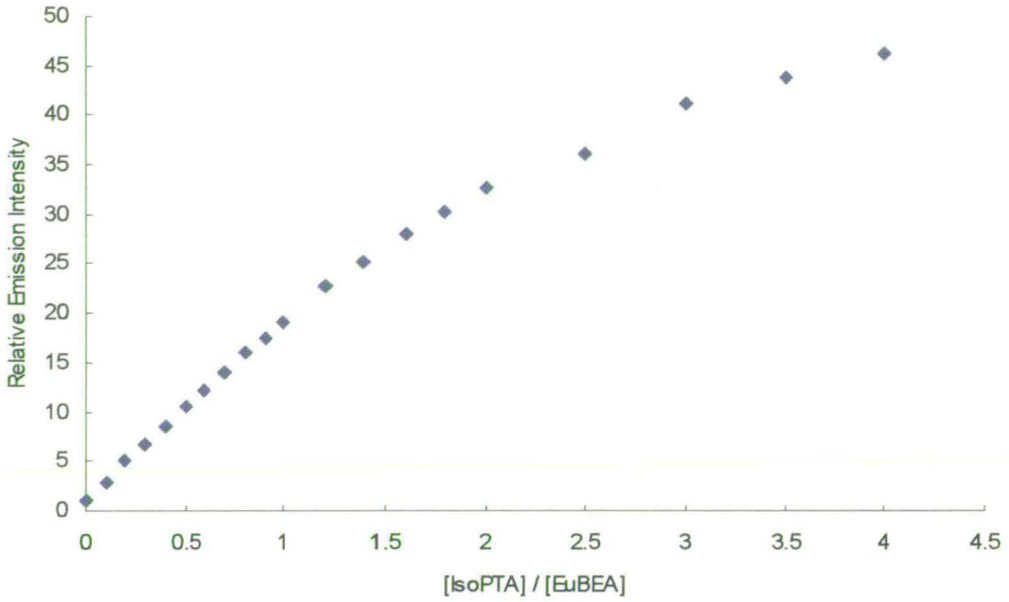

Figure 3-10 Relative emission intensity versus mole ratio for titration of EuBEA ($1.5x10^{-4}$M) with isophthalic acid LHC (λex = 270 nm)

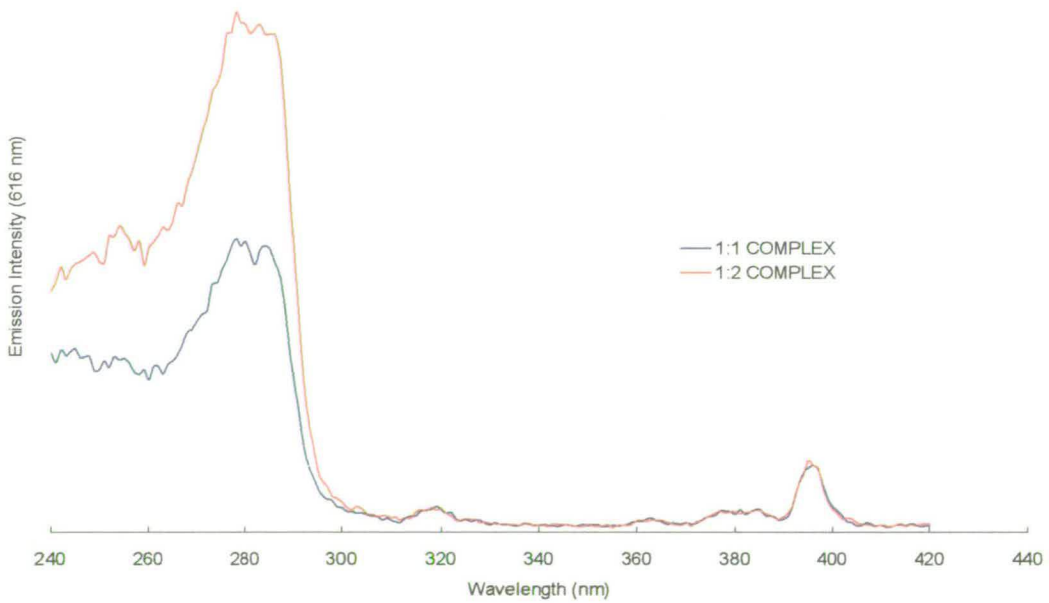

Figure 3-11 Excitation spectra of [EuBEA.IsoPTA] in aqueous solution at 1:1 and 1:2 stoichiometry (λ em = 616 nm), uncorrected for lamp response

The binding of EuBEA by isophthalic acid is clearly different from that of PTA, as illustrated by the emission plot (Figure 3-10). Stoichiometry of the mixed ligand species is not well defined, and saturation of the coordination sphere is not achieved upon titration of EuBEA with the acid. The steeper gradient of the binding plot, and the greater relative emission intensity observed upon recognition of the acid, suggests that the interaction between this LHC and EuNAL is stronger than that of phthalic acid. At experimental pH both carboxylate residues are deprotonated but only one can coordinate the metal.

It has been shown[147] that electronic resonance effects from the *meta* carboxylate increase the stability of the monodentate binding interaction with the metal. This can contribute to the strong increase in emission intensity observed. The absence of a plateau in the emission plot indicates the likelihood of metal coordination by more than one isophthalic acid LHC unit. Multinuclear complex formation may occur in solution, with each isophthalate acting as a bridging ligand between discrete EuNAL complexes.

3.2.5 Dipicolinic Acid Binding

Dipicolinic acid was selected as a light harvesting centre based on its potential for terdentate interaction with the metal. Formation of intensely luminescent Ln(III) complexes with dipicolinic acid are well documented in the literature, in general exhibiting approximately 1:3 stoichiometry. Molecular recognition between EuBEA and diPCA was followed by luminescence spectroscopy. Intense europium emission was observed and sample dilution required in order to prevent detector saturation. No plateau was observed in the binding plot (Figure 3-12), in contrast to the well defined interaction between EuBEA and PCA (Figure 3-8).

It is possible that diPCA is able to extract the metal from the highly stable EuNAL chelate, (Log K ~ 15). Formation constants for the interaction between Ln(III) and diPCA are reported[148] (Log K_1 8.83; Log K_2 15.98; Log K_3 21.00). We conclude that the bis(*ortho)* positioning of the acid residues prevents the acid from fulfilling its terdentate binding potential and facilitates formation of multinuclear species in solution as observed with isophthalic acid. No further studies were undertaken with this acid.

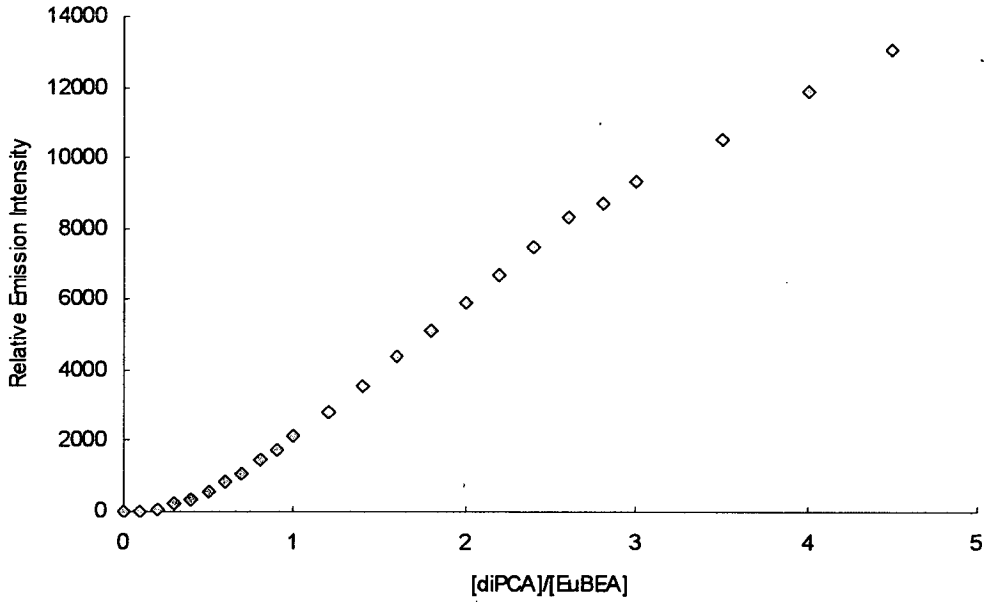

Figure 3-12 Relative emission intensity versus mole ratio for titration of EuBEA ($1.5x10^{-4}M$) with dipicolinic acid LHC ($\lambda ex = 270$ nm)

3.3 Ternary Complex Formation – Electrospray Mass Spectrometry

Additional evidence for mixed ligand complex formation between these simple aryl acid LHCs and the EuDTPA-AM_2 NAL species is provided by electrospray mass spectrometry. Peaks corresponding to sodium adducts of the anionic ternary species are detected in the positive ES-MS and the mixed ligand complex $[EuBEA.PCA]^-$ is observed by negative ion mass spectrometry (Table 3-2).

Acid	Peak (m/z)	Assignment
BZA	762/764	$[(EuBEA.BZA)^- + 2Na^+]^+$
	784/786	$[(EuBEA.BZA)^- - H^+ + 3Na^+]^+$
	906/908	$[(EuBEA.BZA_2)^{2-} + 3Na^+]^+$
PTA	828/830	$[(EuBEA.PTA)^{2-} + 3Na^+]^+$
PCA	763/765	$[(EuBEA.PCA)^- + 2Na^+]^+$
	717/719	$[EuBEA.PCA]^-$

Table 3-2 Electrospray mass spectrometry of ternary luminescent complexes in aqueous solution

3.4 Ternary Complex Formation – ^{1}H NMR Studies

Additional evidence supporting mixed ligand complex formation in aqueous solution between EuBEA and PCA is obtained form ^{1}H NMR studies performed on the analogous diamagnetic La(III) system. The complex is formed in an NMR tube upon addition of one equivalent of deprotonated PCA (pD 7-8) to a preformed solution of LaBEA (pD 7-8) in D_2O/NaOD.

Comparison of the ternary complex spectra, [LaBEA•PCA]$^-$, with that of LaBEA at the corresponding pD shows significant sharpening of the resonances upon PCA recognition. The LaBEA regions of the spectra are shown below in Figure 3-9. The spectra are complicated due to the observation of geminal coupling between the methylene protons of the ligand diethylenetriamine backbone, as observed by correlation spectroscopy (COSY). The unresolved nature of the spectra is due to line broadening effects induced by the metal ion. The sharpening of the resonances upon addition of PCA is attributed to recognition of the LaNAL binding pocket causing a conformational locking effect. It has been shown that LnDTPA-AM_2 complexes exist in solution as eight diasteriomeric pairs in fast exchange.[121, 130, 134, 136] The rotational isomerism of the tricapped trigonal prismatic coordination polyhedron of LaBEA is restricted upon interaction with picolinic acid, and the resonances of the diethylenetriamine backbone become more clearly defined. This observation provides further evidence for molecular recognition between the NAL complex and LHC in aqueous solution. Further NMR investigations with into the ternary complex formation with Yb(III)BEA are underway, in collaboration with Vincent Jaques at the University of Liege in Belgium.

These results indicate that DTPA-AM_2 ligands can be successfully employed as NALs in the controlled formation of mixed ligand luminescent species with a variety of simple aromatic carboxylic acid LHCs. Following the success of these initial investigations we were keen to evaluate the influence of the amide arms of the ligand on the binding interaction. A library of several DTPA-AM_2 derivatives was prepared in order to introduce structural and electronic diversity to the LnNAL chelate binding pocket. Synthetic methods are discussed in Chapter 4. Molecular recognition between these chelates and the simple but effective LHC, picolinic acid, was investigated by several spectroscopic techniques. Combinatorial screening technologies were then employed in evaluating the binding interaction with a library of aromatic carboxylic acids designed to introduce molecular diversity and allow identification of potential LHC units. Results of the screening experiment are considered in Chapter 5 and observations made from further binding studies discussed in Chapter 6.

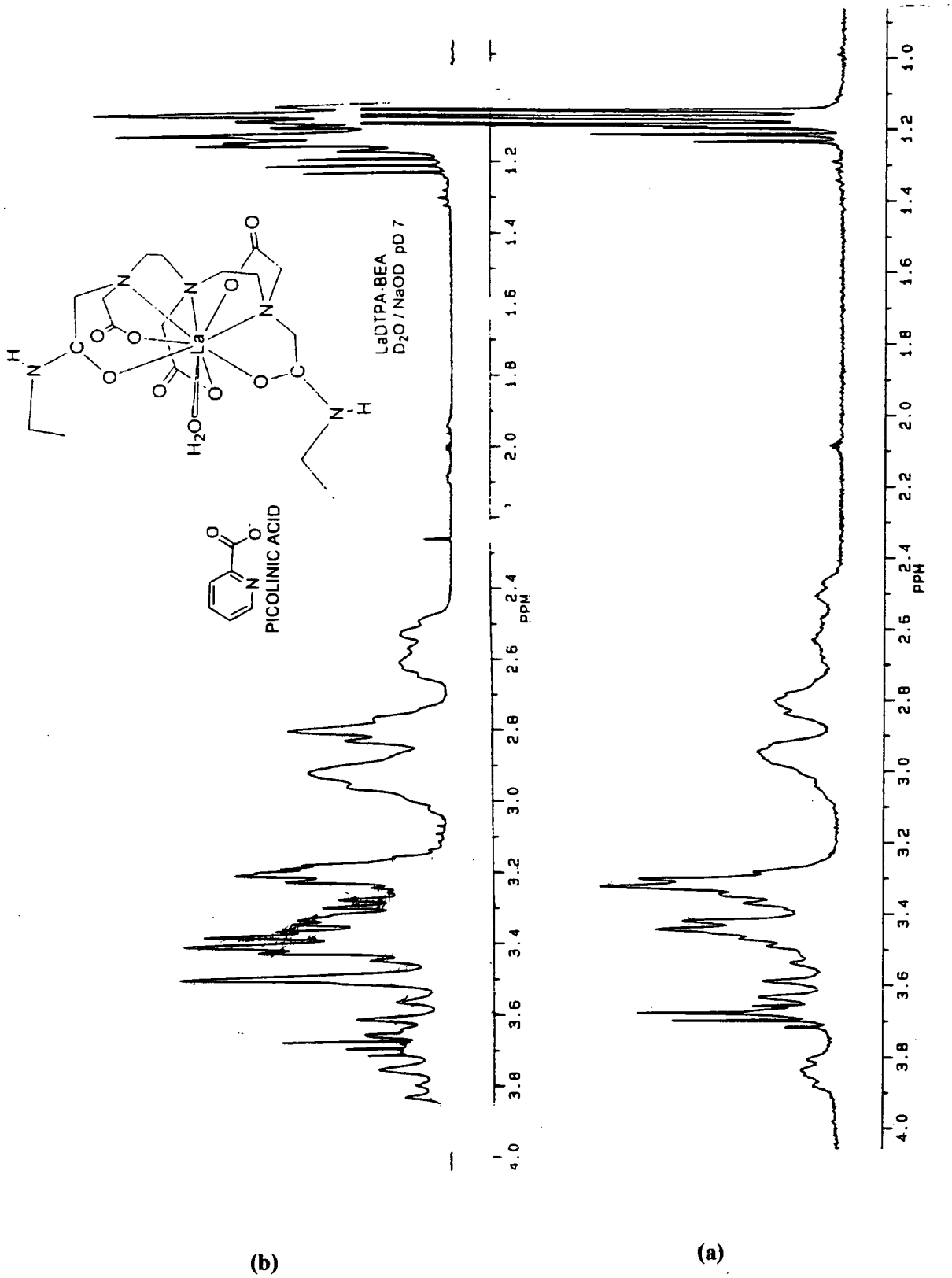

Figure 3-13 ^{1}H NMR spectra of (a) LaBEA and (b) [LaBEA.PCA]$^{-}$ (200 MHz, 25°C, D_2O/NaOD, pD 7-8)

4 Comments on Synthetic Methods

4.1 Ligand Synthesis

Preparation of the DTPA-AM_2 derivatives was performed following the procedure developed by Konings et al.[117-119] The DTPA-AM_2 species was formed by reaction of the cyclic anhydride of DTPA with excess amine (Scheme 2-1). Acidification of the reaction mixture to pH ~2 following dilution with water initiated crystallisation/precipitation of the ligand. Below pH ~ 2 protonation of the amide nitrogen atoms occurs disrupting the H-bonding network (Figure 4-1) between the carboxylate functional groups and the tertiary amine N of the diethylenetriamine backbone facilitating dissolution of the ligand.

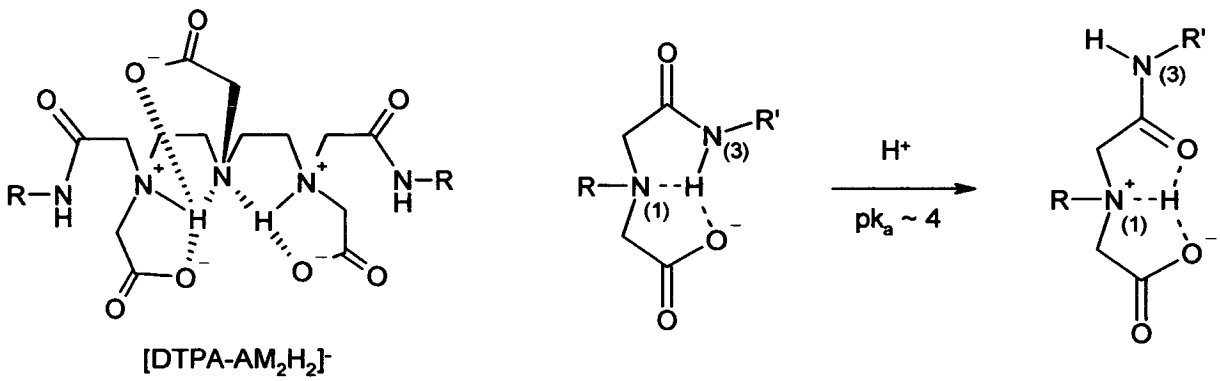

Figure 4-1 H-bonding network established upon second protonation event in DTPA-AM_2 ligands

Preparation of the higher alkyl and aryl DTPA-AM_2 ligands (cyHA, mcyHA, PYA and cyOA) was attempted in isopropanol due to the hydrophobicity of the amines employed. The reaction between the dianhydride and amine occurred forming the desired DTPA-AM_2 product (NMR, MS) but problems were encountered in purification of the ligand due to the association between the excess amine and the carboxylate groups. Crystallisation could not be induced upon acidification with HCl. Trituration of the mixture with an organic solvent[119] such as acetonitrile or acetone was required to precipitate the compound. Recrystallisation of the solid was attempted from water, water/acetone or water/ethanol mixtures but proved to be an inefficient method of removing the excess amine. It was found that these higher alkyl and aryl DTPA-AM_2 ligands could be successfully formed in water, DMF or pyridine and isolated by aqueous acidic work up (2.3.2.13, DTPA-BTA).

Several attempts were made to prepare the pyridine derivative, DTPA-PYA (Chapter 2.3.2, Figure 4-2). This heterocyclic ligand was chosen to enable investigation of H-bonding effects on molecular recognition.

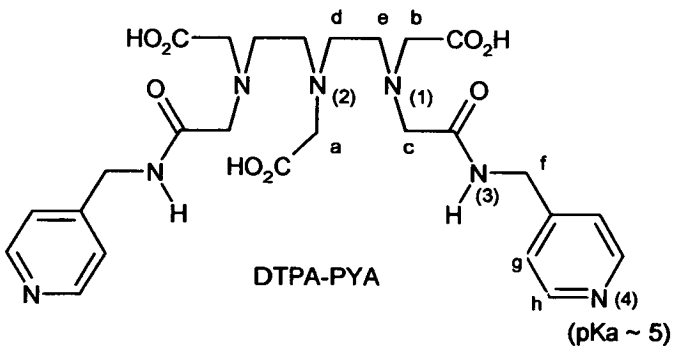

Figure 4-2 Pyridine DTPA-AM_2 derivative, DTPA-PYA

The reaction between 4-picolylamine and DTPA-dianhydride at 60°C in pyridine resulted in formation of penta-, tetra-, tris-, bis- and mono amide products (FAB-MS), none of which were isolated. At lower temperatures and lesser excess of amine the desired bis-amide product could be obtained (solvents attempted: propan-2-ol, water, pyridine, DMF). The acidic aqueous work-up followed in the synthesis of aliphatic and aromatic DTPA-AM_2 species (Chapter 2) was unsuccessful in this case due to the presence of the heterocyclic N atom (pKa ~5). Protonation of this residue is expected to occur prior to protonation of the second carboxylate (pH ~ 4.6) increasing the solubility of the ligand in aqueous media. Any solid obtained from the reaction by trituration with an organic solvent was extremely hygroscopic.[137] Problems were also encountered in removal of the excess amine, which associated with the carboxylates forming $RNH_3^+CO_2^-$ salts. Removal of the excess amine could be achieved using an aldehyde scavenger resin[92, 97] to form an imine supported on the solid phase (Figure 4-3). Filtration of the reaction mixture afforded clean DTPA-PYA in solution (DMF).

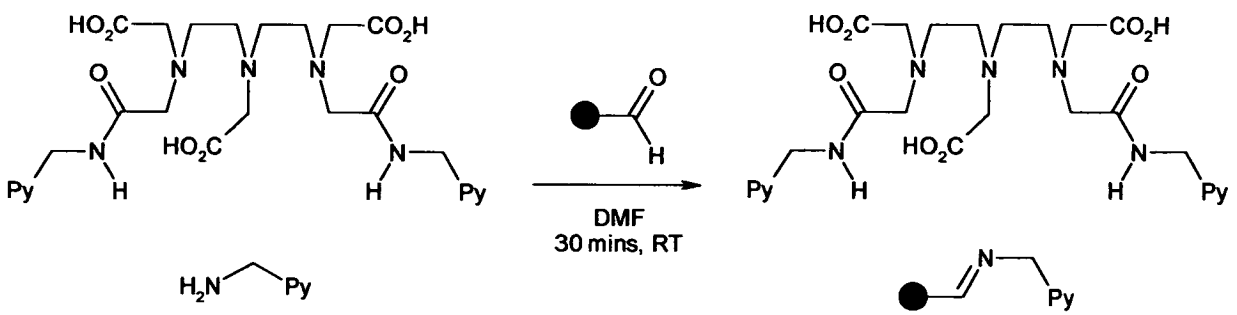

Figure 4-3 Use of a scavenger resin to remove excess amine from the reaction mixture

The principle was applied to the solution phase reaction, employing benzaldehyde as the scavenger (Figure 4-4) and extracting the imine into chloroform. No free amine ^1H resonances were observed in the NMR spectrum of the product (Figure 4-5).

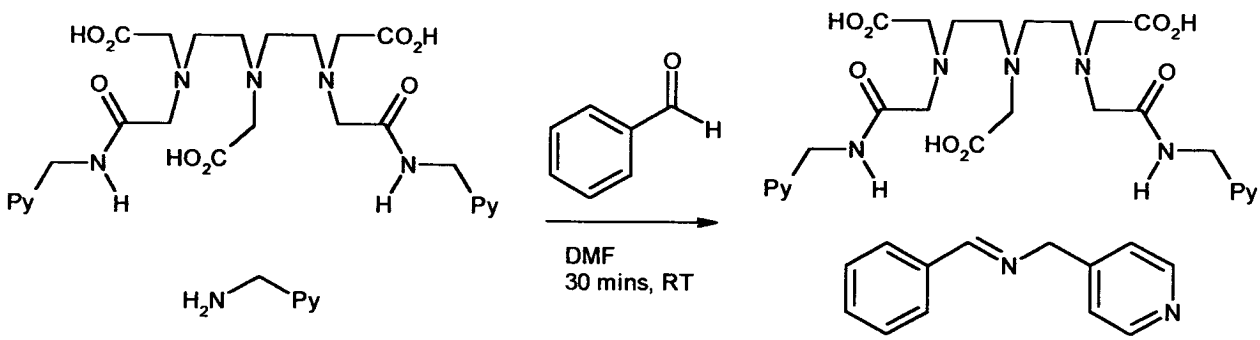

Figure 4-4 Imine scavenging in the solution phase purification of DTPA-PYA

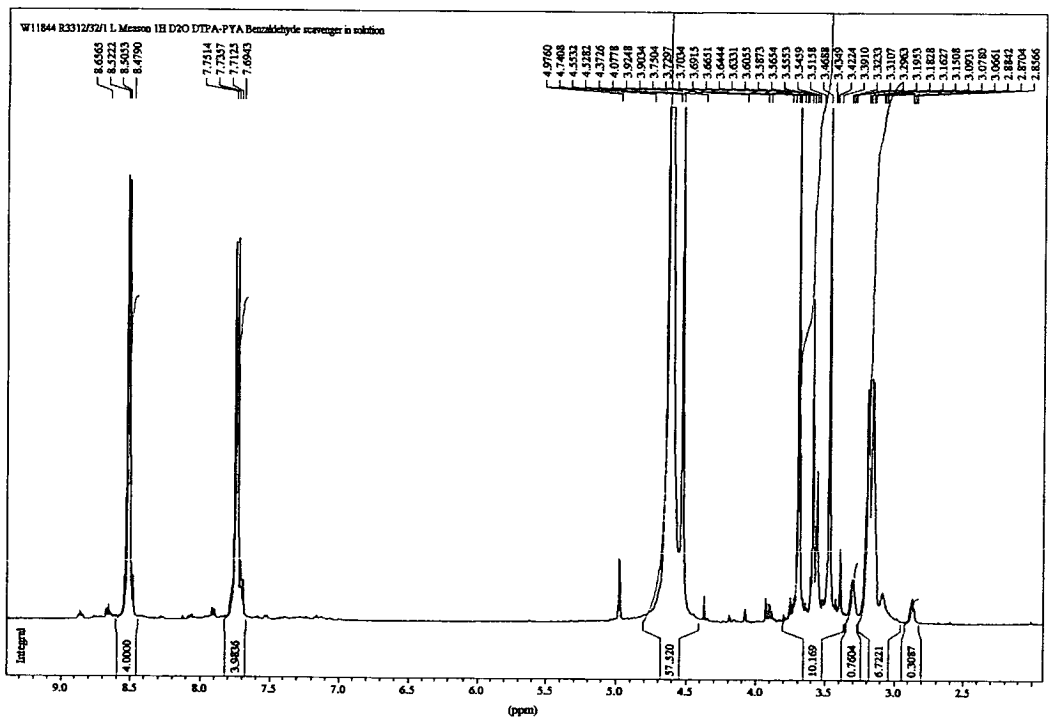

Figure 4-5 ^1H NMR spectrum of DTPA-PYA following treatment with benzaldehyde scavenger

Whilst scavenging using an aldehyde reagent is an option with aromatic amines this is not the case when simple aliphatic primary amines are employed, due to the reduced stability of the product imine. Solid phase synthesis using inert resin supports was attempted offering a potential synthetic route to asymmetric DTPA-bis(amides) (Figure 4-6) (Scheme 2-3). Such methods are routinely applied in the generation of large compound libraries in drug discovery and new technologies are continually evolving.[92, 97, 149-150]

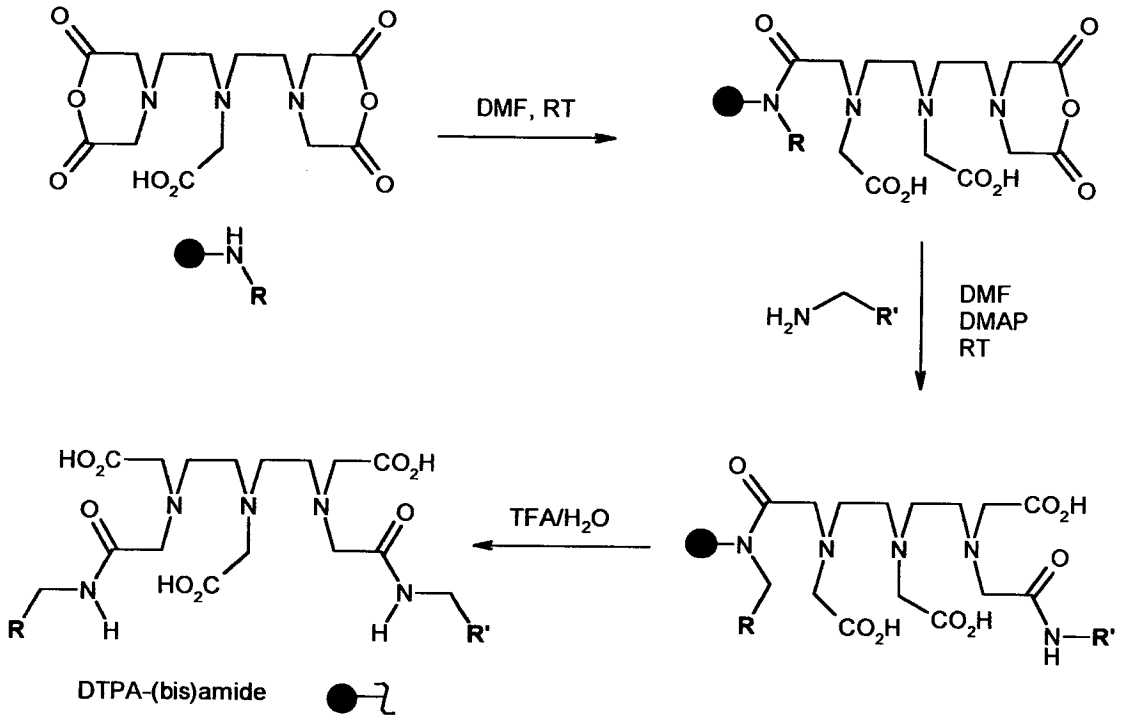

Figure 4-6 Schematic solid phase synthesis of asymmetric DTPA-AM_2 ligands

Conventional methods for attachment of metal (Ln^{3+} and radioisotope) DTPA chelates to biological molecules of interest proceeding via the dianhydride reagent are generally non-specific and allow multiple labelling to occur.[61-83]

By forming asymmetric DTPA-bis(amide) ligands the potential to introduce such functional groups as amines, N-hydroxysuccinimide esters and isothiocyanates selectively to one arm of the ligand, specific functionalities within the biological molecule of interest can be targeted (e.g. -SH in cysteins, N=C=S + NH_2 of lysine etc) (Figure 4-7, Scheme 1-1).[9]

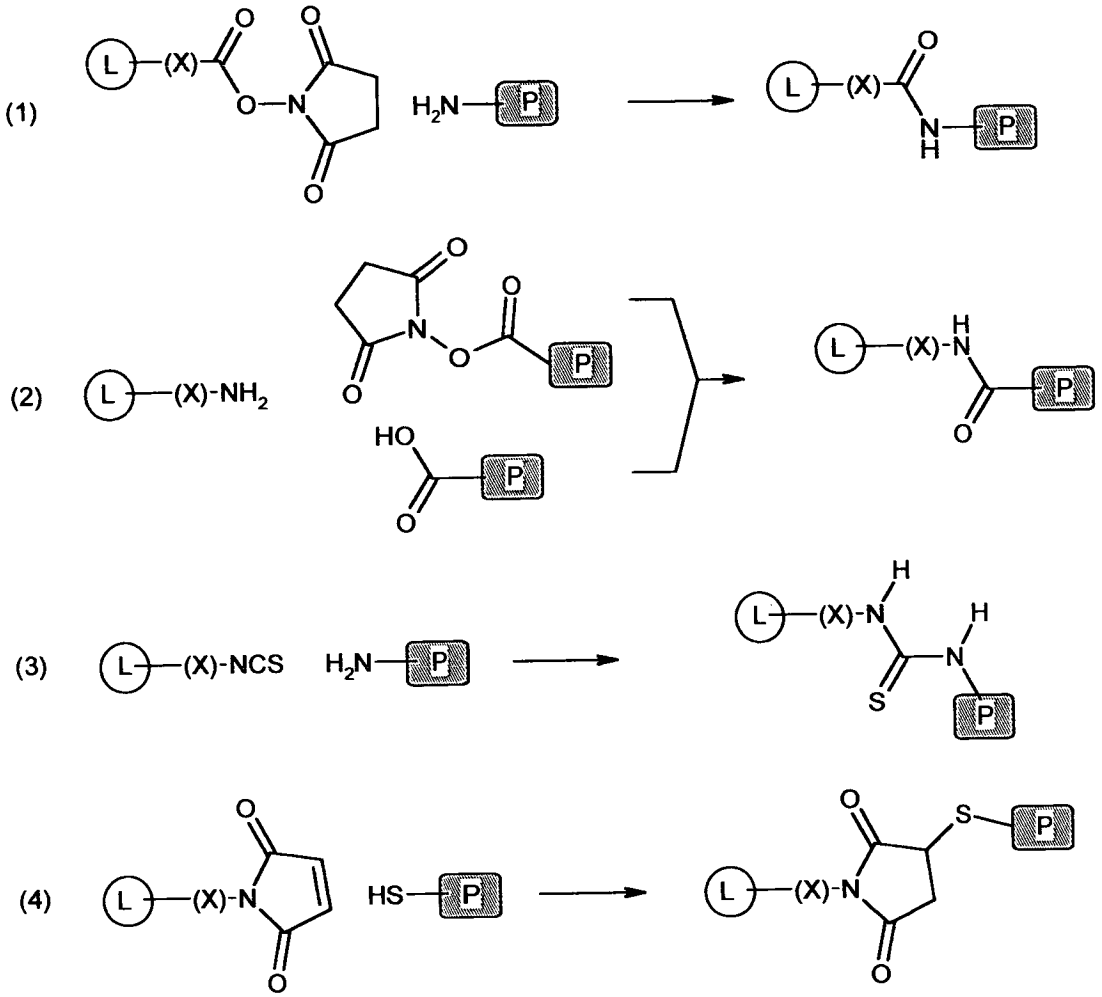

Figure 4-7 Schematic labelling processes: L = label; P = protein; X= spacer unit

The solid phase synthesis (Scheme 2-3, Figure 4-6) was initially performed using only one amine reagent in order to optimise reaction conditions. The amine (4-methylbenzylamine) was loaded on to the resin using conventional solid phase methodology.[149] This was then reacted with an excess of DTPA-dianhydride in dry DMF forming the DTPA-mono(amide) on the solid support. Unreacted dianhydride was washed from the resin with DMF prior to addition of the second equivalent of amine. Careful rinsing of the resin was required following reaction of the amine to ensure removal of the excess reagent. This was achieved using EtOAc/AcOH to form the acetate salt of the amine. Any remaining acid was then removed as the ammonium salt upon washing with EtOAc/NH_3. The resin was finally washed with DCM and MeOH to rinse off all excess reagents prior to cleavage of the product from the resin. Cleavage was performed using TFA (95): H_2O (5) breaking the

secondary amide bond between the linker and product. NMR analysis (Figure 4-8) and LCMS confirmed the formation of DTPA-bis(tolylamide).

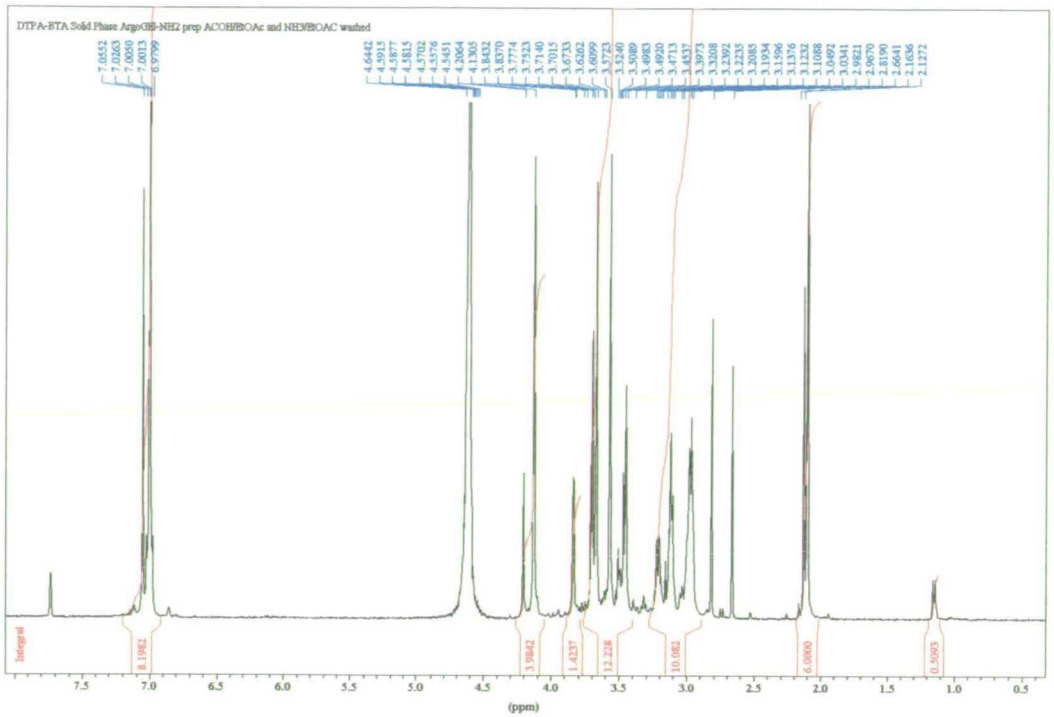

Figure 4-8 ^{1}H NMR spectrum of DTPA-BTA prepared using solid phase methodology

Preparation of asymmetric DTPA-AM_2 ligands by this method was found to be unsuccessful. The major reaction product was the symmetrical amide formed during the first step of the reaction due to rapid coupling between the dianhydride and solid-supported amine. This rapid coupling was found to occur in both pyridine and DMF and in the presence of a large excess of DTPA-dianhydride reagent. The subsequent steps attempted with primary amines (1-butylamine, cyclohexylamine, benzylamine and 4-picolylamine) simply resulted in symmetrical amide products (LCMS, NMR) with little or no evidence of reaction of the second amine added.

This route offers potential but requires much further development. It may be possible to devise a synthesis employing different resins and linkers[92, 97, 149-151] to alter the reactivity of the solid supported resin.

4.2 Complex Preparation

The methods employed in formation and isolation of the LnNAL chelates were developed due to inconsistent results obtained upon formation of the species *in situ* in the cuvette. The problems encountered were found to be a consequence of ionic strength of the solution - variable due to the method of formation. Ligand solutions (~ 0.01 M, pH 7-8) were prepared in standard volumetric flasks, into which the solid ligand was accurately weighed, deprotonated with NaOH, then diluted to volume with deionised water. The complex of interest was formed in the cuvette by combining ligand and aqueous rare earth salt solutions (~ 0.1 mM) in equimolar amounts. The pH of the final solution was then adjusted to pH ~ 7 with NaOH. In forming the chelate complex in this way the ionic strength of the solution is unknown and variations exist between samples. In addition, Na^+ association with the ligand carboxylate groups forming the salt may prevent complete ligand-Ln(III) coordination. The presence of Na^+ in high concentrations was also found to have a bearing on ternary complex formation. Variations between the Ln(III)NAL chelate species present in solution and changes in the hydration state can alter the extent to which the complex can interact with the introduced LHC binding unit. At higher Na^+ concentration the presence of free Ln(III) cations cannot be disregarded, interaction of which with the added LHC can lead to greater enhancement of the luminescence and differences in the peak ratios observed (592:616 nm). Such inconsistencies can be minimised by isolation and characterisation (MS, CHN, and NMR) of the chelate complexes prior to their use in photophysical studies. Complexes can be isolated by precipitation from a concentrated aqueous solution upon addition of an organic solvent.

Initial attempts to isolate the Ln(III)NAL chelates gave mixed results. Deprotonation of the ligand with NaOH prior to combination with the metal salt in aqueous solution and subsequent adjustment of the pH to neutrality resulted in the formation of excess NaCl. This co-precipitated with the LnNAL species giving erroneous elemental analyses and unexpectedly large Na^+ peaks in the FAB and ES-MS. The high ionic strength of solutions prepared with these chelates was found to be detrimental to the LHC binding interaction required to form the ternary complex. In addition association between the sodium ion and carboxylate functional groups of the NAL may prevent complete chelation of the metal, as discussed above, although NMR studies with diamagnetic yttrium and lanthanum discussed in Chapter 6 suggest that this is less problematic.

Preparation of EuDTPA-bis(amide) chelates was also attempted using Eu_2O_3 starting material[119] thus eliminating the formation of inorganic salts of the counter ions encountered

in the previous preparations. The metal oxide and appropriate ligand were combined in water and refluxed for approximately 1 hour forming a colourless solution (pH ~ 12). The volume of the mixture was reduced to 1-2 ml and addition of acetonitrile to the concentrated solution instantly afforded a colourless solid. This was collected by filtration, washed with ACN and diethyl ether then dried under vacuum. Mass spectrometry and elemental analysis revealed the compounds obtained in this way to have the expected composition. Luminescence spectroscopy showed characteristic red Eu(III) emission upon excitation at 394 nm. Binding studies with picolinic acid showed some ternary complex formation in aqueous solution, but with very little Eu(III) emission enhancement. This is attributed to the coordination of OH to the metal during complex preparation. Although the formation and co-precipitation of NaCl is avoided, the coordination of OH is not, as shown by the equation for the reaction (Equation 4-1):

$$Eu_2O_3 + 2\ H_3DTPA\text{-}AM_2 \rightarrow 2\ EuDTPA\text{-}AM_2 + 3\ OH^- \qquad \textbf{Equation 4-1}$$

The release of OH^- accompanying the formation of the chelate raises the solution pH. This free OH^- can compete with the bulk solvent H_2O for the ninth coordination site of the lanthanide.[21, 152] This stronger binding interaction between the anionic hydroxide ligand and the metal (relative to neutral water) is more difficult to perturb, thus LHC binding is inhibited and the luminescence of any mixed ligand species is weak. When a more hydrophobic ligand such as DTPA-cyHA or DTPA-BBZA is employed, addition of base to the Eu_2O_3 ligand mixture is required to aid dissolution. The stable H-bonding network present in the solid ligand must be disrupted for solvation to occur as the influence of the metal oxide alone is insufficient. Addition of the base (aqueous TBAOH) to the reaction accentuates the problems encountered due to hydroxide coordination. Using TBAOH in place of NaOH in preparation of the complexes from the Ln(III) chloride salts facilitates removal of the counter-ion salts after precipitation of the chelate. The solubility of TBACl in acetonitrile allows the excess salt formed during the reaction to be removed by washing of the solid obtained.

Exceeding pH 6.5 during preparation results in formation of species containing coordinated OH. Eu(III) has a pK_a value of about 6.5 in water and $Eu(OH)_3$ is known to precipitate from solutions at high pH (>8).[21, 148] In some cases the pH reached was as high as 12 or 13 and a fine suspension was observed in the solution which was attributed to formation of insoluble metal hydroxide species. The DTPA-AM_2 ligands coordinate the metal in an octadentate manner through the 3 carboxylates, 2 amide carbonyls and 3 diethylenetriamine nitrogen

atoms. A water molecule occupies the ninth coordination site of the metal.[117] At high pH this water can form a more strongly coordinating hydroxide, displacement of which by a competing ligand (LHC) is more difficult. Consequently, ternary complex formation becomes more difficult and the resultant species is less luminescent than the corresponding complex prepared at lower pH.

The anionic complexes of $[LnDTPA]^{2-}$ have been studied extensively as a result of their application in MRI[108-116]. The crystal structure of the Nd(III) complex[113] and NMR relaxation studies (H_2O exchange and ^{17}O NMR spectroscopy) show that only one water molecule coordinates the metal in aqueous solution.[108] Supporting evidence is provided by potentiometric titrations and studies of luminescence as a function of pH, in which it was established that formation of the 1:1 complex is complete by pH ~ 3 and that the luminescence intensities and lifetimes are unchanged between pH 3 and pH 12. This is in contrast to the ligands EDTA, HEDTA and TTHA which each exhibit variation in the photophysical properties with pH, due to oligomer formation at high pH, confirmed by energy transfer studies in mixed Eu^{3+}/Tb^{3+} systems.[152]

Similar studies performed with DTPA-bis(amide) ligands[117-128, 130-137] reveal that they fulfil their octadentate binding potential with Ln(III) cations in aqueous solution, with only one water molecule coordinated. NMR relaxation experiments simply reveal that the water molecule is coordinated to the metal centre, and do not permit differentiation between OH and H_2O. Similarly, lifetime measurements on the chelates in solution cannot distinguish between a coordinating OH ligand and a water molecule. Mass spectrometry does not detect the OH/H_2O and the difference in composition of only one proton cannot be established by elemental analysis. The situation is further complicated by the fact that Ln-OH formation is a process in equilibrium, the position of which, and hence the percentage of chelate in the OH form is unknown.

All chelates used in the screening experiment (Chapter 5) and photophysical studies discussed in Chapter 6 were precipitated from water with acetonitrile at pH 5-6 following pH adjustment with TBAOH (40 % w/w H_2O). The ligand was dissolved in the $LnCl_3$ solution prior to addition of base. The chelates were characterised in full by mass spectrometry (ES-MS), NMR (Y^{3+} and La^{3+} diamagnetic analogues) and elemental analysis. The photophysical properties were studied by luminescence spectroscopy (under steady state and pulsed excitation).

Attempted formation of the diamagnetic lanthanum complexes with the more hydrophobic DTPA-AM_2 ligands (cyHA, BTA, NBA) for NMR analysis was in many cases unsuccessful due to their limited solubility in aqueous media. A colourless solid immediately precipitated upon combination of DTPA-cyHA and $LaCl_3$ in water. Similarly, DTPA-BTA resulted in formation of an insoluble colourless solid with La(III) that could not be analysed by NMR. The Y(III)DTPA-AM_2 analogues were prepared successfully and were soluble in concentrations suitable for study by NMR. It was hoped that some interaction between the protons of the amide arms and the aromatic LHC could be detected upon molecular recognition. With La(III) some splitting and sharpening of the NAL resonances was observed, attributed to a conformational locking effect (Chapter 3) discussed in more detail in Chapter 6, but no such splitting/sharpening was seen with the Y^{3+} complexes.

In conclusion, the method of preparation of the Ln(III)DTPA-AM_2 chelates has a large influence on the molecular recognition processes involved in ternary complex formation. The pH of the EuNAL solution must not exceed pH 5-6 prior to precipitation of the complex, minimising the extent of Eu-OH coordination. Tetrabutylammonium hydroxide solution can be employed to raise the pH of the solution thus avoiding the problems of NaCl co-precipitation encountered when NaOH is used.

5 Combinatorial Screening

5.1 The Experiment

A novel approach to the development of highly luminescent mixed ligand chelates is to employ combinatorial screening technologies – well-established methods in modern drug discovery.[15-18] The process is shown schematically in Figure 5-1. Screening of diverse compound libraries enables identification of potential LHCs in a manner analogous to the initial discovery and target validation in pharmacophore identification. Performing spectroscopic studies in microplate format (96 well) allows the luminescence triggered upon recognition between a large number of LnNAL/LHC combinations to be studied in a short space of time. Potential light harvesting centres can be identified quickly, the effect of the NAL on the interaction evaluated, and structure/activity relationships determined.

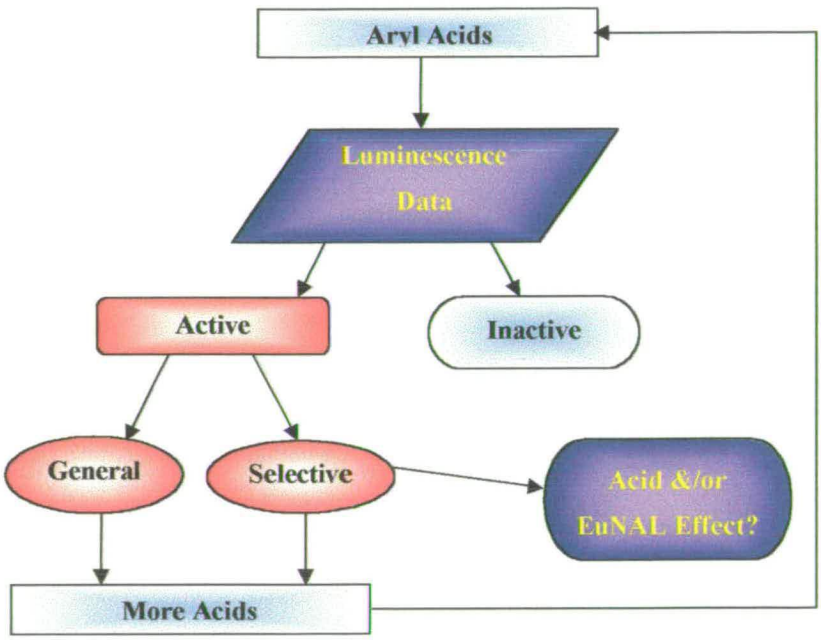

Figure 5-1 Schematic Representation of High Throughput Screening as applied to the development of novel luminescent mixed ligand chelates

A selection of DTPA-bis(amide) derivatives were prepared in order to introduce a variety of structural and electronic properties to the LnNAL chelates. The amide nitrogen of the ligand does not participate in coordination to the metal, thus leaving the arms free to form a cavity occupied by one water molecule in the absence of a competing ligand. The NALs chosen for study by combinatorial screening methods are shown in Figure 5-2 below.

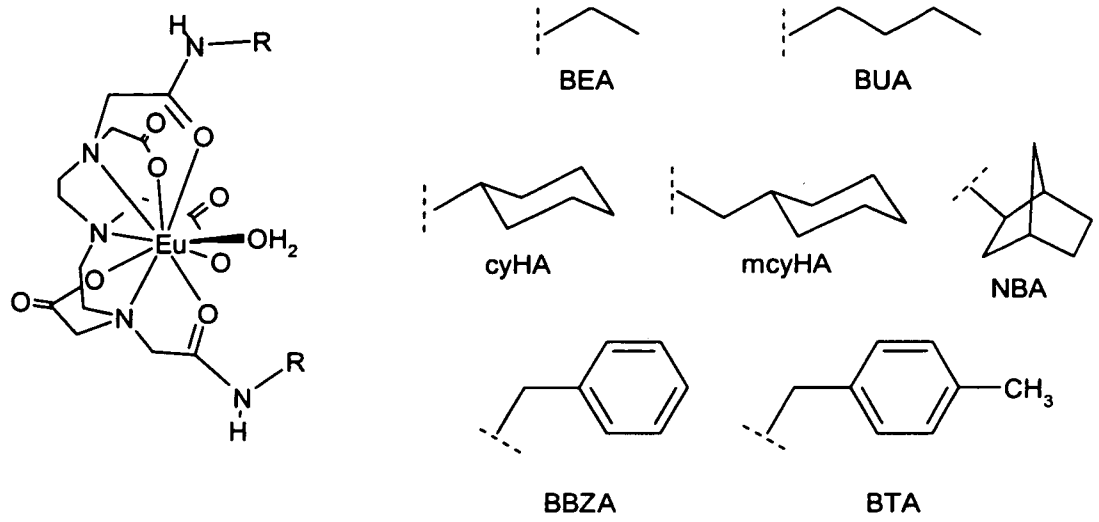

Figure 5-2 Structures of EuDTPA-bis(amide) derivatives screened for molecular recognition with aromatic carboxylic acids by combinatorial methods

The effects of hydrophobicity, rigidity, steric hindrance and π-interactions on the formation of mixed ligand species were investigated by comparison of the luminescence observed upon molecular recognition between aryl acids and the chosen LnNAL chelates. Potential LHCs were chosen on the basis of the ternary complex model system discussed in Chapter 3. The "model" chelate, EuBEA, demonstrated recognition at a molecular level with the simple aromatic carboxylic acids shown in Figure 5-3. Picolinic acid is a better sensitiser of Ln(III) emission than either the bidentate phthalic acid or the weakly binding monodentate benzoate LHC.

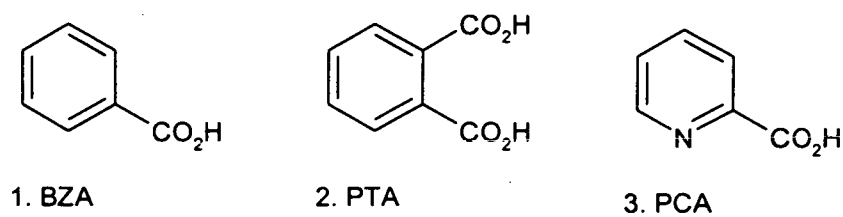

Figure 5-3 Benzoic (BZA), phthalic (PTA) and picolinic (PCA) acids

Aromatic acids bearing at least one carboxylate substituent covalently attached to the ring were selected to provide a representative set of the potential LHC compounds available within GlaxoWellcome's structural database. The chosen acids represent a wide range of

structural and electronic characteristics and were chosen to ascertain which features are important to the molecular recognition processes involved in the controlled formation of luminescent mixed ligand species. Structures of the acids screened in the three iterations of the assay and the experimental results obtained are shown as SMILES strings in Appendix 2. Due to the large volume of data generated only the more interesting observations are discussed. Data directly compared were obtained under the same experimental conditions on the same day. The excitation wavelength employed (275 +/- 10 nm) was selected using the fixed wavelength filter slides provided by *Tecan*. Consequently, variations in λ_{max} and/or ε_{max} of the acids are not accommodated for in the screen. The experiment was performed around neutral pH.

The assay results are discussed in two sections, treating individually the selectivity induced by LHC and NAL characteristics. Consideration is given to a series of physicochemical effects:

1) Hydrophobicity
2) Carboxylate stability
3) Triplet state energies
4) Triplet yield
5) Molar absorptivity at the excitation wavelength
6) Micelle formation

5.2 *LHC Induced Molecular Recognition*

5.2.1 Saturated Alkyl Substitution on the Phenyl LHC Unit

We know from our preliminary experiments with EuBEA (Chapter 3) that benzoic acid binds the metal centre weakly, resulting in a 10-coordinate ternary species with 1:2 stoichiometry. The effect of substitution on this simple aromatic acid was investigated. Firstly we noticed that when an aliphatic "tail" is incorporated on to the LHC the luminescence of the mixed ligand species is greatly enhanced relative to the mixed ligand EuBEA:BZA complex. Compounds GR203309X, GR241592X, GR207127X and GW399139X (Figure 5-4) best illustrate this effect.

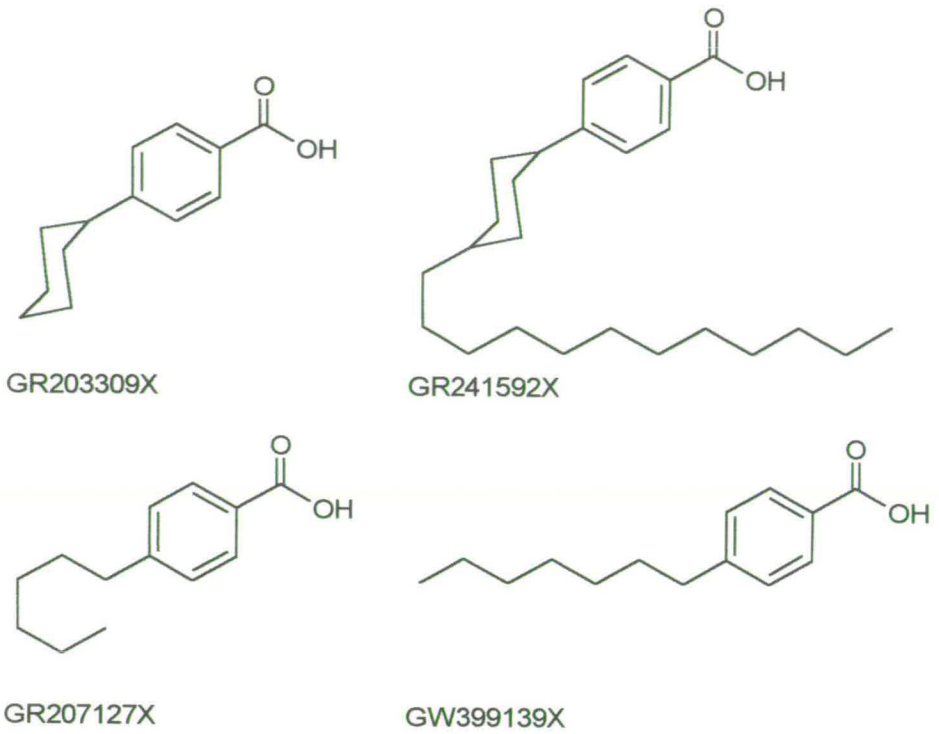

Figure 5-4 4-alkyl-substituted benzoic acids

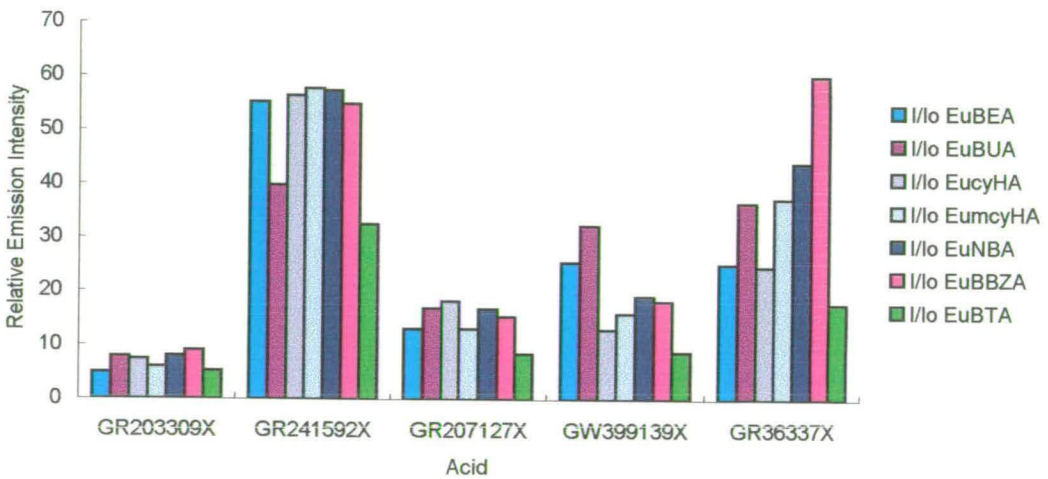

Chart 5-1 Relative emission intensity (I/I_0) upon interaction of acids GR203309X, GR241592X, GR207127X and GW399139X with the EuNALs

With a straight chain alkyl substituent at the 4-position of the aromatic ring a dramatic improvement in the luminescence of the ternary complexes formed with our EuNALs is

observed. The relative emission intensities arising upon molecular recognition with the chelates are shown in Chart 5-1.

Compound GR207127X (4-hexylbenzoic acid) affords ~ 15-fold enhancement of the parent EuNAL emission, as does acid GW399139X (4-heptylbenzoic acid), pictured above in Figure 5-4. The acid chromophore and binding unit are unchanged with respect to benzoic acid (Figure 5-3) as the effect of alkylation on the electronic properties of the system is negligible. We therefore attribute the marked improvement in activity observed with these acids to a "shielding" effect introduced by the aliphatic chain. The hydrophobic nature of the substituent group protects the cavity from attack by outer-sphere solvent molecules, which can quench Eu(III) luminescence by non-radiative energy transfer to the O-H oscillators.[44, 45] Further evidence in support of this is provided by the most effective of the acids illustrated here, GR241592X, which results in a 60-fold increase in sensitised Eu(III) emission under the same experimental conditions.

It is proposed that introduction of the cyclohexyl component to the aliphatic tail provides additional protection from the outer sphere solvent molecules due to the increased rigidity, hydrophobicity and steric bulk of the substituent. It is interesting to note that with only a cyclohexyl ring, acid GR203309X is much less efficient as a sensitiser for our EuNALs. We attribute this observation to two possible factors:

1) The steric bulk of the cyclohexyl group, without the further alkyl substitution can readily undergo ring-flip isomerisation, clashing with the amide arms of the NAL. Consequently the strength of the binding interaction and the degree of orbital overlap is likely to be diminished with respect to the straight chain alkyl derivatives. Despite this impediment, acid GR203309X remains a much better LHC for our EuNALs than unsubstituted benzoic acid.

2) The long chain substituent group at the 4-position on the cyclohexyl ring of acid GR241592X (twelve carbons in length) is likely to be quite surfactant-like in character, encouraging micelle formation with the effect of excluding outer sphere water molecules from the Eu(III) coordination environment.

Another acid of this type exhibiting good potential as a sensitiser for our mixed ligand system is GR36337X (3-octylbenzoic acid, Figure 5-5). This acid bears an *n*-octyl

substituent in the 3-position. The relative emission increase observed upon molecular recognition with the EuNALs is of similar magnitude to the 4-substituted acids discussed above (~50-fold) – but slightly stronger than the hexyl and heptyl derivatives (I/I_0 ~30).

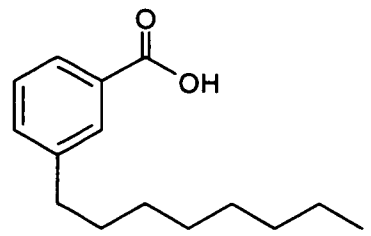

GR36337X

Figure 5-5 3-octylbenzoic acid

The efficiency of this acid as a LHC for the EuNALs studied is again due to the presence of the aliphatic tail, providing an "umbrella" type effect, since the chromophore and binding unit are unchanged with respect to benzoic acid.

The "umbrella" effect has been observed in other cases. The DELFIA immunoassay system, discussed in Chapter 1.1.4, also exploits a mixed ligand Eu(III) chelate. The enhancement solution contains a tris-*n*-octyl phosphine ligand (topo) in addition to the sensitising β-diketonate, the purpose of which is to form an "umbrella" around the complex excluding outer-sphere solvent molecules.[74] Previous research in the Pikramenou group into novel luminescent lanthanide assemblies has lead to the design of luminescent spheres, in which the steric bulk of the tetraphenylimidophosphine (tpip) antenna ligand (Figure 5-6) was increased such that no water molecules could approach the metal centre.[153]

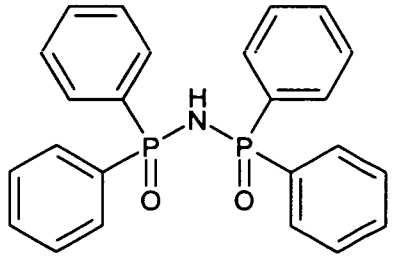

tpip

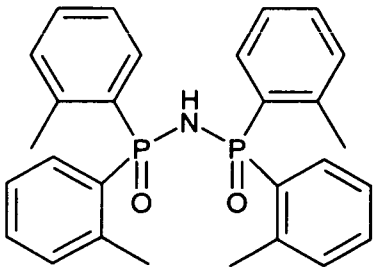

mtpip

Figure 5-6 Antenna ligands tpip and mtpip. Outer sphere water molecules are excluded from the core upon increasing the steric bulk of the aromatic substituents.

Another example of such a phenomenon is in the shielding of the triplet state of bromonaphthalene from the quenching effects of molecular oxygen by the protective hydrophobic cavity of cyclodextrin molecules.

The effect of straight chain and cyclic aliphatic substituents is also observed with the picolinate (PCA) binding unit (Figure 5-7). Under continuous excitation we observe PCA to form a highly luminescent ternary complex with EuBEA in aqueous solution (Chapter 3), attributed to the strength of its bidentate binding interaction with the metal, and closely matched excited state energies facilitating efficient intramolecular energy transfer.

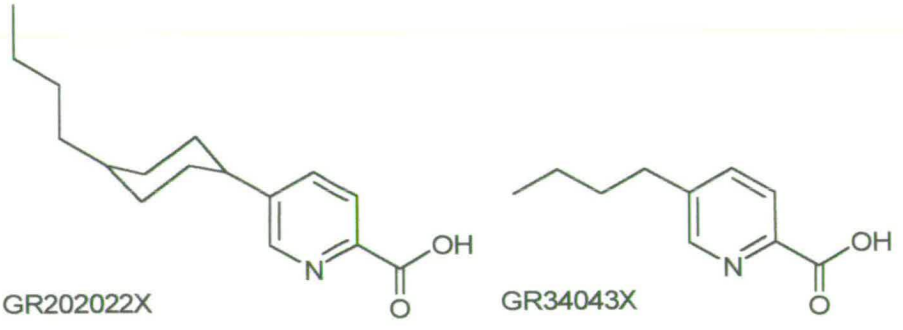

Figure 5-7 5-alkyl pyridine2-carboxylic acids

Here it is noted that acid GR202022X gives rise to an intensely luminescent species, increasing the EuNAL emission ~ 120-fold (Chart 5-2). In common with GR241592X this acid bears a substituted cyclohexyl ring in the aliphatic tail group, acting as an efficient shield. The smaller *n*-butyl derivative GR34043X, whilst enhancing the emission ~ 20-fold, is a less efficient sensitiser than its bulkier counterpart.

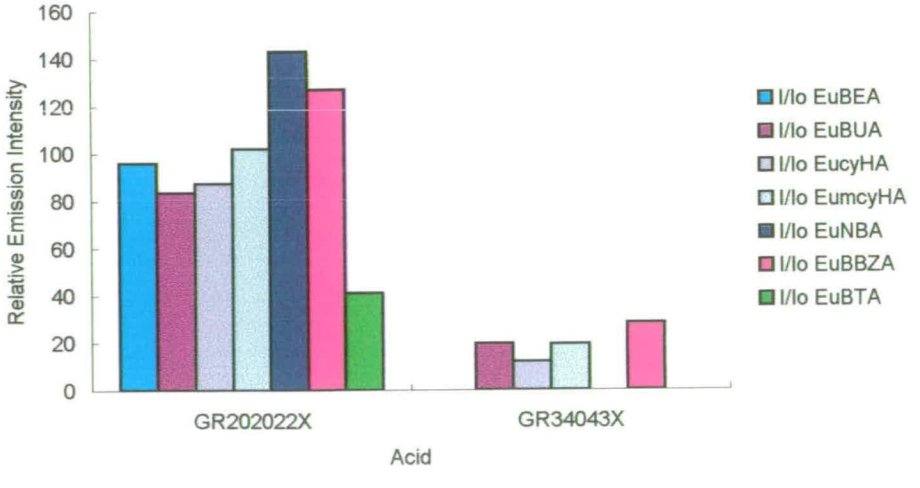

Chart 5-2 Relative Emission Intensities observed upon recognition between EuNALs and alkyl-substituted picolinic acids

5.2.2 Unsaturated Substitution on the Phenyl LHC

A logical progression from the saturated substituents is to investigate the influence of unsaturated alkyl substituents (Figure 5-8) upon a molecular recognition event.

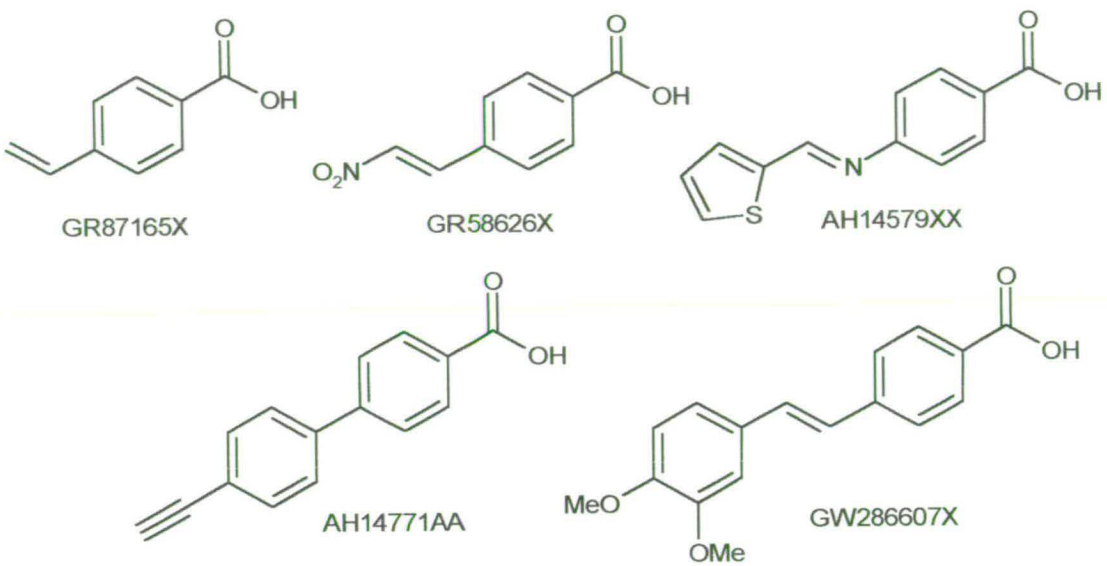

Figure 5-8 Benzoic acids bearing unsaturated substituents

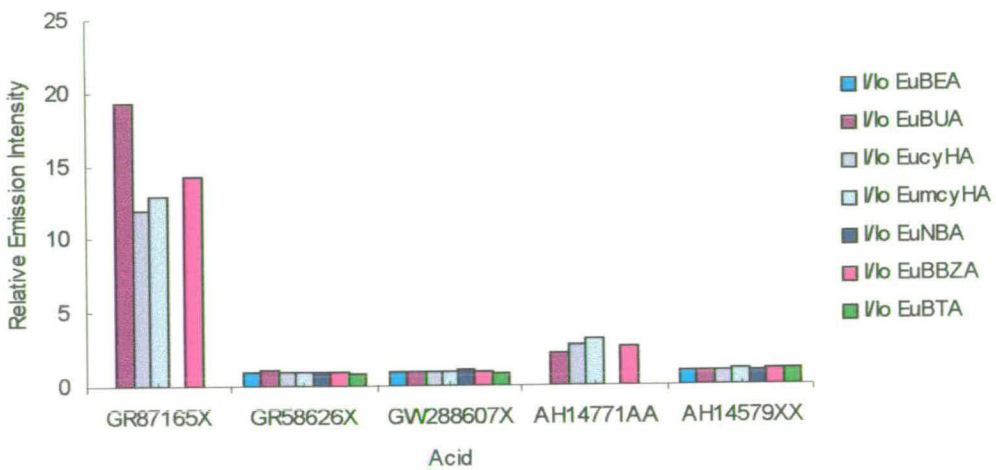

Chart 5-3 Relative emission intensities observed upon interaction between the EuNALs and the acids bearing unsaturated substituent groups

It is notable that only one of these acids (GR87165X) interacts with the EuNAL resulting in sensitised metal emission, as illustrated by Chart 5-3.

In contrast to the saturated substituents that have little effect on the electronic structure of the acids, the functional groups chosen can withdraw electron density from the aromatic ring. Whilst such an effect lends stability to the carboxylate anion relative to the protonated form, the extended conjugation reduces the energy of the aromatic system. The triplet-state therefore may be expected to lie at a lower energy than that of the parent acid. Only one of these acids results in any sensitised EuNAL luminescence. Compound GR87165X bears one double bond in addition to the aromatic system and enhances the emission ~15-fold. In this case, the electronic influence of the unsaturated substituent is likely to be responsible for an improved binding interaction with the metal relative to benzoic acid. The 15-fold increase is of similar magnitude to that observed with acids GR207127X and GW399139X (Figure 5-4) bearing straight chain alkyl substituents in the 4-position, in which electronic influences of the substituent are negligible. The other unsaturated acids tested exhibit extended conjugation, reducing the triplet state energy to a level too low for efficient intramolecular energy transfer to the metal. Here we have our first encounter with a nitrated aryl acid, GR58626X, and note that the Eu(III) emission is not enhanced with respect to the parent chelate. The powerfully electron withdrawing nitro substituent lowers the overall energy of the aromatic system. Low energy $n\pi^*$ transitions lower the sensitiser triplet state energy of the compound, rendering it inactive towards our EuNAL chelates. Competitive coordination by the nitro group is unlikely to occur in aqueous solution, thus the influence of excited state LMCT between the nitro functionality and Eu(III) on the system can be disregarded under these experimental conditions.

5.2.3 Alkoxy-subsituted Benzoic Acids

Introduction of an ether linkage between the aryl head group and the substituent allows the influence of a wide variety of substituent tails on the formation of mixed ligand complexes to be investigated. Several aromatic and aliphatic derivatives were studied and a striking array of activities observed. Firstly we will examine the straight and branched chain saturated derivatives of the generic structure shown in Figure 5-9.

Acid	n	Chain	I/I0 EuNAL
GR34543X	0	1	1
GR30476X	3	4	2
GR208752X	4	5	9
GR30894X	5	6	12
GR30893X	7	8	29
AH20078XX	9	10	28
GR33911X	11	12	24
GR65884X	13	14	28
GR65815X	15	16	20
GR208554X	17	18	12

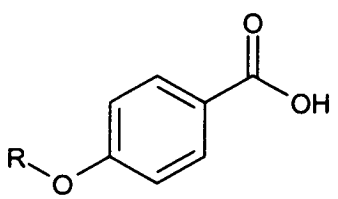

$R = -(CH_2)_nCH_3$

Figure 5-9 4-alkoxy-benzoic acids

in solution cannot be disregarded, which would lead to false signals, the result of scattering from colloidal particles.

A variety of compounds bearing chains of 3-6 carbon atoms in length (Figure 5-10) were studied and a range of activities observed as expected. For example, acid GR155589X bears a primary alcohol functionality at the terminus of the substituent chain and does not form luminescent ternary species with the EuNALs studied here. We propose that this is the result of non-radiative energy transfer from the Eu(III) excited state to the higher vibrational overtones of the OH oscillator, depopulating the emissive state of the metal preventing observation of sensitised emission. Although not likely to penetrate the inner coordination sphere of the metal, the hydrophilicity of the substituent chains may encourage outer sphere water molecules to solvate the metal via hydrogen bonding interactions. Acids CCI9740 and GR53056X provide evidence in support of this. Both bear at least one OH substituent in the "tail" group and neither form luminescent mixed ligand complexes with our EuNAL chelates in aqueous solution.

In contrast, 4-hexyloxy-3,5-dimethylbenzoic acid, GW288377X, (Figure 5-10) improves the interaction relative to the mono-substituted acid due to the increased degree of protection provided by the methyl groups either side of the tail, which bears no additional hydrophilic substituents.

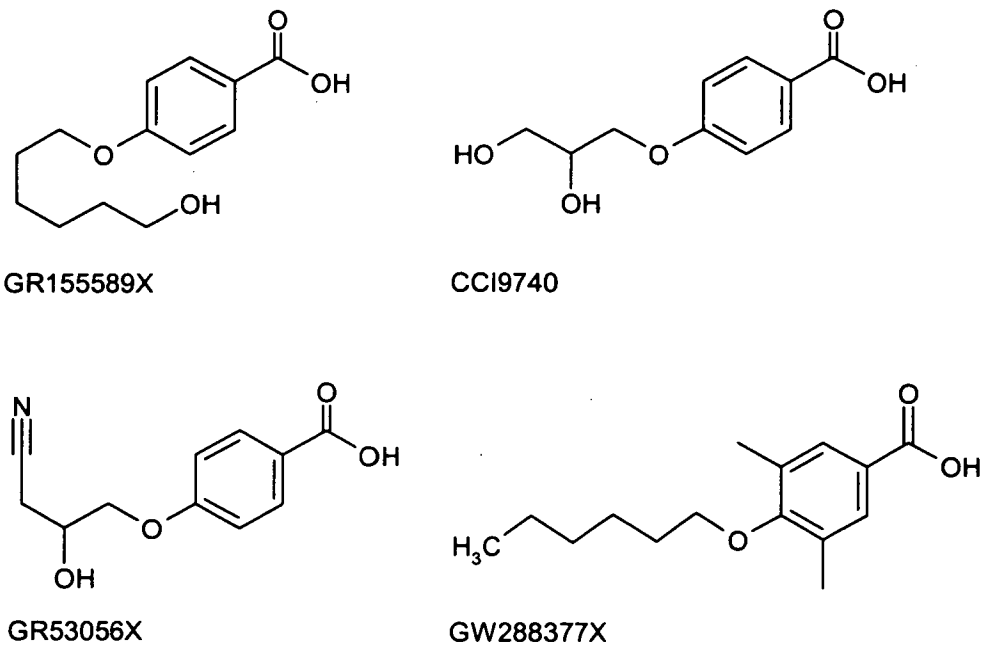

Figure 5-10 Alkoxy-substituted benzoic acids – the presence of the OH functionality in the tail group is detrimental to the luminescence of the ternary complex

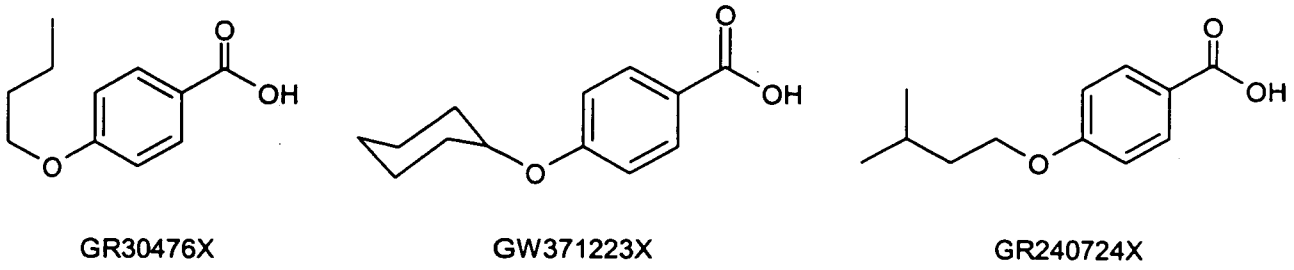

Figure 5-11 4-alkoxybenzoic acids which weakly enhance the chelate emission

In common with acid GR203309X (Figure 5-4) discussed in 5.2.1, the presence of a simple mono-substituted cyclohexyl group on the acid (GW371223X) does not enhance the sensitisation upon molecular recognition with the EuNALs, and the signal detected is similar to that observed with the straight chain *n*-butyl derivative GR30476X (Figure 5-11).

With a branched chain substituent a range of activities is observed, the best of which is obtained with GR54392X (Figure 5-12). This acid bears a methylated alkyl chain and a cyclohexyl group, and is capable of excluding outer-sphere solvent molecules to the extent that the benzoate/EuNAL interaction enhances EuNBA luminescence almost 200-fold (Chart 5-5).

The analogous acid GR57352X (Figure 5-12), without the methyl group at the 2-position of the alkyl chain achieves less than half this effect. The selectivity is attributed to additional protection of the cavity provided by the methyl substituent. Similarly the isopentyl derivative, GR240724X (Figure 5-11) forms luminescent mixed ligand complexes, and is observed to be about twice as effective as the straight chain butyl compound, GR30476X.

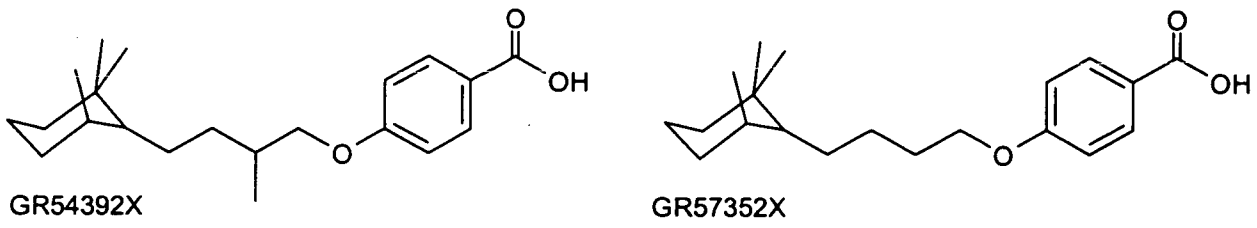

Figure 5-12 4-alkoxybenzoic acids which greatly enhance the chelate emission

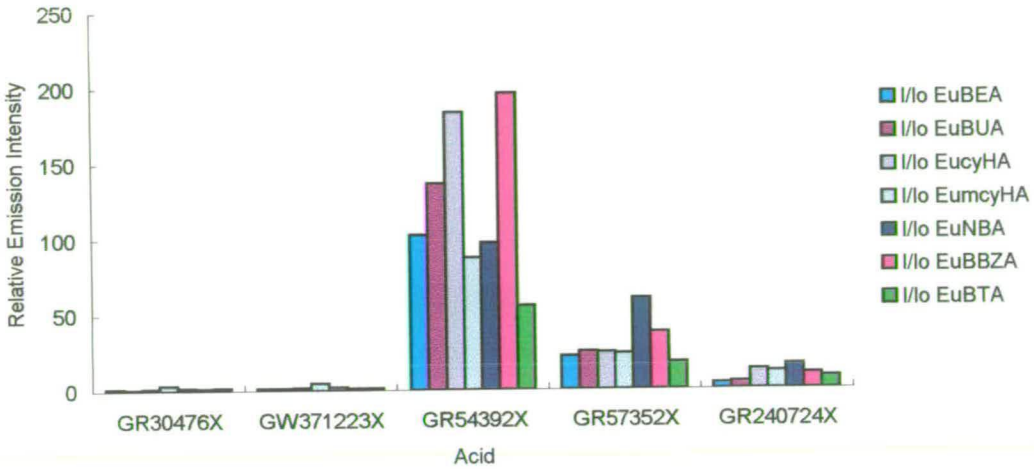

Chart 5-5 I/I_0 observed upon interaction between alkoxy substituted aryl-acid LHCs and the EuNALs

The influence of the alkoxy substituent position on the luminescence of the mixed ligand complex has also been considered. The relative emission intensity observed upon combination of the acid and the chelate is plotted below in Chart 5-6. Upon comparison of the *meta* and *para* substituted acids, the maximum emission intensity is achieved for an alkyl chain length of 10-12 carbon atoms.

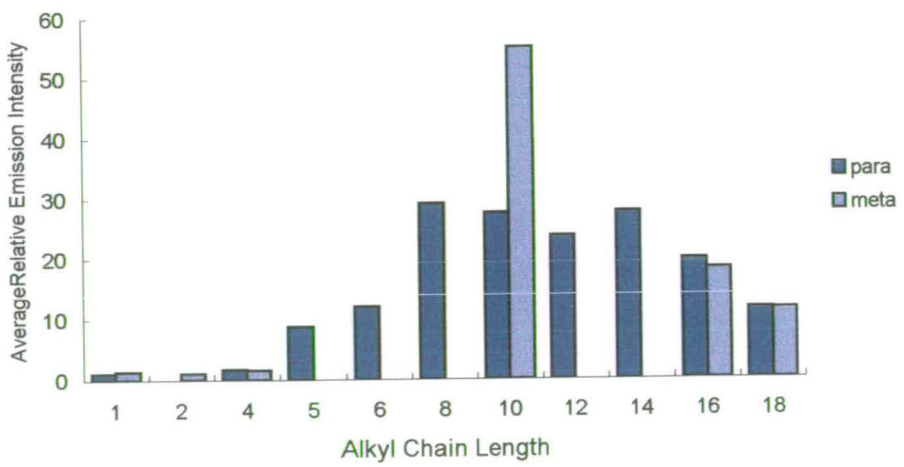

Chart 5-6 Average EuNAL relative emission increase versus chain length: comparison between *meta* and *para* substitution

5.2.4 Aromatic Substituents on the Phenyl LHC Unit

Another interesting class of acids bearing long chain substituents incorporates those with a second, propyl-substituted aromatic ring (Figure 5-13).

Acid	n
GR64693X	2
GR55424X	4
GR55422X	5
GR55423X	6
GR61326X	8
GR61891X	9
GR61984X	10
GR61985X	12

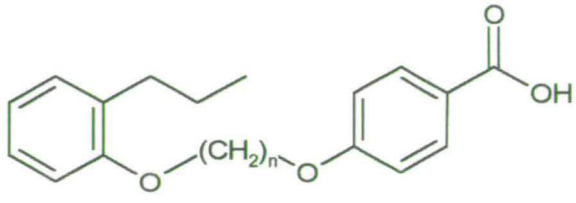

n = 2,4,5,6,8,9,10,12

Figure 5-13 4-alkoylbenzoic acids bearing a substituted phenoxy tail group

The average relative emission increase upon molecular recognition with the EuNALs is presented below in Chart 5-7. Firstly we note the decrease in EuNAL emission observed between a spacer chain length of two and six carbon atoms. With only an ethylene bridge between the two aromatic rings the energy absorbed by the second π-electron system can be transferred to the Eu(III) metal centre to be re-emitted as characteristic red light. As the distance between the two absorbing units is increased the efficiency of intramolecular energy transfer to the metal is decreased, hence the smaller relative emission intensity observed for the LHC with the six-atom spacer relative to that observed with the two-carbon link.[154]

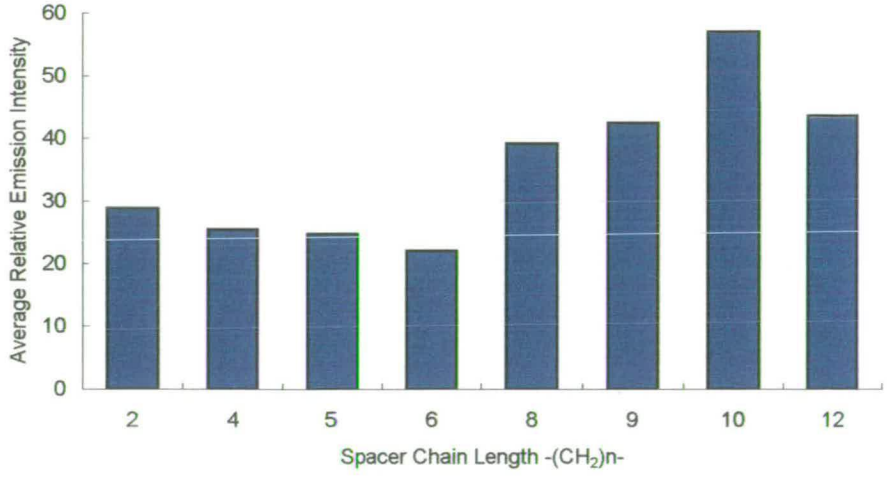

Chart 5-7 The effect of spacer chain length on the emission intensity observed from EuNAL chelates upon molecular recognition with aryl acids bearing a second aromatic ring as part of the substituent chain

As the aliphatic chain between the aryl rings is extended, the lipophilicity of the LHC is increased. We propose that the increasing relative emission intensities observed with the acids bearing a substituent chain of eight or more carbon atoms is due to the improved capacity of the LHC to act as a shield, protecting the metal centre from the quenching effects of outer sphere solvent molecules. The importance of the propyl group on the second aromatic ring is highlighted by the fact that acid GR84408X, without the additional alkyl substituent enhances the EuNAL luminescence by only 5-fold, in contrast to the approximately 30-fold increase observed with compound GR64693X (Figure 5-14).

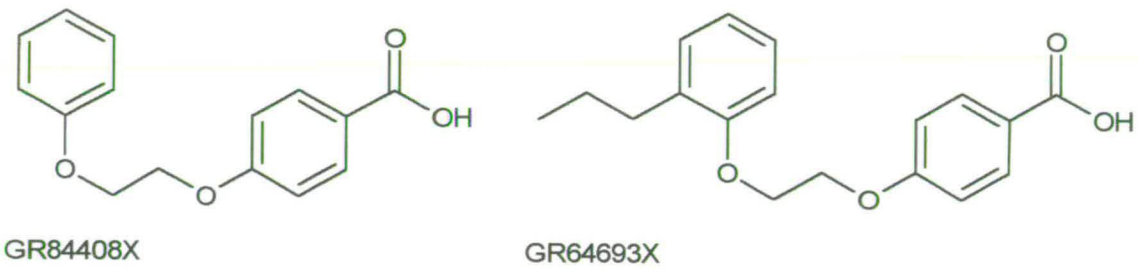

GR84408X GR64693X

Figure 5-14 Additional shielding provided by the propyl substituent on the phenoxy ring is demonstrated by the increased activity of compound GR64693X over GR84408X

The selectivity of molecular recognition with the EuNALs is illustrated below (Chart 5-8). All exhibit good general activity towards the chelates. It is interesting to note that these mono-substituted benzoic acids display a similar pattern of selectivity towards the EuNAL chelate cavity. More intensely luminescent species are formed upon molecular recognition between the acids and the complexes exhibiting well-defined binding cavities (EuBBZA and EuNBA) as expected, an effect discussed in more detail in section 5.3.1 and Chapter 6.

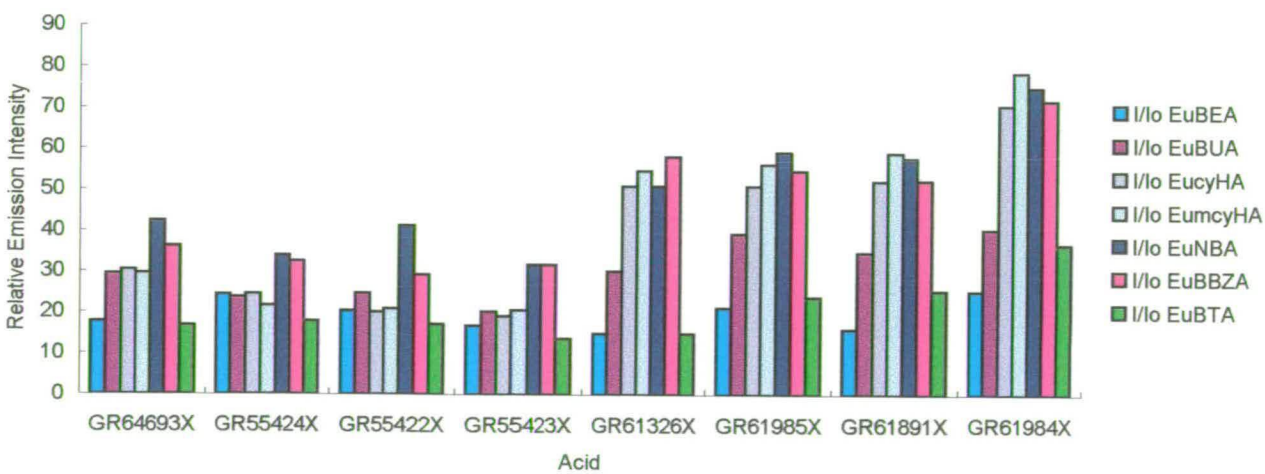

Chart 5-8 Mono-substituted benzoic acids (Figure 5-13, 14) interact well with the EuNALs to form ternary luminescent complexes.

5.2.5 Multiple Substitution on the Phenyl LHC Unit

Interpretation of the influence of multiple LHC substituents on molecular recognition is more complex than evaluation of the effects of mono-substitution. The characteristic Eu(III) emission triggered upon formation of the mixed ligand species is indicative of a molecular recognition event resulting in sensitised europium luminescence. A measure of the strength of any such interaction can be gained from the intensity of the light emitted and direct comparisons between EuNAL/LHC combinations can be made from the qualitative data obtained. Variation in absorbance characteristics of the acids upon substitution of the aryl ring is not accounted for under the experimental conditions since the excitation wavelength is constant at 275 ± 10 nm during the assay. Any subtle but characteristic shifts in the absorption band due to altered electronic properties of the acid are undetected.

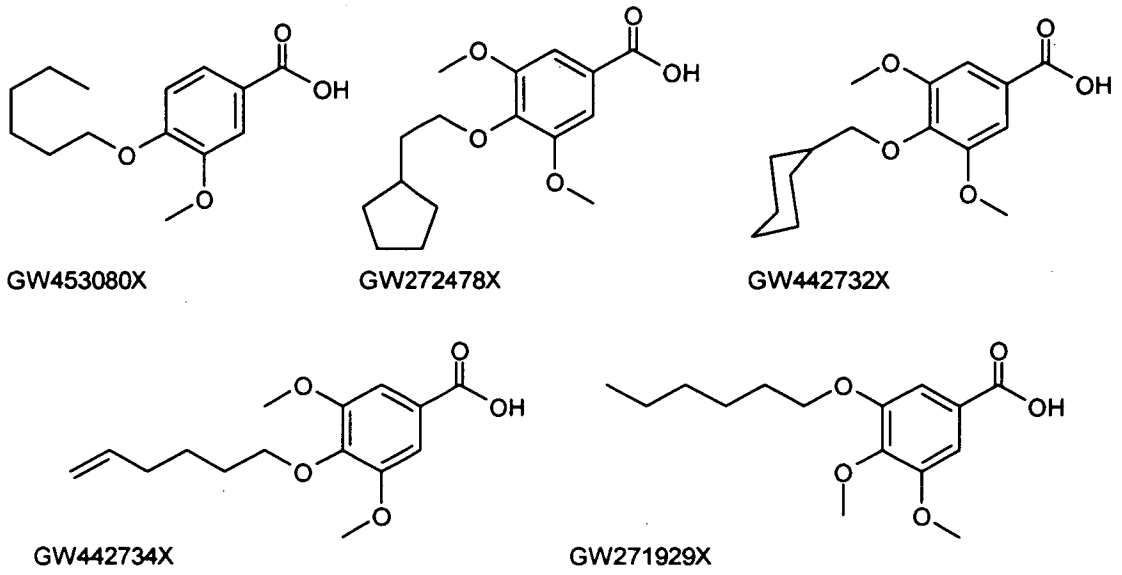

Figure 5-15 Benzoic acids bearing multiple alkoxy substituents

We have demonstrated that the presence of an alkyl chain *meta* or *para* to the carboxylate is beneficial to the luminescence of the ternary complex (5.2 – 5.4) due to its capacity to act as a shield protecting the metal centre from the quenching effects of outer sphere solvent molecules. We have also shown that the electron donating effect of a simple methoxy substituent can destabilise an interaction between the EuNAL and the acid LHC. The

counter-influence of these effects can be evaluated upon considering the interaction between the EuNALs and the acids shown in Figure 5-15.

From the assay data (Table 5-1) it is clear that none of these acids trigger the characteristic Eu(III) emission indicative of ternary complex formation, in contrast to the mono-alkoxybenzoic acids discussed in 5.2.1 and 5.2.3, which on average enhance the chelate luminescence by approximately 30-fold. This can be attributed to a shift in the absorption band away from λ_{exc}.

	Relative Emission Intensity (I/I_0)							
ACID	**EuBEA**	**EuBUA**	**EucyHA**	**EumcyHA**	**EuNBA**	**EuBBZA**	**EuBTA**	**Mean EuNAL**
GW453080X	2	3	2	4	3	3	2	3
GW442734X	2	2	2	4	3	2	2	2
GW272478X	2	2	2	3	3	2	2	2
GW442732X	2	2	2	3	3	2	2	2
GW271929X	2	3	2	3	3	2	2	3

Table 5-1 Relative emission intensity upon interaction between EuNALs and the aryl acids pictured in Figure 5-15. No significant enhancement of Eu(III) luminescence is observed.

In contrast to the mono and di-methoxy substituted compounds (Figure 5-15) which do not sensitise our EuNALs under the experimental conditions, tri-substituted acids GW415699X and GW369764X (Figure 5-16) show good potential as light harvesting units, enhancing the chelate emission significantly (~ 50 and 40-fold respectively, for EuNBA and EuBBZA (Chart 5-9).

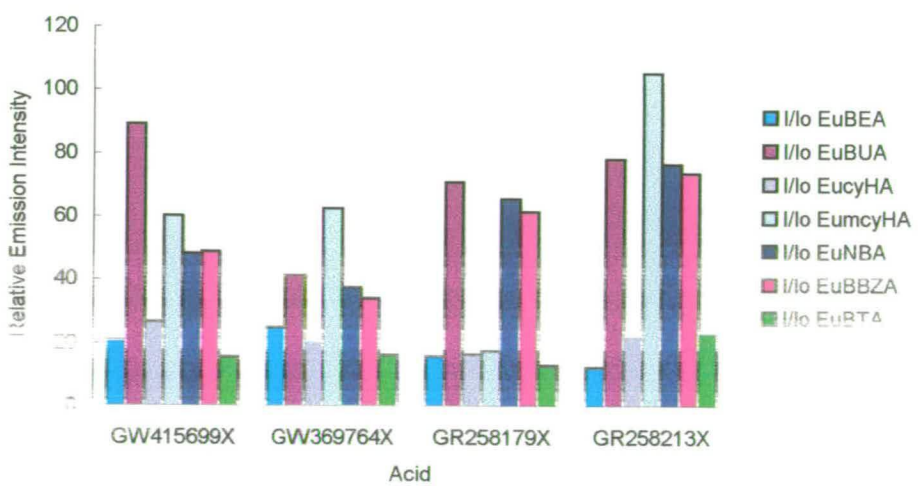

Chart 5-9 The relative emission intensities observed upon recognition of the trisubstituted acids illustrated in Figure 5-16

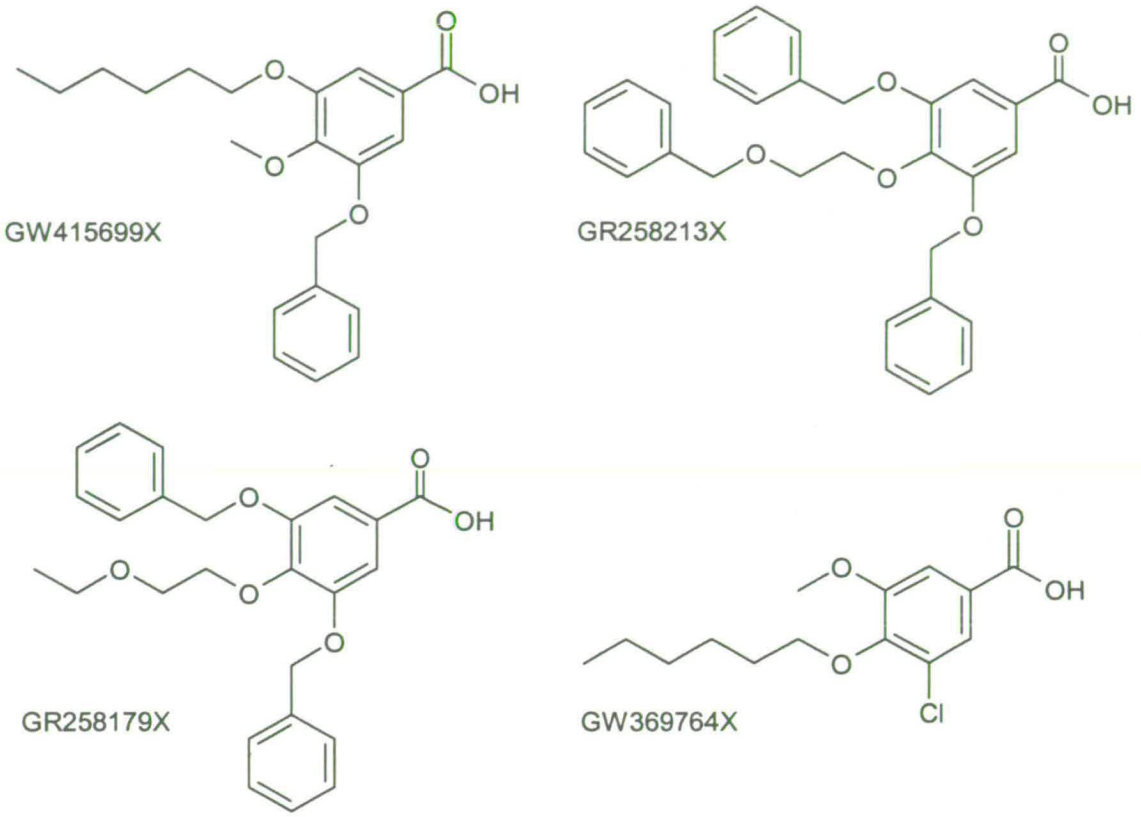

Figure 5-16 Tri-substituted benzoic acid LHCs resulting in enhanced Eu(III) emission upon molecular recognition.

Similarly, acids GR258179X and GR258213X (Figure 5-16) result in luminescent mixed ligand species with approximately 70 and 80-fold enhancement of europium emission respectively (Chart 5-9) for chelates EuNBA and EuBBZA. Interestingly, the best sensitisation is observed with EuBUA and EucyHA. The phenoxy ether substituents are not detrimental to the chelate emission under the experimental conditions. Energy transfer to the metal is feasible from the benzyl-ether substituent groups and their steric bulk provides a shield around the cavity. As expected, the presence of a fourth aromatic ring in GR258213X increases the relative emission intensity of the mixed ligand complex with respect to GR258179X. The molecule contains an extra antenna unit absorbing around 275 nm.

Evidence supporting the importance of electron withdrawing groups on ternary complex formation is provided by acid GW369764X (Figure 5-16), which bears no other aromatic substituents on the benzene ring. The luminescence arising upon molecular recognition between this acid and the EuNALs is compared in Chart 5-10 below with the analogous alkyl

(GW207127X, GW399139X) and alkoxy (GW30894X, GW288377X) substituted LHCs discussed earlier. Structures are pictured in Figure 5-17. The LHC GW369764X bears no absorbing groups in addition to the benzoate chromophore, yet can result in sensitised Eu(III) luminescence. In contrast to the phenoxy substituents, which can absorb UV radiation, the halide is inductively electron withdrawing and cannot absorb the UV excitation energy (275 nm). The positive influence of the chloride substituent on sensitised Eu(III) emission can be attributed to the heavy atom effect, favouring a higher triplet yield and increased luminescence.

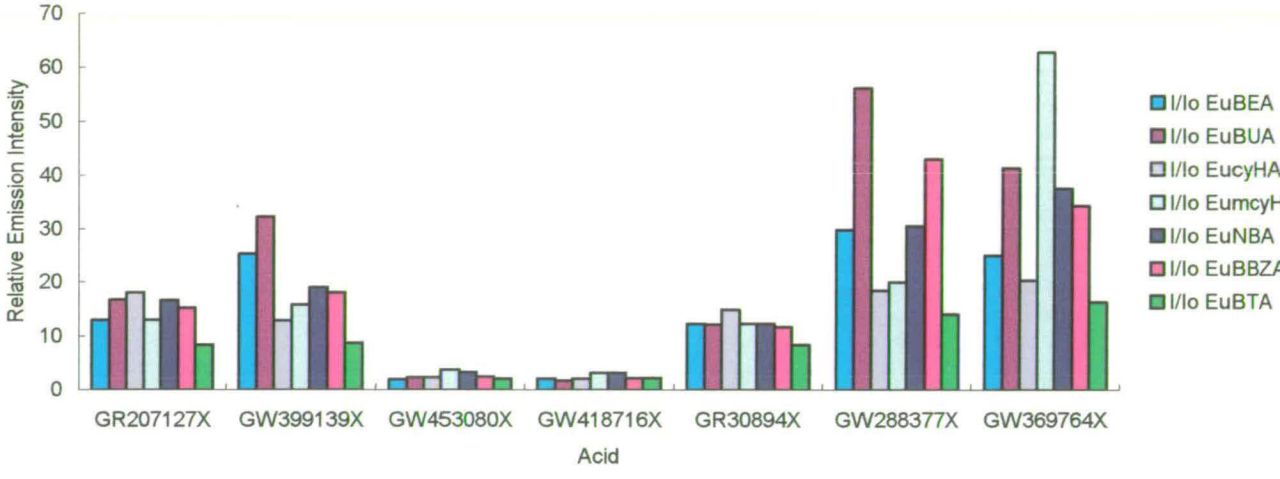

Chart 5-10 I/I_0 observed for alkyl and alkoxy substituted benzoic acids. Comparison between mono- and multiple substituted acids (Figure 5-17)

Acids AH14879X and GR34041X (Figure 5-18), with a *meta* benzyl-ether or phenoxy substituent respectively, do not increase the EuNAL luminescence. These aromatic substituent groups withdraw electron density from the ring, such that the absorption maximum of the molecule is shifted off the excitation wavelength at 275 nm. The resonance effect of such substituents may have been expected to strengthen the binding interaction between the metal and LHC[147] at the under the neutral pH conditions of the experiment. It appears, however, that the substituent lowers the triplet energy to a level below that of the Eu(III) $^5D_0$ excited state. Incorporation of a methoxy group restores some of the electron density, raising the energy of the excited state to a level appropriate for sensitisation at the excitation wavelength allowing intramolecular energy transfer to the metal centre.

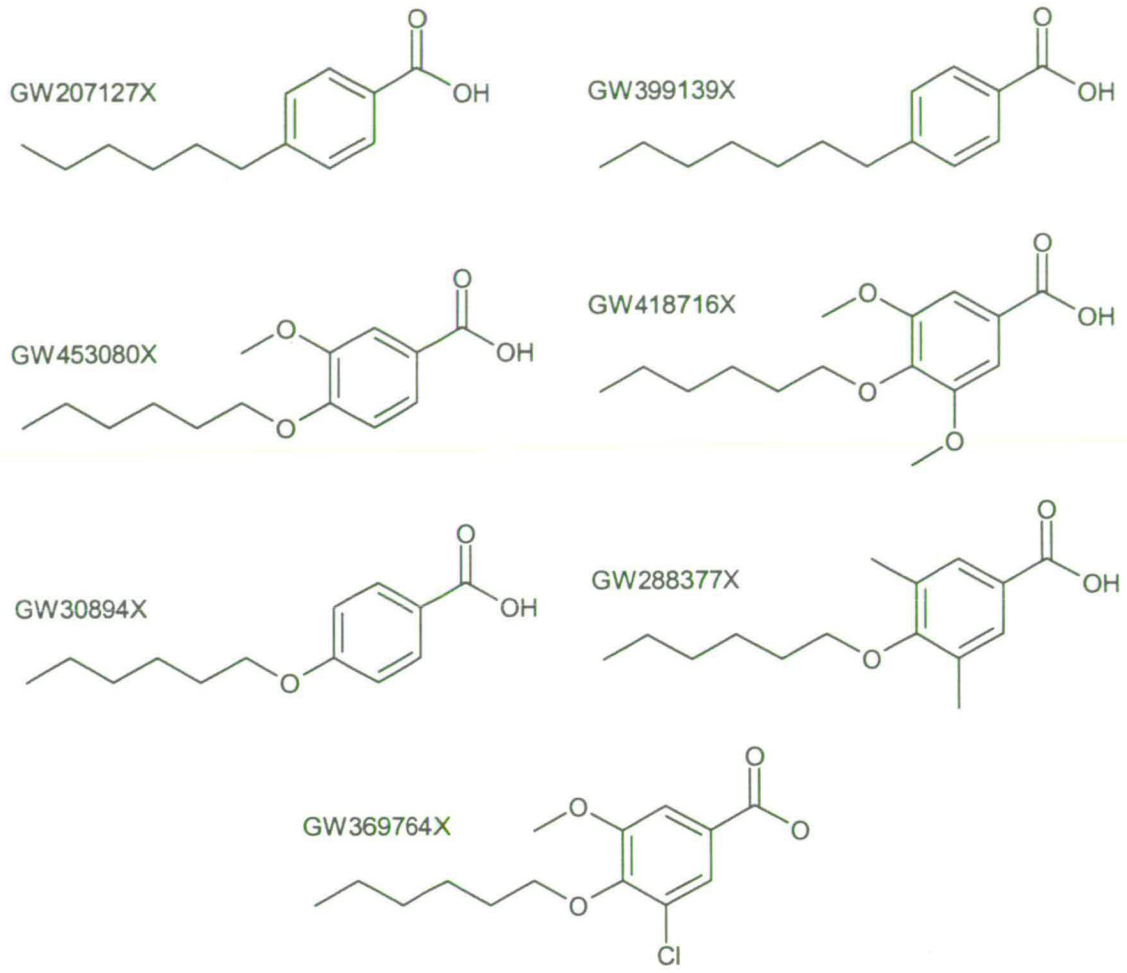

Figure 5-17 Mono and multiple substituted benzoic acids showing some activity as LHCs for the EuNALs studied

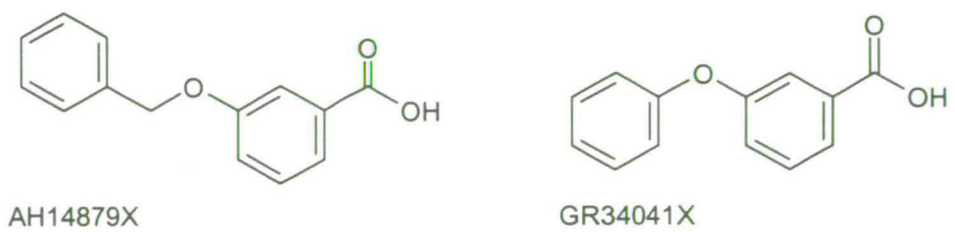

AH14879X GR34041X

Figure 5-18 3-benzyloxybenzoic acid AH14879X and 3-phenoxybenzoic acid GR34041X

5.2.6 Dicarboxylic Aromatic Acids

It has been shown with isophthalic acid[147] that resonance electron withdrawing effects, arising from incorporation of a second carboxylate unit in the 3-position, result in a stronger interaction with the Eu(III) metal centre. The stoichiometry of the luminescent complex in aqueous solution is poorly defined since the formation of multinuclear species is possible (Chapter 3). Upon comparison of acids GR38662X and GR203875X (Figure 5-19), it is apparent that the incorporation of a second carboxylate group facilitates a 3-fold enhancement in emission over the ternary complex formed with the mono-substituted acid.

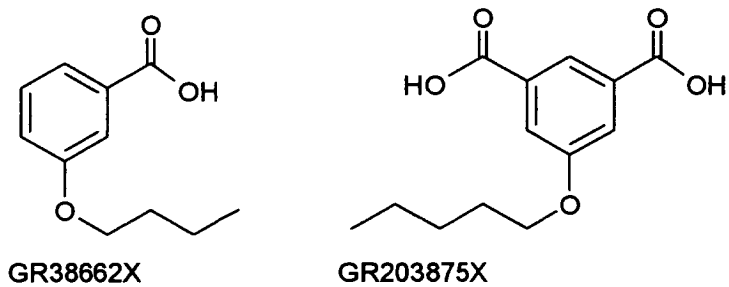

Figure 5-19 4-butoxybenzoic acid (GR38662X) and 5-pentoxy-1,3-benzene-dicarboxylic acid (GR203875X)

Steric constraints prevent the 1,3-dicarboxylic acid from fulfilling its bidentate binding potential and coordination is via a single carboxylate functionality. The stronger interaction with GR203875X may also be attributed to the resonance effect of the second carboxylate group. The emission intensity of the ternary complex, relative to the parent chelate, upon interaction of compounds GR38662X and GR203875X is illustrated in Chart 5-11 below.

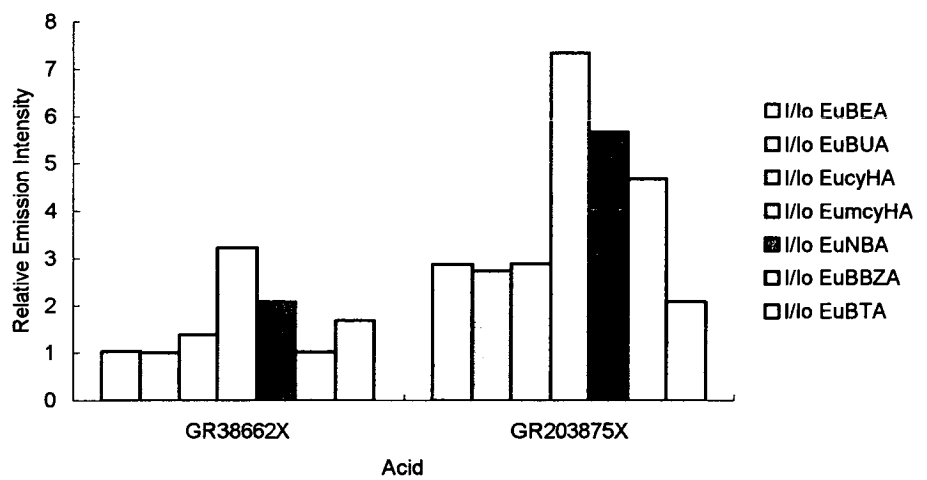

Chart 5-11 I/I_0 upon interaction aromatic acids GR38662X and GR203875X (Figure 5-19)

5.2.7 Heterocyclic acids (I) – Picolinic Acid Derivatives

As discussed in Chapter 3, pyridine-2-carboxylic acid was identified as a particularly good example of a simple LHC for our EuNALs. We were interested in investigating how the recognition between the EuNAL and the picolinate binding unit could be improved to give better sensitisation. The effects of substitution and extended conjugation on the interaction were studied. The influence of simple substituent groups on PCA was evaluated initially. The structures of some of the derivatives studied are shown below in Figure 5-20 and assay results presented in Table 5-2.

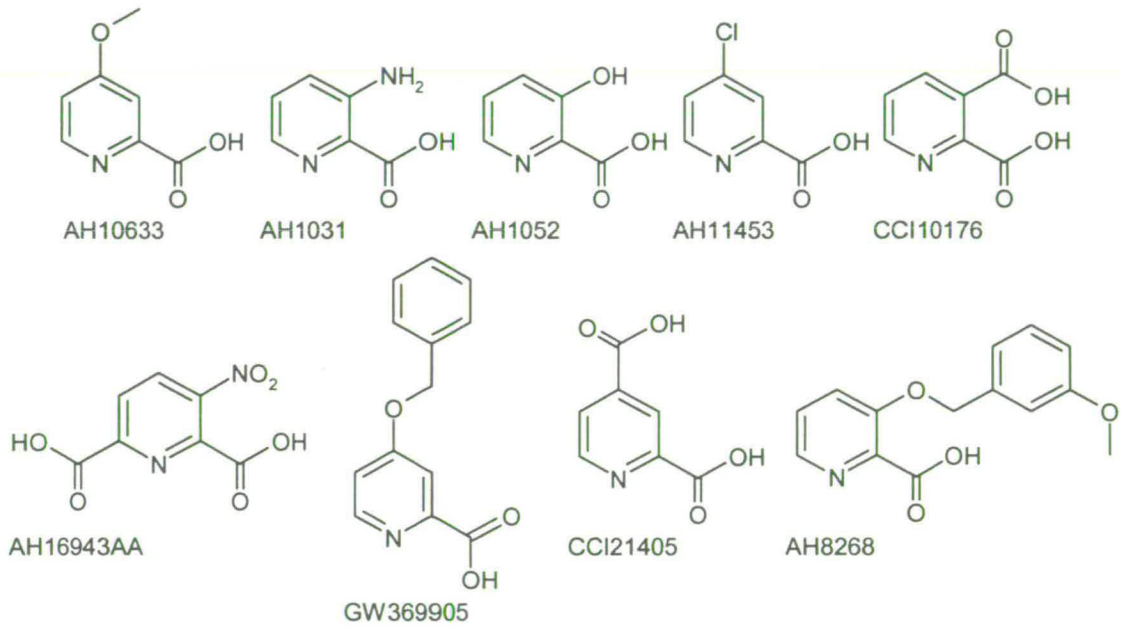

Figure 5-20 substituted picolinic acids

	Relative Emission Intensity							
ACID	**EuBEA**	**EuBUA**	**EucyHA**	**EumcyHA**	**EuNBA**	**EuBBZA**	**EuBTA**	**Mean EuNAL**
AH10633	4	4	3	4	6	5	3	4
AH1052	7	9	5	7	14	12	15	10
AH1031	-	1	1	1	-	1	-	1
AH11453	-	1	1	1	-	1	-	1
CCI10176	3	3	2	3	7	6	3	4
AH16943AA	2	2	2	3	2	2	2	2
GW369905	7	15	4	5	14	14	-	10
AH8268A	1	1	1	1	1	1	1	1
GR202022X	96	84	87	102	143	127	41	97
GR34043X	-	19	12	19	-	28	-	20

Table 5-2 Relative Emission Intensities observed upon combination of substituted picolinic acids and the EuNAL chelates in aqueous solution

Firstly, it is noted that compound AH10633, 4-methoxypyridine-2-carboxylic acid, affords a 4-fold emission enhancement relative to the EuNALs studied. Whilst this increase is considerably less (20%) than that of the unsubstituted picolinic acid (under steady-state illumination, Chapter 3) it is nonetheless proof that an interaction is occurring. In contrast, 4-methoxybenzoate (GR34543X) is not recognised by the chelate cavity. Here the activity can be attributed to the presence of the heteroatom, forming a five member chelate ring with the metal and the carboxylate anion. The increased electron density of the ring system due to the activating influence of the methoxy substituent destabilises the strength of the binding interaction with the metal centre relative to PCA, but the required intramolecular energy transfer is not prevented and sensitised Eu(III) emission is observed. This may also be due in part to increased basicity of the pyridine nitrogen atom.

Similarly, acid AH1052 (3-hydroxypicolinic acid) gives on average a 10-fold increase in emission relative to the EuNAL. With this acid two modes of binding are possible – *via* the "picolinate" or "salicylate" units (Figure 5-21).

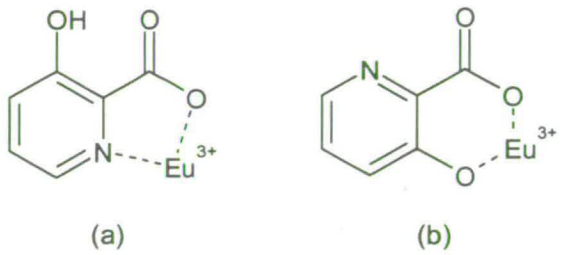

Figure 5-21 (a)"Picolinate" and (b) "Salicylate" bidentate binding units

The binding by "salicylic acids", with a phenol group *ortho* to the carboxylate, is discussed in Chapter 5-10. The sensitised Eu(III) luminescence observed with AH1052 is evidence that the presence of an activating group *ortho* to the binding unit does not greatly impede the molecular recognition required to form the ternary complex.

With acid AH1031, 3-aminopicolinic acid, no sensitised metal luminescence is observed, despite the activating nature of the substituent $-NH_2$ group, increasing the basicity of the pyridine nitrogen atom. This inactivity is attributed to a combination of two factors. Depopulation of the $^5D_0$ excited state by non-radiative energy transfer to higher vibrational overtones of the N-H oscillator is known to occur in many systems, quenching Eu(III) luminescence. In addition to this some amine may be protonated under the slightly acidic assay conditions. The group then becomes deactivating in character, withdrawing electron

density from the aromatic system, and reducing the basicity of the pyridine nitrogen, in turn weakening its activity as a donor ligand to the EuNAL. Proposed binding interactions are shown below (Figure 5-22).

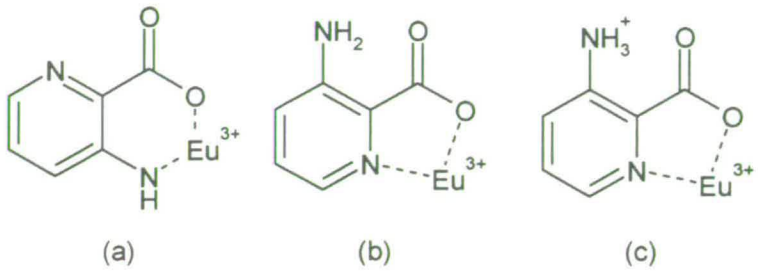

(a) (b) (c)

Figure 5-22 Possible bidentate binding modes in 3-aminopyridine-2-carboxylic acid: (a) via amine and carboxylate; (b) picolinate binding and (c) protonated amine group reducing basicity of pyridine N donor.

Similarly, 4-chloropicolinate (AH11453) does not interact with the EuNALs. Unlike resonance electron withdrawing CO_2H substituents (c.f. isophthalic acid), the inductively electron withdrawing Cl atom does not stabilise the formation of the carboxylate anion, but lowers the energy of the π-system and triplet state, probably to a level below that of the Ln(III) excited state such that the efficiency of intramolecular energy transfer is diminished. In contrast to AH11453, compound CCI21405, pyridine-2,4-dicarboxylic acid, forms ternary luminescent species. We attribute this to the resonance electron withdrawing effect of the second carboxylate substituent, stabilising the binding interaction between the metal centre and the PCA binding unit (c.f. isophthalic and dipicolinic acid binding). Compound CCI10176, pyridine-2,3-dicarboxylic acid, results in a 4-fold enhancement in EuNAL luminescence. Like AH1052, this acid exhibits two potential modes of binding- "picolinate" and "phthalate" (Figure 5-23), the latter of which can result in LMCT with a quenching effect.

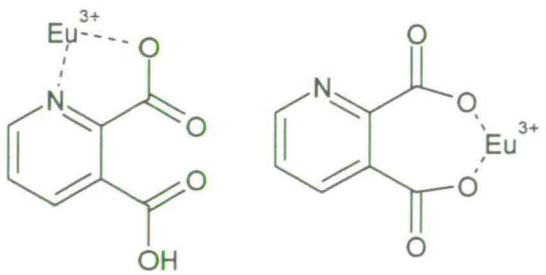

(a) (b)

Figure 5-23 (a) "picolinate" and (b) "phthalate" binding

Dipicolinic acid (pyridine-2,6-dicarboxylic acid) is well known as an excellent LHC for the trivalent lanthanide cations, but here we note with interest that when the acid bears a nitro-substituent (AH16943AA) the chelate luminescence is barely doubled. This can be attributed to the powerful electron-withdrawing influence of the functional group, reducing the basicity of the pyridine N and lowering the triplet-state energy

An interesting observation is that acid GR369905X (Figure 5-20) enhances the emission ~10-fold, but AH8268 does not. These acids differ by both nature and position of the substituent on the pyridine ring. Acid AH8268 bears a *m*-methoxy group on the benzyloxy substituent at the 3-position of the pyridine ring, whereas GR369905X bears an unsubstituted benzyloxy group at the 4-position. It is expected that the resonance electron releasing methoxy group, can raise the energy of the π-system altering the absorption spectrum of the ligand considerably, and lower the carboxylic acid pK_a. A further factor is expected to arise from the relatively high triplet state energy of methoxybenzene, resulting in mismatched triplet excited states. The pyridine substituent position may also influence the extent of interaction/energy transfer. The most efficient LHCs of the substituted picolinic acids tested are those bearing alkyl substituents in the 4 or 5-positions discussed in section 5-2 (Figure 5-24).

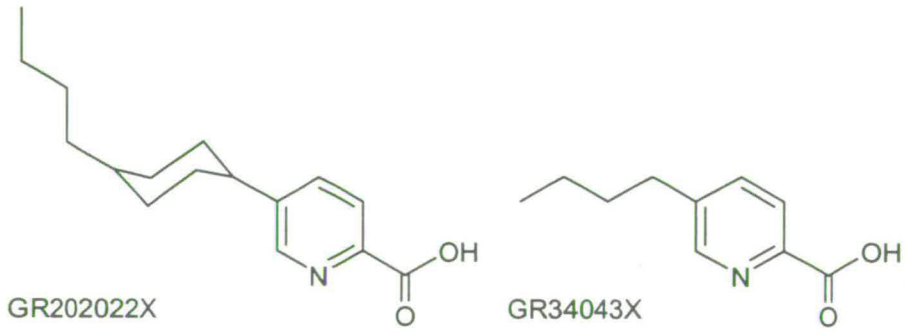

Figure 5-24 Alkyl substituted picolinic acids GR202022X and GR34043X

The presence of a sterically bulky alkyl substituent does not perturb the electronic structure of the acid significantly and the chromophore and binding units are essentially unchanged relative to PCA. The hydrophobic nature of the tail group prevents attack by quenching outer sphere water molecules to the extent that an increase of ~100-fold is observed over the parent chelate under the experimental conditions of the assay. It is also observed that when the alkyl substituent bears an additional carboxylate function (Figure 5-25) the relative emission increase (Chart 5-12) is reduced with respect to the mono-carboxylic acid LHCs.

This can be attributed to competitive coordination of the metal by the aliphatic carboxylate, which cannot facilitate energy transfer to the Eu(III) metal centre.

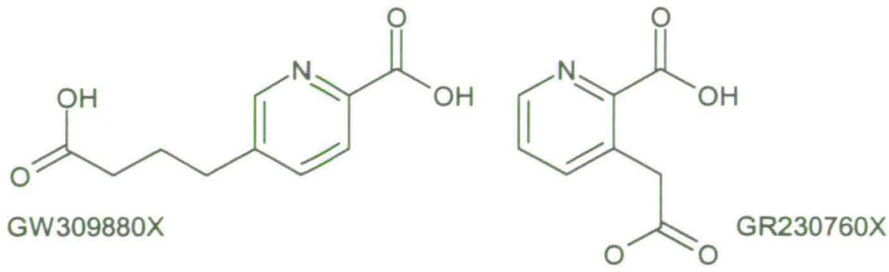

Figure 5-25 Alkyl substituted picolinic acids bearing a second carboxylate functional group. Activity is reduced with respect to the simple alkyl substituted PCA, GR202022X.

5.2.8 Heterocyclic Acids (II) – Quinolinic Acid Derivatives

5.2.8.1 Substituted Quinoline-2-Carboxylic Acid LHC Units

The influence of extended conjugation on the luminescence interaction between the heterocyclic acid LHCs and the EuNAL chelates in aqueous solution was also examined by combinatorial screening techniques. The absorption of the LHC around 270 nm can be varied, and the characteristics of the picolinic binding unit maintained by progressing to quinoline systems with two fused aryl rings.

Quinoline-2-carboxylic acid, AH9727 (Figure 5-26) is observed to form a ternary complex with our EuNALs but the metal centred emission is only enhanced by 3-fold, comparable to the benzoic acid LHC.

A much greater increase may have been expected on account of the extended chromophoric unit; however it is likely that the absorptivity of the acid at 270 nm is diminished slightly due to a red-shift in the absorption maximum. The observed inactivity is attributed to insufficient interaction for intramolecular energy transfer to occur. This is believed to be the result of a repulsive interaction between the Eu(III) metal centre and the proton at the 8-position of the quinolinic acid preventing the acid from fulfilling its bidentate binding potential.

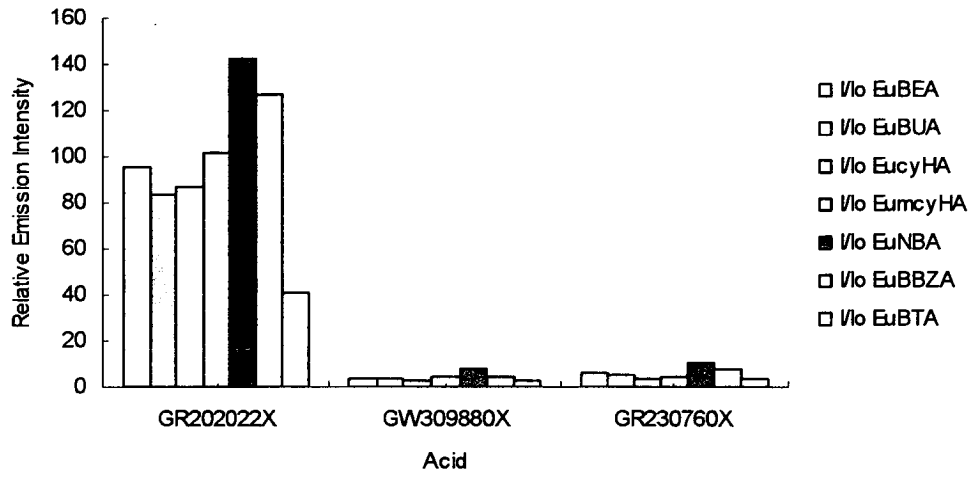

Chart 5-12 Comparison of the relative emision intensity observed upon interaction between alkyl and alkyl-carboxylate substituted picolinic acids

The effect of substitution at the 4-position was investigated to see if the presence of a hydrophobic tail unit would enhance the luminescence of the mixed ligand species. The electronic effects of the substituent groups were also considered. Firstly we will examine the influence of alkoxy-substituents (Figure 5-26).

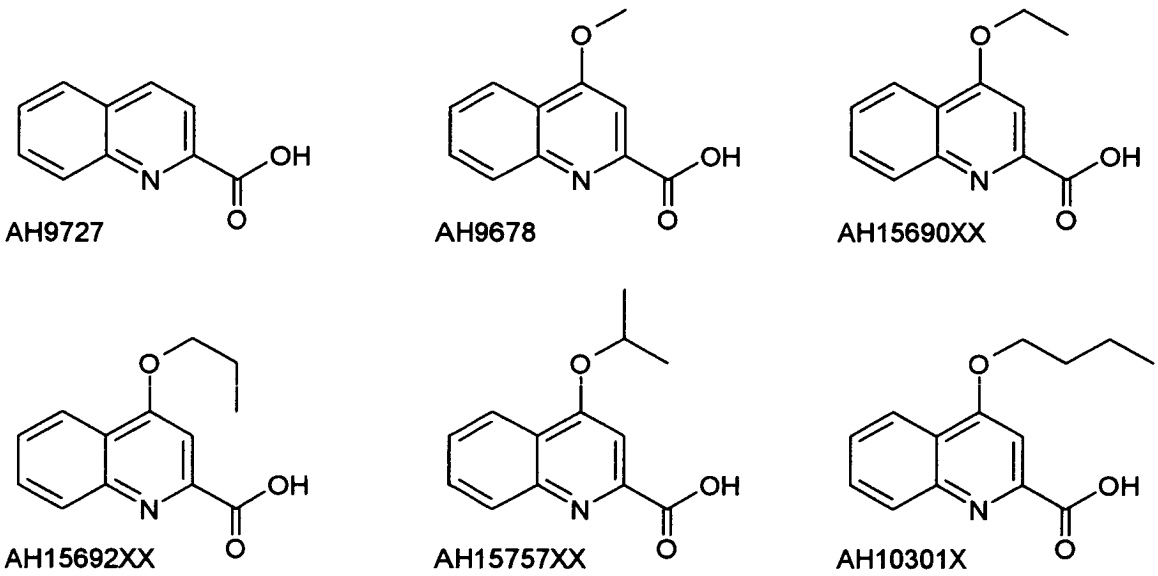

Figure 5-26 4-Alkoxy-substituted quinoline-2-carboxylic acids

	Relative Emission Intensity							
ACID	EuBEA	EuBUA	EucyHA	EumcyHA	EuNBA	EuBBZA	EuBTA	Mean EuNAL
AH9727	-	3	2	3	-	4	-	3
AH9678	2	-	-	-	3	3	-	3
AH15690XX	5	-	-	-	6	6	-	6
AH15692XX	12	-	-	-	13	17	-	14
AH15757XX	7	-	-	-	8	5	-	7
AH10301X	23	23	12	25	60	28	18	27

Table 5-3 I/I_0 upon combination of quinoline-2-carboxylic acids with EuNALs

On average, a 3-fold increase in EuNAL emission is observed with the unsubstituted acid AH9727 as discussed above. Upon addition of an alkoxy group at the 4-position the interaction is improved slightly. Acid AH9678 (4-methoxyquinoline-2-carboxylic acid) results in 2-3-fold enhancement of the EuNAL emission (c.f. benzoate) whereas AH15690 (4-ethoxyquinoline-2-carboxylic acid) gives a relative emission increase of ~ 5-fold, and the propyl derivative AH15692 enhances the luminescence ~ 13-fold. Compound AH15757, 4-isopropyloxyquinoline-2-carboxylic acid, achieves ~ 7-fold enhancement of the metal centred luminescence, less than the straight chain propyl derivative, and likely to be a consequence of adverse steric interactions between the amide arms of the EuNAL and the acid LHC. The straight-chain *n*-butyl derivative, AH10301X, forms a mixed ligand chelate with the EuNALs almost twice as luminescent as those formed with AH15692. The increase in emission intensity relative to the parent quinoline-2-carboxylic acid, AH9729, can be attributed to two factors:

1) The substituents are electron donating in character, and can increase slightly the electronic density of the aryl ring. This in turn increases the basicity of the pyridine nitrogen atom, improving its capacity to act as a donor ligand to the Eu(III) metal centre (section 5.2.7).
2) The second factor is the hydrophobic shielding effect as observed with the benzoic and picolinic acid derivatives discussed earlier in section 5.2.

When an electron withdrawing substituent is placed at the same position, the resultant mixed ligand species exhibits weak metal centred emission. Acids AH12533 and AH12590 (Figure 5-27), which bear unsaturated alkoxy substituents demonstrate this effect (Table 5-4). At best, the alkene derivative, acid AH12533 enhances EuBEA luminescence ~ 6-fold, whereas the alkyne derivative, AH12590, only achieves an average 3-fold emission increase.

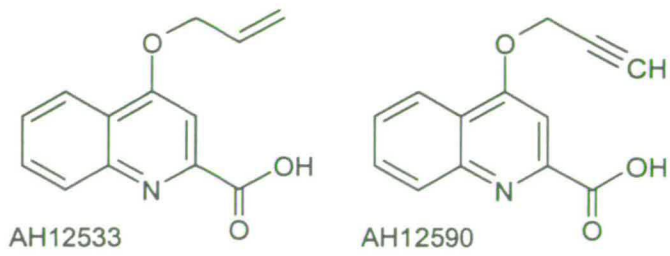

Figure 5-27 Substituted quinoline-2-carboxylic acids AH12533 and AH12590.

	Relative Emission Intensity							
ACID	**EuBEA**	**EuBUA**	**EucyHA**	**EumcyHA**	**EuNBA**	**EuBBZA**	**EuBTA**	**Mean EuNAL**
AH12533	6	-	-	-	8	7	-	7
AH12590	3	-	-	-	5	3	-	4

Table 5-4 Relative emission intensity observed upon interaction between acids AH12533 and AH12590 with the EuNAls

The electron withdrawing group will stabilise the formation of the carboxylate anion with respect to the protonated species, but since this also reduces the basicity of the pyridine nitrogen the binding interaction is weakened.

Introduction of a polyether function to the 4-position (Figure 5-28) of these acids does not improve the interaction and the maximum increase observed upon molecular recognition is ~ 3-fold (Table 5-5). With an OH group incorporated into the substituent chain (AH10978X) the acid results in no increase in EuNAL emission, attributed to additional quenching by non-radiative energy transfer.

	Relative Emission Intensity							
ACID	**EuBEA**	**EuBUA**	**EucyHA**	**EumcyHA**	**EuNBA**	**EuBBZA**	**EuBTA**	**Mean EuNAL**
AH12589	2	2	1	3	3	3	2	2
AH13391	4	3	2	5	5	5	3	4
AH11274	6	5	5	8	8	7	7	7
AH10978	1	-	-	-	2	3	-	2
GR254264X	3	3	3	3	5	3	2	3

Table 5-5 Relative emission intensity observed upon interaction between the EuNALs and quinoline-2-carboxylic acids (Figure 5-28)

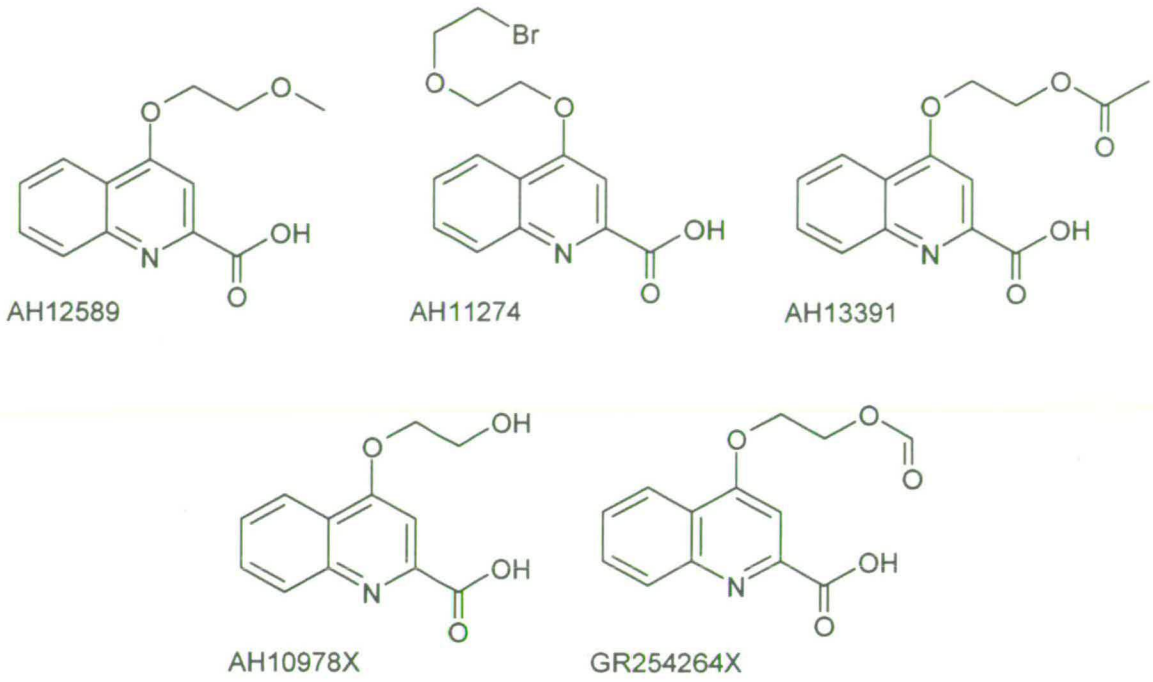

Figure 5-28 Aromatic substituted quinoline2-carboxylic acids

The assay results show that acids AH12695X and AH9676 (Figure 5-29) trigger Eu(III) emission upon molecular recognition with a increase of ~20-fold (Chart 5-13).

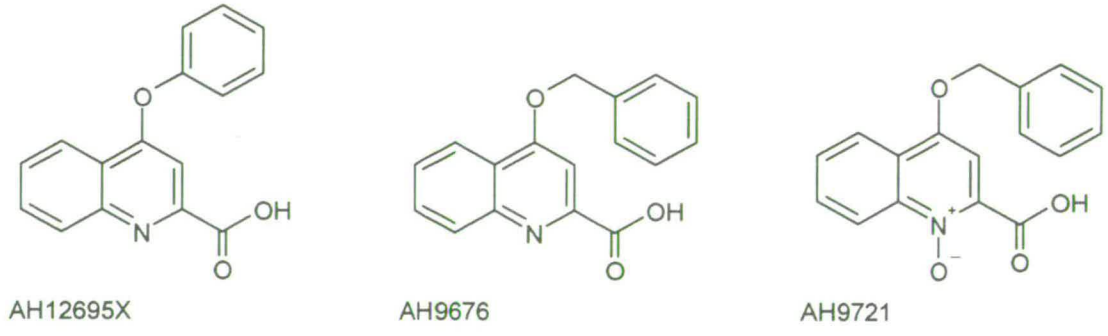

Figure 5-29 Substituted quinoline-2-carboxylic acids resulting in ~ 20-fold enhancement of EuNAL emission (Chart 5-13)

In contrast to the other acids of this type, the substituent in the 4-position is aromatic. This has the effect of increasing the efficiency of photon absorption. This alone is not sufficient, and a strong binding interaction is required, providing good orbital overlap between the

metal centre and the acid. The N-oxide compound, AH9721, has no effect on the lanthanide luminescence. The N lone pair is unable to chelate the metal since the electrons are involved in formation of the N-O bond; however coordination by the $N^{+}O^{-}$ moiety is possible. The inactivity is attributed to electronic factors which can adversely influence the triplet state energy or weaken the interaction with the metal. Acid AH9676 bears a tolyl substituent which can absorb the excitation energy at 275 nm, and transfer it to the Eu(III) *via* the quinoline unit.

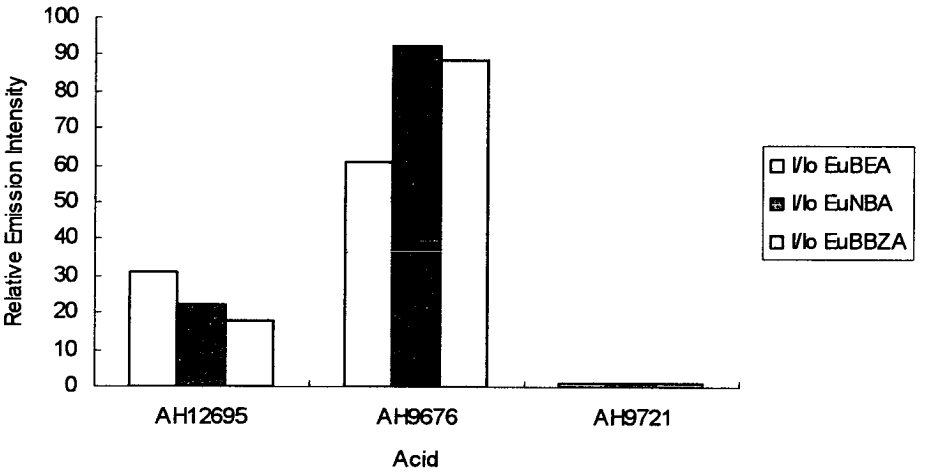

Chart 5-13 Relative emission intensity upon recognition between aryl-acids AH12695X AH9676 and AH9721 (Figure 5-29) and EuBEA, EuNBA and EuBBZA

Acid AH10698V (Figure 5-30) appears to be active as a light-harvesting centre towards our EuNALs (Table 5-6), but as observed with many of the other compounds tested, this is the result of strong organic fluorescence, and not of sensitised Eu(III) emission following a molecular recognition event.

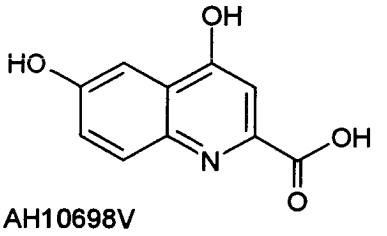

AH10698V

Figure 5-30 Aryl-acid AH10698V exhibiting intense organic fluorescence only

Compounds AH10300, AH10801 and AH9678 (Figure 5-31) all form weakly luminescent ternary complexes, enhancing the lanthanide emission 3 to 5-fold. The feature common to

these acids is the presence of electron donating methoxy substituent groups. Substitution of the second aromatic ring does not greatly influence the interaction of these quinoline-2-carboxylic acids with the EuNALs (Table 5-6).

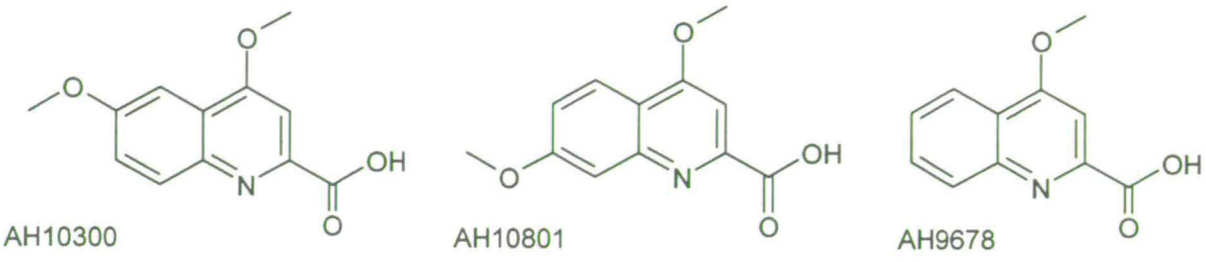

Figure 5-31 Quinoline-2-carboxylic acids – interaction with EuNALs is weak

Acid AH10853 (4,8-dihydroxyquinoline-2-carboxylic acid) and GR92452 (8-hydroxyquinoline-2-carboxylic acid) (Figure 5-32) were tested to ascertain the extent to which a more hydrophilic substituent group at the 8-position would influence the interaction. No sensitised Eu(III) luminescence was observed in either case (Table 5-6). We attribute this to the close proximity of the OH oscillator to the metal centre, which can result in non-radiative energy transfer and depopulation of the Eu(III) excited state. Alternatively, as Eu(III) is coordinating mainly though the carboxylate unit, the 8-hydroxyquinoline moiety is free to lose energy by the internal hydrogen bond with and intervening water leading to exited state intramolecular proton transfer (ESIPT).

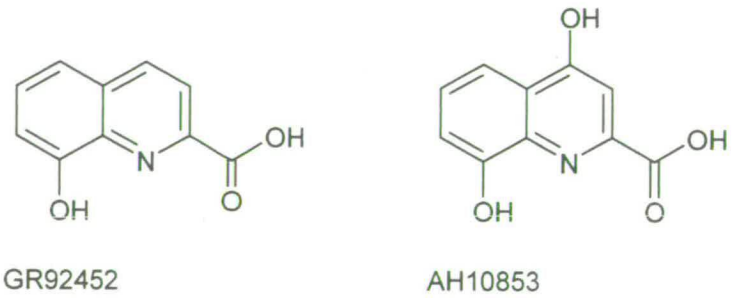

Figure 5-32 7-hydroxyquinoline-2-carboxylic acids GR92452 and AH10853

Further insight into factors governing the activity of substituted quinoline-2-carboxylic acids may be gained upon consideration of compounds bearing alternative functional groups at the 8-position. Amine substituents, like the hydroxide groups, are capable of depopulation of the Eu(III) excited state by non-radiative energy transfer.

	Relative Emission Intensity							
ACID	EuBEA	EuBUA	EucyHA	EumcyHA	EuNBA	EuBBZA	EuBTA	Mean EuNAL
AH10300	3	-	-	-	3	4	-	3
AH10801	5	-	-	-	4	7	-	5
AH9678	2	-	-	-	3	3	-	3
AH10698	57	-	-	-	35	46	-	46
AH10853	1	-	-	-	1	1	-	1
GR92452	1	-	-	-	1	1	-	1

Table 5-6 Relative emission intensity observed upon interaction between substituted quinoline-2-carboxylic acids (Figure 5-30 - 32) and the EuNALs

5.2.8.2 Substituted Hydroxyquinoline-3-Carboxylic Acid LHC Units

One class of acids showing particularly good potential as LHCs for our EuNALs comprises of compounds based on 4-hydroxyquinoline-3-carboxylic acid. Here, the interaction is *via* the bidentate "salicylate" binding unit – with a phenol functionality *ortho* to the carboxylate. The structures of the 4-hydroxyquinoline-3-carboxylic acids tested during the assay experiment are shown below (Figure 5-33).

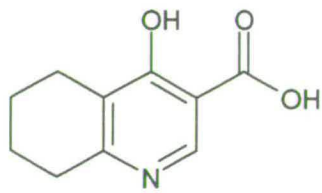

GW304734X

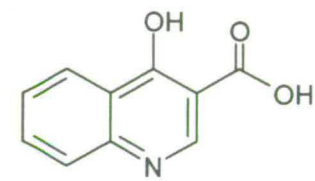

AH10225

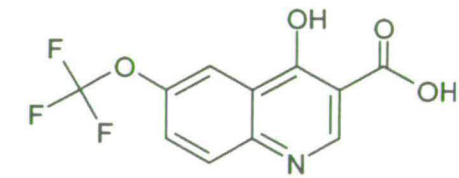

GR258750

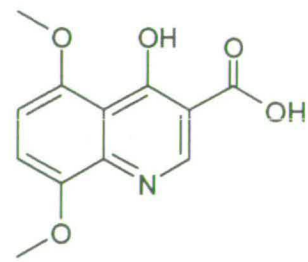

AH11368

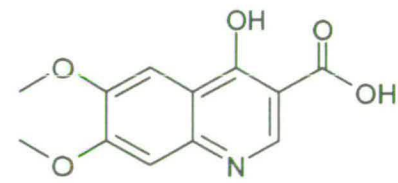

AH11688

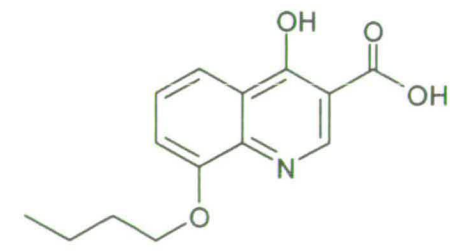

GI266527

Figure 5-33 4-hydroxyquinoline-3-carboxylic acids

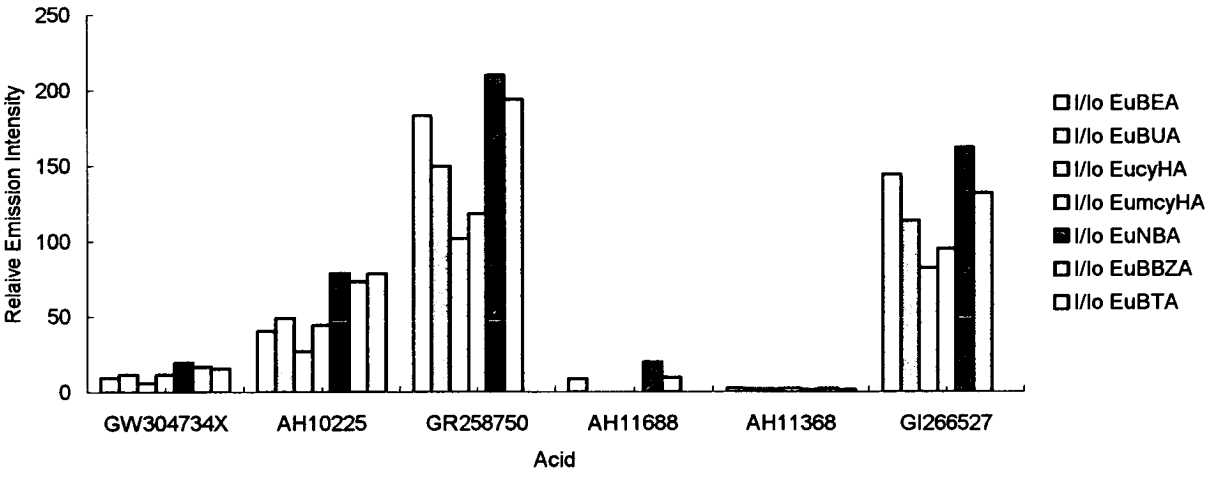

Chart 5-14 I/I_0 observed upon recognition between substituted 4-hydroxyquinoline-3-carboxylic acids and EuDTPA-AM_2 chelates

From the luminescence observed upon the interaction between the EuNALs and acid GW30473X (on average ~13-fold) we know that the binding interaction is strong and that orbital overlap is sufficient to facilitate energy transfer between the acid triplet state and the emissive level of the metal.

Upon extension of the chromophoric unit by fusing a second aryl ring to the heterocyclic acid, we improve the light harvesting ability of the acid as illustrated by AH10225, which forms ternary luminescent complexes with all of the EuNAL chelates studied here, enhancing the characteristic red Eu(III) emission by ~ 50-fold under the experimental conditions of the assay. Similarly, acid GR258750 exhibits excellent sensitiser behaviour towards our EuNALs, resulting in mixed ligand species ~ 200-fold more emissive than the parent chelate. This dramatic improvement is owed to the presence of the strongly electronegative -OCF_3 substituent in the 6-position of the acid. The triplet energy is affected greatly to the extent that an excellent match is established with the $^5D_0$ excited state of the Eu(III) ion.

The binding interaction may also be strengthened by the presence of the trifluoromethoxy substituent, since inductive withdrawal of electron density from the aromatic system is likely to lower the acid pK_a. Such an influence is expected to drive the equilibrium towards

formation of the deprotonated species, under the neutral pH conditions of the assay, thus more acid is available to form the ternary complex.

It is also interesting to note that when the acid bears two electrons donating methoxy substituents on the second aromatic ring (AH11368 and AH11688) that the interaction is diminished greatly. These groups have the opposite effect to the $-OCF_3$ substituent of GR258750 and increase the electron density of the system, raising the pK_a of the acid and the phenol with respect to the unsubstituted acid AH10225. This is expected to weaken the interaction with the metal centre and reduce the efficiency of intramolecular energy transfer to the excited state of the europium ion. The electron donating influence of the *n*-butoxy substituent in the 8-position (GI266527) does not destabilise the interaction significantly. This acid is observed to bind the EuNAL resulting in a ~150-fold increase in metal emission. The alkyl chain substituent is also likely to provide addition protection to the metal centre from any quenching by outer sphere solvent molecules as discussed in section 5.2.1.

5.2.8.3 "Salicylic Acid" LHC Units

It is important to note that salicylic acid (Figure 5-34) is not observed to increase the emission of the EuNAL chelates, and does not form luminescent mixed ligand lanthanide complexes in aqueous solution.

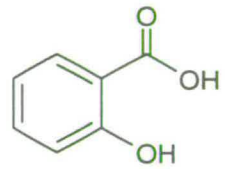

CCI4008

Figure 5-34 Salicylic acid, CCI4008

This is attributed to the high pKa value of the phenol hydroxide, pK_a 13.4 for salicylic acid (CCI4008, Figure 5-34). The oxygen atom remains protonated at the neutral pH of the chelate solution. Any interaction between the carboxylate anion and the metal centre does not result in sensitised Eu(III) luminescence, as the close proximity of the O-H oscillator can effectively depopulate the excited state of the metal by non-radiative energy transfer. The inactivity of Eu(III) with salicylic acid derivatives may also be due to formation of charge transfer states with the phenolate anion (possibly deprotonated under the influence of the Eu^{3+}closeby. The commercial assay, EALL, (Chapter 1.3.3) utilises a salicylic acid derivative in formation of highly luminescent Tb(III) ternary complexes. It should be noted however, that the TbDTPA-AM_2 chelates tested during the assay did not give rise to

sensitised emission with the salicylic acid derivatives. Preliminary research in the Pikramenou research group revealed the mechanism by which ternary complex formation occurs with charged LnNAL species ($[LnDTPA]^{2-}$, $[LnEDTA]^{-}$) to differ from that by which molecular recognition occurs with the neutral chelates.

Similarly, *ortho*-hydroxynaphthoic acids (Figure 5-35) do not result in enhanced Eu(III) emission under our assay conditions. A weak interaction (~2-3 fold increase) was observed between the EuNALs and the acids CCI17440 and GR68891X (Table 5-7) in contrast to the 4-hydroxyquinoline-3-carboxylic acids (Figure 5-33, Chart 5-14).

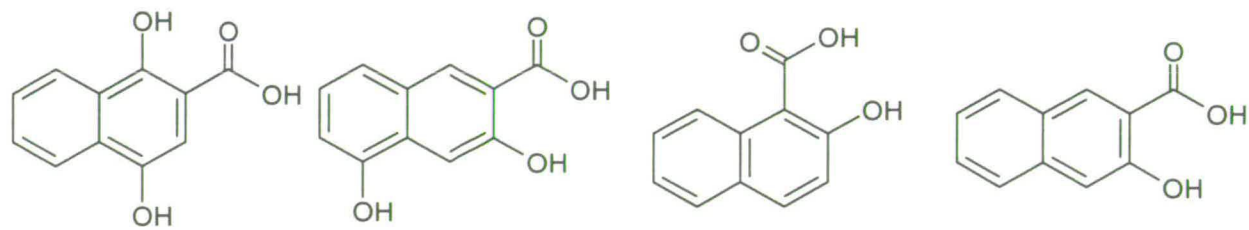

Figure 5-35 *ortho*-hydroxynaphthoic acids – no interacton is observed with the EuNALs (Table 5-7)

	Relative Emission Intensity							
ACID	**EuBEA**	**EuBUA**	**EucyHA**	**EumcyHA**	**EuNBA**	**EuBBZA**	**EuBTA**	**Mean EuNAL**
CCI4008	1	1	1	2	1	1	1	1
CCI17440	3	4	4	4	3	3	3	3
GR68891	1	4	4	4	5	4	-	4
GI148915	1	-	-	-	2	1	-	1
GR207121	6	4	5	5	6	5	-	5

Table 5-7 Relative emission intensity observed upon combination of *ortho*-hydroxynaphthoic acids with the EuNALs

The small enhancement of Eu(III) emission observed with acid CCI17440 can be attributed to the presence of a second hydroxide substituent increasing the electron density of the aromatic system. It is proposed that the presence of the activating substituent results in a slight increase of electron density located at the oxygen atom of the *ortho* hydroxide group. This in turn improves the ability of the oxygen to act as a donor ligand to the hard Eu(III) metal centre, strengthens the interaction and facilitates more efficient intramolecular energy transfer.

5.2.9 Naphthyridine Carboxylic Acids

When a second heteroatom is introduced to the aromatic system using naphthyridine carboxylic acids we observe a dramatic change in the molecular recognition between the acids and our EuNAL chelates. The 4-hydroxyquinoline-3-carboxylic acid binding unit remains unchanged with respect to the acids discussed above, but the pattern of activity with the metal chelates is quite different (discussed in Chapter 5.3 below).

Both acids AH11967 and AH12133 (Figure 5-36) exhibit excellent potential as light harvesting units on account of the well-matched triplet energy levels and strong binding interaction with the metal centre.

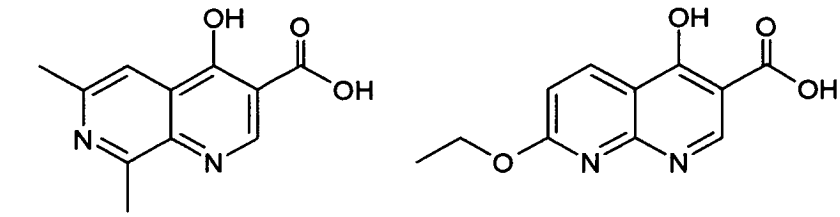

Figure 5-36 Naphthyridine carboxylic acids which show excellent LHC potential for the EuNALs and marked selectivity towards EuNBA and EuBTA

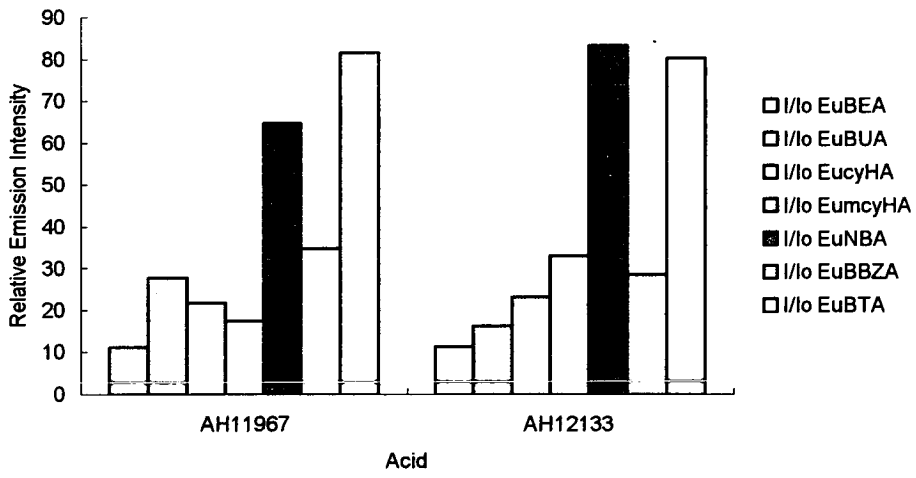

Chart 5-15 Selectivity of interaction between EuNALs and naphthyridine acids AH11967 and AH12133 (Figure 5-36)

It is noted that a non-chelating substituent group *ortho* to the carboxylate unit inhibits the interaction between the EuNAL and simple naphthyridine acids, as observed with GR216655X and GR220880X (Figure 5-37).

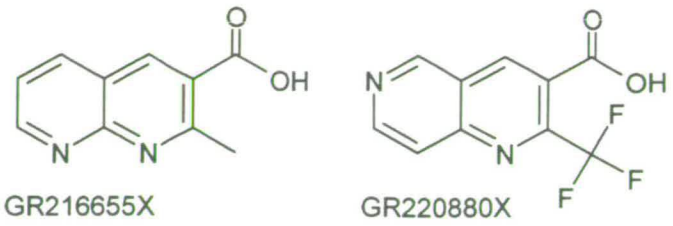

Figure 5-37 Naphthyridine acids bearing non-chelating substituents *ortho* to the carboxylate binding unit

Neither of these acids results in any increase in metal centred emission. Steric effects impede the interaction between the carboxylate and the EuNAL, preventing orbital overlap and energy transfer. As a result no sensitised Eu(III) luminescence is observed.

5.2.10 Sulphur and Oxygen Heterocyclic Acid LHC Units

An interesting range of activity is observed when we study the recognition between other heterocyclic acids (Figure 5-38) and our EuNAL chelates (Chart 5-16).

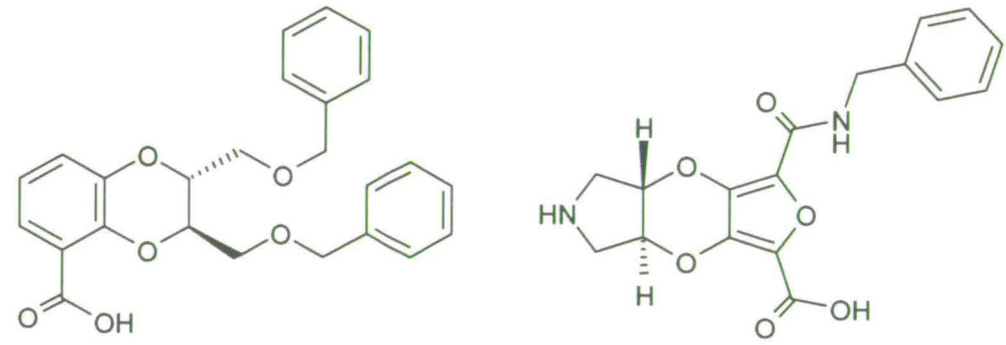

Figure 5-38 Oxygen containing heterocyclic carboxylic acids

We note that the mono-carboxylic acid GR50838A interacts weakly with EuNALs forming mixed ligand species only 5-times more luminescent than the parent chelate. This acid exhibits bidentate binding potential via the lone pairs of the dioxane oxygen, but in water this interaction is very weak, and expected to be insignificant. Acid GR69421X, like GR50838A, forms weakly emissive ternary species in solution, coordinating via the carboxylate. The furan heteroatom is unlikely to bind the metal in aqueous solution. The

electron withdrawing amide group can stabilise the negative charge on the carboxylate under assay conditions driving the equilibrium towards formation of the mixed ligand complex.

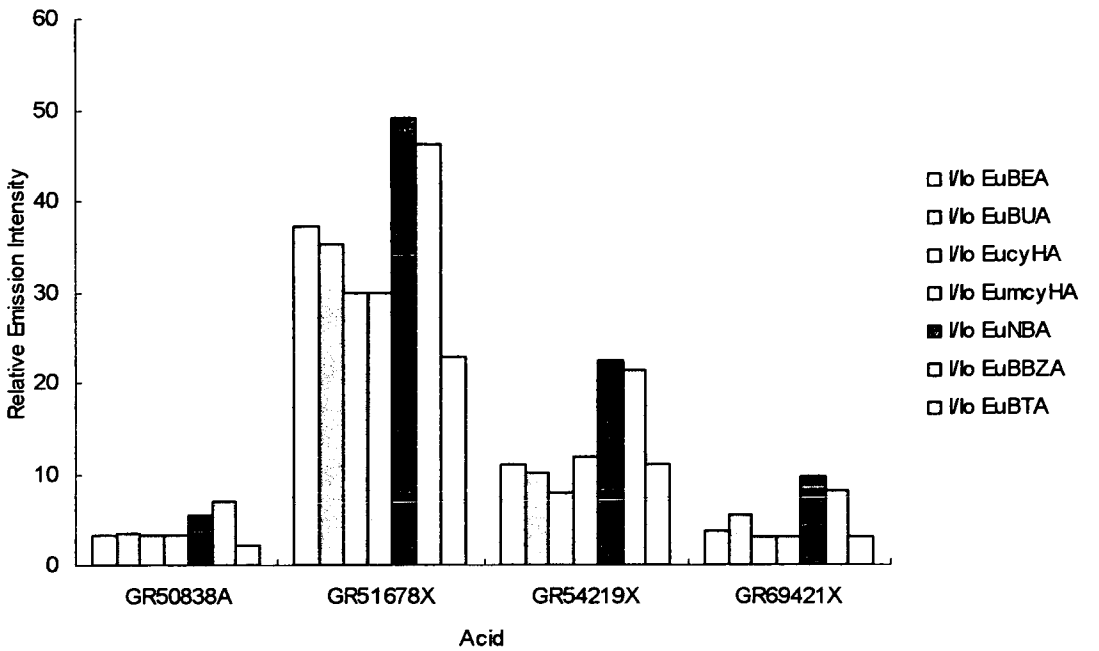

Chart 5-16 I/I_0 observed upon combination of sulphur and oxygen heterocyclic acid LHCs with the EuNALs

In contrast, hetero-dicarboxylic acids (Figure 5-39) result in much more luminescent ternary complexes in solution (Chart 5-16). It is initially surprising that the thiophene derivative, GR51678X, forms more intensively emissive species with the EuNALs than the analogous furan compound, GR54219X. The relative emission intensities observed for EuNBA and EuBBZA with each acid are ~ 50 and 20-fold respectively.

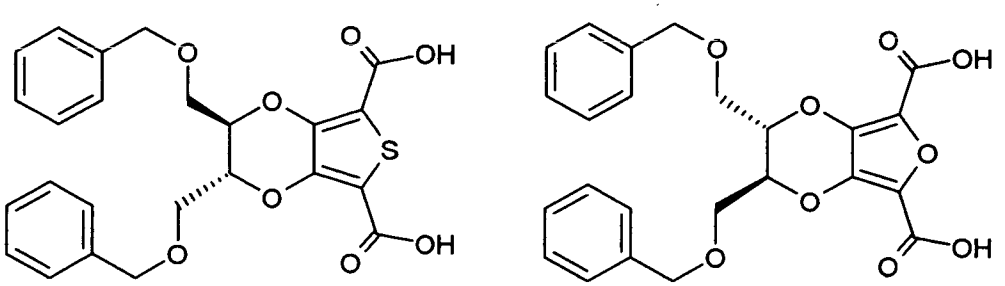

Figure 5-39 Acid GR51678X and GR54219X – thiophene and furan dicarboxylic acids

Europium, a "hard" acid by definition, normally preferentially binds "hard" donor ligands such as O^-, O and N over the softer elements like sulphur. We may have therefore expected GR69421X to be a better LHC towards out EuNALs than GR54219X. Dipicolinic acid (pyridine-2,6-dicarboxylic acid) is an efficient LHC for our LnNALs in aqueous solution forming highly luminescent mixed ligand complexes, but the stoichiometry of the interaction is poorly defined. The potentially terdentate acid is capable of bridging between metal centres forming multinuclear species as observed with isophthalic acid (Chapter 3).

The key to the apparent anomaly observed here might lie in the comparative atomic radii of oxygen and sulphur. The larger element, sulphur, forms longer bonds to carbon then the smaller oxygen atom (1.856 Å and 1.421 Å respectively), therefore distorting the chelate bite-angle forcing a bidentate binding interaction. In contrast, the smaller oxygen atom of the furan-2,5-dicarboxylic acid analogue may facilitate a terdentate binding interaction with the metal. Should both the carboxylate groups coordinate the metal excited state LMCT states may be established. Thermal population of the low lying excited states from the $^5D_1$ leel depopulates the emissive stae and sensitised Eu(III) emission is not detected.

The differing interactions between these two acids and our EuNALs can perhaps be explained by the relative aromaticity of the chromophore upon consideration of the 5-membered parent heterocyclic compounds thiophene and furan (Figure 5-40). Furan, with the harder oxygen heteroatom, is quite diene like in character, with the oxygen reluctant to surrender its electrons to the aromatic ring. In contrast, the softer sulphur heteroatom of thiophene is less electronegative and better able to donate its electrons to the conjugated aromatic system.

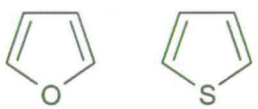

furan thiophene

Figure 5-40

Evidence in support of this is provided by the observation that several thiophene-2-carboxylic acids (Figure 5-41) interact with the EuNALs giving rise to ternary luminescent complexes (Chart 5-17). In contrast, the analogous furan-2-carboxylic acids (Figure 5-42) do not result in sensitised Eu(III) emission (Table 5-8).

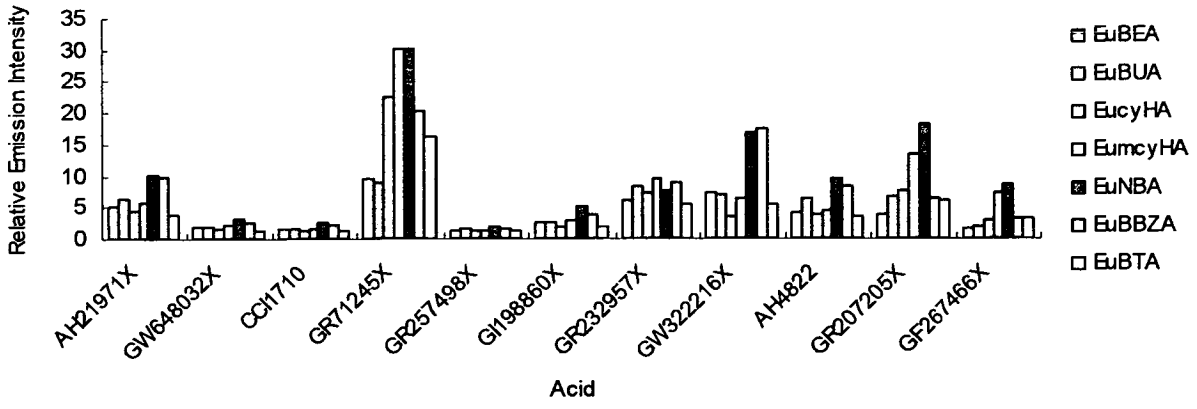

Chart 5-17 Relative emission intensities observed upon interaction of the EuNAL chelates with thiophene-2-carboxylic acids

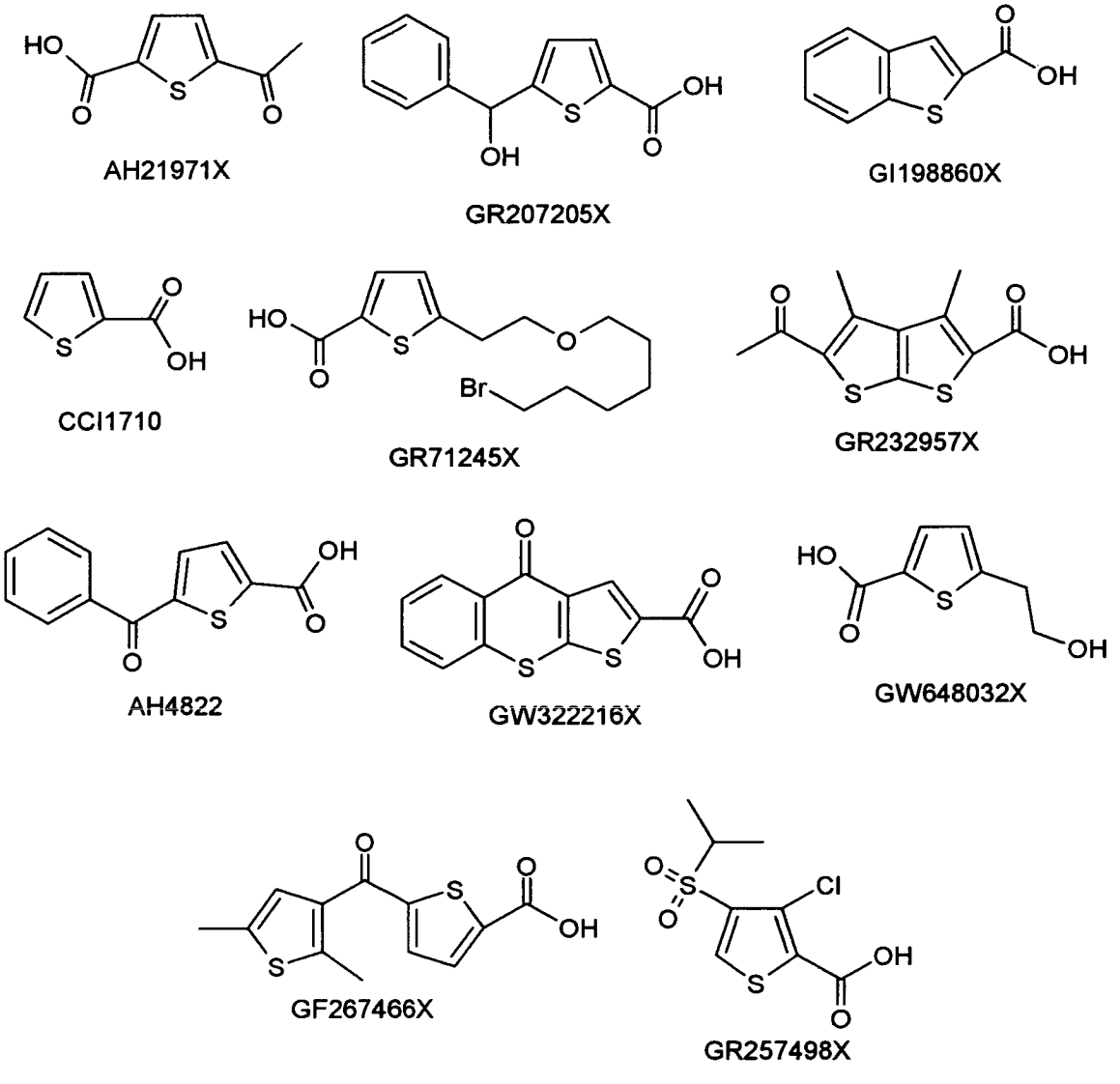

Figure 5-41 Thiophene-2-carboxylic acids

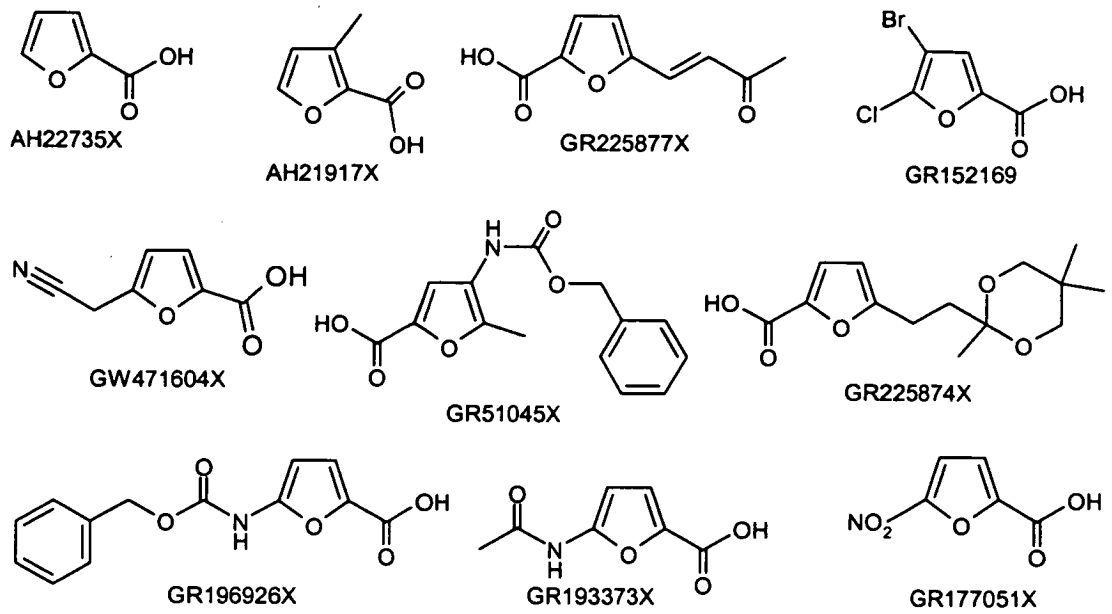

Figure 5-42 Furan-2-carboxylic acids

	Relative Emission Intensity (I/I_0)						
ACID	**EuBEA**	**EuBUA**	**EucyHA**	**EumcyHA**	**EuNBA**	**EuBBZA**	**EuBTA**
AH21917X	1	1	1	1	1	1	1
AH22735X	1	1	1	1	1	1	1
GR177051X	1	1	1	1	1	1	1
GW471604X	2	2	2	2	2	2	1
GR152169X	1	1	1	1	1	1	1
GR225877X	1	1	1	1	1	1	1
GR225874X	1	1	1	1	1	1	1
GR51045X	1	1	1	1	1	1	1
GR193373X	1	1	1	1	1	1	1
GR196926X	1	1	1	1	1	1	1

Table 5-8 I/I_0 upon combination of furan-2-carboxylic acids and EuNALs

Several substituted indole-2-carboxylic acids (Figure 5-43, Appendix 2) were also tested by combinatorial screening methods, none of which exhibited any activity towards the EuNALs. Under the assay conditions the lone pair electrons of the nitrogen heteroatom is and delocalised in the ring, maintaining the aromatic character. Consequently, these acids are unable to chelate the metal and any interaction would be mono-dentate via the carboxylate alone. In addition to this, the NH oscillator is capable of depopulating the Eu(III) excited state by non-radiative energy transfer. Coordination by the acid in the 2-position would bring the N-H bond into close proximity with the metal centre facilitating thermal

depopulation of the emissive $^5D_0$ state (see salicylic acid 5.2.8.3). The absence of sensitised Eu(III) emission can be attributed to PET (photoinduced electron transfer) from indole to Eu^{3+}.[155]

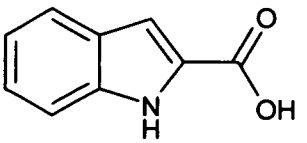

Indole-2-carboxylic acid

Figure 5-43

5.2.11 Anthraquinone Carboxylic Acids

A variety of anthraquinone acids were also studied as potential LHCs. At first glance it would appear that these acids exhibit great promise as light-harvesting centres for our EuNAL chelates in aqueous solution. However, closer examination of the results reveals that much of the light emitted arises from organic fluorescence, not from the metal centre following intramolecular energy transfer, attributed to mismatched triplet state energies. The delayed organic fluorescence may be E-type, due to thermally-assisted back intersystem crossing from the triplet to the singlet, or by P-type, upon recombination of two triplets to produce a singlet.

Anthraquinone carboxylic acids have a pK_a value of ~ 3.4 and as a result are fully deprotonated under experimental conditions with the DMSO/H_2O solvent mixture stabilising the charge formation. Upon excitation at 275 nm, compounds of this type are known to undergo photochemical transformations and are unlikely to exist in the keto-form. Differing results are obtained upon excitation at 340 nm, although in each case the signal detected was predominately due to organic acid fluorescence. This is largely due to differences in molar absorption coefficients of the acids and is also attributable to instrumental factors. For each emission/excitation wavelength pair, the Tecan Ultra automatically selects the appropriate mirror type. For 275/612 nm this is a 50% mirror, allowing transmission of only half the light. At λex = 340 nm a dichroic mirror is selected, allowing transmission of nearly 100% of the light, hence stronger signals are observed.

In all but three cases the signal detected is due to long lived organic fluorescence arising from excitation of the anthraquinone acids at 275 nm (Table 5-9). The feature common to these active acids, AH7652, AH7697 and AH7552 (Figure 5-44) is the presence of a second chromophore in addition to the anthraquinone moiety.

Attached in the 8-position via an ether linkage, these substituents can alter the photophysical properties of the acids relative to the inactive parent acid and the saturated alkyl derivatives, from which only organic fluorescence is observed under the assay conditions.

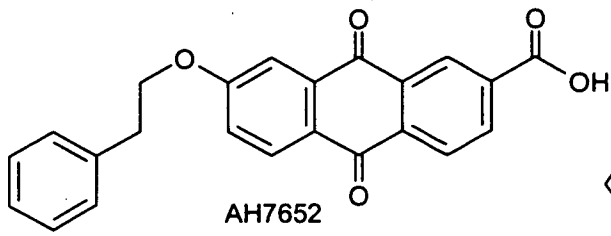

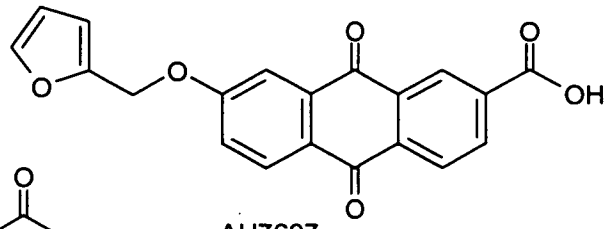

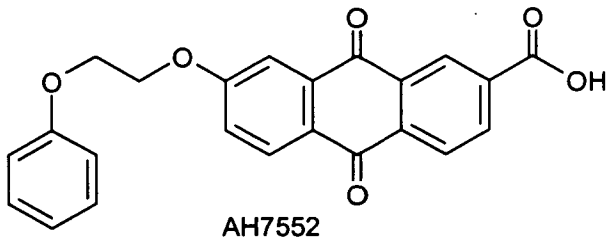

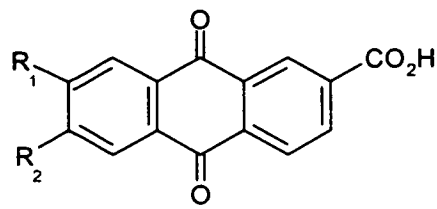

ACID	R_1	R_2
AH11654	$-OCH(CH_3)_2$	-H
AH14868XX	-H	$-OCH(CH_3)_2$
AH7167	$-O(CH_2)_3OH$	-H
AH7792Z	-H	$-O(CH_2)_3OH$
AH7650	$-O(CH_2)_2CH_3$	-H
AH6730	-H	$-OCH_3$
AH7290A	$-O(CH_2)_2NMe_2$	-H
AH7414Z	$-O(CH_2)_2OMe$	-H
AH7621Z	-H	$-O(CH_2)_2OH$
AH7651	$-O(CH_2)_2O(CH_2)_2OMe$	-H

Figure 5-44 Substituted anthraquinone carboxylic acids

	Emission Intensity (I)							
ACID	**Acids**	**EuBEA**	**EuBUA**	**EucyHA**	**EumcyHA**	**EuNBA**	**EuBBZA**	**EuBTA**
AH7652	310	1169	1891	1157	935	2010	2205	1256
AH7697	50	140	179	149	112	253	293	227
AH7552	59	513	749	416	406	1044	1367	638
AH11654	194	365	797	291	1747	2320	1562	1392
AH14868XX	502	843	863	663	1339	1404	1352	918
AH7167	840	921	833	801	845	893	906	869
AH7792Z	407	390	501	491	533	598	589	555
AH7650	816	950	960	869	955	1064	1100	955
AH6730	607	643	613	540	582	674	682	598
AH7290A	106	134	136	129	109	130	136	172
AH7414Z	880	843	879	852	821	863	832	788
AH7621Z	575	587	597	584	589	571	584	570
AH7651	700	759	744	735	753	782	738	778

Table 5-9 Emission intensity (I) recorded upon excitation of 1:1 anthraquinone carboxylic acid:EuNAL solutions at 275 nm.

It is a logical progression from these anthraquinone carboxylic acids to the cyclic γ-lactone xanthone derivatives as represented by the generic structure shown in Figure 5-45. As observed with the anthraquinone compounds, organic fluorescence is strong under experimental conditions and we must not only examine the relative emission increase with respect to the EuNAL, but also the raw luminescence signal from the assay giving rise to the following observations.

ACID	**R_1**	**R_2**	**R_3**
AH15201XX	-OH	-H	-H
AH6859	-OMe	-H	-H
AH15203XX	$-OCH(CH_3)_2$	-H	-H
GW314581X	-OEt	-H	-H
GW294655X	$-O(CH_2)_2OH$	-H	-H
GW328088X	$-OCH_2CH(CH_3)_2$	-H	-H
GW312792X	$-O(CH_2)_3CH_3$	-H	-H
GW294322X	$-O(CH_2)_2NMe_2$	-H	-H
GW304858X	$-O(CH_2)_2O(CH_2)_2OH$	-H	-H
GW312329X	$-O(CH_2)_2O(CH_2)_2OAc$	-H	-H
AH15400XX	$-OCH(CH_3)_2$	-Br	-H
GW314526X	-Et	-H	-OMe
GW324336X	-Me	-H	-OMe

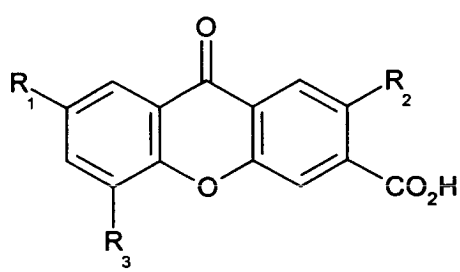

Figure 5-45 Generic structure of xanthone carboxylic acid derivatives

At first glance it appears that this group of acids exhibit great promise as light harvesting centres for our system. This is in fact misleading since each of the acids emits strong organic fluorescence still detected after a 20μs time delay following the excitation flash (Chart 5-18).

Only three of the acids of this type tested enhance the luminescence from the EuNAL chelate in aqueous solution, distinct from the background organic emission. These acids, GW312792X, GW312329X and GW314526X (Figure 5-46), in common with the substituted benzoic acids discussed earlier bear a saturated aliphatic tail group, beneficial to the formation of the ternary species.

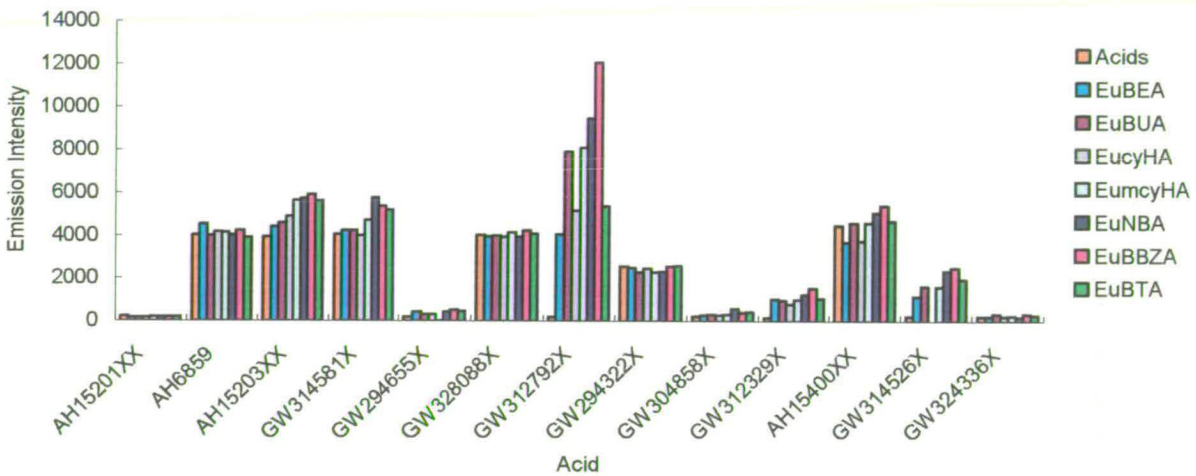

Chart 5-18 Emission intensity observed upon excitation of 1:1 solutions of EuNAL/LHC at 275 nm. Predominantly organic fluorescence is observed.

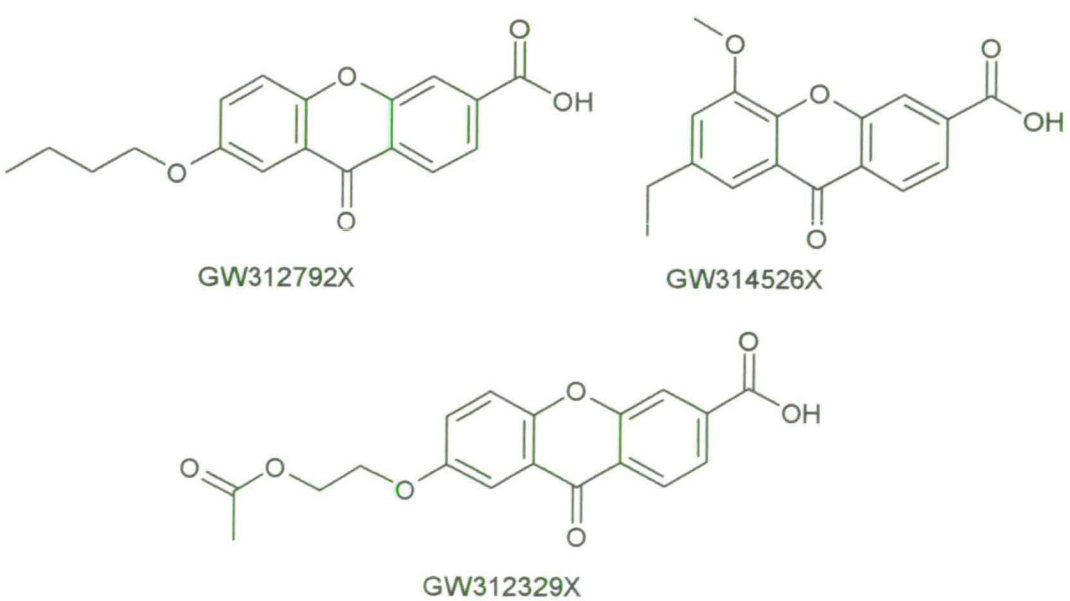

Figure 5-46 Xanthone carboxylic acids resulting in enhanced metal centred emission

It is uncertain at this stage whether the activity of these acids is due to an alteration in the triplet-state of the LHC allowing more efficient energy transfer to the metal centre, a hydrophobic shielding effect, or an increased binding interaction.

The location of electron density on the oxygen atom, discussed above when considering the furan derivatives (5.2.10), is likely to affect the distribution of electronic density in these acids. The π-electron density of these xanthone carboxylic acids is quite delocalised over the system, analogous to benzophenone, and have triplet state energies of similar value. In contrast, in the analogous thiaxanthone compounds (Figure 5-47) the π-electron density is delocalised over all three rings. This is an important consideration as it is noted that the thiaxanthone carboxylic acids are better sensitisers for our EuNALs than the harder oxygen counterparts.

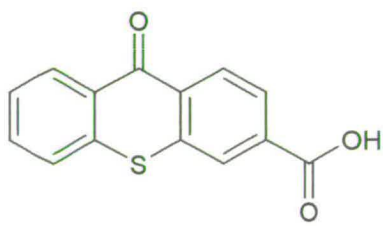

Figure 5-47 Thiaxanthone carboxylic acid

In common with the xanthone acids shown in Figure 5-45, the thiaxanthone acids bearing alkoxy substituents in the 6, 7 or 8 (Figure 5-48) positions give rise to strong, long-lived organic fluorescence under experimental conditions. We do, however observe a significant degree of sensitised Eu(III) emission with acid GW323591X, in which the chelate luminescence is enhanced 140-fold for EuNBA and EuBBZA. This increase is double that observed with EucyHA, EuBEA and EuBTA (~60-fold). EuBUA and EumcyHA emission is increased ~100-fold.

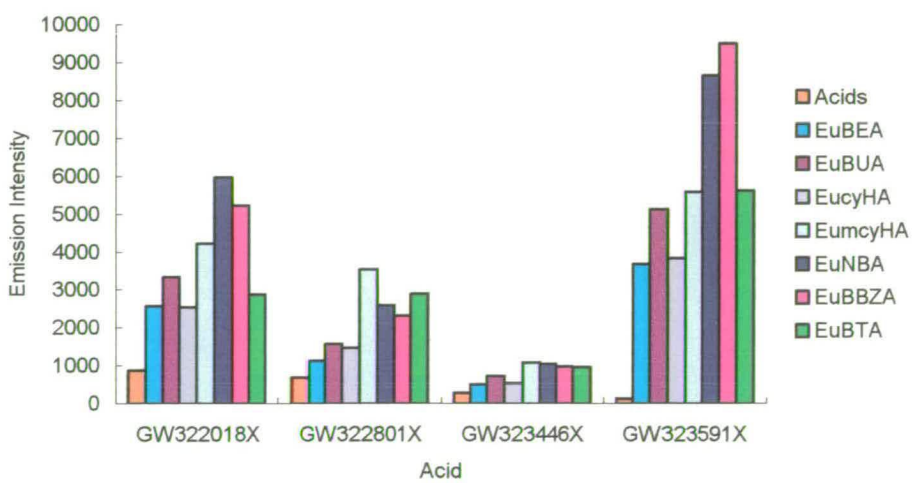

Chart 5-19 Relative Emission Intensity observed upon excitation of 1:1 solutions of EuNAL: LHC at 275 nm

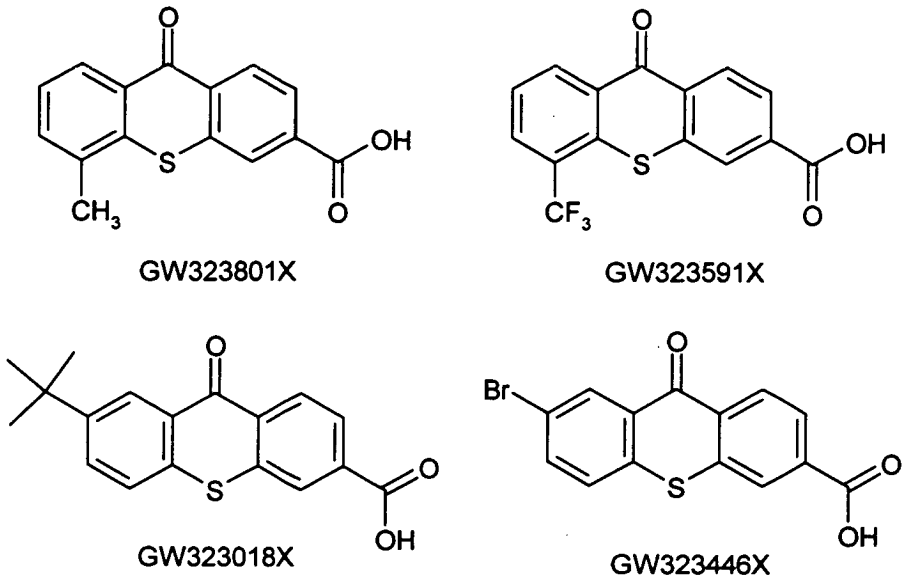

Figure 5-48 Thioxanthone derivatives showing activity towards the EuDTPA-AM_2 chelates

The background acid fluorescence at the detection wavelength is significantly less than that of many of the other acids of this type, reading 139 counts in comparison to an average of ~1000 counts.

We attribute the strong interaction of this acid with the EuNAL to the presence of the powerfully electron withdrawing $-CF_3$ substituent in the 9-position. This group efficiently removes electron density from the aromatic system, stabilising the formation of the carboxylate anion with respect to the protonated species. Not only does this strengthen the binding interaction with the metal centre, but by altering the triplet state seems to lead to an excellent match of excited state energy levels, increasing the efficiency of intramolecular energy transfer. The low intensity of organic fluorescence observed with these thiaxanthone derivatives in combination with the intense sensitised Eu(III) emission is evidence for efficient energy transfer between the LHC triplet-state and metal centre. Similarly, acid GW323446X, bearing a bromide substituent in the 7-position is active as an LHC but the relative emission intensity observed is much weaker than that of the trifluoromethane derivative GW323591X. The activity of GW323446X may also be due to an increased triplet yield due to the heavy atom effect with the bromide substituent. The good activity of compounds GW323801X and GW323018X can be attributed to the steric bulk of the alkyl substituents in the 9 and 6-positions respectively. As expected, the tertiary butyl derivative, GW323018X, interacts with the EuNALs to form ternary complexes more intensely luminescent than the $-CH_3$ derivative, GW323801X. As previously observed, these LHCs demonstrate selectivity towards EuBBZA and EuNBA, the more rigid and hydrophobic EuNALs.

5.3 LnNAL Chelate Induced Selectivity

The aromatic carboxylic acids screened for their ability to form ternary luminescent complexes with EuDTPA-AM_2 chelates in aqueous solution have thus far been considered only from the perspective of the LHC binding and chromophoric units. We now turn our attention to the influence of the amide arms of the NAL on molecular recognition. It is noted from the assay data presented in the preceding section that several of the acids display good general activity towards all the EuNALs under investigation, whereas others interact more selectively, influenced by characteristics of the DTPA-AM_2 binding cavity.

5.3.1 EuNAL Molecular Recognition with Substituted Phenyl LHC Units

A feature of the substituted phenyl LHC units which result in increased sensitised Eu(III) emission discussed in sections is their good general activity towards the EuNALs under investigation, as discussed in sections 5.2.1 – 5.2.5. Interestingly, a degree of selectivity is seen towards EuNAL chelates by several of these LHCs, some of which form more intensely luminescent ternary complexes with EuNBA and EuBBZA than with the straight chain and cyclic aliphatic EuDTPA-AM_2 derivatives. It is proposed the rigidity of the amide residues of DTPA-NBA and DTPA-BBZA results in a binding cavity with better definition than those presented by EuNALs formed from the more flexible aliphatic NALs. The effect is illustrated well by the benzoic acid derivatives LHCs discussed in section 5.2.4. Chelates EuNBA and EuBBZA interact with these acids to form ternary luminescent complexes exhibiting at least twice the degree of sensitisation afforded by the model chelate, EuBEA (Chart 5-8). A striking observation is that although there is evidence for ternary complex formation with EuBTA with these LHCs, the luminescence arising from this interaction is comparatively weak (10-20 - fold). This remarkable difference is attributable to the influence of the tolyl groups on the NAL cavity. A stronger background signal is detected with EuBTA than from the other EuNALs, due to energy transfer from the tolyl rings of the NAL. The molar extinction coefficient of DTPA-BTA is expected to remain unchanged with respect to DTPA-BBZA, since the influence of the methyl substituents on the electronic structure of the aromatic ring is negligible. The increased background signal with EuBTA relative to the other EuNALs is attributed to a combination of two effects:

1) Energy transfer to the metal from the aromatic amide arms

2) Increased protection of the metal centre from quenching by outer sphere solvent molecules provided by the methyl groups.

Consequently, the relative emission increase observed upon molecular recognition is reduced with respect to the other EuNAL chelates. Energy transfer from the aromatic amide arms complicates determination of sensitisation by new LHCs.

The selectivity towards EuBUA over EuBEA may be explained by consideration of the amide arm length. By increasing the aliphatic chain from the two-carbon ethyl to four-carbon butyl we enhance the lipophilicity of the chelate, encouraging inclusion of the acid into the cavity. It is apparent that lipophilicity alone is not sufficient to drive the interaction, as EucyHA would also be expected to interact more strongly than the ethyl derivative EuBEA. This clearly is not the case, and is suspected to be due to steric crowding imparted on the cavity by cyclohexyl ring-flip isomerisation (Figure 5-49). Incorporation of a methylene spacer between the cyclic aliphatic group and the amide bond introduces an additional degree of rotational freedom to the chelate cavity and may account for the increased activity observed with EumcyHA over EucyHA.

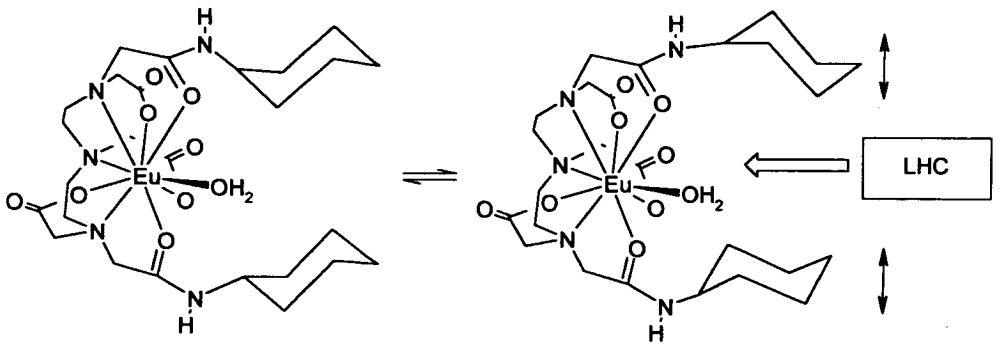

Figure 5-49 Schematic Representation of ring-flip isomerisation in EucyHA, which may serve to impede the molecular recognition between EuNAL and LHC

5.3.2 EuNAL Molecular Recognition with Quinoline Carboxylic Acid LHC Units

The selectivity of the hydroxyquinoline acid LHCs is best illustrated by Chart 5-14 (section 5.2.8.2). It is apparent from the bar charts that 4-hydroxyquinoline-3-carboxylic acids (Figure 5-35) exhibit good general activity towards our EuNAL chelates. As with the substituted phenyl LHC units discussed above, the maximum emission increase is observed upon recognition with EuNBA, due to the more rigid and well-defined binding cavity of the complex. It is interesting to note that the simple chelate, EuBEA, with the shortest amide arms is also strongly active with these acids. One striking observation is that EucyHA and

EumcyHA result in mixed ligand luminescent complexes with almost half the relative emission intensity of EuNBA. We attribute this observation to ring-flip isomerisation within the cyclohexyl (Figure 5-49) and methylenecyclohexyl amide substituent arms of the NAL, which may serve to impede the acid recognition process.

5.3.3 EuNAL Molecular Recognition with Naphthyridine Carboxylic Acid LHC Units

With these LHCs (Section 5.2.9, Figure 5-36), the selectivity towards EuNBA is observed as expected (Chart 5-15). This is attributed as before to the rigid nature of the amide arms, unable to isomerise and therefore capable of forming a well-defined cavity for recognition by the LHC. The interaction with the smaller aliphatic EuNALs is weaker, as the arms of the NAL do not lend themselves to the formation of a pre-defined approach path for the acid LHC to the same extent as the norbornyl derivative does.

The naphthyridine carboxylic acids (Figure 5-36) display a marked difference in activity, favouring EuBTA over EuBBZA under the experimental conditions. It was previously observed that the relative emission intensities recorded with the tolyl derivative are generally lower than those of the benzyl EuNAL, due to the stronger background chelate luminescence (I_0) detected from EuBTA. In this case we believe that the strength of the recognition with EuBTA is due to π-π electronic interactions between the acid chromophore and the tolyl arms of the NAL. The additional methyl substituents on the aromatic ring give the cavity some protection against quenching by outer sphere solvent molecules. The results from these assay experiments do not provide us with sufficient information to draw any firm conclusions as to what is governing this selectivity and further experiments under different conditions are required. The results of subsequent binding studies are discussed in Chapter 6.

5.3.4 EuNAL Molecular Recognition with Sulphur and Oxygen Heterocyclic Carboxylic Acid LHCs

Many of the sulphur and oxygen containing heterocyclic carboxylic acid LHC units screened for their ability to form luminescent ternary complexes with our EuNAL chelates exhibit only organic fluorescence under the experimental conditions. It is noted that those enhancing the metal centred emission display some selectivity towards the more rigid chelates, EuNBA and EuBBZA, consistent with our previous observations. Results are presented and discussed in sections 5.2.10 and 5.2.11.

5.4 Conclusions and Predictions

In conclusion, by employing combinatorial screening techniques in the development of highly luminescent lanthanide chelates, we have demonstrated that selective molecular recognition may be achieved based on both the acid LHC and EuNAL chelate properties. By screening a large library of aromatic carboxylic acids versus a selection of EuDTPA-AM_2 chelates in aqueous solution, chosen to represent a variety of different binding sites, some general structural and electronic trends have been identified.

5.4.1 The Aromatic Acid LHC

It has been shown that incorporating a hydrophobic aliphatic alkyl or alkoxy substituent to the simple acid LHC (benzoate or picolinate) can dramatically enhance the luminescence of the ternary complex formed upon molecular recognition. The presence of resonance electron withdrawing substituents often strengthened the binding interaction observed between the metal and the LHC, whereas electron donating groups such as -OMe, -OH and $-NH_2$ exhibited the opposite effect. By striking a balance between these two influences it is possible to manipulate the ground state energy of the π-electronic systems of simple acids. The triplet state energy is in turn modified to afford a good match with the excited state of the metal centre, resulting in highly luminescent chelates in aqueous solution.

It was noted that increasing the conjugation of the picolinic binding unit by progression to quinoline-2-carboxylic acids does not produce the expected increase in activity. Conversely the interaction is weakened relative to PCA and very little sensitised Eu(III) emission is observed. Interestingly, 4-hydroxyquinoline-3-carboxylic acids were shown to be consistently good light harvesters for our EuDTPA-AM_2 chelates. Considering these observations we wish to predict an ideal aromatic carboxylic acid LHC for optimum ternary complex luminescence upon interaction with the EuDTPA-AM_2 chelates (Figure 5-50).

The binding unit should be based on the 4-hydroxypyridine-3-carboxylic acid moiety. Extension of the conjugation to the quinoline system will increase the molar absorptivity of the acid, in turn favouring the efficiency of energy transfer to the metal. The efficiency of energy transfer can be modified by subtle alterations to the triplet energy of the acid – achieved by incorporation of such inductively electron withdrawing substituents as $-OCF_3$ and $-CF_3$ to achieve a good match of triplet LHC and Ln(III)* excited states energies. Finally, attaching an alkyl or alkoxy hydrophobic chain to the acid chromophore/binding unit may reduce the quenching influence of outer sphere solvent molecules giving an overall increase in Eu(III) emission.

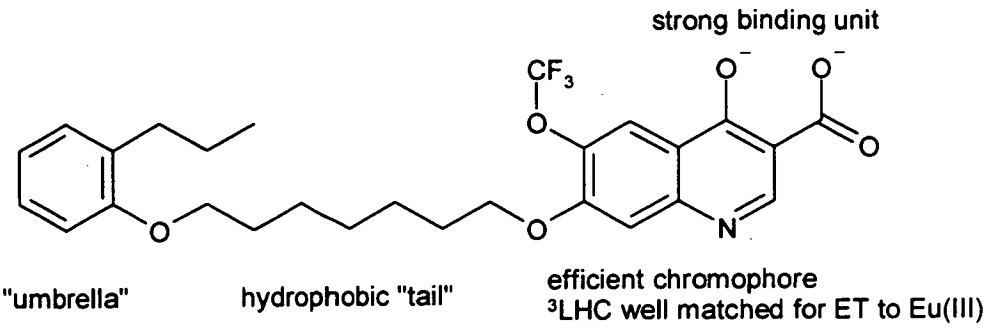

Figure 5-50 Predicted model of an aromatic acid LHC for efficient molecular recognition and optimum luminescence with EuDTPA-AM_2 NAL chelates

5.4.2 The EuNAL

During the combinatorial screening experiment the more rigid and sterically bulky EuNALs emerged as better receptors for the aryl acid LHCs than their smaller, less rigid counterparts. Molecular recognition between the well-defined cavity of EuNBA and the LHCs consistently resulted in intensely luminescent ternary species in aqueous solution. Similarly, a strong interaction is observed between EuBBZA and many of the LHCs screened. At the wavelength employed (275 ± 10 nm) the benzyl rings of the NAL absorb some of the excitation flash. By shifting the excitation wavelength further into the red (~ 30 nm) such absorption by the NAL can be avoided, thus minimising the background Eu(III) emission sensitised by excitation of the aromatic NAL. With the aromatic NALs BTA and BBZA π-π interactions are possible and may enhance the efficiency of energy transfer from the LHC to the metal centre. In view of improvement in luminescence upon substitution of the LHC with an alkyl or alkoxy tail, it might be expected that addition of such substituents to the amide arms of the NAL should have a similar effect. The rigidity of the cavity must be maintained to provide a facile approach route for the LHC upon molecular recognition. Progression to a more rigid sterically bulky aliphatic DTPA-bis(amide) such as an adamantane derivative would also be expected to improve the interaction. Extending the cavity using biphenyl or fused aromatics such as anthracene, naphthalene or pyrene is possible, but enhances the problems of NAL absorption encountered with BBZA and BTA although the triplet states of anthracene and pyrene are known to be too low in energy to sensitise Eu(III) emission. The binding interactions between the acid LHCs identified here and the chelates are studied in more detail by luminescence spectroscopy under steady state and time resolved excitation and the results discussed in Chapter 6.

6 Binding Studies

The specific molecular interactions leading to controlled self assembly of luminescent ternary complexes between LnDTPA-AM_2 chelates and aromatic carboxylic acid LHC units in aqueous solution were investigated using a variety of spectroscopic techniques. Electrospray mass spectrometry was employed in identification of ternary complexes formation. The strength of the binding interaction and intramolecular energy transfer processes were evaluated by luminescence spectroscopy under steady-state monochromatic excitation. Time-resolved emission spectroscopy, monitoring the luminescence decay at a fixed wavelength upon pulsed laser excitation was used to determine the hydration state of the metal and elucidate potential binding mechanisms. Ternary complex formation is also observed by ^{1}H and ^{13}C NMR spectroscopy.

6.1 Aromatic Acid Recognition with EuBEA

In Chapter 3, initial emission studies on the model mixed ligand system revealed the different modes of molecular recognition between EuBEA and the simple aromatic acid LHCs, PCA, PTA, BZA, IsoPTA and DiPCA. Binding of the EuNAL by the LHC is accompanied by increasing metal centred luminescence, as the strongly absorbing moiety chelates to the metal, allowing intramolecular energy transfer to occur. The observed emission intensity is a function of the efficiency of all the photophysical processes occurring within the system, including ligand absorption, intersystem crossing from S_1 to T_1, intramolecular energy transfer to the metal emissive state, non-radiative depopulation, and radiative decay of the luminescent level. Equilibrium constants for formation of 1:1 ternary complexes between the EuNAL and LHC are obtained by fitting of the spectroscopic data to Equation 2-4 by the method on non-linear least squares analysis. The estimated equilibrium constants for the formation of ternary species in aqueous solution between EuBEA and simple aromatic acids BZA, PTA and PCA are given in Table 6-1. The emission spectra obtained upon titration of the EuNAL with the LHC under investigation are integrated (572 – 640 nm) and the change, $\Delta I = I-I_0$, plotted versus the total acid concentration ($molL^{-1}$). Results are illustrated in Figure 6-1.

EuBEA + Acid = [EuBEA.ACID]			
Acid	**K (M^{-1})**	**Log K**	**(±)**
PCA	8.8×10^4	4.95	0.14 (3%)
PTA	7.3×10^4	4.86	0.19 (4%)
BZA	3.9×10^4	4.60	0.02 (0.6%)

Table 6-1 Estimated formation constants for 1:1 EuBEA.LHC in aqueous solution at 0.15 mM (EuNAL chelate formed in solution in cuvette prior to titration with acid)

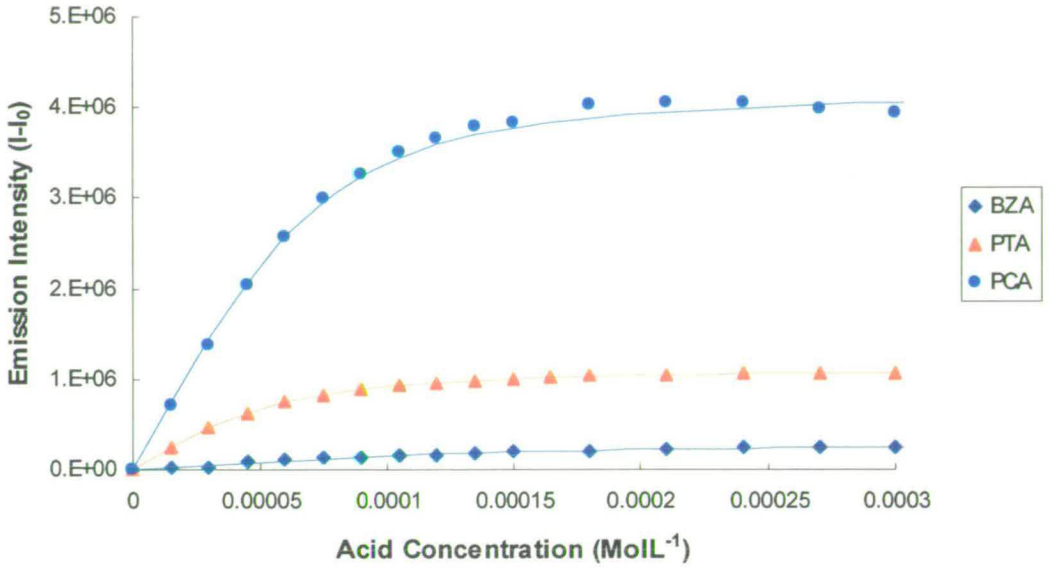

Figure 6-1 Plot of $I-I_0$ versus [LHC] ($molL^{-1}$) for the interaction between EuBEA (0.15 mM aq) and benzoic, phthalic and picolinic acids in aqueous solution (pH 7-8). Binding constant curve fits are in solid lines.

These results demonstrate that PCA is a better sensitiser than PTA or BZA. This can be attributed to three different factors.

1) The recognition between PCA and EuBEA is stronger than that occurring between the chelate and the dicarboxylate PTA or monocarboxylate BZA, due to the better coordinating unit. Conformational analysis (Chem 3D) shows a planar conjugated system to exist between Eu(III) and PCA (Figure 6-2). Similarly, BZA-Eu(III) binding results in a planar structural arrangement. Steric and electronic constraints prevent establishment of such a system with phthalate as the 7-membered chelate ring is likely to be puckered in its lowest energy conformational form.

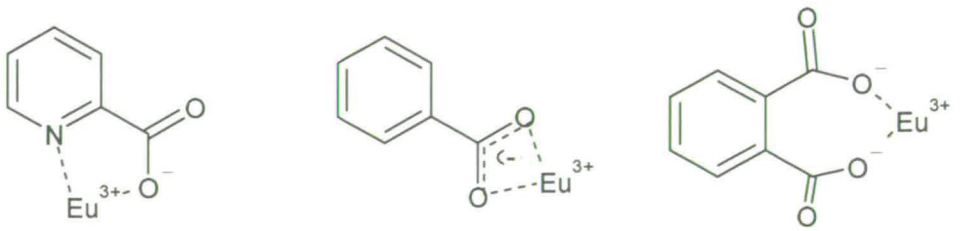

Figure 6-2 Model PCA, BZA and PTA binding interactions with Eu(III)

2) Comparison of the molar absorptivity of the acids reveals that PCA (ε = 3830 $M^{-1}cm^{-1}$) absorbs a slightly greater cross section of the excitation energy (λex = 270 nm) than either PTA (ε = 3200 $M^{-1}cm^{-1}$) or BZA (ε = 2930 $M^{-1}cm^{-1}$).

3) The intramolecular energy transfer between the triplet state of PCA and Eu(III) is more efficient due to the short distance between the chromophoric donor ligand and metal acceptor established upon nitrogen coordination (Eu-N ~ 2.4 Å). In contrast, the energy absorbed by the benzoate and phthalate antenna ligands must travel over three bonds, a total distance of greater than 5 Å.

Picolinic acid was therefore selected as a model LHC with which to study the influence of the amide arms on the LnDTPA-AM_2 binding cavity.

An error involved in the experimental conditions is the formation of the EuNAL in solution. The chelate was formed *in situ* upon addition of one equivalent of the deprotonated NAL (H_2O/NaOH) to aqueous $EuCl_3$ (2 ml, 0.15 mM) in the cuvette prior to titration with the acid of interest. Although the major species present in solution under these conditions is the EuNAL complex (Log K ~ 15), Na^+ also interacts with the ligand (as discussed in Chapter 4) and the ionic strength of the solution is not controlled.

6.2 Factors Affecting Picolinic Acid LHC Recognition

As discussed in Chapter 4, the preparative method employed in isolation of the EuNAL influences the ternary complex formation with PCA. It should be noted that the binding between picolinic acid and the EuNAL chelates isolated at pH 7 or greater, (and those from the Eu_2O_3 starting material) was much weaker than expected, on average resulting in a 5-6 fold increase in emission intensity for both EuBEA and EucyHA. Emission spectra obtained upon excitation of equimolar EuNAL:PCA samples show the observed increase in sensitised Eu(III) luminescence (Figure 6-3). The characteristic absorption of PCA around 270 nm present in the excitation spectra (Figure 6-4) when emission is monitored at 616 nm provides unequivocal evidence for the intramolecular absorption energy transfer emission (AETE) mechanism. The comparatively inefficient intramolecular energy transfer is a consequence of the mode of LHC binding, influenced by the presence of hydroxide ions.

Picolinic acid coordination is expected to occur *via* the carboxylate group only, with the nitrogen unable to participate in chelation. The luminescence lifetime measurements discussed below shed some light on the possible mechanism of interaction.

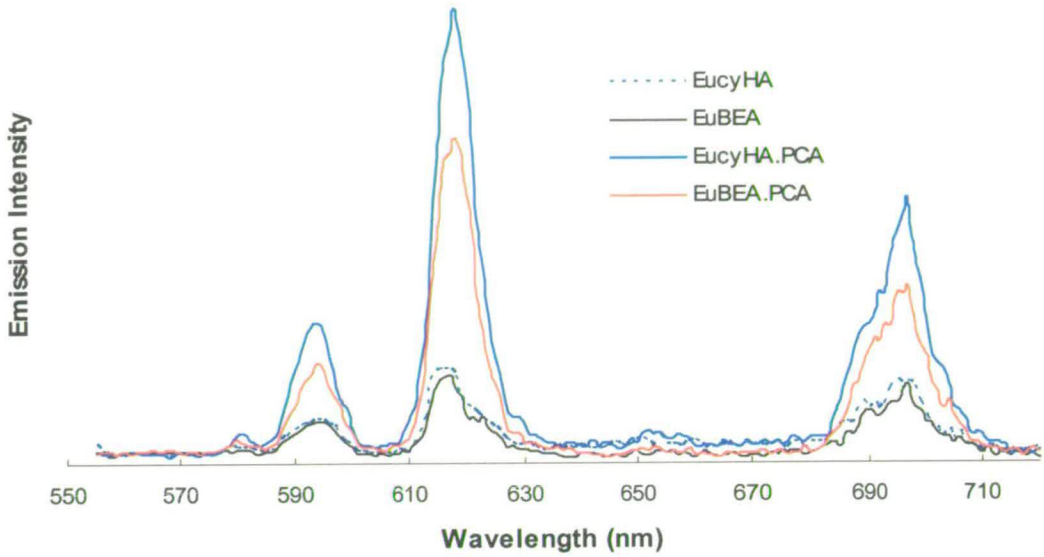

Figure 6-3 Emission spectra obtained upon combination of EuBEA and EucyHA (0.1 mM aq) with 1 equivalent of PCA (λ ex = 270 nm)

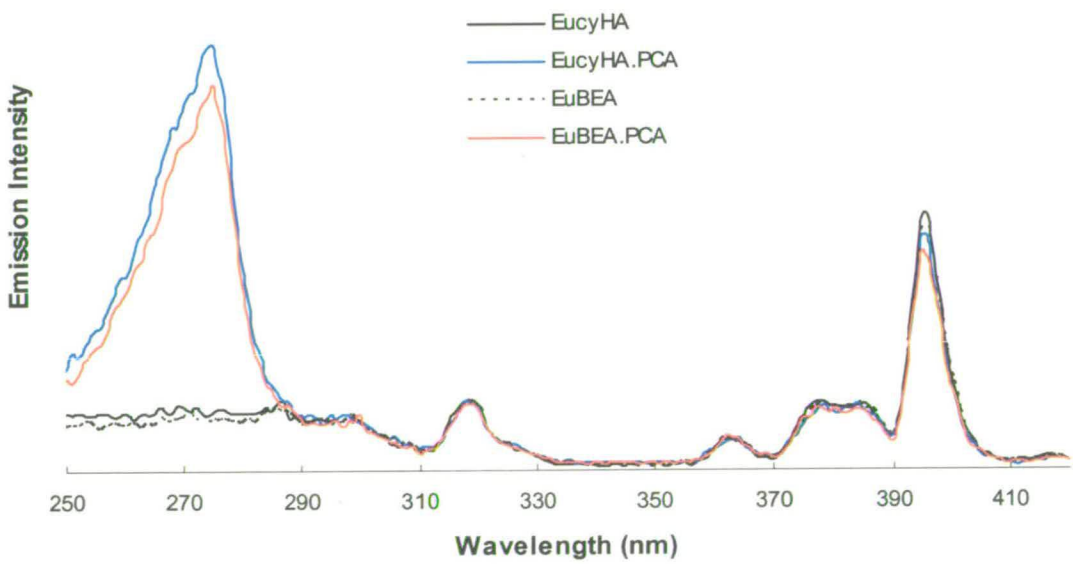

Figure 6-4 Excitation spectra (no correction for lamp response) of EuBEA and EucyHA in aqueous solution (0.1 mM, pH 7) with 1 equivalent PCA (λ em = 616 nm)

Luminescence lifetime data obtained upon pulsed laser excitation of the sample at 355 nm, as detailed in section 2.6.4, is fitted by the method of non-linear least squares curve fitting to a single or bi-exponential decay model (Equation 2-5), is given in Table 6-2. Molecular recognition between the EuNAL and picolinic acid is accompanied by an increase in the luminescence lifetime of the metal, evidence that high energy OH oscillators are displaced from the primary coordination sphere of the metal. For the chelate complexes prepared and isolated from solutions of $EuCl_3$ and the appropriate ligand in the presence of TBAOH (pH ~7) an increase in lifetime of approximately 50 μs is observed upon the LHC binding event. Examples of typical EuNAL and [EuNAL.PCA]$^-$ luminescence decay curves and fits are illustrated in Figure 6-5.

EuNAL + PCA (λex = 355 nm)				**TbNAL + PCA (λex = 355 nm)**			
Chelate	**LHC**	**τ (ms)**	**+/-**	**Chelate**	**LHC**	**τ (ms)**	**+/-**
EuBEA	-	0.574	0.001	**TbBEA**	-	1.710	0.0024
	PCA	0.630	0.001		1 PCA	1.698	0.0025
	2 PCA	0.629	0.000		2 PCA	1.689	0.0020
	3 PCA	0.626	0.000		3 PCA	1.684	0.0026
EuBUA	-	0.578	0.001	**TbBUA**	-	1.699	0.0021
	PCA	0.635	0.001		1 PCA	1.689	0.0018
	2 PCA	0.643	0.001		2 PCA	1.679	0.0017
	3 PCA	0.643	0.001		3 PCA	1.671	0.0018
EuBBZA	-	0.524	0.001	**TbBBZA**	-	1.588	0.0022
	PCA	0.776	0.015		1 PCA	1.611	0.0028
	2 PCA	0.877	0.025		2 PCA	1.587	0.0036
	3 PCA	0.707	0.356		3 PCA	1.564	0.0024
EucyHA	-	-	-	**TbcyHA**	-	1.647	0.0020
	PCA	-	-		1 PCA	1.627	0.0020
	2 PCA	-	-		2 PCA	1.620	0.0018
	3 PCA	-	-		3 PCA	1.610	0.0024

Table 6-2 Luminescence lifetimes for EuNAL and TbNAL ternary complexes formed upon molecular recognition with the PCA binding unit.

The corresponding terbium chelates do not show a measurable increase in the luminescence lifetime upon picolinic acid recognition. This is a reflection of the relative quenching power of the OH oscillator towards Eu^{3+} ($^5D_0$) and Tb^{3+} ($^5D_4$) respectively. The observed luminescence lifetime of the TbNAL species in aqueous solution measured upon excitation at 355 nm is circa 1.6 ms. This is significantly longer than that observed for the

EuNAL species, (0.5 ms), exhibiting the same coordination polyhedron. Picolinic acid binding, displacing the remaining H_2O from the coordination sphere, has a less significant bearing on the luminescent lifetime of the TbNAL•LHC ternary complex than that of the corresponding Eu(III) analogue.

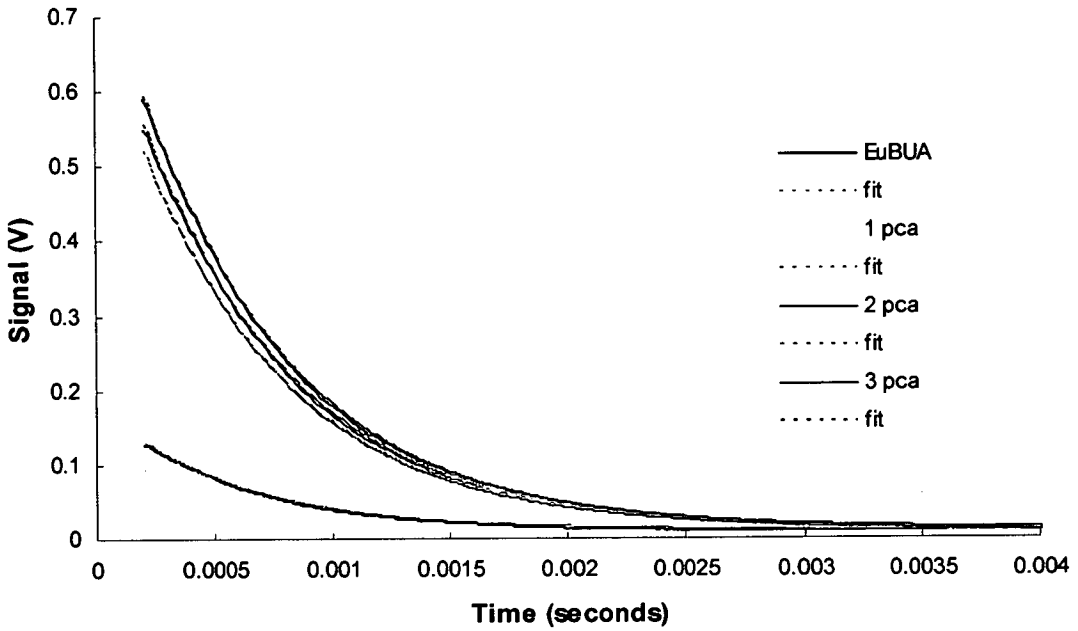

Figure 6-5 Linear plot: Luminescence decay curves of EuBUA and [EuBUA.PCA] mixed ligand complexes in aqueous solution (0.01 M, λex = 355 nm, λem = 616 nm)

It is clear from the above observations that PCA is forming ternary luminescent complexes in the presence of competing hydroxide ligands, however, the relative emission intensity is somewhat diminished. The consequences of OH coordination are evaluated in Chapter 6.2.1 below.

6.2.1 Competing Coordination by Hydroxide Ligands

Regardless of the mechanism of OH coordination to the EuNAL, whether by displacement of the neutral coordinating water molecule by the anionic hydroxide ligand or by proton transfer, the equilibrium is expected to lie to the side of the $[EuNAL.OH]^-$ species at high pH.

NMR studies reported[156] on GdDTPA-AM and GdDTPA-AM_2 (Log K_{GdL} ~ 15) chelates describe an increase in the relaxation time of the protons of the coordinated water molecule in comparison with the anionic chelate $[GdDTPA]^{2-}$ (Log K_{GdL} ~ 22).[130, 133] Replacement of one ligand carboxylate group with an amide results in a decrease in the

exchange rate of the metal bound water molecule by a factor of approx. 4, attributed to the lower thermodynamic stability of the Gd(III) amide bond with respect to carboxylate coordination. In neutral DTPA-AM_2 species the longer amide Gd-O bond (2.444 Å) (relative to the carboxylate Gd-O (2.40 Å)) results in a less crowded inner coordination sphere than that of the analogous anionic DTPA complexes. It was shown that the dissociatively activated water exchange mechanism was favoured in complexes with a tight inner coordination sphere. Additionally it was proposed that the positively charged metal centre is more exposed to the solvent environment in the amide complexes than in the corresponding aminopolycarboxylate species.

It is therefore reasonable to expect similar behavioural trend when a hydroxide ligand occupies the remaining binding site of the EuDTPA-AM_2 chelates. The less shielded positive charge on the metal is likely to increase the strength of an electrostatic interaction with the anionic hydroxide ligand. The protonation constant of the water in an aqueous solution of the Eu(III) ion[148] is 8.3. It is proposed that the pK_a of the metal bound water in the EuDTPA-AM_2 complex is reduced with respect to the free aqueous ion, an important consideration in the study of controlled mixed ligand complex formation.

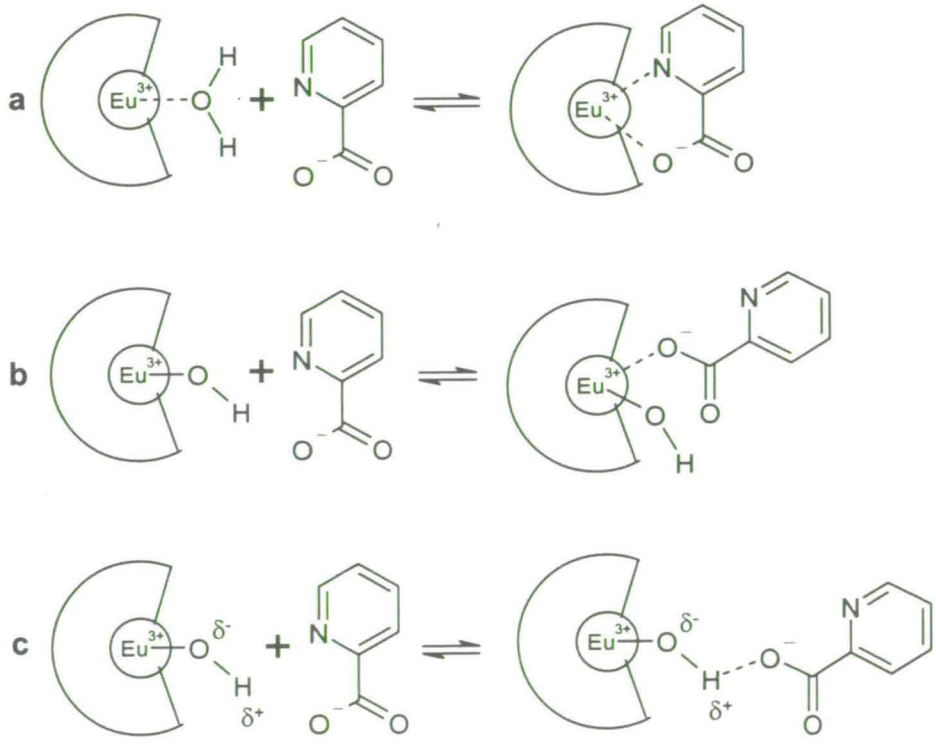

Figure 6-6 EuNAL + PCA binding interactions in the presence of competing hydroxide ligands

Picolinic acid coordination, expected to occur via the bidentate binding unit (comprising the deprotonated carboxylic acid and the nitrogen heteroatom of the aryl ring) becomes increasingly difficult when a hydroxide ligand occupies the ninth coordination site of the EuNAL chelate. Three possible mechanisms of coordination are illustrated above (Figure 6-6) and are discussed below.

Mode (a) is the bidentate interaction forming a 5-membered chelate ring between the metal and the ligand heteroatom and carboxylate, expected to result in increasing metal centred emission. A lengthening of the observed luminescence lifetime[45] by approximately 0.6 ms is predicted as the OH oscillators for one water molecule are displaced from the inner coordination sphere. In mode (b) a hydroxide ligand occupies the ninth coordination site of the metal. The PCA-Eu(III) interaction is not sufficiently strong to displace the OH ligand completely, and any sensitised emission observed is the result of energy transfer occurring via the coordinating monodentate carboxylate group only. The nitrogen heteroatom is not expected to bind the metal in this species, and no increase in the luminescence lifetime is to be expected since the number of OH oscillators in the inner sphere of the metal is unchanged with respect to the EuNAL species. In mode (c) the hydroxide ligand is not displaced from the metal centre, but acts as a bridge forming an H-bonding linkage between the negatively charged carboxylate and the partial positive charge on the coordinated OH. This binding interaction is expected to give rise to an increase in sensitised metal emission. Energy transfer is facilitated by the H-bonding network between the LHC and the EuNAL as the acid is not bound directly to the metal centre. A slight increase in luminescence lifetime is also to be expected. Interaction with the LHC may result in a change in the stretching frequency of the coordinated OH oscillator, thus slightly altering the observed lifetime. As the EuNALs studied exhibit an increased luminescence lifetime upon LHC recognition in aqueous solution, it is proposed that mode (c) is the mechanism by which PCA coordination occurs in the presence of competing hydroxide species. Improved sensitisation of Ln(III) luminescence is observed upon picolinic acid recognition with the chelates which were isolated from aqueous solution at pH 5-6 (avoiding OH coordination: Chapters 2, 4).

Binding studies with analogous TbNAL chelates demonstrated controlled formation of mixed ligand luminescent complexes with PCA. Increasing sensitised terbium emission was observed upon excitation of the sample at λex = 270 nm but no change in luminescence lifetime detected upon molecular recognition. At 20 430 cm^{-1} the $^5D_4$ excited state of Tb(III) is much less susceptible to depopulation by non-radiative energy transfer to OH than the corresponding $^5D_0$ level of Eu(III) (17 250 cm^{-1}). Consequently, a reduction in the

stretching frequency of O-H bond due to interaction with the carboxylate group (Figure 6-6 (c)) will not give rise to a significant change in luminescence lifetime. Intramolecular energy transfer between the LHC and the metal is confirmed by the presence of the characteristic PCA absorption band in the excitation spectra (Appendix 3).

6.3 *Picolinic Acid Molecular Recognition with EuDTPA-AM$_2$ Chelates*

6.3.1 PCA Recognition: Luminescence Studies

The PCA binding unit is observed to recognise the binding cavity of the EuNAL chelates. The effect of the amide arms on this molecular recognition was evaluated using EuNBA, EuBBZA and EuBUA, each forming 1:1 mixed ligand luminescent complexes with PCA (Figure 6-7). In agreement with results of the combinatorial screening experiment, EuNBA is observed to form a more intensely luminescent ternary complex with PCA than EuBUA or EuBBZA.

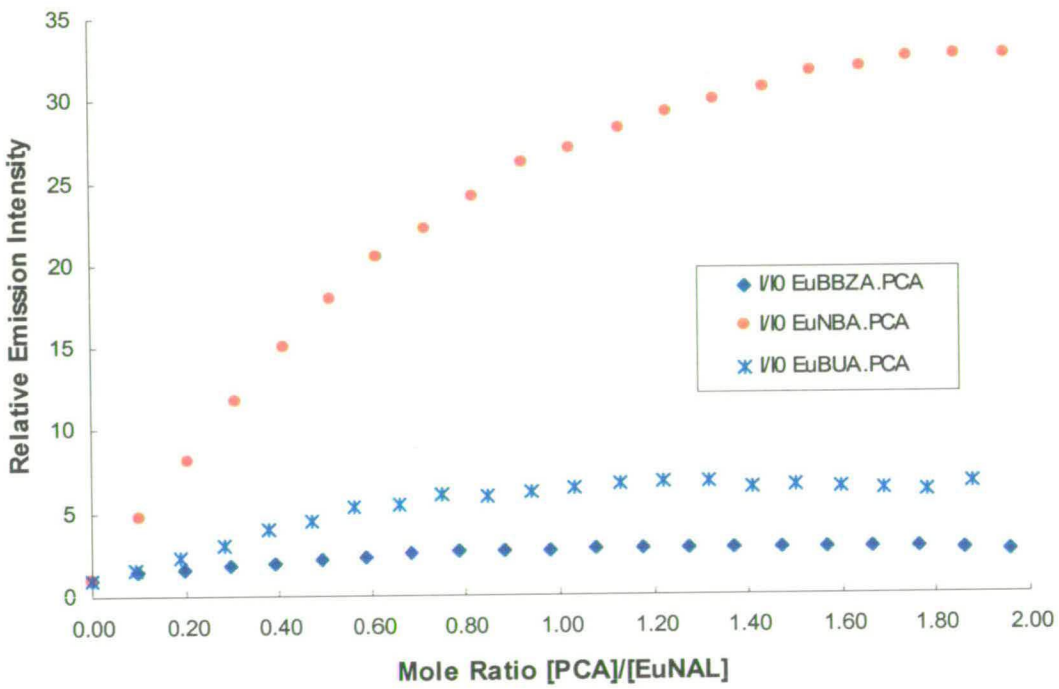

Figure 6-7 Relative emission intensity versus mole ratio [PCA]/[EuNAL] for formation of 1:1 mixed ligand complexes between EuNBA, EuBUA and EuBBZA (0.1 mM aq, pH 7, λ ex 270 nm)

Controlled assembly of the 1:1 mixed ligand species between EuNBA and PCA triggers a 30-fold increase in sensitised Eu(III) emission. In contrast, the analogous ternary species with EuBUA affords approximately 6-fold enhancement under similar experimental

conditions, and PCA recognition with the aromatic derivative, EuBBZA, yields a ternary complex with barely double the emission intensity of the EuNAL chelate upon excitation at 270 nm. Emission spectra are shown in Figure 6-8. The linear plot of the change in emission intensity versus total acid concentration and theoretical curve fits for the binding equation (Equation 2.4) are illustrated in Figure 6-9.

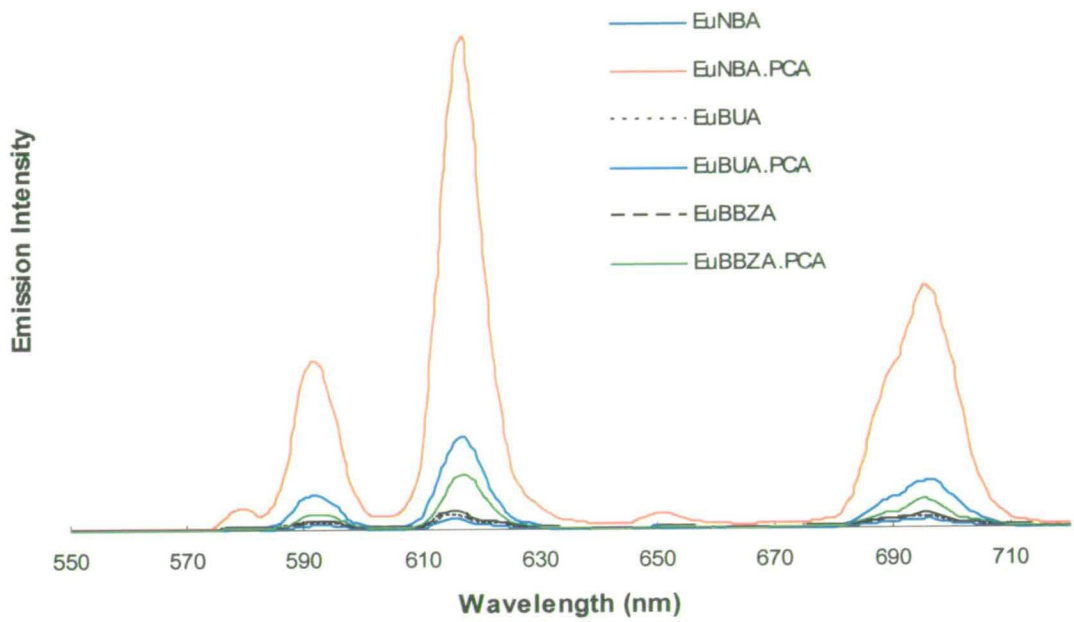

Figure 6-8 Emission Spectra of EuNBA, EuBUA and EuBBZA 1:1 mixed ligand complexes with PCA (0.1 mM aq, pH 7, λ ex = 270 nm)

Chelate	Log K_{PCA}	Error ±	I/I_0
EuNBA	5.12	0.06	32
EuBUA	5.43	0.07	6
EuBBZA	5.18	0.06	2

Table 6-3 EuNAL + PCA = [EuNAL.PCA] binding constants

It is noted that despite the greatly improved luminescence observed upon PCA/EuNBA binding, the estimated formation constant for the interaction (Log K_{PCA}) is of a similar order of magnitude (Table 6-3) to that of PCA recognition with EuBBZA and EuBUA. It is proposed that the strength of molecular recognition is principally governed by

the acid binding unit rather than by hydrophobic, electronic or steric effects imparted on the cavity by the amide arms of the NAL. In contrast, the efficiency of the energy transfer to the metal is affected greatly by the amide ligands.

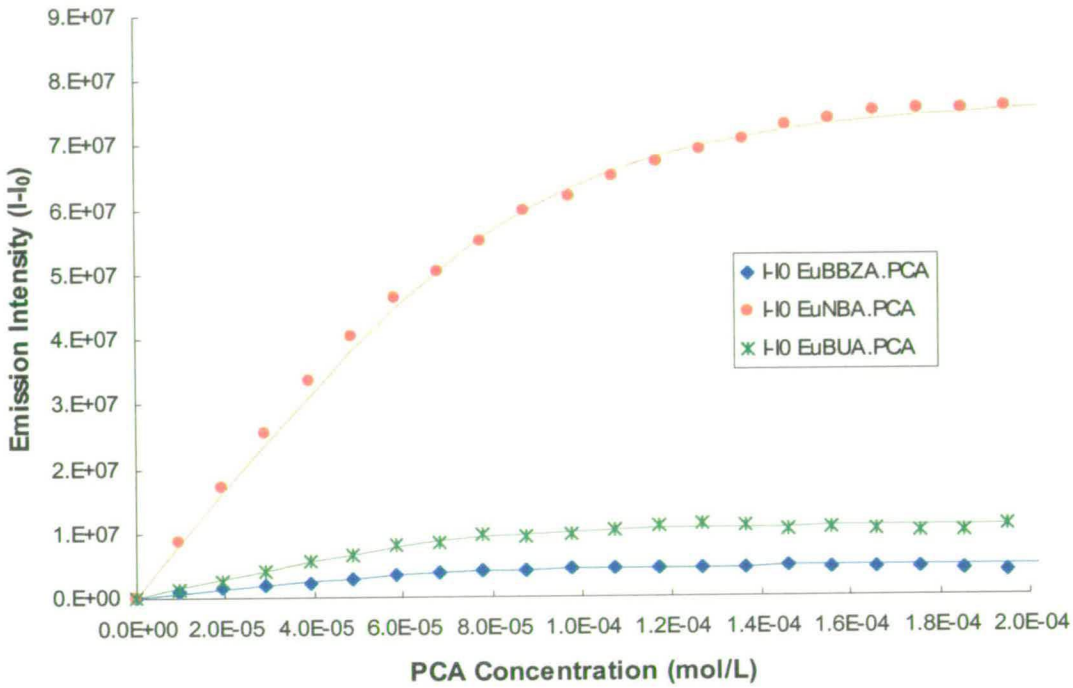

Figure 6-9 Plot of emission intensity ($I-I_0$) of the EuNALs versus PCA concentration ($molL^{-1}$) upon molecular recognition between EuBUA, EuNBA and EuBBZA, (0.1 mM aq, pH 7) and PCA (λ ex = 270 nm)

The flexible *n*-butyl arms of DTPA-BUA are expected to offer less protection to the metal from quenching effects of outer sphere water molecules than the bulky, rigid and hydrophobic DTPA-NBA ligand. It is possible that when PCA coordinates the Eu(III) metal centre in EuBUA, the butyl arms are repelled from the LHC and facilitate approach of high energy OH oscillators. The steric bulk and hydrophobicity of the rigid norbornyl groups is capable of forming a protective shield around the binding cavity. Quenching effects of outer sphere water molecules are minimised and the efficiency of intramolecular energy transfer from the triplet state is maximised. The hydrophobic nature of the amide substituent groups is likely to favour exchange of the of the coordinated water molecule by a dissociative mechanism. Consequently, the rate of exchange between PCA and water in the binding cavity of EuNBA at equilibrium is expected to be slower than the corresponding rate in the acyclic EuBUA system and a better interaction between the nitrogen heteroatom of the

aromatic ring and the emissive metal centre of EuNBA can be established. In addition to the steric and hydrophobic interactions important in molecular recognition with the aliphatic derivatives, electronic effects are expected to be implicated in PCA molecular recognition with aromatic chelates such as EuBBZA.

The relatively small increase in sensitised emission observed upon PCA/EuBBZA recognition is attributed to the residual absorbance of the DTPA-BBZA ligand. The aromatic arms of this ligand absorb UV radiation around 270 nm, the excitation wavelength employed in this study of PCA binding. Some of this energy is transferred to the metal centre resulting in stronger background EuNAL luminescence than observed from the aliphatic chelates under the same experimental conditions. Consequently, the relative emission intensity for the interaction is reduced with respect to the luminescence observed with the aliphatic systems.

Coordination by the aromatic acid LHCs is required in order for intramolecular energy transfer to occur. The carboxylic acid must be deprotonated prior to combination with the EuNAL solution. Maximum emission intensity was observed upon addition of PCA solution at pH 7 (Figure 6-10) to EuBEA (0.1 mM aq, pH 7). At lower pH a greater proportion of the acid is protonated and unable to fulfil its LHC potential (pKa 5.4). At high pH hydroxide ions can compete for the remaining Eu(III) coordination site reducing the overall observed emission intensity, as discussed in 6.2.1.

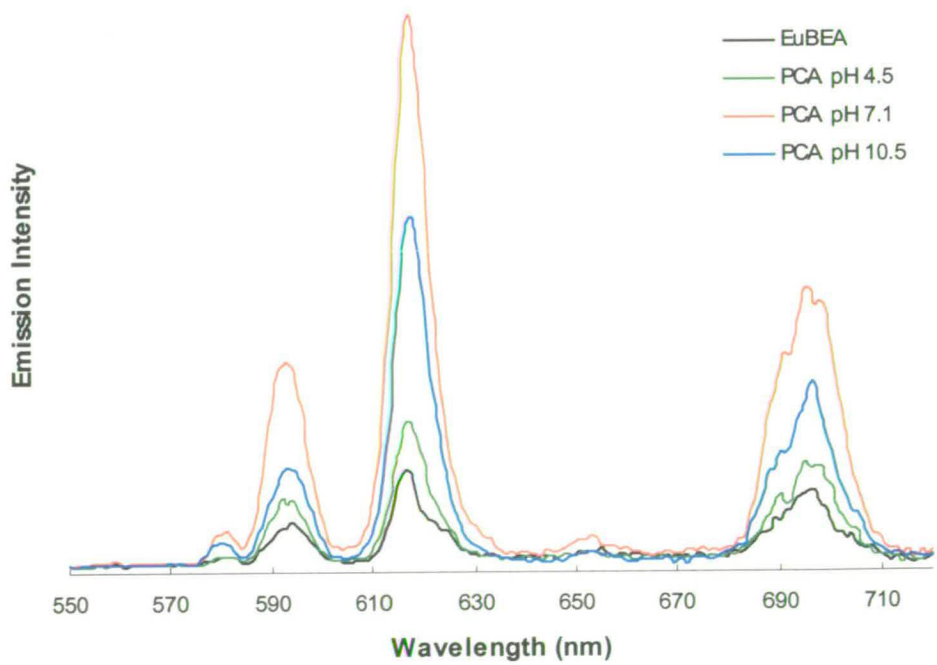

Figure 6-10 Eu(III) emission spectra upon addition of PCA (pH 4.5, pH 7 and pH 10.5) to EuBEA (pH 7, 0.1 mM aq) λ ex 270 nm, corrected for PMT response

In contrast to the aliphatic DTPA-AM_2 chelates, in which coordination of the LHC is prerequisite for AETE, the aromatic derivative, EuBBZA, exhibits an increase in sensitised emission upon addition of toluene (1:1 v/v CH_3CN) to the aqueous chelate sample (Figure 6-11). Characteristic UV absorbance around 270 nm is observed in the excitation spectrum (λem = 616 nm) in addition to the residual absorbance of the benzyl arms of the NAL (Figure 6-12). Toluene bears no lanthanide binding unit and is unable to coordinate the metal centre. The increase in sensitised emission is attributed to π–π electronic interactions occurring between the EuNAL and the LHC. The published crystal structure of the diamagnetic analogue, [YBBZA.H_2O]•$3H_2O$[125] (Figure 6-13) shows a face-edge arrangement of the two aromatic rings of the benzyl arms in the solid state (centroid-centrid 5.511 Å; edge-centroid 4.365 Å). It is proposed that toluene forms an inclusion type complex with EuBBZA in water, and that the observed AETE occurs by an intermolecular FRET mechanism between the aromatic moieties, followed by intramolecular energy transfer between DTPA-BBZA and the $^5D_0$ excited state of the Eu(III) ion. No sensitised emission is observed upon addition of toluene to the cyclic aliphatic derivatives, EucyHA or EumcyHA (Figure 6-14, 15), supporting the observation that the molecular recognition between toluene and EuBBZA is not simply due to hydrophobic interactions.

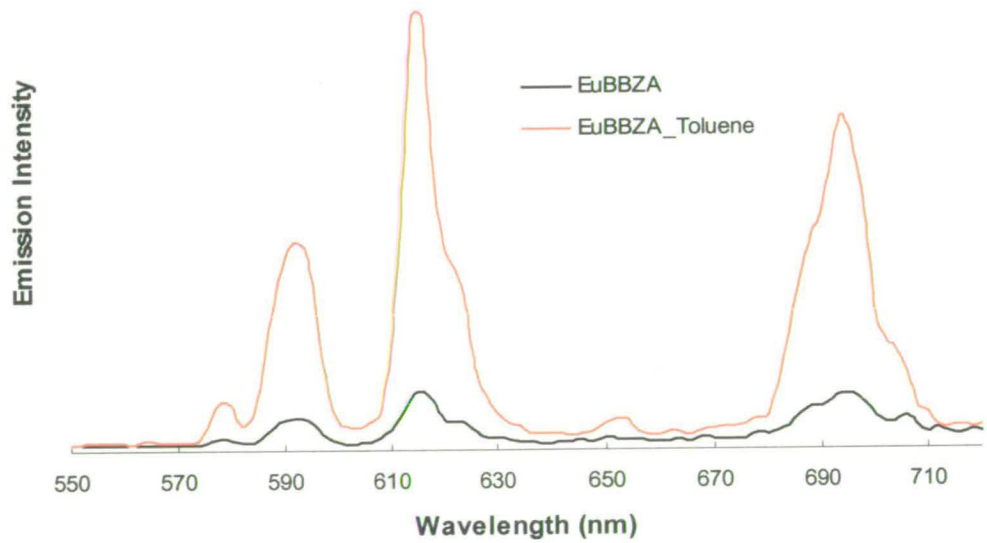

Figure 6-11 Emission spectra of EuBBZA (0.1 mM aq) + toluene (1:1 v/v CH_3CN) (λ ex 270 nm)

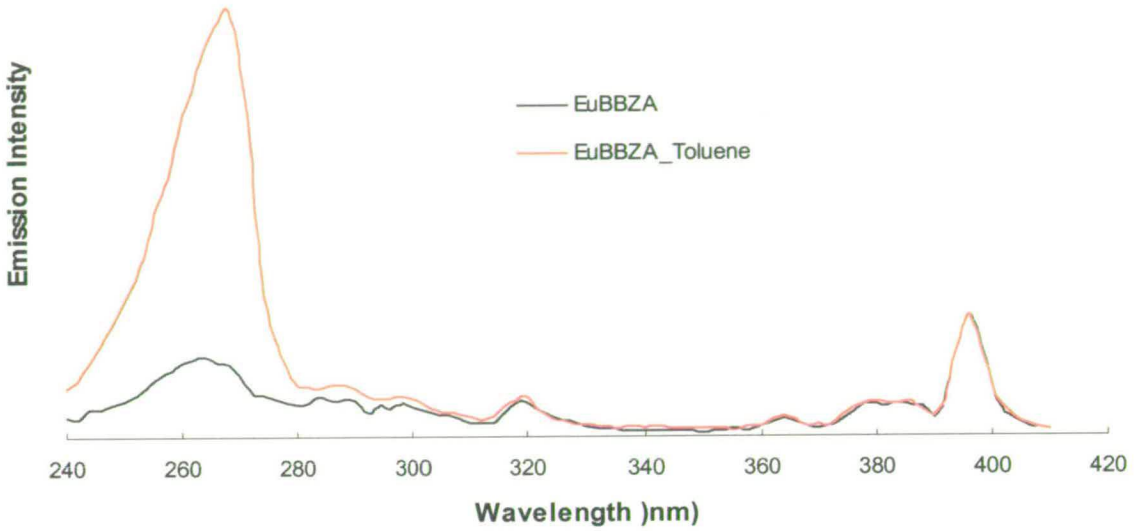

Figure 6-12 Excitation spectra (λ em 616 nm) of EuBBZA (0.1 mM aq) + toluene (1:1 v/v CH_3CN)

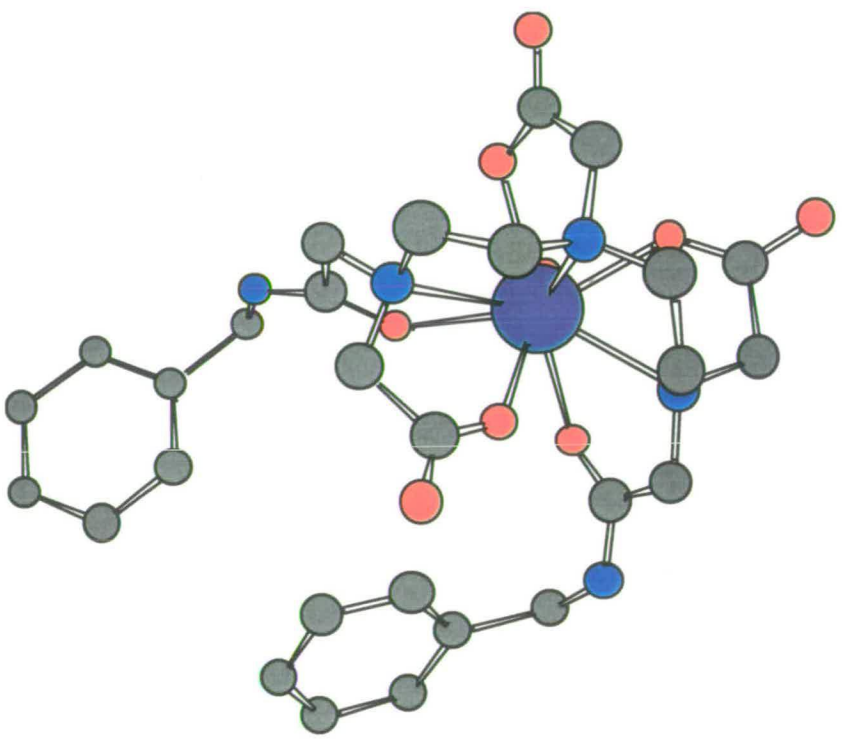

Figure 6-13 [$YBBZAH_2O$] X-ray structure[126] (Chem 3D view)

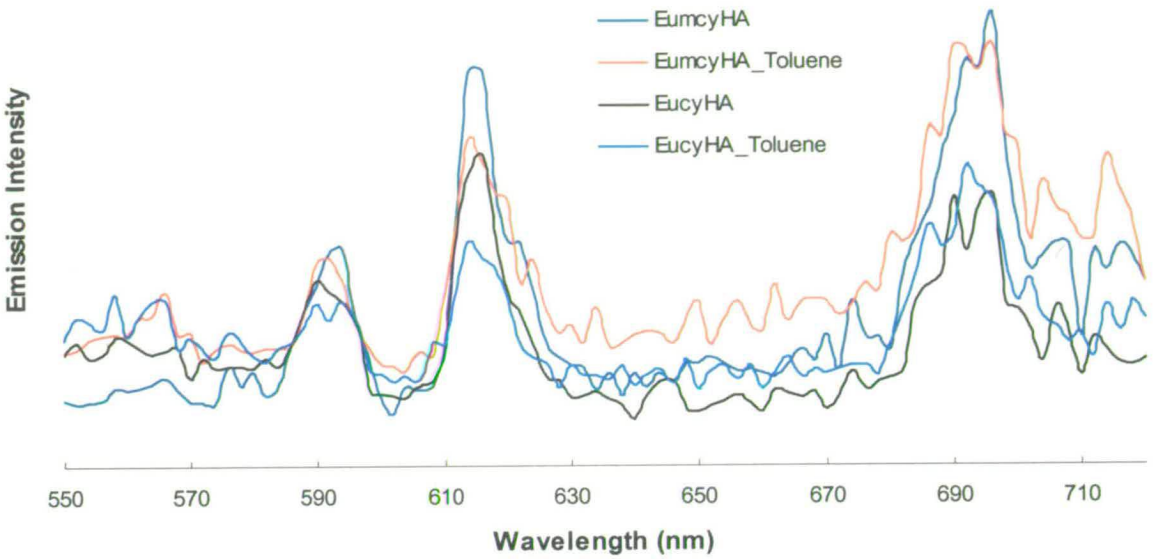

Figure 6-14 Emission spectra (λ ex 270 nm) of EumcyHA and EucyHA (0.1 mM aq) + toluene (1:1 v/v CH_3CN)

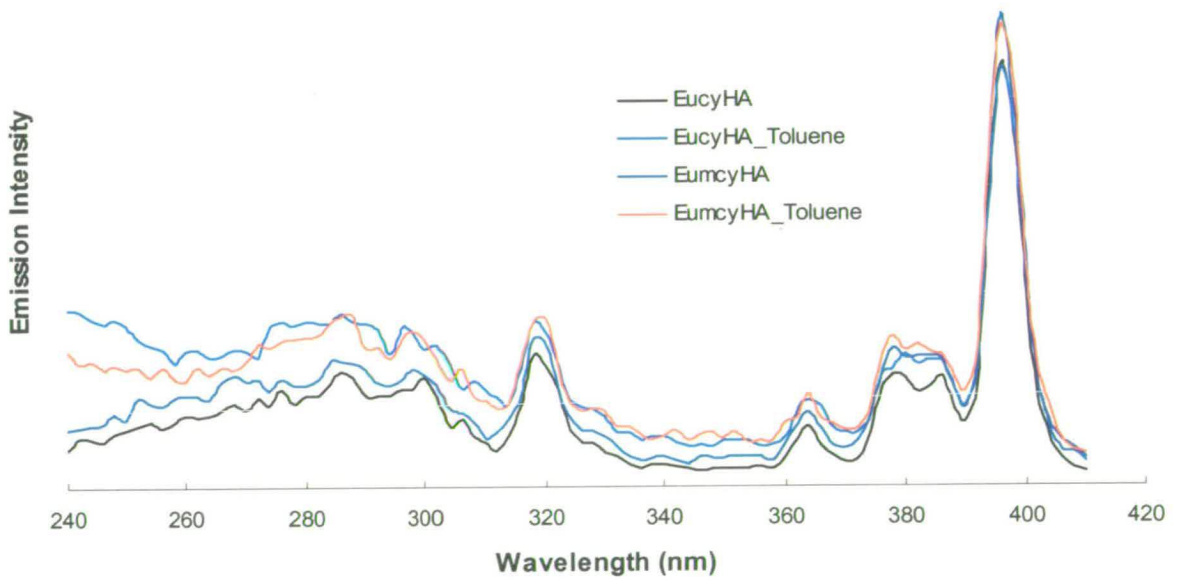

Figure 6-15 Excitation spectra (λ em 616 nm) of EumcyHA and EucyHA (0.1 mM aq) + toluene (1:1 v/v CH_3CN)

To summarise, it is apparent that the model LHC, picolinic acid, is capable of selectively recognising the binding cavity of the EuNAL chelates in the controlled formation of ternary luminescent complexes in aqueous solution. The selectivity induced by the amide ligand is rationalised upon consideration of the properties of the arms. In conclusion, it is observed that increasing the steric bulk and rigidity of the DTPA-AM_2 employed as the NAL greatly benefits luminescent ternary complex formation with the simple aryl carboxylic acid, PCA, consistent with the results of the combinatorial screening experiment.

6.3.2 PCA Recognition: NMR Studies

Further to the preliminary studies described in Chapter 3, whereby the binding of PCA to the diamagnetic chelate, LaBEA, was observed by ^{1}H NMR spectroscopy, an investigation was undertaken to establish the extent of the interaction between the acid and the amide arms of the binding cavity.

$[LnDTPA]^{2-}$ and LnDTPA-AM_2 species have been extensively studied by several research groups whose interest lies in development and characterisation of Gd(III) complexes for application in MRI. Although thermodynamically very stable (Log K ~ 15) the complexes are kinetically quite labile and exist as a series of interchanging conformers in aqueous solution.[121, 130, 134, 136, 156] Isomerism occurs by rearrangement of the coordination polyhedron, involving dissociation of the Ln-O and Ln-N bonds ($\Delta G^{\ddagger}_{283}$ = 71 kJ/mol for La(III)DTPA-bis(*n*-propylamide, from ^{13}C NMR).[134] The rate determining step in the dynamic isomerisation process was found to be inversion of the terminal diethylenetriamine nitrogen atoms (k_{283} = 0.7 s^{-1}). In contrast, carboxylate exchange is rapid on the NMR timescale, and values of $\Delta G^{\ddagger}_{283}$ = < 43 kJ/mol and k_{283} > 9.6 x 10^3 s^{-1} are reported.[134] Consequently, the NMR spectra observed comprise the average of several signals for each distinct nucleus in fast exchange on an NMR timescale.

Several NMR experiments were performed in an attempt to detect an interaction between the aliphatic protons of the amide arms and the aromatic PCA protons. One dimensional NMR (^{1}H and ^{13}C) for LaBUA and [LaBUA.PCA] are shown in Figures 6-16 – 6-21. It is noted that the methylene and terminal -CH_3 protons of the *n*-butyl groups give rise to single resonances, which become multiple signals upon PCA binding (Expanded spectra shown in Figures 6-18 and 6-19). Similarly, a sharpening of the resonances of the diethylenetriamine backbone is observed, indicative of the interaction. The change in the spectra is attributed to a conformational locking effect, which restricts the rotational isomerisation process occurring more rapidly in the LaNAL species. The number of resonances observed in the ^{13}C spectra increase accordingly. The rate of isomerisation is

reduced and the number of distinct nuclei detected at any given point in time increases as the diasteriomers become longer lived on the NMR timescale (The rate is expected to be less than $< 0.7\ s^{-1}$, based on the literature values discussed above).

Preliminary two dimensional NMR preliminary experiments (NOESY) failed to detect any through space interaction between the aromatic resonances of PCA and those of the aliphatic protons of the DTPA-AM_2 arms. Corresponding observations were made with LaBBZA (Appendix 4). The cyclic aliphatic derivatives LacyHA and LaNBA could not be studied due to their limited solubility. In an attempt to overcome these limitations the analogous Y(III) complexes were prepared. Although soluble at concentration suitable for NMR, these chelates did not exhibit any interaction with the added PCA ligand. It was suspected initially that the absence of an interaction was due to the small ionic radius of the Y(III) ion (0.93 Å) in comparison to that of La^{3+} (1.06). Expansion of the Y(III) inner coordination sphere to accommodate 10 ligands is expected to be more difficult for the smaller ion. Upon reflection, it is noted that the ionic radius of Y(III) lies between that of Eu(III) and Tb(III) (0.95 Å and 0.92 Å respectively) both of which exhibit molecular recognition with the PCA binding unit, detected by luminescence. It is more likely that the interaction is inhibited by hydroxide (or OD) coordination under the experimental conditions (pD ~ 7). The formation constants for Ln-OH species are given in Table 6-4.

Metal	Log K_{ML}
Dy	5.2
Er	5.4
Gd	4.6
La	3.3
Lu	6.6
Y	5.0

Table 6-4 Formation constants for Ln (OH^-) species (Lange's Handbook of Chemistry, 13th Ed)[148]

It is noted that the stability constant for OH binding to yttrium (Log 5.0) is of similar magnitude to that of PCA recognition with EuDTPA-AM_2 species (Log ~ 4.9). The binding constants for OH coordination to Eu(III) and Tb(III) are also expected to be of this magnitude. The hydroxide ligand can therefore be expected to compete efficiently with PCA for the remaining coordination site of YNAL chelates, as discussed for Eu(III) and Tb(III) in section 5.2.1. In contrast, the much lower hydroxide binding constant for La (Log 3.3) explains why acid recognition is observed with this metal and not yttrium. No interaction was detected between PCA and the diamagnetic LuBUA derivative, attributed to both the small ionic size (0.85 Å) and the high stability constant for hydroxide binding (Log 6.6).

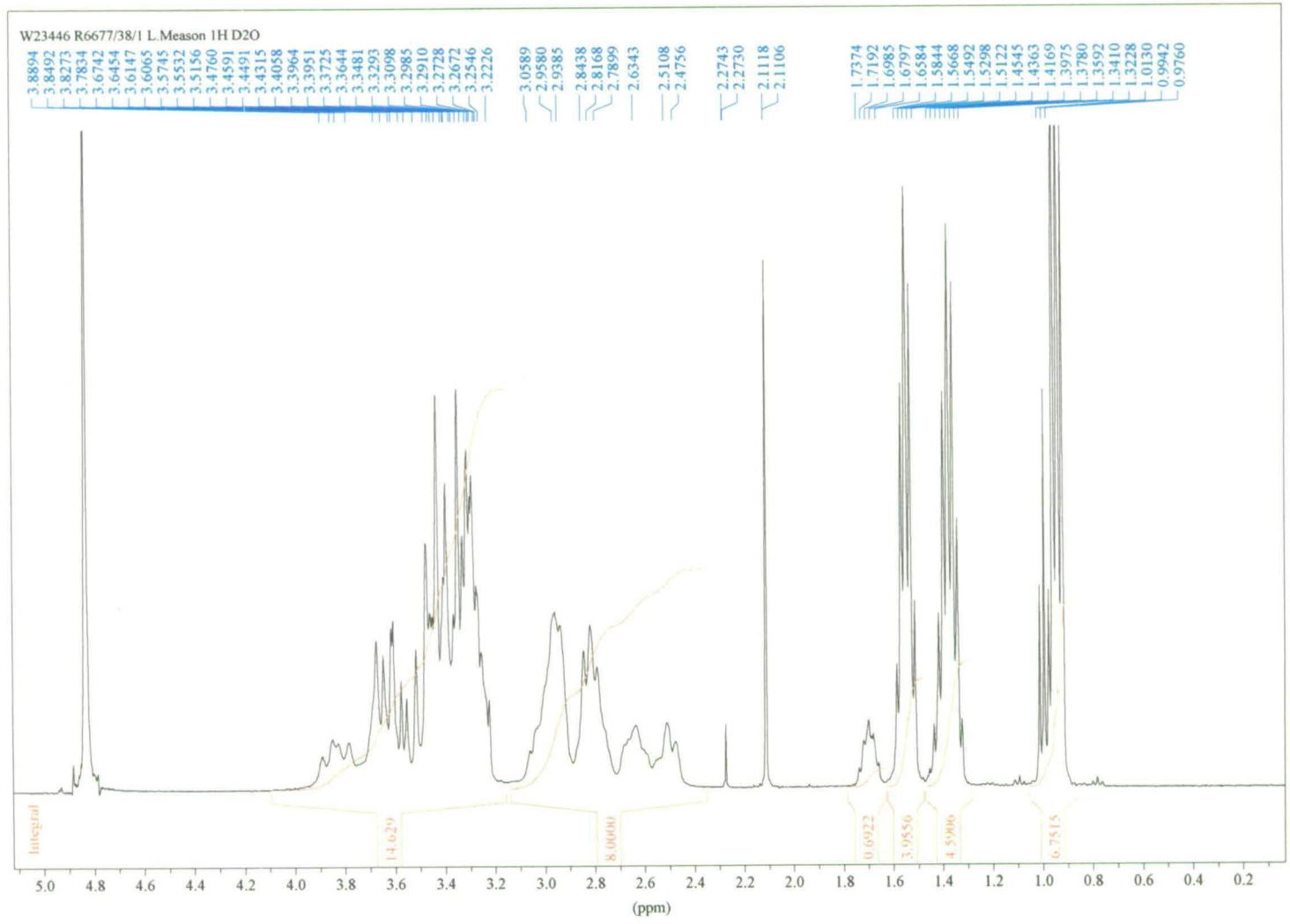

Figure 6-16 ^{1}H NMR spectrum of LaBUA (400 MHz, D_2O, pD 7-8)

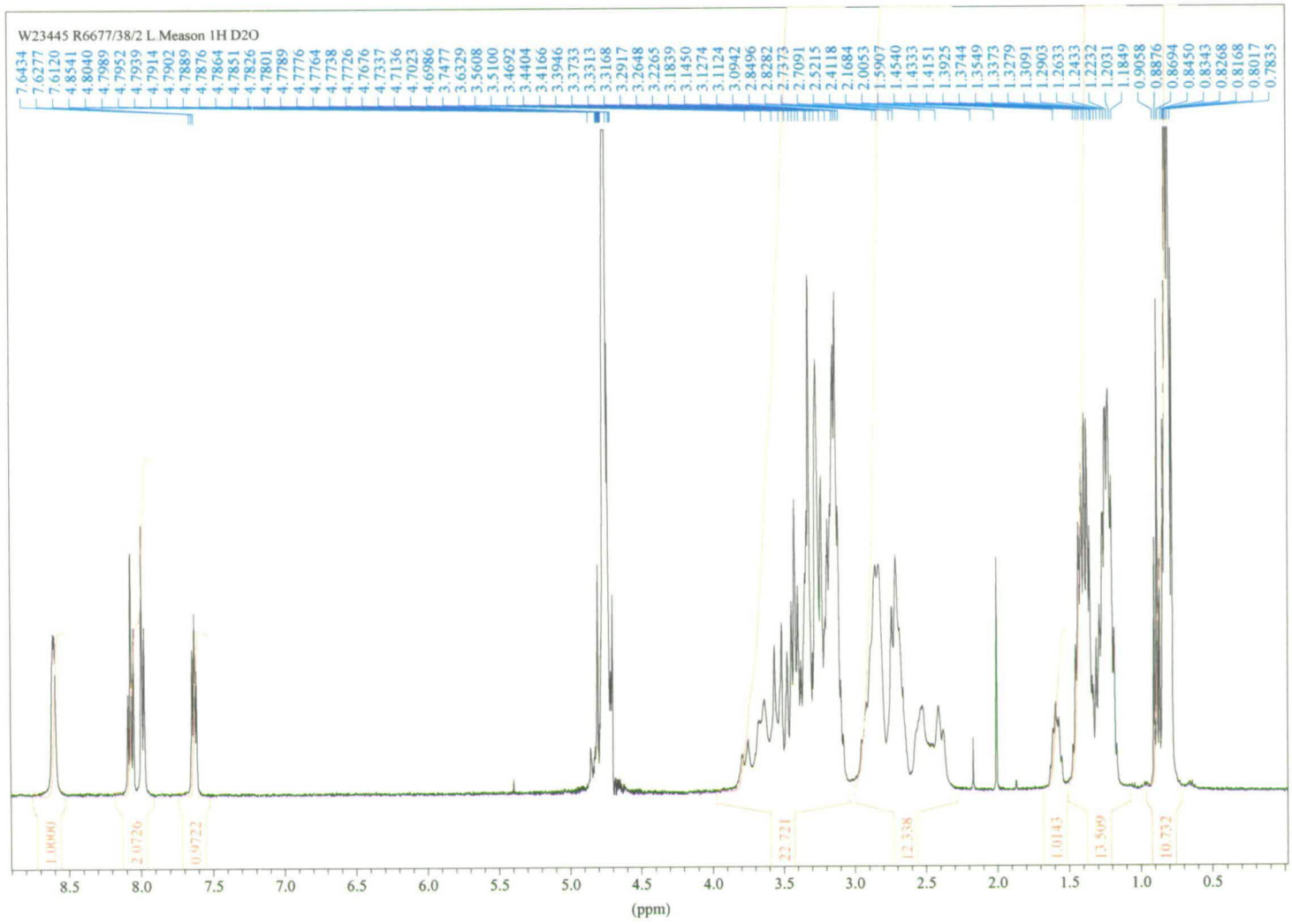

Figure 6-17 ^{1}H NMR spectrum of [LaBUA.PCA] ternary complex (400 MHz, D_2O, pD 7-8)

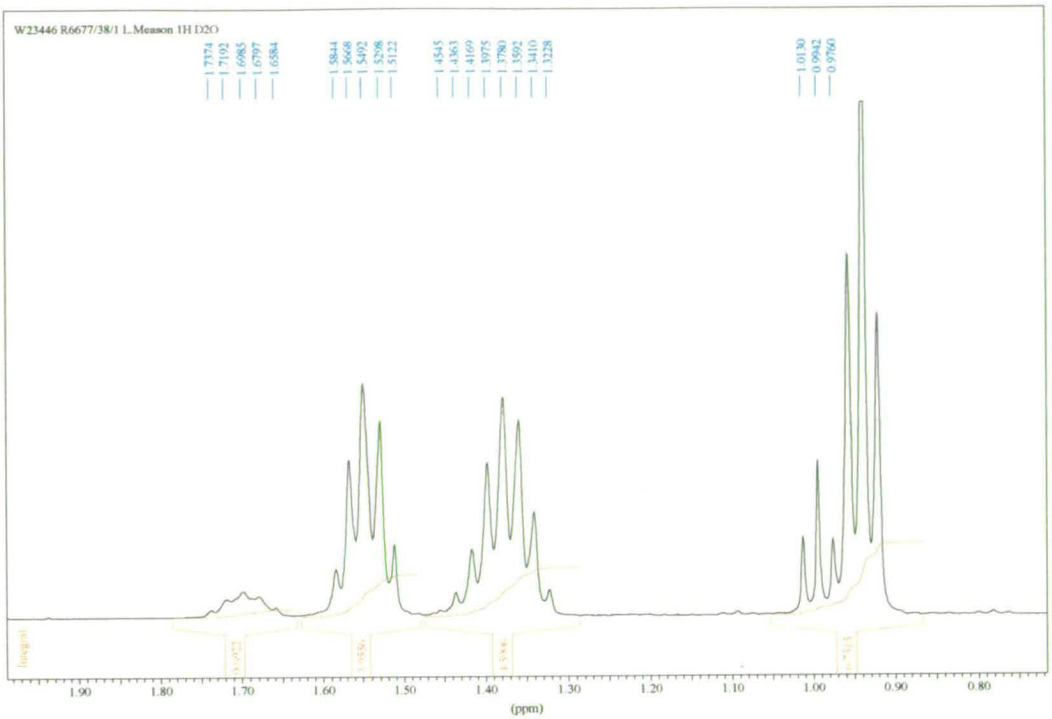

Figure 6-18 Expanded ^{1}H NMR spectrum: LaBUA amide arm region (400 MHz, D_2O)

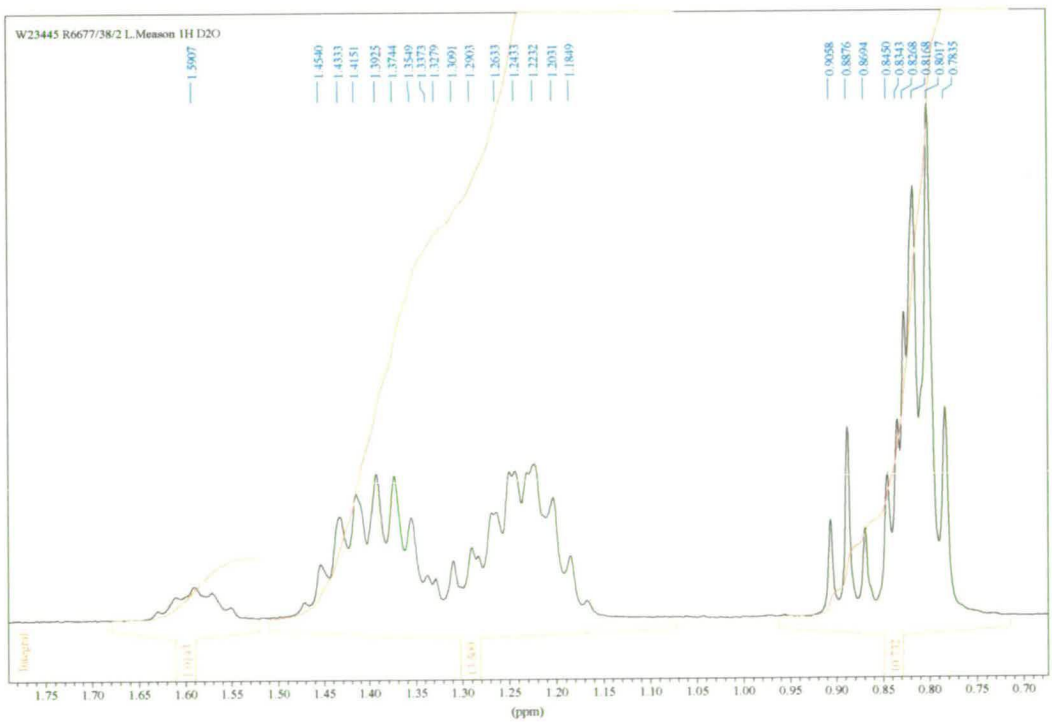

Figure 6-19 Expanded ^{1}H NMR spectrum: [LaBUA.PCA] ternary complex, amide arm region (400 MHz, D_2O)

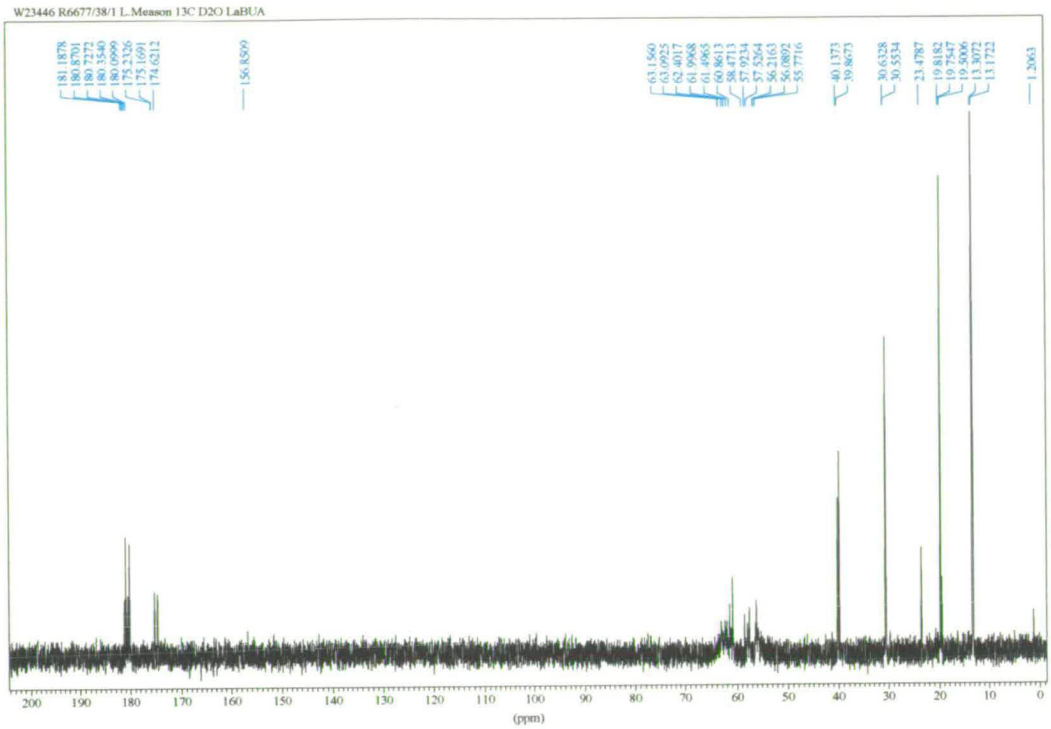

Figure 6-20 ^{13}C NMR spectrum of LaBUA in D_2O (100 MHz)

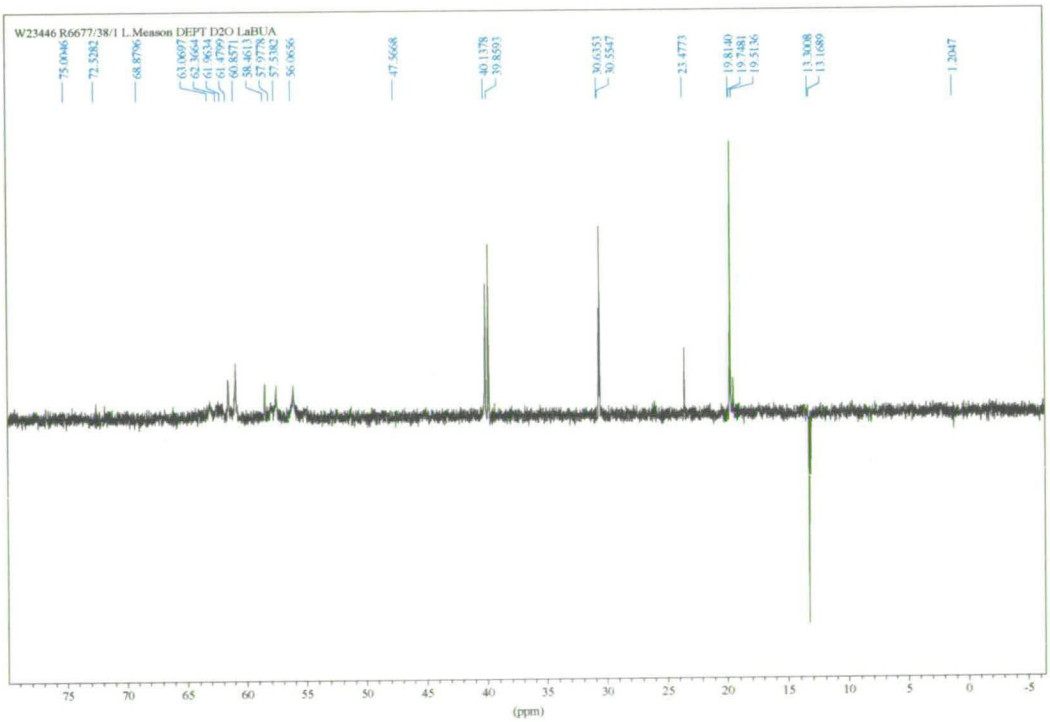

Figure 6-21 ^{13}C NMR DEPT experiment: LaBUA (D_2O)

6.4 Aromatic Acid Recognition with the EuNBA Binding Cavity

Studies into the influence of the amide arms of the EuNAL on picolinic acid molecular recognition revealed that EuNBA consistently afforded more intensely luminescent ternary complexes than the other less rigid EuDTPA-AM_2 chelates. A case study was performed employing EuNBA as a model chelate, providing a well-defined cavity, with which to compare the interaction of aromatic carboxylic acids identified by combinatorial screening as potential LHC units.

6.4.1 Simple Aromatic Acid Recognition

Molecular recognition between the simple aromatic acid LHCs (benzoate, phthalate and picolinate) and EuNBA was investigated by steady-state and time-resolved luminescence spectroscopy. Consistent with initial observations made with EuBEA, PCA was observed to interact more strongly with EuNBA, forming a much more intensely luminescent mixed ligand chelate than that formed upon phthalate or benzoate recognition (Figure 6-22). In addition, it is noted that the binding constants (Table 6-5) for all three acids are greater than those observed for the corresponding molecular recognition with EuBEA.

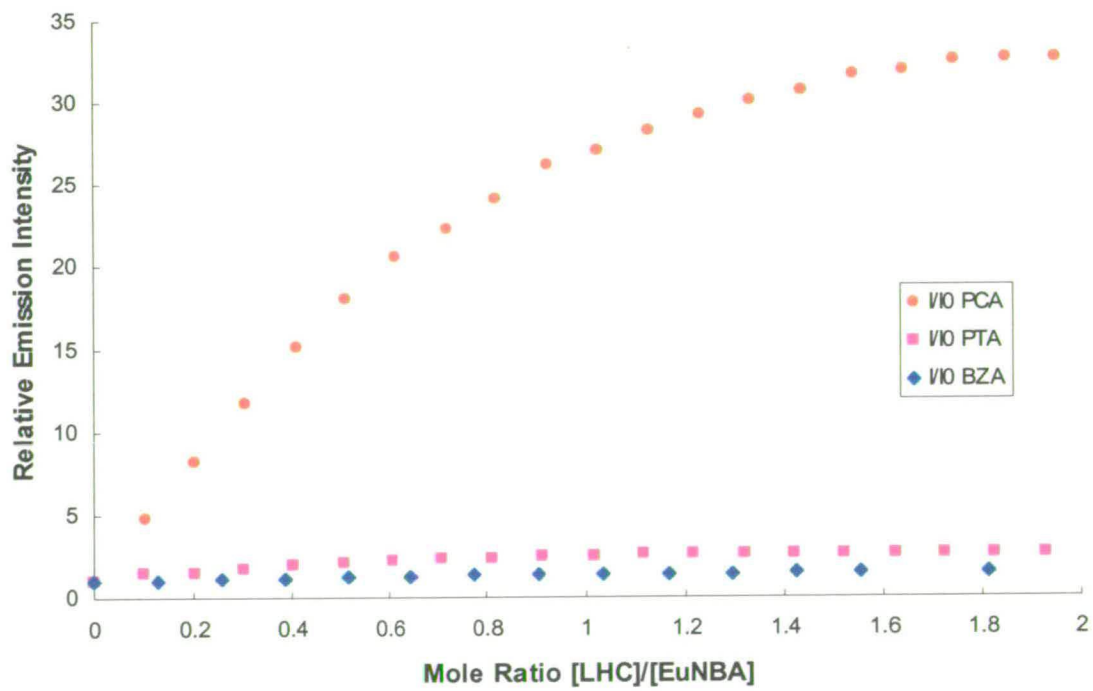

Figure 6-22 Relative emission intensity versus mole ratio of [LHC]/[EuNBA] for PCA, PTA and BZA molecular recognition (0.1 mM aq, pH 7, λ ex 270 nm)

Chelate	Acid	Log K	Error (±)	I/I_0
EuNBA	PCA	5.12	0.06	32
EuNBA	PTA	4.98	0.08	2.5
EuNBA	BZA	4.38	0.5	1.5

Table 6-5 EuNBA+ LHC binding constants

The equilibrium constant for the weak binding interaction between EuNBA and BZA, Log K_{BZA}, is 4.38 ± 0.5 (R = 0.99517). Very little energy transfer is observed between the acid and the Eu(III) metal centre at 1:1 stoichiometry. Benzoic acid is readily displaced upon addition of phthalic acid (Log K_{PTA} 4.98 ± 0.08) to the solution sample. Similarly, the stronger binding between PCA and the EuNAL (Log K_{PCA} = 5.12 ± 0.06) results in a further increase in sensitised emission. Spectra are illustrated in Figure 6-23 below.

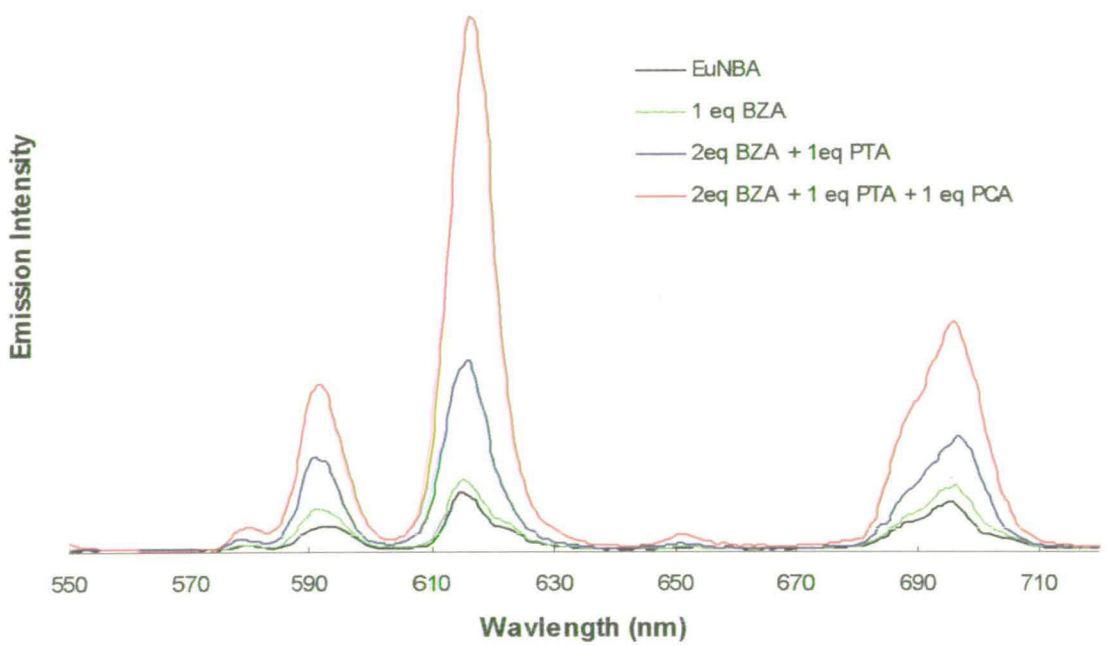

Figure 6-23 Europium emission spectra of EuNBA (0.095 mM aq) upon combination with BZA, PTA and PCA, (pH 7-8) illustrating molecular recognition

Similar behaviour is observed for the aliphatic chelate EuBUA and the aromatic EuNAL species EuBBZA. Lifetime data for the EuBBZA and EuBUA solution samples are presented in Table 6-6.

Chelate	LHC	τ (ms)	Error (±)	%
EuBUA	-	0.83	0.005	0.6%
	2eq PTA + 1eq PCA	1.076	0.005	0.5%
EuBBZA	-	0.779	0.004	0.5%
	1 eq PTA	0.802	0.004	0.5%
	1 eq PTA + 3 eq PCA	1.325	0.01	0.8%

Table 6-6 EuNAL and ternary complex luminescence lifetimes in aqueous solution (0.1 mM, pH 7, λ ex = 532 nm)

Luminescence lifetime measurements confirm the expected mechanism by which controlled assembly of the mixed ligand complexes between the EuNAL and PCA occur. Solution samples irradiated at 532 nm by a pulsed laser excitation source emitted characteristic Eu(III) luminescence at 616 nm, the decay of which was monitored. Under the experimental conditions, the EuNAL lifetime (~ 0.8 ms) is increased substantially (~ 0.6 ms for EuBBZA at saturation concentrations of LHC) upon displacement of the coordinating water in the presence of excess PCA. The observed lifetime of $Eu(PCA)_3$ in aqueous solution is approximately 0.2 – 0.3 ms, much shorter than that of the ternary complexes due to the adverse influence of quenching solvent OH oscillators. The measured EuNAL lifetime is longer than those reported in Table 6-2 due to the measures taken to avoid hydroxide coordination in preparation of the chelates.

Electrospray mass spectrometry of emission samples provides supporting evidence for ternary complex formation (Table 6-7). The mixed ligand species are observed in both the positive and negative ionisation modes. Complexation by all three acids, BZA, PTA and PCA is detected simultaneously, confirmation of competitive binding and the similar magnitude of the equilibrium constants measured by luminescence spectroscopy.

Chelate	ES +/-	Acid	Peak (m/z)	Assignment
EuBUA	+	-	674/676	$[EuBUA + Na]^+$
	+	PCA	819/821	$[EuBUA.PCA + 2Na]^+$
	+	PTA	884/886	$[EuBUA.PTA + 3Na]^+$
	+	BZA	896/898	$[EuBUA.BZA_2+3H]^+$
EuBUA	-	-	650/652	$[EuBUA-H]^-$
	-		817/819	$[EuBUA+PTA]^-$
EuBBZA	+	-	742/744	$[EuBBZA+ Na]^+$
	+	PCA	887/889	$[EuBBZA.PCA + 2Na]^+$
	+	PTA	907/909	$[EuBBZA.PTA+ Na+ 2H]^+$
EuBBZA	-	-	718/720	$[EuBBZA-H]^-$
	-	PTA	885/887	$[EuBBZA.PTA+H]^-$

Table 6-7 Electrospray mass spectrometry data for ternary complex formation in aqueous solution

Several acids bearing the "picolinic" binding unit were identified as potential light-harvesting centres by combinatorial screening under time-resolved conditions (Chapter 5.2.7). The mode of interaction with the EuNAL chelates was studied in greater detail under steady-state monochromatic excitation.

6.4.2 Substituted Picolinic Acid LHCs

The influence of substituent effects on the binding interaction between the PCA unit and EuNALs was briefly investigated during the high throughput screening experiment. The O-CH_2Ph substituted picolinic acid GW369905X (Figure 6-25) facilitates a 5-6 fold enhancement of metal centred emission from each of EuNBA and EuBUA (Figure 6-24). The reduction in activity with respect to PCA is attributed to the electronic influence of the benzyl ether substituent. The resonance effects of the substituent para to the heteroatom must be taken into account when considering the pKa values for GW369905X (Table 6-8). With a pK_a of 6.71 this compound is expected to be protonated to a greater extent than the parent PCA LHC at pH 7. Consequently, the initial interaction between the LHC and EuNAL is expected to be weaker and the acid unlikely to fulfil its bidentate binding potential towards the Eu(III) metal centre. The efficiency of intramolecular AETE is reduced and the

resultant mixed ligand species is considerably less luminescent than the analogous [EuNAL.PCA] complex. In addition, adverse steric interactions between the amide arms and the benzyl-ether group may hinder ternary complex formation.

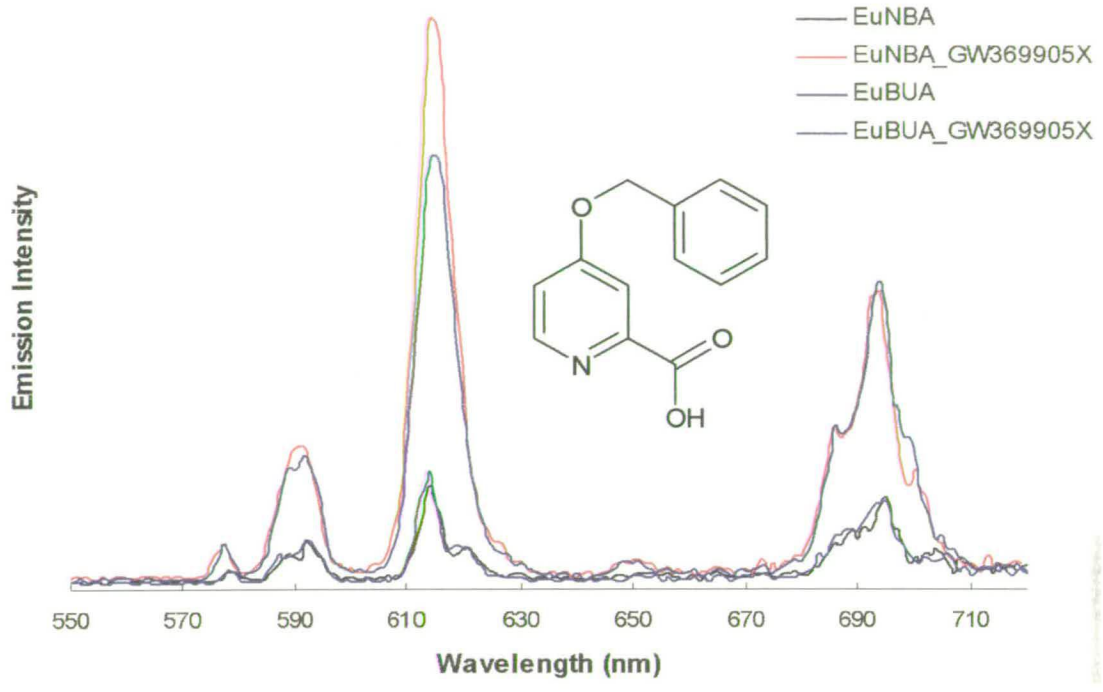

Figure 6-24 Emission spectra for the 1:1 mixed ligand species formed upon combination of EuBUA and EuNBA with acid GW369905X (λ ex 270 nm)

Acid	pK_{a1}	±	pK_{a2}	±
PCA	5.40	0.10	1.00	0.50
GW369905X	6.71	0.1	1.13	0.5

Table 6-8 pK_a values for substituted picolinic acids (calculated using pKadB4.0 software)

EuBUA was titrated with the alkyl substituted picolinic acid, GR34043X (Figure 6-25), and observed to form a 1:1 mixed ligand luminescent species, enhancing the metal emission approximately 10-fold. This increase is comparable to that observed with PCA under the same experimental conditions (0.1 mM aq, pH 6-7, λ ex = 270 nm, 150 W Lamp). The binding constant for the interaction is in each case approximately Log K = 4.9. No detectable difference in the strength of binding interaction or efficiency of energy transfer is observed between these two acids with EuBUA under steady-state excitation. It is

conceivable that an improvement may be detected with the alkyl substituted acid under time-resolved experimental conditions. The luminescence lifetime of EuBUA with GW369905X was not recorded.

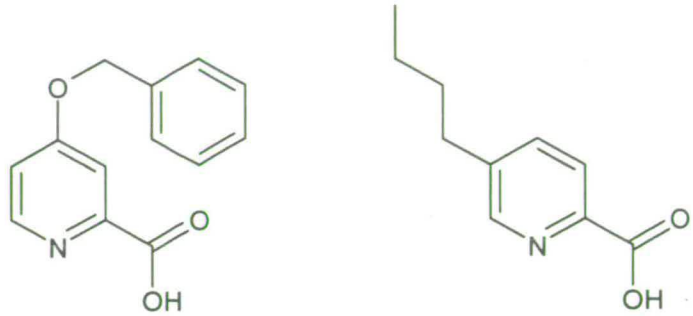

GW369905X GW34043X

Figure 6-25 Substituted picolinic acids

6.4.3 Thiophene and Furan Carboxylic Acids

The thiophene and furan-2,5-carboxylic acids GR51678X and GR54219X (Figure 6-26) were combined with EuBUA in 1:1 stoichiometry. Some interesting differences are observed between the emission spectra of the solution samples (Figure 6-27). An increase in emission intensity of EuBUA is observed upon excitation of the ternary complex at 300 nm.

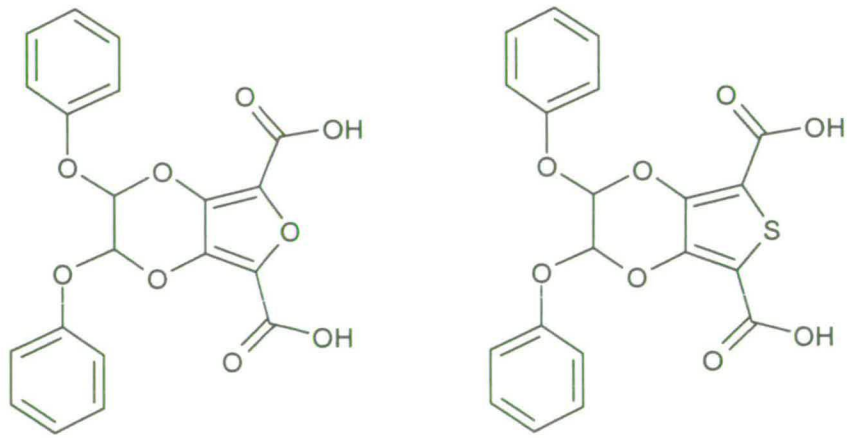

GR54219X GR51678X

Figure 6-26 Thiophene and furan-2,5- dicarboxylic acids

The thiophene derivative GR51678X is more active towards EuBUA than the analogous furan derivative GR54219X. As discussed in Chapter 5.2.10, this is attributed to the relative aromaticity of the heterocyclic ring. The thiophene ring with the softer su;phur heteroatom is more aromatic in character than the furan ring with the harder oxygen heteroatom. The peak ratio 592:616 nm differs slightly between the furan and thiophene dicarboxylic acids, suggesting a change in the ligand environment with respect to the EuNAL chelate, though in both cases the relative intensity 592:616 is roughly equal. In contrast to the nitrogen heterocyclic acids, which act as bidentate binding units, these LHCs are expected to interact via the carboxylate only with little participation by the heteroatom.

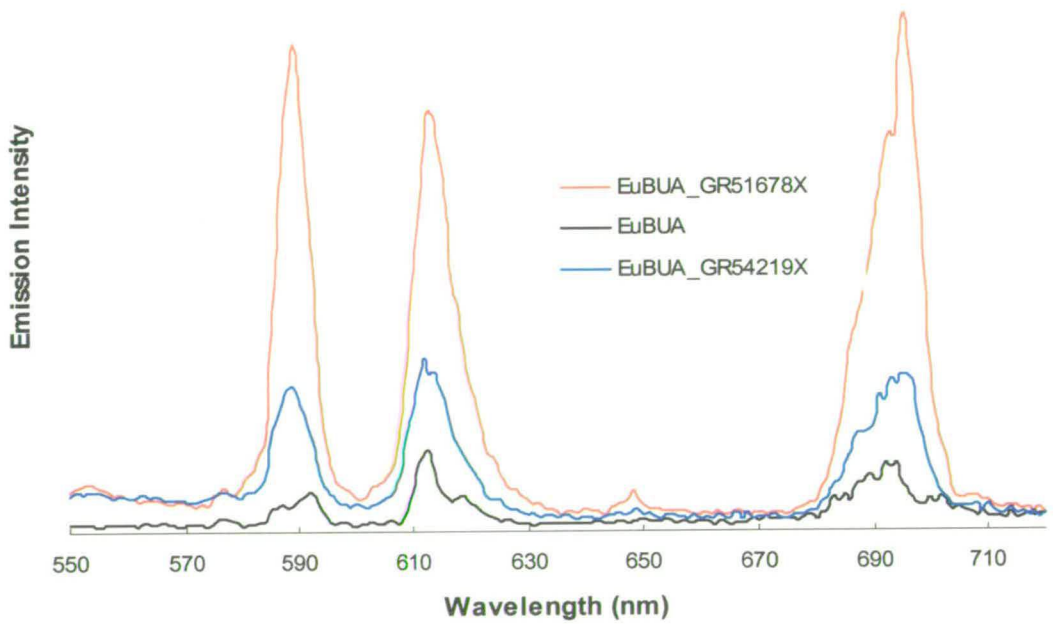

Figure 6-27 Emission Spectra: EuBUA (0.05 mM aq, pH 7) + GR51678X and GR54219X (λex = 300 nm)

6.4.4 Quinoline-2-Carboxylic Acid LHCs

The influence of extension of the chromophoric unit and further substitution of PCA (Figure 6-28) was investigated using EuNBA and EuBUA as model EuNAL chelates. Interestingly, it is observed that these acids are poor sensitisers for Eu(III) ternary complex formation, in contrast to picolinic acid. Estimated pKa values (pKadB 4.0) are given in Table 6-9.

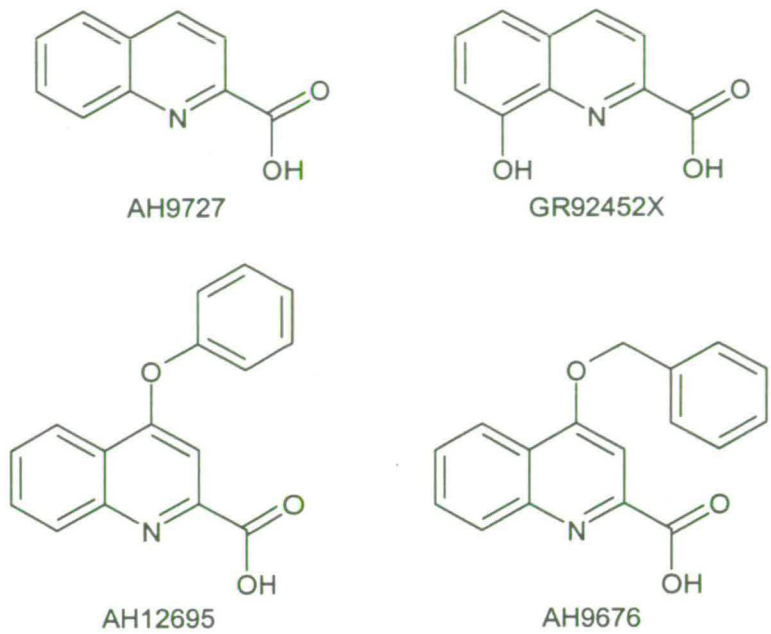

Figure 6-28 Quinoline-2-carboxylic acids

Acid	pK_{a1}	±	pK_{a2}	±	pK_{a3}	±
AH9727	5.34	0.40	1.20	0.30	-	-
AH12695X	5.76	0.50	0.95	0.30	-	-
AH9676X	6.62	0.50	1.05	0.30	-	-
GR92452X	9.98	0.10	4.91	0.40	1.32	0.30

Table 6-9 pK_a values for quinoline-2-carboxylic acids (Figure 6-28) calculated using pKadB 4.0

Acid AH9727, quinoline-2-carboxylic acid, is observed to result in a two-fold enhancement of Eu(III) emission in aqueous solution at neutral pH, forming a 1:1 mixed ligand species with EuBUA. The emission and excitation spectra for the system at equilibrium are obtained upon excitation at 270 nm and monitoring emission at 616 nm respectively are shown below in Figure 6-29 and 6-30. It is noted that the normally hypersensitive transition at 616 nm is less sensitive to AH9727 binding than the 592 nm band, as observed for EuNBA/BZA recognition (Figure 6-31). AH9727 is a poor sensitiser for our EuNAL species, with very little energy transfer observed between the acid and the metal centre.

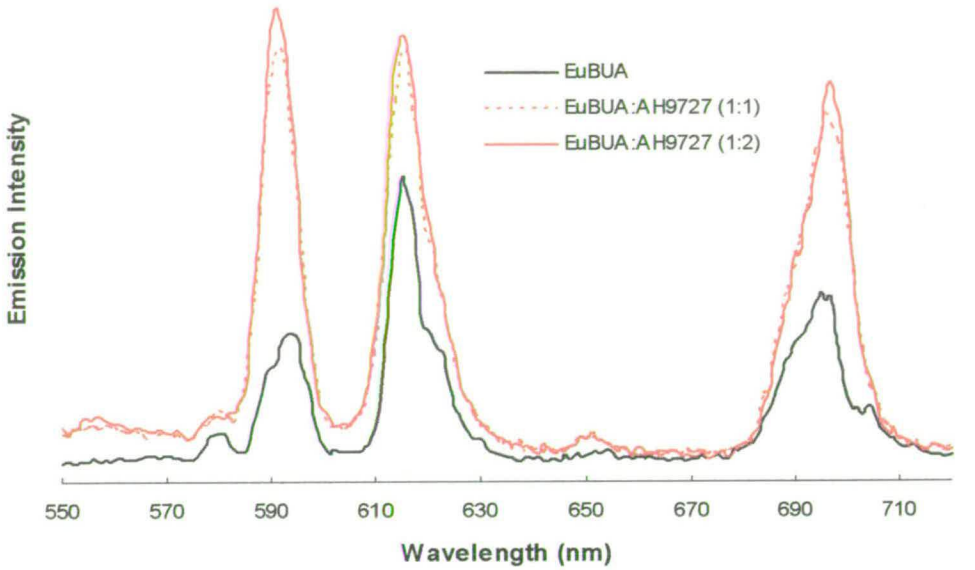

Figure 6-29 Emission spectra of EuNBA (0.1 mM aq) + AH9727 (λex = 270 nm)

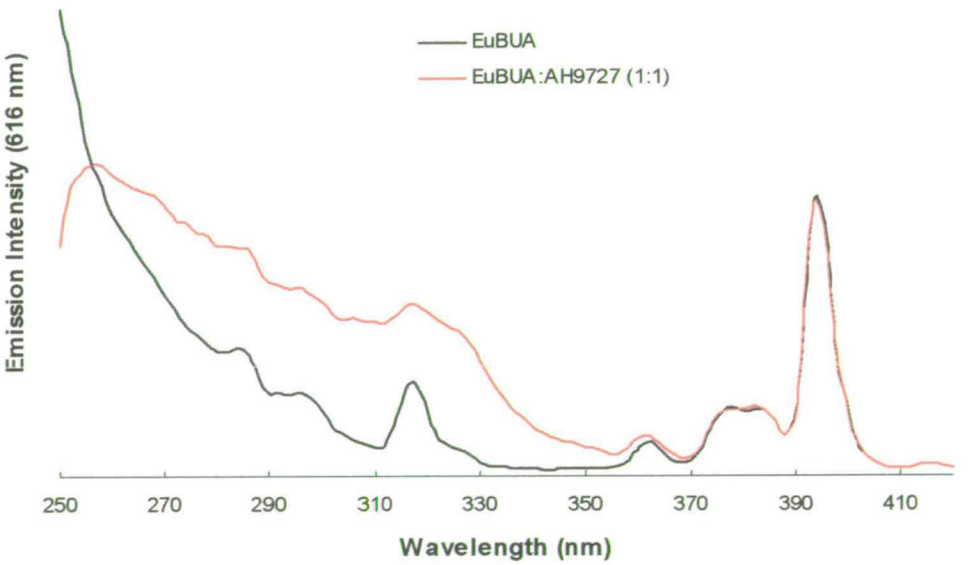

Figure 6-30 Excitation spectra of EuBUA (0.01 mM aq) + 1 eq AH9727 (λem = 616 nm)

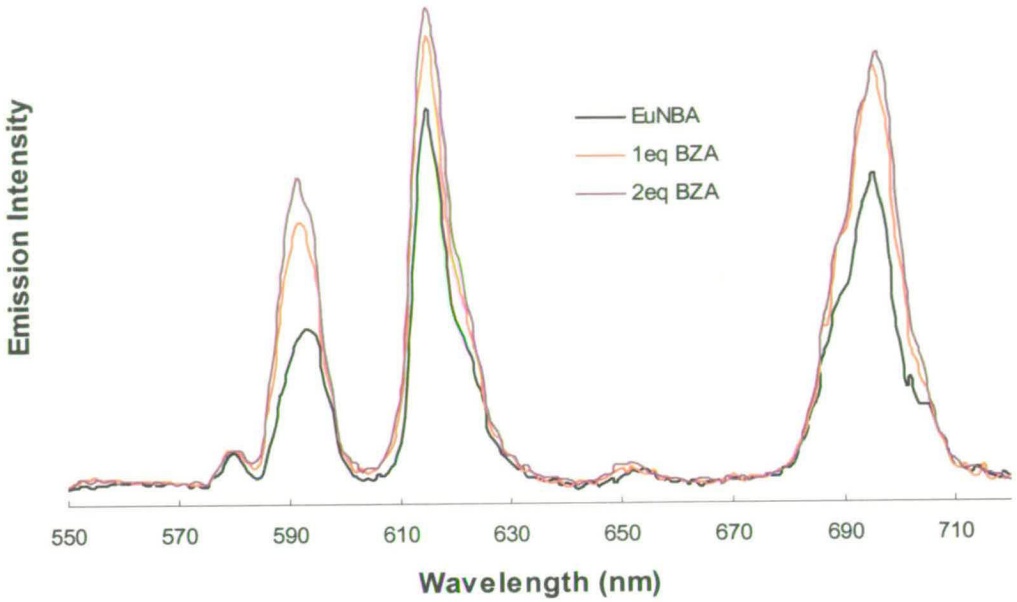

Figure 6-31 Emission spectra of EuNBA (0.05 mM aq) + BZA (λex = 270 nm)

As pKa of acid AH9727 (pK_{a1} 5.34) is similar to that of the efficient LHC, PCA (pK_{a1} 5.40), the LHC is not expected to be significantly protonated under the experimental conditions. The inactivity of AH9727 cannot be directly attributed to the protonation state of the acid and additional factors must be considered. The inefficient interaction is therefore attributed to the hydrophobic nature of the H atom in the 8-position of the acid, impeding bidentate binding via the heteroatom and carboxylate.

The light-harvesting abilities of a selection of the substituted quinoline-2-carboxylic acids (Figure 6-28) evaluated by high throughput screening were studied under steady-state excitation. Consistent with the results of time-resolved assay experiment (Chapter 5.2.8.1), these acids exhibit relatively poor sensitising properties towards the EuNAL chelates with respect to picolinate, attributed to mismatched triplet energy levels.

The difference between the emission spectra obtained from 1:1 solution samples of EuNBA and acids AH9676 and AH12695 (Figure 6-32) is attributed to the influence of the substituent in the 4-position. Whilst both LHCs are poor sensitisers for this system, only

facilitating approximately 4-fold enhancement of Eu(III) emission, it is noted that the mode of binding interaction differs.

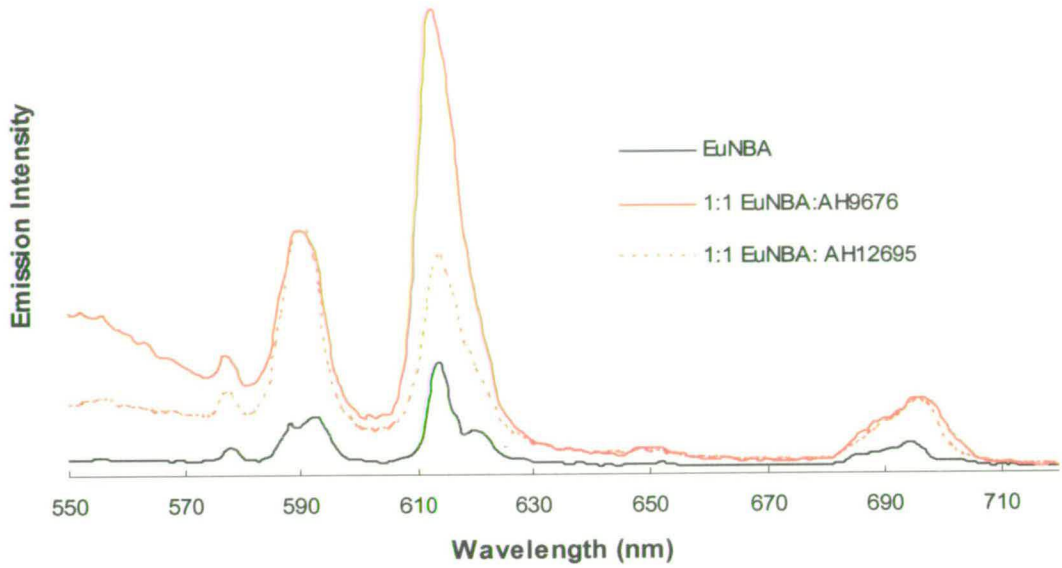

Figure 6-32 Emission spectra of EuNBA (0.05 mM aq) + substituted carboxylic acid LHC units AH12695 and AH9676 (λ ex = 300 nm)

Acid AH12695 bears an aromatic ether -OPh substituent. This group is electron withdrawing, reducing the coordinating ability of the nitrogen heteroatom (pK_{a2} 0.95) with respect to PCA (pK_{a2} 1.0). Consequently, the observed emission spectrum is similar to that observed upon benzoic acid interaction. In contrast, a better interaction is observed between AH9676 and EuNBA. The $-OCH_2Ph$ substituent exerts a lesser influence on the aromatic ring, and the nitrogen heteroatom (pK_{a2} 1.05) is better able to chelate the metal centre in combination with the CO_2^- group. In both cases, the weak intramolecular energy transfer observed is attributed to the weak binding interaction caused by the hydrophobic and steric influences of the proton in the 8-postion. Additional adverse steric interactions are expected between the acid substituent and the norbornyl arms of the EuNAL chelate.

Acid GR92452X (Figure 6-28), bearing a hydroxide substituent in the 8-position is inactive towards the EuNALs. No intramolecular energy transfer is observed between the ligand and the metal centre. It is expected that energy transfer to the luminescent state of the metal will be negated by non-radiative deactivation upon vibronic coupling with the high energy OH oscillator brought into close proximity with the metal centre upon carboxylate recognition. The inactivity of GR92452X may also be attributed to excited state

intramolecular proton transfer, established upon H-bonding interaction between the hydroxide and intervening water leading to depopulation of the acid excited state (as discussed in Chapter 5.2.8).

As the quinoline-2-carboxylic acids were observed to be inefficient LHCs for the controlled assembly of ternary luminescent lanthanide complexes with our EuNALs, the influence of the chelate arms on the binding interaction was not investigated further. Instead, our attention turns to the "salicylate" binding unit and the acids identified by combinatorial screening (Chapters 5.2.8.2-3 and 5.2.9).

6.5 Molecular Recognition between Good LHC Units and a Well Defined Binding Cavity

6.5.1 The 4-Hydroxyquinoline-3-Carboxylic Acid LHC Unit

The 4-hydroxyquinoline-3-carboxylic acid, AH10225, and naphthyridine acids AH12133 and AH11967 were identified during the high throughput screening experiment as excellent candidate LHCs (5.2.8.2) for controlled formation of ternary luminescent complexes in aqueous solution by lanthanide molecular recognition.

It was noted that the parent salicylic and *o*-hydroxynaphthoic acids do not bind the EuNALs to form ternary luminescent complexes (5.2.8.3), whereas their heterocyclic counterparts, in contrast are very efficient LHCs towards Eu(III). The structures and pK_a values for a selection of the acids are given in Figure 6-33 and Table 6-10 respectively.

Fig 6-33	Acid	Tautomer	pK_{a1}	pK_{a2}	pK_{a3}	pK_{a4}
1	Salicylic (SAL)	-	13.70	3.01	-	-
2	1-hydroxy-2-naphthoic	-	10.46	3.02	-	-
3	3-hydroxy-2-naphthoic	-	13.29	3.02	-	-
4	GR340734X	-	7.50	3.58	0.06	-
5	AH10225	Keto	-	3.57	0.80	-
		Enol	12.08	6.26	0.81	-
6	GR258750X	Keto	-	2.72	0.11	-
		Enol	11.07	5.21	0.60	-
7	AH11967	Keto	-	5.08	1.71	-5.29
		Enol	8.05	4.44	0.41	-1.90
8	AH12133	Keto	-	3.07	0.97	-11.57
		Enol	7.32	4.00	0.46	-

Table 6-10 Calculated pK_a values (pKadB 4.0) for "salicylate" LHCs pictured in Figure 6-33

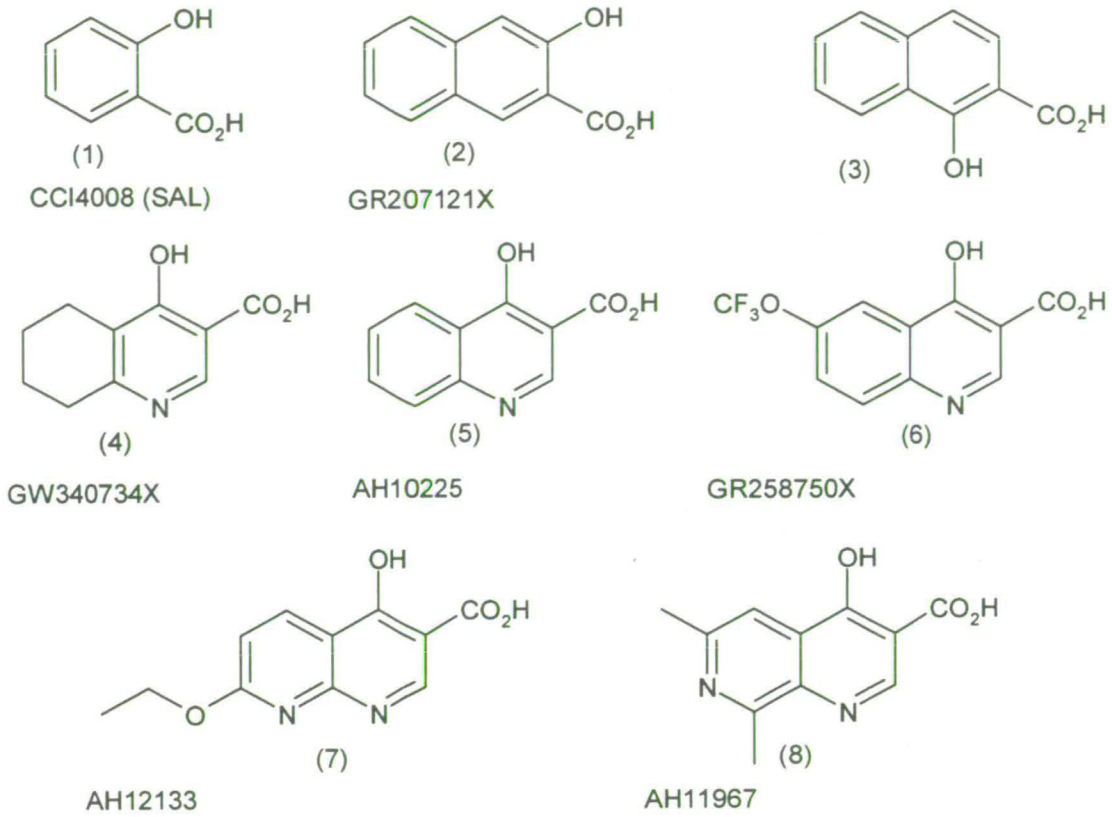

Figure 6-33 Structures of "salicylate" LHCs

It is immediately apparent that the inactivity of salicylate and *o*-hydroxynaphthoic acids is a consequence of the high phenol pK_a. Following the initial deprotonation event, a stable H-bonding network is established between the anionic carboxylate and the phenol group, disruption of which is energetically unfavourable. In addition to this, the high pK_a is indicative of the electron richness of the phenolate, and hence the ease with which LMCT may occur. Commercial assay systems employing salicylate derivatives in detection of biological molecular recognition by Tb(III) luminescence operate at alkaline pH (EALL pH 13, Chapter 1) ensuring a significant fraction of the acid exists in the deprotonated dianionic form (5-FAS: pK_{a1} 13.70, pK_{a2} 2.68; pAS: pK_{a1} 13.75, pK_{a2} 3.58, pK_{a3} 2.21). The 5-FAS ligand is unsuitable for use with Eu(III) due to LMCT.

The model LHC, picolinic acid, is observed to bind the LnNAL chelates (Log K ~ 5) in the presence of excess salicylic acid under neutral experimental conditions. Upon steady-state excitation at 300 nm (λ_{max} SAL) or 270 nm (λ_{max} PCA) strong blue organic fluorescence is observed in the emission cell, the tail of which is seen in the Eu(III) luminescence spectrum, despite the presence of a 550 nm cut-off filter (Figure 6-34, 35). The strength of

the organic fluorescence suggests that the acid does not coordinate the metal. Intersystem crossing to the triplet state, facilitated by the heavy atom effect upon mixing of the metal/ligand orbitals would result in a reduction in the intensity of fluorescence observed. The analogous terbium chelate exhibits similar behaviour to that of the Eu(III) complex, providing evidence that the inactivity of SAL towards LnDTPA-AM_2 is not a consequence of mismatched triplet state energies. In contrast to the TbDTPA-AM_2, covalently bound [$TbDTPA^-$] and [$TbEDTA^-$] chelates interact with pAS or 5-FAS to form highly luminescent lanthanide ternary complexes employed in assay technologies.[66-69] As discussed briefly in Chapter 5, our preliminary investigations have revealed differing mechanisms for ternary complex formation between such charged LnNAL species and the neutral LnDTPA-AM_2 chelates.

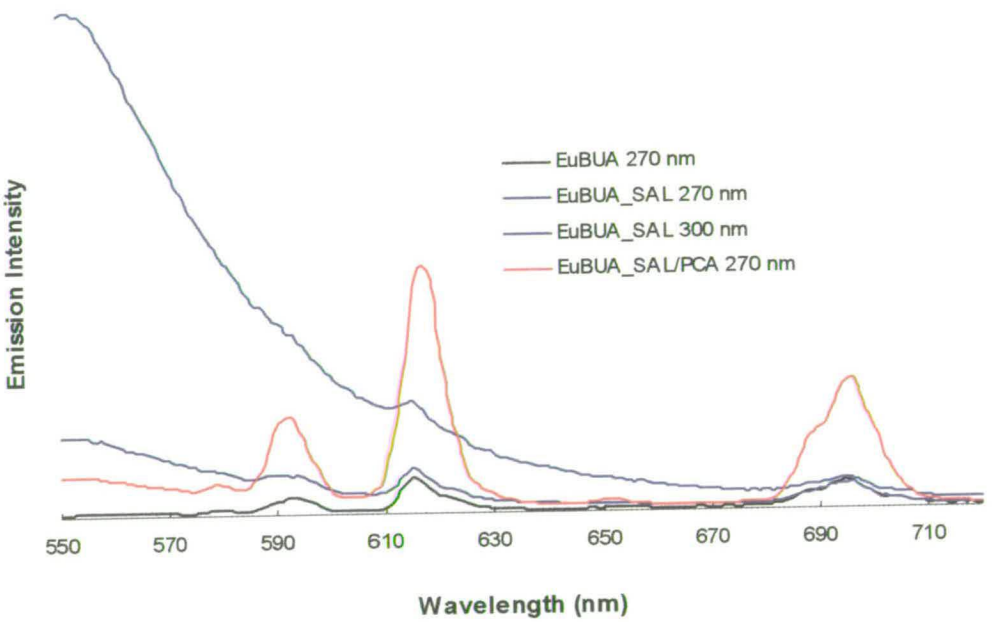

Figure 6-34 Emission spectra of EuBUA (0.1 mM aq) in the presence of excess SAL and 1eq PCA (λex = 720 nm, 300 nm)

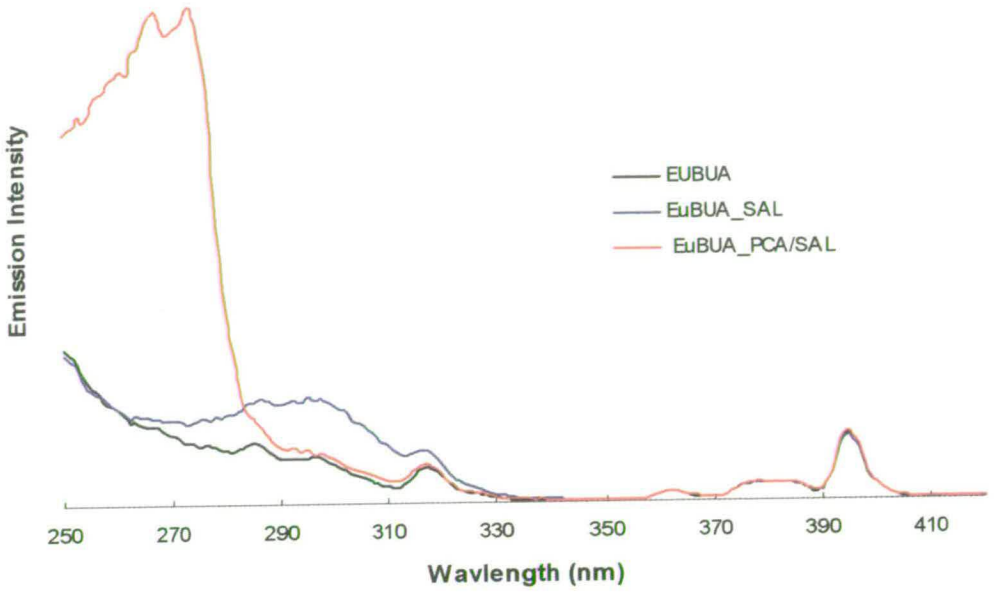

Figure 6-35 Excitation spectra of EuBUA (0.1mM aq) in the presence of excess SAL and 1eq PCA (λ_{em} 616 nm)

The influence of the heteroatom on molecular recognition is clear when the binding between acid GW304734X (Figure 6-33 (4)) and EuDTPA-AM_2 chelates is considered. Emission and excitation spectra for 1:1 solution samples of EuBUA, EuNBA and EuBBZA (0.1 mM aq) upon excitation at 270 nm are shown below (Figure 6-36, 6-37).

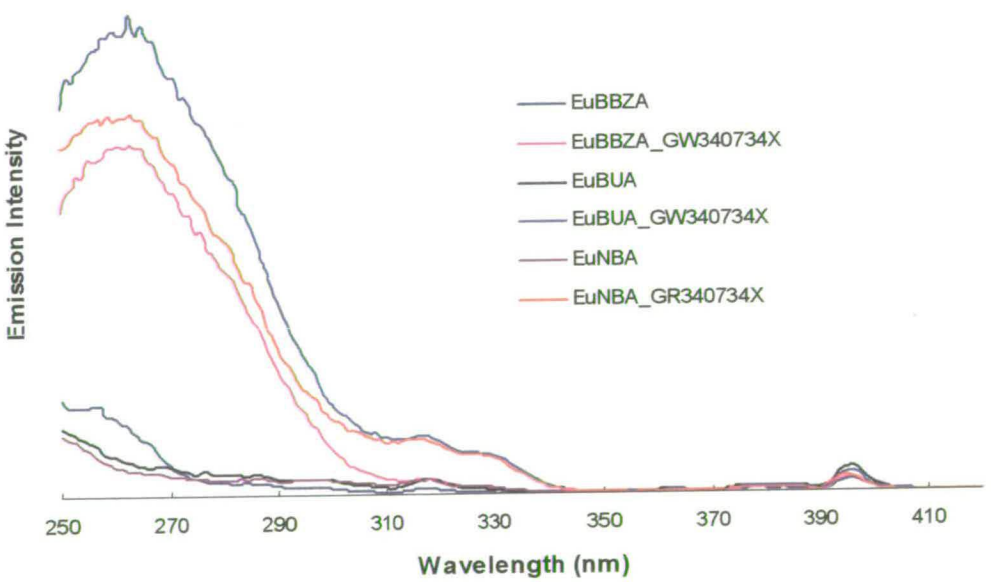

Figure 6-37 Excitation spectra of 1:1 solution samples of EuNBA, EuBBZA and EuBUA (0.1 mM aq, pH 7) + GW304734X (λ em = 616 nm)

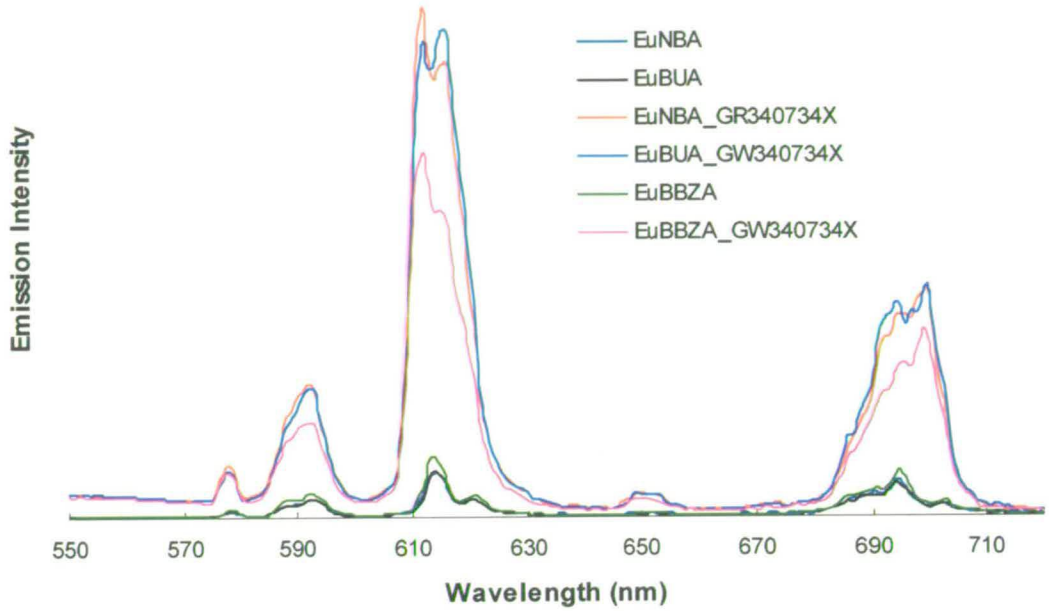

Figure 6-36 Emission spectra of 1:1 solution samples of EuBBZA, EuBUA and EuNBA (0.1 mM aq, pH 7) + GW304734X (λ ex = 270 nm)

The estimated equilibrium constants for the interaction between GW304734X and the EuNAL chelates are given in Table 6-11. It is observed that although the relative increase in sensitised luminescence (Figure 6-38) of EuBBZA is half that afforded by molecular recognition with the aliphatic chelates, (due to DTPA-BBZA residual absorbance) the binding constants for the interaction are of the same order of magnitude (average Log K 5.56 ± 5%), and show a significant improvement relative to PCA (Log K_{pca} ~ 4.9).

Chelate	LHC	K	±	Log K	±	Error	I/I_0
EuBUA	GW304734X	8.35E+05	5.71E+05	5.92	0.36	6%	14
EuNBA		3.79E+05	1.85E+05	5.58	0.23	4%	14
EuBBZA		1.49E+05	7.27E+04	5.17	0.23	4%	7
Average	**GW304734X**	**4.54E+05**	**2.76E+05**	**5.56**	**0.28**	**5%**	**12**

Table 6-11 Estimated formation constants for EuNAL (0.1 mM aq, pH 7) + GR340734X

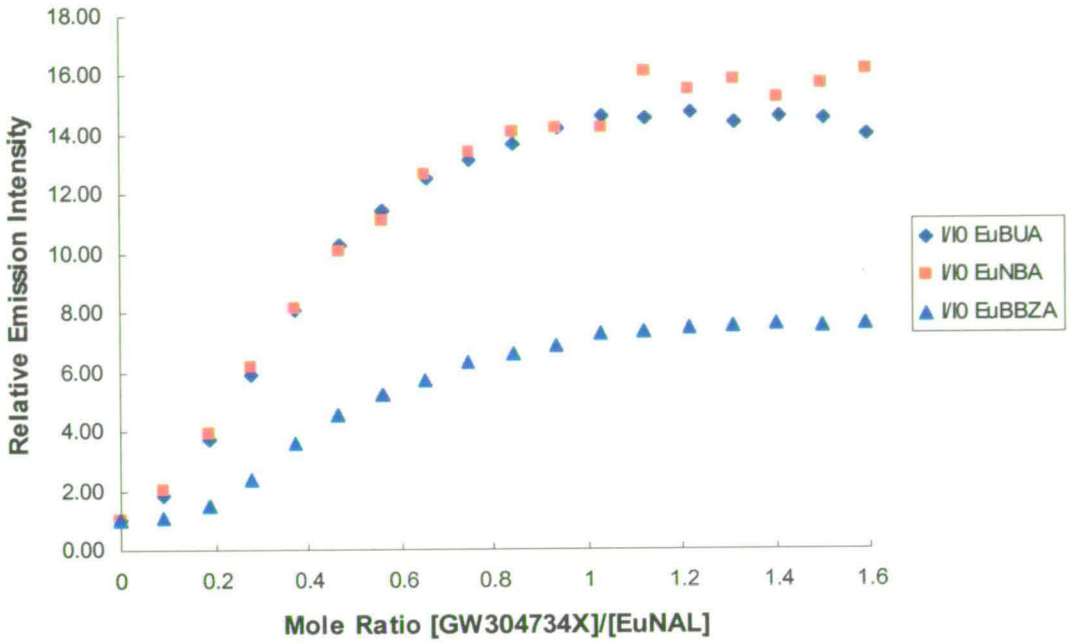

Figure 6-38 Relative emission versus mole ratio of [LHC]/[EuNAL] for GW304734X binding (0.1 mM aq, λ ex 270 nm)

The acid is expected to exist as the enol tautomer (Figure 6-33 (4)), with an estimated phenol pK_a of 3.58. Under the neutral conditions of the binding experiment in aqueous solution we can expect the hydroxide to be fully deprotonated. The ligand, bearing two anionic oxygen donors is ideally suited to Ln(III) coordination. Upon molecular recognition a stable six membered chelate ring is established with almost planar geometry (torsion angles of ca. 15° (Chem 3D)) facilitating efficient intramolecular energy transfer to the metal excited state.

The light harvesting properties of the ligand can be improved by extending the chromophoric unit, as demonstrated by AH10225 (Figure 6-33 (5)) binding. With the absorption maximum around 300 nm, and the same binding unit as acid GW304734X discussed above, this acid interacts strongly with the EuNAL (Table 6-12) to form highly luminescent mixed ligand complexes in 1:1 stoichiometry (Figure 6-39).

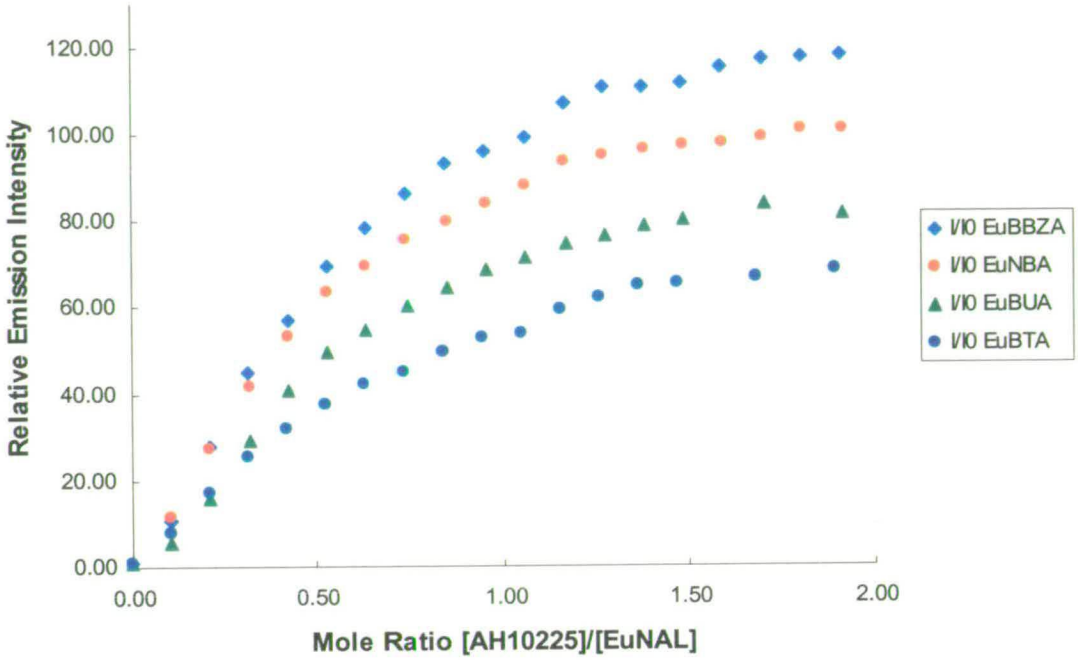

Figure 6-39 Relative emission intensity versus mole ratio [AH10225]/[EuNAL] (0.05 mM aq, pH 7, λ ex 300 nm)

Chelate	LHC	K	±	Log K	±	Error	I/I_0
EuNBA	AH10225	2.55E+05	6.74E+04	5.41	0.12	2%	100
EuBBZA	AH10225	2.01E+05	4.93E+04	5.30	0.11	2%	110
EuBUA	AH10225	1.82E+05	7.81E+04	5.26	0.20	4%	80
EuBTA	AH10225	7.81E+04	2.31E+04	4.89	0.13	3%	70
Average	**AH10225**			**5.22**	**0.14**	**3%**	**90**

Table 6-12 Formation constants for 1:1 EuNAL + AH10225 complexation

The relative emission increase observed for the interaction is on average approximately 100-fold. Interestingly, the LHC displays a degree of selectivity towards the more rigid EuNAL chelate (Figure 6-39), in common with PCA. The enhancement of Eu(III) emission observed for EuBBZA is almost double that of the other aromatic derivative studied, EuBTA, attributed to adverse steric interactions between the LHC and the methyl substituents in the 4-position of the aromatic amide arms. The estimated binding constant for EuBTA and AH10225 is slightly smaller than the other EuNAL chelates studied here. Electronic effects cannot be disregarded when considering the efficiency of energy transfer from the LHC triplet state to the $^5D_0$ emissive level of Eu(III). It is proposed that π–π

interactions between the arms of the aromatic DTPA-AM_2 and the acid may play a role in the pathway of energy transfer from the sensitising ligand to the metal.

The lowest energy conformation of acid AH10225 is expected to be the keto tautomer (Figure 6-40) with a carboxylate pK_a of 3.57. In the minor tautomeric species, the enol, the phenol pK_a is estimated at 6.26. The LHC is therefore expected to be completely deprotonated under the experimental conditions, presenting a dianionic bidentate binding unit to the metal.

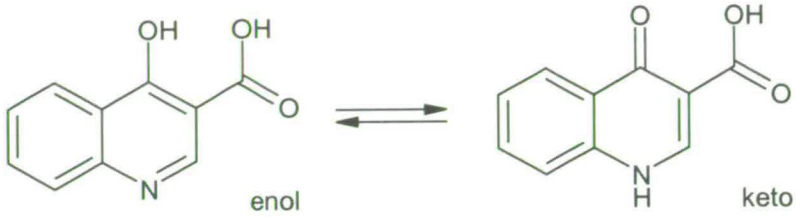

Figure 6-40 Tautomeric structural forms of AH10225

The interaction is strong and energy transfer efficient, as the shortest intramolecular distance between the Eu(III) metal centre and the sensitising ligand (Eu-O) is approximately 3.3 Å (Chem 3D). The stronger emission intensity observed from the $[EuNBA.AH10225]^{2-}$ species relative to the other EuNALs under the same experimental conditions is again attributed to the rigid, hydrophobic arms of the NAL protecting the antenna binding site from quenching effects of the solvent. Emission and excitation spectra are shown below in Figures 6-41 and 6-42 respectively.

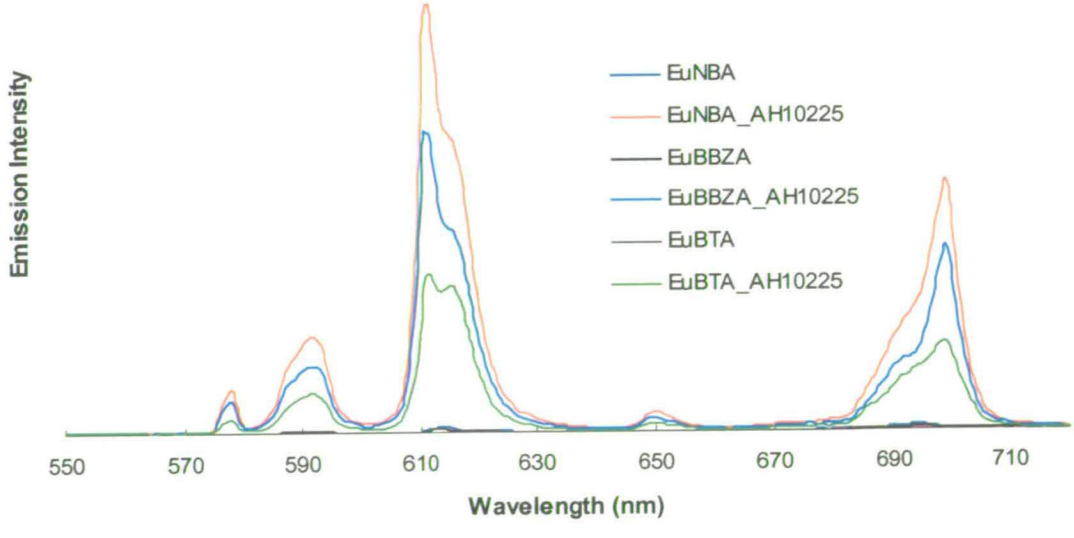

Figure 6-41 Emission spectra of 1:1 solution samples of EuNBA, EuBBZA and EuBUA with 4-hydroxyquinoline-3-carboxylic acid LHC, AH10225 (0.05 mM aq, pH 7, λ ex = 300 nm)

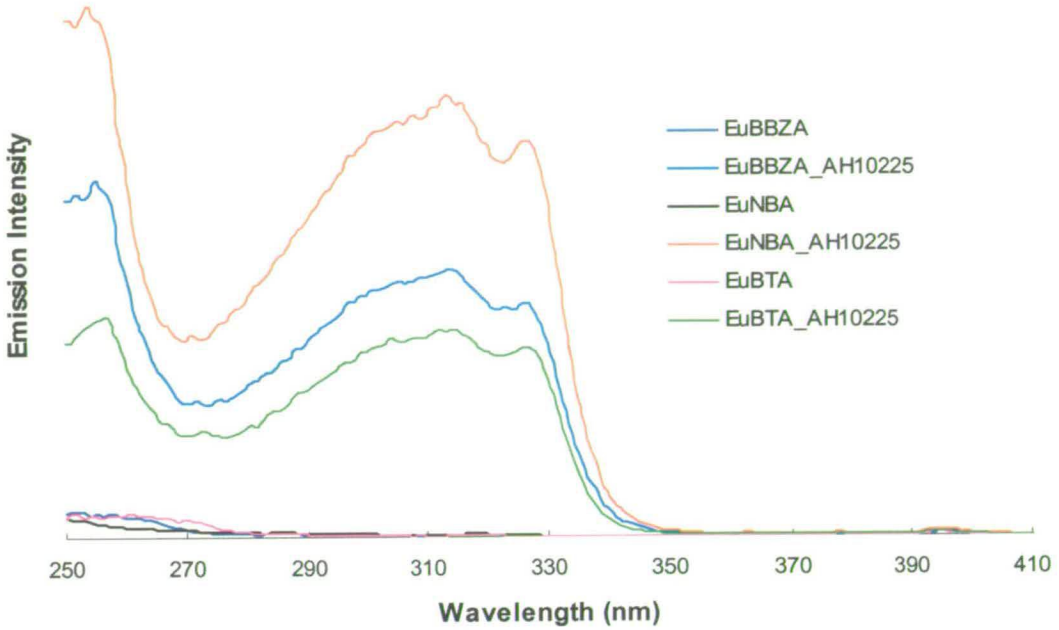

Figure 6-42 Excitation spectra of 1:1 solutions of EuBBZA, EuBTA and EuNBA (0.05 mM) aq + AH10225 (λ em = 616 nm)

6.5.2 Substituted 4-Hydroxyquinoline-3-Carboxylic Acid LHC Units

The trifluoromethoxy derivative of AH10225, compound GR258750X (Figure 6-33 (6)) also exhibits promising light harvesting properties towards the EuNALs for ternary complex formation. The observed emission increase upon interaction with EuBUA under excitation at 300 nm (λ max) is approximately 80-fold (Figure 6-43), and characteristic ligand absorbance bands are observed in the excitation spectrum confirming the intramolecular AETE emission process.

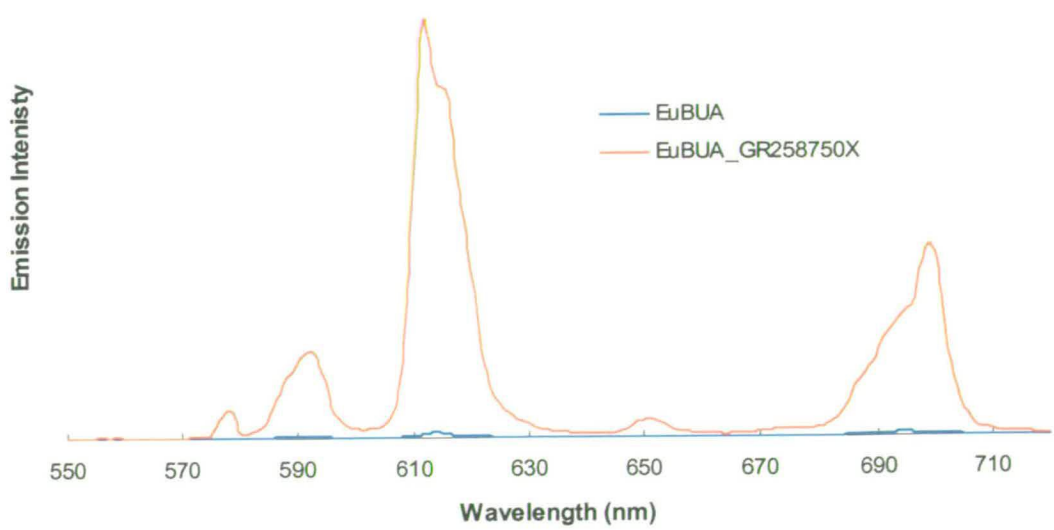

Figure 6-43 Emission spectra of EuBUA (0.1 mM aq, pH 7) + GR258750X (λex = 300 nm)

Formation constants (λ ex 270 nm) are of similar magnitude to AH10225 for both EuNBA and EuBUA, as expected for coordination by the 4-hydroxyquinoline-3-carboxylic acid binding unit, fully deprotonated under the titration conditions.

It can be concluded that the presence of strongly electron withdrawing $-CF_3$ substituent, reduces the resonance electron donating ability of the oxygen in the 6 position of the hydroxyquinoline carboxylic acid, and does not perturb the binding interaction with the EuNAL. The efficiency of intramolecular energy transfer between the LHC and EuBUA is of similar magnitude to that observed with the parent acid, AH10225, under steady-state excitation at 300 nm. In contrast, the substituted acids AH11688 and GI266527 (Figure 6-44) do not recognise the EuNAL binding cavity. Strong blue organic fluorescence is detected upon continuous illumination of the sample at the LHC absorption maximum.

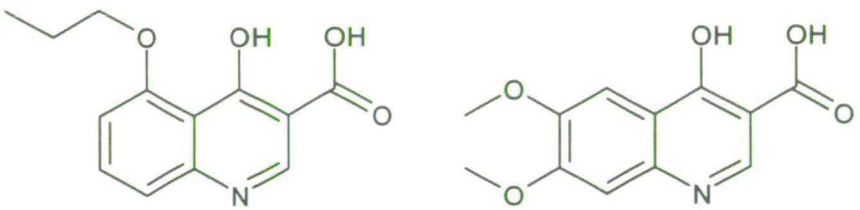

Figure 6-44

In the enol tautomeric species the carboxylate and phenol pK_a values are estimated at approximately 1 and 6 respectively, and the acids are expected to be fully deprotonated under experimental conditions.

Comparison of the emission spectra (Figure 6-45) reveals the different interaction between each of these acids and EuNBA. Acid AH11688 binds the metal centre affording a small increase in sensitised Eu(III) luminescence with residual levels of organic fluorescence. The inefficiency of energy transfer is attributed to inappropriately matched excited state energy levels. Inductive electron donation from the methoxy substituents in the 6 and 7 positions raises the energy of the aromatic system. The emission spectrum of EuNBA + GI265527 shows the strong organic background fluorescence almost obscuring the lanthanide emission bands. The alkoxy group in the 5-position is expected to impede the interaction between the phenolate and the metal centre, impeding the binding interaction. Consequently the efficiency of intersystem crossing is reduced and the singlet excited state of the LHC can decay radiatively.

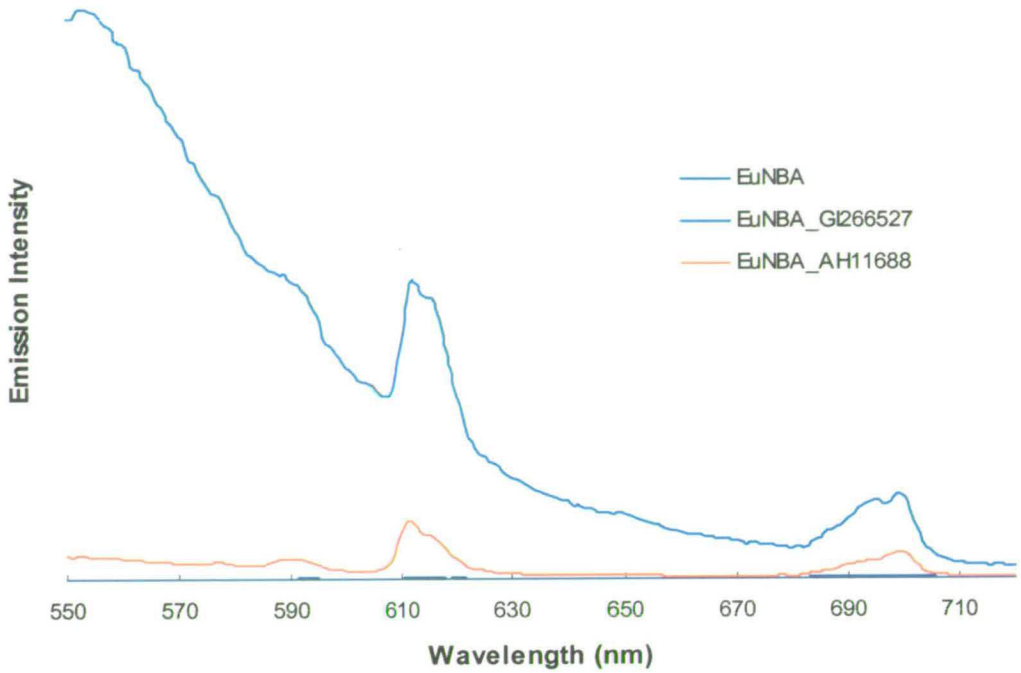

Figure 6-45 Emission spectra of EuNBA (0.05 mM aq) + AH11688 and GI265527 (λex = 300 nm)

6.5.3 Substituted Salicylic Acid LHCs

The salicylic acid derivative, AH9018 (Figure 6-46), appeared to exhibit excellent potential as a light harvesting ligand when studied under the time-resolved conditions of the assay experiment. In contrast, no interaction is observed under steady-state excitation, as any characteristic red sensitised europium emission is obscured by intense organic fluorescence from the acid. This inactivity is attributed to the electron rich phenolate group which can easily establish LMCT states with the Eu(III) centre. In contrast, acid GR94828 (Figure 6-46) increases the emission intensity of the EuNAL (Figure 6-47).

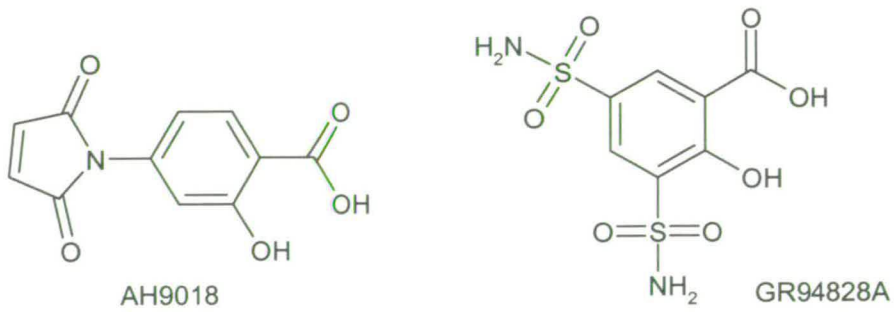

Figure 6-46 Substituted salicylic acid LHC units

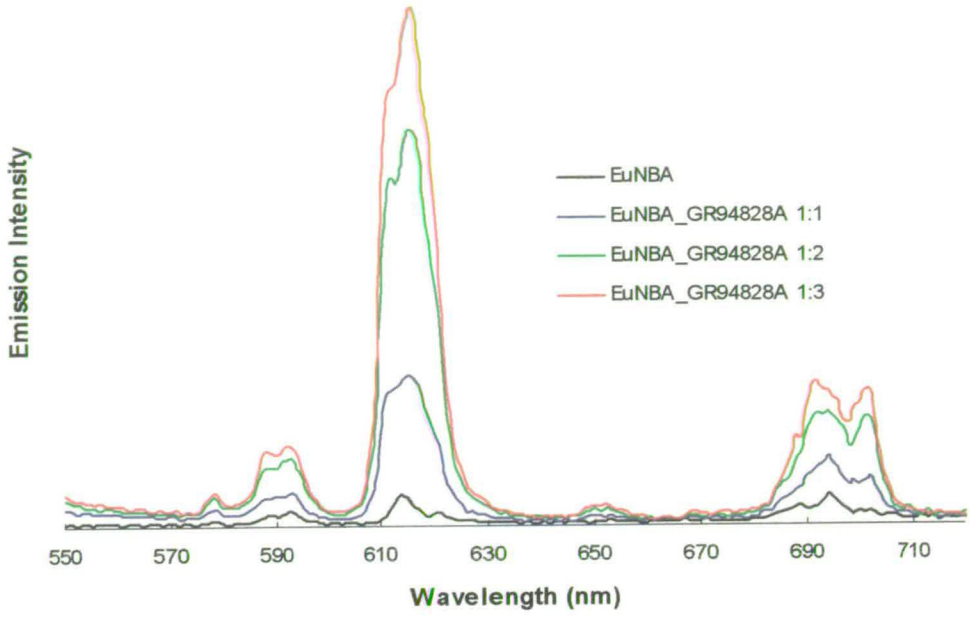

Figure 6-47 Emission Spectra of EuNBA (0.05 mM aq, pH 7) + GR94828A (λ ex = 270 nm)

The stoichiometry of the ternary complex is poorly defined, illustrated by the emission spectra shown in Figure 6-47, and is attributed to the possibility of alternative coordination via the sulphonamide substituents. Under experimental conditions (pH 7) the phenol is substantially deprotonated (predicted pK_a 8.0). This reduction in acid dissociation constant relative to the parent SAL is due to the presence of the electron withdrawing sulphonamide groups *meta* to the carboxylic acid unit (pKa 1.3).

6.5.4 Molecular Recognition with EuBAA

In light of the observations made regarding the steric bulk and rigidity of the NAL and the improved luminescence properties of the mixed ligand chelate in aqueous solution, it was decided to test the bulkier adamantyl DTPA-AM_2 derivative, EuBAA (Figure 6-48).

The chelate (0.05 mM aq, pH 7) was titrated with AH10225 (pH 7-8). Formation of the 1:1 mixed ligand species resulted in a 500 fold increase in sensitised emission of the Eu(III) ion (Figure 6-49). Qualitatively, the experiments confirms the hypothesis that the rigidity and

hydrophobicity imparted on the EuNAL binding cavity by the DTPA-AM_2 chelate arms is greatly beneficial to luminescence of the ternary complex formed upon molecular recognition with 4-hydroxyquinoline-3-carboxylic acid LHCs in aqueous solution. Emission plots for the interaction of AH10225 with chelates EuNBA and EuBAA are shown below (Figure 6-49). Molecular recognition with the well defined binding cavity of EuBAA affords an increase in sensitised luminescence approximately five times that of the corresponding interaction with EuNBA under the same experimental conditions.

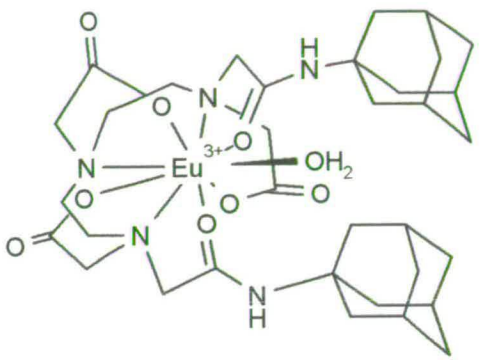

Figure 6-48 [EuBAA.H_2O]

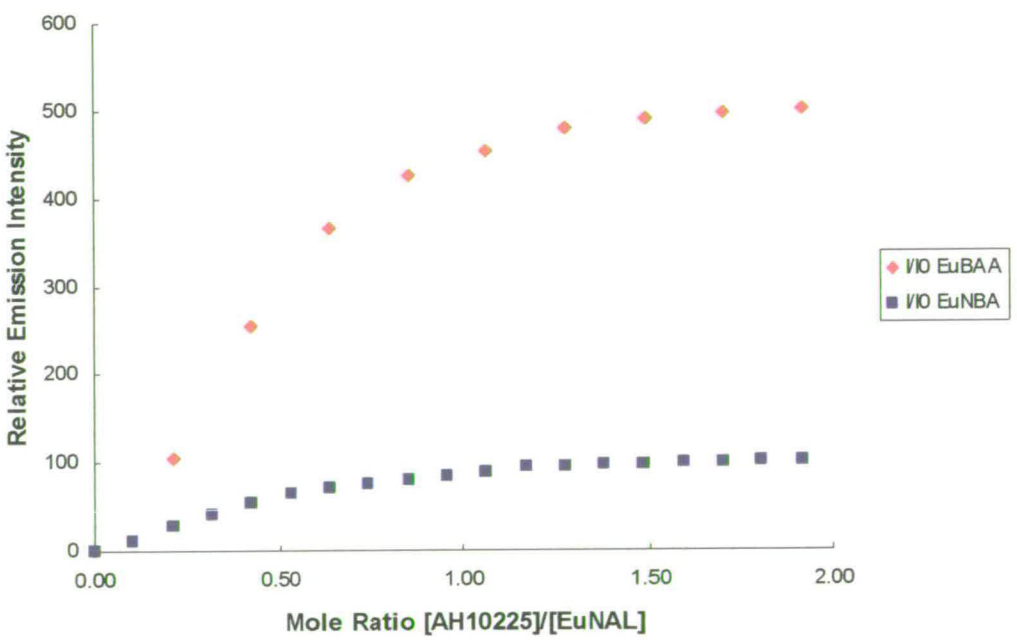

Figure 6-49 Plot of relative emission intensity versus mole ratio for ternary complex formation with EuNBA and EuBAA chelates (0.05 mM aq) and AH10225 (λex = 300 nm)

Acid AH10225 is an excellent light harvesting unit for Eu(III) under these conditions, forming stable mixed ligand, intensely luminescent complexes with the EuNALs in aqueous solution (Log K ~ 5.5). The presence of aromatic absorption bands in the excitation spectra corresponding to AH10225 absorbance provide unequivocal evidence that the increase in emission intensity is due to intramolecular energy transfer from the LHC chromophore.

6.5.5 4-Hydroxynaphthyridine-3-Carboxylic Acid Recognition

The naphthyridine derivatives AH12133 and AH11967 (Figure 6-50) were identified as potentially excellent sensitising ligands for ternary complex formation with Eu(III) DTPA-AM_2 chelates during the high throughput screening experiment (Chapter 5.2.9). Further study into controlled formation of luminescent mixed ligand species with the EuNALs gave interesting results. The acids are predicted to adopt the keto tautomeric structure, of lower energy than the enol conformation, and to be fully deprotonated under experimental conditions (pKa values are given in Table 6-11).

The acids were observed to interact with the metal centre substantially increasing EuNAL emission upon excitation of the chromophoric unit, exhibiting excellent potential as sensitising ligands for our ternary complex system. Emission plots for titration of EuBBZA, EuNBA and EuBUA with AH12133 (Figure 6-51) and EuNBA with AH11967 (Figure 6-52) plateau fairly sharply, indicative of a strong binding interaction. However, instead of forming 1:1 mixed ligand [EuNAL.LHC] complexes, analogous to AH10225 binding as expected, the stoichiometry appears to be 1:0.5. Several controlled experiments were performed in order to check this effect. The behaviour is wavelength independent, observed at λ ex 270 nm, 300 nm and 350 nm, and unlikely to arise from organic photophysical or photochemical processes occurring within the LHC. No signal degradation is observed under steady-state irradiation or pulsed-excitation during the experimental period. Dilution of the sample by a factor of two (0.1 mM $\rightarrow$ 0.05 mM) did not influence the results, confirmation that the behaviour is not the result of instrumental artefacts arising from sample self absorption or inner filter effects.

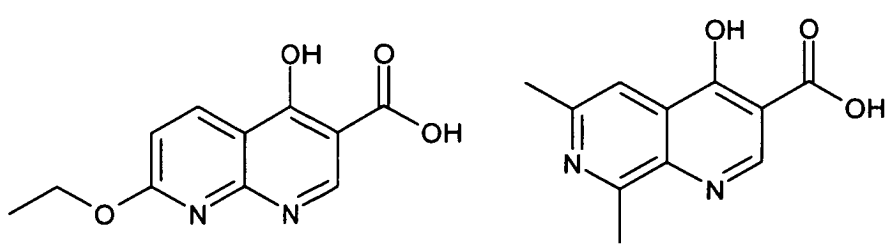

AH12133 AH11967

Figure 6-50 4-hydroxynaphthyridine-3-carboxylic acid LHC units

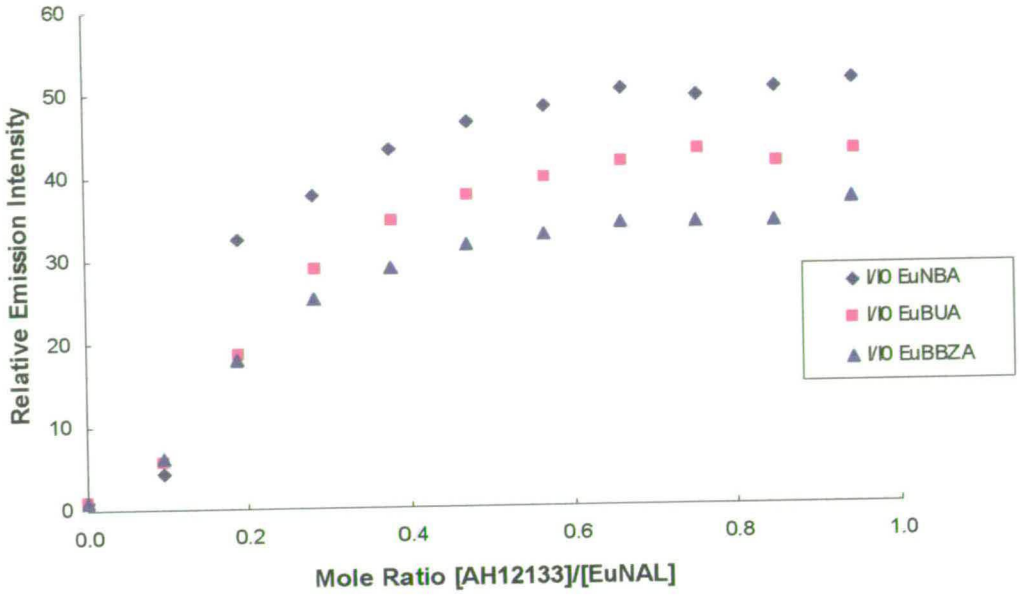

Figure 6-51 Plots of relative emission intensity versus mole ratio LHC:EuNAL for ternary complex formation between EuNALs (EuBUA, EuNBA and EuBBZA, 0.1 mM aq, pH 7) and AH12133 (λ ex = 270 nm)

The interaction between EuNBA and AH11967 is clearly stronger than the corresponding recognition with AH12133, as demonstrated by the sharp plateau in the emission plot (Figure 6-52). Similar behaviour is observed upon excitation off maximum at 350 nm.

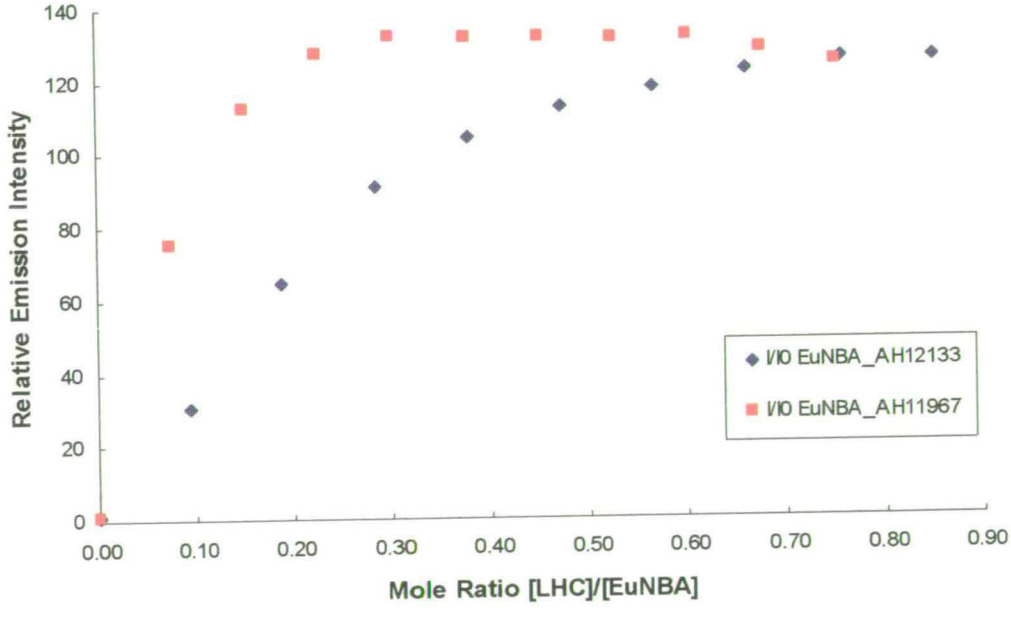

Figure 6-52 Plot of relative emission intensity versus mole ratio LHC:EuNAL for the interaction between EuNBA (0.05 mM aq, pH 7) and naphthyridine acid LHCs, AH12133 and AH11967 (λex = 300 nm)

To the best of our knowledge little attention had been paid to the light harvesting properties of naphthyridine carboxylic acids towards Ln(III) cations. One paper[64] reports the evaluation of 33 potential fluorogenic chelators for europium and terbium towards their application in enzymatic assays (EALL) at alkaline pH. One naphthyridine acid (Figure 6-53) was identified as a good substrate molecule for alkaline phosphatase assays employing Eu(III) or Tb(III) metal lumophores. Characteristic sensitised Ln(III) emission was detected at 616 nm and observed to be stable over time in buffered solution at pH 9 in the presence of excess EDTA (1 mM in LHC; LHC:Ln:Buffer = 1:4:5). No further investigation into the mechanism of luminescent complex formation was reported.

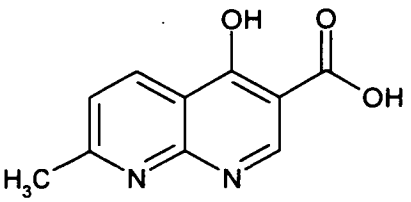

Figure 6-53 4-hydroxy-7-methyl-1,8-naphthyridine-3-carboxylic acid

Luminescence lifetimes of mixed ligand samples (Table 6-12) were measured upon excitation at 355 nm (single photon absorption) or 532 nm (expected to be a two-photon excitation process). The emission detected at 616 nm arises from the sensitised Eu(III) lumophore and the measured lifetime is that of the metal centre. Agreement within experimental error is observed between the two studies.

Chelate	LHC	τ (ms)	Error (±)	%
EuBAA†	-	0.741	0.010	1.3
	AH10225†	0.847	0.007	0.8
	AH11967†	0.556	0.007	1.3
	AH12133†	0.567	0.002	0.4
EuNBA*	-	0.780	0.002	0.3
	AH11967*	0.560	0.001	0.2

Table 6-13 Luminescence lifetimes for [EuNAL.LHC] mixed ligand samples (λex = †355 nm or *532 nm, λem = 616 nm)

The ternary complex formed between the effective sensitising ligand, AH10225,and the well defined binding cavity of EuBAA exhibits a longer luminescence lifetime that the parent chelate ($\Delta\tau \sim 0.1$ ms), confirmation that OH oscillators are displaced from the primary coordination sphere. In contrast, aqueous solution samples containing EuNAL and a

naphthyridine LHC, AH11967 or AH12133, exhibit a significant reduction in the observed luminescent lifetime relative to the parent chelate.

It is possible that the rate of EuNAL isomerisation is reduced upon addition of the second component which may partially associate with the chelate to inhibit rearrangement of the coordination polyhedron. The measured decay constant comprises the average of terms for all the distinct Eu(III) environments present and interchanging on a timescale observable with the laser set-up employed. The kinetic lability of the thermodynamically very stable LnDTPA-AM_2 complexes is well established, as discussed in section 6.3.2. Transient intermediate species that are short lived are not readily observed on the timescale of pulsed laser excitation, and single exponential decay curves are obtained.

Lifetime measurements performed in H_2O and D_2O provide a measure of the number of water molecules occupying coordination sites in the inner sphere of the metal complex. Corrections made to Equation 1-2 allow the influence of closely diffusing OH and proximal XH oscillators to be included in evaluation of the hydration state (q) (Equation 6-1). The parameter A_{Eu} = 1.11 waters•ms, as determined by Horrocks et al.[45] τ^{-1}_{H2O} and τ^{-1}_{D2O} are the reciprocal lifetimes (ms^{-1}) for the species under investigation in H_2O and D_2O respectively, and k_{XH} (ms^{-1}) represents the contribution from other high energy X-H oscillators capable of depopulating the excited state by non-radiative energy transfer.

$$q = A_{Eu}(\tau^{-1}_{H2O} - \tau^{-1}_{D2O} - k_{XH})$$

$$k_{XH} = \alpha + \beta n_{OH} + \gamma n_{NH} + \delta n_{O=CNH} \qquad \textbf{Equation 6-1}$$

The parameters n_{OH}, n_{NH} and $n_{O=CNH}$ represent the number of alcoholic OH, secondary amine NH and amide NH where the carbonyl group coordinates the metal respectively, and α is the de-excitation rate constant for closely diffusing solvent molecules (α = 0.30 ms^{-1}, β = 0.45 ms^{-1}, γ = 0.99 ms^{-1}, δ = 0.075 ms^{-1}). For the DTPA-AM_2 ligands employed in this study k_{XH} adopts the value 0.0525 ms^{-1}.

Chelate	Solvent	τ_1	±	q (± 0.1)
EuBUA	H_2O	0.786	0.003	-
	D_2O	2.414	0.019	0.89
EuNBA	H_2O	0.780	0.002	-
	D_2O	2.297	0.005	0.88
EuBBZA	H_2O	0.956	0.011	-
	D_2O	2.480	0.031	0.65

Table 6-14 Luminescence lifetimes measured in water and D_2O and estimated hydration states (q) for EuNALs (λ ex = 532 nm, λem = 616 nm)

Interaction between the LHC and free Eu(III) was considered but can be disregarded, as the high thermodynamic stability of the EuNAL species (Log K_{GdL} ~ 15) prevents significant dissociation of the metal from the NAL chelate. Under the experimental conditions at pH 7, 0.05 mM, the stability constant for EuNAL formation is 1.37×10^{13} (Log K_{ML} 13.14) (computed from literature values for protonation and formation constants for GdBEA)[120]. The major species present in solution is the EuNAL chelate and the concentration of free Eu(III) estimated at around $2x\ 10^{-9}$ M (~ 0.004 % dissociated). At this concentration the level of free Eu(III) can be regarded as negligible. The possibility of non-specific binding of dissociated Eu(III) with by LHC titrant can be disregarded due to the extremely low level of free Eu(III). The major species detected by electrospray MS analysis of the emission samples is the EuNAL, confirmation that the LHC is not extracting the metal from the aminopolycarboxylate complex. No peaks corresponding to $Eu(LHC)_n$ species are observed.

Luminescence quantum yields were evaluated relative to a $[Ru(bipy)_3Cl_2]$ standard (Φ = 0.028 in water)[153] for the interaction between EuBAA and acids AH10225, AH12133 and AH11967 (1:1 solutions) by the method of Haas and Stein.[158]

Chelate	Acid	Quantum Yield
EuBAA	-	-
	AH10225	0.0016
	AH11967	0.0026
	AH12133	0.0015

Table 6-15 Relative luminescence quantum yields for mixed ligand complexes formed between EuBAA and LHCs AH10225, AH12133 and AH11967 in aqueous solution.

The results are representative of the interaction between the LHC and the metal in aqueous solution and demonstrate that energy transfer between the antenna ligand and the Eu(III) ion is relatively efficient. From the results (Table 6-15) it is obvious that the acids are excellent antenna and sensitiser ligands for Eu(III), but further investigation into ternary complex formation is clearly necessary.

The observations regarding molecular recognition between the EuNALs and 4-hydroxynaphthyridine-3-carboxylic acids suggest that a dinuclear inclusion type complex may be forming, with one naphthyridine LHC unit acting as a bridging ligand between two discrete EuNALs. This was initially thought to be unlikely as the bulk solvent water is a

much better ligand towards Eu(III) than a neutral, heterocyclic nitrogen atom. Bipyridine compounds of Eu(III) are generally unstable in aqueous solution, unless the chromophore is incorporated into a macrobicyclic cryptand structure, rendering dissociation of the metal entropically unfavourable.

Coordination of the second nitrogen atom, normally unfavourable in water, in the absence of a second, anionic donor group, becomes more stable when shielded from the effects of outer sphere solvent molecules by the hydrophobic arms of the DTPA-AM_2 ligand. Whereas an increased lifetime could be expected for a dimeric [$(EuNAL)_2LHC$] species, it is not unreasonable to propose that charge transfer states are established upon heterocyclic nitrogen coordination, resulting in an increased rate of radiative decay and hence a shorter lifetime. The highly conjugated aromatic system may be responsible for establishing resonance structure between the two metal centres (cf isoPTA).

6.6 Conclusions

It can be concluded from these spectroscopic studies that aromatic carboxylic acid binding to LnDTPA-AM_2 chelates can be modified by the structural and electronic properties of the NAL, as initially established during the high throughput screening of a diverse library of potential antenna ligands (Chapter 5). Molecular recognition can be controlled primarily by the choice of LHC binding unit, with additional selectivity imparted by careful NAL design.

7 Luminescent Heterobimetallic 1D Coordination Polymers: Towards New Properties in the Solid State

7.1 Luminescent Materials

Novel functional materials with tuneable luminescent properties are continually in demand[159] to keep abreast with the technological advances in modern display and sensory equipment. Combinatorial approaches adopted in materials research (outlined in Chapter 1.4.4) have accelerated the discovery and optimisation of potentially viable luminescent systems. Lanthanide ions are routinely employed as dopants[160] in inert metal oxide lattices, and have been incorporated into zeolites and colloidal particles to produce luminescent nanomaterials. In contrast to the traditionally trial and error process by which many of today's commercially important luminescent materials evolved, it has been the goal of some researchers to introduce structural control at a molecular level in the design of organic-inorganic hybrid solids.[161] Whereas the photophysical properties of luminescent lanthanide complexes are often thoroughly investigated, much less attention has been paid to the behaviour of such species in the solid state.

An unexpected, but nevertheless very interesting result was obtained whilst attempting to crystallise the luminescent ternary complexes formed upon molecular recognition between the EuNALs and the model LHC, PCA, and is discussed below.

7.2 Structural Studies

Large, well defined, hexagonal single crystals, exhibiting characteristic sensitised Eu(III) emission were grown from aqueous solutions of the EuNAL with a large excess of PCA in the presence of NaOH (pH 7-8). Further investigation demonstrated that mixing concentrated aqueous solutions of $EuCl_3 \bullet 6H_2O$ with excess picolinic acid in the presence of NaOH (pH 7-8) lead to precipitation of a microcrystalline solid, from solutions of which the large hexagonal crystals could be grown by vapour diffusion with acetone (Chapter 2).

Analysis by X-ray diffraction revealed the crystals to have the formulation $[EuNa(PCA)_4H_2O]_n 0.5nH_2O$ with a high degree of structural organisation. The crystal structure (Figre 7-1) shows closely packed polymeric chains comprising of $[Eu(PCA)_4]^-$ units liked together by bridging carboxylate oxygen ligands and the sodium counterions. Each europium is nine coordinate, encapsulated by four bidentate PCA units and one additional carboxylate unit bridging to the Na^+ ion in what can loosely be described as a distorted monocapped square antiprismatic polyhedron. The distance between neighbouring Eu(III)

ions of the $[Eu(PCA)_4]^-$ monomers is 6.3 Å, within the limits of the range covered by Dexter type energy transfer. Interestingly, no quenching water molecules occupy the primary coordination sphere of the Eu(III) centre, despite the presence of H-bonding solvent between the chains. Each sodium ion with only three ligands is unexpectedly low in coordination number. One water molecule and two bridging carboxylate oxygen atoms bind the alkali metal ion. The one dimensional polymers are disposed along a 2_1 screw axis, with the Na^+ adopting a zig-zag motif along the chain. Face-edge π interactions exist (5.1 Å centroid-centroid) between the pyridyl moieties of neighbouring PCA units contributing to the stability of the polymeric structure.

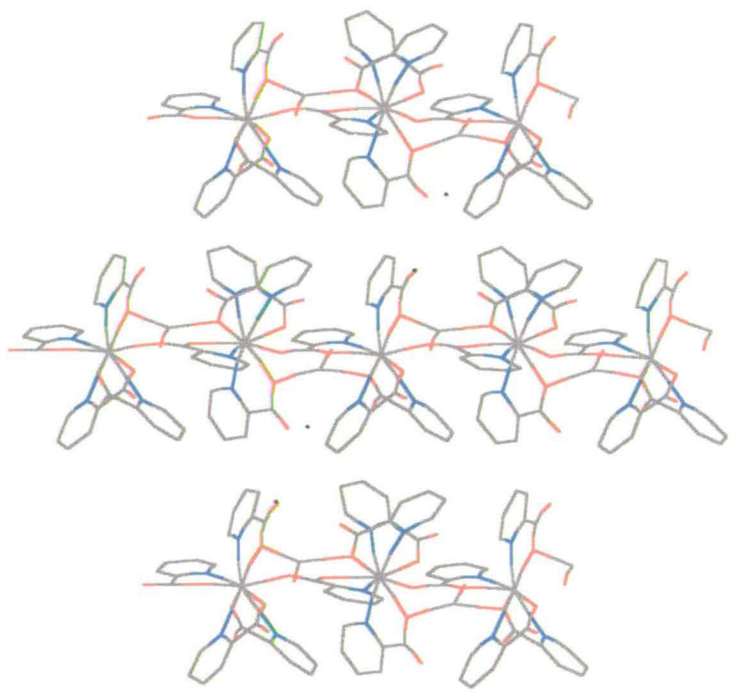

Figure 7-1 Crystal structure of $[EuNa(PCA)_4H_2O]_n0.5nH_2O$

Single crystals of the yttrium and gadolinium species were found to have the same unit cell as the Eu(III) polymer. The X-ray powder diffraction patterns obtained from microcrystalline samples of the Eu(III), Tb(III) and Gd(III) solids (Figure 7-2) matched that predicted from the Eu(III) single crystal structure. It can be concluded from this information that the single crystals obtained are representative of the bulk microcrystalline material.

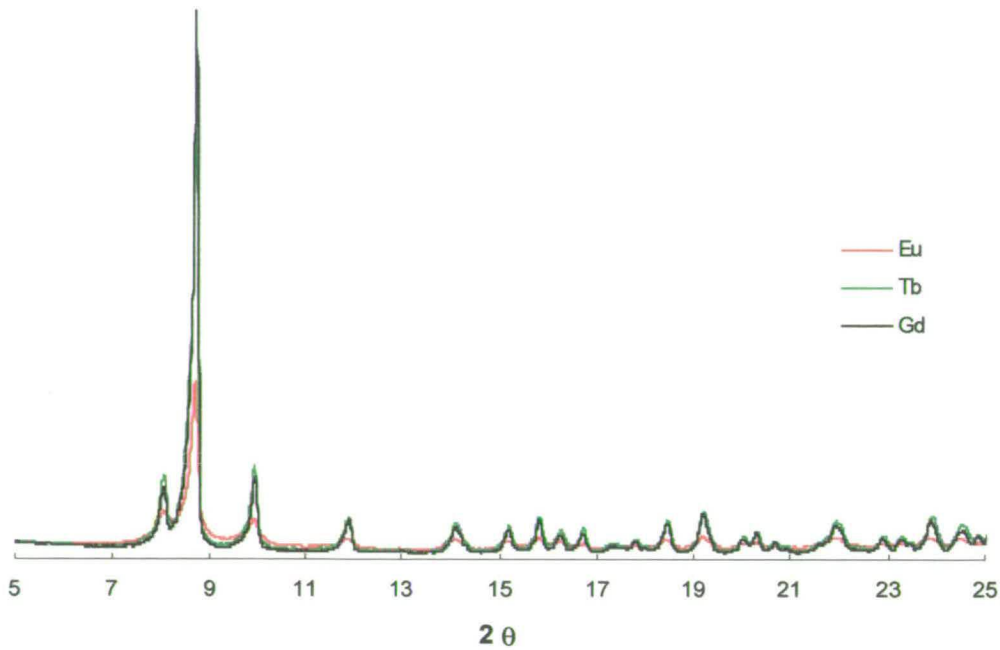

Figure 7-2 Powder XRD patterns obtained from microcrystalline samples of Eu(III), Gd(III) and Tb(III) 1D coordination polymers with PCA and sodium

7.3 Luminescence Studies

The single crystal exhibits characteristic strong red Eu(III) emission (Figure 7-3) upon excitation in the UV and the visible region of the electromagnetic spectrum. Unlike solution samples of Eu(III) and PCA, whose excitation profile match closely that of the ligand absorption spectrum, with a maximum around 270 nm, the crystal excitation spectrum exhibits a broad profile, shifted significantly into the red (Figure 7-4). This unexpected profile is indicative of a new interaction occurring in the single crystal, not present in solution. The interaction is believed to arise from the structural arrangement of the luminescent components in the solid state, with the new state responsible for energy transport to the metal ion.

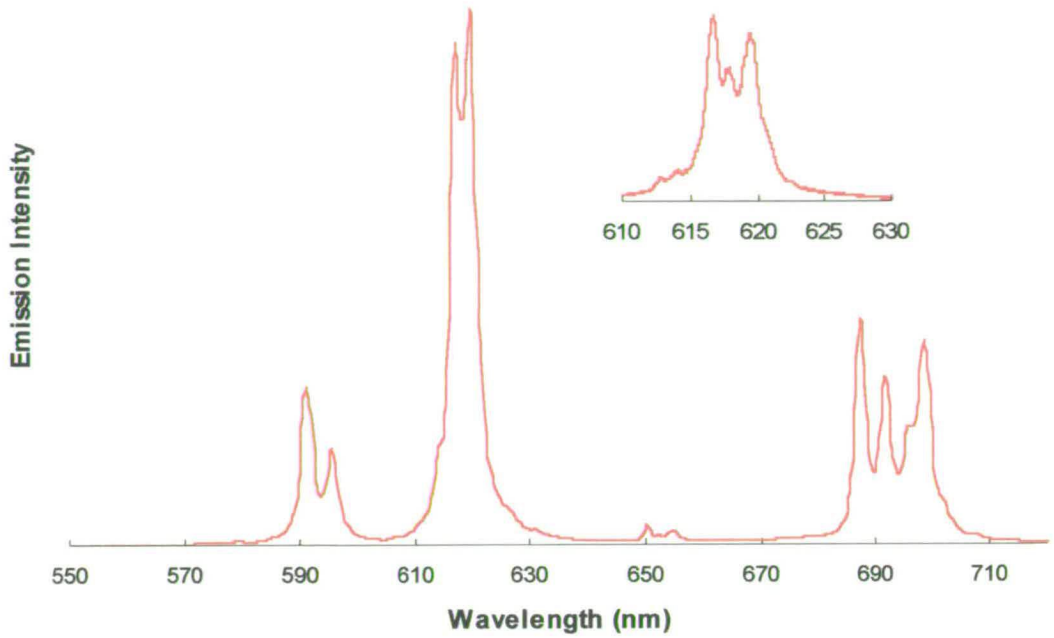

Figure 7-3 Single crystal emission spectrum (corrected for PMT response) upon excitation at 360 nm Inset shows 616 nm peak under high resolution (0.18 nm).

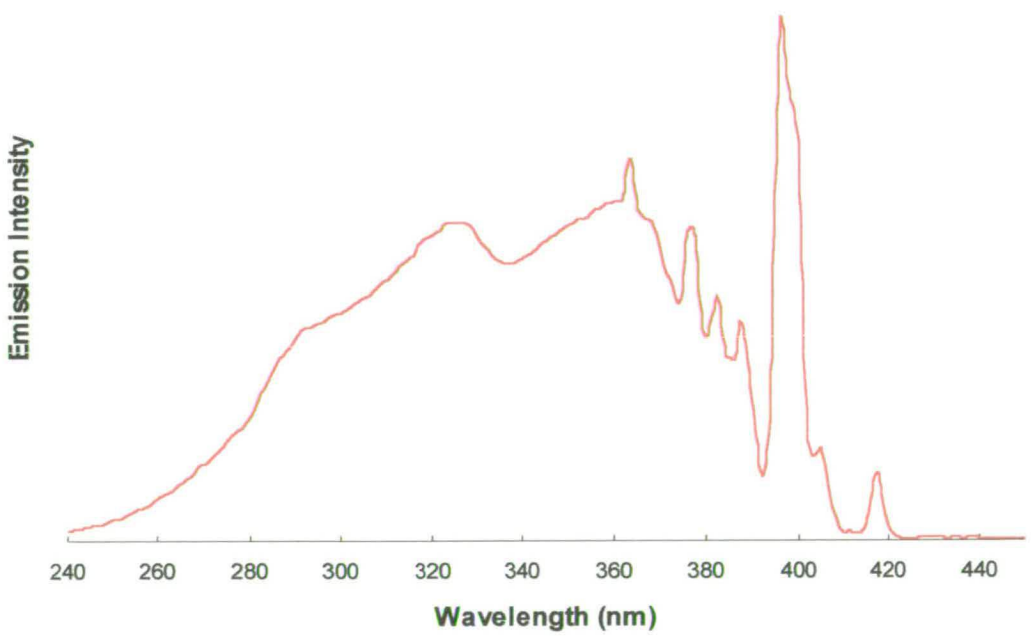

Figure 7-4 Single crystal excitation spectrum, not corrected for lamp response (λem = 616 nm)

The red shifted excitation profile could be attributed to the presence of charge transfer states, however this seems unlikely as such bands are known to quench Eu(III) emission and the solid exhibits a long luminescence lifetime (~ 1.5 ms).

We believe that this new state is arising from π interactions[162] between the closely packed PCA units in the crystal lattice, responsible for ground state interactions enhanced upon irradiation with ultra violet or visible light, leading to new states from which energy transfer to the metal ion then occurs triggering characteristic lanthanide luminescence. When the crystals are washed with water or alcohol the polymeric structure is broken down and the excitation profile reverts back to that of the solution samples. Provisional absorption studies made on KBr disk samples of the single crystal and bulk solids have not detected the presence of any new bands arising from the structural organisation of the PCA units. Spectra exhibit only the UV absorbance around 270 nm attributed to the picolinate residues.

7.4 Further Studies

Initial investigations carried out in the Pikramenou research group[163] into the influence of the counterion on the structural and photophysical properties of the polymeric species formed have revealed some interesting trends relating to the size and charge of the chosen cation.

When the monovalent potassium ion is employed the crystalline one dimensional heterobimetallic coordination polymer obtained is similar to that of the sodium species, exhibiting an analogous red shifted broad excitation profile. This is again attributed to ground state interactions between the closely packed picolinate antennae groups, enhanced upon light excitation allowing new states to form, from which efficient energy transport to the metal centre can occur. In contrast, when $EuCl_3 \bullet 6H_2O$ is combined with PCA in the presence of ammonium hydroxide, the NH_4^+ counterion is not involved in formation of the polymeric structure,[163, 164] and the excitation spectrum exhibits characteristic PCA absorbance around 270 nm. The mechanism by which energy transfer to the metal centre is facilitated clearly differs between these solids prepared in the presence of coordinating and non-coordinating counterions, suggesting that the alkali metals are of importance in influencing the energy transport mechanism within the crystal.

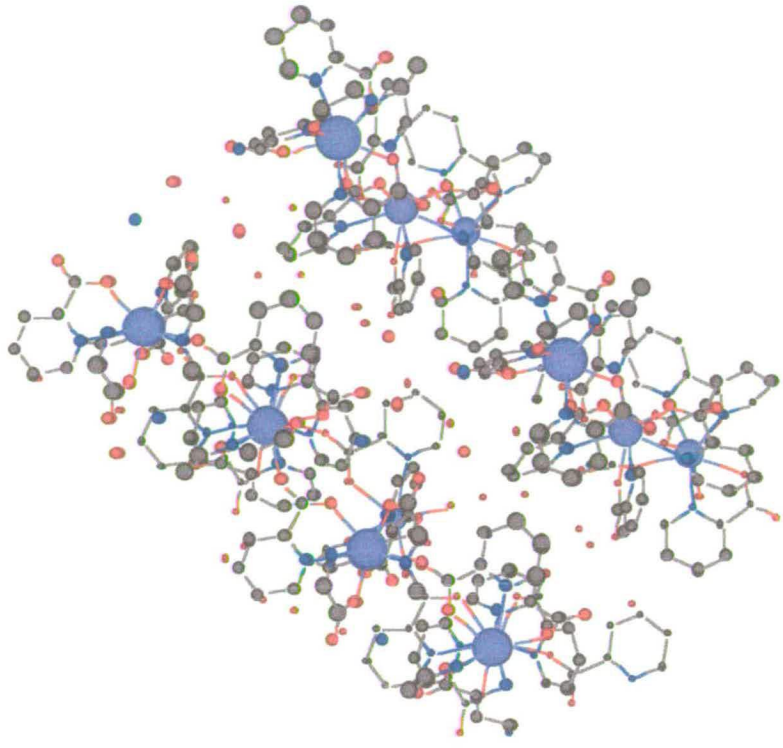

Figure 7-5 Simplified Chem 3D view of polymeric [$EuNH_4(PCA)_4$]

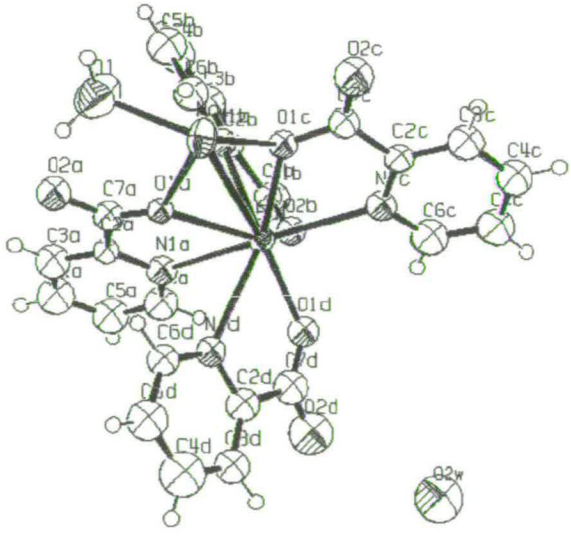

[$EuNa(PCA)4]_n0.5nH_2O$	
Bond	**Length (Å)**
Eu-O1a	2.402
Eu-N1a	2.567
Eu-O1b	2.366
Eu-N1b	2.647
Eu-O1c	2.445
Eu-N1c	2.591
Eu-O1d	2.393
Eu-N1d	2.722

Figure 7-6 Ortep view showing numbered atoms and table with selected bond lengths (Å) for the [$EuNa(PCA)_4$]n$0.5nH_2O$ coordination polymers

Detailed photophysical and structural studies are underway on the coordination solids obtained from trivalent lanthanide cations, the picolinic acid light harvesting ligand and alkali metal (Li, Na, K, and Cs) counterions. The $[Eu(PCA)_4]^-$ crystalline polymer with Ca^{2+} has also been prepared and characterised giving the formulation $[EuCa_{0.5}(PCA)_4 2H_2O]$.[161] In contrast to the linear polymeric chains of the sodium and potassium polymers, the provisional structure of the calcium solid reveals a two dimensional coordination network, with carboxylate oxygen atoms bridging directly between Eu(III) nuclei in one direction, and via the Ca^{2+} counterions in the other. Further photophysical studies are currently underway.

One limiting factor in developing new lanthanide materials has been the inherently weak absorption coefficient of the ions. In solution this has been overcome by designing complexes with light harvesting ligands to act as antennae, populating the emissive states by energy transfer. Such complexes are routinely applied as luminescent sensors in solution (Chapter 1).

Applying the approach commonly adopted in solution, using our simple model light harvesting ligand, picolinic acid (PCA) to overcome the weak absorptivity of the Ln(III) cations, and its characteristic bidentate binding unit to impart control on the coordination environment of the metal centre, it is possible to design structurally organised, highly luminescent solids. It is foreseen that this strategy will allow development of novel luminescent materials with tuneable photophysical properties quite different from the corresponding solution phase species. Microstructural control can be achieved by careful selection of the metal counterion based on its size and charge. The photophysical attributes of the system may also be tailored by choosing suitable light harvesting ligands, analogous to the design now routinely implemented in the solution phase. Moreover, it is possible to modify the macroscopic properties of the coordination complex such that ligands whose absorption band is in the UV can be employed to sensitise Ln(III) luminescence upon excitation in the near UV and visible region.

8 Conclusions and Future Work

We have successfully demonstrated the controlled self-assembly of ternary luminescent lanthanide complexes in aqueous solution, achieved by molecular recognition. The octadentate DTPA-AM_2 ligands are ideal candidate NALs, forming a cavity for LHC binding upon chelation to the trivalent lanthanide cations. A stronger interaction is observed when a more hydrophobic/rigid DTPA-AM_2 ligand is employed, offering a well-defined path by which the LHC can approach the metal centre. Aromatic acid LHCs recognise the LnNAL binding pocket and exhibit a range of sensitising abilities related to their structural and electronic properties.

Several aspects of the molecular recognition observed between the LnNALs and aromatic acid LHC units require further investigation. A detailed investigation into ternary complex formation with naphthyridine carboxylic acids is necessary in order to characterise the species forming in solution.

Computational modelling of the system may provide insight into the steric factors introduced by the amide arms of the DTPA-AM_2 ligand and LHC substituent groups on the binding interaction. Such techniques may also allow prediction of suitable LHC moieties in development and optimisation of specific signalling systems.

It was discovered that molecular recognition is perturbed in the presence of competing hydroxide ligands. NMR relaxivity studies with Gd(III)NAL species are expected to provide better insight into the displacement of water/hydroxide from the inner sphere of the metal upon LHC recognition. Potentiometric studies with the complexes may also allow the local pH at the metal bound water in the neutral chelates to be investigated. It is expected that the EuNALs are better acids than the free Eu^{3+} ion, and that the ninth coordination site is more exposed in the more bulky DTPA-AM_2 chelates. In addition, infra-red spectroscopy may be employed in examination of the isomerisation kinetics, in combination with variable temperature NMR and luminescence studies. An investigation into the formation of ternary complexes with YbNALs by NMR is currently underway in collaboration with the University of Liege.

The effect of ionic strength on the interaction, thus far not considered in any detail, will be further investigated. Signalling systems exhibiting sensitivity to Na^+ and or Cl^- ions are of immense value in the study of biological ion transport channels, often implicated in complex physiological disorders.

The extent to which $\pi-\pi$ interactions influence molecular recognition between the LnNALs and the aromatic acid LHCs will be studied in more detail. We propose to develop the DTPA-AM_2 ligands. Aromatic bis(amide) derivatives incorporating pyrene and anthracene residues exhibiting extended conjugation will be employed. Although not strictly "non-absorbing ligands" the triplet excited states of these chromophores are known to be inappropriately matched for efficient population of the Ln(III) excited state. It is expected that the rigid arms of these ligands will present well-defined binding cavities for LHC recognition. We also expect to observe sensitised emission from non-coordinating aromatic moieties. Two-dimensional NMR (NOESY) will be exploited in the study of the interactions.

Research in the Pikramenou group has shown the mechanism of ternary complex formation to differ considerably when charged LnNAL chelates are employed. We propose further investigation with the more biologically compatible neutral DTPA-AM_2 species, replacing the central NCH_2CO_2H with $NHCH_2OH$. By incorporating non-coordinating residues (alkyl or halide for example) at this position, the influence of both charge and the binding pocket on molecular recognition can be evaluated.

We will also exploit solid-phase and combinatorial methodology in development of asymmetric DTPA-bis(amide) derivatives (see Chapter 4) such that specific bioconjugation may be achieved. Methods for attaching the aromatic LHC to the biomolecule under investigation will also be considered such that targeted labelling will be possible.

In conclusion, a molecular recognition system exhibiting great potential for application in new, homogeneous screening technologies has been developed by adopting a supramolecular approach to lanthanide coordination chemistry in aqueous solution.

9 References

1. Lehn, J. -M. Supramolecular Chemistry, Concepts and Perspectives, VCH, **1995**
2. a) Pietraszkiewicz, M. *Luminescence Probes* in Comprehensive Supramolecular Chemistry, Volume 10, Ch10; 1996, Pergamon, Oxford b) de Silva, A. P.; Fox, D. B; Huxley, A. J.M; Moody, T. S, *Coord. Chem. Rev.* **2000,** *205,* 41-57
3. Diamandis, E. P.; Christopoulos, T. K. *Immunoassay*, Academic Press, San Diego, **1990**
4. Anderson, D. G.; Guo, B.; Xu, Y.; Krika, L. M.; Skogerboe, K. J.; Hage, D. S.; Schoeff, L.; Wang, J.; Cokoll, L. K.; Chang, D. W.; Ward, K. M.; Davis, K. H. *Anal. Chem.* **1997,** *69,* 165R
5. Mogan, C. L.; Newman, D. J.; Price, C. P. *Clin. Chem.*, **1996,** *42,* (2), 193
6. (a) Yalow, R. S.; Berson, S. A. *J. Clin. Invest.* **1959,** *38,* 1996; (b) Yalow, R. S.; Berson, S. A. *J. Clin. Invest.*, **1960,** *39,* 1157
7. (a) Guesdon, J. –L. *J. Histochem. Cytochem.* ***1979,*** *27,* 1131; (b) Brennan, G; Hutchieson, J. S.; Odell, W. D. *Clin. Chem. Winston Salem NC,* **1989,** *35,* 804; (c) Diamandis. E. P.; Chrisopoulos, T. K *Clin. Chem. Winston Salem NC,* **1991,** *37,* 625
8. McDonald, O. B.; Chen, W. J.; Ellis, B.; Hoffan. C.; Overton, L.; Rink, M; Smith, A.; Marshall, C. J.; Wood, E. R. *Anal. Biochem.*, **1999,** *268,* 318
9. Mayer, A.; Neuenhofer, S. *Angew. Chem. Int. Ed. Engl.* **1994,** *33,* 1044
10. Soini, E.; Hemillä, I. *Clin. Chem.* **1979,** *25,* (3), 353
11. Hemillä, I. Applications of Fluorescence in Immunoassays, Wiley, New York, **1991**
12. Sammes, P. G.; Yahoiglie, G. *Nat. Prod. Rep.*, **1996,** *13,* 1
13. Alouani, S; Gaertner, H. F.; Mermod, J. –J.; Power, C. A.; Bacon, K. N.; Wells, T. N. C.; Proudfoot, A. E. I. *Eur. J. Biochem.* **1995,** *227,* 328
14. Coons, A. H.; Creech, H. J.; Jones, R. N. *Proc. R. Soc. Exp. Biol.* (N. Y.) **1941,** *47,* 200
15. Needles, M. C.; Jones, D. G.; Tate, E. H.; Heinkel, G. H.; Kochersperger, L. M.; Dower, W. J.; Barett, R. W.; Gallop, M. A. *Proc. Nat. Acad. Sci. USA* **1993,** *90,* 10700
16. Scott, R. H.; Balasubramanian, S. *Biol. Med. Chem. Let.*, **1997,** *7,* 1567
17. Houston, J. G.; Banks, M. *Current Opinion in Biotechnology,* **1997,** *8,* 734
18. Appel, N. K.; Chung, T. D. Y.; Solly, K.; Chelsky, D. *J. Biomol. Screening,* **1998,** *3,* 19
19. (a) Gould, B. J.; Marks, V. *Non Isotopic Immunoassay,* (Ed. T. T. Ngo), Plenum, New York, **1988,** pp3-26; (b) Engvall, E.; Pearlmann, P. *J. Immunol. Methods,* **1971,** *8,* 871; (c) Engvall. E; Pearlmann, P. *J. Immunol. Methods,* **1971,** *10,* 161 (and references cited in 9)
20. General background in FP assay given at http://www.panvera.com
21. Bunzli, J. –C. G. in *Lanthanide Probes in Life, Chemical and Earth Sciences,* Chapter 7. Eds. Bunzli, J. –C. G.; Choppin, G. R. Elsevier, Amsterdam, **1989**
22. Parker, D.; Williams, J. A. G. *J. Chem. Soc. Dalton Trans.*, **1996,** 3613
23. Richardson, F. S. *Chem. Rev.* **1982,** 541
24. Choppin, G. R.; Peterman, D. R. *Coord. Chem. Rev.* **1999,** *185-186,*283

25. Sabbatini, N.; Guardigli, M.; Lehn, J. –M. *Coord. Chem. Rev.* **1993**, *123*,201;
26. de Silva, A. P.; Fox, D. B.; Huxley, A. J. M.; McClenaghan, N. D.; Rioron, J. *Coord. Chem. Rev.* **1999**, *185-186*,297
27. Dickins, R. S.; Gunnlaugsson, T.; Parker, D.; Peacock, R. D.; *J. Chem. Soc., Chem. Commun.*, **1998**, 1643
28. (a) Parker, D.; Senanayake, P.K.; Williams, J. A. G.; *J. Chem. Soc. Perkin Trans. 2*, **1998**, 2129; (b) Kessler, M. A. *Anal. Chem.*, **1999**, *71*, 1540; (c) Mortellaro, M. A.; Nocera, D. G. *J. Am. Chem. Soc.*, **1996**, *118*, 7417
29. Elbanowski, M.; Mąkowska, B. *J. Photochem. Photobiol. A: Chemistry*, **1996**, 99, 85
30. Hemmilä, I. *J. Alloys and Cpds.*, **1995**, 225, 480
31. (a) Condrau, M. A.; Schwendener, R. A.; Niederer, P.; Anikler, M. *Cytometry*, **1994**, *16*, 187; (b) Condrau, M. A.; Schwendener, R. A.; Zimmerman, M.; Muser, M. H.; Graf, U.; Niederer, P.; Anikler, M. *Cytometry*, **1994**, *16*, 195
32. (a) Marriott, G.; Heidecker, M.; Diamandis, E. P.; Yan-Marriott, Y. *Biophys. J.* **1994**, *67*, 957; (b) Phimphivong, S.; Kölchens, S.; Edminson, P. L.; Saavedra, S. S. *Anal. Chim. Acta*, **1995**, *307*, 403; (c) Delaina, E.; Barbin-Arbogast, A.; Bourgeoise, C. A.; Mathis, G.; Mory, C.; Favard, C.; Vigny, P.; Nivelaue, N. *J. Trace Microprobe Tech.* **1995**, *13*, (3), 371
33. Allen, C.; Chen, Y. –H.; Chen, H. Y.; Shieh, F. –K. *J. Chem. Soc. Dalton Trans.*, **1998**, 3243;
34. Kim, M. J.; Patton, W. F.; Lopez, M. F.; Spofford, K. H.; Shojaee. N.; Shepro, D. *Anal. Biochem.* **1997**, *245*, 184
35. Supkowski, R. M.; Bolender, J. P.; Smith, W. D.; Reynolds, L. E. L.; Horrocks, W. DeW. Jr. *Coord. Chem. Rev.* **1999**, *185-186*, 307
36. Horrocks, W. DeW. Jr.; Sudnick, D. R. *Acc. Chem. Res.* **1981**, *14*, 384
37. Bunzli, J. -C. G.; Pfefferié, J. –M. *Helv. Chim. Acta*, **1994**, *77*, 323
38. Frey, M. W.; Frey, S. T.; Horrocks, W. DeW. Jr.; Kaboord, B. F.; Benkovic, S. J. *Chem. Biol.* **1995**, *3*, (5), 393
39. Horrocks, W. DeW. Jr.; Arkle, V. K.; Liotta, F.; Sudnick, D. R. *J. Am. Chem. Soc.*, **1983**, *105*, 3455
40. Bryden, C. C.; Reilley, C. N. *Anal. Chem.*,**1982**, *54*, 610
41. Tissue, B. M. and Bihari, B. *J. Fluoresc*, **1998**, *8*, (4), 289
42. Aime, S.; Botta, M, Fasano, M.; Terreno, E. *Chem. Soc. Rev.*, **1998**, *27*, 19
43. Cotton, F. A.; Wilkinson, G. *Advanced Inorganic Chemistry*, Wiley, New York
44. Horrocks, W. DeW. Jr.; Sudnick, D. R. *J. Am. Chem. Soc.*, **1979**, *101*, 334
45. Beeby, A.; Clarkson, I. M.; Dickins, R. S.; Faulkner, S.; Parker, D.; Royle, L.; de Sousa, A. S.; Williams, J. A. G.; Woods, M. *J. Chem. Soc., Perkin Trans.*, **1999**, 493; Supkowski, R. M.; Horrocks, W. DeW. Jr. *Inorg. Chem*, **1999**, *38*, (24), 5619
46. Kropp, J. L.; Windsor, M. W. *J. Chem. Phys*, **1963**, *39*, 2769

47. Haas, Y.; Stein, G. *J. Phys. Chem.*, **1972**, *106*, 103
48. Gallacher, P. K., *J. Chem. Phys*, **1964**, *41*, (10), 3061
49. Weissman, S. I. *J. Chem. Phys.* **1942**, *10*, 214
50. Alpha, B.; Balardini, R.; Balzani, V.; Lehn, J. –M.; Perathoner, S.; Sabbatini, N. *Photochem. Photobiol.*, **1990**, *52*,(2), 299
51. Balzani, V.; Ballardini, R. *Photochem. And Photobiol.* **1990**, *52*, 409
52. Pearson, J, *J. Am. Chem. Soc.*, **1963**, *84*, 3533
53. Limaye, S. N.; Saxena, M. C. *Can. J. Chem.*, **1986**, *64*, 865
54. Mathis, G. *Clin. Chem.* **1993**, *39*, 1953
55. Yuan, J; Matsumoto, K. *Anal. Chem.* **1998**, *70*, 596
56. Hnatourich, D. J.; Layne, W. W.; Childs, R L.; Davis, A. M. *Science*, **1983**, *220*, 613
57. Arano, Y.; Uezono, T.; Akizawa, H.; Ono, M.; Wakisaka, K.; Nakayama, M.; Sakahara, H.; Konishi, J.; Yokoyama, A. *J. Med. Chem.*, **1996**, *39*, 3451
58. Gries, H.; Mikautz, H. *Physiol. Chem.Phys. Med. NMR*, **1984**, 16, 105
59. Diamandis E. P.; Christopoulos, T. K. *Anal. Chem.* **1990**, *62*, 1449A
60. H. Karşilayan; Hemmilä, I.; Takalo, H.; Toivonen, A.; Petterson, K. *Bioconjugate Chem*, **1997**, *8*, 71
61. Chen, J.; Selvin, P. R. *Bioconjugate Chem.*, **1999**, *10*, 311
62. Takalo, H.; Mukkala, V. –M.; Mikola, H.; Liiti, P.; Hemmilä, I. *Bioconjugate Chem.*, **1994**, *5*, 278
63. Meltola, N.; Juaria, P.; Saviranta, P.; Mikola, H. *Bioconjugate Chem.* **1999**, *10*, 325
64. Diamandis, E. P. *Analyst*, **1992**, *117*, 1879
65. Diamandis E. P.; Christopoulos, T. K. *Anal. Chem.* **1992**, *64*, 342
66. Canfi, A.; Bailey, M. P.; Rocks, B. F. *Analyst*, **1989**, *114*,1405
67. Saavedra, S. S.; Picozza, E. G. *Analyst*, **1989**, *114*, 835 Siepak, J. *Analyst*, **1989**, *114*,529
68. Bailey, M. P.; Rocks, B. F.; Riley, C. *Analyst*, **1985**, *110*, 603
69. M. P. Bailey; B. F. Rocks and C. Riley, *Analyst*, **1984**, *109*, 1449
70. Wallac-Oy, Eur Pat.; Patent No: 0 103 558
71. Soini, E.; Hemmilä, I. US Patent No 4,374,120, **1983**
72. Soini, E.; Hemmilä, I.; Lövgren, T. European Patent Application No 83850244.1, **1983**. Baxter Travenol Labs, International Publication Number WO 87/07955, **1987**
73. (a) Deary, C. M.; Dysan, R. M.; Hambley, T. W.; Lawreance, M.; Maeder, M.; Tannock, G. A. *Aust. J. Chem.* **1993**, *46*, 577 (b) de Sá, G. F.; de Silva, F. R. G.; Malta, O. L.; *J. Alloys and Compounds*, **1993**, *196*, 17
74. Ingles, J.; Samama, P.; Patel, S.; Burbaum, J.; Stroke, H. L.; Appell, K. C. *Biochemistry*, **1998**, *37*, 2372
75. Diamandis E. P.; Christopoulos, T. K. *Anal. Chem.* **1990**, *62*, 1449A
76. Oser, A.; Valet, G. *Angew. Chem. Int. Ed. Engl.*,**1990**, *29*, (10), 1167

77. Lim, M. J.; Patton, W. F.; Lopez, M. F.; Spofford, K. H.; Shojaww. N.; Shepro, D. *Anal. Biochem.*, **1997,** *245,* 184

78. Diamandis, E. P. *Electophoresis,* **1993,** *14,* 866

79. Geyer, C. R.; Sen, D. *J. Mol. Biol.*, **1998,** *275,* 483

80. Saha, A. K.; Kross, K.; Kloszewaki, E. D.; Upson, D. U.; Toner, J. L.; Snow, R. A.; Black, C. D. V.; Desai, V. C. *J. Am. Chem. Soc.*, **1993,** *115,* 11032

81. S. Sueda; Ihara, T.; Juskowiak, B.; Takagi, M. *Anal. Chim. Acta,* **1998,** *365,* 27

82. Klakamp, S. L.; Horrocks, W.DeW. Jr. *J. Inorg. Biochem.*, **1992,** *46,* 175 & 193

83. Ci, Y. –X.; Li, Y. –Z.; Chang, W. –B. *Anal. Chim. Acta,* **1991,** *248,* 589

84. Förster, T. *Ann Phys*, **1948,** *2,* 55

85. Bolger, R. *DDT,* **1999,** *4,* 251

86. Grepin, C.; Pernelle, C. *DDT,* **2000,** *5,* 212

87. Upham, L. V. *LRA,* **1999,** *11,* 324

88. Swartzman, E. E.; Miraglia, S. J.; Mellentin-Michelotti, J.; Evangelista, L.; Yuan, P. –M. *Anal. Biochem.*, **1999,** *271,* 143

89. Seifert, M.; Haindl, S.; Hock, B. *Anal. Chim. Acta,* **1999,** *386,* 191

90. Gremlich, H. U. *Biotech. Bioeng.* **1999,** *61,* 179

91. Merrifield, R. B., *J. Am. Chem. Soc.*, **1963,** *85,* 2149

92. Hijfte, L. V.; Marciniak, G.; Froloff, N. *J. Chormatogr. B,* **1999,** *725,* 3

93. Hann, M.; B. Hudson; Lewell, X; Lifely, R.; Miller, L; Ramsden, N. *J. Chem. Inf. Comput. Sci.*, **1999,** *39,* 897

94. Flower, D. R. *J. Chem. Inf. Comput. Sci.*, **1998,** 38, 379

95. Packer, M. J.; Hunter, C. A, *J. Am. Chem. Soc.*, **2001,** *123,* 7399

96. Andres, C. J.; Swann, R. T.; Severino, J.; Young, K. G.; Edinger, K.; Monillo, J.; Deshpande, M. S. *Biotech. Bioeng.* **1998,** *61*, 93

97. Gayo, L. M. *Biotech. Bioeng.* **1998,** *61,* 95

98. Newsam, J. M.; Schüth, F. *Biotech. Bioeng.* **1999,** *61*, 201

99. Brouwer, A. J.; van der Linden, H. J.; Liskamp, R. M. *J. Org. Chem.*, **2000,** *65,* 1750

100. Gennari, C.; Ceccarelli, S.; Piarulli, U.; Montalbetti, C. A. G. N.; Jackson, R. F. W. *J. Org. Chem.*, **1998,** *63,* 5312

101. Sui, H.; Yeung, E. S. *J. Am. Chem. Soc.*, **2000,** *122,* 7422

102. Xiang, X. –D. *Chem. Ind.*, **1998,** 800

103. Shaughnessy, K. H.; Kin, P.; Hartwig, J. F. *J. Am. Chem. Soc.*, **1999,** *121,* 2123

104. Blassé, G. Grabmaier, B. C. *Luminescent Materials,* Springer Verlag, Berlin, 1994

105. Newkome, G. R.; Childs, B. J.; Rourk, M. J.; Baker, G. R.; Moorefield, C. N. *Biotech. Bioeng.*, **1999,** *61,* (4), 244 (and several other papers in same issue of journal)

106. (a) de Sá, G. F.; de Silva, F. R. G.; Malta, O. L. *J. Alloys and Cpds.* **1993,** *196,* 17 (b) de Sá, G. F.; Nunes, L. H. A.; Wang, Z. –M.; Choppin, G. R. *J. Alloys and Cpds.* **1994,** *207/208,* 457

107.Coates, J.; Sammes, P. G.; West, R. M.; *J. Chem. Soc. Perkin Trans. 2,* **1996,** 1275 and 1283; Coates, J. Sammes, P. G.; Yahioglu, G.; West, R. M.; Gaman, A. J. *J. Chem. Soc. Chem. Commun.,* **1995,** 1107

108.Letkeman, P.; Martell, A. R. *Inorg. Chem.,* **1979,** *18,* 1284

109.Rizkalla, E. N.; Sullivan, J. C.; Choppin, G. R. *Inorg. Chem.,* **1989,** *28,* 909

110.Laurenczy, G.; Radics, R. Brücher, E. *Inorg. Chim. Acta,* **1983,** *75,* 219

111.Chang, C. A.; Brittain, H. G.; Telser, J.; Tweedle, M. F. *Inorg. Chem.,* **1990,** *29,* 4468

112.Alsaadi, B. M.; Rossotti, F. J. C.; Williams, R. J. P. *J. Chem. Soc. Dalton Trans.* **1980,** 2151

113.Stezowski, J. J.; Hoard, J. L. *Isr. J. Chem.,* **1984,** *24,* 323

114.Lis, S.; Konarski, J.; Hnatejko, Z. Elbanowski, M. *J. Photochem. Photobiol. A: Chem.,* **1994,** *79,* 25

115.Cacheris, W. P.; Nickle, K. S.; Sherry, A. D. *Inorg. Chem.,* **1987,** *26,* 958

116.Wu, S. L.; Johnson, K. A.; Horrocks, W. DeW. Jr. *Inorg. Chem.,* **1997,** *36,* 1884

117.Konings, M. S.; Dow, W. C.; Love, D. B.; Raymond, K. N.; Quay, S. C.; Rocklage, S. M. *Inorg. Chem.,* **1990,** *29,* 1488

118.Quay, S. C. US Patent, No 4 687 659, **1987**

119.Geraldes, C. F. G. C.; Urbano, A. M.; Alpoim, M. C.; Sherry, A. D.; Kuan, K. –T; Rajagopalan, R.; Maton, F.; Muller, R. N. *Magnetic Resonance Imaging,* **1995,** *13,* 401

120.Bligh, S. W. A.; Chowdhury, A. H. M. S.; McPartlin, M.; Scowen, I. J. *Polyhedron,* **1995,** *14,*(4), 567

121.Geraldes, C. F. G. C.; Urbano, A. M.; Alpoim, M. C.; Hoefnagel, M. A.; Peters, J. A. *J. Chem. Soc., Chem. Commun.* , **1991,** 656

122.Wang, Y. –M.; Lin, S. –T.; Wang, Y. –J.; Sheu, R. -S. *Polyhedron,* **1998,** *17,* (11-12), 2021

123.Wang, Y. –M.; Cheng, T. –H.; Lui., G. –C.; Sheu, R. –S. *J. Chem. Soc. Dalton Trans.,* **1997,** 833

124.White, D. H.; deLearie, L. A.; Dunn. T. J.; Rizkalla, E. N.; Imura, H.; Choppin, G. R. *Investigative Radiology,* **1991,** *26,* S229

125.Parker, D.; Pulukkody, K.; Smith, F. C.; Batsanov, A.; Howard, J. A. K. *J. Chem. Soc. Dalton Trans.,* **1994,** *689*

126.Ehnebom, L.; Pedersen, B. F. *Acta Chem. Scand.,* **1992,** *46,* 126

127.Aime, S.; Botta, M.; Fausano, M.; Paoletti, S.; Anelli, P. L. *Inorg Chem.,* **1994,** *33,* 4707

128.Rizkalla, E. N.; Choppin, G. R. *Inorg. Chem.,* **1993,** *32,* 582

129.da Silva, A. P., *Angew. Chem. Int. Ed. Engl.* **1996,** *35,* 2116; *J. Chem. Soc. Chem. Commun.,* **1997,** 1891

130.Lammers, H.; Maton, F.; Pubanz, D.; van Lauren, M. W.; van Bekkum, H.; Merbacj, A. E.; Muller, R. N.; Peters, J. A. *Inorg. Chem.,* **1997,** *36,* 2527

131.Wu, S. L.; Horrocks, W. DeW. Jr. *J. Chem. Soc. Dalton Trans.,* **1997,** 1497

132.Carvalho, R. A.; Peters, J. A.; Geraldes, C. F. G. C. *Inorg. Chim. Acta,* **1997,** *262,* 167

133.C. F. G. C.; Delgado, R.; Urbano, A. M.; Costa, J.; Jasanda, F.; Nepveu, F. *J. Chem. Soc. Dalton Trans.* **1995,** 327

134.Geraldes, C. F. G. C.; Urbano, A. M.; Hoefnagel, M. A.; Peters, J. A. *Inorg. Chem.,* **1993,** *32,* 2426

135.Geze, C.; Mouro, C.; Hindre, F.; Le Plouzennec, M.; Moinet, C.; Rolland, R.; Alderighi, L.; Vacca, A. Simmoneaux, G. *Bull. Chim. Soc. Fr.* **1996,** *133,* 401

136.Franklyn, S. J.; Raymond, K. *Inorg. Chem.* **1994,** *33,* 5794

137.Geogopoulou, A. S.; Ulvenund, S.; Mingos, M. P.; Baxter, I.; Williams, J. D. *J. Chem. Soc. Dalton Trans.* **1999,** 547

138.Xiao, M.; Selvin, P. R. *J. Am. Chem. Soc.,* **2001,** *123,* 7067

139.Selvin, P. R.; Rana, T. M.; Hearst, J. E. *J Am. Chem. Soc.,* **1994,** *116,* 6029

140.Selvin, P. R.; Jancarik, J.; Li, M. Hung, L. –W. *Inorg. Chem.,* **1996,** *35,* 700

141.Spaulding, L; Brittain, H. G. *Inorg. Chem.,* **1983,** *82,* 3486

142.Selvin, P. R.; Hearst, J. E. *Proc. Nat. Acad. Sci. USA,* **1994,** *91,* 10024

143.Li, M.; Selvin, P. R. *J. Am. Chem. Soc.,* **1995,** *117,* 8132

144.Hoshino, H.; Utsumi, S. –Y.; Yosuyangi, T. *Talanta,* **1994,** *41,* (1), 93

145.Chen, J.; Selvin, P. R. *J. Am. Chem. Soc.,* **2000,** *122,* 657

146.Geigy, J. R. A. –G. Fr Patent 1 548 888 (Cl. C 07d), 1968; *Chem. Abstr.* **1969,** *71,* 81380q

147.Brittain, H. G. *Inorg Chem.,* **1978,** *17,* 2762; Choppin, G. R.; Bertrand, P. A.; Hasegawa, Y.; Rizkalla, N., *Inorg., Chem.,* **1982,** *21,* 3722

148.Lange's Handbook of Chemistry, 13th ed., Ed. Dean, J. A.

149.General technical information and collection of references given in Argonaut Technologies Resins and Reagents 2000 catalogue

150.Rebek, J.; Brown, D.; Zimmerman, S. *J. Am. Chem. Soc.,* **1975,** *97,* 4401; Kaldor, S. W.; Fritz, J. E.; Tang, J.; McKenney, E. R. *Bioorg. Med. Chem. Lett.* **1976,** *6,* 3041; Kaldor, S. W.; Fritz, J. E.; Seigel, M. G.; Dressman, B. A.; Hahn, P. J. *Tetrahedron Lett.,* **1996,** *37,* 7193; Booth, J. R. Hodges, J. C. *J. Am. Chem. Soc.,* **1997,** *119,* 4882

151.Lanter, C. L.; Guiles, J. W.; Rivero, R. A. *Mol. Diversity,* **1999,** *4,* 149

152.Chang, A. C.; Brittain, H. G.; Telser, J.; Tweedle, M. F.; *Inorg. Chem.,* **1990,** *29,* 4468

153.Magennis, S. W.; Parsons, S; Corval, A.; Woolins, D. J., Pikramenou, Z. *J. Chem. Soc., Chem. Commun.,* **1999,** 61

154.Pikramenou, Z.; Yu, J. –A.; Lessard, R. B.; Ponce, A.; Wong, P. A.; Nocera, D. G., *Coord. Chem. Rev.,* **1994,** *132,* 181

155.Abu-Saleh, A.; Mears, C. F. *Photochem. Photobiol.* **1984,** *39,* 736

156.Tóth, E.; Burai, L.; Brücher, E.; Merbach, A. E. *J. Chem. Soc., Dalton Trans.,* **1997,** 1587

157.Sheldrick, G. M.; SHELXL-97, Siemens Analytical X-ray, **1995**

158. Haas, Y.; Stein, G. *J. Phys. Chem.* **1971,** *75,* 3668

159. Braga, D.; Orpen, A. G. Eds. NATO Advanced Institute Studies Series; Kluwer: Dordecht, The Netherlands, **1999**; E. J. Cussen

160. Meysammy, H.; Riwotzki, K.; Kornowki, A.; Naused, S.; Hasse, M. *Adv. Mater.* **1999,** *11,* 840; Tissue, B. M.; *Chem. Mater.,* **1998,** *10,* 2387

161. Rosseinsky, M. J.; Battle, P. D.; Burley, J. C.; Spring, L. E.; Vente, S. J.; Coldea, A. I.; Singleton, J., *J. Am. Chem. Soc.,* **2001,** *123,* 1111; Denning, R. J., *J. Mater. Chem.,* **2001,** *11,* 19; Bruce, D. W.; *Acc. Chem. Res.,* **2000,** *33,* 831

162. Energy hopping preceding energy transfer has been previously demonstrated: Jullien, L.; Canciell, J.; Valeur, B.; Berdez, E.; Lefèvre, J. P.; Lehn, J. –M.; Artzner, V. M.; Pansu, R., *J. Am. Chem. Soc.,* **1996,** *118,* 5432

163. Philps, L. (B. Sc. Honours Project, University of Edinburgh, 2000)

164. Starynowicz, P., *Acta Crystallogr., Sect. C (Cr. Str. Comm.)* ***1993, 49,*** 1895; Starynowicz, P., *Acta Crystallogr., Sect. C (Cr. Str. Comm.)* ***1991, 47,*** 294

Appendix 1

LC/MS Analytical Methods

Mass Spectrometer	Micromass series II MS
ELSD	Sedere Sedex 55, 40°C,
Temp	40°C
Gas Flow	2.2 bar N_2
LC/Auto injector	HP1100
Column	3.3 cm x 4.6 mm ID (3 µm particle size) ABZ+PLUS
Flow Rate	3 ml/min
Injection Volume	5 µL
Temp	RT
UV Detection Range	215 – 330 nm
Solvents	A: 0.1% Formic Acid + 10 mM Ammonium Acetate
	B: 95% Acetonitrile + 0.05% Formic Acid

Gradient	Time (mins)	A %	B %
	0.00	100	0
	0.70	100	0
	4.20	0	100
	5.30	0	100
	5.50	100	0

Floinject ES/MS

Mass Spectrometer	Micromass LCTOF
	Electrospray + ve only (Z spray source)
LC/Auto injector	HP1100 + Gilson 233xl Autoinjector
ELSD	Polymer Labs PL-ELS 1000
Temp	55°C
Gas Flow	2.2 bar N_2
Flow Rate	1 ml/min
Injection Volume	5 µL
Temp	RT
Isocratic run	30 % A, 70 % B
Solvents	A: 0.1% Formic Acid + 10 mM Ammonium Acetate
	B: 95% Acetonitrile + 0.05 % Formic Acid

Reg No	Smiles String	Formula	MW
GR207962X	COc1cc(ccc1C)C(=O)O	C9H10O3	166.18
GR212454X	COc1cc(cc(OC)c1C)C(=O)O	C10H12O4	196.21
CCI21177	COc1cc(OC)cc(c1)C(=O)O	C9H10O4	182.18
GR257381X	COc1cc(C)c(OC)c(C)c1C(=O)O	C11H14O4	210.23
AH6621	OC(=O)c1cc(O)cc(c1)C(=O)O	C8H6O5	182.13
GR193563X	COC(=O)c1cc(OC)cc(c1)C(=O)O	C10H10O5	210.19
GF267447X	COc1cc(C#N)ccc1C(=O)O	C9H7NO3	177.16
GW431055X	COc1cc(ccc1C#N)C(=O)O	C9H7NO3	177.16
GR257410X	COC(=O)Oc1ccccc1C(=O)O	C9H8O5	196.16
GW503358X	COc1ccccc1COC(=O)c2ccccc2C(=O)O	C16H14O5	286.29
GW318421X	COc1cc(SC)ccc1C(=O)O	C9H10O3S	198.24
GR50343X	OC(=O)c1ccccc1OP(=O)(O)O	C7H7O6P	218.10
AH14879XX	OC(=O)c1cccc(OCc2ccccc2)c1	C14H12O3	228.25
GR235591X	OC(=O)c1ccc(N(=O)=O)c(OCc2ccccc2)c1	C14H11NO5	273.25
AH3827	CC(=O)c1ccc(OCc2ccccc2)c(c1)C(=O)O	C16H14O4	270.29
GF267697X	OC(=O)c1ccc(COc2cccc(O)c2C=O)cc1	C15H12O5	272.26
GR32114X	OC(=O)c1ccc(OCc2ccccc2)cc1O	C14H12O4	244.25
AH14579XX	OC(=O)c1ccc(N=Cc2cccs2)cc1	C12H9NO2S	231.28
GW288607X	COc1ccc(N=Cc2ccc(cc2)C(=O)O)cc1OC	C16H15NO4	285.30
CCI23883	CNC(=O)Oc1ccc(cc1)C(=O)O	C9H9NO4	195.18
GR30858X	CNC(=O)Oc1ccc(cc1OC(=O)NC)C(=O)O	C11H12N2O6	268.23
CCI3965	COc1cc(N)c(cc1OC)C(=O)O	C9H11NO4	197.19
GI207347X	COc1cc(C(=O)O)c(cc1OC)N(=O)=O	C9H9NO6	227.18
GR38987X	COc1ccc(C(=O)O)c(Br)c1OC	C9H9BrO4	261.07
CCI3923A	O.[Na+].Nc1ccc(C(=O)[O-])c(O)c1	C7H6NO3-.Na+.2.0(H2O)	211.15
GR38954X	COc1cc(N)c(cc1C)C(=O)O	C9H11NO3	181.19
GR251016X	Nc1c(Br)c(O)c(cc1C#N)C(=O)O	C8H5BrN2O3	257.05
AH14993XX	OC(=O)c1ccc(OCCOCCOc2ccc(cc2)C(=O)O)cc1	C18H18O7	346.34
AH14994XX	OC(=O)c1ccc(OCCOc2ccc(cc2)C(=O)O)cc1	C16H14O6	302.29

Reg No	Smiles String	Formula	MW
GR84408X	OC(=O)c1ccc(OCCOc2ccccc2)cc1	C15H14O4	258.28
AH25091X	OC(=O)c1ccc(OCC=C)cc1	C10H10O3	178.19
GR64693X	CCCc1ccccc1OCCOc2ccc(cc2)C(=O)O	C18H20O4	300.36
AH16584XX	OC(=O)c1ccc(Oc2cccc(OCC#C)c2)cc1	C16H12O4	268.27
GR76119A	Cl.CN(C)CC#CCOc1ccc(cc1)C(=O)O	C13H15NO3. HCl	269.73
GI224436X	OC(=O)c1ccc(OC(F)(F)F)cc1	C8H5F3O3	206.12
GR34543	COc1ccc(cc1)C(=O)O	C8H8O3	152.15
GR40314	COc1ccc(C(=O)O)c2ccccc12	C12H10O3	202.21
GR62892	COc1cccc2ccc(cc12)C(=O)O	C12H10O3	202.21
GF133808X	CCOC(=O)Oc1c(OC)cc(cc1OC)C(=O)O	C12H14O7	270.24
GR253989X	COC(=O)Oc1cc(OC)c(C(=O)O)c(c1)C(=O)OC	C12H12O8	284.23
GR215101X	CCOC(=O)c1c(OC)c(O)c(OC)cc1C(=O)O	C12H14O7	270.24
GW322044X	OC(=O)c1cc(Br)c2OCOCc2c1	C9H7BrO4	259.06
GR148285X	CC(=O)Oc1c(Cl)cc(cc1Cl)C(=O)O	C9H6Cl2O4	249.05
GR81142X	CC(=O)Oc1cc(cc(Cl)c1OC(=O)C)C(=O)O	C11H9ClO6	272.64
GR63007X	CCCc1c(Cl)c(OC)c(Cl)c(O)c1C(=O)O	C11H12Cl2O4	279.12
GW423740X	CC(=CCc1cc(ccc1OC(=O)C)C(=O)O)C	C14H16O4	248.28
AH14732XX	COc1ccc(Oc2cc(ccc2C(=O)O)C(=O)O)cc1	C15H12O6	288.26
GW291819X	Cc1ccc(Oc2cc(ccc2C(=O)O)C(=O)O)cc1	C15H12O5	272.26
AH15398XX	COc1ccc(Oc2cc(C(=O)O)c(Br)cc2C(=O)O)cc1	C15H11BrO6	367.16
GW314444X	CSc1ccc(Oc2cc(ccc2C(=O)O)C(=O)O)cc1	C15H12O5S	304.32
GW385245X	NC(=O)c1ccc(cc1Oc2ccc(C=O)cc2)C(=O)O	C15H11NO5	285.26
AH15251XX	OC(=O)c1ccc2Oc3ccccc3Oc2c1	C13H8O4	228.21
AH4591	OC(=O)c1ccccc1Oc2ccccc2	C13H10O3	214.22
AH8259	OC(=O)c1ccc(Oc2ccc(cc2)C(=O)O)cc1	C14H10O5	258.23
GR34041X	OC(=O)c1cccc(Oc2ccccc2)c1	C13H10O3	214.22
GR261706X	COC(=O)c1cc(ccc1Oc2ccc(OC)cc2)N(=O)=O.COc1ccc(Oc2ccc(cc2C(=O)O)N(=O)=O)cc1	C15H13NO6/C14H11NO6	592.52
GR265013X	OC(=O)c1ccc(Cl)cc1Oc2ccc(C#N)cc2	C14H8ClNO3	273.68
GR49081X	Nc1cc(cc(N)c1Oc2ccccc2)C(=O)O	C13H12N2O3	244.25

Reg No	Smiles String	Formula	MW
GW339416X	CC(=O)Nc1ccc(Oc2ccc(cc2)C(=O)O)cc1	C15H13NO4	271.28
GW404922A	Cl.NC(=N)Nc1ccc(Oc2ccc(cc2)C(=O)O)cc1	C14H13N3O3. HCl	307.74
GW409763X	NC(=S)Nc1ccc(Oc2cccc(c2)C(=O)O)cc1	C14H12N2O3S	288.33
AH11164	OC(=O)c1ccc(Cl)c(Cl)c1	C7H4Cl2O2	191.02
GR214770X	OC(=O)c1ccc(F)cc1Cl	C7H4ClFO2	174.56
CCI5134	OC(=O)c1cc(Cl)c(Oc2ccc(O)cc2)c(Cl)c1	C13H8Cl2O4	299.11
GI149795A	O.OC(=O)c1ccc(O)c(Cl)c1	C7H5ClO3. 0.5(H2O)	181.58
GR38988X	OC(=O)c1ccc(O)c(O)c1Cl	C7H5ClO4	188.57
GR39182X	COc1ccc(Cl)cc1C(=O)O	C8H7ClO3	186.60
GW328037X	OC(=O)c1cc(Cl)cc(S)c1O	C7H5ClO3S	204.63
AH9074	OC(=O)c1cc(Br)cc(Br)c1	C7H4Br2O2	279.92
GI160046X	OC(=O)c1cc(Br)ccc1O	C7H5BrO3	217.02
GF253708X	OC(=O)c1cc(Br)ccc1Cl	C7H4BrClO2	235.47
GW328038X	OC(=O)c1cc(Br)cc(S)c1O	C7H5BrO3S	249.08
AH11410	COCc1ccccc1C(=O)O	C9H10O3	166.18
GI166356X	COC(=O)c1ccc(cc1)C(=O)O	C9H8O4	180.16
AH5737	OC(=O)c1cccc(C=O)c1	C8H6O3	150.14
GR239060X	COC(=O)c1cccc(c1)C(=O)O	C9H8O4	180.16
CCI1659	OC(=O)c1ccc(C#C)cc1	C9H6O2	146.15
GR156438X	OC(=O)c1ccc(CS)cc1	C8H8O2S	168.22
GR58626X	OC(=O)c1ccc(C=CN(=O)=O)cc1	C9H7NO4	193.16
GR87165X	OC(=O)c1ccc(C=C)cc1	C9H8O2	148.16
AH18307XX	OC(=O)c1cc(ccc1C(F)(F)F)C(F)(F)F	C9H4F6O2	258.12
GF234517X	OC(=O)c1ccc(cc1F)C(F)(F)F	C8H4F4O2	208.11
GF233960X	OC(=O)c1c(F)cccc1F	C7H4F2O2	158.11
GI220410A	O.OC(=O)c1c(F)c(F)c(O)c(F)c1F	C7H2F4O3. H2O	228.10
GR101348X	OC(=O)c1cc(F)ccc1Br	C7H4BrFO2	219.01
AH14771AA	OC(=O)c1ccc(cc1)c2ccc(C#C)cc2	C15H10O2	222.25
GF241458X	OC(=O)c1ccccc1c2ccccc2C(=O)O	C14H10O4	242.23

Reg No	Smiles String	Formula	MW
GR71072X	OC(=O)c1ccc(cc1)c2ccc(cc2)N(=O)=O	C13H9NO4	243.22
GR93262X	OC(=O)c1ccccc1c2ccc(cc2)N(=O)=O	C13H9NO4	243.22
GW315267X	OC(=O)c1ccc-2c(c1)C(=O)C(=O)c3ccccc32	C15H8O4	252.23
GR59449X	COc1ccc(cc1c2ccccc2)C(=O)O	C14H12O3	228.25
GR59450X	CCOc1ccc(cc1C(=O)O)c2ccccc2	C15H14O3	242.28
CCI17440	OC(=O)c1cc(O)c2ccccc2c1O	C11H8O4	204.18
GR68891	OC(=O)c1cc2cccc(O)c2cc1O	C11H8O4	204.18
GI148915	OC(=O)c1c(O)ccc2ccccc12	C11H8O3	188.19
GR207121	OC(=O)c1cc2ccccc2cc1O	C11H8O3	188.19
GR260810	OC(=O)c1cc2cc3ccccc3cc2cc1O	C15H10O3	238.25
GR66288	OC(=O)c1ccc2ccccc2c1O	C11H8O3	188.19
GI166629	OC(=O)c1ccc2cc(O)ccc2c1	C11H8O3	188.19
GR235507	OC(=O)c1ccc2ccc(O)cc2c1	C11H8O3	188.19
GR38555	OC(=O)c1ccc(O)c2ccccc12	C11H8O3	188.19
GW296997	OC(=O)c1ccc2cccc(O)c2c1	C11H8O3	188.19
CCI4008	OC(=O)c1ccccc1O	C7H6O3	138.12
GR244973	COc1ccc2cc(ccc2c1)C(=O)O	C12H10O3	202.21
GR260719	COc1ccc2ccccc2c1C(=O)O	C12H10O3	202.21
GW317730	COc1cc2ccccc2cc1C(=O)O	C12H10O3	202.21
GW412437	COc1c(ccc2ccccc12)C(=O)O	C12H10O3	202.21
GW369998	COc1cc2c(OC)cccc2cc1C(=O)O	C13H12O4	232.24
GW416206	COc1ccc2cc(O)c(cc2c1)C(=O)O	C12H10O4	218.21
GW315253X	OC(=O)c1ccc2ccc3ccccc3c(=O)c2c1	C16H10O3	250.26
AH16806XX	COc1cccc(c1)C(=O)c2ccc(cc2)C(=O)O	C15H12O4	256.26
AH17157XX	CCCOc1cccc(c1)C(=O)c2ccc(cc2)C(=O)O	C17H16O4	284.32
GW312681X	COc1ccc2Oc3cc(ccc3Cc2c1)C(=O)O	C15H12O4	256.26
AH4366	OC(=O)c1ccc(cc1)C(=O)c2ccccc2	C14H10O3	226.23
AH4367	OC(=O)c1ccccc1C(=O)c2ccccc2	C14H10O3	226.23
AH9991	Cc1ccc(cc1Cl)C(=O)c2ccccc2C(=O)O	C15H11ClO3	274.71

Reg No	Smiles String	Formula	MW
AH9456	Nc1ccccc1C(=O)c2ccccc2C(=O)O	C14H11NO3	241.25
AH7716	OC(=O)c1cc(Cc2ccc(O)c(c2)C(=O)O)ccc1O	C15H12O6	288.26
GR244160X	OC(=O)c1cccc(c1)C(=O)c2ccc(Cl)cc2	C14H9ClO3	260.68
GR30170X	COc1ccc(C(=O)c2ccccc2C(=O)O)c(O)c1	C15H12O5	272.26
GW294785X	COc1ccc(Cc2cc(ccc2C(=O)O)C(=O)O)cc1	C16H14O5	286.29
GR232463X	OC(=O)c1ccc2C(OC(=O)c2c1)c3ccc(F)cc3	C15H9FO4	272.24
GW312679X	COc1ccc(cc1)C2OC(=O)c3ccc(cc23)C(=O)O	C16H12O5	284.27
AH12195	CC(=O)c1cccc2cccc(C(=O)O)c12	C13H10O3	214.22
GR30355X	CC(=O)c1ccc(cc1)C(=O)O	C9H8O3	164.16
GR30686X	OC(=O)c1ccc(cc1)C(=O)C(F)(F)F	C9H5F3O3	218.13
GI221306X	OC(=O)c1ccccc1CCc2ccccc2	C15H14O2	226.28
GR197556X	OC(=O)c1ccc2CCc3cccc1c32	C13H10O2	198.22
GR236886	CC(=O)c1cccc2cc(O)c(cc12)C(=O)O	C13H10O4	230.22
GW432536	COc1cc(ccc1C(=O)O)C(=O)C	C10H10O4	194.19
AH14680XX	Cc1cc(C)c(C(=O)O)c(CC(C)(C)C(=O)O)c1	C14H18O4	250.30
GR215350X	OC(=O)CCc1ccc(cc1)C(=O)O	C10H10O4	194.19
GW413125X	COC(=O)CC(Cc1ccc(cc1)C(=O)O)C(=O)OC(C)(C)C	C17H22O6	322.36
GR203309X	OC(=O)c1ccc(cc1)C2CCCCC2	C13H16O2	204.27
GR241592X	CCCCCCCCCCCCC1CCC(CC1)c2ccc(cc2)C(=O)O	C25H40O2	372.60
GR207127X	CCCCCCc1ccc(cc1)C(=O)O	C13H18O2	206.29
GW399139X	CCCCCCCc1ccc(cc1)C(=O)O	C14H20O2	220.31
GR34040X	CC(C)(C)c1cc(cc(c1O)C(C)(C)C)C(=O)O	C15H22O3	250.34
GW323465X	CC(=O)c1cc(Cl)c(O)c(c1)C(=O)O	C9H7ClO4	214.61
GR36337X	CCCCCCCCc1cccc(c1)C(=O)O	C15H22O2	234.34
GR87232X	OC(=O)c1cccc(CCCCc2ccc(O)cc2)c1	C17H18O3	270.33
GW322742X	CCCCC(=O)c1ccc(O)c(c1)C(=O)O	C12H14O4	222.24
CCI8247	CC(C)(OC(=O)c1ccccc1C(=O)O)C#C	C13H12O4	232.24
GW470564X	CC1(COC(=O)c2ccccc2C(=O)O)CCCC1=O	C15H16O5	276.29
GR136744X	OC(=O)c1cnccc1C2OCCO2	C9H9NO4	195.18

Reg No	Smiles String	Formula	MW
GW398946X	OC(=O)c1ccc(cc1)C2OCCO2	C10H10O4	194.19
GR258074X	OC(=O)/C=C/c1ccccc1C(=O)O	C10H8O4	192.17
GR30298X	OC(=O)C(=Cc1ccc(cc1)C(=O)O)O	C10H8O5	208.17
GW294643X	COc1ccccc1C=CC(=O)c2cc(ccc2O)C(=O)O	C17H14O5	298.30
GW295897X	OC(=O)c1ccccc1C=CC(=O)c2ccccc2	C16H12O3	252.27
AH5119	NC(=O)Cc1ccccc1C(=O)O	C9H9NO3	179.18
GR146857A	O.[Na+].[O-]C(=O)c1ccccc1CC(=O)Nc2ccccc2	C15H12NO3-. Na+. 0.2(H2O)	280.86
GR108821X	OC(CN(=O)=O)c1ccc(cc1)C(=O)O	C9H9NO5	211.18
CCI21441X	OC(=O)Cc1ccccc1C(=O)O	C9H8O4	180.16
GI222965X	OC(=O)Cc1cccc(O)c1C(=O)O	C9H8O5	196.16
GR85032X	COc1cc(CC(=O)O)c(cc1OC)C(=O)O	C11H12O6	240.22
GW317925X	OC(=O)Cc1ccc(cc1C(=O)O)N(=O)=O	C9H7NO6	225.16
GW423592X	CCOC(=O)C(C(=O)C)c1cc(ccc1C(=O)O)N(=O)=O	C13H13NO7	295.25
GR212558X	OC(=O)Cc1cccc(c1)C(=O)O	C9H8O4	180.16
GV98449X	NC(C(=O)O)c1cccc(c1)C(=O)O	C9H9NO4	195.18
GR245353X	OC(=O)C(CC#N)c1cccc2cccc(C(=O)O)c12	C15H11NO4	269.26
AH13207	OC(=O)c1cccc2C(=O)N(Cc3ccccc3)C(=O)c21	C16H11NO4	281.27
GR53007X	OC(=O)c1ccc2C(=O)N(OCc3ccccc3)C(=O)c2c1	C16H11NO5	297.27
AH8335X	OC(=O)c1ccc(cc1)N2C(=O)c3ccccc3C2=O	C15H9NO4	267.24
GR100133X	OC(=O)c1cc(CNC(=O)C(F)(F)F)ccc1Cl	C10H7ClF3NO3	281.62
GR111981X	CC(C)(C)OC(=O)NCc1cccc(c1)C(=O)O	C13H17NO4	251.29
GR124650X	CCOCCOc1ccc(cc1C(=O)N)C(=O)O	C12H15NO5	253.26
GR236342X	CCNC(=O)c1cc(ccc1O)C(=O)O	C10H11NO4	209.20
GR258909	CONC(=O)c1cc(O)c(C(=O)O)c(O)c1	C9H9NO6	227.18
GR265026X	CC(=O)NCc1ccc(cc1)C(=O)O	C10H11NO3	193.20
GR43579X	NCc1ccc(cc1)C(=O)O	C8H9NO2	151.17
GR51409X	NC(=NO)c1ccc(cc1)C(=O)O	C8H8N2O3	180.17
GW273704X	NC(c1ccc(cc1)C(=O)O)P(=O)(O)O	C8H10NO5P	231.15
GW324992X	OC(=O)c1cccc(CP(=O)(O)O)c1	C8H9O5P	216.13

Reg No	Smiles String	Formula	MW
CCI19762	OC(=O)c1cc2ccccc2cc1C(=O)N3CCOCC3	C16H15NO4	285.30
GR249776X	OC(=O)c1ccccc1C(=O)NCCc2ccccc2	C16H15NO3	269.30
GR256398X	C[C@H](NC(=O)c1ccccc1C(=O)O)c2ccccc2	C16H15NO3	269.30
GR269435X	CNC(C(=O)O)c1ccc(Cl)cc1C(=O)O	C10H10ClNO4	243.65
GR180851A	[Ba+2].[O-]C(=O)C1CCCN(Cc2ccccc2C(=O)[O-])C1	C14H15NO4(2-). Ba(2+)	398.62
GR88677X	NC(=O)CC[C@H](NC(=O)c1ccccc1C(=O)O)C(=O)O	C13H14N2O6	294.27
GW401244X	COC(=O)[C@H](Cc1ccc(cc1)C(=O)O)NC(=O)c2ccccc2Cl	C18H16ClNO5	361.79
GW406680X	COC(=O)[C@H](Cc1ccc(cc1)C(=O)O)NC(=O)OC(C)(C)C	C16H21NO6	323.35
GW521849X	COC(=O)[C@H](Cc1ccc(cc1)C(=O)O)NC(=O)OCc2ccccc2	C19H19NO6	357.37
AH13312	OC(=O)CC1=CCCc2cccc(C(=O)O)c12	C13H12O4	232.24
AH14681XX	Cc1cc(C)c(C(=O)O)c2CC(C)(C)C(=O)c21	C14H16O3	232.28
GR130650X	CC1(C)CCc2ccc(cc21)C(=O)O	C12H14O2	190.24
GR99513X	OC(=O)c1ccc2CCC(=O)c2c1	C10H8O3	176.17
AH23294X	OC(=O)c1ccc2CCC(=CC#N)c2c1	C12H9NO2	199.21
GR212000X	Cc1cccc2C3C(C4C3C(=O)c5c4cccc5C(=O)O)C(=O)c21	C20H14O4	318.33
GR116024X	CCN(CC)C(=O)[C@H]1CC[C@H]2[C@@H]3CCc4cc(ccc4[C@H]3CC[C@]12C)C(=O)O	C24H33NO3	383.54
GR58504X	CC1(C)CCC(C)(C)c2cc(ccc21)C(=O)O	C15H20O2	232.33
GW315124X	OC(=O)c1ccc2CCCCc2c1	C11H12O2	176.22
GW442963X	OC(=O)c1ccc2CCCC(=O)c2c1	C11H10O3	190.20
GW342768X	COc1cc2CCCCc2cc1C(=O)O	C12H14O3	206.24
AH25327X	OC(=O)c1ccc(OC(=O)CCC/C=C\CC2C(CC(=O)C2N3CCOCC3)OCc4ccc(cc4)c5ccccc5)cc1	C36H39NO7	597.72
AH25377X	OC(=O)c1cccc(c1)C(=O)CC2C(CC(=O)C2N3CCOCC3)OCc4ccc(cc4)c5ccccc5	C31H31NO6	513.60
GR60468X	OC(=O)c1cccc(CCCOC2C(CCC2N3CCCCC3)OCc4ccccc4)c1	C27H35NO4	437.58
GR223597X	CC1(C)CC(=O)/C/2=C(\C1)/Nc3ccccc3NC2c4ccc(cc4)C(=O)O	C22H22N2O3	362.43
GW543499X	CC1(C)CC(=C(C(C2=C(O)CC(C)(C)CC2=O)c3ccc(cc3)C(=O)O)C(=O)C1)O	C24H28O6	412.49
GR257678X	CC1OC(=O)c2c(O)c(C(=O)O)c(O)cc2C1C	C12H12O6	252.23
GW652716X	CC1(C)Cc2nc(cc(Cl)c2CO1)C(=O)O	C11H12ClNO3	241.68
GW292869X	COc1ccc(CC(C)(CCCC2=NOC(C2)c3ccc(cc3)C(=O)O)C#N)cc1OC	C25H28N2O5	436.51
GW342412X	COc1ccc(CC(C)(CCC2=NOC(C2)c3ccc(cc3)C(=O)O)C#N)cc1OC	C24H26N2O5	422.49

Reg No	Smiles String	Formula	MW
GR232127X	OC(=O)c1ccc2OCCCC(NC(=O)OCc3ccccc3)c2c1	C19H19NO5	341.37
GW309937A	Cl.CN1CCc2cc(C(=O)O)c(O)cc2C1Cc3ccccc3Cl	C18H18ClNO3. HCl	368.26
GR54241	COc1ccc(cc1CCCN(C)C)C(=O)O	C13H19NO3	237.30
GR64138A	I.COc1ccc(cc1CCC2CCCCN2C)C(=O)O	C16H23NO3. HI	405.28
GR81562	CN(C)CCCc1cc(ccc1N(C)C)C(=O)O	C14H22N2O2	250.34
GW424484X	OC(=O)c1cccc(CC2NC(=O)NC2=O)c1	C11H10N2O4	234.21
GW294777X	COc1ccc(cc1)C2COc3ccc(cc3C2=O)C(=O)O	C17H14O5	298.30
GW313525X	OC(=O)c1ccc2OC(CCc2c1)c3ccccc3	C16H14O3	254.29
GW321902X	OC(=O)c1ccc2OCCCc2c1	C10H10O3	178.19
GR194866A	O[C@@H](CNC1CCC(CC1)c2ccc(cc2)C(=O)O)c3cccc(Cl)c3.OC(=O)C(F)(F)F	C21H24ClNO3. C2HF3O2	487.91
GR65644X	Nc1c(Cl)cc(cc1Cl)C(O)CNCCCCCCOCCCc2ccc(cc2)C(=O)O	C24H32Cl2N2O4	483.44
GW553810A	Cl.Nc1c(Cl)cc(cc1Cl)[C@@H](O)CNCCCCCCOCCCc2ccc(cc2)C(=O)O	C24H32Cl2N2O4. HCl	519.90
GW549758A	Cl.Nc1c(Cl)cc(cc1Cl)[C@@H](O)CNCCCCCOCCCc2ccc(cc2)C(=O)O	C23H30Cl2N2O4. HCl	505.87
GW550038A	Cl.Nc1c(Cl)cc(cc1Cl)[C@@H](O)CNCCCCCCOCCCc2cccc(c2)C(=O)O	C24H32Cl2N2O4. HCl	519.90
GR70745X	Nc1c(Cl)cc(cc1Cl)C(O)CNCCCCCCOCCCc2cncc(c2)C(=O)O	C23H31Cl2N3O4	484.43
GR69220X	Nc1c(Cl)cc(cc1Cl)C(O)CNCCCCCOCCCc2ccc(o2)C(=O)O	C21H28Cl2N2O5	459.37
AH11291	NS(=O)(=O)c1cc(ccc1C(=O)O)C(=O)O	C8H7NO6S	245.21
GR94828A	N.NS(=O)(=O)c1cc(C(=O)O)c(O)c(c1)S(=O)(=O)N	C7H8N2O7S2. H3N	313.31
AH12740	COc1cc(ccc1C(=O)O)S(=O)(=O)N	C8H9NO5S	231.23
AH12757	NS(=O)(=O)c1ccc(cc1)C(=O)O	C7H7NO4S	201.20
GR199839X	Cc1ccc(cc1)S(=O)(=O)Nc2ccccc2C(=O)O	C14H13NO4S	291.33
GR58191X	OC(=O)c1ccc(CCCNS(=O)(=O)c2ccccc2)o1	C14H15NO5S	309.34
GR87036X	CCCN(CCC)S(=O)(=O)c1ccc(cc1)C(=O)O	C13H19NO4S	285.37
GW415452X	OC(=O)c1cc(ccc1O)S(=O)(=O)N2CCCCC2	C12H15NO5S	285.32
AH8294	CS(=O)(=O)c1ccc(cc1)C(=O)O	C8H8O4S	200.22
GR39220X	OC(=O)c1ccc(cc1)S(=O)c2ccc(cc2)C(=O)O	C14H10O5S	290.30
GI101694A	[K+].OC(=O)c1ccc(cc1)S(=O)(=O)[O-]	C7H5O5S-. K+	240.28
GR50961A	N.OC(=O)c1ccccc1S(=O)(=O)O	C7H6O5S. H3N	219.22
GR147168X	Nc1cc(C(=O)O)c(O)c(c1)S(=O)(=O)O	C7H7NO6S	233.20

Reg No	Smiles String	Formula	MW
GR51196X	Nc1cc(Cl)c(cc1C(=O)O)S(=O)(=O)O	C7H6ClNO5S	251.65
GR117463X	OC(=O)c1ccccc1SCc2ccccc2	C14H12O2S	244.32
GR208696X	OCCSc1ccccc1C(=O)O	C9H10O3S	198.24
GR32768A	[Na+].CSc1ccccc1C(=O)[O-]	C8H7O2S-. Na+	190.20
GW432313X	CC(=O)NCSc1ccccc1C(=O)O	C10H11NO3S	225.27
GR266494X	CSc1ccc(Cl)c(c1)C(=O)O	C8H7ClO2S	202.66
GW298250X	OC(=O)CCSc1cccc(c1)C(=O)O	C10H10O4S	226.25
GR125017X	CC(C)(C)OC(=O)NCCSc1ccc(cc1)C(=O)O	C14H19NO4S	297.38
GW370018X	OC(=O)c1ccccc1SCC(=O)Nc2ccccc2	C15H13NO3S	287.34
GW315103X	OC(=O)c1ccc2c(CCCS2(=O)=O)c1	C10H10O4S	226.25
GW321966X	OC(=O)c1ccc2C(=O)CCSc2c1	C10H8O3S	208.24
GF233961X	OC(=O)c1ccccc1Sc2ccccc2C#N	C14H9NO2S	255.30
GI230797A	[Na+].[O-]C(=O)c1ccccc1Sc2ccc(cc2)N(=O)=O	C13H8NO4S-. Na+	297.27
GR140164X	OC(=O)c1ccccc1Sc2ccc(Cl)cc2	C13H9ClO2S	264.73
GW290604X	OC(=O)c1ccc2Sc3ccccc3Sc2c1	C13H8O2S2	260.34
GW291821X	OC(=O)c1cccc(Sc2ccccc2C(=O)O)c1	C14H10O4S	274.30
GW361278X	OC(=O)c1ccc(C(=O)O)c(Sc2ccccc2)c1	C14H10O4S	274.30
GW336990X	OC(=O)c1ccc(C(=O)O)c(Sc2cccc3ccccc23)c1	C18H12O4S	324.36
GW295365X	CCc1ccc(Sc2cc(ccc2C(=O)O)C(=O)O)cc1	C16H14O4S	302.35
GW292911X	OC(=O)c1cc(ccc1O)S(=O)(=O)c2ccccc2	C13H10O5S	278.29
GW294867X	Cc1ccc(cc1S(=O)(=O)c2ccccc2)C(=O)O	C14H12O4S	276.31
GW322405X	Cc1ccc(cc1)S(=O)(=O)c2cc(ccc2C)C(=O)O	C15H14O4S	290.34
GW315228X	OC(=O)c1ccc2Oc3ccc(cc3Sc2c1)C(=O)O	C14H8O5S	288.28
GW321601X	OC(=O)c1ccc2-c3ccccc3S(=O)(=O)c2c1	C13H8O4S	260.27
GI230786	OC(=O)c1cscc1Sc2ccc(Cl)cc2	C11H7ClO2S2	270.76
GW295364	OC(=O)c1ccc(C(=O)O)c(Sc2ccsc2)c1	C12H8O4S2	280.32
AH7066	OC(=O)c1ccc2c(c1)C(=O)c3ccccc3S2(=O)=O	C14H8O5S	288.28
GF234516X	OC(=O)c1ccc2C(=O)c3ccccc3S(=O)(=O)c2c1	C14H8O5S	288.28
GF269343X	OC(=O)c1ccc2Cc3ccccc3S(=O)(=O)c2c1	C14H10O4S	274.30

Reg No	Smiles String	Formula	MW
GW314651X	OC(=O)c1ccc2C(=O)c3cc(F)ccc3S(=O)(=O)c2c1	C14H7FO5S	306.27
GW311857X	Nc1ccc2C(=O)c3ccc(cc3S(=O)(=O)c2c1)C(=O)O	C14H9NO5S	303.30
GW323587X	CCc1ccc2c(c1)C(=O)c3ccc(cc3S2(=O)=O)C(=O)O	C16H12O5S	316.34
GW294790X	OC(=O)c1ccc2Cc3cc(Cl)ccc3Sc2c1	C14H9ClO2S	276.74
GW322118X	OC(=O)c1ccc2Cc3ccccc3Sc2c1	C14H10O2S	242.30
GW312723X	OCCOc1ccc2Cc3ccc(cc3S(=O)(=O)c2c1)C(=O)O	C16H14O6S	334.35
GW432537X	CCOc1ccc2Cc3ccc(cc3S(=O)(=O)c2c1)C(=O)O	C16H14O5S	318.35
GW322502X	OCCOc1ccc2C(=O)c3ccc(cc3S(=O)(=O)c2c1)C(=O)O	C16H12O7S	348.33
GW312725X	OC(=O)c1ccc2Cc3ccc(O)cc3S(=O)(=O)c2c1	C14H10O5S	290.30
GW322531X	COc1ccc2C(=O)c3ccc(cc3S(=O)(=O)c2c1)C(=O)O	C15H10O6S	318.31
GW314663X	CCCOc1ccc2c(c1)C(=O)c3ccc(cc3S2(=O)=O)C(=O)O	C17H14O6S	346.36
GW323690X	CCOc1ccc2c(c1)C(=O)c3ccc(cc3S2(=O)=O)C(=O)O	C16H12O6S	332.33
GW323328X	COc1cccc2C(=O)c3ccc(cc3S(=O)(=O)c12)C(=O)O	C15H10O6S	318.31
AH10503	OC(=O)C=CC(=O)Nc1ccc(cc1)C(=O)O	C11H9NO5	235.20
AH25564X	CN(C(=O)C)c1ccc(cc1)C(=O)O	C10H11NO3	193.20
CCI7155	CC(=O)Nc1ccc(C(=O)O)c(O)c1	C9H9NO4	195.18
GR51515	CC(=O)Nc1ccc(C(=O)O)c(c1)N(=O)=O	C9H8N2O5	224.18
GW363503A	CN(C)CCO.CC(=O)Nc1ccc(C(=O)O)c(F)c1	C9H8FNO3. C4H11NO	286.31
GR253714X	CC(=O)Nc1c(Cl)cc(cc1Cl)C(=O)O	C9H7Cl2NO3	248.07
AH9018	OC(=O)c1ccc(cc1O)N2C(=O)C=CC2=O	C11H7NO5	233.18
AH12070	CC(=O)Nc1cc(Cl)ccc1C(=O)O	C9H8ClNO3	213.62
GI123058	CC(=O)Nc1ccccc1C(=O)O	C9H9NO3	179.18
GR55509	CC(=O)Nc1cc2ccccc2cc1C(=O)O	C13H11NO3	229.24
GR50239	CC(=O)Nc1ccc(C)cc1C(=O)O	C10H11NO3	193.20
GR87121	OC(=O)c1ccccc1NC(=O)C(F)(F)F	C9H6F3NO3	233.15
AH2951	CN(C=O)c1ccccc1C(=O)O	C9H9NO3	179.18
GR199994	CC(=O)N(CC(=C)Cl)c1ccccc1C(=O)O	C12H12ClNO3	253.69
AH12275	OC(=O)c1ccccc1N2C(=O)CCC2=O	C11H9NO4	219.20
GR173757	CC(C)(C)C(=O)Nc1cccc(c1C(=O)O)C(F)(F)F	C13H14F3NO3	289.26

Reg No	Smiles String	Formula	MW
GR161201X	COC(=O)CNC(=O)Nc1ccccc1C(=O)O	C11H12N2O5	252.23
AH12764	OC(=O)C(Nc1ccccc1C(=O)O)c2ccccc2	C15H13NO4	271.28
AH17306AB	[Na+].[O-]C(=O)CNc1ccccc1C(=O)[O-]	C9H7NO4(2-). 2(Na+)	239.14
GR161186X	CCOC(=O)CNc1ccccc1C(=O)O	C11H13NO4	223.23
AH15079XX	Cc1ccc(N(CC#C)CC#C)c(c1)C(=O)O	C14H13NO2	227.27
GR35117X	OC(=O)c1ccc(NCC#Cc2ccccc2)cc1	C16H13NO2	251.29
AH21453	OC(=O)CCNc1ccccc1C(=O)O	C10H11NO4	209.20
GR178029	OC(=O)c1ccccc1NCCC#N	C10H10N2O2	190.20
GR33748	CCNc1ccccc1C(=O)O	C9H11NO2	165.19
GI152672	CC(=O)Nc1ccc(N)c(c1)C(=O)O	C9H10N2O3	194.19
GR141743	CC(=O)Nc1cccc(c1)C(=O)O	C9H9NO3	179.18
GR39406	CC(=O)Nc1cc(N)cc(c1)C(=O)O	C9H10N2O3	194.19
GR214280	CC(=O)Nc1cc(ccc1C)C(=O)O	C10H11NO3	193.20
GR226270	OC(=O)C(=O)Nc1cccc(c1)C(=O)O	C9H7NO5	209.16
GR78537	CC(C)CC(=O)Nc1cccc(c1)C(=O)O	C12H15NO3	221.26
GR189793	CC(=O)Nc1ccc(cc1NC(=O)C)C(=O)O	C11H12N2O4	236.23
GR263804X	CC(=O)Nc1cc(ccc1C(C)(C)C)C(=O)O	C13H17NO3	235.29
GW324674	CC(=O)Nc1ccc(N(=O)=O)c(c1)C(=O)O	C9H8N2O5	224.18
GW410247	CC(=O)Nc1cccc(C(=O)O)c1N(=O)=O	C9H8N2O5	224.18
GR38461X	CC(=O)Nc1cc(C(=O)O)c(O)cc1O	C9H9NO5	211.18
GW340239X	CC(=O)Nc1ccc(OCC=C)c(c1)C(=O)O	C12H13NO4	235.24
GR73169X	OC(=O)c1cccc(NC(=O)CCc2ccc(O)cc2)c1	C16H15NO4	285.30
AH15491XX	OC(=O)c1ccccc1C(=O)Nc2ccccc2F	C14H10FNO3	259.24
GR107832X	OC(=O)c1ccc(NC(=O)c2ccccc2)cc1	C14H11NO3	241.25
GR231878X	OC(=O)c1ccccc1NC(=O)c2ccccc2	C14H11NO3	241.25
GR137556X	OC(=O)c1cccc(NC(=O)c2ccc(C#N)cc2)c1	C15H10N2O3	266.26
GF146238	OC(=O)c1cc(NCc2cc(O)ccc2O)ccc1O	C14H13NO5	275.26
GW295088	COc1ccc(O)c(CNc2ccc(O)c(c2)C(=O)O)c1	C15H15NO5	289.29
GF267572X	COc1ccc(CNc2ccc(cc2)C(=O)O)cc1OC	C16H17NO4	287.32

Reg No	Smiles String	Formula	MW
GW323141X	OC(=O)c1ccc(NCc2ccc3OCCOc3c2)cc1	C16H15NO4	285.30
GF267575X	CCOC(=O)Nc1ccc(cc1)C(=O)O	C10H11NO4	209.20
GR76319X	OC(=O)c1cccc(NC(=O)OCc2ccccc2)c1	C15H13NO4	271.28
GR78359X	OC(=O)c1ccccc1NC(=O)OCc2ccccc2	C15H13NO4	271.28
GI170475X	CN(C)c1ccc(N=Nc2ccccc2C(=O)O)cc1	C15H15N3O2	269.31
GW275669A	[Na+].CN(C)c1ccc(N=Nc2ccc(cc2)C(=O)[O-])cc1	C15H14N3O2-. Na+	291.29
GR205623X	CN(C)N=Nc1ccccc1C(=O)O	C9H11N3O2	193.21
GR53844X	CN(C)C=Nc1cccc(C)c1C(=O)O	C11H14N2O2	206.25
GW298071X	OC(=O)c1ccccc1NC=CN(=O)=O	C9H8N2O4	208.18
GI199827X	NC(=S)Nc1ccc(cc1)C(=O)O	C8H8N2O2S	196.23
GR141837X	NC(=S)Nc1cccc(c1)C(=O)O	C8H8N2O2S	196.23
GW323802A	[Na+].[O-]C(=O)c1ccc(NCS(=O)(=O)[O-])cc1	C8H7NO5S(2-). 2(Na+)	275.19
GW329522X	NC(=N)NC(=O)Nc1ccc(C(=O)O)c(Cl)c1	C9H9ClN4O3	256.65
GR251266A	CNC(=O)c1ccc(cc1NC(=N)N)C(=O)O.OC(=O)C(F)(F)F	C10H12N4O3. C2HF3O2	350.26
GR265018A	Cc1ccc(cc1NC(=N)N)C(=O)O.OC(=O)C(F)(F)F	C9H11N3O2. C2HF3O2	307.23
GR253017X	COc1ccc(cc1NC(=N)N)C(=O)O	C9H11N3O3	209.21
GW425183X	Cc1ccc(cc1NC(=NC(=O)OC(C)(C)C)NC(=O)OC(C)(C)C)C(=O)O	C19H27N3O6	393.44
GR267248A	NC(=N)Nc1cc(ccc1CNC(=O)C(F)(F)F)C(=O)O.OC(=O)C(F)(F)F	C11H11F3N4O3. C2HF3O2	418.26
GW425181X	OC(=O)c1ccc(CNC(=O)C(F)(F)F)c(c1)N(=O)=O	C10H7F3N2O5	292.17
AH17295XX	Nc1c(cccc1N(=O)=O)C(=O)O	C7H6N2O4	182.14
AH26206X	CN(C)c1ccc(cc1N(=O)=O)C(=O)O	C9H10N2O4	210.19
AH20560XX	NNc1ccc(cc1N(=O)=O)C(=O)O	C7H7N3O4	197.15
GR97173X	CC(C)(CN)CNc1ccc(cc1N(=O)=O)C(=O)O	C12H17N3O4	267.29
AH21291X	OC(=O)c1cc(Br)cc(c1)N(=O)=O	C7H4BrNO4	246.02
GW471254X	CN1CCN(CC1)c2ccc(cc2C(=O)O)N(=O)=O	C12H15N3O4	265.27
AH17365XX	Nc1cccc(N(=O)=O)c1C(=O)O	C7H6N2O4	182.14
GI198830X	OC(=O)c1ccc(cc1N(=O)=O)C(F)(F)F	C8H4F3NO4	235.12
AH7669	OC(=O)c1cc(N=Nc2ccc(cc2)N(=O)=O)ccc1O	C13H9N3O5	287.23
GI221325A	OC(=O)c1cc(N(=O)=O)c(O)c(c1)N(=O)=O.c1ccncc1	C7H4N2O7. C5H5N	307.22

Reg No	Smiles String	Formula	MW
GI95276X	OC(=O)c1ccc(N(=O)=O)c(O)c1	C7H5NO5	183.12
CCI7978	Nc1ncnc(Nc2cc(ccc2Cl)C(=O)O)n1	C10H8ClN5O2	265.66
GF267691X	OC(=O)c1cc(N(=O)=O)c(Cl)cc1Cl	C7H3Cl2NO4	236.01
GI147499A	Nc1ccc(Cl)c(c1)C(=O)O.OS(=O)(=O)O	C7H6ClNO2. H2O4S	269.66
AH21350X	OC(=O)c1ccc(Nc2ccccc2C(=O)O)cc1	C14H11NO4	257.25
GW321669X	OC(=O)c1ccc(Nc2ccccc2)cc1	C13H11NO2	213.24
GW323630X	COc1ccc(Nc2ccc(cc2C(=O)O)C(=O)O)cc1	C15H13NO5	287.28
CCI1914	OC(=O)c1ccc(cc1Nc2ccccc2)N(=O)=O	C13H10N2O4	258.24
GF146728X	OC(=O)c1ccccc1Nc2cccc(c2)C(F)(F)F	C14H10F3NO2	281.24
GR86838X	OC(=O)c1cc(Nc2ccc(Nc3ccccc3)cc2)c(cc1Nc4ccc(Nc5ccccc5)cc4)C(=O)O	C32H26N4O4	530.59
AH5502	Nc1cc(ccc1C(=O)O)C(=O)O	C8H7NO4	181.15
GR141836	Cc1ccc(cc1N)C(=O)O	C8H9NO2	151.17
GR248323	COC(=O)c1ccc(cc1N)C(=O)O	C9H9NO4	195.18
AH6472	Nc1cc(cc(c1)C(=O)O)C(=O)O	C8H7NO4	181.15
GR141839	Nc1ccc(cc1N)C(=O)O	C7H8N2O2	152.15
GR31162	Nc1cccc(c1)C(=O)O	C7H7NO2	137.14
GR40490	Nc1cc(N)cc(c1)C(=O)O	C7H8N2O2	152.15
GR40028	Nc1ccc(cc1)C(=O)O	C7H7NO2	137.14
GI149060	Nc1cccc(C(=O)O)c1C(=O)O	C8H7NO4	181.15
GI153357	Cc1c(N)cccc1C(=O)O	C8H9NO2	151.17
GV95604	Nc1ccc(C(=O)O)c(c1)C(=O)O	C8H7NO4	181.15
GI119939X	Nc1cc(F)ccc1C(=O)O	C7H6FNO2	155.13
GI147798	Cc1cc(ccc1N)C(=O)O	C8H9NO2	151.17
GR113723	Cc1cc(cc(C)c1N)C(=O)O	C9H11NO2	165.19
GI150183	Cc1ccc(N)c(c1)C(=O)O	C8H9NO2	151.17
GR259835	Cc1cc(C)c(N)c(c1)C(=O)O	C9H11NO2	165.19
GR197159	Cc1cccc(C(=O)O)c1N	C8H9NO2	151.17
GR118329	Nc1ccc(cc1C(=O)O)C(=O)O	C8H7NO4	181.15
GI151314	Cc1cccc(N)c1C(=O)O	C8H9NO2	151.17

Reg No	Smiles String	Formula	MW
GR214686	Cc1ccc(C(=O)O)c(N)c1	C8H9NO2	151.17
GR89164	Nc1ccccc1C(=O)O	C7H7NO2	137.14
GR261930	Nc1cc2ccccc2cc1C(=O)O	C11H9NO2	187.20
GR31787A	Cl.NNc1ccc(cc1)C(=O)O	C7H8N2O2. HCl	188.62
CCI8566	CS(=O)(=O)Nc1ccccc1C(=O)O	C8H9NO4S	215.23
GR32579	CS(=O)(=O)Nc1ccc(cc1)C(=O)O	C8H9NO4S	215.23
GW286126	CS(=O)(=O)Nc1ccc(C(=O)O)c(Cl)c1	C8H8ClNO4S	249.67
GW422957	NS(=O)(=O)Nc1ccc(cc1)C(=O)O	C7H8N2O4S	216.22
GR123674	CS(=O)(=O)Nc1cccc(c1)C(=O)O	C8H9NO4S	215.23
GR146669	CS(=O)(=O)Nc1cc(ccc1O)C(=O)O	C8H9NO5S	231.23
CCI9041	CS(=O)(=O)Nc1ccc(C(=O)O)c(O)c1	C8H9NO5S	231.23
GW296344	COc1cc(NS(=O)(=O)C)ccc1C(=O)O	C9H11NO5S	245.26
GR154729	CS(=O)(=O)Nc1ccc(cc1O)C(=O)O	C8H9NO5S	231.23
GR171932	OC(=O)c1ccc(NS(=O)(=O)C(F)(F)F)c(O)c1	C8H6F3NO5S	285.20
AH13018	OC(=O)c1cc2ccccc2o1	C9H6O3	162.15
GV140840X	OC(=O)c1cc2cc(ccc2o1)N(=O)=O	C9H5NO5	207.14
GR207209X	CCC(O)CCc1c(oc2ccccc12)C(=O)O	C14H16O4	248.28
GR112257X	OC(=O)c1cc(O)c2ccoc2c1	C9H6O4	178.15
GR263152X	OC(=O)c1cc2oc3ccccc3c2cc1O	C13H8O4	228.21
GR112259X	COc1cc(cc2occc12)C(=O)O	C10H8O4	192.17
GR185905X	COc1ccc2occc2c1C(=O)O.COc1cc2ccoc2cc1C(=O)O	C10H8O4/C10H8O4	384.35
GR186845X	Cc1cccc2c(coc12)C(=O)O	C10H8O3	176.17
GR219630X	OC(=O)c1coc2cccc(O)c12	C9H6O4	178.15
GW541786X	Cc1oc2cc(ccc2c1C)C(=O)O	C11H10O3	190.20
GW560094X	Cc1coc2cc(ccc12)C(=O)O	C10H8O3	176.17
GR53539X	OC(=O)c1ccc2oc(=O)oc2c1	C8H4O5	180.12
AH15201XX	OC(=O)c1ccc2c(=O)c3cc(O)ccc3oc2c1	C14H8O5	256.22
AH6859	COc1ccc2oc3cc(ccc3c(=O)c2c1)C(=O)O	C15H10O5	270.24
AH15203XX	CC(C)Oc1ccc2oc3cc(ccc3c(=O)c2c1)C(=O)O	C17H14O5	298.30

Reg No	Smiles String	Formula	MW
GW314581X	CCOc1ccc2oc3cc(ccc3c(=O)c2c1)C(=O)O	C16H12O5	284.27
GW294655X	OCCOc1ccc2oc3cc(ccc3c(=O)c2c1)C(=O)O	C16H12O6	300.27
GW328088X	CC(O)COc1ccc2oc3cc(ccc3c(=O)c2c1)C(=O)O	C17H14O6	314.30
GW312792X	CCCCOc1ccc2oc3cc(ccc3c(=O)c2c1)C(=O)O	C18H16O5	312.33
GW294322X	CN(C)CCOc1ccc2oc3cc(ccc3c(=O)c2c1)C(=O)O	C18H17NO5	327.34
GW304858X	OCCOCCOc1ccc2oc3cc(ccc3c(=O)c2c1)C(=O)O	C18H16O7	344.32
GW312329X	CC(=O)OCCOc1ccc2oc3cc(ccc3c(=O)c2c1)C(=O)O	C18H14O7	342.31
AH15400XX	CC(C)Oc1ccc2oc3cc(C(=O)O)c(Br)cc3c(=O)c2c1	C17H13BrO5	377.19
GW314526X	CCc1cc(OC)c2oc3cc(ccc3c(=O)c2c1)C(=O)O	C17H14O5	298.30
GW324336X	COc1cc(C)cc2c(=O)c3ccc(cc3oc12)C(=O)O	C16H12O5	284.27
AH5558	OC(=O)c1ccc2oc3ccccc3c(=O)c2c1	C14H8O4	240.22
AH5950	OC(=O)c1ccc2c(=O)c3ccccc3oc2c1	C14H8O4	240.22
GW312371X	OC(=O)c1ccc2c(=O)c3cc(C=O)ccc3oc2c1	C15H8O5	268.23
GW315227X	Cc1ccc2oc3cc(ccc3c(=O)c2c1)C(=O)O	C15H10O4	254.25
GW312460X	COCc1ccc2oc3cc(ccc3c(=O)c2c1)C(=O)O	C16H12O5	284.27
GW312437X	CCCc1ccc2oc3cc(ccc3c(=O)c2c1)C(=O)O	C17H14O4	282.30
GW312435X	Nc1ccc2oc3cc(ccc3c(=O)c2c1)C(=O)O	C14H9NO4	255.23
GF267701X	CSc1ccc2oc3cc(ccc3c(=O)c2c1)C(=O)O	C15H10O4S	286.31
GR189755X	OC(=O)c1ccc(C(=O)O)c(c1)c2c3ccc(O)cc3oc4cc(=O)ccc24.OC(=O)c1cccc(C(=O)O)c1c2c3ccc(O)cc3oc4cc(=O)ccc24	C21H12O7/C21H12O7	752.65
GW313003X	OC(=O)c1ccc2occ(c3ccc(O)cc3)c(=O)c2c1	C16H10O5	282.26
GR256734X	Cc1cc(O)c(C(=O)O)c2oc(=O)cc(C)c12	C12H10O5	234.21
GW321218X	OC(=O)c1ccc2oc3CCCCc3c(=O)c2c1	C14H12O4	244.25
AH6372	OC(=O)c1ccc2c(=O)cc(oc2c1)c3ccccc3	C16H10O4	266.26
GI205545X	Cc1c(oc2c(cccc2c1=O)C(=O)O)c3ccccc3	C17H12O4	280.28
GW312626X	OC(=O)c1ccc2oc(cc2c1)c3ccc(Cl)cc3	C15H9ClO3	272.69
GR230571X	OC(=O)c1ccc(o1)c2cc3ccccc3oc2=O	C14H8O5	256.22
AH21917X	Cc1ccoc1C(=O)O	C6H6O3	126.11
AH22735X	OC(=O)c1ccco1	C5H4O3	112.09

Reg No	Smiles String	Formula	MW
GR177051X	OC(=O)c1ccc(o1)N(=O)=O	C5H3NO5	157.08
GW471604X	OC(=O)c1ccc(CC#N)o1	C7H5NO3	151.12
GR152169X	OC(=O)c1cc(Br)c(Cl)o1	C5H2BrClO3	225.43
GR225877X	CC(=O)/C=C/c1ccc(o1)C(=O)O	C9H8O4	180.16
GR255442X	COc1c(OC)c(oc1C(=O)O)C(=O)O	C8H8O7	216.15
CCI2180	CCOC(=O)c1cocc1C(=O)O	C8H8O5	184.15
GR121162X	OC(=O)c1coc(Br)c1	C5H3BrO3	190.98
GW308403X	OC(=O)c1ccoc1C(=O)c2ccccc2	C12H8O4	216.20
GR114265X	C[C@H](Cc1ccccc1)[C@H](OC(=O)C)C(=C)CCc2ccc(o2)C(=O)O	C21H24O5	356.42
GR225874X	CC1(C)COC(C)(CCc2ccc(o2)C(=O)O)OC1	C14H20O5	268.31
GR51045X	Cc1oc(cc1NC(=O)OCc2ccccc2)C(=O)O	C14H13NO5	275.26
GW521143X	COc1cc(cc(OC)c1OCc2ccc(o2)C(=O)C(F)(F)F)C(=O)O	C16H13F3O7	374.27
GR200308X	CC1=C2CC(C)(C)CC2Cc3coc(C(=O)O)c13.CC1=C2CC(C)(CO)CC2Cc3coc(C(=O)O)c13.CC1(C)CC2C(C1)C(C)(O)c3c(occ3C2O)C(=O)O	C15H20O5/C15H18O4/C15H1	788.94
GR32131X	OC(=O)c1coc2CCCC(=O)c12	C9H8O4	180.16
AH2599	OC(=O)c1cc(Cl)ccc1NCc2ccco2	C12H10ClNO3	251.67
AH7307	OC(=O)c1cc(Cl)ccc1NC(=O)c2ccco2	C12H8ClNO4	265.66
GR121876X	OC(=O)c1ccc(NC(=O)c2ccccc2)o1	C12H9NO4	231.21
GR193373X	CC(=O)Nc1ccc(o1)C(=O)O	C7H7NO4	169.14
GR196926X	OC(=O)c1ccc(NC(=O)OCc2ccccc2)o1	C13H11NO5	261.24
GW426030X	CC(C)(C)OC(=O)Nc1ccc(o1)C(=O)O	C10H13NO5	227.22
AH21971X	CC(=O)c1ccc(s1)C(=O)O	C7H6O3S	170.19
GW648032X	OCCc1ccc(s1)C(=O)O	C7H8O3S	172.20
CCI1710	OC(=O)c1cccs1	C5H4O2S	128.15
GR71245X	OC(=O)c1ccc(CCOCCCCCCBr)s1	C13H19BrO3S	335.26
GR173914X	Cc1ccc(C)n1c2ccsc2C(=O)O	C11H11NO2S	221.28
GR257498X	CC(C)S(=O)(=O)c1csc(C(=O)O)c1Cl	C8H9ClO4S2	268.74
AH23040X	OC(=O)c1ccsc1	C5H4O2S	128.15
GR36682X	OC(=O)c1csc(c1)N(=O)=O	C5H3NO4S	173.15

Reg No	Smiles String	Formula	MW
GR47574X	OC(=O)c1ccc(s1)N(=O)=O	C5H3NO4S	173.15
GR215566X	COc1c(Cl)scc1C(=O)O	C6H5ClO3S	192.62
GI198860X	OC(=O)c1cc2ccccc2s1	C9H6O2S	178.21
GR74829X	OC(=O)c1csc2ccccc12	C9H6O2S	178.21
GW271761X	COc1ccc2sc(C(=O)O)c(OC(C)C)c2c1	C13H14O4S	266.32
GR232957X	CC(=O)c1sc2sc(C(=O)O)c(C)c2c1C	C11H10O3S2	254.33
GW322216X	OC(=O)c1cc2c(=O)c3ccccc3sc2s1	C12H6O3S2	262.31
AH4822	OC(=O)c1ccc(s1)C(=O)c2ccccc2	C12H8O3S	232.26
GR207205X	OC(c1ccc(s1)C(=O)O)c2ccccc2	C12H10O3S	234.28
GF267466X	Cc1cc(C(=O)c2ccc(s2)C(=O)O)c(C)s1	C12H10O3S2	266.34
GW328094A	Cl.Cc1ccc(cc1)/C(=C/CN2CCCC2)/c3ccc(s3)C(=O)O	C19H21NO2S. HCl	363.91
GW418822A	Cl.Cc1ccc(cc1)/C(=C\CN2CCCC2)/c3ccc(s3)C(=O)O	C19H21NO2S. HCl	363.91
GW448911X	Cc1ccc(cc1)C(=CCN2CCCC2)c3ccc(s3)C(=O)O	C19H21NO2S	327.45
GI198877X	OC(=O)c1ccc(s1)c2ccccn2	C10H7NO2S	205.24
GR267007X	OC(=O)c1cc(nc2ccccc12)c3cccs3	C14H9NO2S	255.30
GW340373X	OC(=O)c1ccc(s1)c2ccccc2	C11H8O2S	204.25
GR256536X	Cn1nc(cc1c2ccc(s2)C(=O)O)C(F)(F)F	C10H7F3N2O2S	276.24
GR192153X	COC(=O)c1sccc1c2ccc(o2)C(=O)O	C11H8O5S	252.25
GW321193X	OC(=O)c1cc-2c(s1)C(=O)c3ccccc23	C12H6O3S	230.24
AH23064X	CSc1sc(C(=O)O)c(C)c1C(=O)C	C9H10O3S2	230.31
GW279435X	CSc1sc(C(=O)O)c2CCCC(=O)c12	C10H10O3S2	242.32
GW279438X	CS(=O)(=O)c1sc(C(=O)O)c2CCC=Cc12	C10H10O4S2	258.32
GW279439X	CSc1sc(C(=O)O)c2CCC=Cc12	C10H10O2S2	226.32
GR127482A	[Na+].CC(=O)Nc1sc(cc1C(=O)[O-])C(=O)C	C9H8NO4S-. Na+	249.22
GR262262X	CCCN(CCC)C(=O)c1c(C)c(sc1NC(=O)C)C(=O)O	C15H22N2O4S	326.42
GR262264X	CCCNC(=O)c1c(C)c(sc1NC(=O)C)C(=O)O	C12H16N2O4S	284.34
GR267264X	CCCN(CCc1ccccc1)C(=O)c2c(C)c(sc2NC(=O)C)C(=O)O	C20H24N2O4S	388.49
AH8425	COc1ccc2sc3ccc(cc3c(=O)c2c1)C(=O)O	C15H10O4S	286.31
GW314731X	COc1cccc2c(=O)c3ccc(cc3sc12)C(=O)O	C15H10O4S	286.31

Reg No	Smiles String	Formula	MW
GW314830X	COc1ccc2sc3cc(ccc3c(=O)c2c1)C(=O)O	C15H10O4S	286.31
GW320557X	CCOc1ccc2sc3cc(ccc3c(=O)c2c1)C(=O)O	C16H12O4S	300.34
GW323721X	CCCOc1ccc2sc3cc(ccc3c(=O)c2c1)C(=O)O	C17H14O4S	314.36
GW314662X	CCc1cccc2c(=O)c3ccc(cc3sc12)C(=O)O	C16H12O3S	284.34
GW314681X	CCc1ccc2sc3cc(ccc3c(=O)c2c1)C(=O)O	C16H12O3S	284.34
GW314793X	CC(C)c1ccc2sc3cc(ccc3c(=O)c2c1)C(=O)O	C17H14O3S	298.36
GW322018X	CC(C)(C)c1ccc2sc3cc(ccc3c(=O)c2c1)C(=O)O	C18H16O3S	312.39
GW314751X	Cc1ccc2sc3cc(ccc3c(=O)c2c1)C(=O)O	C15H10O3S	270.31
GW315158X	OC(=O)c1ccc2c(=O)c3ccccc3sc2c1	C14H8O3S	256.28
GW322801X	Cc1cccc2c(=O)c3ccc(cc3sc12)C(=O)O	C15H10O3S	270.31
GW323040X	Cc1cc(C)c2sc3cc(ccc3c(=O)c2c1)C(=O)O	C16H12O3S	284.34
GW321891X	OC(=O)c1ccc2c(=O)c3ccccc3s(=O)c2c1	C14H8O4S	272.28
GW323845X	OC(=O)c1ccc2c(=O)c3cc(F)ccc3sc2c1	C14H7FO3S	274.27
GW323446X	OC(=O)c1ccc2c(=O)c3cc(Br)ccc3sc2c1	C14H7BrO3S	335.18
GW323591X	OC(=O)c1ccc2c(=O)c3cccc(c3sc2c1)C(F)(F)F	C15H7F3O3S	324.28
GW315075X	OC(=O)c1ccc2c(=O)c3cc(Cl)ccc3sc2c1	C14H7ClO3S	290.73
GW322693X	OC(=O)c1ccc2c(=O)c3c(Cl)ccc(Cl)c3sc2c1	C14H6Cl2O3S	325.17
GW321808X	Cc1ccc(Cl)c2c(=O)c3ccc(cc3sc12)C(=O)O	C15H9ClO3S	304.75
GW322384X	OC(=O)c1ccc2c(=O)c3sccc3sc2c1	C12H6O3S2	262.31
GW321800A	Cl.CCN(CC)CCNc1ccc(C)c2sc3cc(ccc3c(=O)c12)C(=O)O	C21H24N2O3S. HCl	420.96
GW322628X	CSc1ccc2sc3cc(ccc3c(=O)c2c1)C(=O)O	C15H10O3S2	302.37
GW322988X	CS(=O)c1ccc2sc3cc(ccc3c(=O)c2c1)C(=O)O	C15H10O4S2	318.37
AH15466AA	OCC(O)COc1ccccc1C(=O)O.C1CCC(CC1)NC2CCCCC2	C10H12O5. C12H23N	393.53
AH2565	CC(C)(C)C(=O)Oc1ccccc1C(=O)O	C12H14O4	222.24
GW366246	CCCCCCCOc1ccc(N)cc1C(=O)O	C14H21NO3	251.33
CCI17196	CC1(C)C2CCC1(CC2)C(=O)Oc3ccccc3C(=O)O	C17H20O4	288.35
AH20078XX	CCCCCCCCCCOc1ccc(cc1)C(=O)O	C17H26O3	278.40
GR208554X	CCCCCCCCCCCCCCCCCCCCOc1ccc(cc1)C(=O)O	C25H42O3	390.61
GR230104X	OC(=O)c1ccc(OCCCCCCCCCCCCCCOc2ccc(cc2)C(=O)O)cc1	C26H34O6	442.56

Reg No	Smiles String	Formula	MW
GR30893X	CCCCCCCCOc1ccc(cc1)C(=O)O	C15H22O3	250.34
GR33911X	CCCCCCCCCCCCOc1ccc(cc1)C(=O)O	C19H30O3	306.45
GR62459X	OC(=O)c1ccc(OCCCCCCCCCCOc2ccc(cc2)C(=O)O)cc1	C23H28O6	400.48
GR65815X	CCCCCCCCCCCCCCCCCOc1ccc(cc1)C(=O)O	C23H38O3	362.56
GR65884X	CCCCCCCCCCCCCCCOc1ccc(cc1)C(=O)O	C21H34O3	334.50
GW385846X	OC(=O)c1ccc(OCCCCCCCOc2ccc(cc2)C(=O)O)cc1	C21H24O6	372.42
GR155589X	OCCCCCCOc1ccc(cc1)C(=O)O	C13H18O4	238.29
GR30894X	CCCCCCOc1ccc(cc1)C(=O)O	C13H18O3	222.29
GR208752X	CCCCCOc1ccc(cc1)C(=O)O	C12H16O3	208.26
GW288377X	CCCCCCOc1c(C)cc(cc1C)C(=O)O	C15H22O3	250.34
GR34968X	CCOCCCCCCOc1ccc(cc1)C(=O)O	C15H22O4	266.34
GR54392X	CC(CCC1C(C)CCCC1(C)C)COc2ccc(cc2)C(=O)O	C21H32O3	332.49
GR57352X	CC1CCCC(C)(C)C1CCCCOc2ccc(cc2)C(=O)O	C20H30O3	318.46
GW371223X	OC(=O)c1ccc(OC2CCCCC2)cc1	C13H16O3	220.27
CCI9740	OCC(O)COc1ccc(cc1)C(=O)O	C10H12O5	212.20
GR240724X	CC(C)CCOc1ccc(cc1)C(=O)O	C12H16O3	208.26
GR30476X	CCCCOc1ccc(cc1)C(=O)O	C11H14O3	194.23
GR53056X	OC(COc1ccc(cc1)C(=O)O)CC#N	C11H11NO4	221.22
GR136670X	OC(=O)c1cc(I)c(OC2CCCC=C2)c(I)c1	C13H12I2O3	470.05
GR34039X	OC(=O)c1ccc(OC2CCCC=C2)cc1	C13H14O3	218.26
AH24908A	CCCc1c(O)c(ccc1OCCCCCCCCCCOc2ccc(C(=O)O)c(O)c2)C(=O)C	C27H36O7	472.58
GR49928X	CCCc1c(O)c(ccc1OCCCCOc2ccc(C(=O)O)c(O)c2)C(=O)C	C22H26O7	402.45
AH25368X	CCCCC(CCOc1ccc(C(=O)O)c(O)c1)Oc2ccc(C(=O)C)c(O)c2	C22H26O7	402.45
GR55422X	CCCc1ccccc1OCCCCCOc2ccc(cc2)C(=O)O	C21H26O4	342.44
GR55423X	CCCc1ccccc1OCCCCCCOc2ccc(cc2)C(=O)O	C22H28O4	356.47
GR61326X	CCCc1ccccc1OCCCCCCCCOc2ccc(cc2)C(=O)O	C24H32O4	384.52
GR61891X	CCCc1ccccc1OCCCCCCCCCCOc2ccc(cc2)C(=O)O	C26H36O4	412.57
GR61984X	CCCc1ccccc1OCCCCCCCCCCCCOc2ccc(cc2)C(=O)O	C28H40O4	440.63
GR61985X	CCCc1ccccc1OCCCCCCCCCOc2ccc(cc2)C(=O)O	C25H34O4	398.55

Reg No	Smiles String	Formula	MW
GR55424X	CCCc1ccccc1OCCCCOc2ccc(cc2)C(=O)O	C20H24O4	328.41
AH5157	CC(C)(C)NCC(O)COc1ccc(O)c(c1)C(=O)O	C14H21NO5	283.33
AH6770	COC(=O)c1ccc(cc1OC(=O)C)C(=O)O	C11H10O6	238.20
AH9603	OCCOc1cccc(c1)C(=O)O	C9H10O4	182.18
GW315367X	OC(=O)c1cc(OCCOc2ccc(O)c(c2)C(=O)O)ccc1O	C16H14O8	334.29
GR219955X	OCCOc1cc(cc(O)c1C(=O)O)C(=O)O	C10H10O7	242.19
GR120092X	CC(C)(C)OC(=O)COc1ccc(N)c(c1)C(=O)O	C13H17NO5	267.28
GR75258X	OC(=O)C(=C)Oc1cc(ccc1O)C(=O)O	C10H8O6	224.17
GF233967X	CCOc1ccc(cc1OCC)C(=O)O	C11H14O4	210.23
GW641533X	OC(=O)c1ccc2OCCOCCOc3ccc(cc3OCCOCCOc2c1)C(=O)O	C22H24O10	448.43
GW321911X	OC(=O)c1ccc2OCCCOc2c1	C10H10O4	194.19
GW402775X	CCCOc1cc(cc(CCC)c1OCCC)C(=O)O	C16H24O4	280.37
GR258179X	CCOCCOc1c(OCc2ccccc2)cc(cc1OCc3ccccc3)C(=O)O	C25H26O6	422.48
GR258213X	OC(=O)c1cc(OCc2ccccc2)c(OCCOCc3ccccc3)c(OCc4ccccc4)c1	C30H28O6	484.55
GF267695X	OC(=O)c1ccc2OCCOc2c1	C9H8O4	180.16
GW322088X	Cc1cc2OCCOc2cc1C(=O)O	C10H10O4	194.19
GW322112X	OC(=O)c1cc2OCCOc2cc1C(=O)O	C10H8O6	224.17
GW322316X	COc1cc(cc2OCCOc12)C(=O)O	C10H10O5	210.19
GW322086X	CC1Oc2ccc(cc2OC1C)C(=O)O	C11H12O4	208.22
GR222247X	COc1ccc(Nc2ccc3OCOc3c2)c(c1)C(=O)O	C15H13NO5	287.28
GR53849X	CC1(C)Oc2cc(N)c(cc2O1)C(=O)O	C10H11NO4	209.20
GR99312X	Cc1ccc(C(=O)O)c2OC(C)(C)Oc21	C11H12O4	208.22
GR57082X	OC(=O)c1ccc(OC2CCCCO2)cc1	C12H14O4	222.24
GW320929X	OC(=O)c1cc(OC2CCCCO2)cc(OC3CCCCO3)c1	C17H22O6	322.36
GW412113X	OC[C@H]1O[C@@H](Oc2ccc(cc2)C(=O)O)[C@H](O)[C@@H](O)[C@@H]1O	C13H16O8	300.27
GR215780X	CN(C)C(=O)c1c(O)cc(cc1OCCO)C(=O)O	C12H15NO6	269.26
GR219957X	CNC(=O)c1c(O)cc(cc1OCCO)C(=O)O	C11H13NO6	255.23
GR219958X	CNC(=O)c1c(O)cc(cc1OCCOCCO)C(=O)O	C13H17NO7	299.28
GR216184X	CCCCOc1cc(cc(OCCCC)c1C(=O)N(C)C)C(=O)O	C18H27NO5	337.42

Reg No	Smiles String	Formula	MW
GR216186X	CCCCOc1cc(cc(O)c1C(=O)N(C)C)C(=O)O	C14H19NO5	281.31
GR218004X	CCCCOc1cc(cc(OCCCC)c1C(=O)NC)C(=O)O	C17H25NO5	323.39
GR218005X	CCCCOc1cc(cc(O)c1C(=O)NC)C(=O)O	C13H17NO5	267.28
GR133748X	CCCCOc1cc(OCCCC)cc(c1)C(=O)O	C15H22O4	266.34
GR82836X	CC(C)CCOc1cc(OCCC(C)C)cc(c1)C(=O)O	C17H26O4	294.39
GR38662X	CCCCOc1cccc(c1)C(=O)O	C11H14O3	194.23
GW292734X	OC(=O)c1cccc(OCCCCCOc2cccc(c2)C(=O)O)c1	C19H20O6	344.37
GW322234X	CCCCOc1ccc(O)c(c1)C(=O)O	C11H14O4	210.23
GR79956X	CC(=C)COc1cc(OCC(=C)C)cc(c1)C(=O)O	C15H18O4	262.31
GR203866X	CCCCCCCCCCCCCCCCCCCCOc1cc(cc(c1)C(=O)O)C(=O)O	C26H42O5	434.62
GR203872X	CCCCCCCCCOc1cc(cc(c1)C(=O)O)C(=O)O	C16H22O5	294.35
GR203875X	CCCCCOc1cc(cc(c1)C(=O)O)C(=O)O	C13H16O5	252.27
GR204301X	CCCCCCCCCCOc1cccc(c1)C(=O)O	C17H26O3	278.40
GR65881X	CCCCCCCCCCCCCCCCCCCCOc1cccc(c1)C(=O)O	C25H42O3	390.61
GR65883X	CCCCCCCCCCCCCCCCCCOc1cccc(c1)C(=O)O	C23H38O3	362.56
GR65885X	CCCCCCCCCCCCCCCCOc1cccc(c1)C(=O)O	C21H34O3	334.50
GR188442X	CCCCCCOc1cc(C(=O)O)c(OCCCCCC)cc1C(=O)O	C20H30O6	366.46
GW322235X	CCCCOc1ccc(OC(=O)C)c(c1)C(=O)O	C13H16O5	252.27
GW327773X	OC(=O)CCCCOc1cccc(C(=O)O)c1C=O	C13H14O6	266.25
GW643493X	CCCCCCOc1c(C(=O)O)c(C(=O)O)c(OCCCCCC)c2ccccc12	C24H32O6	416.52
GW643495X	CCCCOc1c(C(=O)O)c(C(=O)O)c(OCCCC)c2ccccc12	C20H24O6	360.41
GR215459A	CC(C)CCCOc1cc(NC(=N)N)cc(c1)C(=O)O.OC(=O)C(F)(F)F	C14H21N3O3. C2HF3O2	393.37
GW280814	Nc1ccc(cc1OCCCCCC(=O)O)C(=O)O	C13H17NO5	267.28
GW290851X	Nc1ccc(cc1OCCCCC(=O)O)C(=O)O	C12H15NO5	253.26
GW290862X	Nc1ccc(cc1OCCCC(=O)O)C(=O)O	C11H13NO5	239.23
GW326112X	CCCCCC(=O)Oc1ccc(CC(=O)Nc2ccccc2)c(c1)C(=O)O	C21H23NO5	369.42
GW271929X	CCCCCCOc1cc(cc(OC)c1OC)C(=O)O	C15H22O5	282.34
GW317768X	COc1cc(cc(OCCCCCCCCCCCCCCCCOc2cc(cc(OC)c2OC)C(=O)O)c1OC)C(=O)O	C32H46O10	590.72
GW272447X	COc1cc(cc(OC)c1OCCCCCOc2c(OC)cc(cc2OC)C(=O)O)C(=O)O	C23H28O10	464.47

Reg No	Smiles String	Formula	MW
GW326127X	COc1cc(cc(OC)c1OCCCCCCCCCCCCOc2c(OC)cc(cc2OC)C(=O)O)C(=O)O	C30H42O10	562.66
GW440381X	CCCCCCCCCCCCCCCCOc1c(OC)cc(cc1OC)C(=O)O	C25H42O5	422.61
GW418716X	CCCCCCOc1c(OC)cc(cc1OC)C(=O)O	C15H22O5	282.34
GW453080X	CCCCCCOc1ccc(cc1OC)C(=O)O	C14H20O4	252.31
GW442734X	COc1cc(cc(OC)c1OCCCCC=C)C(=O)O	C15H20O5	280.32
GW272478X	COc1cc(cc(OC)c1OCCC2CCCC2)C(=O)O	C16H22O5	294.35
GW442732X	COc1cc(cc(OC)c1OCC2CCCCC2)C(=O)O	C16H22O5	294.35
GW415699X	CCCCCCOc1cc(cc(OCc2ccccc2)c1OC)C(=O)O	C21H26O5	358.44
GW369764X	CCCCCCOc1c(Cl)cc(cc1OC)C(=O)O	C14H19ClO4	286.76
GR50838A	NCc1ccccc1.OC(=O)c1cccc2OC(COCc3ccccc3)C(COCc4ccccc4)Oc12	C25H24O6. C7H9N	527.62
GR51678X	OC(=O)c1sc(C(=O)O)c2OC(COCc3ccccc3)C(COCc4ccccc4)Oc12	C24H22O8S	470.50
GR54219X	OC(=O)c1oc(C(=O)O)c2OC(COCc3ccccc3)C(COCc4ccccc4)Oc12	C24H22O9	454.44
GR69421X	OC(=O)c1oc(C(=O)NCc2ccccc2)c3OC4CNCC4Oc13	C17H16N2O6	344.33
GW317904X	CC(C)N1CC(COc2cc(cc3ccccc23)C(=O)O)OC1=O	C18H19NO5	329.36
GW411913X	COc1ccc(cc1OCC2CN(C(C)C)C(=O)O2)C(=O)O	C15H19NO6	309.32
GW327989X	CC(C)N1CC(COc2ccc(cc2)C(=O)O)OC1=O	C14H17NO5	279.30
GW414889X	COc1cc(OCC2CN(C(C)C)C(=O)O2)ccc1C(=O)O	C15H19NO6	309.32
AH10104A	Cl.CN(C)CCN(C)c1ccc2C(=O)c3ccc(cc3C(=O)c2c1)C(=O)O	C20H20N2O4. HCl	388.85
AH7702	OCCN(CCO)c1ccc2C(=O)c3ccc(cc3C(=O)c2c1)C(=O)O	C19H17NO6	355.35
AH7559	CN(C)c1ccc2C(=O)c3ccc(cc3C(=O)c2c1)C(=O)O	C17H13NO4	295.30
AH10011A	Cl.OCCN1CCN(CC1)c2ccc3C(=O)c4ccc(cc4C(=O)c3c2)C(=O)O	C21H20N2O5. HCl	416.87
AH7724Z	CN(C)CCO.OC(=O)c1ccc2C(=O)c3cc(ccc3C(=O)c2c1)N4CCCCC4	C20H17NO4. C4H11NO	424.50
GW575621X	OCCNc1c(ccc2C(=O)c3ccccc3C(=O)c12)C(=O)O	C17H13NO5	311.30
AH10424A	Cl.OC(=O)c1ccc2C(=O)c3ccc(NCCN4CCOCC4)cc3C(=O)c2c1	C21H20N2O5. HCl	416.87
AH7620Z	CN(C)CCO.OC(=O)c1ccc2C(=O)c3cc(ccc3C(=O)c2c1)N4CCOCC4	C19H15NO5. C4H11NO	426.47
AH7699	CC1CN(CC(C)O1)c2ccc3C(=O)c4ccc(cc4C(=O)c3c2)C(=O)O	C21H19NO5	365.39
AH5961	OC(=O)c1ccc2C(=O)c3ccccc3C(=O)c2c1N(=O)=O	C15H7NO6	297.23
AH6102	Nc1c(ccc2C(=O)c3ccccc3C(=O)c12)C(=O)O	C15H9NO4	267.24
AH7647	Nc1cc2C(=O)c3ccccc3C(=O)c2cc1C(=O)O	C15H9NO4	267.24

Reg No	Smiles String	Formula	MW
AH9531	CCOc1ccc(Nc2c(ccc3C(=O)c4ccccc4C(=O)c23)C(=O)O)cc1	C23H17NO5	387.40
GR199045X	OC(=O)c1ccc2C(=O)c3ccccc3C(=O)c2c1Nc4ccc-5c(Cc6ccccc65)c4	C28H17NO4	431.45
AH5724	OC(=O)c1ccc2C(=O)c3ccccc3C(=O)c2c1	C15H8O4	252.23
GW295014X	Cc1ccc2C(=O)c3ccc(cc3C(=O)c2c1)C(=O)O	C16H10O4	266.26
GW315237X	OC(=O)c1ccc2C(=O)c3cc(ccc3C(=O)c2c1)C(=O)O	C16H8O6	296.24
GW315238X	OC(=O)c1ccc2C(=O)c3ccc(cc3C(=O)c2c1)C(=O)O	C16H8O6	296.24
AH6593	OC(=O)c1cc2C(=O)c3ccccc3C(=O)c2cc1C(=O)O	C16H8O6	296.24
GW315239X	Cc1cc2C(=O)c3ccccc3C(=O)c2cc1C(=O)O	C16H10O4	266.26
AH6247	OC(=O)c1ccc2Cc3ccccc3C(=O)c2c1	C15H10O3	238.25
AH6313	OC(=O)c1ccc2C(=O)c3ccccc3Cc2c1	C15H10O3	238.25
AH6072	OC(=O)c1cccc2C(=O)c3ccccc3C(=O)c12	C15H8O4	252.23
AH6624	NC(=O)c1cc2C(=O)c3ccccc3C(=O)c2cc1C(=O)O	C16H9NO5	295.25
AH7013Z	CN(C)CCO.OC(=O)c1ccc2C(=O)c3ccc(F)cc3C(=O)c2c1	C15H7FO4. C4H11NO	359.36
AH7014Z	CN(C)CCO.OC(=O)c1ccc2C(=O)c3cc(F)ccc3C(=O)c2c1	C15H7FO4. C4H11NO	359.36
AH6198	OC(=O)c1ccc2C(=O)c3ccccc3C(=O)c2c1Cl	C15H7ClO4	286.67
AH6248	OC(=O)c1ccc2C(=O)c3c(Cl)cccc3C(=O)c2c1	C15H7ClO4	286.67
AH7031Z	CN(C)CCO.OC(=O)c1ccc2C(=O)c3cccc(Cl)c3C(=O)c2c1	C15H7ClO4. C4H11NO	375.81
AH7029	OC(=O)c1ccc2Cc3c(Cl)cccc3C(=O)c2c1	C15H9ClO3	272.69
AH6292	OC(=O)c1cc2C(=O)c3ccccc3C(=O)c2cc1Cl	C15H7ClO4	286.67
AH6570	OC(=O)c1ccc2C(=O)c3ccc(Cl)cc3C(=O)c2c1	C15H7ClO4	286.67
AH7083Z	CN(C)CCO.OC(=O)c1ccc2C(=O)c3cc(Cl)ccc3C(=O)c2c1	C15H7ClO4. C4H11NO	375.81
GR240517X	OC(=O)c1ccc2Cc3ccc(Cl)cc3C(=O)c2c1	C15H9ClO3	272.69
AH6169K	[K+].OC(=O)c1ccc2C(=O)c3ccccc3C(=O)c2c1S(=O)(=O)[O-]	C15H7O7S-. K+	370.39
GW315217X	OC(=O)c1ccc2C(=O)c3cc(ccc3C(=O)c2c1)S(=O)(=O)O	C15H8O7S	332.29
AH11654	CC(C)Oc1ccc2C(=O)c3ccc(cc3C(=O)c2c1)C(=O)O	C18H14O5	310.31
AH14868XX	CC(C)Oc1ccc2C(=O)c3cc(ccc3C(=O)c2c1)C(=O)O	C18H14O5	310.31
AH7167	OCCCOc1ccc2C(=O)c3ccc(cc3C(=O)c2c1)C(=O)O	C18H14O6	326.31
AH7792Z	CN(C)CCO.OCCCOc1ccc2C(=O)c3cc(ccc3C(=O)c2c1)C(=O)O	C18H14O6. C4H11NO	415.45
AH7650	CCCOc1ccc2C(=O)c3ccc(cc3C(=O)c2c1)C(=O)O	C18H14O5	310.31

Reg No	Smiles String	Formula	MW
AH6730	COc1ccc2C(=O)c3cc(ccc3C(=O)c2c1)C(=O)O	C16H10O5	282.26
AH7290A	Cl.CN(C)CCOc1ccc2C(=O)c3ccc(cc3C(=O)c2c1)C(=O)O	C19H17NO5. HCl	375.81
AH7652	OC(=O)c1ccc2C(=O)c3ccc(OCCc4ccccc4)cc3C(=O)c2c1	C23H16O5	372.38
AH7414Z	COCCOc1ccc2C(=O)c3ccc(cc3C(=O)c2c1)C(=O)O.CN(C)CCO	C18H14O6. C4H11NO	415.45
AH7621Z	CN(C)CCO.OCCOc1ccc2C(=O)c3cc(ccc3C(=O)c2c1)C(=O)O	C17H12O6. C4H11NO	401.42
AH7552	OC(=O)c1ccc2C(=O)c3ccc(OCCOc4ccccc4)cc3C(=O)c2c1	C23H16O6	388.38
AH7651	COCCOCCOc1ccc2C(=O)c3ccc(cc3C(=O)c2c1)C(=O)O	C20H18O7	370.36
AH7697	OC(=O)c1ccc2C(=O)c3ccc(OCc4ccco4)cc3C(=O)c2c1	C20H12O6	348.32
AH6276	OC(=O)c1cc(O)c2C(=O)c3ccccc3C(=O)c2c1	C15H8O5	268.23
GR85411X	OC(=O)c1cc(O)c2C(=O)c3c(O)cccc3C(=O)c2c1	C15H8O6	284.23
AH6390	OC(=O)c1ccc2C(=O)c3c(O)ccc(O)c3C(=O)c2c1	C15H8O6	284.23
GR65254X	OC(=O)c1ccc2C(=O)c3c(O)cccc3C(=O)c2c1	C15H8O5	268.23
AH6535	OC(=O)c1ccc2C(=O)c3ccccc3C(=O)c2c1O	C15H8O5	268.23
AH6712	OC(=O)c1ccc2C(=O)c3c(O)cc(O)cc3C(=O)c2c1	C15H8O6	284.23
AH7646	OC(=O)c1cc2C(=O)c3ccccc3C(=O)c2cc1O	C15H8O5	268.23
GR257968X	CC1(O)c2cccc(O)c2C(=O)c3c(O)c(C(=O)O)c(cc31)C(=O)O	C17H12O8	344.28
AH6342	COc1cc(cc2C(=O)c3ccccc3C(=O)c12)C(=O)O	C16H10O5	282.26
AH6572	COc1cccc2C(=O)c3cc(ccc3C(=O)c12)C(=O)O	C16H10O5	282.26
AH7133	COc1cccc2C(=O)c3ccc(cc3C(=O)c12)C(=O)O	C16H10O5	282.26
GW321108X	COc1c(ccc2C(=O)c3ccccc3C(=O)c12)C(=O)O	C16H10O5	282.26
AH6550	COc1ccc(OC)c2C(=O)c3cc(ccc3C(=O)c12)C(=O)O	C17H12O6	312.28
GR242642X	COc1cc(OC)c2C(=O)c3ccc(cc3C(=O)c2c1)C(=O)O	C17H12O6	312.28
AH6573	CCCOc1cccc2C(=O)c3cc(ccc3C(=O)c12)C(=O)O	C18H14O5	310.31
AH6714	CCOc1cccc2C(=O)c3cc(ccc3C(=O)c12)C(=O)O	C17H12O5	296.28
AH6759	OCCCOc1c(ccc2C(=O)c3ccccc3C(=O)c12)C(=O)O	C18H14O6	326.31
AH6713	OC(=O)c1ccc2C(=O)c3c(Oc4ccccc4)cccc3C(=O)c2c1	C21H12O5	344.33
AH7696	COc1ccccc1Oc2ccc3C(=O)c4ccc(cc4C(=O)c3c2)C(=O)O	C22H14O6	374.35
AH7731	OC(=O)c1ccc2C(=O)c3ccc(Oc4ccccc4O)cc3C(=O)c2c1	C21H12O6	360.33
AH2671	OC(=O)c1cccc2C(=O)c3ccccc3-c21	C14H8O3	224.22

Reg No	Smiles String	Formula	MW
GR139602	OC(=O)c1cccc2Cc3ccccc3-c21	C14H10O2	210.24
GW433974	OC1c2ccccc2-c3c1cccc3C(=O)O	C14H10O3	226.23
GW321876	OC(=O)c1ccc-2c(c1)C(=O)c3cccc(C(=O)O)c32	C15H8O5	268.23
GR139604	Cc1ccc(C(=O)O)c-2c1Cc3ccccc32	C15H12O2	224.26
GW321338X	Cc1c2C(=O)c3ccccc3-c2ccc1C(=O)O	C15H10O3	238.25
GW343619X	OC1c2cccc(c2-c3ccc(cc13)C(=O)O)C(F)(F)F	C15H9F3O3	294.23
AH2672	OC(=O)c1ccc-2c(c1)C(=O)c3ccccc32	C14H8O3	224.22
GR85308	OC(=O)c1ccc-2c(c1)C(=O)c3cc(ccc32)C(=O)O	C15H8O5	268.23
GW321553X	OC(=O)c1ccc-2c(c1)C(=O)c3cc(ccc32)C(=O)c4ccccc4	C21H12O4	328.33
GW368591A	NCCO.OC(=O)c1ccc-2c(c1)C(=O)c3cc(Cc4ccc-5c(c4)C(=O)c6cc(ccc65)C(=O)O)ccc32	C29H16O6. 2(C2H7NO)	582.62
GR115690	OC(=O)c1ccc-2c(Cc3cc(C=O)ccc32)c1	C15H10O3	238.25
GR176137	OC(=O)c1ccc-2c(Cc3ccccc32)c1	C14H10O2	210.24
GW321167	OC(=O)c1ccc-2c(Cc3cc(ccc32)C(=O)O)c1	C15H10O4	254.25
GW320968X	OC1c2ccccc2-c3ccc(cc13)C(=O)O	C14H10O3	226.23
GW321421	OC(=O)c1ccc-2c(c1)C(=O)c3cc(C#N)ccc32	C15H7NO3	249.23
GW315288X	OC(=O)c1ccc-2c(c1)C(=O)c3cc(Br)ccc32	C14H7BrO3	303.11
GW315296X	OC(=O)c1ccc-2c(c1)C(=O)c3cc(Cl)ccc32	C14H7ClO3	258.66
GW288615	CCC(=O)c1ccc-2c(c1)C(=O)c3cc(ccc32)C(=O)O	C17H12O4	280.28
GW321424X	CCC(=O)c1ccc-2c(Cc3cc(ccc32)C(=O)O)c1	C17H14O3	266.30
GW321634X	CCCCc1ccc-2c(c1)C(=O)c3cc(ccc32)C(=O)O	C18H16O3	280.33
GW321145	CC(=O)c1ccc-2c(Cc3cc(ccc32)C(=O)O)c1	C16H12O3	252.27
GW321168X	CC(=O)c1ccc-2c(c1)C(=O)c3cc(ccc32)C(=O)O	C16H10O4	266.26
GW321422X	CCc1ccc-2c(c1)C(=O)c3cc(ccc32)C(=O)O	C16H12O3	252.27
GW322230X	OC(=O)c1ccc-2c(c1)C(=O)c3cc(ccc32)c4nnn[nH]4	C15H8N4O3	292.26
GW314379	CCCOc1ccc-2c(c1)C(=O)c3cc(ccc32)C(=O)O	C17H14O4	282.30
GW314406X	CCCOc1ccc-2c(Cc3cc(ccc32)C(=O)O)c1	C17H16O3	268.32
GW321354X	COc1ccc-2c(c1)C(=O)c3cc(ccc32)C(=O)O	C15H10O4	254.25
GW321243X	CC(=O)OC1c2ccccc2-c3ccc(cc13)C(=O)O	C16H12O4	268.27
GW321742X	CCCCOC(=O)c1ccc-2c(c1)C(=O)c3cc(ccc32)C(=O)O	C19H16O5	324.34

Reg No	Smiles String	Formula	MW
GW321779X	CCC(C)OC(=O)c1ccc-2c(c1)C(=O)c3cc(ccc32)C(=O)O	C19H16O5	324.34
GW321755X	CCCCCCOC(=O)c1ccc-2c(c1)C(=O)c3cc(ccc32)C(=O)O	C21H20O5	352.39
GW410928X	CC(C)OC(=O)c1ccc-2c(c1)C(=O)c3cc(ccc32)C(=O)O	C18H14O5	310.31
GW324540X	CCCOC(=O)c1ccc-2c(c1)C(O)c3cc(ccc32)C(=O)O	C18H16O5	312.33
GW322198X	OC(=O)c1ccc-2c(c1)C(=O)c3cc(ccc32)S(=O)(=O)C(Br)(Br)Br	C15H7Br3O5S	539.00
GW322492X	CS(=O)(=O)c1ccc-2c(c1)C(=O)c3cc(ccc32)C(=O)O	C15H10O5S	302.31
GW320926X	ON=C1c2ccccc2-c3ccc(cc13)C(=O)O	C14H9NO3	239.23
GW321470X	ON=C1c2cc(ccc2-c3ccc(cc13)C(=O)O)C(=O)O	C15H9NO5	283.24
GW321607X	CON=C1c2ccccc2-c3ccc(cc13)C(=O)O	C15H11NO3	253.26
GW323008X	CCCOC(=O)c1ccc-2c(c1)C(=NO)c3cc(ccc32)C(=O)O	C18H15NO5	325.32
GR175627	OC(=O)c1cccc-2c1Cc3ccccc32	C14H10O2	210.24
GR175628	OC(=O)c1cccc2-c3ccccc3C(=O)c21	C14H8O3	224.22
GR196922	NN=C1c2ccccc2-c3cccc(C(=O)O)c13	C14H10N2O2	238.25
GR256963	OC(=O)c1ccc2C(=O)c3ccccc3-c2c1	C14H8O3	224.22
GW321245X	OC(=O)c1cc2C(=O)c3ccccc3-c2cc1C(=O)O	C15H8O5	268.23
GW321912X	OC(=O)c1ccc-2c(c1)C(=O)c3ccc(cc32)C(=O)O	C15H8O5	268.23
AH10033	COc1ccc(Nc2cc(Cl)ccc2C(=O)O)cn1	C13H11ClN2O3	278.70
GR237865X	Cc1cc(Nc2ccccc2C(=O)O)n(C)n1	C12H13N3O2	231.26
AH15255XX	CC(=O)Nc1ccc(cn1)C(=O)O	C8H8N2O3	180.17
GR68357X	OC(=O)c1cccnc1Nc2cccc(c2)C(F)(F)F	C13H9F3N2O2	282.22
GW320801X	OC(=O)c1ccc(NC(=N)c2ccccn2)cc1	C13H11N3O2	241.25
GW385455A	Cl.OC(=O)c1ccc(NCc2nc3ccccc3[nH]2)cc1	C15H13N3O2. HCl	303.75
AH11305	OC(=O)c1cc(nc2ccccc12)N3CCCCC3	C15H16N2O2	256.31
AH9723	CC(=O)Nc1cc(nc2ccccc12)C(=O)O	C12H10N2O3	230.23
GW655414X	CCn1cc(N2CCN(CC2)C(=S)N)c(=O)c3c(F)cc(cc13)C(=O)O	C17H19FN4O3S	378.43
GR107114X	CCCCc1nc2ccc(cc2n1Cc3ccc(cc3)C(=O)c4ccccc4C(=O)O)N(=O)=O.CCCCc1nc2cc(ccc2n1Cc3ccc(cc3)C(=O)c4ccccc4C(=O)O)N(=O)=O	C26H23N3O5/C26H23N3O5	914.98
GR138809X	COc1cc(ccc1Cc2cn(C)c3ccc(NC(=O)OC4CCCC4)cc23)C(=O)O	C24H26N2O5	422.49
GW295817X	CC(=O)c1ccc2NC(=O)c3ccc(cc3Sc2c1)C(=O)O	C16H11NO4S	313.33

Reg No	Smiles String	Formula	MW
GW365467X	OC(=O)c1ccc2Sc3ccccc3Nc2c1	C13H9NO2S	243.29
GW311376X	NC1=NN(CC1)c2ccc(cc2)C(=O)O	C10H11N3O2	205.22
GW397304X	COC(=O)CC1Nc2ccc(cc2CN(C)C1=O)C(=O)O	C14H16N2O5	292.29
GW584442X	OC(=O)c1cc2NCCC(=O)c2cc1Cl	C10H8ClNO3	225.63
GW635258X	CC(C)(C)C(=O)C(Oc1ccc(cc1)C(=O)O)C(=O)Nc2cc(N)ccc2Cl	C20H21ClN2O5	404.85
GW635452X	CC(C)(C)C(=O)C(Oc1ccc(cc1)C(=O)O)C(=O)Nc2ccc(Cl)cc2Cl	C20H19Cl2NO5	424.28
GR269503X	COC(=O)C1=CO[C@H](O)[C@H]2[C@@H]1Cc3nc(cc4c5cc(O)ccc5n([C@@H]2C)c34)C(=O)O	C22H20N2O7	424.41
GR223454A	Cl.COc1ccc2C[C@H]3N(C)CC[C@]4([C@H]5Oc1c24)[C@@]3(O)Cc6c5[nH]c7ccc(cc67)C(=O)O	C25H24N2O5. HCl	468.94
GW580127X	OC(=O)c1ccc(s1)C2N(CCc3c2[nH]c4ccccc34)C(=O)/C=C/c5ccccc5	C25H20N2O3S	428.51
GW623142A	CC(=O)O.OC(=O)c1ccc(s1)C2NCCc3c2[nH]c4ccccc34	C16H14N2O2S. C2H4O2	358.42
GW624854X	Nc1c(sc2nc(c3ccccc3)c4CCCCc4c12)C(=O)O	C18H16N2O2S	324.40
GW663118X	CCc1nc2sc(C(=O)O)c(N)c2c3CCCCc13	C14H16N2O2S	276.36
GW652611X	OC(=O)c1c(SCc2ccc(C#N)cc2)nc3CCCCc3c1c4ccccs4	C22H18N2O2S2	406.53
GR151827X	CCCCc1nn(CC)c(/C=C(/Cc2cccs2)\C(=O)O)c1Cc3ccc(cc3)C(=O)O	C25H28N2O4S	452.58
GR152989X	CCCCc1n[nH]c(/C=C(/Cc2cccs2)\C(=O)O)c1Cc3ccc(cc3)C(=O)O	C23H24N2O4S	424.52
AH11426	OC(=O)c1cnnc2ccccc12	C9H6N2O2	174.16
GR37359X	OC(=O)c1ccc2cn[nH]c2c1	C8H6N2O2	162.15
GW321066X	OC(=O)c1ccc2cnn(C(=O)OCc3ccccc3)c2c1	C16H12N2O4	296.29
CCI8732	OC(=O)c1ccc2nnn(O)c2c1	C7H5N3O3	179.14
GW312666X	COc1ccc(cc1)c2n[nH]c(=O)c3ccc(cc23)C(=O)O	C16H12N2O4	296.29
GW424662X	COc1ccc2c(C(=O)O)c(nn2n1)c3ccc(F)cc3	C14H10FN3O3	287.25
AH8940	OC(=O)c1cc(C(=O)O)c(cc1C(=O)Nc2nnn[nH]2)C(=O)Nc3nnn[nH]3.OC(=O)c1cc(C(=O)Nc2nnn[nH]2)c(cc1C(=O)Nc3nnn[nH]3)C(=O)O	C12H8N10O6/C12H8N10O6	776.52
GR258784X	OC(=O)c1ccccc1Oc2ccc(cc2)c3nnn[nH]3	C14H10N4O3	282.26
GW322374X	OC(=O)c1ccc(cc1Sc2ccccc2)c3nnn[nH]3	C14H10N4O2S	298.33
AH8076	COc1ccc2Cc3[nH]c(C)c(C(=O)O)c3-c2c1	C14H13NO3	243.27
GW315274X	OC(=O)c1ccn-2c1C(=O)c3ccccc32	C12H7NO3	213.20
GW650524X	Cc1[nH]c(C(=O)O)c(C#N)c1C(=O)c2ccccc2	C14H10N2O3	254.25
GW650525X	CCn1c(C)c(C(=O)c2ccccc2)c(C#N)c1C(=O)O	C16H14N2O3	282.30

Reg No	Smiles String	Formula	MW
AH9033	OC(=O)c1ccc2C(=O)c3ccccc3-c4ncnc1c24	C16H8N2O3	276.25
GW649399X	OC(=O)c1ccc2C(=O)c3ccccc3-c4n[nH]c1c42	C15H8N2O3	264.24
AH9527	OC(=O)c1ccc2-c3ccccc3C(=O)c4cccc1c42	C18H10O3	274.28
CCI4563	OC(=O)c1ccnc(c1)n2nnc3ccccc23	C12H8N4O2	240.22
GR154660A	Cl.Cc1ccc(c(c1)C(=O)O)n2ccc(=O)cc2	C13H11NO3. HCl	265.70
GR177049X	OC(=O)c1ccc(nc1)n2cccc2	C10H8N2O2	188.19
GR219652X	COc1ccc(cc1C(=O)O)n2nnnc2C	C10H10N4O3	234.22
GR249207X	Cc1c(cnn1c2ccccc2)C(=O)O	C11H10N2O2	202.22
GR118330	OC(=O)c1ccc2[nH]c(=O)oc(=O)c2c1	C9H5NO5	207.14
GW276690	Cc1nc2ccc(cc2c(=O)o1)C(=O)O	C10H7NO4	205.17
GR242234X	Cc1nn(Cc2ccc(o2)C(=O)O)c(C)c1Br	C11H11BrN2O3	299.13
GW283348X	CCn1ncc2c(NCc3ccccc3)c(cnc12)C(=O)O	C16H16N4O2	296.33
GW318076X	CCn1cc(C(=O)O)c(=O)c2cc(oc12)C(=O)O	C11H9NO6	251.20
GR37727X	Nc1nc(CC(=O)O)c(o1)C(=O)O	C6H6N2O5	186.13
GR53040X	OC(=O)c1cnc(Cc2ccccc2)o1	C11H9NO3	203.20
AH7643	OC(=O)c1cc(no1)c2ccccc2	C10H7NO3	189.17
AH9554	Cc1onc(c1C(=O)O)c2ccccc2	C11H9NO3	203.20
GR152077X	Cc1nc(no1)c2ccc(c(C)c2)c3ccc(cc3)C(=O)O	C17H14N2O3	294.31
GM189907X	Cc1noc(C)c1C(=O)O	C6H7NO3	141.13
GR39699X	Cc1cc(on1)C(=O)O	C5H5NO3	127.10
GR114312X	OC(=O)c1noc2ccccc12	C8H5NO3	163.13
AH11195B	Br.OC(=O)c1nc2ccccn2c1c3ccccc3	C14H10N2O2. HBr	319.16
GR239106X	Cc1nc2cccc(C)n2c1C(=O)O	C10H10N2O2	190.20
GR106841X	OC(=O)c1ncn2cc(ccc12)N(=O)=O	C8H5N3O4	207.15
AH6081A	Cl.Nc1ncnc2[nH]c(nc12)c3cccc(c3)C(=O)O	C12H9N5O2. HCl	291.70
GR240822X	OC(=O)c1ncnc2[nH]cnc12	C6H4N4O2	164.12
GW327515X	COc1cc(ccc1c2nc3cnccc3[nH]2)C(=O)O	C14H11N3O3	269.26
GW416086	COc1ccc(c2nc3cc(cnc3[nH]2)C(=O)O)c(OC)c1	C15H13N3O4	299.29
AH9652	OC(=O)c1nc[nH]c1C(=O)O	C5H4N2O4	156.10

Reg No	Smiles String	Formula	MW
GR44240X	Cn1c(S)ncc1C(=O)O	C5H6N2O2S	158.18
GR103163A	Cl.OC(=O)c1ccc(OCCn2ccnc2)cc1	C12H12N2O3. HCl	268.70
GW327758A	Cl.OC(=O)c1ccc(/C=C/Cn2ccnc2)cc1	C13H12N2O2. HCl	264.71
GW312641A	Cl.OC(=O)c1ccc(Cn2ccnc2)cc1	C11H10N2O2. HCl	238.68
GI138330X	OC(=O)c1cnc(S)nc1O	C5H4N2O3S	172.16
GW329078X	OC(=O)c1c(Cl)ncnc1Cl	C5H2Cl2N2O2	192.99
GR240576X	CCSc1ncc(C(=O)O)c(N)n1	C7H9N3O2S	199.23
GW315215	Cc1ncc(C(=O)O)c(N)n1	C6H7N3O2	153.14
GW412098	Cc1ncc(C(=O)O)c(NC(=S)S)n1	C7H7N3O2S2	229.28
GR108394X	CSc1ncc(Br)c(n1)C(=O)O	C6H5BrN2O2S	249.09
GR245706X	OC(=O)c1ncnc(O)c1Br	C5H3BrN2O3	219.00
GR117055X	OC(=O)c1ccnc(n1)c2ccccc2	C11H8N2O2	200.20
AH7461	CCCc1cc(Nc2ccccc2C(=O)O)nc(N)n1	C14H16N4O2	272.31
GW341377	Cc1cnc(N)nc1Nc2ccc(cc2)C(=O)O	C12H12N4O2	244.26
GW365140	Cc1cc(Nc2ccc(cc2)C(=O)O)nc(N)n1	C12H12N4O2	244.26
GW365173	Cc1nc(N)nc(Nc2ccc(cc2)C(=O)O)c1C	C13H14N4O2	258.28
GI261653	OC(=O)c1ccc(Nc2ncnc3ccccc23)cc1O	C15H11N3O3	281.27
GR242078X	Nc1ncnc(N)c1N=Cc2cccc(c2)C(=O)O	C12H11N5O2	257.25
GW308852X	Nc1nc(N)c(c2ccc(Cl)cc2Cl)c(n1)C(=O)O	C11H8Cl2N4O2	299.12
GW307512X	Nc1nc(N)c(CCCOc2ccc(cc2)C(=O)O)c(=O)[nH]1	C14H16N4O4	304.31
GW311866X	CC1(C)Nc2nc(N)[nH]c(=O)c2N=C1CCc3ccc(cc3)C(=O)O	C17H19N5O3	341.37
GW319241X	OC(=O)c1ccc(cc1O)n2cc(C#N)c(=O)[nH]c2=O	C12H7N3O5	273.21
GW448056X	CC(=O)c1cn(c2ccc(o2)C(=O)O)c(=O)[nH]c1=O	C11H8N2O6	264.20
GR258734A	CCN(CC)CC.OC(=O)c1ccc2c(=O)[nH]c(=N)[nH]c2c1	C9H7N3O3. C6H15N	306.37
GR264071A	Cn1c(=N)[nH]c2cc(ccc2c1=O)C(=O)O.OC(=O)C(F)(F)F	C10H9N3O3. C2HF3O2	333.23
GR263255X	OC(=O)c1ccc2c(=O)[nH]c(=O)[nH]c2c1	C9H6N2O4	206.16
GR43767X	OC(=O)c1ccc2nc[nH]c2c1	C8H6N2O2	162.15
GW472535X	OC(=O)c1ccc2c(O)ncnc2c1	C9H6N2O3	190.16
GW288946X	Cn1c2cc(nn2c(=O)c3cc(N)ccc13)C(=O)O	C12H10N4O3	258.24

Reg No	Smiles String	Formula	MW
GW324060X	OC(=O)c1cccc2nc3CCCn3c(=O)c12	C12H10N2O3	230.23
AH10315	Nc1c(nnn1Cc2ccccc2)C(=O)O	C10H10N4O2	218.22
AH10461	Nc1c(nnn1C2CCCCC2)C(=O)O	C9H14N4O2	210.24
GR105716X	Cn1ncc(n1)C(=O)O	C4H5N3O2	127.10
GR212122X	OC(=O)c1[nH]nnc1Nc2ccccc2	C9H8N4O2	204.19
AH22431B	[K+].Cc1cc(n[nH]1)C(=O)[O-]	C5H5N2O2-. K+	164.21
GR109361X	OC(=O)c1n[nH]cc1N(=O)=O	C4H3N3O4	157.09
GR60436X	CCCCCCCCCCCCCc1cc(n[nH]1)C(=O)O	C17H30N2O2	294.44
AH6087	Cn1ncc(C(=O)O)c1N	C5H7N3O2	141.13
GI163641X	OC(=O)c1cn[nH]c1	C4H4N2O2	112.09
CCI153	OC(=O)c1csnn1	C3H2N2O2S	130.13
GR128873	OC(=O)c1nnsc1CN=[N+]=[N-]	C4H3N5O2S	185.17
GR75538X	OC(=O)c1snnc1c2ccccc2	C9H6N2O2S	206.22
GR35345A	[Na+].Oc1nsnc1C(=O)[O-]	C3HN2O3S-. Na+	168.11
GR49747X	CCSc1snc(O)c1C(=O)O	C6H7NO3S2	205.26
GR51603A	N.OC(=O)c1nonc1O	C3H2N2O4. 2(H3N)	164.12
GR85161X	OC(=O)c1nonc1OCc2ccc(Cl)c(Cl)c2	C10H6Cl2N2O4	289.08
AH10536	OC(=O)c1nc2ccccc2nc1O	C9H6N2O3	190.16
AH10767	OC(=O)c1cnc2ccccc2n1	C9H6N2O2	174.16
AH9356	OC(=O)c1nc2ccccc2nc1C(=O)O	C10H6N2O4	218.17
GW316125	CCOC(=O)c1nc2cc(ccc2nc1O)C(=O)O	C12H10N2O5	262.22
CCI10174	OC(=O)c1nccnc1C(=O)O	C6H4N2O4	168.11
GR263958X	NC(=O)c1nccnc1C(=O)O	C6H5N3O3	167.13
GW433821A	Cl.OC(=O)c1cncc(n1)c2ccc(F)cc2	C11H7FN2O2. HCl	254.65
CCI10446	CC(=O)Nc1ncc(s1)C(=O)O	C6H6N2O3S	186.19
GR138218X	OC(=O)c1ccccc1C(=O)Nc2nccs2	C11H8N2O3S	248.26
GW349042X	OC(=O)c1ccc2ncsc2c1	C8H5NO2S	179.20
GR44479X	Cc1nc(C)c(s1)C(=O)O	C6H7NO2S	157.19
GR66484X	OC(=O)c1cscn1	C4H3NO2S	129.14

Reg No	Smiles String	Formula	MW
GW449422A	Cl.CC(C)C(N)c1nc(cs1)C(=O)O	C8H12N2O2S. HCl	236.72
GI204510X	OC(=O)c1csc(n1)c2cccnc2	C9H6N2O2S	206.22
GR239579X	OC(=O)c1csc(n1)c2ccc3nonc3c2	C10H5N3O3S	247.23
GW352006X	OC(=O)c1csc(n1)c2sccc2Br	C8H4BrNO2S2	290.16
GI233445X	OC(=O)c1csc(n1)C2COc3ccccc3O2	C12H9NO4S	263.27
GR239577X	Cc1nc(COc2ccc3nonc3c2)sc1C(=O)O	C12H9N3O4S	291.29
AH1010	Nc1cnccc1C(=O)O	C6H6N2O2	138.13
CCI21414	OC(=O)c1ccncc1	C6H5NO2	123.11
GI222692X	Cc1cc(cc(Cl)n1)C(=O)O	C7H6ClNO2	171.58
GR84679X	CN(C)CC#Cc1cc(ccn1)C(=O)O	C11H12N2O2	204.23
GR84985A	Cl.CN(C)CCCc1cc(ccn1)C(=O)O	C11H16N2O2. 2(HCl)	281.18
AH10182	OC(=O)c1ccncc1C(=O)c2ccccc2	C13H9NO3	227.22
GR203336X	OC(=O)c1ccnc(c1)C(=O)c2ccccc2	C13H9NO3	227.22
AH20998XX	COC(=O)c1ccn(=O)cc1C(=O)O	C8H7NO5	197.15
AH6595	OC(=O)c1cccn(=O)c1	C6H5NO3	139.11
AH21933X	OC(=O)c1ccc(Cl)nc1	C6H4ClNO2	157.56
GR154396X	OC(=O)c1cncc(Br)c1	C6H4BrNO2	202.01
GW408146X	OC(=O)c1ccc(C#N)nc1	C7H4N2O2	148.12
AH6732	OC(=O)c1cccnc1Sc2ccccc2	C12H9NO2S	231.28
GR208133X	OC(=O)c1cccnc1S	C6H5NO2S	155.18
AH1031	Nc1cccnc1C(=O)O	C6H6N2O2	138.13
AH16943AA	OC(=O)c1ccc(N(=O)=O)c(n1)C(=O)O	C7H4N2O6	212.12
AH1052	OC(=O)c1ncccc1O	C6H5NO3	139.11
CCI21405	OC(=O)c1ccnc(c1)C(=O)O	C7H5NO4	167.12
AH11453	OC(=O)c1cc(Cl)ccn1	C6H4ClNO2	157.56
CCI10176	OC(=O)c1cccnc1C(=O)O	C7H5NO4	167.12
AH10633	COc1ccnc(c1)C(=O)O	C7H7NO3	153.14
GW369905	OC(=O)c1cc(OCc2ccccc2)ccn1	C13H11NO3	229.24
AH8268A	Cl.COc1cccc(COc2cccnc2C(=O)O)c1	C14H13NO4. HCl	295.73

Reg No	Smiles String	Formula	MW
GR202022X	CCCCC1CCC(CC1)c2ccc(nc2)C(=O)O	C16H23NO2	261.37
GR34043X	CCCCc1ccc(nc1)C(=O)O	C10H13NO2	179.22
GR247048X	CCCCCc1c(N)c(nc2cc(C)c(C)cc12)C(=O)O	C17H22N2O2	286.38
GW309880X	OC(=O)CCCCc1ccnc(c1)C(=O)O	C11H13NO4	223.23
GR230760X	OC(=O)Cc1cccnc1C(=O)O	C8H7NO4	181.15
GW299526X	CCOC(=O)Cc1ncccc1C(=O)O	C10H11NO4	209.20
AH10225	OC(=O)c1cnc2ccccc2c1O	C10H7NO3	189.17
AH11688	COc1cc2ncc(C(=O)O)c(O)c2cc1OC	C12H11NO5	249.23
GR258750	OC(=O)c1cnc2ccc(OC(F)(F)F)cc2c1O	C11H6F3NO4	273.17
AH11368	COc1ccc(OC)c2c(O)c(cnc12)C(=O)O	C12H11NO5	249.23
GI266527	CCCCOc1cccc2c(O)c(cnc12)C(=O)O	C14H15NO4	261.28
AH11967	Cc1cc2c(O)c(cnc2c(C)n1)C(=O)O	C11H10N2O3	218.21
GR140330X	CC(C)c1cc(C(=O)O)c2ccccn12	C12H13NO2	203.24
GR216655X	Cc1nc2ncccc2cc1C(=O)O	C10H8N2O2	188.19
GR220880X	OC(=O)c1cc2cnccc2nc1C(F)(F)F	C10H5F3N2O2	242.16
GR232939X	OC(=O)c1cc2sccc2nc1C(F)(F)F	C9H4F3NO2S	247.20
AH1053	OC(=O)c1cccnc1O	C6H5NO3	139.11
AH6596	OC(=O)c1cccnc1Oc2ccccc2	C12H9NO3	215.21
AH12133	CCOc1ccc2c(O)c(cnc2n1)C(=O)O	C11H10N2O4	234.21
AH13394	OC(=O)c1cccnc1OCCc2ccccc2	C14H13NO3	243.27
GW299375X	CCCCOc1ccc(cn1)C(=O)O	C10H13NO3	195.22
AH3663	OC(=O)COc1cnccc1C(=O)O	C8H7NO5	197.15
GR239599X	CCOc1cc(cnc1C(=O)O)C(F)(F)F	C9H8F3NO3	235.16
AH11395	OC(=O)c1cc(O)nc2ccccc12	C10H7NO3	189.17
AH13826XX	OC(=O)c1c2ccccc2nc3ccccc13	C14H9NO2	223.23
GR54987X	OC(=O)c1cc(Cl)nc2ccccc12	C10H6ClNO2	207.62
GW471049X	Cc1cc(C(=O)O)c2ccc(C)c(Br)c2n1	C12H10BrNO2	280.12
GW320828X	OC(=O)c1ccc2[nH]c3ccccc3c(=O)c2c1	C14H9NO3	239.23
GW321479X	Cn1c2ccccc2c(=O)c3ccc(cc13)C(=O)O	C15H11NO3	253.26

Reg No	Smiles String	Formula	MW
GR101886	OC(=O)c1ccc2nc(Cl)c(Cl)nc2c1	C9H4Cl2N2O2	243.05
GR82448	OC(=O)c1ccc2nc(O)c(O)nc2c1	C9H6N2O4	206.16
GW294831	Cc1ccc2nc3ccc(cc3n(=O)c2c1)C(=O)O	C14H10N2O3	254.25
AH12975	OC(=O)c1ccccc1c2nc3ccc(Cl)cc3[nH]2	C14H9ClN2O2	272.69
GW312607X	OC(=O)c1ccc2[nH]c(cc2c1)c3ccc(Cl)cc3	C15H10ClNO2	271.71
AH17009XX	OC(=O)c1cc(nc2ccccc12)c3ccccc3	C16H11NO2	249.27
GW314282X	OC(=O)c1c(cnc2ccccc12)c3ccccc3	C16H11NO2	249.27
GW355545X	OC(=O)c1cc(nc2ccccc12)c3ccco3	C14H9NO3	239.23
AH3705A	Cl.OC(=O)c1cnccc1c2ccccc2	C12H9NO2. HCl	235.67
CCI10881	OC(=O)c1ccccc1c2ccccn2	C12H9NO2	199.21
AH10300	COc1ccc2nc(cc(OC)c2c1)C(=O)O	C12H11NO4	233.23
AH10801	COc1ccc2c(OC)cc(nc2c1)C(=O)O	C12H11NO4	233.23
AH9678	COc1cc(nc2ccccc12)C(=O)O	C11H9NO3	203.20
AH10698	OC(=O)c1cc(O)c2cc(O)ccc2n1	C10H7NO4	205.17
AH10853	OC(=O)c1cc(O)c2cccc(O)c2n1	C10H7NO4	205.17
GR92452	OC(=O)c1ccc2cccc(O)c2n1	C10H7NO3	189.17
AH9727	OC(=O)c1ccc2ccccc2n1	C10H7NO2	173.17
AH12695	OC(=O)c1cc(Oc2ccccc2)c3ccccc3n1	C16H11NO3	265.27
AH13070	OC(=O)c1nc2ccccc2c(O)c1CC=C	C13H11NO3	229.24
AH9676	OC(=O)c1cc(OCc2ccccc2)c3ccccc3n1	C17H13NO3	279.30
AH9721	OC(=O)c1cc(OCc2ccccc2)c3ccccc3n1=O	C17H13NO4	295.30
AH10301X	CCCCOc1cc(nc2ccccc12)C(=O)O	C14H15NO3	245.28
AH15692	CCCOc1cc(nc2ccccc12)C(=O)O	C13H13NO3	231.25
AH12533	OC(=O)c1cc(OCC=C)c2ccccc2n1	C13H11NO3	229.24
AH12590	OC(=O)c1cc(OCC#C)c2ccccc2n1	C13H9NO3	227.22
AH15690	CCOc1cc(nc2ccccc12)C(=O)O	C12H11NO3	217.23
AH15757	CC(C)Oc1cc(nc2ccccc12)C(=O)O	C13H13NO3	231.25
AH10978	OCCOc1cc(nc2ccccc12)C(=O)O	C12H11NO4	233.23
AH11275	OC(=O)c1cc(OCCOc2cc(nc3ccccc23)C(=O)O)c4ccccc4n1	C22H16N2O6	404.38

Reg No	Smiles String	Formula	MW
AH12589	COCCOc1cc(nc2ccccc12)C(=O)O	C13H13NO4	247.25
AH11274	OC(=O)c1cc(OCCOCCBr)c2ccccc2n1	C14H14BrNO4	340.18
AH13391	CC(=O)OCCOc1cc(nc2ccccc12)C(=O)O	C14H13NO5	275.26
GR254264X	OC(=O)c1cc(OCCOC=O)c2ccccc2n1	C13H11NO5	261.24
AH10616T	CN(C)CCO.OC(=O)c1cc(O)c2cc(ccc2n1)N(=O)=O	C10H6N2O5. C4H11NO	323.31
AH7490	OC(=O)c1cc2cc(ccc2[nH]1)N(=O)=O	C9H6N2O4	206.16
AH18515XX	OC(=O)c1cc2ccccc2c(Cl)n1	C10H6ClNO2	207.62
AH22573X	OC(=O)c1cc2c(Cl)cccc2[nH]1	C9H6ClNO2	195.61
AH8588	OC(=O)c1cc2ccccc2[nH]1	C9H7NO2	161.16
AH8601	COc1ccc2[nH]c(cc2c1)C(=O)O	C10H9NO3	191.19
GR32737X	OC(=O)c1ccc[nH]1	C5H5NO2	111.10
AH23288X	CCOC(=O)c1c[nH]c2cc(ccc12)C(=O)O	C12H11NO4	233.23
GI149558	OC(=O)c1c[nH]c2ccccc12	C9H7NO2	161.16
GR133921	Cc1ccc2[nH]cc(C(=O)O)c2c1	C10H9NO2	175.19
GR134971	OC(=O)c1cccc2cc[nH]c12	C9H7NO2	161.16
GR65242X	Cn1cc(C(=O)O)c2ccccc12	C10H9NO2	175.19
AH26099	OC(=O)c1ccc2cc[nH]c2c1	C9H7NO2	161.16
GR116365X	Cc1[nH]c2cc(ccc2c1C)C(=O)O	C11H11NO2	189.22
GW541785X	Cc1cc2ccc(cc2[nH]1)C(=O)O	C10H9NO2	175.19
GR31004	OC(=O)c1ccc2[nH]ccc2c1	C9H7NO2	161.16
GW278395	OC(=O)c1ccc2[nH]c3ccc(cc3c2c1)C(=O)O	C14H9NO4	255.23
GR110635X	Cn1cc(C(=O)O)c2cc(CNS(=O)(=O)C)ccc12	C12H14N2O4S	282.32
GR116353X	CCOC(=O)Cc1c(C(=O)O)c2ccccc2n1C	C14H15NO4	261.28
GR125882X	COCc1c(C(=O)O)c2ccccc2n1C	C12H13NO3	219.24
GW294490X	CC(C)(C)OC(=O)n1c(cc2ccccc12)C(=O)O	C14H15NO4	261.28
GW589997X	Cc1c(C(=O)O)c2cccc3CCn1c32	C12H11NO2	201.23
AH20902	NCCc1c[nH]c2ccc(cc12)C(=O)O	C11H12N2O2	204.23
GR36456	CN(C)CCc1c[nH]c2ccc(cc12)C(=O)O	C13H16N2O2	232.29
AH20984	NCCc1c([nH]c2ccc(cc12)C(=O)O)C(=O)O	C12H12N2O4	248.24

Reg No	Smiles String	Formula	MW
AH21852	CC(=O)c1ccc2[nH]c(C(=O)O)c(CCN)c2c1	C13H14N2O3	246.27
GR252017	NCCc1c([nH]c2ccccc12)C(=O)O	C11H12N2O2	204.23
GR58047	CN1CCOC(C1)c2c[nH]c3ccc(cc23)C(=O)O	C14H16N2O3	260.30
GR44857A	Cl.CN1CCC(=CC1)c2c[nH]c3ccc(cc23)C(=O)O	C15H16N2O2. HCl	292.77
GR207154	COc1ccc2[nH]c(C(=O)O)c(CCNC(=O)C)c2c1	C14H16N2O4	276.30
GR78684X	COc1ccc2[nH]c(C(=O)O)c(CCC(=O)O)c2c1	C13H13NO5	263.25
AH2426A	Cl.OC(=O)c1c2CCCCc2nc3ccccc13	C14H13NO2. HCl	263.73
AH3116	OC(=O)c1ccc2[nH]c3CCCCc3c2c1	C13H13NO2	215.25
GW304734X	OC(=O)c1cnc2CCCCc2c1O	C10H11NO3	193.20
GW661447X	OC(=O)c1cc2CCCCc2[nH]1	C9H11NO2	165.19
GR173175X	CCOC(=O)c1[nH]c(C)c(C(=O)O)c1C	C10H13NO4	211.22
GR254404X	CC(=O)c1c(C)[nH]c(C(=O)O)c1C	C9H11NO3	181.19
GW275105X	CCOCc1[nH]c(C(=O)O)c(C)c1C(=O)C	C11H15NO4	225.25
GW299610X	CC(=O)OCc1[nH]c(C(=O)O)c(C)c1C(=O)C	C11H13NO5	239.23
GW298781X	COCc1[nH]c(C(=O)O)c(C)c1C(=O)C	C10H13NO4	211.22
GW470761X	CC(=O)OCCc1c(C)[nH]c(C(=O)O)c1C	C11H15NO4	225.25
GW369798X	CCc1[nH]c(C(=O)O)c(C)c1C(=O)O	C9H11NO4	197.19
GW659802X	CC(=O)c1[nH]c(C(=O)O)c(C(=O)O)c1C	C9H9NO5	211.18

Compound			Emission Intensity (616 nm +/- 10 nm)							
Reg_No	Cluster	Rank	Acids	EuBEA	EuBUA	EucyHA	EumcyHA	EuNBA	EuBBZA	EuBTA
GR207962X	1	1	43	95	81	93	185	102	110	171
GR212454X	1	2	44	88	84	104	184	103	108	162
CCI21177	1	3	47	77	68	69	60	71	80	91
GR257381X	1	4	41	77	73	90	85	76	99	138
AH6621	1	5	44	71	63	57	56	64	74	81
GR193563X	1	6	39	75	67	71	61	61	78	87
GF267447X	1	7	50	77	67	62	62	72	80	87
GW431055X	1	8	44	55	45	64	58	59	65	81
GR257410X	2	1	39	66	64	60	61	63	78	84
GW503358X	2	2	36	74	65	58	62	75	76	85
GW318421X	2	3	41	78	67	61	60	74	78	84
GR50343X	3	1	45	95	81	78	65	102	118	95
AH14879XX	4	1	45	73	64	67	96	118	94	98
GR235591X	4	2	33	65	63	58	52	56	71	75
AH3827	5	1	35	159	136	104	166	286	228	211
GF267697X	5	2	66	75	58	61	61	70	80	64
GR32114X	5	3	47	69	60	63	61	71	72	65
AH14579XX	6	1	41	68	59	58	55	60	72	79
GW288607X	6	2	35	62	63	57	59	59	70	67
CCI23883	7	1	50	79	64	66	62	69	73	92
GR30858X	7	2	44	78	72	67	58	83	91	87
CCI3965	8	1	56	72	64	67	61	64	65	79
GI207347X	8	2	48	73	61	62	54	58	69	80
GR38987X	8	3	43	72	56	58	53	57	69	71
CCI3923A	9	1	49	69	60	63	58	70	77	70
GR38954X	9	2	51	72	61	62	59	66	73	88
GR251016X	9	3	45	67	59	67	61	67	75	66
AH14993XX	10	1	51	192	176	99	161	269	223	210
AH14994XX	10	2	44	63	57	61	73	88	83	93
GR84408X	10	3	38	736	351	215	170	230	321	229
AH25091X	10	4	44	73	59	59	63	68	66	87
GR64693X	10	5	39	813	1525	1606	1647	2371	2095	1327
AH16584XX	10	6	47	329	158	344	399	618	338	326
GR76119A	10	7	43	74	58	65	56	65	74	85

Compound			Emission Intensity (616 nm +/- 10 nm)							
Reg_No	Cluster	Rank	Acids	EuBEA	EuBUA	EucyHA	EumcyHA	EuNBA	EuBBZA	EuBTA
GI224436X	11	1	48	76	63	61	81	78	77	95
GR34543	11	2	9	8	13	15	10	15	13	-
GR40314	11	3	11	8	18	15	22	37	18	-
GR62892	11	4	544	524	-	-	-	486	651	-
GF133808X	12	1	49	86	70	62	66	68	82	93
GR253989X	12	2	37	74	72	65	68	67	85	90
GR215101X	12	3	43	72	63	65	64	85	86	76
GW322044X	13	1	32	72	60	53	69	68	71	80
GR148285X	14	1	38	88	76	82	102	133	108	107
GR81142X	14	2	40	72	53	64	53	64	71	83
GR63007X	14	3	44	72	58	60	59	68	77	66
GW423740X	15	1	42	87	86	75	118	112	100	108
AH14732XX	16	1	38	49	44	43	65	56	57	75
GW291819X	16	2	42	73	76	84	86	79	97	123
AH15398XX	16	3	40	49	51	44	73	61	65	78
GW314444X	16	4	36	50	52	54	52	56	53	68
GW385245X	16	5	47	94	87	81	115	141	130	119
AH15251XX	17	1	95	122	101	123	163	143	167	129
AH4591	17	2	41	74	62	60	54	72	74	95
AH8259	17	3	62	476	351	279	242	379	265	224
GR34041X	17	4	46	71	60	55	59	60	68	82
GR261706X	18	1	39	55	61	59	51	57	72	78
GR265013X	18	2	41	83	88	75	109	132	116	120
GR49081X	19	1	42	76	56	63	53	69	70	81
GW339416X	19	2	39	65	60	58	64	66	66	79
GW404922A	19	3	34	88	68	66	70	82	83	93
GW409763X	19	4	36	67	58	50	62	65	61	73
AH11164	20	1	42	-	71	65	98	-	85	-
GR214770X	20	2	39	-	64	60	57	-	64	-
CCI5134	20	3	56	82	73	76	67	83	88	79
GI149795A	20	4	43	67	60	60	54	64	72	68
GR38988X	20	5	44	69	55	63	54	67	74	62
GR39182X	20	6	49	70	61	61	55	60	72	82
GW328037X	20	7	45	62	53	58	53	62	63	59

Compound			Emission Intensity (616 nm +/- 10 nm)							
Reg_No	Cluster	Rank	Acids	EuBEA	EuBUA	EucyHA	EumcyHA	EuNBA	EuBBZA	EuBTA
AH9074	21	1	40	-	57	56	69	-	64	-
GI160046X	21	2	49	73	66	66	62	67	81	67
GF253708X	21	3	43	-	65	60	62	-	63	-
GW328038X	21	4	45	93	88	79	118	132	140	125
AH11410	22	1	44	75	64	58	59	71	74	88
GI166356X	22	2	46	79	65	65	62	73	83	90
AH5737	22	3	43	67	62	60	61	71	74	80
GR239060X	22	4	40	69	76	69	69	71	85	84
CCI1659	22	5	54	-	88	66	85	-	96	-
GR156438X	22	6	39	73	53	56	55	67	68	78
GR58626X	23	1	45	67	55	60	47	63	69	68
GR87165X	23	2	40	-	1174	695	709	-	938	-
AH18307XX	24	1	40	-	69	63	66	-	74	-
GF234517X	24	2	41	-	69	66	70	-	84	-
GF233960X	25	1	43	-	59	58	55	-	63	-
GI220410A	25	2	45	68	60	62	55	68	72	62
GR101348X	25	3	40	-	60	62	59	-	64	-
AH14771AA	26	1	40	-	136	161	170	-	167	-
GF241458X	26	2	49	89	72	69	73	84	101	99
GR71072X	26	3	42	228	126	197	219	374	331	289
GR93262X	26	4	56	74	61	71	61	76	74	83
GW315267X	27	1	38	56	56	57	50	59	57	67
GR59449X	28	1	42	85	61	69	78	81	93	95
GR59450X	28	2	51	144	298	75	282	667	334	91
CCI17440	29	1	57	235	231	211	195	197	221	187
GR68891	29	2	50	11	53	47	50	48	50	-
GI148915	29	3	81	157	-	-	-	194	186	-
GR207121	29	4	56	57	55	57	55	56	54	-
GR260810	29	5	17	9	14	14	15	14	15	-
GR66288	29	6	9	14	15	18	16	23	13	-
GI166629	29	7	65	68	83	69	75	78	80	-
GR235507	29	8	41	48	55	53	46	48	49	-
GR38555	29	9	22	21	27	25	21	23	24	-
GW296997	29	10	71	70	81	72	70	73	75	-

Compound			Emission Intensity (616 nm +/- 10 nm)							
Reg_No	Cluster	Rank	Acids	EuBEA	EuBUA	EucyHA	EumcyHA	EuNBA	EuBBZA	EuBTA
CCl4008	29	11	69	92	82	85	79	89	99	90
GR244973	29	12	11	15	25	16	30	26	26	-
GR260719	29	13	11	9	13	13	11	12	15	-
GW317730	29	14	19	21	28	23	26	25	27	-
GW412437	29	15	-	-	-	-	-	-	-	-
GW369998	29	16	17	17	23	21	19	22	25	-
GW416206	29	17	-	-	-	-	-	-	-	-
GW315253X	29	18	52	118	147	187	283	264	227	239
AH16806XX	30	1	45	87	80	69	86	143	96	92
AH17157XX	30	2	47	388	202	507	768	1755	1751	742
GW312681X	30	3	50	102	194	149	201	140	213	204
AH4366	31	1	38	173	169	120	196	370	291	206
AH4367	31	2	41	76	64	61	59	69	74	86
AH9991	31	3	42	90	80	87	129	147	115	120
AH9456	31	4	46	70	62	56	60	69	71	73
AH7716	32	1	49	97	99	111	151	135	125	149
GR244160X	32	2	40	70	77	63	72	66	80	84
GR30170X	32	3	44	62	51	55	50	58	71	59
GW294785X	32	4	38	75	74	89	98	92	102	133
GR232463X	33	1	37	79	73	68	115	125	101	112
GW312679X	33	2	43	73	100	140	197	280	131	213
AH12195	34	1	47	180	134	118	139	159	289	153
GR30355X	34	2	43	163	129	104	165	249	239	159
GR30686X	34	3	47	70	56	61	53	60	76	81
GI221306X	34	4	42	-	69	72	100	-	78	-
GR197556X	34	5	44	-	90	82	91	-	85	-
GR236886	35	1	629	606	552	589	623	680	589	489
GW432536	35	2	-	-	-	-	-	-	-	-
AH14680XX	36	1	42	71	64	60	56	67	74	81
GR215350X	36	2	37	89	78	68	79	71	105	90
GW413125X	36	3	43	76	86	100	116	108	114	136
GR203309X	37	1	38	366	597	629	485	622	882	687
GR241592X	37	2	41	4134	3020	4788	4666	4469	5374	4317
GR207127X	37	3	39	979	1280	1541	1060	1309	1503	1118

Compound			Emission Intensity (616 nm +/- 10 nm)							
Reg_No	Cluster	Rank	Acids	EuBEA	EuBUA	EucyHA	EumcyHA	EuNBA	EuBBZA	EuBTA
GW399139X	37	4	45	1397	1809	870	939	1033	1249	804
GR34040X	38	1	42	82	67	70	83	95	97	92
GW323465X	38	2	48	68	61	65	66	70	76	64
GR36337X	38	3	43	1149	1899	1302	2084	2457	3483	1401
GR87232X	38	4	35	60	58	136	94	154	74	140
GW322742X	38	5	1603	54	55	69	165	82	63	120
CCI8247	39	1	51	72	61	60	57	62	76	83
GW470564X	39	2	34	96	75	62	85	108	94	99
GR136744X	40	1	37	71	56	64	56	67	61	83
GW398946X	40	2	34	78	66	62	66	82	85	88
GR258074X	41	1	43	58	62	58	53	55	67	73
GR30298X	41	2	44	70	58	61	56	58	68	81
GW294643X	42	1	72	77	53	78	63	71	90	85
GW295897X	42	2	38	68	75	54	56	58	66	74
AH5119	43	1	45	86	73	63	77	93	88	101
GR146857A	43	2	40	72	53	61	49	70	73	86
GR108821X	43	3	40	74	56	68	61	76	74	86
CCI21441X	44	1	47	91	75	64	67	82	99	95
GI222965X	44	2	51	73	64	61	58	64	71	88
GR85032X	44	3	40	71	53	61	50	62	71	78
GW317925X	45	1	37	83	58	56	52	59	72	73
GW423592X	45	2	34	54	57	48	54	53	59	68
GR212558X	46	1	37	92	79	74	85	70	105	90
GV98449X	46	2	40	74	70	64	65	60	86	84
GR245353X	46	3	38	319	285	166	457	236	447	215
AH13207	47	1	44	94	78	66	69	86	88	88
GR53007X	47	2	42	137	105	94	99	159	160	115
AH8335X	47	3	44	78	87	75	96	121	133	79
GR100133X	48	1	41	72	56	59	54	69	74	82
GR111981X	48	2	41	80	63	66	78	94	94	94
GR124650X	49	1	37	80	79	85	74	103	113	118
GR236342X	49	2	53	74	64	74	58	74	79	71
GR258909	50	1	50	329	361	331	348	377	335	342
GR265026X	50	2	41	74	77	63	73	67	91	95

Compound			Emission Intensity (616 nm +/- 10 nm)							
Reg_No	Cluster	Rank	Acids	EuBEA	EuBUA	EucyHA	EumcyHA	EuNBA	EuBBZA	EuBTA
GR43579X	50	3	41	-	61	60	64	-	65	-
GR51409X	50	4	41	66	55	61	48	61	65	71
GW273704X	51	1	38	72	75	67	70	64	108	92
GW324992X	51	2	42	93	83	68	72	110	112	107
CCI19762	52	1	44	153	123	100	131	203	192	155
GR249776X	53	1	36	70	65	62	62	64	79	83
GR256398X	53	2	39	72	73	65	72	68	86	89
GR269435X	53	3	37	65	61	59	53	56	71	76
GR180851A	54	1	37	64	66	63	48	59	79	82
GR88677X	54	2	42	73	56	63	55	69	77	86
GW401244X	55	1	40	57	54	67	64	63	64	84
GW406680X	55	2	38	62	54	73	78	74	80	96
GW521849X	55	3	40	65	68	75	97	89	85	109
AH13312	56	1	52	122	76	76	92	117	131	104
AH14681XX	57	1	36	69	67	45	75	86	89	85
GR130650X	57	2	36	154	145	227	270	395	288	326
GR99513X	57	3	42	85	83	80	57	104	98	104
AH23294X	57	4	49	78	76	94	114	96	93	95
GR212000X	58	1	38	114	122	104	125	148	171	247
GR116024X	59	1	36	905	1041	796	461	535	1063	583
GR58504X	59	2	39	310	315	326	286	386	407	333
GW315124X	59	3	42	67	68	71	109	88	89	110
GW442963X	59	4	45	88	102	100	130	159	152	159
GW342768X	59	5	38	59	57	70	72	62	67	94
AH25327X	60	1	36	81	117	85	92	134	188	142
AH25377X	60	2	35	108	90	57	88	120	114	121
GR60468X	61	1	38	156	145	93	158	180	174	183
GR223597X	62	1	38	74	66	78	82	73	80	110
GW543499X	63	1	40	54	50	64	74	66	63	116
GR257678X	64	1	49	70	61	66	61	68	75	61
GW652716X	65	1	46	77	77	81	74	74	95	97
GW292869X	66	1	39	160	172	244	426	384	403	326
GW342412X	66	2	42	175	75	79	236	233	279	169
GR232127X	67	1	38	744	323	578	446	482	506	608

Compound			Emission Intensity (616 nm +/- 10 nm)							
Reg_No	Cluster	Rank	Acids	EuBEA	EuBUA	EucyHA	EumcyHA	EuNBA	EuBBZA	EuBTA
GW309937A	68	1	42	68	67	75	79	73	83	97
GR54241	69	1	43	76	63	64	54	68	78	84
GR64138A	69	2	45	50	58	62	71	58	64	86
GR81562	69	3	108	-	88	82	88	-	92	-
GW424484X	70	1	40	83	71	61	63	83	84	98
GW294777X	71	1	44	77	86	93	131	89	106	181
GW313525X	71	2	43	325	310	195	395	432	419	317
GW321902X	71	3	42	63	58	68	81	79	66	81
GR194866A	72	1	33	77	78	98	99	75	108	156
GR65644X	72	2	37	53	46	58	74	60	57	77
GW553810A	72	3	37	96	60	77	111	152	167	102
GW549758A	72	4	45	105	93	120	113	115	111	146
GW550038A	72	5	45	195	212	218	179	188	262	205
GR70745X	72	6	35	129	107	121	81	120	140	112
GR69220X	72	7	39	88	90	117	138	107	109	119
AH11291	73	1	58	158	124	103	108	178	160	131
GR94828A	73	2	47	779	57	321	399	565	1029	331
AH12740	73	3	45	91	76	67	67	97	105	90
AH12757	73	4	43	83	68	65	64	83	96	88
GR199839X	73	5	56	84	85	80	71	80	95	100
GR58191X	74	1	37	58	54	75	64	64	60	82
GR87036X	75	1	41	74	58	61	54	66	72	91
GW415452X	75	2	46	74	60	68	71	81	80	67
AH8294	76	1	44	77	67	60	62	76	94	87
GR39220X	76	2	51	149	128	95	134	184	188	133
GI101694A	76	3	45	75	63	66	57	64	74	91
GR50961A	76	4	43	125	115	102	98	176	173	126
GR147168X	77	1	1267	1308	1222	1240	1288	1252	1310	1253
GR51196X	77	2	43	69	56	62	52	67	67	80
GR117463X	78	1	38	67	57	61	64	64	69	75
GR208696X	78	2	39	66	66	61	60	60	77	87
GR32768A	78	3	45	72	58	62	53	57	72	81
GW432313X	78	4	37	73	66	65	62	65	74	88
GR266494X	79	1	-	-	-	-	-	-	-	-

Compound			Emission Intensity (616 nm +/- 10 nm)							
Reg_No	Cluster	Rank	Acids	EuBEA	EuBUA	EucyHA	EumcyHA	EuNBA	EuBBZA	EuBTA
GW298250X	79	2	38	66	64	58	57	67	69	78
GR125017X	80	1	41	104	88	127	244	152	132	178
GW370018X	80	2	35	66	62	59	64	64	65	78
GW315103X	81	1	39	85	79	65	77	72	94	91
GW321966X	81	2	74	96	103	120	155	213	177	264
GF233961X	82	1	50	76	61	60	59	62	72	87
GI230797A	82	2	43	69	57	60	52	53	64	78
GR140164X	82	3	41	77	64	61	82	81	82	99
GW290604X	83	1	1174	1119	1042	1008	2234	1924	1502	1486
GW291821X	83	2	41	64	63	57	55	67	70	79
GW361278X	83	3	44	63	67	63	73	60	65	87
GW336990X	83	4	45	54	65	73	74	86	71	86
GW295365X	83	5	50	85	86	100	202	101	114	136
GW292911X	84	1	57	79	125	76	94	82	84	74
GW294867X	84	2	39	98	95	159	277	207	193	254
GW322405X	84	3	40	90	100	146	292	277	161	336
GW315228X	85	1	219	235	282	299	219	305	241	260
GW321601X	86	1	51	189	159	132	206	243	282	213
GI230786	87	1	47	72	57	58	63	78	73	88
GW295364	87	2	84	106	110	103	99	109	111	121
AH7066	88	1	39	68	60	61	55	65	69	107
GF234516X	88	2	38	41	41	53	90	67	54	121
GF269343X	88	3	38	62	67	75	90	109	86	90
GW314651X	88	4	2037	57	61	70	141	127	75	120
GW311857X	88	5	61	89	84	91	85	87	101	113
GW323587X	88	6	35	1346	1650	1370	1996	2361	2952	1500
GW294790X	88	7	76	477	1246	919	897	1425	1446	919
GW322118X	88	8	39	180	221	245	351	439	271	343
GW312723X	89	1	41	95	119	130	196	192	179	189
GW432537X	89	2	67	117	191	142	166	166	224	189
GW322502X	89	3	36	98	107	117	153	157	148	201
GW312725X	89	4	37	51	65	73	88	72	91	111
GW322531X	89	5	47	75	83	81	126	175	122	127
GW314663X	89	6	71	551	998		1054	1504	1420	895

Compound			Emission Intensity (616 nm +/- 10 nm)							
Reg_No	Cluster	Rank	Acids	EuBEA	EuBUA	EucyHA	EumcyHA	EuNBA	EuBBZA	EuBTA
GW323690X	89	7	195	482	532	461	619	643	743	624
GW323328X	89	8	82	123	122	135	178	175	165	153
AH10503	90	1	41	62	54	52	47	56	63	69
AH25564X	90	2	49	74	55	59	52	57	68	85
CCI7155	90	3	58	83	71	76	68	78	89	81
GR51515	90	4	39	67	51	61	46	59	48	74
GW363503A	90	5	37	81	75	58	66	86	86	82
GR253714X	90	6	35	67	62	57	57	60	75	75
AH9018	90	7	50	3067	2980	1504	2485	4646	5336	5486
AH12070	91	1	106	138	119	129	132	144	134	142
GI123058	91	2	147	168	-	-	-	178	201	-
GR55509	91	3	27	22	27	29	38	33	30	-
GR50239	91	4	18	15	18	21	16	20	17	-
GR87121	91	5	79	128	-	-	-	114	129	-
AH2951	91	6	48	86	68	61	63	75	79	88
GR199994	91	7	40	69	64	61	62	62	76	87
AH12275	91	8	66	100	87	84	83	94	97	104
GR173757	91	9	80	124	103	104	103	111	105	113
GR161201X	91	10	41	72	55	65	50	68	71	78
AH12764	92	1	65	90	87	87	83	81	83	96
AH17306AB	92	2	53	75	66	64	62	66	78	80
GR161186X	92	3	51	73	66	68	59	69	72	83
AH15079XX	93	1	43	-	66	58	61	-	64	-
GR35117X	93	2	38	-	61	61	70	-	61	-
AH21453	93	3	60	83	69	69	68	72	90	98
GR178029	93	4	122	156	-	-	-	150	171	-
GR33748	93	5	43	525	823	590	1046	1075	1140	491
GI152672	94	1	113	133	122	121	122	114	129	149
GR141743	94	2	11	13	11	12	10	12	14	-
GR39406	94	3	9	10	13	15	11	11	11	-
GR214280	94	4	39	93	83	94	95	82	101	145
GR226270	94	5	13	10	13	12	10	12	15	-
GR78537	94	6	11	8	12	11	10	17	12	-
GR189793	94	7	86	129	-	-	-	122	136	-

Compound			Emission Intensity (616 nm +/- 10 nm)							
Reg_No	Cluster	Rank	Acids	EuBEA	EuBUA	EucyHA	EumcyHA	EuNBA	EuBBZA	EuBTA
GR263804X	94	8	42	58	60	68	58	60	75	94
GW324674	94	9	12	10	11	14	11	11	12	-
GW410247	94	10	-	-	-	-	-	-	-	-
GR38461X	94	11	46	72	63	64	70	79	82	72
GW340239X	94	12	39	74	65	58	59	65	70	81
GR73169X	94	13	46	72	58	62	53	67	82	66
AH15491XX	95	1	45	73	63	57	53	68	79	82
GR107832X	95	2	39	62	50	55	51	60	64	64
GR231878X	95	3	40	57	52	54	64	67	69	57
GR137556X	95	4	40	66	48	59	46	67	68	76
GF146238	96	1	444	441	319	395	424	386	449	372
GW295088	96	2	72	72	72	67	75	63	65	-
GF267572X	96	3	56	72	63	63	62	62	72	80
GW323141X	96	4	51	75	69	63	71	72	75	89
GF267575X	97	1	98	102	93	101	98	94	106	110
GR76319X	97	2	48	294	316	664	1223	1511	1246	1430
GR78359X	97	3	83	115	101	101	107	117	114	121
GI170475X	98	1	42	-	68	57	55	-	64	-
GW275669A	98	2	43	-	62	53	54	-	61	-
GR205623X	98	3	43	-	70	59	63	-	62	-
GR53844X	99	1	43	-	68	62	63	-	66	-
GW298071X	100	1	41	67	63	59	51	59	74	78
GI199827X	101	1	44	65	54	56	49	57	62	75
GR141837X	101	2	39	57	48	52	46	55	67	64
GW323802A	101	3	41	75	73	59	63	67	72	82
GW329522X	102	1	38	67	57	56	57	72	64	78
GR251266A	103	1	99	94	119	100	83	101	126	143
GR265018A	103	2	39	55	58	71	58	61	79	97
GR253017X	103	3	39	68	66	59	61	62	82	87
GW425183X	104	1	37	174	165	156	194	189	183	192
GR267248A	105	1	42	55	60	74	60	63	74	100
GW425181X	105	2	35	67	61	58	58	63	70	82
AH17295XX	106	1	42	66	60	54	53	57	68	71
AH26206X	106	2	44	58	53	51	49	55	59	69

Compound			Emission Intensity (616 nm +/- 10 nm)							
Reg_No	Cluster	Rank	Acids	EuBEA	EuBUA	EucyHA	EumcyHA	EuNBA	EuBBZA	EuBTA
AH20560XX	106	3	42	68	53	58	49	57	62	71
GR97173X	106	4	39	61	50	55	48	57	57	63
AH21291X	106	5	43	65	56	57	47	61	63	71
GW471254X	106	6	40	72	63	61	56	64	70	80
AH17365XX	107	1	45	66	55	57	49	58	64	77
GI198830X	107	2	45	63	56	57	51	56	66	71
AH7669	107	3	45	53	52	55	50	58	66	58
GI221325A	107	4	50	62	55	57	56	63	69	64
GI95276X	107	5	38	65	53	59	54	61	70	59
CCI7978	108	1	43	-	63	61	81	-	63	-
GF267691X	108	2	47	71	59	57	54	65	71	87
GI147499A	108	3	47	-	68	66	69	-	68	-
AH21350X	109	1	41	67	50	53	71	54	62	76
GW321669X	109	2	51	-	66	62	64	-	71	-
GW323630X	109	3	49	60	55	54	56	59	65	75
CCI1914	109	4	59	54	46	44	42	47	54	58
GF146728X	109	5	45	-	65	60	59	-	66	-
GR86838X	109	6	43	55	49	49	47	54	51	56
AH5502	110	1	129	136	133	134	115	126	130	128
GR141836	110	2	117	148	-	-	-	143	170	-
GR248323	110	3	21	19	24	22	17	24	19	-
AH6472	110	4	101	149	-	-	-	146	160	-
GR141839	110	5	76	159	-	-	-	163	170	-
GR31162	110	6	16	13	14	15	12	17	16	-
GR40490	110	7	15	11	14	14	13	13	14	-
GR40028	110	8	8	8	11	9	7	11	10	-
GI149060	110	9	314	456	-	-	-	382	422	-
GI153357	110	10	136	165	-	-	-	163	177	-
GV95604	110	11	38	40	42	42	40	42	42	-
GI119939X	110	12	49	-	67	64	69	-	68	-
GI147798	110	13	78	112	-	-	-	112	126	-
GR113723	110	14	79	113	-	-	-	104	125	-
GI150183	110	15	103	137	-	-	-	131	149	-
GR259835	110	16	15	13	14	15	11	16	13	-

Compound			Emission Intensity (616 nm +/- 10 nm)							
Reg_No	Cluster	Rank	Acids	EuBEA	EuBUA	EucyHA	EumcyHA	EuNBA	EuBBZA	EuBTA
GR197159	110	17	106	145	-	-	-	133	141	-
GR118329	110	18	119	171	-	-	-	154	194	-
GI151314	110	19	102	143	-	-	-	138	157	-
GR214686	110	20	13	10	15	12	11	16	16	-
GR89164	110	21	101	143	-	-	-	129	153	-
GR261930	110	22	53	64	60	67	59	60	61	-
GR31787A	110	23	41	-	59	60	55	-	58	-
CCI8566	111	1	101	133	114	113	111	117	123	140
GR32579	111	2	11	12	11	12	9	11	11	-
GW286126	111	3	38	131	164	354	320	280	264	144
GW422957	111	4	-	-	-	-	-	-	-	-
GR123674	111	5	87	130	-	-	-	122	149	-
GR146669	111	6	89	122	-	-	-	119	136	-
CCI9041	111	7	60	90	75	77	76	74	78	96
GW296344	111	8	8	8	12	12	9	16	9	-
GR154729	111	9	90	127	-	-	-	113	146	-
GR171932	111	10	94	118	-	-	-	114	125	-
AH13018	112	1	39	164	149	106	106	217	225	124
GV140840X	112	2	40	58	65	56	50	57	61	71
GR207209X	112	3	36	155	175	135	325	253	268	245
GR112257X	113	1	48	70	62	62	51	63	70	81
GR263152X	113	2	258	260	314	275	262	255	262	285
GR112259X	113	3	40	64	69	64	53	76	73	79
GR185905X	113	4	46	83	86	82	71	107	111	103
GR186845X	113	5	38	86	86	105	238	94	115	138
GR219630X	113	6	39	61	65	55	50	57	66	70
GW541786X	113	7	44	75	87	148	840	203	100	227
GW560094X	113	8	43	75	79	95	222	114	106	99
GR53539X	114	1	44	68	52	64	50	61	65	77
AH15201XX	115	1	225	178	170	189	217	220	196	216
AH6859	115	2	4042	4523	3997	4167	4159	4019	4224	3917
AH15203XX	115	3	3941	4430	4596	4896	5629	5717	5908	5625
GW314581X	115	4	4049	4225	4237	3997	4729	5774	5367	5189
GW294655X	115	5	206	433	325	317	17	440	548	486

Compound			Emission Intensity (616 nm +/- 10 nm)							
Reg_No	Cluster	Rank	Acids	EuBEA	EuBUA	EucyHA	EumcyHA	EuNBA	EuBBZA	EuBTA
GW328088X	115	6	4021	3968	4006	3952	4153	3932	4224	4094
GW312792X	115	7	208	4057	7914	5158	8084	9459	12074	5383
GW294322X	115	8	2559	2508	2301	2488	2289	2322	2576	2602
GW304858X	115	9	228	304	323	295	333	597	417	441
GW312329X	115	10	182	1045	998	809	1024	1254	1559	1088
AH15400XX	115	11	4490	3712	4594	3752	4600	5074	5391	4697
GW314526X	115	12	231	1176	1646	-	1615	2366	2512	1956
GW324336X	115	13	230	234	372	242	266	221	368	310
AH5558	116	1	42	94	79	62	86	119	107	93
AH5950	116	2	37	158	197	158	180	321	355	278
GW312371X	116	3	37	156	186	143	189	331	328	286
GW315227X	116	4	141	211	366	282	399	189	643	499
GW312460X	116	5	44	341	806	681	632	1138	1366	1083
GW312437X	116	6	49	921	1026	938	2567	2690	1655	1593
GW312435X	116	7	47	65	73	76	81	75	77	101
GF267701X	116	8	1226	799	959	1021	1144	1242	1054	1117
GR189755X	117	1	4826	5117	5043	4212	4353	4915	4022	4235
GW313003X	117	2	36	55	48	52	51	66	61	55
GR256734X	117	3	42	86	80	84	87	83	97	138
GW321218X	118	1	41	130	142	116	196	231	221	177
AH6372	119	1	47	228	210	152	136	1265	601	249
GI205545X	119	2	46	76	60	55	55	61	72	80
GW312626X	119	3	41	139	135	105	240	134	220	139
GR230571X	119	4	108	163	170	170	185	171	190	222
AH21917X	120	1	49	74	62	57	51	66	68	78
AH22735X	120	2	40	72	58	55	55	65	74	87
GR177051X	120	3	40	59	48	58	48	58	61	67
GW471604X	120	4	50	101	101	111	98	132	139	125
GR152169X	120	5	36	68	56	63	49	62	52	74
GR225877X	121	1	41	74	76	69	65	66	88	90
GR255442X	121	2	39	519	738	456	676	1162	1179	590
CCI2180	122	1	48	74	60	59	55	66	73	78
GR121162X	122	2	42	72	56	63	57	63	70	77
GW308403X	123	1	36	137	129	88	164	114	175	134

Compound			Emission Intensity (616 nm +/- 10 nm)							
Reg_No	Cluster	Rank	Acids	EuBEA	EuBUA	EucyHA	EumcyHA	EuNBA	EuBBZA	EuBTA
GR114265X	124	1	39	149	164	143	114	175	202	149
GR225874X	124	2	43	83	80	86	81	90	111	139
GR51045X	125	1	43	64	48	59	61	64	62	81
GW521143X	126	1	55	65	60	66	64	64	72	79
GR200308X	127	1	32	118	148	121	183	205	194	162
GR32131X	127	2	47	90	73	65	66	92	90	93
AH2599	128	1	97	120	115	113	116	114	121	135
AH7307	128	2	77	243	-	-	-	387	360	-
GR121876X	129	1	42	70	59	60	55	68	69	70
GR193373X	129	2	36	61	64	65	62	60	82	98
GR196926X	129	3	40	63	66	74	73	62	76	102
GW426030X	129	4	34	82	73	65	69	78	85	86
AH21971X	130	1	40	235	326	240	314	565	565	292
GW648032X	130	2	42	107	114	98	126	167	179	129
CCI1710	130	3	45	118	100	81	86	153	147	105
GR71245X	130	4	36	589	510	1347	1294	1684	1378	1305
GR173914X	131	1	47	77	67	71	75	87	85	87
GR257498X	132	1	34	86	93	70	102	81	120	96
AH23040X	133	1	45	72	60	56	56	63	70	72
GR36682X	133	2	47	65	55	56	53	57	67	117
GR47574X	133	3	43	68	56	65	49	62	70	80
GR215566X	134	1	39	68	66	60	56	58	74	77
GI198860X	135	1	44	179	151	109	149	291	265	164
GR74829X	135	2	43	95	74	85	97	139	107	114
GW271761X	135	3	41	71	75	62	68	81	83	87
GR232957X	136	1	96	366	468	431	415	433	600	433
GW322216X	136	2	111	487	440	200	373	1052	1267	440
AH4822	137	1	35	255	370	234	189	530	552	283
GR207205X	137	2	39	285	507	642	1081	1426	624	791
GF267466X	137	3	48	104	108	161	373	486	221	245
GW328094A	138	1	35	43	48	41	51	52	52	66
GW418822A	138	2	37	45	45	59	58	55	61	83
GW448911X	138	3	42	59	59	65	59	60	72	91
GI198877X	139	1	49	152	144	105	112	202	217	140

Compound			Emission Intensity (616 nm +/- 10 nm)							
Reg_No	Cluster	Rank	Acids	EuBEA	EuBUA	EucyHA	EumcyHA	EuNBA	EuBBZA	EuBTA
GR267007X	139	2	144	249	320	240	392	281	332	231
GW340373X	139	3	33	69	64	59	60	61	67	77
GR256536X	140	1	39	249	304	371	883	774	493	365
GR192153X	141	1	43	93	111	98	122	118	142	137
GW321193X	142	1	41	53	51	52	50	52	57	67
AH23064X	143	1	45	67	55	60	62	58	68	73
GW279435X	143	2	42	54	54	66	67	60	65	88
GW279438X	144	1	42	68	79	89	85	98	107	107
GW279439X	144	2	38	72	83	172	366	344	100	244
GR127482A	145	1	45	70	55	64	60	68	70	82
GR262262X	145	2	37	50	47	43	48	50	54	73
GR262264X	145	3	39	44	50	56	53	53	61	78
GR267264X	145	4	38	40	41	40	44	51	52	67
AH8425	146	1	2762	3113	3111	3196	3310	3862	3281	3186
GW314731X	146	2	2548	2241	1881	2001	2639	2593	2090	2189
GW314830X	146	3	6721	5113	4012	-	5768	5319	5839	5210
GW320557X	146	4	5393	5488	4477	4768	5348	5412	4734	5606
GW323721X	146	5	5682	5843	4959	4362	5392	5961	5197	5334
GW314662X	147	1	566	1219	2747	1890	3690	4083	3696	3619
GW314681X	147	2	982	1361	1449	1840	3202	2410	2538	2367
GW314793X	147	3	897	1047	1429	-	3234	1610	1960	2590
GW322018X	147	4	874	2568	3333	2538	4222	5959	5215	2878
GW314751X	147	5	860	1202	1326	1091	2476	1626	1421	2001
GW315158X	147	6	408	800	890	-	1454	1211	1182	1028
GW322801X	147	7	690	1133	1581	1473	3545	2590	2318	2900
GW323040X	147	8	1655	2566	2697	2977	4423	4055	4088	3261
GW321891X	147	9	48	57	54	70	62	60	65	84
GW323845X	147	10	300	326	383	358	387	309	392	456
GW323446X	147	11	284	501	729	541	1084	1043	983	970
GW323591X	147	12	139	3679	5117	3832	5583	8644	9493	5617
GW315075X	147	13	403	604	643	643	1076	947	793	941
GW322693X	147	14	145	444	586	482	859	805	846	734
GW321808X	147	15	504	916	934	775	2567	1837	1621	1358
GW322384X	147	16	178	418	435	444	584	865	765	622

Compound			Emission Intensity (616 nm +/- 10 nm)							
Reg_No	Cluster	Rank	Acids	EuBEA	EuBUA	EucyHA	EumcyHA	EuNBA	EuBBZA	EuBTA
GW321800A	147	17	190	182	83	208	203	214	270	179
GW322628X	147	18	2174	1915	1671	1538	1900	1788	1702	1837
GW322988X	147	19	343	450	494	426	556	585	681	706
AH15466AA	148	1	46	72	62	60	59	66	82	79
AH2565	148	2	45	70	61	58	55	71	78	94
GW366246	148	3	125	141	144	128	129	137	142	140
CCI17196	148	4	39	179	199	173	207	264	133	170
AH20078XX	149	1	58	747	1438	1115	1957	2264	1917	1556
GR208554X	149	2	41	1008	1030	1008	1041	1012	876	1034
GR230104X	149	3	43	546	750	699	1035	808	1110	663
GR30893X	149	4	45	1121	1366	2060	1648	2164	1529	1603
GR33911X	149	5	41	625	828	1465	1894	1550	1688	1413
GR62459X	149	6	60	4918	6321	5597	6617	6705	7165	5595
GR65815X	149	7	42	966	851	1136	1596	764	1403	1040
GR65884X	149	8	46	1114	1087	1886	2067	1750	1805	1152
GW385846X	149	9	75	3774	4733	3810	4020	4779	6426	3709
GR155589X	149	10	37	103	85	117	129	158	161	173
GR30894X	149	11	43	569	638	793	692	688	680	670
GR208752X	149	12	46	282	592	680	686	1308	872	994
GW288377X	149	13	64	1638	3143	1240	1183	1645	2966	1286
GR34968X	149	14	40	191	210	220	311	320	267	275
GR54392X	149	15	56	4718	7088	9723	4899	5444	11384	4384
GR57352X	149	16	58	1021	1290	1299	1320	3363	2179	1403
GW371223X	149	17	44	71	67	100	270	112	84	108
CCI9740	149	18	49	81	61	64	62	70	79	86
GR240724X	149	19	43	274	343	1071	926	1263	988	1093
GR30476X	149	20	39	57	54	72	200	92	77	122
GR53056X	149	21	41	66	53	70	53	60	58	81
GR136670X	150	1	44	140	214	106	82	132	185	108
GR34039X	150	2	46	98	70	102	189	191	115	143
AH24908A	151	1	107	113	209	160	261	213	204	167
GR49928X	151	2	104	91	145	119	216	167	151	154
AH25368X	151	3	56	200	378	401	481	454	505	252
GR55422X	151	4	58	938	1278	1062	1172	2305	1690	1355

Compound			Emission Intensity (616 nm +/- 10 nm)							
Reg_No	Cluster	Rank	Acids	EuBEA	EuBUA	EucyHA	EumcyHA	EuNBA	EuBBZA	EuBTA
GR55423X	151	5	51	773	1053	1017	1154	1774	1834	1078
GR61326X	151	6	40	688	1566	2701	3061	2857	3376	1175
GR61891X	151	7	148	734	1804	2766	3312	3242	3040	2006
GR61984X	151	8	70	1158	2101	3745	4412	4210	4178	2915
GR61985X	151	9	81	973	2048	2702	3150	3315	3171	1888
GR55424X	151	10	51	1117	1231	1293	1211	1900	1882	1408
AH5157	152	1	87	98	98	98	95	102	130	105
AH6770	152	2	40	78	70	59	60	73	80	85
AH9603	152	3	42	71	65	57	53	71	69	78
GW315367X	152	4	70	89	84	86	74	84	84	97
GR219955X	152	5	46	83	78	91	88	81	92	124
GR120092X	152	6	39	58	57	64	50	62	65	74
GR75258X	152	7	43	31687	25909	22016	21843	21961	26775	18051
GF233967X	153	1	42	71	54	61	57	61	71	82
GW641533X	153	2	43	67	63	69	73	67	79	89
GW321911X	153	3	39	70	66	58	60	69	81	87
GW402775X	153	4	39	195	202	167	239	228	236	201
GR258179X	154	1	42	1193	5398	1395	1421	5128	6037	1730
GR258213X	154	2	58	687	4385	1490	6215	4141	5093	2125
GF267695X	155	1	41	48	53	62	62	60	56	63
GW322088X	155	2	38	60	61	63	63	63	67	81
GW322112X	155	3	38	83	92	83	92	110	123	114
GW322316X	155	4	35	54	50	53	61	54	56	74
GW322086X	155	5	34	71	61	54	69	63	67	82
GR222247X	156	1	41	61	61	59	48	58	70	72
GR53849X	156	2	47	74	55	68	56	65	71	82
GR99312X	156	3	45	60	61	65	48	56	66	79
GR57082X	157	1	35	61	52	64	66	67	62	87
GW320929X	157	2	34	45	54		88	62	68	102
GW412113X	157	3	46	57	55	68	63	60	99	214
GR215780X	158	1	41	85	81	90	87	82	111	147
GR219957X	158	2	47	90	94	98	94	85	108	135
GR219958X	158	3	46	92	87	97	104	94	104	147
GR216184X	158	4	42	301	260	256	350	521	470	622

Compound			Emission Intensity (616 nm +/- 10 nm)							
Reg_No	Cluster	Rank	Acids	EuBEA	EuBUA	EucyHA	EumcyHA	EuNBA	EuBBZA	EuBTA
GR216186X	158	5	41	85	80	90	85	83	99	141
GR218004X	158	6	43	91	113	107	210	218	172	262
GR218005X	158	7	44	99	108	125	201	161	111	246
GR133748X	159	1	-	-	-	-	-	-	-	-
GR82836X	159	2	45	1661	1864	1468	1261	1821	2826	1207
GR38662X	159	3	40	48	53	74	181	117	60	134
GW292734X	159	4	42	160	165	350	346	384	380	347
GW322234X	159	5	87	100	104	107	105	97	108	131
GR79956X	159	6	42	153	131	111	148	179	186	169
GR203866X	159	7	41	468	1057	568	846	885	1156	587
GR203872X	159	8	39	348	297	204	665	466	626	295
GR203875X	159	9	40	216	208	245	594	442	458	278
GR204301X	159	10	39	3060	4370	2459	3727	8871	7392	2975
GR65881X	159	11	47	299	209	118	554	1679	1003	803
GR65883X	159	12	44	343	639	1609	1171	1313	1201	986
GR65885X	159	13	48	388	699	428	776	1074	1417	842
GR188442X	160	1	46	103	118	107	141	141	130	184
GW322235X	160	2	36	58	57	60	67	63	66	85
GW327773X	160	3	39	60	61	66	80	77	72	96
GW643493X	160	4	149	442	592	382	454	704	772	516
GW643495X	160	5	59	91	90	90	99	94	122	140
GR215459A	161	1	39	104	111	113	120	97	162	168
GW280814	161	2	37	62	63	55	53	57	71	78
GW290851X	161	3	38	48	55	60	52	59	61	83
GW290862X	161	4	42	44	54	60	55	54	62	85
GW326112X	161	5	37	110	120	122	216	282	187	262
GW271929X	162	1	38	111	164	137	202	173	159	189
GW317768X	162	2	49	1464	2122	1515	1882	2923	2166	1079
GW272447X	162	3	42	93	130	122	257	173	140	220
GW326127X	162	4	43	242	548	387	592	556	579	355
GW440381X	162	5	51	255	551	524	1328	673	407	428
GW418716X	162	6	43	120	102	142	191	173	155	202
GW453080X	162	7	44	114	134	162	226	177	176	199
GW442734X	162	8	42	83	97	138	216	168	115	220

Compound			Emission Intensity (616 nm +/- 10 nm)							
Reg_No	Cluster	Rank	Acids	EuBEA	EuBUA	EucyHA	EumcyHA	EuNBA	EuBBZA	EuBTA
GW272478X	162	9	42	82	89	117	197	154	131	182
GW442732X	162	10	46	100	99	127	203	144	137	187
GW415699X	162	11	45	1145	4990	1790	3551	2612	3377	1422
GW369764X	162	12	53	1380	2312	1370	3700	2027	2363	1485
GR50838A	163	1	42	151	184	175	182	311	407	177
GR51678X	163	2	44	1710	1833	1590	1674	2745	2683	1807
GR54219X	164	1	34	510	530	425	664	1252	1238	860
GR69421X	164	2	38	228	311	189	129	537	554	245
GW317904X	165	1	38	83	95		223	233	140	187
GW411913X	165	2	39	57	54	72	69	60	66	92
GW327989X	165	3	41	77	86	102	123	155	112	114
GW414889X	165	4	43	57	59	70	56	58	74	98
AH10104A	166	1	38	60	48	46	53	61	61	79
AH7702	166	2	35	48	43	46	38	39	45	51
AH7559	166	3	38	54	50	49	39	46	50	53
AH10011A	166	4	39	47	44	39	51	50	52	59
AH7724Z	166	5	33	41	46	43	35	42	49	47
GW575621X	166	6	41	49	48	59	49	49	58	68
AH10424A	166	7	39	40	41	34	50	49	46	50
AH7620Z	166	8	37	52	45	50	39	46	56	63
AH7699	166	9	36	50	52	46	40	49	52	58
AH5961	167	1	39	62	54	49	49	55	60	129
AH6102	167	2	94	119	109	108	104	96	123	117
AH7647	167	3	37	52	47	49	38	40	53	58
AH9531	168	1	43	48	46	32	43	50	43	53
GR199045X	168	2	50	42	49	41	45	45	51	44
AH5724	169	1	36	99	120	71	63	449	545	220
GW295014X	169	2	37	124	150	123	277	343	410	289
GW315237X	169	3	41	67	78	57	55	100	179	104
GW315238X	169	4	34	50	74	-	91	89	105	100
AH6593	169	5	38	103	129	90	78	161	170	124
GW315239X	169	6	34	268	438	-	634	428	287	436
AH6247	169	7	741	514	463	444	449	372	546	434
AH6313	169	8	191	171	158	172	146	144	163	160

Compound			Emission Intensity (616 nm +/- 10 nm)							
Reg_No	Cluster	Rank	Acids	EuBEA	EuBUA	EucyHA	EumcyHA	EuNBA	EuBBZA	EuBTA
AH6072	169	9	164	199	358	272	294	318	353	348
AH6624	169	10	30	54	58	48	40	59	60	130
AH7013Z	169	11	40	56	52	54	39	46	60	74
AH7014Z	169	12	35	50	50	52	38	48	62	67
AH6198	170	1	38	63	57	62	47	55	61	109
AH6248	170	2	34	203	193	161	213	630	684	356
AH7031Z	170	3	39	58	58	60	44	51	69	90
AH7029	170	4	871	526	515	489	532	421	611	520
AH6292	170	5	33	51	48	46	45	58	61	164
AH6570	170	6	43	214	274	143	130	409	479	265
AH7083Z	170	7	37	77	76	61	52	70	80	87
GR240517X	170	8	69	76	70	72	79	77	83	100
AH6169K	171	1	39	61	53	56	45	54	62	59
GW315217X	171	2	28	45	37	-	57	48	59	74
AH11654	172	1	194	365	797	291	1747	2320	1562	1392
AH14868XX	172	2	502	843	863	663	1339	1404	1352	918
AH7167	172	3	840	921	833	801	845	893	906	869
AH7792Z	172	4	407	390	501	491	533	598	589	555
AH7650	172	5	816	950	960	869	955	1064	1100	955
AH6730	172	6	607	643	613	540	582	674	682	598
AH7290A	172	7	106	134	136	129	109	130	136	172
AH7652	172	8	310	1169	1891	1157	935	2010	2205	1256
AH7414Z	172	9	880	843	879	852	821	863	832	788
AH7621Z	172	10	575	587	597	584	589	571	584	570
AH7552	172	11	59	513	749	416	406	1044	1367	638
AH7651	172	12	700	759	744	735	753	782	738	778
AH7697	172	13	50	140	179	149	112	253	293	227
AH6276	173	1	422	511	350	415	403	279	458	430
GR85411X	173	2	341	326	341	373	339	344	303	289
AH6390	173	3	1651	1693	1586	1647	1606	1225	1787	1458
GR65254X	173	4	308	218	243	252	244	243	244	259
AH6535	173	5	113	113	106	113	97	97	115	109
AH6712	173	6	50	62	60	61	47	60	61	68
AH7646	173	7	39	50	50	53	47	57	52	87

Compound			Emission Intensity (616 nm +/- 10 nm)							
Reg_No	Cluster	Rank	Acids	EuBEA	EuBUA	EucyHA	EumcyHA	EuNBA	EuBBZA	EuBTA
GR257968X	173	8	45	63	76	75	85	101	113	96
AH6342	173	9	44	112	174	192	177	272	288	295
AH6572	173	10	93	113	118	110	114	136	113	141
AH7133	173	11	65	85	88	93	96	114	144	169
GW321108X	173	12	42	58	54	62	63	64	63	78
AH6550	173	13	1134	1191	1300	1247	1307	1253	1401	1176
GR242642X	173	14	49	71	68	73	71	74	81	103
AH6573	173	15	190	225	218	198	175	187	217	221
AH6714	173	16	117	125	117	140	116	132	129	131
AH6759	173	17	52	75	65	70	56	67	71	80
AH6713	174	1	39	60	56	59	44	62	73	71
AH7696	174	2	47	180	244	153	130	284	315	187
AH7731	174	3	38	35	42	26	51	50	47	50
AH2671	175	1	43	70	63	56	56	63	72	83
GR139602	175	2	80	154	-	-	-	224	199	-
GW433974	175	3	-	-	-	-	-	-	-	-
GW321876	175	4	65	71	80	82	82	73	79	91
GR139604	175	5	38	74	84	98	72	112	111	124
GW321338X	175	6	51	62	65	68	90	74	68	89
GW343619X	175	7	37	333	837	1642	1967	2384	1376	1721
AH2672	175	8	48	66	62	61	50	61	69	71
GR85308	175	9	67	80	83	81	73	82	85	86
GW321553X	175	10	175	203	221	225	411	266	248	321
GW368591A	175	11	49	67	70	75	72	63	76	96
GR115690	175	12	250	404	587	390	473	835	831	496
GR176137	175	13	120	502	-	-	-	2330	1568	-
GW321167	175	14	10	68	118	49	162	62	158	-
GW320968X	175	15	33	75	82	-	184	121	122	115
GW321421	175	16	127	131	143	-	172	144	144	162
GW315288X	175	17	55	58	62	-	66	62	75	74
GW315296X	175	18	80	81	91	-	140	100	104	110
GW288615	175	19	114	230	311	219	605	782	670	499
GW321424X	175	20	3792	599	1042	554	1013	1227	1348	1042
GW321634X	175	21	142	140	316	349	225	139	207	250

Compound			Emission Intensity (616 nm +/- 10 nm)							
Reg_No	Cluster	Rank	Acids	EuBEA	EuBUA	EucyHA	EumcyHA	EuNBA	EuBBZA	EuBTA
GW321145	175	22	105	882	746	-	847	1234	1402	748
GW321168X	175	23	227	165	189	-	223	243	190	227
GW321422X	175	24	130	180	179	-	286	242	208	254
GW322230X	175	25	61	82	75	73	70	72	82	78
GW314379	176	1	180	185	293	302	182	246	203	194
GW314406X	176	2	55	1522	1613	-	1397	2562	2917	1436
GW321354X	176	3	66	56	72	74	67	57	72	75
GW321243X	177	1	35	84	86	-	242	202	125	228
GW321742X	177	2	101	109	121	113	116	103	117	122
GW321779X	177	3	158	151	144	144	152	162	153	181
GW321755X	177	4	145	159	160	171	171	159	167	184
GW410928X	177	5	155	127	129	128	130	114	131	147
GW324540X	177	6	193	447	431	430	623	541	543	316
GW322198X	178	1	201	260	227	243	527	324	367	362
GW322492X	178	2	98	220	224	183	228	401	310	245
GW320926X	179	1	293	278	251	229	274	269	259	292
GW321470X	179	2	110	114	96	104	108	114	101	118
GW321607X	179	3	367	377	333	391	340	332	325	391
GW323008X	179	4	109	127	118	125	133	141	133	140
GR175627	180	1	46	-	311	347	899	-	397	-
GR175628	180	2	98	137	-	-	-	140	150	-
GR196922	180	3	19	17	20	19	18	20	23	-
GR256963	180	4	11	10	9	17	9	14	13	-
GW321245X	180	5	65	77	99		108	131	139	105
GW321912X	180	6	39	107	95	160	321	272	208	292
AH10033	181	1	46	62	58	57	54	63	61	64
GR237865X	182	1	37	62	61	63	45	60	67	71
AH15255XX	183	1	45	75	64	64	61	74	82	85
GR68357X	184	1	40	-	89	78	76	-	103	-
GW320801X	185	1	38	-	59	54	49	-	58	-
GW385455A	185	2	36	60	54	50	55	58	62	76
AH11305	186	1	118	-	116	110	132	-	109	-
AH9723	186	2	46	238	279	149	234	497	493	248
GW655414X	187	1	222	5321	6663	-	7226	7154	8208	5525

Compound			Emission Intensity (616 nm +/- 10 nm)							
Reg_No	Cluster	Rank	Acids	EuBEA	EuBUA	EucyHA	EumcyHA	EuNBA	EuBBZA	EuBTA
GR107114X	188	1	40	69	55	63	53	64	74	81
GR138809X	189	1	45	95	117	104	80	100	121	98
GW295817X	190	1	37	69	71	113	90	138	121	160
GW365467X	191	1	327	345	319	284	314	312	324	323
GW311376X	192	1	43	-	61	55	57	-	61	-
GW397304X	193	1	35	63	58	54	56	58	63	73
GW584442X	194	1	878	830	837	880	844	849	860	843
GW635258X	195	1	44	50	52	64	69	58	64	92
GW635452X	195	2	42	233	255	248	237	307	327	244
GR269503X	196	1	314	325	342	343	296	296	342	356
GR223454A	197	1	38	59	62	65	67	76	78	87
GW580127X	198	1	54	113	207	138	135	218	267	123
GW623142A	198	2	42	56	61	66	64	60	72	87
GW624854X	199	1	48	76	114	86	182	124	110	97
GW663118X	199	2	38	49	44	-	70	63	63	95
GW652611X	200	1	47	391	1091	609	777	1452	1487	640
GR151827X	201	1	62	235	235	162	145	196	312	196
GR152989X	201	2	48	309	775	513	460	1334	1040	409
AH11426	202	1	45	-	63	60	53	-	61	-
GR37359X	202	2	47	79	72	66	59	74	82	89
GW321066X	203	1	71	257	250	288	543	542	547	655
CCI8732	204	1	46	71	60	59	56	58	71	78
GW312666X	205	1	44	167	299	171	146	235	206	209
GW424662X	206	1	216	332	269	296	296	379	340	329
AH8940	207	1	42	86	95	60	62	102	109	92
GR258784X	208	1	46	70	75	64	65	75	76	83
GW322374X	208	2	33	71	60	54	64	64	68	77
AH8076	209	1	48	64	53	52	52	61	63	68
GW315274X	210	1	40	66	59	55	50	58	66	71
GW650524X	211	1	44	54	59	69	70	60	73	88
GW650525X	211	2	46	58	57	68	86	64	75	93
AH9033	212	1	43	82	67	63	63	74	76	85
GW649399X	212	2	2448	2037	2009	1654	1600	1460	1792	1908
AH9527	212	3	13186	12768	-	-	-	10757	10238	-

Compound			Emission Intensity (616 nm +/- 10 nm)							
Reg_No	Cluster	Rank	Acids	EuBEA	EuBUA	EucyHA	EumcyHA	EuNBA	EuBBZA	EuBTA
CCI4563	213	1	48	68	55	55	54	54	62	75
GR154660A	214	1	45	77	62	77	64	88	92	81
GR177049X	214	2	44	76	56	65	55	67	77	80
GR219652X	215	1	41	69	69	60	58	57	77	86
GR249207X	216	1	40	65	69	68	59	66	80	103
GR118330	217	1	112	153	123	142	135	135	145	154
GW276690	217	2	26	31	40	30	42	36	43	-
GR242234X	218	1	39	76	79	69	71	67	93	88
GW283348X	219	1	38	70	71	62	79	91	80	85
GW318076X	220	1	60	1675	2369	-	2693	4301	4911	2316
GR37727X	221	1	43	71	59	63	56	57	68	82
GR53040X	222	1	39	72	52	59	49	66	74	79
AH7643	223	1	45	83	78	67	67	92	94	89
AH9554	223	2	41	66	53	58	54	62	66	66
GR152077X	224	1	40	715	599	283	470	395	707	513
GM189907X	225	1	46	74	58	60	56	60	67	85
GR39699X	225	2	46	71	63	58	53	60	70	86
GR114312X	226	1	39	67	53	61	48	62	51	77
AH11195B	227	1	47	81	69	64	57	78	81	81
GR239106X	227	2	37	67	70	60	57	67	79	84
GR106841X	228	1	67	78	69	76	70	82	80	95
AH6081A	229	1	122	177	168	188	189	222	207	207
GR240822X	229	2	38	262	251	160	353	203	399	209
GW327515X	230	1	100	209	253	205	279	308	367	276
GW416086	230	2	40	82	69	73	69	75	79	95
AH9652	231	1	44	124	105	83	91	163	162	107
GR44240X	231	2	41	62	51	62	50	62	62	73
GR103163A	232	1	41	71	52	63	49	68	50	80
GW327758A	232	2	37	67	57	52	53	58	67	77
GW312641A	232	3	40	66	66	56	63	63	76	85
GI138330X	233	1	41	230	228	147	195	395	395	401
GW329078X	233	2	40	-	66	64	62	-	70	-
GR240576X	234	1	48	86	85	74	93	87	100	99
GW315215	234	2	62	-	91	78	82	-	81	-

Compound			Emission Intensity (616 nm +/- 10 nm)							
Reg_No	Cluster	Rank	Acids	EuBEA	EuBUA	EucyHA	EumcyHA	EuNBA	EuBBZA	EuBTA
GW412098	234	3	68	111	97	87	96	103	107	115
GR108394X	235	1	44	72	58	68	59	71	78	75
GR245706X	235	2	45	67	58	62	53	67	76	68
GR117055X	236	1	39	-	94	85	92	-	110	-
AH7461	237	1	86	125	-	-	-	126	145	-
GW341377	237	2	12	11	9	13	10	12	8	-
GW365140	237	3	13	8	12	12	11	14	14	-
GW365173	237	4	10	8	10	11	10	14	12	-
GI261653	237	5	47	68	60	61	54	64	80	60
GR242078X	238	1	46	-	69	65	61	-	62	-
GW308852X	239	1	72	-	86	76	82	-	79	-
GW307512X	240	1	41	72	65	86	95	82	76	95
GW311866X	241	1	38	51	64	69	74	63	85	110
GW319241X	242	1	39	67	55	53	58	68	66	74
GW448056X	243	1	45	81	83	84	83	91	103	114
GR258734A	244	1	53	69	66	71	67	66	80	101
GR264071A	244	2	59	80	84	95	81	85	101	119
GR263255X	244	3	45	63	65	72	65	67	76	104
GR43767X	245	1	41	93	69	73	67	90	78	91
GW472535X	245	2	43	71	67	64	65	83	89	89
GW288946X	246	1	7487	6701	6936	7347	6519	8116	7340	6621
GW324060X	247	1	47	101	88	72	73	99	112	108
AH10315	248	1	46	72	63	59	57	66	67	81
AH10461	248	2	43	74	61	58	56	67	72	80
GR105716X	249	1	40	72	51	67	50	63	71	80
GR212122X	249	2	42	68	70	59	51	59	80	80
AH22431B	250	1	46	76	63	58	55	65	83	107
GR109361X	250	2	39	64	51	60	49	60	63	69
GR60436X	250	3	37	137	108	118	123	190	114	162
AH6087	251	1	50	71	61	56	55	62	67	77
GI163641X	251	2	47	75	59	65	60	62	76	84
CCI153	252	1	47	76	60	60	53	65	73	87
GR128873	252	2	82	113	109	113	100	108	124	124
GR75538X	253	1	40	64	53	61	48	63	68	70

Compound			Emission Intensity (616 nm +/- 10 nm)							
Reg_No	Cluster	Rank	Acids	EuBEA	EuBUA	EucyHA	EumcyHA	EuNBA	EuBBZA	EuBTA
GR35345A	254	1	46	212	169	131	144	273	289	265
GR49747X	255	1	65	83	72	75	73	80	87	75
GR51603A	256	1	45	65	59	56	54	68	78	64
GR85161X	256	2	43	69	58	61	52	68	70	83
AH10536	257	1	216	444	-	-	-	749	757	-
AH10767	257	2	99	254	-	-	-	469	356	-
AH9356	257	3	42	285	275	146	199	498	573	254
GW316125	257	4	106	129	114	127	118	153	136	135
CCI10174	258	1	49	249	229	140	168	375	411	192
GR263958X	258	2	40	76	80	66	70	70	91	80
GW433821A	259	1	39	-	142	106	133	-	210	-
CCI10446	260	1	45	71	58	60	53	70	78	80
GR138218X	260	2	41	67	51	53	48	69	72	78
GW349042X	261	1	35	110	107	76	86	143	152	104
GR44479X	262	1	40	70	57	60	49	62	75	74
GR66484X	262	2	43	76	57	66	54	70	76	82
GW449422A	262	3	37	74	68	60	64	66	75	92
GI204510X	263	1	43	88	64	65	59	75	90	76
GR239579X	263	2	339	381	361	345	278	325	319	315
GW352006X	263	3	34	66	69	60	102	124	87	105
GI233445X	264	1	48	74	59	63	53	62	70	78
GR239577X	265	1	38	64	67	60	56	62	71	79
AH1010	266	1	38	-	60	56	58	-	59	-
CCI21414	266	2	41	-	60	56	52	-	55	-
GI222692X	266	3	47	-	66	61	64	-	69	-
GR84679X	267	1	46	-	67	66	62	-	72	-
GR84985A	267	2	41	-	64	63	53	-	67	-
AH10182	268	1	40	61	59	51	54	61	59	65
GR203336X	268	2	39	64	68	60	53	55	76	74
AH20998XX	269	1	45	71	62	62	54	64	71	78
AH6595	269	2	44	84	79	63	62	88	88	84
AH21933X	269	3	38	-	84	67	73	-	100	-
GR154396X	269	4	44	-	61	60	59	-	64	-
GW408146X	269	5	39	92	80	66	70	101	104	92

Compound			Emission Intensity (616 nm +/- 10 nm)							
Reg_No	Cluster	Rank	Acids	EuBEA	EuBUA	EucyHA	EumcyHA	EuNBA	EuBBZA	EuBTA
AH6732	270	1	41	66	58	57	65	66	72	84
GR208133X	270	2	34	75	75	63	73	72	86	92
AH1031	271	1	38	-	61	56	53	-	66	-
AH16943AA	271	2	44	133	95	130	135	136	136	181
AH1052	271	3	49	485	497	300	354	887	813	970
CCI21405	271	4	48	513	466	221	363	799	929	425
AH11453	271	5	41	-	65	57	53	-	60	-
CCI10176	271	6	44	238	180	131	147	392	424	242
AH10633	272	1	44	290	227	153	197	391	382	197
GW369905	272	2	12	66	191	52	136	63	173	-
AH8268A	272	3	43	77	68	67	59	73	100	72
GR202022X	273	1	36	7197	6348	7418	8270	11143	12427	5451
GR34043X	273	2	39	-	1189	699	1056	-	1867	-
GR247048X	274	1	44	80	79	86	85	82	98	142
GW309880X	274	2	39	266	267	206	334	595	410	304
GR230760X	275	1	41	381	350	197	569	283	584	278
GW299526X	275	2	36	69	68	63	63	59	83	79
AH10225	276	1	47	2820	2843	1625	2219	4972	5053	5087
AH11688	276	2	172	1145	-	-	-	2525	1233	-
GR258750	276	3	11	1831	1946	1219	2096	1419	2323	-
AH11368	276	4	130	167	119	119	123	114	173	103
GI266527	276	5	32	1441	1477	988	1619	1138	1581	-
AH11967	277	1	50	779	1606	1310	878	4075	2405	5299
GR140330X	277	2	468	515	461	405	520	511	428	532
GR216655X	277	3	43	-	90	79	90	-	126	-
GR220880X	277	4	41	-	65	57	55	-	65	-
GR232939X	278	1	40	98	103	99	100	121	141	164
AH1053	279	1	49	767	700	342	490	1225	1207	1196
AH6596	279	2	43	67	60	56	53	65	70	76
AH12133	280	1	45	785	945	1392	1647	5235	1969	5210
AH13394	280	2	42	359	273	215	264	544	525	278
GW299375X	280	3	40	98	89	80	110	195	118	106
AH3663	281	1	44	89	73	79	77	79	97	100
GR239599X	281	2	42	85	84	73	101	81	113	96

Compound			Emission Intensity (616 nm +/- 10 nm)							
Reg_No	Cluster	Rank	Acids	EuBEA	EuBUA	EucyHA	EumcyHA	EuNBA	EuBBZA	EuBTA
AH11395	282	1	54	143	56	104	135	228	184	179
AH13826XX	282	2	54	-	79	72	66	-	73	-
GR54987X	282	3	38	-	69	60	73	-	82	-
GW471049X	282	4	43	-	91	76	112	-	135	-
GW320828X	282	5	319	425	445	442	440	617	557	456
GW321479X	282	6	1046	1043	1117	-	1349	1336	1188	1279
GR101886	283	1	123	-	155	145	165	-	158	-
GR82448	283	2	98	120	193	102	108	117	134	123
GW294831	283	3	178	200	204	211	223	187	197	-
AH12975	284	1	127	155	138	146	152	174	175	161
GW312607X	284	2	63	86	125	113	232	203	163	215
AH17009XX	285	1	41	-	111	110	283	-	167	-
GW314282X	285	2	39	-	64	57	56	-	58	-
GW355545X	285	3	699	745	709	735	679	770	768	684
AH3705A	286	1	40	-	66	57	63	-	74	-
CCI10881	286	2	37	-	62	52	59	-	63	-
AH10300	287	1	194	396	-	-	-	387	445	-
AH10801	287	2	101	595	-	-	-	534	841	-
AH9678	287	3	91	251	-	-	-	416	399	-
AH10698	287	4	6890	7190	-	-	-	4464	5857	-
AH10853	287	5	96	121	-	-	-	114	149	-
GR92452	287	6	80	113	-	-	-	104	122	-
AH9727	287	7	43	-	176	106	166	-	259	-
AH12695	287	8	86	3900	-	-	-	2837	2250	-
AH13070	287	9	42	69	72	64	60	76	79	70
AH9676	287	10	80	7701	-	-	-	11749	11235	-
AH9721	287	11	90	119	-	-	-	108	122	-
AH10301X	288	1	40	1035	1216	656	1425	3332	1645	1402
AH15692	288	2	77	1465	-	-	-	1699	2145	-
AH12533	288	3	82	705	-	-	-	1069	869	-
AH12590	288	4	85	400	-	-	-	587	429	-
AH15690	288	5	84	676	-	-	-	770	711	-
AH15757	288	6	87	886	-	-	-	953	666	-
AH10978	288	7	82	181	-	-	-	307	317	-

Compound			Emission Intensity (616 nm +/- 10 nm)							
Reg_No	Cluster	Rank	Acids	EuBEA	EuBUA	EucyHA	EumcyHA	EuNBA	EuBBZA	EuBTA
AH11275	288	8	39	733	1222	1894	1855	2572	2763	1119
AH12589	288	9	42	109	112	72	171	192	170	143
AH11274	288	10	43	278	280	283	465	426	420	524
AH13391	288	11	43	176	164	107	277	263	267	265
GR254264X	288	12	38	212	225	216	245	366	342	277
AH10616T	289	1	45	60	54	59	54	62	73	53
AH7490	289	2	39	53	49	46	51	51	50	56
AH18515XX	290	1	40	-	287	161	247	-	503	-
AH22573X	290	2	52	69	62	64	129	80	73	86
AH8588	290	3	47	74	69	68	76	71	78	77
AH8601	290	4	269	280	347	315	336	304	302	287
GR32737X	290	5	44	65	58	57	54	53	69	72
AH23288X	291	1	41	49	48	61	71	58	59	72
GI149558	291	2	85	130	-	-	-	118	119	-
GR133921	291	3	88	125	-	-	-	117	137	-
GR134971	291	4	146	182	-	-	-	197	218	-
GR65242X	291	5	43	73	56	62	52	66	72	77
AH26099	291	6	157	172	161	179	185	162	176	163
GR116365X	291	7	243	353	399	371	261	299	251	274
GW541785X	291	8	59	69	71	86	93	76	80	106
GR31004	291	9	13	15	13	17	14	16	12	-
GW278395	291	10	89	108	131	118	114	111	121	-
GR110635X	292	1	40	66	51	63	50	65	70	72
GR116353X	292	2	41	65	49	58	63	69	71	71
GR125882X	292	3	40	71	53	64	63	68	70	78
GW294490X	292	4	39	65	66	59	55	60	73	82
GW589997X	293	1	38	49	52	63	61	50	63	79
AH20902	294	1	84	114	103	98	98	99	108	122
GR36456	294	2	19	20	20	21	16	20	21	-
AH20984	294	3	86	118	-	-	-	113	138	-
AH21852	294	4	85	130	-	-	-	118	139	-
GR252017	294	5	22	22	26	27	28	29	25	-
GR58047	294	6	45	73	58	65	56	65	77	85
GR44857A	295	1	227	267	238	208	214	231	241	266

Compound			Emission Intensity (616 nm +/- 10 nm)							
Reg_No	Cluster	Rank	Acids	EuBEA	EuBUA	EucyHA	EumcyHA	EuNBA	EuBBZA	EuBTA
GR207154	296	1	54	88	85	78	71	76	97	94
GR78684X	296	2	269	275	248	269	270	262	246	273
AH2426A	297	1	39	-	67	63	58	-	71	-
AH3116	297	2	165	174	157	168	166	197	181	179
GW304734X	297	3	49	683	689	383	585	1263	1161	1029
GW661447X	297	4	61	77	72	-	92	80	94	95
GR173175X	298	1	42	69	56	66	52	67	73	72
GR254404X	298	2	39	63	63	54	56	62	68	79
GW275105X	298	3	42	54	54	65	76	61	65	83
GW299610X	298	4	37	79	70	86	100	88	88	127
GW298781X	298	5	40	48	44	40	48	54	55	72
GW470761X	298	6	40	48	45	56	51	48	56	65
GW369798X	298	7	42	57	56	66	61	60	71	88
GW659802X	298	8	39	45	40	-	56	46	62	64
GR221928X	299	1	43	75	72	86	126	84	83	121
GW470720X	300	1	56	58	59	93	86	66	69	92
GW641296X	300	2	46	49	41	52	60	55	52	67

Comound			Relative Emission Intensity (I/I_0)							
Reg_No	Cluster	Rank	EuBEA	EuBUA	EucyHA	EumcyHA	EuNBA	EuBBZA	EuBTA	Average EuNAL
GR207962X	1	1	1	1	1	2	1	1	1	1
GR212454X	1	2	1	1	1	2	1	1	1	1
CCI21177	1	3	1	1	1	1	1	1	1	1
GR257381X	1	4	1	1	1	1	1	1	1	1
AH6621	1	5	1	1	1	1	1	1	1	1
GR193563X	1	6	1	1	1	1	1	1	1	1
GF267447X	1	7	1	1	1	1	1	1	1	1
GW431055X	1	8	1	1	1	1	1	1	1	1
GR257410X	2	1	1	1	1	1	1	1	1	1
GW503358X	2	2	1	1	1	1	1	1	1	1
GW318421X	2	3	1	1	1	1	1	1	1	1
GR50343X	3	1	1	2	1	1	2	2	1	1
AH14879XX	4	1	1	1	1	2	2	1	1	1
GR235591X	4	2	1	1	1	1	1	1	1	1
AH3827	5	1	2	2	2	3	5	3	3	3
GF267697X	5	2	1	1	1	1	1	1	1	1
GR32114X	5	3	1	1	1	1	1	1	1	1
AH14579XX	6	1	1	1	1	1	1	1	1	1
GW288607X	6	2	1	1	1	1	1	1	1	1
CCI23883	7	1	1	1	1	1	1	1	1	1
GR30858X	7	2	1	1	1	1	1	1	1	1
CCI3965	8	1	1	1	1	1	1	1	1	1
GI207347X	8	2	1	1	1	1	1	1	1	1
GR38987X	8	3	1	1	1	1	1	1	1	1
CCI3923A	9	1	1	1	1	1	1	1	1	1
GR38954X	9	2	1	1	1	1	1	1	1	1
GR251016X	9	3	1	1	1	1	1	1	1	1
AH14993XX	10	1	4	3	2	3	5	4	3	3
AH14994XX	10	2	1	1	1	1	2	1	1	1
GR84408X	10	3	12	6	4	4	4	5	3	5
AH25091X	10	4	1	1	1	1	1	1	1	1
GR64693X	10	5	18	29	30	29	42	36	17	29
AH16584XX	10	6	5	3	6	8	10	5	4	6
GR76119A	10	7	1	1	1	1	1	1	1	1

Comound			Relative Emission Intensity (I/I_0)							
Reg_No	Cluster	Rank	EuBEA	EuBUA	EucyHA	EumcyHA	EuNBA	EuBBZA	EuBTA	Average EuNAL
GI224436X	11	1	1	1	1	2	1	1	1	1
GR34543	11	2	1	1	1	1	1	1	-	1
GR40314	11	3	1	1	1	3	2	2	-	2
GR62892	11	4	4	-	-	-	4	5	-	4
GF133808X	12	1	1	1	1	1	1	1	1	1
GR253989X	12	2	1	1	1	1	1	1	1	1
GR215101X	12	3	1	1	1	1	1	1	1	1
GW322044X	13	1	1	1	1	1	1	1	1	1
GR148285X	14	1	1	1	1	2	2	2	1	2
GR81142X	14	2	1	1	1	1	1	1	1	1
GR63007X	14	3	1	1	1	1	1	1	1	1
GW423740X	15	1	1	1	1	2	2	1	1	2
AH14732XX	16	1	1	1	1	1	1	1	1	1
GW291819X	16	2	1	1	1	1	1	1	1	1
AH15398XX	16	3	1	1	1	1	1	1	1	1
GW314444X	16	4	1	1	1	1	1	1	1	1
GW385245X	16	5	1	2	1	2	2	2	2	2
AH15251XX	17	1	2	2	2	3	2	2	2	2
AH4591	17	2	1	1	1	1	1	1	1	1
AH8259	17	3	7	6	5	5	6	4	3	5
GR34041X	17	4	1	1	1	1	1	1	1	1
GR261706X	18	1	1	1	1	1	1	1	1	1
GR265013X	18	2	1	1	1	2	2	2	2	2
GR49081X	19	1	1	1	1	1	1	1	1	1
GW339416X	19	2	1	1	1	1	1	1	1	1
GW404922A	19	3	1	1	1	1	1	1	1	1
GW409763X	19	4	1	1	1	1	1	1	1	1
AH11164	20	1	-	1	1	2	-	1	-	1
GR214770X	20	2	-	1	1	1	-	1	-	1
CCI5134	20	3	1	1	1	1	1	1	1	1
GI149795A	20	4	1	1	1	1	1	1	1	1
GR38988X	20	5	1	1	1	1	1	1	1	1
GR39182X	20	6	1	1	1	1	1	1	1	1
GW328037X	20	7	1	1	1	1	1	1	1	1

Comound			Relative Emission Intensity (I/I_0)							
Reg_No	Cluster	Rank	EuBEA	EuBUA	EucyHA	EumcyHA	EuNBA	EuBBZA	EuBTA	Average EuNAL
AH9074	21	1	-	1	1	1	-	1	-	1
GI160046X	21	2	1	1	1	1	1	1	1	1
GF253708X	21	3	-	1	1	1	-	1	-	1
GW328038X	21	4	1	2	1	2	2	2	2	2
AH11410	22	1	1	1	1	1	1	1	1	1
GI166356X	22	2	1	1	1	1	1	1	1	1
AH5737	22	3	1	1	1	1	1	1	1	1
GR239060X	22	4	1	1	1	1	1	1	1	1
CCI1659	22	5	-	1	1	2	-	1	-	1
GR156438X	22	6	1	1	1	1	1	1	1	1
GR58626X	23	1	1	1	1	1	1	1	1	1
GR87165X	23	2	-	19	12	13	-	14	-	15
AH18307XX	24	1	-	1	1	1	-	1	-	1
GF234517X	24	2	-	1	1	1	-	1	-	1
GF233960X	25	1	-	1	1	1	-	1	-	1
GI220410A	25	2	1	1	1	1	1	1	1	1
GR101348X	25	3	-	1	1	1	-	1	-	1
AH14771AA	26	1	-	2	3	3	-	3	-	3
GF241458X	26	2	1	1	1	1	1	2	1	1
GR71072X	26	3	3	2	3	4	6	5	4	4
GR93262X	26	4	1	1	1	1	1	1	1	1
GW315267X	27	1	1	1	1	1	1	1	1	1
GR59449X	28	1	1	1	1	2	1	1	1	1
GR59450X	28	2	2	6	1	6	11	5	1	4
CCI17440	29	1	3	4	4	4	3	3	3	3
GR68891	29	2	1	4	4	4	5	4	-	4
GI148915	29	3	1	-	-	-	2	1	-	1
GR207121	29	4	6	4	5	5	6	5	-	5
GR260810	29	5	1	1	1	1	2	1	-	1
GR66288	29	6	1	1	2	2	2	1	-	1
GI166629	29	7	7	6	6	7	8	7	-	7
GR235507	29	8	5	4	4	4	5	4	-	4
GR38555	29	9	2	2	2	2	2	2	-	2
GW296997	29	10	7	6	6	6	7	6	-	6

Comound			Relative Emission Intensity (I/I_0)							
Reg_No	Cluster	Rank	EuBEA	EuBUA	EucyHA	EumcyHA	EuNBA	EuBBZA	EuBTA	Average EuNAL
CCl4008	29	11	1	1	1	2	1	1	1	1
GR244973	29	12	2	2	1	2	3	2	-	2
GR260719	29	13	1	1	1	1	1	1	-	1
GW317730	29	14	2	2	2	2	3	2	-	2
GW412437	29	15	-	-	-	-	-	-	-	#DIV/0!
GW369998	29	16	2	2	2	2	2	2	-	2
GW416206	29	17	-	-	-	-	-	-	-	#DIV/0!
GW315253X	29	18	2	3	3	5	4	4	3	3
AH16806XX	30	1	1	1	1	2	2	1	1	1
AH17157XX	30	2	6	3	9	14	28	25	10	14
GW312681X	30	3	1	3	2	2	2	2	2	2
AH4366	31	1	2	3	2	4	6	4	3	3
AH4367	31	2	1	1	1	1	1	1	1	1
AH9991	31	3	1	1	2	2	2	2	2	2
AH9456	31	4	1	1	1	1	1	1	1	1
AH7716	32	1	1	2	2	3	2	2	2	2
GR244160X	32	2	1	1	1	1	1	1	1	1
GR30170X	32	3	1	1	1	1	1	1	1	1
GW294785X	32	4	1	1	1	1	1	1	1	1
GR232463X	33	1	1	1	1	2	2	1	1	2
GW312679X	33	2	1	1	2	2	4	1	2	2
AH12195	34	1	3	2	2	3	3	4	2	3
GR30355X	34	2	2	2	2	3	4	4	2	3
GR30686X	34	3	1	1	1	1	1	1	1	1
GI221306X	34	4	-	1	1	2	-	1	-	1
GR197556X	34	5	-	1	1	2	-	1	-	1
GR236886	35	1	9	10	10	12	11	9	8	10
GW432536	35	2	-	-	-	-	-	-	-	#DIV/0!
AH14680XX	36	1	1	1	1	1	1	1	1	1
GR215350X	36	2	1	1	1	1	1	1	1	1
GW413125X	36	3	1	2	1	2	2	2	1	2
GR203309X	37	1	5	8	7	6	8	9	5	7
GR241592X	37	2	55	40	56	58	57	55	32	50
GR207127X	37	3	13	17	18	13	17	15	8	15

Comound			Relative Emission Intensity (I/I_0)							
Reg_No	Cluster	Rank	EuBEA	EuBUA	EucyHA	EumcyHA	EuNBA	EuBBZA	EuBTA	Average EuNAL
GW399139X	37	4	25	32	13	16	19	18	9	19
GR34040X	38	1	1	1	1	2	2	1	1	1
GW323465X	38	2	1	1	1	1	1	1	1	1
GR36337X	38	3	25	37	25	37	44	60	18	35
GR87232X	38	4	1	1	2	2	3	1	2	2
GW322742X	38	5	1	1	1	3	1	1	1	1
CCI8247	39	1	1	1	1	1	1	1	1	1
GW470564X	39	2	1	1	1	1	2	1	1	1
GR136744X	40	1	1	1	1	1	1	1	1	1
GW398946X	40	2	1	1	1	1	1	1	1	1
GR258074X	41	1	1	1	1	1	1	1	1	1
GR30298X	41	2	1	1	1	1	1	1	1	1
GW294643X	42	1	1	1	1	1	1	1	1	1
GW295897X	42	2	1	1	1	1	1	1	1	1
AH5119	43	1	1	1	1	1	1	1	1	1
GR146857A	43	2	1	1	1	1	1	1	1	1
GR108821X	43	3	1	1	1	1	1	1	1	1
CCI21441X	44	1	1	1	1	1	1	1	1	1
GI222965X	44	2	1	1	1	1	1	1	1	1
GR85032X	44	3	1	1	1	1	1	1	1	1
GW317925X	45	1	1	1	1	1	1	1	1	1
GW423592X	45	2	1	1	1	1	1	1	1	1
GR212558X	46	1	1	1	1	1	2	1	1	1
GV98449X	46	2	1	1	1	1	1	1	1	1
GR245353X	46	3	5	4	3	4	8	6	3	5
AH13207	47	1	1	1	1	1	1	1	1	1
GR53007X	47	2	2	2	2	2	3	2	1	2
AH8335X	47	3	1	1	1	2	2	2	1	2
GR100133X	48	1	1	1	1	1	1	1	1	1
GR111981X	48	2	1	1	1	2	2	1	1	1
GR124650X	49	1	1	1	1	2	2	2	1	2
GR236342X	49	2	1	1	1	1	1	1	1	1
GR258909	50	1	5	6	6	7	6	5	5	6
GR265026X	50	2	1	1	1	1	1	1	1	1

Comound			Relative Emission Intensity (I/I_0)							
Reg_No	Cluster	Rank	EuBEA	EuBUA	EucyHA	EumcyHA	EuNBA	EuBBZA	EuBTA	Average EuNAL
GR43579X	50	3	-	1	1	1	-	1	-	1
GR51409X	50	4	1	1	1	1	1	1	1	1
GW273704X	51	1	1	1	1	1	1	2	1	1
GW324992X	51	2	1	1	1	1	2	2	1	1
CCI19762	52	1	2	2	2	3	4	3	2	2
GR249776X	53	1	1	1	1	1	1	1	1	1
GR256398X	53	2	1	1	1	1	1	1	1	1
GR269435X	53	3	1	1	1	1	1	1	1	1
GR180851A	54	1	1	1	1	1	1	1	1	1
GR88677X	54	2	1	1	1	1	1	1	1	1
GW401244X	55	1	1	1	1	1	1	1	1	1
GW406680X	55	2	1	1	1	1	1	1	1	1
GW521849X	55	3	1	1	1	2	2	1	1	1
AH13312	56	1	2	1	1	2	2	2	1	2
AH14681XX	57	1	2	1	1	1	2	2	1	1
GR130650X	57	2	3	3	4	6	7	4	4	4
GR99513X	57	3	1	1	1	1	2	1	1	1
AH23294X	57	4	2	1	2	2	2	2	1	2
GR212000X	58	1	2	2	1	2	2	2	2	2
GR116024X	59	1	15	18	13	11	10	16	7	13
GR58504X	59	2	7	6	6	5	7	7	4	6
GW315124X	59	3	1	1	1	2	1	1	1	1
GW442963X	59	4	2	2	1	2	3	2	2	2
GW342768X	59	5	1	1	1	1	1	1	1	1
AH25327X	60	1	2	2	2	2	2	3	2	2
AH25377X	60	2	2	2	1	2	2	2	2	2
GR60468X	61	1	3	3	2	3	3	3	2	3
GR223597X	62	1	1	1	1	1	1	1	1	1
GW543499X	63	1	1	1	1	1	1	1	1	1
GR257678X	64	1	1	1	1	1	1	1	1	1
GW652716X	65	1	1	1	1	1	1	1	1	1
GW292869X	66	1	3	3	4	7	7	6	4	5
GW342412X	66	2	3	1	1	4	4	4	2	3
GR232127X	67	1	10	4	7	6	6	5	5	6

Comound			Relative Emission Intensity (I/I_0)							
Reg_No	Cluster	Rank	EuBEA	EuBUA	EucyHA	EumcyHA	EuNBA	EuBBZA	EuBTA	Average EuNAL
GW309937A	68	1	1	1	1	1	1	1	1	1
GR54241	69	1	1	1	1	1	1	1	1	1
GR64138A	69	2	1	1	1	1	1	1	1	1
GR81562	69	3	-	1	1	2	-	1	-	1
GW424484X	70	1	1	1	1	1	1	1	1	1
GW294777X	71	1	1	1	1	2	1	1	1	1
GW313525X	71	2	5	5	3	7	7	6	4	5
GW321902X	71	3	1	1	1	1	1	1	1	1
GR194866A	72	1	1	1	1	1	1	1	1	1
GR65644X	72	2	1	1	1	1	1	1	1	1
GW553810A	72	3	2	1	1	2	3	2	1	2
GW549758A	72	4	2	2	2	2	2	2	2	2
GW550038A	72	5	4	4	3	3	3	4	2	3
GR70745X	72	6	2	2	2	2	2	2	1	2
GR69220X	72	7	2	2	2	2	2	2	2	2
AH11291	73	1	2	2	2	2	3	2	2	2
GR94828A	73	2	11	1	5	8	9	15	5	8
AH12740	73	3	1	1	1	1	2	2	1	1
AH12757	73	4	1	1	1	1	1	1	1	1
GR199839X	73	5	1	1	1	1	1	1	1	1
GR58191X	74	1	1	1	1	1	1	1	1	1
GR87036X	75	1	1	1	1	1	1	1	1	1
GW415452X	75	2	1	1	1	1	1	1	1	1
AH8294	76	1	1	1	1	1	1	1	1	1
GR39220X	76	2	2	2	2	3	3	3	2	2
GI101694A	76	3	1	1	1	1	1	1	1	1
GR50961A	76	4	2	2	2	2	3	2	2	2
GR147168X	77	1	19	23	20	26	20	19	16	20
GR51196X	77	2	1	1	1	1	1	1	1	1
GR117463X	78	1	1	1	1	1	1	1	1	1
GR208696X	78	2	1	1	1	1	1	1	1	1
GR32768A	78	3	1	1	1	1	1	1	1	1
GW432313X	78	4	1	1	1	1	1	1	1	1
GR266494X	79	1	-	-	-	-	-	-	-	#DIV/0!

Comound			Relative Emission Intensity (I/I_0)							
Reg_No	Cluster	Rank	EuBEA	EuBUA	EucyHA	EumcyHA	EuNBA	EuBBZA	EuBTA	Average EuNAL
GW298250X	79	2	1	1	1	1	1	1	1	1
GR125017X	80	1	2	2	2	5	2	2	2	2
GW370018X	80	2	1	1	1	1	1	1	1	1
GW315103X	81	1	1	1	1	1	1	1	1	1
GW321966X	81	2	2	2	2	3	4	3	3	3
GF233961X	82	1	1	1	1	1	1	1	1	1
GI230797A	82	2	1	1	1	1	1	1	1	1
GR140164X	82	3	1	1	1	2	1	1	1	1
GW290604X	83	1	17	16	17	32	41	21	19	23
GW291821X	83	2	1	1	1	1	1	1	1	1
GW361278X	83	3	1	1	1	1	1	1	1	1
GW336990X	83	4	1	1	1	1	1	1	1	1
GW295365X	83	5	1	1	1	2	1	1	1	1
GW292911X	84	1	1	2	1	2	1	1	1	1
GW294867X	84	2	1	1	2	3	3	2	2	2
GW322405X	84	3	2	2	2	5	5	3	4	3
GW315228X	85	1	4	4	5	5	4	3	3	4
GW321601X	86	1	3	3	2	4	4	4	3	3
GI230786	87	1	1	1	1	1	1	1	1	1
GW295364	87	2	2	2	2	2	2	2	2	2
AH7066	88	1	1	1	1	1	1	1	1	1
GF234516X	88	2	1	1	1	2	1	1	2	1
GF269343X	88	3	1	1	1	2	2	1	1	1
GW314651X	88	4	1	1	1	2	2	1	1	1
GW311857X	88	5	1	1	1	1	1	1	1	1
GW323587X	88	6	24	29	23	34	39	47	18	31
GW294790X	88	7	6	16	11	11	18	15	7	12
GW322118X	88	8	3	4	4	6	7	4	4	5
GW312723X	89	1	1	2	2	2	2	2	1	2
GW432537X	89	2	2	3	2	3	3	3	2	3
GW322502X	89	3	2	2	2	3	3	2	2	2
GW312725X	89	4	1	1	1	1	1	1	1	1
GW322531X	89	5	1	1	1	2	3	2	2	2
GW314663X	89	6	11	20	-	18	31	22	12	19

Comound			Relative Emission Intensity (I/I_0)							
Reg_No	Cluster	Rank	EuBEA	EuBUA	EucyHA	EumcyHA	EuNBA	EuBBZA	EuBTA	Average EuNAL
GW323690X	89	7	8	10	8	11	11	12	7	9
GW323328X	89	8	2	2	2	3	3	3	2	2
AH10503	90	1	1	1	1	1	1	1	1	1
AH25564X	90	2	1	1	1	1	1	1	1	1
CCI7155	90	3	1	1	1	1	1	1	1	1
GR51515	90	4	1	1	1	1	1	1	1	1
GW363503A	90	5	1	1	1	1	1	1	1	1
GR253714X	90	6	1	1	1	1	1	1	1	1
AH9018	90	7	44	51	25	50	74	77	84	58
AH12070	91	1	2	2	2	2	2	2	2	2
GI123058	91	2	1	-	-	-	1	2	-	1
GR55509	91	3	2	2	2	3	4	3	-	3
GR50239	91	4	2	1	2	2	2	1	-	2
GR87121	91	5	1	-	-	-	1	1	-	1
AH2951	91	6	1	1	1	1	1	1	1	1
GR199994	91	7	1	1	1	1	1	1	1	1
AH12275	91	8	1	1	1	2	1	1	1	1
GR173757	91	9	2	2	2	2	2	2	1	2
GR161201X	91	10	1	1	1	1	1	1	1	1
AH12764	92	1	1	1	2	2	1	1	1	1
AH17306AB	92	2	1	1	1	1	1	1	1	1
GR161186X	92	3	1	1	1	1	1	1	1	1
AH15079XX	93	1	-	1	1	1	-	1	-	1
GR35117X	93	2	-	1	1	1	-	1	-	1
AH21453	93	3	1	1	1	1	1	1	1	1
GR178029	93	4	1	-	-	-	1	1	-	1
GR33748	93	5	11	16	11	19	19	20	6	15
GI152672	94	1	2	2	2	2	2	2	2	2
GR141743	94	2	1	1	1	1	1	1	-	1
GR39406	94	3	1	1	1	1	1	1	-	1
GR214280	94	4	1	1	1	1	1	1	1	1
GR226270	94	5	1	1	1	1	1	1	-	1
GR78537	94	6	1	1	1	1	1	1	-	1
GR189793	94	7	1	-	-	-	1	1	-	1

Comound			Relative Emission Intensity (I/I_0)							
Reg_No	Cluster	Rank	EuBEA	EuBUA	EucyHA	EumcyHA	EuNBA	EuBBZA	EuBTA	Average EuNAL
GR263804X	94	8	1	1	1	1	1	1	1	1
GW324674	94	9	1	1	1	1	1	1	-	1
GW410247	94	10	-	-	-	-	-	-	-	#DIV/0!
GR38461X	94	11	1	1	1	1	1	1	1	1
GW340239X	94	12	1	1	1	1	1	1	1	1
GR73169X	94	13	1	1	1	1	1	1	1	1
AH15491XX	95	1	1	1	1	1	1	1	1	1
GR107832X	95	2	1	1	1	1	1	1	1	1
GR231878X	95	3	1	1	1	1	1	1	1	1
GR137556X	95	4	1	1	1	1	1	1	1	1
GF146238	96	1	6	6	7	8	6	7	6	6
GW295088	96	2	7	6	6	5	8	5	-	6
GF267572X	96	3	1	1	1	1	1	1	1	1
GW323141X	96	4	1	1	1	1	1	1	1	1
GF267575X	97	1	1	2	2	2	2	2	1	2
GR76319X	97	2	5	6	11	28	27	18	18	16
GR78359X	97	3	2	2	2	2	2	2	2	2
GI170475X	98	1	-	1	1	1	-	1	-	1
GW275669A	98	2	-	1	1	1	-	1	-	1
GR205623X	98	3	-	1	1	1	-	1	-	1
GR53844X	99	1	-	1	1	1	-	1	-	1
GW298071X	100	1	1	1	1	1	1	1	1	1
GI199827X	101	1	1	1	1	1	1	1	1	1
GR141837X	101	2	1	1	1	1	1	1	1	1
GW323802A	101	3	1	1	1	1	1	1	1	1
GW329522X	102	1	1	1	1	1	1	1	1	1
GR251266A	103	1	2	2	2	1	2	2	2	2
GR265018A	103	2	1	1	1	1	1	1	1	1
GR253017X	103	3	1	1	1	1	1	1	1	1
GW425183X	104	1	3	3	2	3	4	3	2	3
GR267248A	105	1	1	1	1	1	1	1	1	1
GW425181X	105	2	1	1	1	1	1	1	1	1
AH17295XX	106	1	1	1	1	1	1	1	1	1
AH26206X	106	2	1	1	1	1	1	1	1	1

Comound			Relative Emission Intensity (I/I_0)							
Reg_No	Cluster	Rank	EuBEA	EuBUA	EucyHA	EumcyHA	EuNBA	EuBBZA	EuBTA	Average EuNAL
AH20560XX	106	3	1	1	1	1	1	1	1	1
GR97173X	106	4	1	1	1	1	1	1	1	1
AH21291X	106	5	1	1	1	1	1	1	1	1
GW471254X	106	6	1	1	1	1	1	1	1	1
AH17365XX	107	1	1	1	1	1	1	1	1	1
GI198830X	107	2	1	1	1	1	1	1	1	1
AH7669	107	3	1	1	1	1	1	1	1	1
GI221325A	107	4	1	1	1	1	1	1	1	1
GI95276X	107	5	1	1	1	1	1	1	1	1
CCI7978	108	1	-	1	1	1	-	1	-	1
GF267691X	108	2	1	1	1	1	1	1	1	1
GI147499A	108	3	-	1	1	1	-	1	-	1
AH21350X	109	1	1	1	1	1	1	1	1	1
GW321669X	109	2	-	1	1	1	-	1	-	1
GW323630X	109	3	1	1	1	1	1	1	1	1
CCI1914	109	4	1	1	1	1	1	1	1	1
GF146728X	109	5	-	1	1	1	-	1	-	1
GR86838X	109	6	1	1	1	1	1	1	1	1
AH5502	110	1	2	2	2	2	2	2	2	2
GR141836	110	2	1	-	-	-	1	1	-	1
GR248323	110	3	2	2	2	2	2	2	-	2
AH6472	110	4	1	-	-	-	1	1	-	1
GR141839	110	5	1	-	-	-	1	1	-	1
GR31162	110	6	1	1	1	1	1	1	-	1
GR40490	110	7	1	1	1	1	1	1	-	1
GR40028	110	8	1	1	1	1	1	1	-	1
GI149060	110	9	4	-	-	-	3	3	-	3
GI153357	110	10	1	-	-	-	1	1	-	1
GV95604	110	11	4	3	4	4	4	4	-	4
GI119939X	110	12	-	1	1	1	-	1	-	1
GI147798	110	13	1	-	-	-	1	1	-	1
GR113723	110	14	1	-	-	-	1	1	-	1
GI150183	110	15	1	-	-	-	1	1	-	1
GR259835	110	16	1	1	1	1	1	1	-	1

Comound			Relative Emission Intensity (I/I_0)							
Reg_No	Cluster	Rank	EuBEA	EuBUA	EucyHA	EumcyHA	EuNBA	EuBBZA	EuBTA	Average EuNAL
GR197159	110	17	1	-	-	-	1	1	-	1
GR118329	110	18	1	-	-	-	1	2	-	1
GI151314	110	19	1	-	-	-	1	1	-	1
GR214686	110	20	1	1	1	1	1	1	-	1
GR89164	110	21	1	-	-	-	1	1	-	1
GR261930	110	22	6	5	6	5	6	5	-	5
GR31787A	110	23	-	1	1	1	-	1	-	1
CCI8566	111	1	2	2	2	2	2	2	2	2
GR32579	111	2	1	1	1	1	1	1	-	1
GW286126	111	3	2	3	6	5	6	4	2	4
GW422957	111	4	-	-	-	-	-	-	-	#DIV/0!
GR123674	111	5	1	-	-	-	1	1	-	1
GR146669	111	6	1	-	-	-	1	1	-	1
CCI9041	111	7	1	1	1	1	1	1	1	1
GW296344	111	8	1	1	1	1	1	1	-	1
GR154729	111	9	1	-	-	-	1	1	-	1
GR171932	111	10	1	-	-	-	1	1	-	1
AH13018	112	1	2	2	2	2	3	3	2	2
GV140840X	112	2	1	1	1	1	1	1	1	1
GR207209X	112	3	2	2	2	4	3	3	2	3
GR112257X	113	1	1	1	1	1	1	1	1	1
GR263152X	113	2	5	6	4	4	5	4	3	4
GR112259X	113	3	1	1	1	1	1	1	1	1
GR185905X	113	4	1	2	1	2	2	2	1	2
GR186845X	113	5	1	1	1	3	1	1	1	1
GR219630X	113	6	1	1	1	1	1	1	1	1
GW541786X	113	7	1	2	2	14	4	1	2	4
GW560094X	113	8	1	1	1	4	2	2	1	2
GR53539X	114	1	1	1	1	1	1	1	1	1
AH15201XX	115	1	4	3	4	4	4	3	3	4
AH6859	115	2	74	70	69	97	72	62	48	70
AH15203XX	115	3	96	88	92	101	102	102	71	93
GW314581X	115	4	74	76	68	82	96	85	62	77
GW294655X	115	5	6	4	4	0	6	6	4	4

Comound			Relative Emission Intensity (I/I_0)							
Reg_No	Cluster	Rank	EuBEA	EuBUA	EucyHA	EumcyHA	EuNBA	EuBBZA	EuBTA	Average EuNAL
GW328088X	115	6	70	72	67	72	66	67	49	66
GW312792X	115	7	54	104	61	100	121	123	40	86
GW294322X	115	8	46	41	37	39	43	37	29	39
GW304858X	115	9	4	4	3	4	8	4	3	4
GW312329X	115	10	14	13	10	13	16	16	8	13
AH15400XX	115	11	81	88	71	82	91	93	59	81
GW314526X	115	12	24	34	-	28	48	39	26	33
GW324336X	115	13	4	7	4	5	4	6	4	5
AH5558	116	1	1	1	1	2	2	2	1	1
AH5950	116	2	3	3	3	4	6	5	3	4
GW312371X	116	3	2	2	2	2	4	3	2	3
GW315227X	116	4	4	7	5	7	3	10	6	6
GW312460X	116	5	5	11	8	8	15	14	8	10
GW312437X	116	6	12	14	11	32	34	17	12	19
GW312435X	116	7	1	1	1	1	1	1	1	1
GF267701X	116	8	17	18	19	20	22	18	14	19
GR189755X	117	1	80	79	73	82	81	56	54	72
GW313003X	117	2	1	1	1	1	1	1	1	1
GR256734X	117	3	1	1	1	1	1	1	1	1
GW321218X	118	1	2	3	2	3	4	4	2	3
AH6372	119	1	4	4	3	3	23	9	3	7
GI205545X	119	2	1	1	1	1	1	1	1	1
GW312626X	119	3	2	2	2	2	4	3	2	3
GR230571X	119	4	2	2	2	2	2	2	2	2
AH21917X	120	1	1	1	1	1	1	1	1	1
AH22735X	120	2	1	1	1	1	1	1	1	1
GR177051X	120	3	1	1	1	1	1	1	1	1
GW471604X	120	4	2	2	2	2	2	2	1	2
GR152169X	120	5	1	1	1	1	1	1	1	1
GR225877X	121	1	1	1	1	1	1	1	1	1
GR255442X	121	2	7	10	5	8	15	12	4	9
CCI2180	122	1	1	1	1	1	1	1	1	1
GR121162X	122	2	1	1	1	1	1	1	1	1
GW308403X	123	1	2	2	2	2	3	2	2	2

Comound			Relative Emission Intensity (I/I_0)							
Reg_No	Cluster	Rank	EuBEA	EuBUA	EucyHA	EumcyHA	EuNBA	EuBBZA	EuBTA	Average EuNAL
GR114265X	124	1	2	3	2	3	3	3	2	3
GR225874X	124	2	1	1	1	1	1	1	1	1
GR51045X	125	1	1	1	1	1	1	1	1	1
GW521143X	126	1	1	1	1	1	1	1	1	1
GR200308X	127	1	2	2	1	2	3	2	1	2
GR32131X	127	2	1	1	1	1	2	1	1	1
AH2599	128	1	2	2	2	2	2	2	2	2
AH7307	128	2	2	-	-	-	3	3	-	3
GR121876X	129	1	1	1	1	1	1	1	1	1
GR193373X	129	2	1	1	1	1	1	1	1	1
GR196926X	129	3	1	1	1	1	1	1	1	1
GW426030X	129	4	1	1	1	1	1	1	1	1
AH21971X	130	1	5	6	5	6	10	10	4	6
GW648032X	130	2	2	2	1	2	3	3	1	2
CCI1710	130	3	2	2	1	2	3	2	1	2
GR71245X	130	4	10	9	22	30	30	20	16	20
GR173914X	131	1	1	1	1	2	1	1	1	1
GR257498X	132	1	1	1	1	1	2	2	1	1
AH23040X	133	1	1	1	1	1	1	1	1	1
GR36682X	133	2	1	1	1	1	1	1	1	1
GR47574X	133	3	1	1	1	1	1	1	1	1
GR215566X	134	1	1	1	1	1	1	1	1	1
GI198860X	135	1	3	3	2	3	5	4	2	3
GR74829X	135	2	1	1	1	2	2	2	1	2
GW271761X	135	3	1	1	1	1	1	1	1	1
GR232957X	136	1	6	8	7	10	8	9	5	8
GW322216X	136	2	7	7	4	6	17	18	5	9
AH4822	137	1	4	6	4	4	9	8	3	6
GR207205X	137	2	4	7	8	13	18	6	6	9
GF267466X	137	3	1	2	3	7	9	3	3	4
GW328094A	138	1	1	1	1	1	1	1	1	1
GW418822A	138	2	1	1	1	1	1	1	1	1
GW448911X	138	3	1	1	1	1	1	1	1	1
GI198877X	139	1	2	2	2	2	4	3	2	2

Comound			Relative Emission Intensity (I/I_0)							
Reg_No	Cluster	Rank	EuBEA	EuBUA	EucyHA	EumcyHA	EuNBA	EuBBZA	EuBTA	Average EuNAL
GR267007X	139	2	4	5	4	5	7	5	3	5
GW340373X	139	3	1	1	1	1	1	1	1	1
GR256536X	140	1	4	5	6	13	16	7	5	8
GR192153X	141	1	1	1	1	2	2	1	1	1
GW321193X	142	1	1	1	1	1	1	1	1	1
AH23064X	143	1	1	1	1	1	1	1	1	1
GW279435X	143	2	1	1	1	1	1	1	1	1
GW279438X	144	1	1	1	1	1	2	2	1	1
GW279439X	144	2	1	1	3	6	7	1	3	3
GR127482A	145	1	1	1	1	1	1	1	1	1
GR262262X	145	2	1	1	1	1	1	1	1	1
GR262264X	145	3	1	1	1	1	1	1	1	1
GR267264X	145	4	1	1	1	1	1	1	1	1
AH8425	146	1	44	52	55	62	61	47	42	52
GW314731X	146	2	39	34	34	46	43	33	26	36
GW314830X	146	3	104	82	-	99	109	91	69	92
GW320557X	146	4	96	80	81	92	90	75	67	83
GW323721X	146	5	103	89	74	93	99	82	64	86
GW314662X	147	1	21	49	32	64	68	59	43	48
GW314681X	147	2	24	26	31	55	40	40	28	35
GW314793X	147	3	21	29	-	56	33	31	34	34
GW322018X	147	4	45	60	43	73	99	83	34	62
GW314751X	147	5	21	24	18	43	27	23	24	26
GW315158X	147	6	16	18	-	25	25	18	14	19
GW322801X	147	7	20	28	25	61	43	37	35	36
GW323040X	147	8	45	48	50	76	68	65	39	56
GW321891X	147	9	1	1	1	1	1	1	1	1
GW323845X	147	10	6	7	6	7	5	6	5	6
GW323446X	147	11	9	13	9	19	17	16	12	13
GW323591X	147	12	65	91	65	96	144	151	67	97
GW315075X	147	13	11	11	11	19	16	13	11	13
GW322693X	147	14	8	10	8	15	13	13	9	11
GW321808X	147	15	16	17	13	44	31	26	16	23
GW322384X	147	16	7	8	8	10	14	12	7	10

Comound			Relative Emission Intensity (I/I_0)							
Reg_No	Cluster	Rank	EuBEA	EuBUA	EucyHA	EumcyHA	EuNBA	EuBBZA	EuBTA	Average EuNAL
GW321800A	147	17	3	1	4	4	4	4	2	3
GW322628X	147	18	34	30	26	33	30	27	22	29
GW322988X	147	19	8	9	7	10	10	11	8	9
AH15466AA	148	1	1	1	1	1	1	1	1	1
AH2565	148	2	1	1	1	1	1	1	1	1
GW366246	148	3	2	2	2	2	2	2	2	2
CCI17196	148	4	3	3	3	4	5	2	2	3
AH20078XX	149	1	16	28	21	35	40	33	20	28
GR208554X	149	2	13	14	12	13	13	9	8	12
GR230104X	149	3	7	10	8	13	10	11	5	9
GR30893X	149	4	24	26	39	29	39	26	20	29
GR33911X	149	5	14	16	28	34	28	29	18	24
GR62459X	149	6	107	122	106	118	120	124	71	109
GR65815X	149	7	21	16	21	29	14	24	13	20
GR65884X	149	8	24	21	36	37	31	31	15	28
GW385846X	149	9	69	85	57	68	89	93	41	72
GR155589X	149	10	2	1	2	3	3	2	2	2
GR30894X	149	11	12	12	15	12	12	12	8	12
GR208752X	149	12	4	8	8	8	17	9	7	9
GW288377X	149	13	30	56	19	20	30	43	14	30
GR34968X	149	14	4	4	4	6	6	5	3	5
GR54392X	149	15	103	136	183	87	97	196	55	123
GR57352X	149	16	22	25	25	24	60	38	18	30
GW371223X	149	17	1	1	1	5	2	1	1	2
CCI9740	149	18	1	1	1	1	1	1	1	1
GR240724X	149	19	4	5	13	11	16	10	8	10
GR30476X	149	20	1	1	1	4	2	1	2	2
GR53056X	149	21	1	1	1	1	1	1	1	1
GR136670X	150	1	2	4	2	2	2	3	1	2
GR34039X	150	2	1	1	2	4	3	2	2	2
AH24908A	151	1	2	4	3	5	4	4	2	3
GR49928X	151	2	2	3	2	4	3	3	2	3
AH25368X	151	3	4	7	8	9	8	9	3	7
GR55422X	151	4	20	25	20	21	41	29	17	25

Comound			Relative Emission Intensity (I/I_0)							
Reg_No	Cluster	Rank	EuBEA	EuBUA	EucyHA	EumcyHA	EuNBA	EuBBZA	EuBTA	Average EuNAL
GR55423X	151	5	17	20	19	21	32	32	14	22
GR61326X	151	6	15	30	51	55	51	58	15	39
GR61891X	151	7	16	35	52	59	58	52	25	43
GR61984X	151	8	25	40	71	79	75	72	37	57
GR61985X	151	9	21	39	51	56	59	55	24	44
GR55424X	151	10	24	24	24	22	34	32	18	25
AH5157	152	1	1	2	2	2	2	2	2	2
AH6770	152	2	1	1	1	1	1	1	1	1
AH9603	152	3	1	1	1	1	1	1	1	1
GW315367X	152	4	2	2	1	1	1	1	1	1
GR219955X	152	5	1	1	1	1	1	1	1	1
GR120092X	152	6	1	1	1	1	1	1	1	1
GR75258X	152	7	459	489	355	437	354	383	231	387
GF233967X	153	1	1	1	1	1	1	1	1	1
GW641533X	153	2	1	1	1	1	1	1	1	1
GW321911X	153	3	1	1	1	1	1	1	1	1
GW402775X	153	4	3	3	3	4	4	3	2	3
GR258179X	154	1	16	71	16	18	66	62	13	37
GR258213X	154	2	12	78	22	105	77	74	23	56
GF267695X	155	1	1	1	1	1	1	1	1	1
GW322088X	155	2	1	1	1	1	1	1	1	1
GW322112X	155	3	1	2	1	2	2	2	1	2
GW322316X	155	4	1	1	1	1	1	1	1	1
GW322086X	155	5	1	1	1	1	1	1	1	1
GR222247X	156	1	1	1	1	1	1	1	1	1
GR53849X	156	2	1	1	1	1	1	1	1	1
GR99312X	156	3	1	1	1	1	1	1	1	1
GR57082X	157	1	1	1	1	1	1	1	1	1
GW320929X	157	2	1	1	-	2	1	1	1	1
GW412113X	157	3	1	1	1	1	1	1	2	1
GR215780X	158	1	1	1	1	1	1	1	1	1
GR219957X	158	2	1	1	1	1	1	1	1	1
GR219958X	158	3	1	1	1	1	1	1	1	1
GR216184X	158	4	4	3	3	4	7	5	5	4

Comound			Relative Emission Intensity (I/I_0)							
Reg_No	Cluster	Rank	EuBEA	EuBUA	EucyHA	EumcyHA	EuNBA	EuBBZA	EuBTA	Average EuNAL
GR216186X	158	5	1	1	1	1	1	1	1	1
GR218004X	158	6	1	1	1	3	3	2	2	2
GR218005X	158	7	1	1	1	2	2	1	2	2
GR133748X	159	1	-	-	-	-	-	-	-	-
GR82836X	159	2	27	33	24	29	33	42	15	29
GR38662X	159	3	1	1	1	3	2	1	2	2
GW292734X	159	4	3	3	5	6	7	6	4	5
GW322234X	159	5	2	2	2	2	2	2	2	2
GR79956X	159	6	2	2	2	3	3	3	2	2
GR203866X	159	7	6	14	7	10	11	12	4	9
GR203872X	159	8	5	4	2	8	6	6	2	5
GR203875X	159	9	3	3	3	7	6	5	2	4
GR204301X	159	10	41	58	29	46	114	75	22	55
GR65881X	159	11	7	4	2	10	30	17	10	11
GR65883X	159	12	7	12	30	21	23	21	12	18
GR65885X	159	13	8	13	8	14	19	24	11	14
GR188442X	160	1	1	2	1	2	2	1	1	1
GW322235X	160	2	1	1	1	1	1	1	1	1
GW327773X	160	3	1	1	1	1	1	1	1	1
GW643493X	160	4	8	11	6	8	13	11	6	9
GW643495X	160	5	2	2	1	2	2	2	2	2
GR215459A	161	1	1	1	1	1	1	2	1	1
GW280814	161	2	1	1	1	1	1	1	1	1
GW290851X	161	3	1	1	1	1	1	1	1	1
GW290862X	161	4	1	1	1	1	1	1	1	1
GW326112X	161	5	2	2	2	4	5	3	3	3
GW271929X	162	1	2	3	2	3	3	2	2	3
GW317768X	162	2	26	38	26	32	49	34	13	31
GW272447X	162	3	2	2	2	4	3	2	2	3
GW326127X	162	4	4	10	7	10	9	9	4	8
GW440381X	162	5	5	10	8	23	12	6	5	10
GW418716X	162	6	2	2	2	3	3	2	2	2
GW453080X	162	7	2	2	2	4	3	3	2	3
GW442734X	162	8	2	2	2	4	3	2	2	2

Comound			Relative Emission Intensity (I/I_0)							
Reg_No	Cluster	Rank	EuBEA	EuBUA	EucyHA	EumcyHA	EuNBA	EuBBZA	EuBTA	Average EuNAL
GW272478X	162	9	1	2	2	3	3	2	2	2
GW442732X	162	10	2	2	2	3	3	2	2	2
GW415699X	162	11	21	89	27	60	48	49	16	44
GW369764X	162	12	25	41	20	63	38	34	16	34
GR50838A	163	1	3	4	3	3	6	7	2	4
GR51678X	163	2	37	35	30	30	49	46	23	36
GR54219X	164	1	11	10	8	12	22	21	11	14
GR69421X	164	2	4	5	3	3	10	8	3	5
GW317904X	165	1	2	2	-	4	5	2	2	3
GW411913X	165	2	1	1	1	1	1	1	1	1
GW327989X	165	3	1	2	2	2	3	2	1	2
GW414889X	165	4	1	1	1	1	1	1	1	1
AH10104A	166	1	1	1	1	1	1	1	1	1
AH7702	166	2	1	1	1	1	1	1	1	1
AH7559	166	3	1	1	1	1	1	1	1	1
AH10011A	166	4	1	1	1	1	1	1	1	1
AH7724Z	166	5	1	1	1	1	1	1	1	1
GW575621X	166	6	1	1	1	1	1	1	1	1
AH10424A	166	7	1	1	1	1	1	1	1	1
AH7620Z	166	8	1	1	1	1	1	1	1	1
AH7699	166	9	1	1	1	1	1	1	1	1
AH5961	167	1	1	1	1	1	1	1	2	1
AH6102	167	2	2	2	2	2	2	2	1	2
AH7647	167	3	1	1	1	1	1	1	1	1
AH9531	168	1	1	1	1	1	1	1	1	1
GR199045X	168	2	1	1	0	1	1	1	0	1
AH5724	169	1	2	2	1	1	8	8	3	4
GW295014X	169	2	2	2	1	3	4	4	2	3
GW315237X	169	3	1	1	1	1	2	3	1	1
GW315238X	169	4	1	2	-	2	2	2	1	1
AH6593	169	5	2	2	2	2	3	3	2	2
GW315239X	169	6	5	9	-	11	9	4	6	7
AH6247	169	7	8	8	7	10	7	8	5	8
AH6313	169	8	3	3	3	3	3	2	2	3

Comound			Relative Emission Intensity (I/I_0)							
Reg_No	Cluster	Rank	EuBEA	EuBUA	EucyHA	EumcyHA	EuNBA	EuBBZA	EuBTA	Average EuNAL
AH6072	169	9	3	6	5	6	5	5	5	5
AH6624	169	10	1	1	1	1	1	1	2	1
AH7013Z	169	11	1	1	1	1	1	1	1	1
AH7014Z	169	12	1	1	1	1	1	1	1	1
AH6198	170	1	1	1	1	1	1	1	1	1
AH6248	170	2	3	3	3	5	11	10	4	6
AH7031Z	170	3	1	1	1	1	1	1	1	1
AH7029	170	4	9	9	8	12	8	9	6	9
AH6292	170	5	1	1	1	1	1	1	2	1
AH6570	170	6	4	5	2	3	7	7	3	4
AH7083Z	170	7	1	1	1	1	1	1	1	1
GR240517X	170	8	1	1	1	1	1	1	1	1
AH6169K	171	1	1	1	1	1	1	1	1	1
GW315217X	171	2	1	1	-	1	1	1	1	1
AH11654	172	1	8	15	5	31	41	27	18	21
AH14868XX	172	2	18	17	13	24	25	23	12	19
AH7167	172	3	15	15	13	20	16	13	11	15
AH7792Z	172	4	8	10	9	10	11	10	7	9
AH7650	172	5	16	17	14	22	19	16	12	17
AH6730	172	6	11	11	9	14	12	10	7	10
AH7290A	172	7	2	2	2	3	2	2	2	2
AH7652	172	8	19	33	19	22	36	32	16	25
AH7414Z	172	9	14	15	14	19	15	12	10	14
AH7621Z	172	10	10	10	10	14	10	9	7	10
AH7552	172	11	8	13	7	9	19	20	8	12
AH7651	172	12	12	13	12	18	14	11	10	13
AH7697	172	13	2	3	2	3	5	4	3	3
AH6276	173	1	8	6	7	9	5	7	5	7
GR85411X	173	2	5	6	6	8	6	4	4	6
AH6390	173	3	28	28	27	37	22	26	18	27
GR65254X	173	4	5	5	5	4	4	4	3	4
AH6535	173	5	2	2	2	2	2	2	1	2
AH6712	173	6	1	1	1	1	1	1	1	1
AH7646	173	7	1	1	1	1	1	1	1	1

Comound			Relative Emission Intensity (I/I_0)							
Reg_No	Cluster	Rank	EuBEA	EuBUA	EucyHA	EumcyHA	EuNBA	EuBBZA	EuBTA	Average EuNAL
GR257968X	173	8	1	1	1	1	1	1	1	1
AH6342	173	9	2	3	3	4	5	4	4	4
AH6572	173	10	2	2	2	3	2	2	2	2
AH7133	173	11	1	2	2	2	2	2	2	2
GW321108X	173	12	1	1	1	1	1	1	1	1
AH6550	173	13	20	23	21	30	22	21	15	22
GR242642X	173	14	1	1	1	1	1	1	1	1
AH6573	173	15	4	4	3	4	3	3	3	3
AH6714	173	16	2	2	2	3	2	2	2	2
AH6759	173	17	1	1	1	1	1	1	1	1
AH6713	174	1	1	1	1	1	1	1	1	1
AH7696	174	2	3	4	3	3	5	5	2	4
AH7731	174	3	1	1	0	1	1	1	1	1
AH2671	175	1	1	1	1	1	1	1	1	1
GR139602	175	2	1	-	-	-	2	2	-	2
GW433974	175	3	-	-	-	-	-	-	-	#DIV/0!
GW321876	175	4	1	1	1	1	1	1	1	1
GR139604	175	5	1	1	2	2	2	2	2	2
GW321338X	175	6	1	1	1	2	1	1	1	1
GW343619X	175	7	6	15	28	34	40	22	20	24
AH2672	175	8	1	1	1	1	1	1	1	1
GR85308	175	9	1	1	1	2	1	1	1	1
GW321553X	175	10	4	4	4	7	4	4	4	4
GW368591A	175	11	1	1	1	1	1	1	1	1
GR115690	175	12	7	10	7	11	15	12	6	10
GR176137	175	13	4	-	-	-	18	12	-	12
GW321167	175	14	7	9	4	5	16	13	-	9
GW320968X	175	15	2	2	-	3	2	2	2	2
GW321421	175	16	3	3	-	3	3	2	2	3
GW315288X	175	17	1	1	-	1	1	1	1	1
GW315296X	175	18	2	2	-	2	2	2	1	2
GW288615	175	19	4	6	3	10	14	10	5	8
GW321424X	175	20	11	19	9	17	20	21	12	16
GW321634X	175	21	2	6	6	4	2	3	3	4

Comound			Relative Emission Intensity (I/I_0)							
Reg_No	Cluster	Rank	EuBEA	EuBUA	EucyHA	EumcyHA	EuNBA	EuBBZA	EuBTA	Average EuNAL
GW321145	175	22	18	15	-	15	25	22	10	17
GW321168X	175	23	3	4	-	4	5	3	3	4
GW321422X	175	24	4	4	-	5	5	3	3	4
GW322230X	175	25	1	1	1	1	1	1	1	1
GW314379	176	1	3	5	5	4	3	3	2	4
GW314406X	176	2	31	33	-	24	52	46	19	34
GW321354X	176	3	1	1	1	1	1	1	1	1
GW321243X	177	1	2	2	-	4	4	2	3	3
GW321742X	177	2	2	2	2	2	2	2	1	2
GW321779X	177	3	3	3	2	3	3	2	2	3
GW321755X	177	4	3	3	3	3	3	3	2	3
GW410928X	177	5	2	2	2	2	2	2	2	2
GW324540X	177	6	8	8	7	11	9	9	4	8
GW322198X	178	1	5	4	4	9	5	6	4	5
GW322492X	178	2	4	4	3	4	7	5	3	4
GW320926X	179	1	5	4	4	5	4	4	3	4
GW321470X	179	2	2	2	2	2	2	2	1	2
GW321607X	179	3	7	6	7	6	6	5	5	6
GW323008X	179	4	2	2	2	2	2	2	2	2
GR175627	180	1	-	5	6	16	-	6	-	8
GR175628	180	2	1	-	-	-	1	1	-	1
GR196922	180	3	2	2	2	2	2	2	-	2
GR256963	180	4	1	1	1	1	1	1	-	1
GW321245X	180	5	2	2	-	2	3	2	1	2
GW321912X	180	6	2	2	3	6	5	3	3	3
AH10033	181	1	1	1	1	1	1	1	1	1
GR237865X	182	1	1	1	1	1	1	1	1	1
AH15255XX	183	1	1	1	1	1	1	1	1	1
GR68357X	184	1	-	1	1	1	-	2	-	1
GW320801X	185	1	-	1	1	1	-	1	-	1
GW385455A	185	2	1	1	1	1	1	1	1	1
AH11305	186	1	-	2	2	2	-	2	-	2
AH9723	186	2	3	5	3	4	8	7	3	5
GW655414X	187	1	109	136	-	125	146	128	73	119

Comound			Relative Emission Intensity (I/I_0)							
Reg_No	Cluster	Rank	EuBEA	EuBUA	EucyHA	EumcyHA	EuNBA	EuBBZA	EuBTA	Average EuNAL
GR107114X	188	1	1	1	1	1	1	1	1	1
GR138809X	189	1	2	2	2	2	2	2	1	2
GW295817X	190	1	1	1	1	1	2	1	1	1
GW365467X	191	1	5	5	5	5	5	5	4	5
GW311376X	192	1	-	1	1	1	-	1	-	1
GW397304X	193	1	1	1	1	1	1	1	1	1
GW584442X	194	1	15	15	13	14	16	12	9	14
GW635258X	195	1	1	1	1	1	1	1	1	1
GW635452X	195	2	4	5	4	4	6	5	3	4
GR269503X	196	1	6	6	5	5	5	5	4	5
GR223454A	197	1	1	1	1	1	1	1	1	1
GW580127X	198	1	2	4	2	2	4	4	1	3
GW623142A	198	2	1	1	1	1	1	1	1	1
GW624854X	199	1	1	2	1	3	2	2	1	2
GW663118X	199	2	1	1	-	1	1	1	1	1
GW652611X	200	1	7	19	9	13	27	22	7	15
GR151827X	201	1	4	4	3	3	4	5	2	4
GR152989X	201	2	7	15	10	8	24	18	5	12
AH11426	202	1	-	1	1	1	-	1	-	1
GR37359X	202	2	1	1	1	1	1	1	1	1
GW321066X	203	1	5	4	5	9	9	9	8	7
CCI8732	204	1	1	1	1	1	1	1	1	1
GW312666X	205	1	2	4	2	2	3	2	2	2
GW424662X	206	1	5	4	5	5	6	5	4	5
AH8940	207	1	1	2	1	1	2	2	1	1
GR258784X	208	1	1	1	1	1	1	1	1	1
GW322374X	208	2	1	1	1	1	1	1	1	1
AH8076	209	1	1	1	1	1	1	1	1	1
GW315274X	210	1	1	1	1	1	1	1	1	1
GW650524X	211	1	1	1	1	1	1	1	1	1
GW650525X	211	2	1	1	1	1	1	1	1	1
AH9033	212	1	1	1	1	1	1	1	1	1
GW649399X	212	2	37	36	25	27	27	26	21	28
AH9527	212	3	101	-	-	-	85	81	-	89

Comound			Relative Emission Intensity (I/I_0)							
Reg_No	Cluster	Rank	EuBEA	EuBUA	EucyHA	EumcyHA	EuNBA	EuBBZA	EuBTA	Average EuNAL
CCl4563	213	1	1	1	1	1	1	1	1	1
GR154660A	214	1	1	1	1	1	1	1	1	1
GR177049X	214	2	1	1	1	1	1	1	1	1
GR219652X	215	1	1	1	1	1	1	1	1	1
GR249207X	216	1	1	1	1	1	1	1	1	1
GR118330	217	1	2	2	2	3	2	2	2	2
GW276690	217	2	3	3	3	3	4	4	-	3
GR242234X	218	1	1	1	1	1	1	1	1	1
GW283348X	219	1	1	1	1	2	1	1	1	1
GW318076X	220	1	34	48	-	46	88	77	30	54
GR37727X	221	1	1	1	1	1	1	1	1	1
GR53040X	222	1	1	1	1	1	1	1	1	1
AH7643	223	1	1	1	1	1	1	1	1	1
AH9554	223	2	1	1	1	1	1	1	1	1
GR152077X	224	1	10	11	5	9	6	10	7	8
GM189907X	225	1	1	1	1	1	1	1	1	1
GR39699X	225	2	1	1	1	1	1	1	1	1
GR114312X	226	1	1	1	1	1	1	1	1	1
AH11195B	227	1	1	1	1	1	1	1	1	1
GR239106X	227	2	1	1	1	1	1	1	1	1
GR106841X	228	1	1	1	1	1	1	1	1	1
AH6081A	229	1	3	3	3	4	4	3	3	3
GR240822X	229	2	4	4	3	3	7	6	3	4
GW327515X	230	1	4	5	3	5	5	6	3	4
GW416086	230	2	1	1	1	1	1	1	1	1
AH9652	231	1	2	2	1	2	3	2	1	2
GR44240X	231	2	1	1	1	1	1	1	1	1
GR103163A	232	1	1	1	1	1	1	1	1	1
GW327758A	232	2	1	1	1	1	1	1	1	1
GW312641A	232	3	1	1	1	1	1	1	1	1
GI138330X	233	1	3	4	2	4	6	6	6	5
GW329078X	233	2	-	1	1	1	-	1	-	1
GR240576X	234	1	1	1	1	1	2	1	1	1
GW315215	234	2	-	1	1	1	-	1	-	1

Comound			Relative Emission Intensity (I/I_0)							
Reg_No	Cluster	Rank	EuBEA	EuBUA	EucyHA	EumcyHA	EuNBA	EuBBZA	EuBTA	Average EuNAL
GW412098	234	3	2	2	2	2	2	1	1	2
GR108394X	235	1	1	1	1	1	1	1	1	1
GR245706X	235	2	1	1	1	1	1	1	1	1
GR117055X	236	1	-	2	1	2	-	2	-	2
AH7461	237	1	1	-	-	-	1	1	-	1
GW341377	237	2	1	1	1	1	1	1	-	1
GW365140	237	3	1	1	1	1	1	1	-	1
GW365173	237	4	1	1	1	1	1	1	-	1
GI261653	237	5	1	1	1	1	1	1	1	1
GR242078X	238	1	-	1	1	1	-	1	-	1
GW308852X	239	1	-	1	1	1	-	1	-	1
GW307512X	240	1	1	1	1	1	1	1	1	1
GW311866X	241	1	1	1	1	1	1	1	1	1
GW319241X	242	1	1	1	1	1	1	1	1	1
GW448056X	243	1	1	1	1	1	2	1	1	1
GR258734A	244	1	1	1	1	1	1	1	1	1
GR264071A	244	2	1	2	1	1	2	1	1	1
GR263255X	244	3	1	1	1	1	1	1	1	1
GR43767X	245	1	1	1	1	1	1	1	1	1
GW472535X	245	2	1	1	1	1	1	1	1	1
GW288946X	246	1	105	108	127	135	121	102	85	112
GW324060X	247	1	2	1	1	1	2	2	1	1
AH10315	248	1	1	1	1	1	1	1	1	1
AH10461	248	2	1	1	1	1	1	1	1	1
GR105716X	249	1	1	1	1	1	1	1	1	1
GR212122X	249	2	1	1	1	1	1	1	1	1
AH22431B	250	1	1	1	1	1	1	1	1	1
GR109361X	250	2	1	1	1	1	1	1	1	1
GR60436X	250	3	2	2	2	2	3	2	2	2
AH6087	251	1	1	1	1	1	1	1	1	1
GI163641X	251	2	1	1	1	1	1	1	1	1
CCI153	252	1	1	1	1	1	1	1	1	1
GR128873	252	2	2	2	2	2	2	2	2	2
GR75538X	253	1	1	1	1	1	1	1	1	1

Comound			Relative Emission Intensity (I/I_0)							
Reg_No	Cluster	Rank	EuBEA	EuBUA	EucyHA	EumcyHA	EuNBA	EuBBZA	EuBTA	Average EuNAL
GR35345A	254	1	3	3	2	3	4	4	4	3
GR49747X	255	1	1	1	1	1	1	1	1	1
GR51603A	256	1	1	1	1	1	1	1	1	1
GR85161X	256	2	1	1	1	1	1	1	1	1
AH10536	257	1	3	-	-	-	6	6	-	5
AH10767	257	2	2	-	-	-	4	3	-	3
AH9356	257	3	4	5	3	4	8	8	3	5
GW316125	257	4	2	2	2	2	2	2	2	2
CCI10174	258	1	4	4	2	3	7	6	2	4
GR263958X	258	2	1	1	1	1	1	1	1	1
GW433821A	259	1	-	2	2	2	-	3	-	2
CCI10446	260	1	1	1	1	1	1	1	1	1
GR138218X	260	2	1	1	1	1	1	1	1	1
GW349042X	261	1	2	2	1	1	2	2	1	2
GR44479X	262	1	1	1	1	1	1	1	1	1
GR66484X	262	2	1	1	1	1	1	1	1	1
GW449422A	262	3	1	1	1	1	1	1	1	1
GI204510X	263	1	1	1	1	1	1	1	1	1
GR239579X	263	2	6	6	6	5	5	4	4	5
GW352006X	263	3	1	1	1	2	2	1	1	1
GI233445X	264	1	1	1	1	1	1	1	1	1
GR239577X	265	1	1	1	1	1	1	1	1	1
AH1010	266	1	-	1	1	1	-	1	-	1
CCI21414	266	2	-	1	1	1	-	1	-	1
GI222692X	266	3	-	1	1	1	-	1	-	1
GR84679X	267	1	-	1	1	1	-	1	-	1
GR84985A	267	2	-	1	1	1	-	1	-	1
AH10182	268	1	1	1	1	1	1	1	1	1
GR203336X	268	2	1	1	1	1	1	1	1	1
AH20998XX	269	1	1	1	1	1	1	1	1	1
AH6595	269	2	1	1	1	1	1	1	1	1
AH21933X	269	3	-	1	1	1	-	2	-	1
GR154396X	269	4	-	1	1	1	-	1	-	1
GW408146X	269	5	1	1	1	1	2	1	1	1

Comound			Relative Emission Intensity (I/I_0)							
Reg_No	Cluster	Rank	EuBEA	EuBUA	EucyHA	EumcyHA	EuNBA	EuBBZA	EuBTA	Average EuNAL
AH6732	270	1	1	1	1	1	1	1	1	1
GR208133X	270	2	1	1	1	1	1	1	1	1
AH1031	271	1	-	1	1	1	-	1	-	1
AH16943AA	271	2	2	2	2	3	2	2	2	2
AH1052	271	3	7	9	5	7	14	12	15	10
CCI21405	271	4	7	8	4	7	14	14	5	8
AH11453	271	5	-	1	1	1	-	1	-	1
CCI10176	271	6	3	3	2	3	7	6	3	4
AH10633	272	1	4	4	3	4	6	5	3	4
GW369905	272	2	7	15	4	5	14	14	-	10
AH8268A	272	3	1	1	1	1	1	1	1	1
GR202022X	273	1	96	84	87	102	143	127	41	97
GR34043X	273	2	-	19	12	19	-	28	-	20
GR247048X	274	1	1	1	1	1	1	1	1	1
GW309880X	274	2	4	4	2	4	8	4	2	4
GR230760X	275	1	6	5	3	5	11	8	4	6
GW299526X	275	2	1	1	1	1	1	1	1	1
AH10225	276	1	41	49	27	44	79	73	78	56
AH11688	276	2	9	-	-	-	20	10	-	13
GR258750	276	3	183	150	102	118	210	194	-	159
AH11368	276	4	2	2	2	2	2	3	2	2
GI266527	276	5	144	114	82	95	162	132	-	121
AH11967	277	1	11	28	22	18	65	35	82	37
GR140330X	277	2	7	9	7	10	8	6	7	8
GR216655X	277	3	-	1	1	2	-	2	-	2
GR220880X	277	4	-	1	1	1	-	1	-	1
GR232939X	278	1	1	1	1	1	2	1	1	1
AH1053	279	1	11	12	6	10	19	17	18	13
AH6596	279	2	1	1	1	1	1	1	1	1
AH12133	280	1	11	16	23	33	83	29	80	39
AH13394	280	2	5	5	4	5	9	8	4	5
GW299375X	280	3	2	1	1	3	2	2	1	2
AH3663	281	1	1	1	1	1	1	1	1	1
GR239599X	281	2	1	1	1	1	2	2	1	1

Comound			Relative Emission Intensity (I/I_0)							
Reg_No	Cluster	Rank	EuBEA	EuBUA	EucyHA	EumcyHA	EuNBA	EuBBZA	EuBTA	Average EuNAL
AH11395	282	1	2	1	2	3	4	3	3	2
AH13826XX	282	2	-	1	1	1	-	1	-	1
GR54987X	282	3	-	1	1	1	-	1	-	1
GW471049X	282	4	-	-	-	-	-	-	-	#DIV/0!
GW320828X	282	5	6	7	8	8	10	8	6	7
GW321479X	282	6	21	23	23	27	19	17	-	22
GR101886	283	1	-	3	3	3	-	2	-	3
GR82448	283	2	2	3	2	2	2	2	2	2
GW294831	283	3	20	16	18	16	22	16	-	18
AH12975	284	1	2	2	3	3	3	3	2	2
GW312607X	284	2	1	2	2	3	4	2	3	3
AH17009XX	285	1	-	2	2	5	-	3	-	3
GW314282X	285	2	-	1	1	1	-	1	-	1
GW355545X	285	3	11	11	13	12	12	11	8	11
AH3705A	286	1	-	1	1	1	-	1	-	1
CCI10881	286	2	-	1	1	1	-	1	-	1
AH10300	287	1	3	-	-	-	3	4	-	3
AH10801	287	2	5	-	-	-	4	7	-	5
AH9678	287	3	2	-	-	-	3	3	-	3
AH10698	287	4	57	-	-	-	35	46	-	46
AH10853	287	5	1	-	-	-	1	1	-	1
GR92452	287	6	1	-	-	-	1	1	-	1
AH9727	287	7	-	3	2	3	-	4	-	3
AH12695	287	8	31	-	-	-	22	18	-	24
AH13070	287	9	1	1	1	1	1	1	1	1
AH9676	287	10	61	-	-	-	93	88	-	81
AH9721	287	11	1	-	-	-	1	1	-	1
AH10301X	288	1	23	23	12	25	60	28	18	27
AH15692	288	2	12	-	-	-	13	17	-	14
AH12533	288	3	6	-	-	-	8	7	-	7
AH12590	288	4	3	-	-	-	5	3	-	4
AH15690	288	5	5	-	-	-	6	6	-	6
AH15757	288	6	7	-	-	-	8	5	-	7
AH10978	288	7	1	-	-	-	2	2	-	2

Comound			Relative Emission Intensity (I/I_0)							
Reg_No	Cluster	Rank	EuBEA	EuBUA	EucyHA	EumcyHA	EuNBA	EuBBZA	EuBTA	Average EuNAL
AH11275	288	8	16	24	36	33	46	48	14	31
AH12589	288	9	2	2	1	3	3	3	2	2
AH11274	288	10	6	5	5	8	8	7	7	7
AH13391	288	11	4	3	2	5	5	5	3	4
GR254264X	288	12	3	3	3	3	5	3	2	3
AH10616T	289	1	1	1	1	1	1	1	1	1
AH7490	289	2	1	1	1	1	1	1	1	1
AH18515XX	290	1	-	5	3	4	-	8	-	5
AH22573X	290	2	1	1	1	2	1	1	1	1
AH8588	290	3	1	1	1	1	1	1	1	1
AH8601	290	4	4	6	5	6	5	4	4	5
GR32737X	290	5	1	1	1	1	1	1	1	1
AH23288X	291	1	1	1	1	1	1	1	1	1
GI149558	291	2	1	-	-	-	1	1	-	1
GR133921	291	3	1	-	-	-	1	1	-	1
GR134971	291	4	1	-	-	-	2	2	-	2
GR65242X	291	5	1	1	1	1	1	1	1	1
AH26099	291	6	2	3	3	4	3	3	2	3
GR116365X	291	7	6	7	6	6	5	4	3	5
GW541785X	291	8	1	1	1	2	1	1	1	1
GR31004	291	9	2	1	1	1	1	1	-	1
GW278395	291	10	11	10	10	9	11	10	-	10
GR110635X	292	1	1	1	1	1	1	1	1	1
GR116353X	292	2	1	1	1	1	1	1	1	1
GR125882X	292	3	1	1	1	1	1	1	1	1
GW294490X	292	4	1	1	1	1	1	1	1	1
GW589997X	293	1	1	1	1	1	1	1	1	1
AH20902	294	1	2	2	2	2	2	2	2	2
GR36456	294	2	2	2	2	2	2	2	-	2
AH20984	294	3	1	-	-	-	1	1	-	1
AH21852	294	4	1	-	-	-	1	1	-	1
GR252017	294	5	2	2	2	2	3	2	-	2
GR58047	294	6	1	1	1	1	1	1	1	1
GR44857A	295	1	4	4	3	4	4	3	3	4

Comound			Relative Emission Intensity (I/I_0)							
Reg_No	Cluster	Rank	EuBEA	EuBUA	EucyHA	EumcyHA	EuNBA	EuBBZA	EuBTA	Average EuNAL
GR207154	296	1	1	1	1	1	1	1	1	1
GR78684X	296	2	4	5	4	5	4	4	4	4
AH2426A	297	1	-	1	1	1	-	1	-	1
AH3116	297	2	3	3	3	4	4	3	2	3
GW304734X	297	3	10	12	6	12	20	17	16	13
GW661447X	297	4	2	1	-	2	2	1	1	1
GR173175X	298	1	1	1	1	1	1	1	1	1
GR254404X	298	2	1	1	1	1	1	1	1	1
GW275105X	298	3	1	1	1	1	1	1	1	1
GW299610X	298	4	1	1	1	1	1	1	1	1
GW298781X	298	5	1	1	1	1	1	1	1	1
GW470761X	298	6	1	1	1	1	1	1	1	1
GW369798X	298	7	1	1	1	1	1	1	1	1
GW659802X	298	8	1	1	-	1	1	1	1	1
GR221928X	299	1	1	1	1	2	1	1	1	1
GW470720X	300	1	1	1	1	1	1	1	1	1
GW641296X	300	2	1	1	1	1	1	1	1	1

Appendix 3

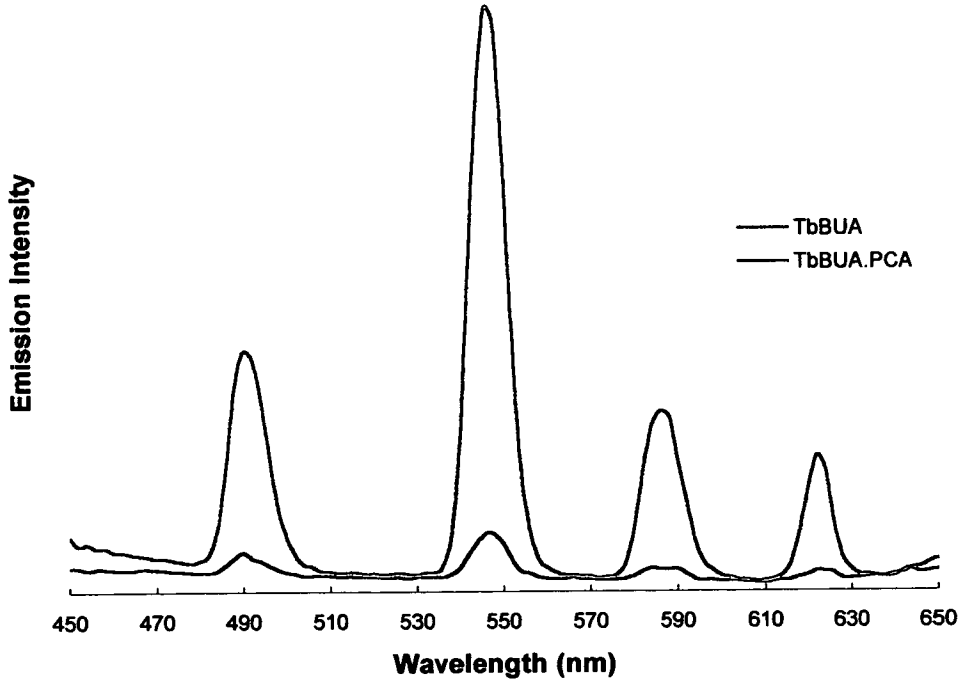

Figure 1 Emission spectrum (corrected for PMT response) of TbBUA (0.1 mM aq, pH 7) + PCA (λex = 270 nm)

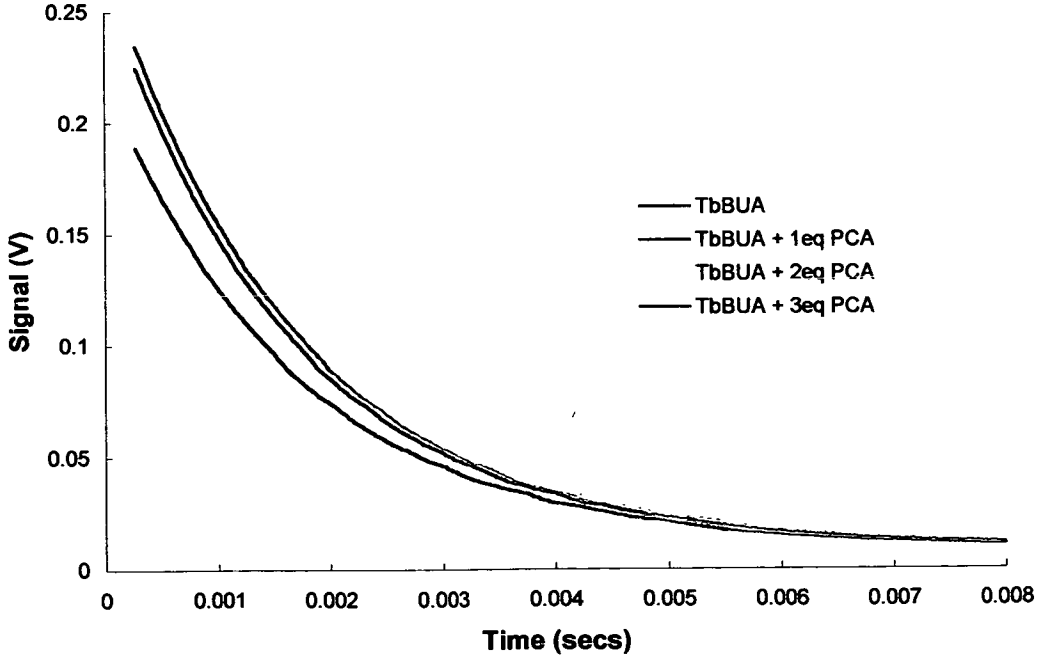

Figure 2 Lifetime decay curves for TbBUA (0.1 mM aq) + PCA

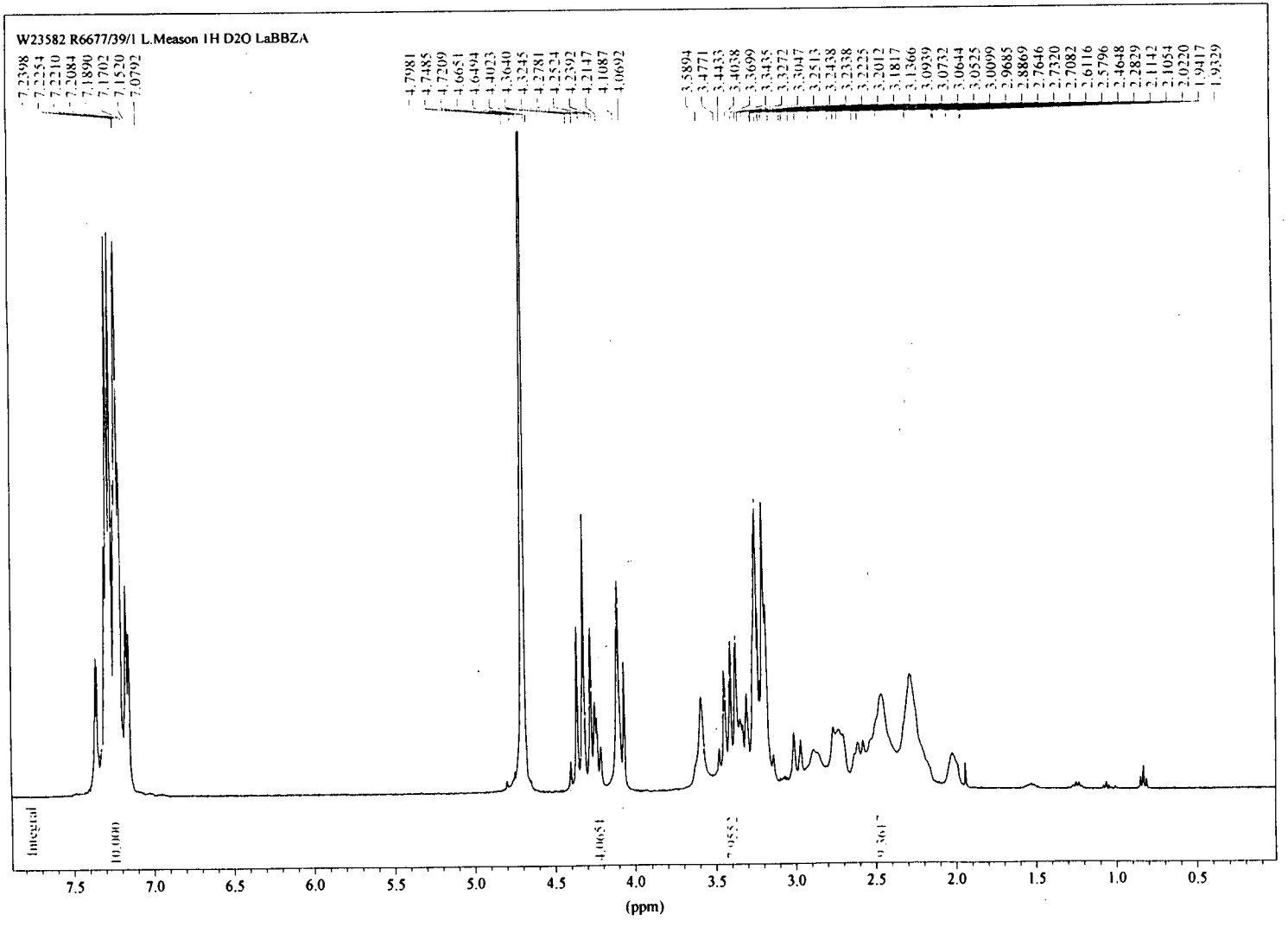

Figure 1 LaBBZA ^{1}H NMR spectrum (400 MHz, D_2O)

Appendix 4: LaBBZA NMR

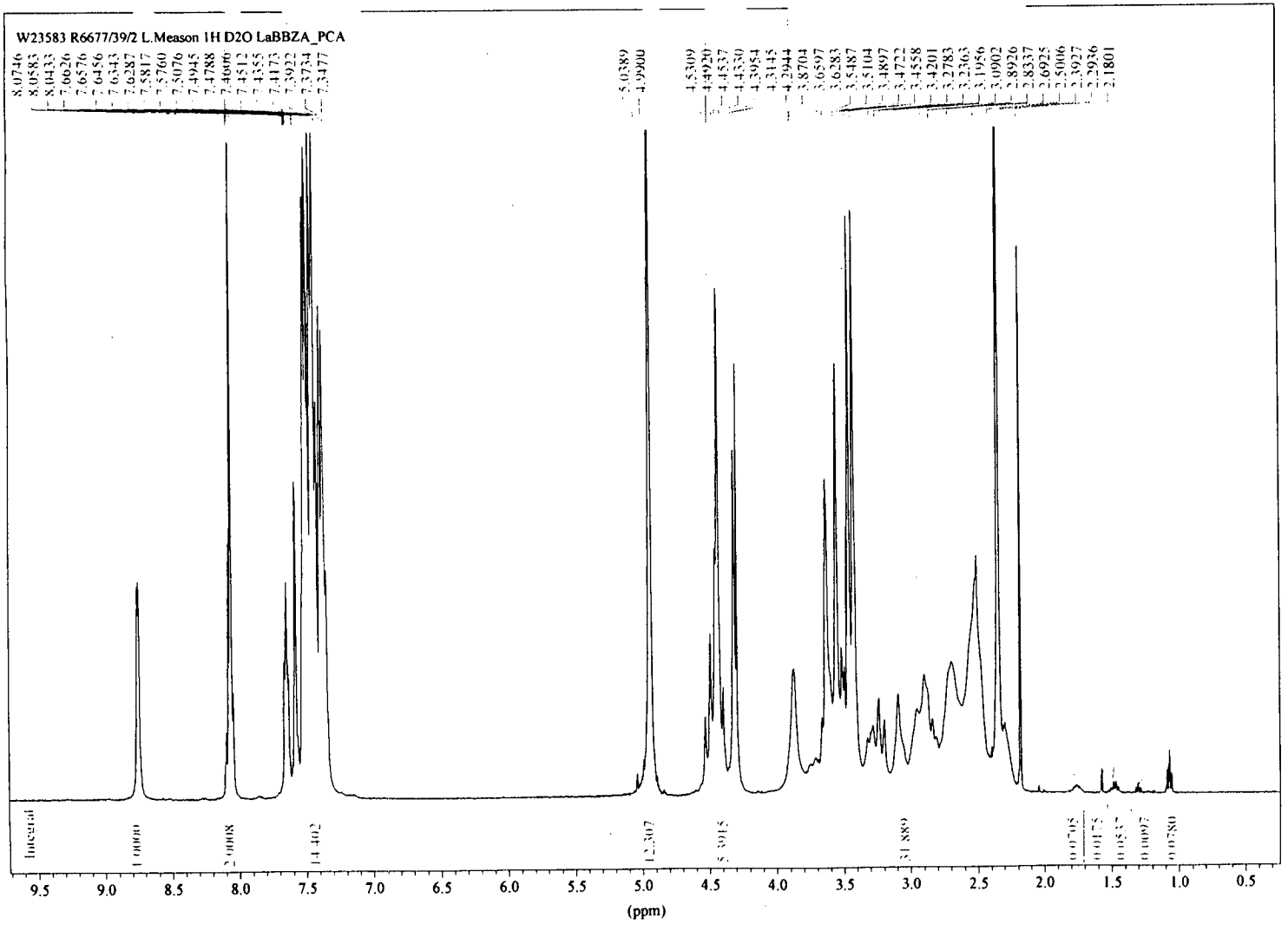

Figure 2 ^{1}H NMR spectrum of LaBBZA + PCA (400 MHz, D_2O)

Appendix 4: LaBBZA NMR

Appendix 5

Model for calculation of polyprotic acid speciation versus solution pH

L = DTPA-BEA

Protonation Equilibria:

$$H_3L \overset{K_{a1}}{\rightleftharpoons} H_2L^- \overset{K_{a2}}{\rightleftharpoons} HL^{2-} \overset{K_{a3}}{\rightleftharpoons} L^{3-}$$

$K_{a1} = [H_2L^-]/[H_3L]$; $K_{a2} = [HL^{2-}]/[H_2L^-]$; $K_{a3} = [L^{3-}]/[HL^{2-}]$

Protonation Constants:

Protonation Event	*Ka*	*pKa*
1	*6.31E-04*	*3.2*
2	*2.51E-05*	*4.6*
3	*6.31E-10*	*9.2*

$pH = -Log_{10}[H_3O^+]$

$[H_3O^+] = 10^{(-pH)}$

Mass Balance Equation:

$[L]_T = [H_3L] + [H_2L^-] + [HL^{2-}] + [L^{3-}]$

Species Fraction (α)

$\alpha_0 = [H_3L]/[L]_T$; $\alpha_1 = [H_2L^-]/[L]_T$;; $\alpha_2 = [HL^{2-}]/[L]_T$; $\alpha_3 = [L^{3-}]/[L]_T$

$\alpha_0 = [H_3O^+]^3/([H_3O^+]^3 + K_{a1}[H_3O^+]^2 + K_{a1}K_{a2}[H_3O^+] + K_{a1}K_{a2}K_{a3})$

$\alpha_1 = K_{a1}[H_3O^+]^2/([H_3O^+]^3 + K_{a1}[H_3O^+]^2 + K_{a1}K_{a2}[H_3O^+] + K_{a1}K_{a2}K_{a3})$

$\alpha_2 = K_{a1}K_{a2}[H_3O^+]/([H_3O^+]^3 + K_{a1}[H_3O^+]^2 + K_{a1}K_{a2}[H_3O^+] + K_{a1}K_{a2}K_{a3})$

$\alpha_3 = K_{a1}K_{a2}K_{a3}/([H_3O^+]^3 + K_{a1}[H_3O^+]^2 + K_{a1}K_{a2}[H_3O^+] + K_{a1}K_{a2}K_{a3})$

Conditional Stability Constants

The conditional stability constant (K'_{ML}) for an aminopolycarboxylate complex in aqueous solution at a fixed pH is calculated from the thermodynamic stability constant (K_{ML}) for the complex and the species fraction of the fully deprotonated ligand. For DTPA-BEA, the thermodynamic stability constant with Gd(III) is 2.19×10^{15} ($LogK_{GdL} = 15.34$).

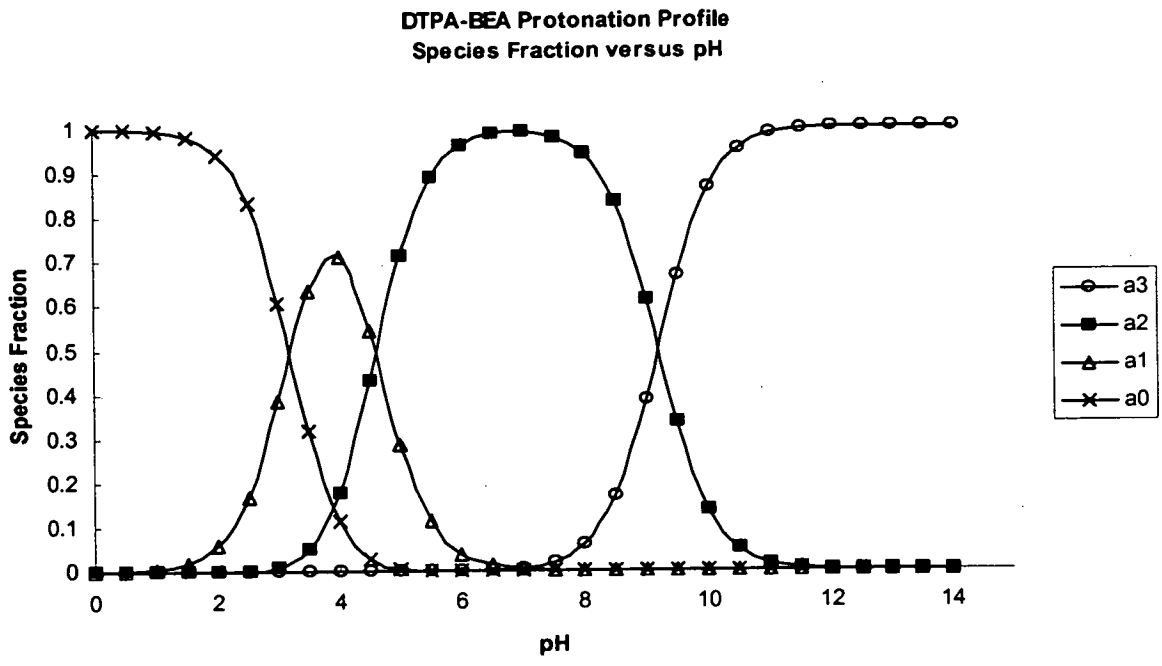

Figure 1 DTPA-BEA protonation equilibria: Species fraction versus pH

pH	$[H_3O^+]$	α_3	α_2	α_1	α_0	K'_{ML}	$Log\ K_{ML}$
0	*1.00E+00*	*9.99E-18*	*1.58E-08*	*6.31E-04*	*9.99E-01*	*2.19E-02*	*-1.66*
1	*1.00E-01*	*9.94E-15*	*1.57E-06*	*6.27E-03*	*9.94E-01*	*2.17E+01*	*1.34*
2	*1.00E-02*	*9.41E-12*	*1.49E-04*	*5.93E-02*	*9.41E-01*	*2.06E+04*	*4.31*
3	*1.00E-03*	*6.07E-09*	*9.62E-03*	*3.83E-01*	*6.07E-01*	*1.33E+07*	*7.12*
4	*1.00E-04*	*1.12E-06*	*1.78E-01*	*7.09E-01*	*1.12E-01*	*2.46E+09*	*9.39*
5	*1.00E-05*	*4.49E-05*	*7.12E-01*	*2.83E-01*	*4.49E-03*	*9.83E+10*	*10.99*
6	*1.00E-06*	*6.06E-04*	*9.61E-01*	*3.83E-02*	*6.06E-05*	*1.33E+12*	*12.12*
7	***1.00E-07***	***6.25E-03***	***9.90E-01***	***3.94E-03***	***6.25E-07***	***1.37E+13***	***13.14***
8	*1.00E-08*	*5.93E-02*	*9.40E-01*	*3.74E-04*	*5.93E-09*	*1.30E+14*	*14.11*
9	*1.00E-09*	*3.87E-01*	*6.13E-01*	*2.44E-05*	*3.87E-11*	*8.46E+14*	*14.93*
10	*1.00E-10*	*8.63E-01*	*1.37E-01*	*5.45E-07*	*8.63E-14*	*1.89E+15*	*15.28*
11	*1.00E-11*	*9.84E-01*	*1.56E-02*	*6.21E-09*	*9.84E-17*	*2.15E+15*	*15.33*
12	*1.00E-12*	*9.98E-01*	*1.58E-03*	*6.30E-11*	*9.98E-20*	*2.18E+15*	*15.34*
13	*1.00E-13*	*1.00E+00*	*1.58E-04*	*6.31E-13*	*1.00E-22*	*2.19E+15*	*15.34*
14	*1.00E-14*	*1.00E+00*	*1.58E-05*	*6.31E-15*	*1.00E-25*	*2.19E+15*	*15.34*

Dissociation Equilibrium

EuNAL = Eu + NAL (Eu = NAL = x) $K^{-1} = 1/K'_{ML} = 7.32 \times 10^{-14}$

$[EuNAL] = [EuNAL]_0 - [Eu]$; $[EuNAL] = [EuNAL]_0 - x$

$K^{-1} = x^2/([EuNAL]_0 - x)$

$x^2 - K^{-1}[EuNAL]_0 + K^{-1}x = 0$ (solved for x; $[EuNAL]_0$ and K^{-1} are constants to give the extent of complex dissociation in solution)

Lecture Courses, Conferences and Presentations

Lectures

Supramolecular Coordination Chemistry (Oct-Dec 98) Dr Zoe Pikramenou

Modern NMR Spectroscopy, Jan-Apr 98,

Basic principles (5hrs)

Special topics (2 hrs)

Quadrupolar nuclei

Paramagnetic NMR

Current Awareness in Organic Chemistry (2hrs)

Metallation of Aryl and Hetaryl Ring Systems using Alkyl Lithium Reagents

New Aromatic Substitution Reactions

Computers in Chemistry Workshops (July 98)

Molecular Mechanics, Steve Harris (3hrs)

Ames Symposium, Inaugural Lecture of Prof. P. Sadler. (6/98)

Walker Memorial Lecture, Prof. J. -M. Lehn, Perspectives in Supramolecular Chemistry, 17/4/98

R. S. C. lectures by: Prof. Zare,

Prof. K. Wieghardt

Inorganic Colloquia terms 1,2 and 3. (Wed, 11.10am)

Prof. M. Walkinshaw (C. A. Beevers lecture)

Inorganic Section Meetings, Thursdays 5pm (97/98, 98/99, 99/00)

Conferences

ICCC 34
Edinburgh, July 2000
"New Chelators in the Development of Highly Luminescent Lanthanide Complexes for Biomolecule Labelling"

RSC Young Researchers Meeting
Heriot Watt University, Sept 1999
"Ternary Luminescent Lanthanide Complexes: New Light Bulbs"

University of Edinburgh Inorganic Section Meetings
Firbush Outdoor Centre, April 1998 and 1999
"Ternary Luminescent Lanthanide Complexes: New Light Bulbs"

RSC Dalton Meetings: St Andrews University, April 1999
University of Glasgow, April 1998

5th International Symposium on Biotechnological and Spectroscopic Chemistry
Greece, March 1999
Poster Prize: *"Ternary Luminescent Lanthanide Complexes for Biomolecule Labelling"*

RSC "New Chemistry, New People"
RSC, London; Dec 1998
"Ternary Luminescent Lanthanide Complexes: New Light Bulbs"

USIC 98
University of Strathclyde, Sept 1998
"Ternary Luminescent Lanthanide Complex Formation by Lanthanide Molecular Recognition"

UK Macrocycles and Supramolecular Chemistry Group, Annual Conference
University of Nottingham, Jan 1998,
Poster prize: *"The Design of Luminescent, Mixed Ligand Lanthanide Complexes"*

Presentations

Glaxo Wellcome, Stevenage

June 2000	"New Chelators for the Development of Highly Luminescent Complexes for Biomolecule Labelling"
May 1999	"Lanthanide Molecular Recognition Towards the Luminescent Labelling of Biomolecules"

University of Edinburgh

Feb 2000	"Ligands for Lanthanide Molecular Recognition"
May 1999	"Ternary Luminescent Lanthanide Complexes: New Light Bulbs"
March 1998	"The Design of Luminescent Mixed Ligand Lanthanide Comlpexes"